Navigating the immuno-epidemiology of malaria: Potential metrics for surveillance and cluster randomised trials

Lindsey Wu

Thesis submitted in accordance with the requirements for the degree of
Doctor of Philosophy

July 2018

DEPARTMENT OF IMMUNOLOGY AND INFECTION
FACULTY OF INFECTIOUS AND TROPICAL DISEASES
LONDON SCHOOL OF HYGIENE & TROPICAL MEDICINE
UNIVERSITY OF LONDON

Funded by the UK Medical Research Council

Supervisors: Professor Chris Drakeley, Faculty of Infectious and Tropical Diseases
Professor Immo Kleinschmidt, Faculty of Epidemiology and Population Health

Declaration

I, *Lindsey Wu*, confirm that the work presented in this thesis is my own. Where information has been derived from other sources, I confirm that this has been indicated in the thesis.

Signed 

July 2018

Abstract

As malaria endemic countries progress towards elimination, accurately measuring community-level transmission is critical for monitoring control strategies and the design of efficacy trials. However, measuring malaria transmission often faces challenges in pre-elimination settings due to the complexity of human immunity and its interaction with vector and parasite dynamics. This study evaluates current and emerging epidemiological measures of malaria transmission, and explores the use of novel serological markers of malaria infection as metrics in surveillance and cluster-randomised trials (CRTs).

The relative sensitivity of commonly used surveillance diagnostics - polymerase chain reaction (PCR), rapid diagnostic tests (RDTs), and microscopy – are cross-compared with respect to their accuracy in quantifying cluster-level prevalence of malaria infection. These are further evaluated against immunological measures of transmission based on antibody responses to two malaria parasite antigens - *Pf*MSP1$_{19}$ and *Pf*AMA1 - used extensively in serological surveillance for the last decade.

To investigate novel serological markers of malaria infection, a multiplexed immunoassay was used to characterise post-infection antibody dynamics to 20 *Plasmodium falciparum* antigens. This was based on a subset of 192 individuals from an all-age longitudinal cohort study in The Gambia. Antibody responses against several antigens showed accuracy in detecting infection in the preceding six months. These may have potential utility in measuring time since infection or short-term changes in transmission. However, variations in immune response by age and transmission intensity were observed and should be taken into consideration for future optimisation of serological assays.

Antigens identified as the most promising biomarkers of recent infection were used to estimate cluster-level transmission in four villages in The Gambia. Serological responses are compared between dry and wet season and geographical regions of low and high transmission intensity. Their application was also extended to compare study arms of a cluster-randomised trial in the Zambezi Region, Namibia, comparing the effectiveness of reactive focal case detection, reactive focal mass drug administration, and reactive vector control.

These findings may help to inform the development of new serological diagnostic assays for malaria, their use in future malaria surveillance and elimination strategies, and the design of cluster-randomised trials in low transmission settings.

Acknowledgements

". . . if there had been a way to get to success without traveling through disaster someone would have already done it and thus rendered the experiments unnecessary. . .there's still no journal where I can tell the story of how my science is done with both the heart and the hands."

- Hope Jahren

It is certainly true that without the heart and hands of so many people, the research presented in this thesis would not have been possible. First and foremost, I'm extremely grateful for the support and guidance of my supervisors – Chris Drakeley and Immo Kleinschmidt - from whom I've learned an incredible amount in the past four years. Not only have they given me endless advice, opportunities, and encouragement, but have taught by example the importance of pursuing research with true scientific curiosity and humility.

A huge thanks to Lucy Okell and Nuno Sepulveda, who have been an enormous help on statistics and modelling, and to Kevin Tetteh, Tom Hall, and Lotus van den Hoogen for teaching me the basics of lab serology (and for being on standby as I set it up in The Gambia!). Thanks to Jackie Cook and Bronner Gonçalves, who have always been willing to give advice on epidemiology, no matter the topic, and were a source of great scientific discussion and friendship through the years. Thanks to the rest of my LSHTM / Imperial malaria family, who I've been lucky to learn from and laugh with.

My time working in the field with the MRC Gambia was a truly wonderful experience with the support of Julia Mwesigwa, Muna Affara, and Umberto D'Alessandro. My gratitude especially to Julia, who was a great mentor and friend throughout my research time there. Special thanks to Simon Correa and Mamadou Bah for the dedication, fresh mangoes, chakri, and chats that got me through lab work and the rainy season. And, of course, to Manchester House & Co for all the laughs and amazing road trips.

With the support of Lisa Prach and Michelle Hsiang, I gained excellent trial experience in Namibia, and I'm extremely thankful for the opportunity (and faith they put in my abilities!). To my Katima family - Leah, Joy, Val, Henry, Tererai, and Miriam - life in Namibia would not have been the same without our moments dodging goats and impalas driving back from the field and much needed sundowners on the Zambezi after a hard day's work.

I've had the privilege to share this PhD journey with Mateusz Hasso Agopsowicz and Lisa Stockdale, whose friendship and support academically and personally have been invaluable; I could not have asked for two better LSHTM companions. Thanks also to Lilly, Adarsh, Tilly, Mariella, Ingram, and Peggy - friends who have been there for me throughout, and to Sonal, who was a great support and idea generation buddy during the thesis writing process!

To my family: Christine, an amazing sister and role model my whole life who continues to inspire me as a scientist and person; and, of course, to mom and dad, who, as both my strongest disciplinarians and my biggest cheerleaders, taught me the value of hard work, grit, and compassion.

Last but not least, to the study communities and villages in The Gambia and Zambezi, for whom I hope this research can make a difference.

Statement of Contributions

Chapter 3 was co-authored by myself and Lotus van den Hoogen[1], with equal contributions to final data analysis and writing. Lucy Okell[2] and Chris Drakeley[1] provided guidance on study design and analysis, with support from Patrick Walker[2], Hannah Slater[2] and Azra Ghani[2].

Chapter 4 all analysis and writing was conducted by myself. Lucy Okell, Jamie Griffin[3], and Nuno Sepulveda[1] provided guidance on statistical analysis. Lucy Okell, Immo Kleinschmidt[1], and Chris Drakeley provided comments on data analysis and interpretation. Lotus van den Hoogen and Jackie Cook[1] provided support in the data compilation process.

Chapters 5 and 6 are based on a longitudinal cohort study conducted in The Gambia. Laboratory procedures were part of previous and ongoing work to optimise the Luminex assay for malaria serology. Contributions of colleagues involved in both are summarised below.

- Study design, field activities, sample collection, and laboratory analysis for the Malaria Transmission Dynamics project were coordinated by Julia Mwesigwa, Umberto D'Alessandro, Jane Achan and Muna Affara at the Medical Research Council Unit, The Gambia.
- PCR, microscopy, community-based RDT testing, and clinical case management, were the work of numerous laboratory staff, field workers, and nurses at the MRC Gambia, of which there are too many to name here, but their dedication should be fully acknowledged. I am particularly grateful for all that I learned from the field team at Besse health facility, and the microscopy and PCR labs in Fajara with Sarjo Njie, Simon Correa and Fatoumatta Kanuteh.
- Luminex assay procedures were optimised by Kevin Tetteh and Tom Hall[1]. Antigens were designed/produced by Kevin Tetteh[1], with the exception of EBA175/181/140 (James Beeson[4]), Rh5 (Simon Draper[5]), $MSP1_{19}$ (Anthony Holder[6]), AMA1 (Michael Blackman[6]), GLURP (Michael Theisen[7]) and CSP (Gennova Biopharmaceuticals).
- Luminex procedures were adapted/coordinated at the MRC Gambia by myself and Muna Affara. Assays were conducted by Simon Correa, Mamadou Bah, and myself.
- Study design for the analysis in this chapter was conceived by myself with support from Chris Drakeley, Umberto D'Alessandro, Julia Mwesigwa, Muna Affara, Immo Kleinschmidt, and Davis Nwakwanma.
- Isabel Rodriguez[8], Bryan Greenhouse[8], and Nuno Sepulveda provided advice on statistical analyses and R code.
- All final analyses, code, and writing was conducted by myself, with comments by Chris Drakeley, Immo Kleinschmidt, Lucy Okell, Umberto D'Alessandro, Julia Mwesigwa and Muna Affara.

[1] London School of Hygiene & Tropical Medicine

[2] Department of Infectious Disease Epidemiology, Imperial College London

[3] Queen Mary University of London

[4] Burnet Institute

[5] Jenner Institute, University of Oxford

[6] The Francis Crick Institute

[7] Department for Congenital Disorders, Statens Serum Institut. Centre for Medical Parasitology at Department of International Health, Immunology and Microbiology, University of Copenhagen

Chapter 7 is based on a cluster-randomised trial conducted in the Zambezi Region, Namibia.

- Study design, field activities, sample collection, and laboratory analysis for the cluster-randomised trial were coordinated by Michelle Hsiang[8,9], Henry Ntuku[8], Kathryn Roberts[8], Oliver Medzihradsky[8], Lisa Prach[8], Bryan Greenhouse, Hugh Sturrock[8], Adam Bennett[8], Jennifer Smith[8], Valerie Scott[8], Davis Mumbengegwi[10], Immo Kleinschmidt, and Roly Gosling[8].
- Samples for analyses are from the end-line cross-sectional survey (of the CRT), which was designed by Lisa Prach, Michele Hsiang, and Kathryn Roberts.
- Field activities and sample collection for the end-line survey were coordinated in Katima, Namibia by Lisa Prach, Leah Schrubbe[8], Joy Yala[11] and myself:
    - From April – July, I served as on-site data manager, trained field staff, and co-supervised survey activities with Leah Schrubbe.
- Plasma samples collected in Namibia were sent to London via San Francisco by UCSF, and Luminex assays were conducted in the Drakeley Lab at LSHTM by Katie Patterson[1], Joseph Biggs[1], Tom Hall, and myself.
- All final analysis and writing in this chapter was conducted by myself, with comments by Chris Drakeley, Immo Kleinschmidt, Lisa Prach, Michelle Hsiang, and Roly Gosling.

Additional Publications

I also contributed to the following manuscripts, which were not a part of my PhD.

- The malERA Refresh Consultative Panel on Characterising the Reservoir and Measuring Transmission. 2017. "MalERA: An Updated Research Agenda for Characterising the Reservoir and Measuring Transmission in Malaria Elimination and Eradication." *PLOS Medicine* 14 (11). Public Library of Science: e1002452. doi:10.1371/journal.pmed.1002452.
    - For this publication, I was a rapporteur for the consultative panel and part of the writing group that prepared the final manuscript. I prepared Tables 1-3, which built on previous work from my upgrading report. These have been included in Chapter 1 of this thesis.
- Floyd, Jessica*, **Lindsey Wu***, Deborah Hay Burgess, Rasa Izadnegahdar, David Mukanga, and Azra C. Ghani. 2015. "Evaluating the Impact of Pulse Oximetry on Childhood Pneumonia Mortality in Resource-Poor Settings." *Nature* 528 (7580): S53–59. doi:10.1038/nature16043.

  *co-first-author

[8] Malaria Elimination Initiative, University of California, San Francisco (UCSF)
[9] University of Texas, Southwestern
[10] University of Namibia (UNAM)
[11] Kent State University

Table of Contents

List of Figures

CHAPTER 1

CHAPTER 2

No figures

CHAPTER 3

Publication

CHAPTER 4

CHAPTER 5

CHAPTER 6

CHAPTER 7

CHAPTER 8

List of Tables

CHAPTER 1

CHAPTER 2

No figures

CHAPTER 3

Publication

CHAPTER 4

CHAPTER 5

CHAPTER 6

CHAPTER 7

Abbreviations

ACD	Active case detection
ACTs	Artemisinin-based combination therapies
AL	Artemether-lumefantrine
AMA1	Apical membrane antigen 1
API	Annual parasite incidence / index
ASCs	Antibody-secreting plasma cells
AUC	Area under the curve
CBA	Cytometric bead assay
CRT	Cluster randomised trial
DBS	Dried blood spot
DDT	Dichloro-diphenyl-trichloroethane
DIC	Deviance information criterion
DHS	Demographic and Health Surveys
EA	Enumeration area
EIR	Entomological inoculation rate
ELISA	Enzyme-linked immunosorbent assay
FACS	Fluorescence-activated cell sorting
FMM	Finite mixture model
FOI	Force of infection
FSAT / FTAT	Focal screen and treat / focal test and treat
GEE	Generalised estimating equations
GMEP	Global Malaria Eradication Program 1955-1969
GST	Glutathione S-transferase
HLA	Human leukocyte antigen
HLOQ / LLOQ	Higher / Lower limit of quantification
HRP2	Histidine-rich protein 2
HSRDT	Highly sensitive rapid diagnostic test
ICC	Intra-cluster coefficient of variation
IFAT	Immunofluorescence antibody test
IgG	Immunoglobulin
IHA	Indirect haemagglutination assay
IPT	Intermittent preventive treatment
IRR	Incidence rate ratio
IRS	Indoor residual spraying
ITN	Insecticide-treated bed net
ITT	Intention-to-treat
LAMP	Loop-mediated isothermal amplification
LDH	Lactate dehydrogenase
LFA	Lateral flow assay
LLINs	Long-lasting insecticidal nets
LLPCs	Long-lived plasma cells
LOB	Limit of blank / background
Luminex	Luminex MAGPIX©
MAP	Malaria Atlas Project
MBCs	Memory B cells
MCMC	Markov Chain Monte Carlo
MDA / rfMDA	Mass drug administration / reactive focal mass drug administration
MFI	Median fluorescence intensity
MICS	UNICEF Multiple Indicators Cluster Surveys
MIS	Malaria Indicators Surveys
MHC	Major histocompatibility complex
MOI	Multiplicity of infection
$_{mol}$FOI	Molecular force of infection
MSAT / MTAT	Mass screen and treat / mass test and treat

$MSP1_{19}$	Merozoite surface protein 1, C-terminal 19-kilodalton region
NAATs	Nucleic acid amplification techniques
nPCR	Nested polymerase chain reaction
OD	Optical density
OR	Odds Ratio
PACD	Proactive case detection
PCD	Passive case detection
PCR	Polymerase chain reaction
PMBCs	Peripheral blood mononuclear cells
PP	Per-protocol
PR	Parasite rate
Pf	*Plasmodium falciparum*
Pv	*Plasmodium vivax*
Pm	*Plasmodium malariae*
Po	*Plasmodium ovale*
Pk	*Plasmodium knowlesi*
$PfPR_{2-10}$	*P.falciparum* parasite rate in 2-10 year olds
*Pf*EMP1	*P.falciparum* erythrocyte membrane protein 1
qSAT	Quantitative suspension array technology
R_0	Basic reproductive rate/number
R_C	Basic reproductive rate/number under malaria control measures
RACD	Reactive case detection
RAVC	Reactive focal vector control
RBCs / iRBCs	Red blood cells / infected red blood cells
RDT	Rapid diagnostic test
ROC	Receiver operating characteristics
SCR / SRR	Sero-conversion rate / sero-reversion rate
SD	Standard deviation
SE	Standard error
SMC	Seasonal malaria chemoprevention
SP	Sero-prevalence
TBV	Transmission-blocking vaccine
Th	T-helper cells
TNF-α	Tumour necrosis factor alpha
TPE	Targeted parasite elimination
$t_{0.5}$	Half-life
URR	Upper River (Administrative) Region South, The Gambia
VIMTs	Vaccines interrupting malaria transmission
WCR	West Coast (Administrative) Region, The Gambia
WHO	World Health Organization
µL	Micro-litre
95%CI	95% confidence interval or 95% credible interval (if based on posterior distribution of MCMC estimates)

Chapter 1 Introduction

1.1 Malaria elimination – past, present and future

"Not only does malaria persist; it thrives."[1]

In fact, the human battle against *Plasmodia* has endured for millennia.[2] In 2007, when Bill and Melinda Gates challenged scientists to eradicate malaria in their lifetimes,[3] it was not the first time the world had made this pursuit. Nonetheless, it signalled a renewed paradigm shift from control to elimination in the modern era of malaria. In the years since, consistent financial investment and political will have enabled sizeable reductions in malaria at national and regional levels. As part of the Global Technical Strategy for Malaria endorsed by the World Health Organization (WHO) in 2015, the malaria community set targets to achieve elimination in over 35 countries by 2030. A number of countries have already been declared no longer endemic or free of indigenous cases since 2000,[4] and 32 currently endemic countries are pursuing national policies for elimination[5] (Figure 1.1).

Yet, perhaps the most distinguishing characteristic of current malaria efforts is the recognition that multi-faceted approaches are crucial (Figure 1.2). Countries currently on or considering the path to elimination possess a much larger range of intrinsic transmission potential than countries that have eliminated since the Global Malaria Eradication Program (GMEP) of 1955-1969.[5–9] These variations are driven by complex environmental, biological, and health system factors.[10,11] Today, a better appreciation for these differences across epidemiological settings means that implementing an optimal set of strategies for elimination will require a tailored effort for many countries. In light of this, well-designed and consistent methods for measuring malaria transmission are needed to assess the effectiveness of strategies in varied settings and to monitor progress towards elimination.

In this chapter, I review strategies for malaria elimination (past and present) and the challenges posed by the changing landscape of malaria epidemiology. I will also discuss current and emerging diagnostic tools for measuring transmission, including the application of immunoassays to serological surveillance. Finally, I describe the history of epidemiology in The Gambia and Namibia - two sub-Saharan African countries currently on the path to malaria elimination - and how their experience with community-based interventions may help illustrate what is required going forward.

Figure 1.1 Map of 21 countries with the potential to eliminate malaria by 2020

As described by Rabinovich, R.N. et al in "malERA: An updated research agenda for malaria elimination and eradication." *PLOS Med*. 14, e1002456 (2017)[12], there are 91 countries and territories with ongoing malaria transmission. As of November 2017, analysis by WHO identified 21 countries with the potential to eliminate by 2020: Algeria, Belize, Bhutan, Botswana, Cabo Verde, China, Comoros, Costa Rica, Ecuador, El Salvador, Iran (Islamic Republic of), Malaysia, Mexico, Nepal, Paraguay, Republic of Korea, Saudi Arabia, South Africa, Suriname, Swaziland, and Timor-Leste. Countries and territories that have been certified malaria-free since 2007 are the United Arab Emirates (2007), Morocco (2010), Turkmenistan (2010), Armenia (2011), Maldives (2015), Sri Lanka (2016), Kyrgyzstan (2016), and Paraguay (2018). Argentina has formally requested certification of malaria elimination and is in the process. Note that not all countries that have achieved zero indigenous cases for 3 consecutive years have sought certification from WHO.

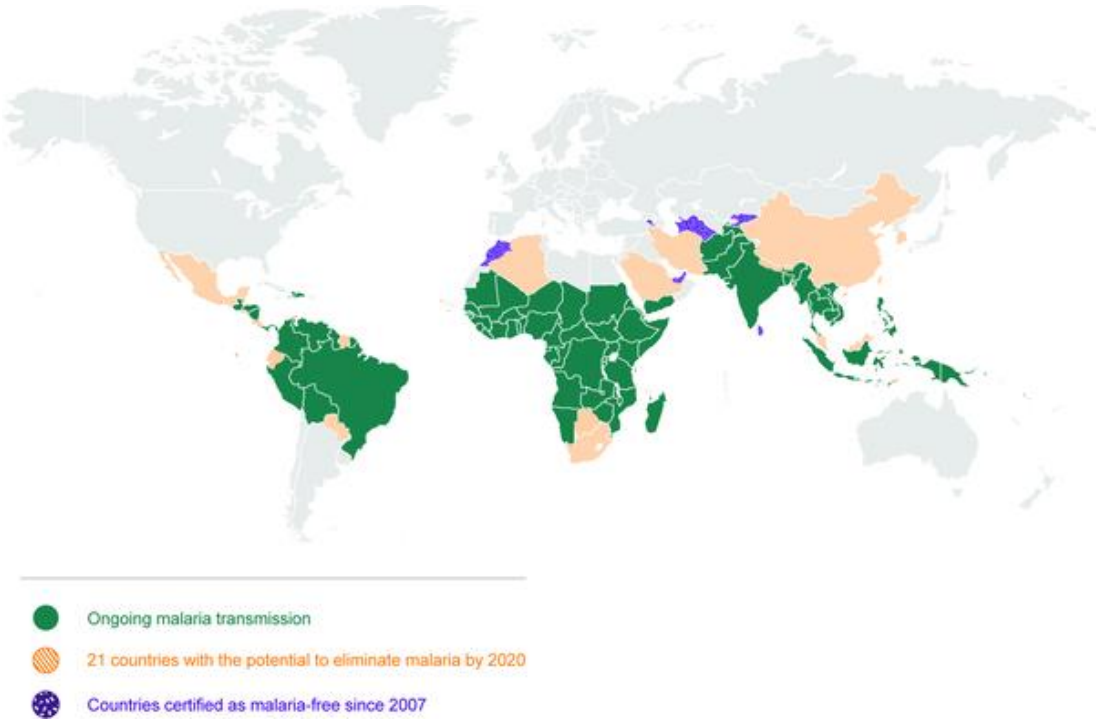

1.2 Strategies for malaria elimination

The eradication of malaria was first considered a feasible objective after the development and application of dichloro-diphenyl-trichloroethane (DDT) in the 1940s as a long-lasting residual insecticide. Numerous field trials and the integration of DDT spraying into national malaria control programmes demonstrated that it was extremely effective in interrupting transmission.[13,14] Furthermore, the early work of Ronald Ross and George Macdonald on mathematical models of mosquito-borne pathogens brought to the centre stage principles of vectorial capacity, methods for measuring mosquito-driven transmission, and quantitative theories of vector control.[15,16]

Consequently, GMEP interventions were based entirely around indoor residual spraying (IRS) with DDT and other insecticides, abandoning other methods of malaria control such as

prevention of mosquito biting and the destruction of vector breeding sites. Even the use of antimalarial drugs was initially considered unnecessary. The campaign's emphasis on intervention coverage and operational efficiency galvanised countries with the existing infrastructure and resources to eliminate regionally. The impact on the global burden of malaria was clear; the geographical distribution of malaria shrank, albeit primarily due to reduction in areas with strong control programmes.[17,18]

As with any disease elimination effort, however, GMEP eventually faced diminishing returns. The importance of reported treatment failures and the documentation of chloroquine resistance in Venezuela and Thailand as early as the 1950s was overlooked, and evidence of vector avoidance of insecticide contact in Mexico also emerged. By the 1960s, a number of areas failed to reduce malaria at rates originally predicted, and other regions experienced unexpected resurgences after long periods of interrupted transmission. As countries began to revert from "consolidation" to "attack" phase (Figure 1.3) and financial constraints grew, the global eradication campaign lost momentum.[19] The 1968-1969 epidemic in Sri Lanka, the poster child for malaria research and control at the time, may have foreshadowed what was to come - formal recognition by the WHO in 1969 that short-term eradication in many countries was not feasible.[20]

Figure 1.2 Framework for malaria elimination established by the WHO in 2017

As described by the WHO Global Malaria Programme in "A framework for malaria elimination" (2017)[4], the figure below illustrates a package of intervention strategies that can be adapted for different geographical areas in a country. It is recommended that the choice of interventions be based on transmission intensity (from "high" to "very low" to zero and maintaining zero) and also on operational capacity and system readiness. The diagram is presented as illustrative rather than prescriptive, as the onset and duration of interventions depends on local circumstances. Shading of boxes indicates enhancements and quality required as programmes progress towards elimination, with more intense actions indicated with darker colours and shading from light to dark indicating enhancement of quality and scale or focus of work.

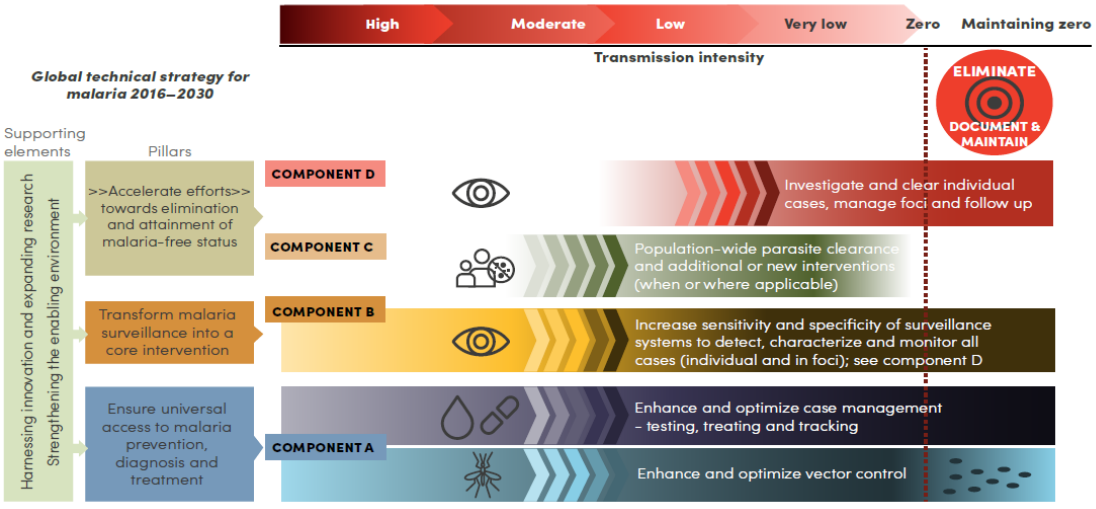

Acceleration – as represented by arrow bars (>>>>>) here - relates to time-limited efforts made across all components in order to (1) achieve universal/optimal coverage in malaria prevention and case management (Component A**), and increase sensitivity and specificity of surveillance systems so they are able to detect, characterize and monitor all malaria cases and foci (**Component B**); and (2) bring malaria transmission to sufficiently low levels (with or without population-wide parasite clearance and other strategies, **Component C as an option**) where remaining cases can be investigated/cleared and foci can be managed and followed up (**Component D**).*

Figure 1.3 Phases of the Malaria Eradication Campaign as established by the WHO in 1963

As described in the report of the World Health Assembly "Re-examination of the global strategy of malaria eradication" published in 1969[19], the figure below illustrates the phases of malaria control and elimination under the Global Malaria Eradication Programme (GMEP).

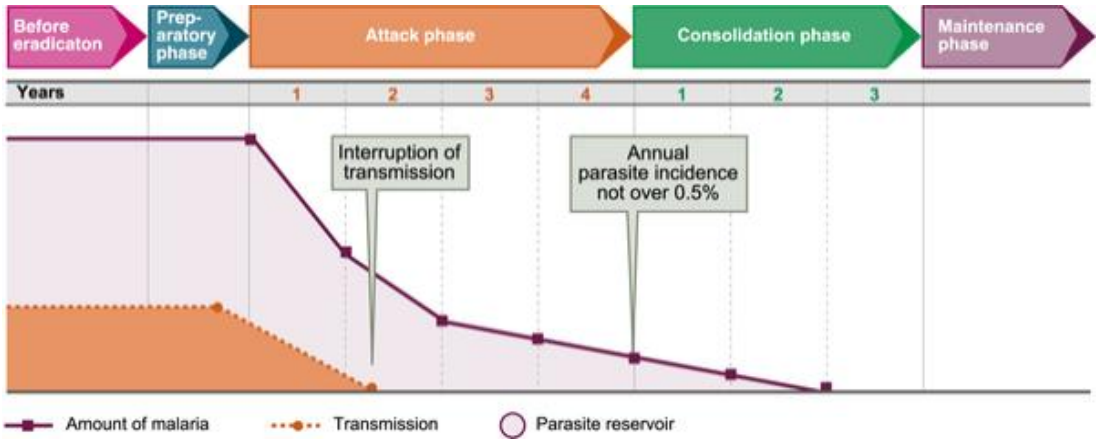

Today, there are a number of elimination strategies and interventions aimed at community-based reduction of transmission (Table 1.1). These range from vector control, surveillance, and case management to the development of novel drugs and vaccines to reduce human-to-mosquito transmission. All of them will require robust methods for measuring transmission, either as a means of focally targeting interventions or tracking impact over time.

Table 1.1 Elimination strategies and interventions for reducing malaria transmission

*Interventions discussed in subsequent research-specific chapters are underlined for emphasis.

Intervention	Description
Vector control	***Long-lasting insecticidal nets (LLINs) and indoor residual spraying (IRS)*** have been the mainstay of malaria control and elimination, accounting for an estimated 78% of malaria cases averted globally since 2000.[21] However, new vector control products and methods will need to address insecticide resistance, outdoor resting and biting species, and other constraints. Potential innovations and strategies include (but are not limited to) improved larval source management, ground or aerial spray delivery of insecticides, housing modifications such as window screening, sealed eaves and closed ceilings, insecticide treated clothing, odour- or sugar-baited traps, and veterinary insecticides to target livestock feeding vectors.[22] Studies are also on-going on the mass drug administration of ivermectin as both vector control and a sporontocidal transmission-interrupting drug.[23,24] ***Reactive vector control (RAVC).*** Vector control measures can also face coverage challenges or risk of resistance if insecticides are not rotated. Reactive vector control is one strategy for spatially targeting households with increased risk of infection based on entomological or clinical surveillance data.

Population-wide drug-based strategies	***Mass drug administration (MDA).*** Studies have suggested that in populations with a large proportion of low-density asymptomatic infections below the detection limit of microscopy and rapid diagnostic tests (RDTs), mass screen and treat (MSAT) is not effective in reducing transmission.[25,26] This has renewed the interest in the administration of chemoprophylaxis to entire populations to prevent transmission. Due to concerns over safety and drug resistance, variations also include presumptive treatment directed at potentially high-risk populations or targeted parasite elimination (TPE).[27] ***Reactive focal mass drug administration (rfMDA).*** If population-wide MDA is not feasible or unpopular due to the risks associated with treating uninfected populations or the potential for drug resistance, chemoprophylaxis can be administered only to individuals with increased risk of infection based on proximity to passively-detected index cases from the health facility. ***Seasonal malaria chemoprevention (SMC).*** In areas where malaria transmission is highly seasonal, SMC has been used to provide preventive treatment specifically during months of peak transmission. Studies have shown that this is highly effective in reducing clinical incidence in young children[28–30] and, in 2012, the WHO recommended implementation in children under age five in countries of the Sahel sub-region of Africa.[31] SMC is used primarily for malaria control and reduction of morbidity and is contra-indicated in areas with low or perennial transmission, though it is currently being implemented in countries with large heterogeneities in transmission and may impact on bordering areas being targeted for elimination sub-nationally (e.g., Senegal, The Gambia). Studies have also suggested that SMC is effective when administered to individuals up to 10 years of age, though this is not yet recommended by the WHO.[32] It is also not yet recommended for use in southern or eastern Africa due to high levels of resistance to amodiaquine and sulfadoxine-pyrimethamine and lack of efficacy and safety data on the use of other antimalarials in SMC.[33]
Enhanced surveillance and case management	***Case management through passive and active case detection.*** Passive case detection (PCD) based on health facility cases is used for malaria surveillance at all transmission intensities. For malaria-eliminating countries, however, clinical cases are increasingly rare, and active case detection (ACD) by health workers is used to identify infections in the community or households that may not present directly to the health systems. It is used primarily as a strategy for targeting asymptomatic reservoirs of infection.[34] ***Mass screening and treatment (MSAT) / Mass testing and treatment (MTAT).*** This strategy involves screening for risk factors or symptoms (in the case of MSAT), following by testing and treating (MTAT), of an entire population. The objective is to target the parasite reservoir in areas of low parasite prevalence or where MDA is not feasible or acceptable. ***Reactive case detection (RACD) and focal screening/testing and treatment (FSAT/FTAT).*** Focal and reactive strategies are a subset of MSAT/MTAT strategies, where interventions are in limited geographical areas or communities. RACD, also referred to as reactive case investigation[34], involves the screening and/or testing of household members, neighbours, and other contacts - typically with RDTs - around a passively detected case

	and treating those who are positive, while FSAT/FTAT may be based on known high-risk areas or foci. This is motivated by evidence in multiple settings that malaria cases tend to be spatially clustered[35–39], but limited impact studies are available. ***Pro-active case detection (PACD).*** Also a form of MSAT/MTAT, PACD is not prompted by an index case, but focused on populations with limited access to the health system, poor health-seeking behaviour, or in particularly high-risk groups (e.g., migrants and refugees, forest or mine workers). Compared to FSAT/FTAT, it is similar to a form of ACD conducted periodically (weekly or monthly) during high transmission season.
Transmission-blocking pharmaceutical products	***Transmission blocking drugs.*** Human-to-mosquito transmission involves the uptake of gametocytes, the sexual stage of the parasite. Single low-dose primaquine has been shown to be active against this stage. This regimen was recommended for addition to artemisinin-based combination therapies (ACTs) by the WHO in 2012.[40] Research has shown that this can reduce infectiousness to mosquitoes, but there are limited studies that demonstrate a reduction of malaria transmission in communities.[41] ***Vaccines interrupting malaria transmission (VIMTs).*** To date, most vaccines have focused on reducing morbidity and mortality, with only one vaccine candidate, RTS,S/AS01, reaching phase III clinical trials. VIMTs typically refer to "classical" transmission-blocking vaccines (TBVs) that directly target sexual or mosquito stage parasite antigens, but may also include pre-erythrocytic or asexual stage vaccines that inhibit parasite densities enough to indirectly reduce the presence of gametocytes.[42,43] There are a limited number of candidate-TBVs in early stage R&D,[44] with leading candidates based on *Pfs25*[45] as well as *Pfs48/45*, *Pfs230*[46], *Pfs28,* and *APN1*.
Other strategies	***Surveillance as an intervention***. There has been an increased emphasis on strategies to detect all infections as early as possible. Therefore, the strength of health systems to identify, investigate, classify, and manage foci more efficiently has been highlighted as critical for countries aiming to eliminate. ***Testing of co-travellers.*** This strategy is similar to RACD, but focused on imported cases or those that occur outside the household, such a forest-workers. ***Border screening***. To reduce the risk of imported malaria to eliminating countries, the screening and/or testing of any individuals entering eliminating countries from endemic areas has been suggested, but there have not been formal impact evaluations of this strategy.

1.3 The challenge of measuring malaria transmission for elimination

Getting to zero – a matter of debate (and definitions)?

The difference between global eradication, elimination, and control has been described as "the difference between absolute zero, nearly zero, and low."[47] Eradication is the permanent reduction to zero of worldwide incidence of all human malaria parasite species. On the other hand, elimination has been more difficult to delineate. Formally, the WHO defines elimination as the interruption of local transmission of a specified malaria parasite species in a defined geographical area. Certification requires proof of zero incidence of indigenous cases for at least three consecutive years.[4]

However, elimination has also been described as a state of interrupted endemic transmission below a threshold at which risk of re-establishment is minimised.[47] This relates to the concept of "malariogenic potential", a combination of an ecosystem's receptivity to malaria transmission (e.g., presence of competent vectors, a suitable climate, and a susceptible population) and vulnerability or "importation risk" due to the influx of infected individuals, groups, and/or infective mosquitoes.[4,47] Debates around the qualitative and quantitative concept of elimination are not purely academic, but critical for both policy and research. The subtleties of various definitions imply that elimination is linked to *risk* of transmission, and must therefore involve much more than monitoring of infections or cases, as WHO certification requirements imply.

The epidemiology of malaria in a landscape of declining transmission

What is clear in recent decades is the rapidly changing epidemiology of malaria. There are five *Plasmodium* species known to infect humans [*P.falciparum (Pf), P.vivax (Pv), P.malariae (Pm), P. ovale (Po), and P.knowlesi (Pk)]*[48]. *Pf,* which this report exclusively focuses on, is most associated with severe disease, clinical symptoms, and mortality, particularly in sub-Saharan Africa[49]. It also has the greatest global distribution. Geospatial methods developed by the Malaria Atlas Project (MAP) have utilised malariometric information from multi-year national surveys, routine health facility data, and a range of environmental covariates. In 2010, they estimated that 2.57 billion people worldwide were at risk of *Pf* transmission. Of these, 1.13 billion lived in areas of unstable and very low transmission (where case incidence is unlikely to exceed 10,000 per annum), primarily in Asia (91%). In the same year, 1.44 billion people still resided in areas of stable transmission, with the majority located in Africa (52%) or Central, South and East Asia (46%).[50]

Within sub-Saharan Africa, updated geospatial estimates in 2015 (Figure 1.4) reported a 50% reduction in *Pf* parasite rate in children aged 2 to 10 ($PfPR_{2\text{-}10}$) since 2000, with three-quarters of

the decline occurring between 2005 and 2015 alone.[21] The population of stable endemic Africa experiencing *Pf*PR$_{2-10}$ less than 1% also increased six-fold in that time (faster that the underlying rate of population growth). Based on these figures, Bhatt et al suggest that 121 million people are currently living in areas where elimination campaigns are feasible.[21] They attribute these changes in prevalence to the distribution of insecticide treated bednets (ITNs), estimated to account for 62-72% of *Pf*PR declines, while access to artemisinin combination therapies (ACTs) and IRS have also contributed, but to a lesser degree (15-24% and 11-16% respectively). In 2014, based on spatial temporal analysis of *Pf* parasite prevalence, Noor et al also observed a shift towards populations residing in areas of lower transmission intensity across Africa between 2000 and 2010 (Table 1.2).[51]

Figure 1.4 Changing infection prevalence in Africa 2000-2015

As described by Bhatt, S et al in "The effect of malaria control on *Plasmodium falciparum* in Africa between 2000 and 2015." *Nature* 526, 207-2011 (2015)[21], the figure below includes (a) *Pf*PR$_{2-10}$ for the year 2000 predicted at 5×5 km resolution, (b) *Pf*PR$_{2-10}$ for the year 2015 predicted at 5×5 km resolution, (c) absolute reduction in *Pf*PR$_{2-10}$ from 2000 to 2015, and (d) smoothed density plot showing the relative distribution of endemic populations by *Pf*PR$_{2-10}$ in the years 2000 (red line) and 2015 (blue line).

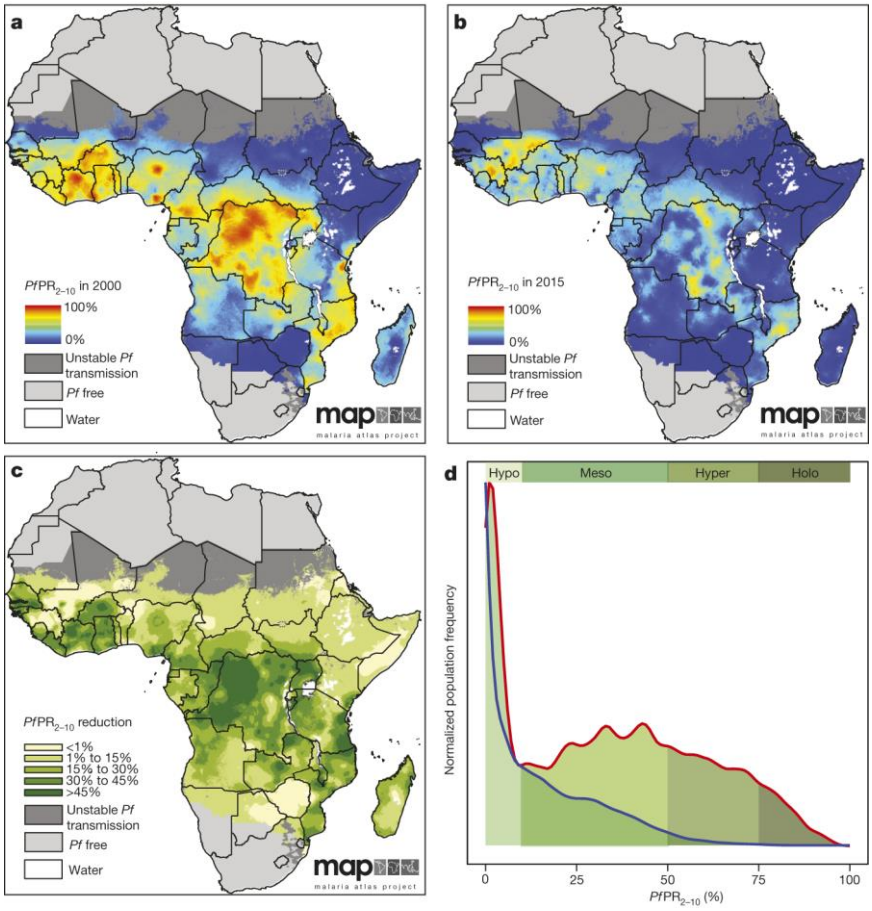

Table 1.2 2010 population (millions) in malaria endemic countries in Africa by the *Plasmodium falciparum* parasite rate endemicity class in 2000 and 2010

As described by Noor, A.M. et al in "The changing risk of *Plasmodium falciparum* malaria infection in Africa: 2000-10: a spatial and temporal analysis of transmission intensity." *Lancet* 383, 1739-1747 (2014)[51], the table below includes green shaded cells showing the number of people (millions) in 2010 who lived in areas where malaria endemicity declined least one level from 2000. Pink shaded areas are where endemicity increased by at least one level from 2000. Estimates do not include Burundi, Central African Republic, Congo, Mauritania, and Niger, for which there was insufficient data to predict change. PAR=populations at risk. *Pf*$PR_{2–10}$=community *Plasmodium falciparum* parasite rate standardised to the age group 2–10 years.

	2010								
	Malaria free	Unstable	<1% *Pf*PR_{2-10}	1% to <5% *Pf*PR_{2-10}	5–10% *Pf*PR_{2-10}	>10% to 50% *Pf*PR_{2-10}	>50% to 75% *Pf*PR_{2-10}	>75% to 100% *Pf*PR_{2-10}	Total PAR
2000									
Malaria free	98·7	0	0	0	0	0	0	0	**98·7**
Unstable	0	16·7	0	0	0	0	0	0	**16·7**
<1% *Pf*PR_{2-10}	0	2·1	67·7	7·4	0·6	0·6	0	0	**78·4**
1% to <5% *Pf*PR_{2-10}	0	0·7	24·4	38·7	3·6	2·3	0·2	0·1	**70·0**
5–10% *Pf*PR_{2-10}	0	0	7·9	19·6	7·5	5·0	0·4	0·2	**40·6**
>10% to 50% *Pf*PR_{2-10}	0	0	7·2	24·2	21·9	166·7	23·3	2·7	**246·0**
>50% to 75% *Pf*PR_{2-10}	0	0	1·5	0·9	0·8	105·3	121·2	16·5	**246·2**
>75% to 100% *Pf*PR_{2-10}	0	0	0	0	0	0·2	0·9	18·0	**19·1**
Total PAR	**98·7**	**19·5**	**108·7**	**90·8**	**34·4**	**280·1**	**146·0**	**37·5**	**815·7**
PAR transitioned from a higher endemicity	**0**	**2·8**	**41·0**	**44·7**	**22·7**	**105·5**	**0·9**	**0**	**217·6**

Heterogeneity in malaria transmission

It is easy to making sweeping generalisations at the global or regional level, especially when gains have been impressive. However, as a caveat to their estimates, Noor et al describe a central challenge to malaria elimination: "Why the intensity of malaria has changed so dramatically in some areas and seems to be intractable in others over the past decade is a fundamental question for future investment in malaria control in Africa." One reason may be our limited understanding of the malaria ecotypes that correlate most with the feasibility of interrupting transmission, but more importantly, the risk of resurgence. In fact, the most recent World Malaria Report suggests that progress in malaria control may be stalling, with 5 million more cases in 2016 than 2015 (though this may potentially be an artefact of improved surveillance).

Following GMEP, malaria resurgence was experienced widely in sub-Saharan Africa (Kenya, Nigeria, Sudan, Mauritius, Madagascar, and Swaziland), Asia (India, Pakistan, Sri Lanka, Thailand, Indonesia), and Latin America (Brazil, Mexico, Peru, Colombia). Causes have been attributed to the cessation of pilot programmes and control activities, increased human or mosquito movement, development and land-use changes, as well as war and civil strife and the associated worsening of socio-economic conditions.[52]

Terms classically used to describe malaria transmission are hypo, meso, hyper, and holo-endemic based on spleen and parasite rate. Today, transmission intensity is similarly defined as high, moderate, low, and very low, based on annual parasite incidence (API) and parasite prevalence (Figure 1.2).[4] Despite advancements in geospatial mapping described above, not explicitly

embedded in these categories are geographical and socio-demographic characteristics that determine the rate of change in transmission intensity. Ecology-based classifications of malarious zones fell out of popularity during GMEP. This was largely due to the fact that control and elimination in sub-Saharan Africa - which exhibits a diversity of environments and, therefore, malariogenic potential - was largely ignored. However, francophone scientists working in tropical Africa at the time did develop categories of *faciès épidèmiologique*, based on:

- Natural regions
    - Equatorial with forest or savannah - perennial transmission
    - Tropical and humid savannah - transmission season exceeding 6 months
    - Sahelian with dry savannahs - transmission season lasting less than 6 months
    - Desert – short or absent transmission season
    - Southern (plateaus of southern African) – seasonal transmission interrupted with winter
    - Highland (1000-2000m altitude) – highly variable transmission limited by temperature and surface declination
- Secondary factors
    - Natural - landform, water bodies, soil characteristics
    - Anthropic factors - modification of vegetation, water bodies, urbanisation, habitat of humans and cattle
    - Dynamic factors – natural disasters, climate change, malaria control, population movement, development of transport networks

Malaria ecotypes are most useful if they can demarcate areas most responsive to intervention strategies and if there are methods for measuring risk factors as they change. Heterogeneity and hotspots of transmission are increasingly common as malaria burden declines in many regions (Figure 1.5). Micro-epidemiological variations in malaria infection are frequently observed in areas of low to moderate transmission intensity.[53–56] Here, large proportions of the population may remain malaria free for years, while subpopulations experience multiples episodes.[54,55,57] For example, a study in Kilifi, Kenya found that 20% of homesteads experiencing a febrile case of malaria during the dry season later experienced 65% of all febrile malaria episodes the following year.[58] Malaria hotspots have been described previously as a geographical area where transmission intensity exceeds the average level, and, in fact, several hotspots of malaria transmission can occur in a single defined region,[55,56] resulting in much higher localised reproductive rate (R_0) estimates compared to broader intervention focus areas.[59]

Figure 1.5 Malaria heterogeneity across the transmission continuum

As described by the WHO in "Malaria surveillance, monitoring & evaluation: a reference manual" (2018)[60], the schematic below illustrates the increasingly focal nature of malaria as transmission decreases, requiring increased intensity and frequency of reporting from large geographical areas (e.g., district) to reporting near-real-time individual case data in small areas.

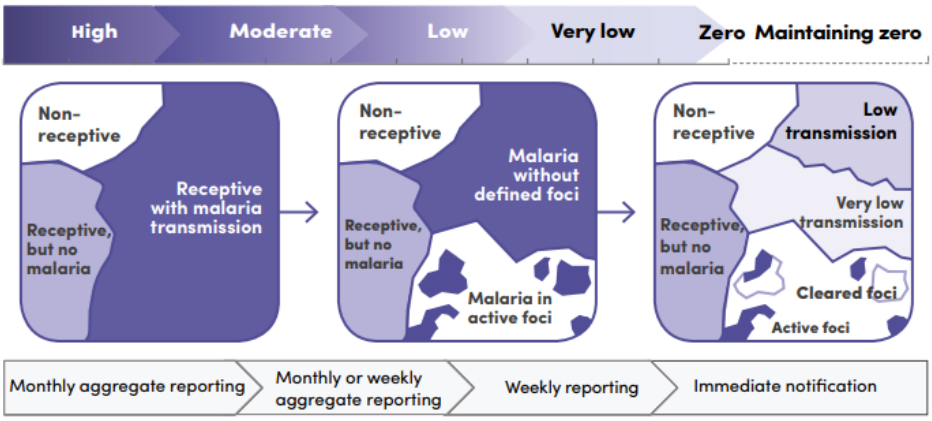

1.4 Implications for surveillance and the evaluation of transmission-reducing interventions

A major shortfall of GMEP was the lack of strong surveillance systems and strategies for detecting the last remaining cases. Many health systems lacked the geographical coverage required to achieve effective surveillance for elimination.[61] In fact, the resurgence of malaria in Sri Lanka is credited to the failure of the surveillance system to respond to decades of evidence on the periodic nature of epidemic risk in the country. One underlying principle behind other eradication campaigns, such as smallpox and polio, is a focus on outbreak investigation or clustering of cases, before attempting to identify individual cases.[17]

The current epidemiology of malaria poses several challenges for surveillance. These include the changing demographics of high-risk populations or occupations (e.g., forest and mine workers), increased migration and imported malaria, hard to reach populations, and the increasing prevalence of asymptomatic low-density infections.[62] The latter of these may also vary at the sub-national and regional level. This has implications for the effectiveness of intervention packages that need to adapt to the diversity of transmission intensity. The WHO framework for malaria elimination suggests that stratification to differentiate transmission risk can be thought of in sequential stages (Figure 1.6):

1. Receptive and non-receptive areas
2. Receptive areas with and without ongoing transmission
3. Transmission with or without foci
4. Degree of transmission in diffuse or focal areas

In many instances, a number of elimination strategies and interventions described above (Table 1.1) have provided valuable data via health-facility surveillance and active household surveys. This surveillance data in various forms has allowed evidence-based stratification or identification of transmission foci for targeted community-interventions.[63,64]

Figure 1.6 Sequential stratification according to receptivity and transmission intensity

As described by the WHO in "A framework for malaria elimination" (2017)[4], the schematic below illustrates the geographically focal or diffuse nature of transmission in areas targeted for malaria elimination.

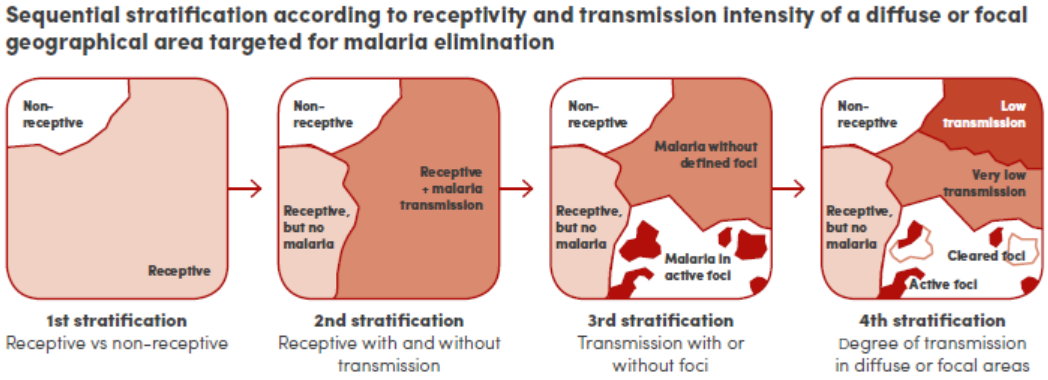

Challenges facing cluster randomised trials for transmission-blocking interventions

Testing the effectiveness of transmission interrupting interventions (drug, vaccine, or vector control) requires measuring the indirect reduction of infection at the community level to evaluate herd effects. In low transmission settings, measuring clinical incidence may require large samples sizes. Furthermore, active surveillance may have the effect of altering patterns of clinical disease.[65]

Cluster randomised trials (CRTs) are practical for measuring the indirect and/or herd immunity effects of interventions, and they have been used previously to evaluate intermittent preventive treatment (IPT),[66–69] ITNs[70–73] and MDA[74,75]. CRTs achieve study power by increasing the number of clusters rather than increasing cluster size,[76,77] which will also be influenced by the intervention-independent malaria transmission and risk of infection between clusters. In a CRT, the degree of variability between clusters in the outcome of interest has a large impact on the precision and power of the trial.[76] While conducting a trial across many heterogeneous settings may improve the generalisability of the study findings, this will impact on the value of the intra-cluster coefficient of variation (ICC), which reduces the power and precision at a given sample size. One method of accounting for this is to match or stratify study communities with respect to the primary outcome.[77] The effectiveness of this stratification, however, will depend on the accuracy of the metric that is used as the proxy for the expected primary outcome levels.

It is also likely that movement of people and/or mosquitoes between clusters will occur during the trials and the contamination of infection from control clusters, or spill-over protective effects from intervention clusters, may lead to an underestimation of impact. For example, one study evaluating the effectiveness of permethrin-treated ITNs in Asembo and Gem, Kenya, showed a protective effect against child mortality, moderate anaemia, and high-density parasitaemia in control clusters within a particular distance of the intervention clusters.[72] A standard analysis of the effect of the control vs. intervention clusters without accounting for these spatial spill-over effects would have led to an underestimation of the intervention's community effect. Therefore, several cluster designs have been suggested to address this issue that involve the inclusion of buffer zones in various forms (discussed further in Chapter 7).[65]

Heterogeneity in transmission and hotspots present challenges for both the implementation of interventions[78] and clinical trial design to evaluate them. If untargeted, residual transmission is most likely to persist in these areas.[56] Studies have observed instances in which hotspots of malaria intensity remained unaltered even after overall transmission is reduced.[35,37,79] In the context of cluster trials, heterogeneity will exists between and within clusters and needs to be accounted for either in the stratification or analysis of trial outcomes. The ability to detect heterogeneities will vary depending on transmission intensity and the discriminatory power of the metrics used to identify differences in malaria infection.

Accurate measures of malaria transmission are also essential to the design of CRTs. Firstly, baseline measures of transmission intensity can be used to select appropriate trial sites. Transmission intensity influences not only the sample size required to demonstrate an intervention's effectiveness, but the choice of diagnostic to be used. Furthermore, these baseline measures of transmission intensity can be used to classify clusters into strata to improve study power. However, inaccurate measurement can lead to inefficient stratification and an under- or over-estimation of intervention effect. Finally, evaluation of an intervention effect on transmission requires accurate measures of infection incidence. This can include a combination of primary and secondary endpoints. If surrogate entomological endpoints are to be measured prior to phase III trials, for example, it may also be important to understand how these relate to primary human endpoints. These factors will influence decisions on the frequency of sampling and the sample size required for each endpoint.

1.5 Diagnostics and tools for measuring transmission

As best described by Tusting et al, "measuring malaria transmission is intrinsically noisy."[80,81] We currently have a wide range of malaria diagnostics at our disposal, but they vary in their suitability as metrics of transmission or as endpoints in efficacy trials. Historically, malaria transmission has been measured using the entomological inoculation rate (EIR), or the number of infective bites per person per unit of time.[80] In humans, infection prevalence can be directly measured using parasite prevalence, the proportion of individuals with parasitaemia at a given point in time, and its accuracy varies depending on the measurement method used.[80] These range in sensitivity from light microscopy[82] and RDTs[83] to nucleic acid amplification tests (NAATs), such as polymerase chain reaction (PCR)[84–87]. The relative sensitivity of these measures will be discussed further in Chapter 3.

Active and passive case detection based on clinical cases or annual parasite index (API) are the cornerstone of national malaria control programmes.[81] More recently, they have also been improved and complemented by the widespread use of RDTs in health facilities and large-scale surveys such as the Demographic and Health Surveys (DHS), Malaria Indicators Surveys (MIS) and UNICEF Multiple Indicators Cluster Surveys (MICS).[88] Currently used human and entomological metrics are summarised in Tables 1.3 and 1.4[88], which also describe their discriminatory power in different settings.

Recently, there have been a number of new approaches used to monitor changes in malaria epidemiology using both molecular and serological methods (Table 1.5[88]), though they have been limited to research settings. For example, molecular force of infection ($_{mol}$FOI) can be estimated through the genotyping of individual parasite infections.[89–91] Broadly, force of infection (FOI) is defined as the number of new infections per person per unit time, while $_{mol}$FOI specifically is the number of new parasite clones acquired per unit time.[89] These methods can distinguish multiple co-infecting parasite clones within one host.[89,92,93] Another molecular measure being used is the multiplicity of infection (MOI), the number of concurrent parasite clones per parasite-positive host.[80] Additionally, the use of single nucleotide polymorphism (SNP) barcode assays has been suggested for measuring changes in malaria infection in low transmission settings. Studies in Senegal have used a 24-SNP barcode assay to correlate parasite population diversity with longitudinal changes in disease transmission.[94,95]

Serology, which indirectly measures infection using human antibody (Ab) responses to malaria parasite antigens, has been used extensively in malaria epidemiology in the last decade, primarily through FOI estimates derived from age-dependent measures of sero-prevalence. These and other serological methods are discussed in more detail below and in Chapters 4-7.

In low transmission settings, the prevalence of asymptomatic infections with parasite densities below the detection limit of conventional diagnostics such as microscopy and RDTs has been observed. Nearly 50% of infections identified by nested PCR (nPCR) are undetectable by light microscopy, and this proportion also varies by endemicity and population groups.[96,97] The factors influencing the relative sensitivities of these diagnostics, and their relationship with asymptomatic infections, are discussed further in Chapter 3.

Table 1.3 Summary of currently available malaria transmission metrics in humans

As described in "malERA: An updated research agenda for characterising the reservoir and measuring transmission in malaria elimination and eradication." *PLOS Med.* 14, e1002452 (2017)[88], the table below outlines currently available metrics for measuring malaria transmission in humans.

Metric	Definition [3]	Measure of transmission	Method	Discriminatory power
Annual blood examination rate (ABER)	The number of people receiving a parasitological test for malaria per unit population per year	Level of diagnostic monitoring activity	Microscopy or RDT	• Dependent on health-system provision
Case, confirmed	Malaria case (or infection) in which the parasite has been detected in a diagnostic test	Current transmission or incidence if data collection is repeated or routine	Microscopy or RDT positive	• Insensitive at low transmission; saturates at high transmission • Underestimates due to system inadequacies and poor health-seeking behaviour
Case, fever	The occurrence of fever (current or recent) in a person	Current transmission or incidence if data collection is repeated or routine	Reported or observed fever	• Overestimates malaria infection
Proportion of fevers parasitaemic (PFPf) *	Proportion of fever cases found to be positive for *Plasmodium*	Current transmission or incidence if data collection is repeated or routine	Microscopy; RDT; NAAT	• Depends on diagnostic sensitivity • Insensitive at low transmission
Slide positivity rate (SPR)	Proportion of blood smears found to be positive for *Plasmodium* among all blood smears examined	Current transmission or incidence if data collection is repeated or routine	Microscopy	• Depends on ABER • Insensitive at low transmission
RDT positivity rate (RDT-PR)	Proportion of positive results among all RDTs performed	Current transmission or incidence if data collection is repeated or routine	RDT	• Depends on RDT sensitivity • Insensitive at low transmission
Parasite rate (PR)	Proportion of the population found to carry asexual blood-stage parasites	Current transmission or incidence if data collection is repeated or routine	Microscopy; RDT; NAAT	• Depends on diagnostic sensitivity • Insensitive at low transmission
Gametocyte rate (GR)	Percentage of individuals in a defined population in whom sexual forms of malaria parasites have been detected	Potentially infectious human population	Microscopy; NAAT	• Depends on diagnostic sensitivity • Insensitive at low transmission

*No WHO definition is available for this term.

Abbreviations: ABER, annual blood examination rate; GR, gametocyte rate; NAAT, nucleic acid amplification test; PF*Pf*, proportion of fevers parasitaemic; PR, parasite rate; RDT, rapid diagnostic test; RDT-PR, RDT positivity rate; SPR, slide positivity rate.

Table 1.4 Summary of currently available entomological malaria transmission metrics

As described in "malERA: An updated research agenda for characterising the reservoir and measuring transmission in malaria elimination and eradication." *PLOS Med*. 14, e1002452 (2017) [88], the table below outlines currently available entomological measures of malaria transmission.

Metric	Definition [3]	Measure of transmission	Sampling method and resolution	Discriminatory power
Entomological inoculation rate (EIR)	Number of infective bites received per person in a given unit of time, in a human population	Transmission intensity	• Human landing collection; light traps • Resolution: Household or community level	• Insensitive at low transmission • Lack of standardised sampling design • Collected by malaria control programmes
Sporozoite rate (SR)	Percentage of female *Anopheles* mosquitoes with sporozoites in the salivary glands	Risk of infection	• Human landing catch; baited traps; gravid traps • Resolution: Community level	• Insensitive at low transmission
Human biting rate (HBR)	Average number of mosquito bites received by a host in a unit of time, specified according to host and mosquito species	Risk of exposure	• Human landing collection • Resolution: Person or community level	• Allows determination of the primary vector
Vectorial capacity	Rate at which given vector population generates new infections caused by a currently infectious human case	Efficiency of transmission	• Derived from human biting rate, parasite inoculation period, mosquito to human density and mosquito survival • Resolution: Community level	• Measures potential, not actual, rate of transmission—includes no parasitological information • Sensitive to changes in mosquito survival and biting behaviour but may not translate to significant change in human incidence • Can be useful when infection rates are low and mosquito sampling difficult

Table 1.5 Advances in the development of metrics for measuring malaria transmission

As described in "malERA: An updated research agenda for characterising the reservoir and measuring transmission in malaria elimination and eradication." *PLOS Med*. 14, e1002452 (2017)[88], the table below summarises recent advances in the development of new metrics for measuring malaria transmission.

Metric	Definition	Measure of transmission	Method	Discriminatory power
Force of infection	Rate at which susceptible individuals contract malaria	• Probability of transmission	Time from birth to first malaria episode; microscopic detection of parasites following successful antimalarial treatment	• Difficult to measure • Difficult to standardise • Depends on diagnostic sensitivity • Cannot differentiate superinfections
mFOI	The number of new parasite clones acquired by a host over time	• Population-level transmission intensity • Transmission heterogeneity	Cohort study >6 months with parasite genotyping	• Highly sensitive for monitoring changes in malaria exposure • Superinfections can be differentiated
MOI	The number of different parasite strains coinfecting a single host	• Population-level transmission intensity • Transmission heterogeneity	Parasite genotyping of positive samples	• Saturates at high transmission • Restricted by age dependency • Insensitive at low transmission • Highly sensitive to spatial heterogeneity • Highly sensitive to increases in imported infection • Less sensitive to changes in seasonality
Genotyping: SNPs or amplicon sequencing	• Genetic diversity, i.e., number of alleles in a population • Parasite signatures to map geographical relatedness of infection (i.e., spatial–temporal transmission)	• Population-level transmission intensity • Transmission heterogeneity • Geographical tracking of transmission patterns	• Haplotypes composed of >12 informative SNPs from single clone infections • Haplotypic signatures from highly variable loci	• Sensitive to changes in malaria exposure and spatial–temporal flow of infection • Standardisation of measures needed • Methods for analysis and interpretation of data needed
Antibody seroprevalence	The percentage of seropositive individuals in a population	• Population-level transmission intensity	Seronegative or seropositive defined using appropriate cutoff points	• Dependent on antibody target tested • Saturates at high transmission • Sensitive at low transmission
SCR	The rate (typically annual) by which seronegative individuals become seropositive upon malaria exposure	• Population-level transmission intensity • Temporal changes in transmission can be detected from a single sampling time point	Detection of antibodies in sera using serological assay (IFAT, ELISA, bead-based assays microarray)	• Dependent on antibody target tested • Restricted by age dependency • Saturates at high transmission • Sensitive at low transmission • Sensitive to risk of malaria in absence of transmission

Abbreviations: ELISA, enzyme-linked immunosorbant assay; IFAT, Immunofluorescence Antibody Test; mFOI, molecular force of infection; MOI, multiplicity of infection; SCR, seroconversion rate.

1.6 Leveraging the human immune response for surveillance

The use of serological data in epidemiological analysis

Sero-epidemiology, or the measure of population-wide Ab responses in serum, has been widely used to study the prevalence of infection for a number of diseases. Sero-prevalence surveys have helped to guide vaccination strategies as well as disease control and elimination programmes[98] for polio[99,100], measles,[101] rubella,[102] diphtheria,[103] *Haemophilus influenza* type B (*Hib*)[104], and pertussis[105]. It has been used extensively in tropical infectious diseases such a dengue, trachoma, chikungunya, and helminths infections.[106–111]

For infections that lead to lifelong or persistent antibodies, the application to sero-epidemiology is primarily through measures of Ab prevalence by age in mathematical models used to estimate an age-specific FOI[112]. It is particularly useful for pathogens such as hepatitis B[113] and rubella where serology is a strong marker for subclinical infections. It is less suitable for infections that do not generate stable Ab responses, such as cholera, human papillomavirus (HPV), rotavirus, and typhoid.

In malaria, the use of sero-epidemiology has also focused on measuring age-related sero-prevalence and FOI through community or household surveys. Over the past 10 years, substantial work has shown that serological evaluation of cross-sectional Ab prevalence can provide medium- and long-term temporal measures of transmission intensity,[114–121] and correlate well with within-study estimates of EIR, PR, and clinical incidence.[121] In particular, the ability to standardise the use of the *Pf* blood-stage antigens *Pf*AMA1 and P*f*MSP1$_{19}$ due to their long half-life, moderate levels of immunogenicity, and limited polymorphisms, has allowed the use of immunological assays that measure human Ab responses to these antigens as a practical epidemiological tool.

As a proxy for malaria transmission intensity, age-stratified sero-prevalence data are used to fit reverse catalytic models and estimate population-level FOI or a seroconversion rate (SCR) - the rate at which sero-negative individuals become sero-positive after infection by malaria parasites.[122] More recently, new approaches have been applied using serological data to measure population Ab responses to malaria. These include adaptations of the reverse catalytic model with the use of Ab titre measurements rather than sero-positivity[123] and Ab acquisition models[124]. These and other malaria sero-epidemiology models will be discussed in more detail in Chapters 4 – 7.

Naturally acquired immunity to malaria

Most successful vaccines have been against pathogens that induce long-lived protective Abs upon a single infection, such as smallpox, measles, and yellow fever.[125,126] Pathogens that do not induce

sterile immunity, including malaria as well as human immunodeficiency virus type-1 (HIV-1) and *Mycobacterium tuberculosus* (Mtb), are much more challenging for vaccine development.

Currently, we still have an incomplete understanding of the dynamics of immune responses to *Pf.* While sterilising immunity to malaria is almost never achieved, it is generally understood that partial immunity against high-density parasitaemia and clinical disease is developed through repeated and cumulative infection (Figure 1.7[127]). This has been illustrated through studies of non-immune individuals challenged with malaria infection[128], passive transfer of immune serum to malaria-infected children,[129,130] and more broadly through epidemiological and clinical observations in malaria endemic populations.

Epidemiological data across medium-high transmission intensities in Africa indicate that clinical immunity in these settings is acquired after 10 to 15 years of exposure and severe malaria is rare in older children and adults.[8,131,132] There is also large variability in disease episodes among children within the same transmission setting. At the individual level, studies have shown that those repeatedly exposed have lower parasite densities and less frequent clinical episodes.[133–140] In high transmission settings, severe malaria is only generally observed in children under age five.[8,133] On the other hand, in some low transmission settings, limited exposure has been found to result in low effective immunity and higher rates of symptomatic and severe malaria in adults.[141,142] Several longitudinal studies suggest that "premunition"[143], or persistent low-density asymptomatic infection, is important for maintaining Ab responses through repeated immune boosting.[144–150] After the re-emergence of malaria in Madagascar after 30 years of control, individuals exposed when transmission intensity was previously higher were more resistant to clinical disease than their younger counterparts.[151] As transmission declines, shifts in age distribution are also observed, with a higher frequency of clinical disease in older individuals compared to high transmission settings where symptomatic episodes are primarily experienced in children under age 10-15 years.[152,153]

What determines the rate at which naturally acquired immunity develops has been a subject of debate for some time. One hypothesis is that the slow onset of clinical immunity in holo-endemic areas is due to parasite diversity, where cumulative exposure to multiple parasite infections over time yields a suitable diverse repertoire of strain-specific immune responses.[154–156] One of the best examples of *Pf* polymorphisms are the approximately 60 *var* genes that encode the hypervariable surface protein known as the *Pf* erythrocyte membrane protein 1 (*Pf*EMP1), critical for malaria pathogenesis and immune evasion.[157–159]

A competing hypothesis is that immunity is less dependent on parasite-specific exposure, but instead due to cross-reactive strain-transcending immune responses associated with age-related maturation of the immune system. This is motivated by data from trans-migrants in Indonesian

Papua, where malaria-naïve adults initially experienced parasitaemia at the same rates as children, but rapidly acquired protective immunity such that age-specific prevalence paralleled those of lifelong residents in the area within two years, suggesting innate age-dependent factors associated with immunity.[160,161] This has also been observed in studies in Tanzania.[162,163]

However, the influence of age on the pathophysiology of malaria has also been found to be important. It has been observed that, relative to children, adults are more tolerant of chronic infection but less able to withstand acute infection. For example, Griffin et al investigated the effect of age on different severe malaria syndromes across transmission intensities in Tanzania based on mathematical models and found that infection at later ages was associated with a higher proportion of cerebral malaria regardless of exposure.[164] Field-based studies by Reyburn et al found that this age effect was observed primarily in low and moderate transmission settings.[141] This could be driven by T-cell mediated immune responses or an increased production of tumour necrosis factor alpha (TNF-α) by adults in response to primary infection that may wane with continued exposure (Figure 1.8[1]).[165] What is key is how these biological mechanisms will manifest themselves as transmission declines.[132] While the overall risk of clinical disease across the population will inevitably decline with malaria intensity, empirical studies are conflicting on whether a loss of immunity in older children and adults will render a large proportion of at-risk individuals more vulnerable to severe and fatal malaria.

Implications of antibody longevity on serological markers of immunity and exposure

What is still the subject of on-going research is how the effect of age and exposure on the acquisition of immunity differs between antigens. Characterising these dynamics for specific target antigens is fundamental to how measures of human immune response can be used epidemiologically. Antigens will fall along a continuum of suitability as a biomarker of acute infection / recent exposure to a correlate of protective clinical or parasitic immunity.

While low antibody levels are not protective against malaria, they will increase with age and/or exposure and, once it reaches a theoretical threshold to confer protection against clinical disease are most suitable as biomarkers of immunity (Figure 1.9[166]). Conversely, antibody levels below the threshold of protection can be useful as biomarkers of previous infection in populations with limited exposure, such as young children or areas of low transmission intensity. It may also be possible that antibody responses that boost above the threshold of protective immunity, but decay rapidly in the absence of infection, can also be used as markers of recent infection.

Figure 1.7 The acquisition of immunity to malaria in the context of intense seasonal *Pf* transmission

As described by Crompton, P.D. et al in "Malaria immunity in man and mosquito: Insights into unsolved mysteries of a deadly infectious disease". *Annu Rev. Immunol*. 32, 157-187 (2014)[127], the figure below seeks to illustrate that in areas of intense malaria transmission, immunity to severe life-threatening malaria is generally acquired by the age of five years. Children remain susceptible to repeated episodes of febrile malaria into adolescence, eventually acquiring near complete immunity to the symptoms of malaria by adulthood, but remaining susceptible to infection by blood-stage parasites. The mechanisms of immunity to severe malaria are unclear but may involve the acquisition of "strain-specific" antibodies that neutralise key *P. falciparum* variant antigens, which drive the pathogenesis of severe disease (e.g., subset of *Pf*EMP1s that mediate sequestration), and the induction of "strain-transcendent" regulatory mechanisms that control excessive *P. falciparum*-induced inflammation. Both of these mechanisms may depend on ongoing *P. falciparum* exposure to be maintained. In young children, *P. falciparum*-specific antibody responses to acute infection are generally short-lived, but with each year of exposure, there is a gradual increase in the breadth of antigen specificity and serum levels of *P. falciparum*-specific IgG that persists in the absence of transmission (i.e., during the dry season in the case of seasonal malaria). Protection against malaria symptoms is only conferred when an, as yet ill-defined, threshold is surpassed.

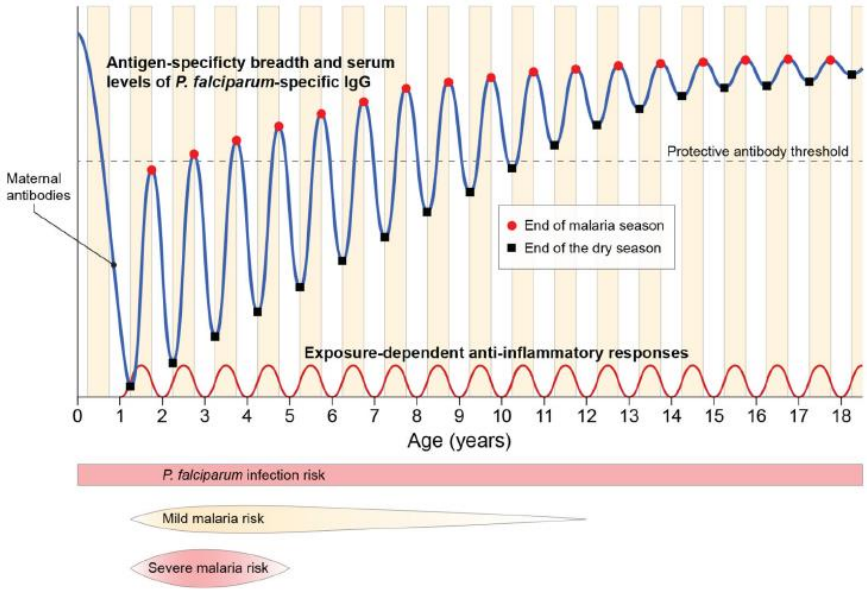

Figure 1.8 Hypothetical basis of age-dependent inversion of susceptibility to disease with acutve vs. chronic exposure in children and adults

As described by Doolan et al in "Acquired immunity to malaria. " *Clin. Microbiol. Rev*. 22, 13-36 (2009)[1], the figure below illustrates the hypothetical basis of an age-dependent inversion of susceptibility to disease with respect to acute versus chronic exposure in children and adults. Th1- and Th2-type immune responses are surrogates for immune responses that change with age-dependent exposure and play a critical role in infection outcomes. Th1-driven effectors may dominate the immune response of children, while Th2-driven effectors may dominate adult immune responses.

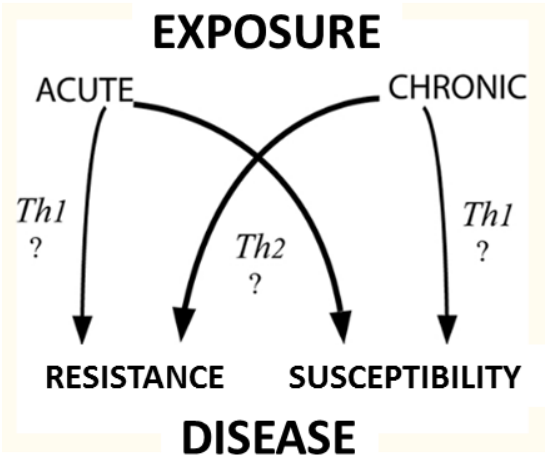

Figure 1.9 Models of the evolving role of antibodies to *Plasmodium falciparum* merozoite antigens with changing malaria exposure and antibody levels

As described by Stanisic, D.I. et al in "Acquisition of antibodies against *Plasmodium falciparum* merozoites and malaria immunity in young children and the influence of age, force of infection, and magnitude of response." *Infect. Immun*. 83, 646-60 (2015)[166], the figure below illustrates models of the evolving role of antibodies to *Plasmodium falciparum* merozoite antigens with changing malaria exposure and antibody levels, where (a) low antibody levels are not protective against malaria, but as antibody levels increase (with age and/or exposure) and reach a theoretical threshold, antibodies contribute to protection and serve as biomarkers of malaria immunity, and (b) antibody levels may also serve as biomarkers to predict malaria risk or protective immunity by identifying individuals who have been exposed to infection. In young children or those with limited exposure, antibodies have a high predictive value for increased risk of malaria and poor predictive value for protective immunity. As age or cumulative exposure or both increase, the predictive value of antibodies for increased risk of malaria declines, reaching a point where antibodies become better markers of protection.

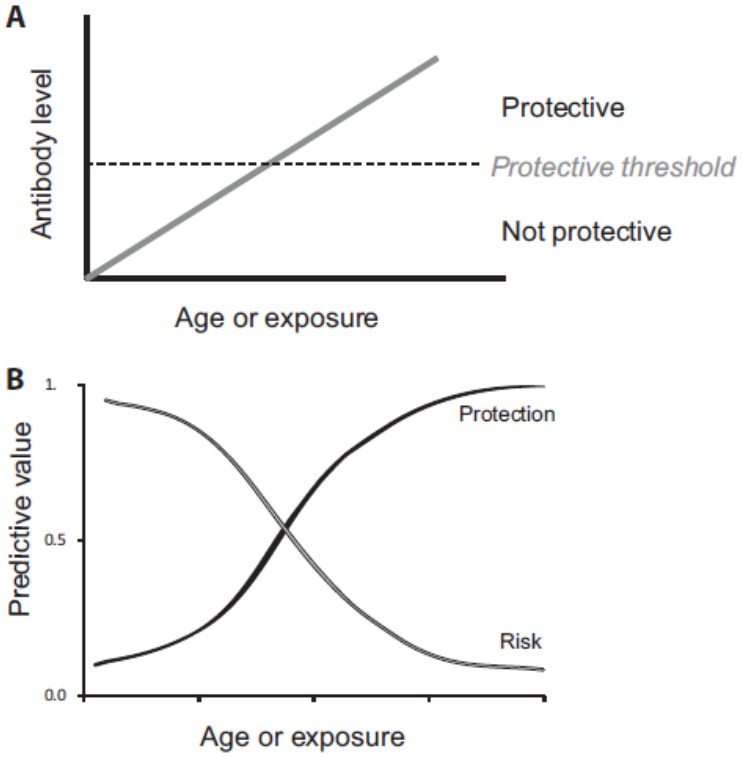

Only 1% of the roughly 5,000 antigens encoded by the malaria parasite have been studied so far.[167,168] Blood stage infection is the primary target of acquired human immunity and antigens expressed by the merozoite, the erythrocyte infecting extracellular form of *Plasmodium*, are particularly important immune targets and vaccine candidates.[169,170] These are assumed to be humoral responses because human leukocyte antigen (HLA) class I and II molecules associated with cell-mediated immune responses are absent from the surface of the parasite and infected red blood cells (RBCs).[167]

The invasion of erythrocytes is a multi-step process involving several interactions with proteins on the merozoite surface as well as those associated with invasion organelles – micronemes and rhoptries (a schematic of the specific proteins investigated in this thesis are illustrated in Figure 1.10).[171] Due to their direct exposure to the host immune system and their roles in invasion, these antigens are major targets for protective Abs, which can act either by inhibiting parasite replication (opsonising merozoites for uptake by phagocytes and antibody-dependent cellular inhibition), blocking binding of merozoite ligands to their receptor or binding partners, or blocking processes required for parasite function.[170,172–178] Developments in genomics, proteomics, and innovations in protein expression have allowed a much wider identification and expression of antigens that may be potential vaccine candidates, but also markers of immunity or exposure.[179,180] However, gaps still remain between the expression of recombinant proteins and natural antigens.

Upon initial exposure and binding to parasite antigens, naïve B cells begin to differentiate into either short-lived plasma cells that function to control initial infection or long-lived plasma cells and memory B cells (MBCs) that contribute to the maintenance of sustained antibody-based immunity.[125,181] Research suggests that short-lived plasma cells secrete primarily immunoglobulin-M (IgM), while long-lived plasma cells and MBCs secrete immunoglobulin-G (IgG) and immunoglobulin-A (IgA).[182] Given that IgM only persists for several days to a month, IgG antibodies are typically used to measure historical transmission intensity as they tend to be associated with protective immunity and are detectable for a longer period, replacing IgM once parasite load begins to fall.

Figure 1.10 *Plasmodium falciparum* parasite life cycle and antigens as potential biomarkers of malaria exposure

Adapted from Winzeler et al in "Applied systems biology and malaria." *Nat. Rev Microbiol*. 4, 145-151 (2006)[183] and Cowman et al in "Invasion of red blood cells by malaria parasites." *Cell* 124, 755-766 (2006)[171]. Original figures have been modified to include specific antigens discussed in following chapters of this report (blue boxes).

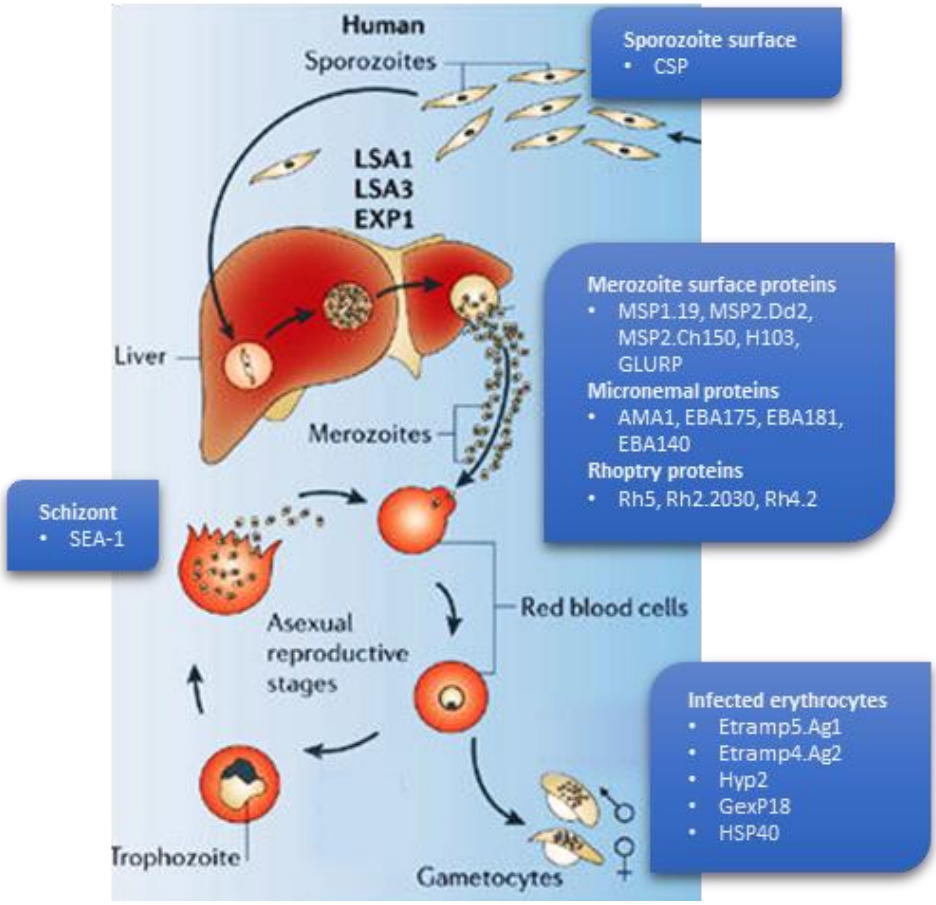

1.7 The role of multiplex immunoassays

Several types of assays have been used to quantify Ab responses to malaria and other infectious pathogens. As early as the 1900s, Ab quantification methods were found to be more sensitive than microscopy in detecting current infection in the form of complement fixation and precipitin tests[184–186]. These were designed to photo-metrically measure reductions in complement concentrations that are specific or "fix" to target antigen-antibody complexes of interest in serum and resulted in an increase of RBC lysis in an indicator system. This was later replaced by the indirect haemagglutination assay (IHA)[187], where malaria antigen-coated tests reacted with anti-malarial Abs in serum samples, resulting in agglutination that was measured visually. This method allowed improvements in high throughput analysis given that antigen was easily prepared on micro-titre plates to test several samples at once.

By the 1960s, Ab quantification tests were modified again in favour of immunofluorescence antibody tests (IFAT). Here, antigens of interest (usually whole parasitised RBCs as opposed to the antigen extracts used in IHA) are fixed to a glass slide, incubated with human serum samples, and a secondary Ab coupled with a fluorescent compound added and reactivity measured visually with a fluorescence microscope. Both IHA and IFAT methods are difficult to standardise, however, because reactivity was measured visually and were therefore subjective.[119,188]

IFAT tests were widely used in malaria surveillance for some time.[189–193] However, in the last decade they have been supplanted by enzyme-linked immunosorbent assays (ELISA). Similar to IFAT, but rather than glass slides, recombinant antigens are coated to micro-titre plates, which are incubated with human sera followed by an enzyme-coupled secondary Ab. Upon addition of an enzymatic substrate, a colour change proportional to the amount of antigen-specific Ab in the sample is measured with a spectrophotometer.[119,188]

More recently, cytometric bead assays (CBA) and protein microarray have been used as multiplex platforms to measure responses to multiple antigen-specific responses in a single sample. CBAs use measurement techniques similar to fluorescence-activated cell sorting (FACS). Recombinant antigens are conjugated to distinctly coloured microspheres or beads (a combination of fluorescent dyes), allowing a unique spectral address for each analyte of interest. This allows a dual-detection flow cytometer to identify the bead-specific colour and to quantify the associated analyte concentration.[194] Current CBA platforms allow measurement of up to 500 different analytes simultaneously. CBA assays will be discussed in more detail in Chapter 5.

In a revisit to IFAT methods, protein microarrays bind (or print) recombinant proteins to microscopy slides, but with only nano- or pico-gram volumes of antigen. Like CBAs, it has the advantages of a larger dynamic range compared to ELISA and multiplexing up to 1,000s of antigens at a time. However, high start-up costs make it impractical for field-based surveillance. It also suffers from variability in signal between slides and large volumes of data, leading to data standardisation and processing challenges. For these reason, it is used primarily for broad screening of immune responses or antigen discovery in research settings.[188,195]

While ELISA has been the assay of choice for sero-epidemiological studies, the proliferation of newer multiplex technologies are allowing surveillance tools to be more refined in the breadth of malaria exposure that is measured. However, it also introduces new challenges in assay validation and standardisation. Nonetheless, these tools may become increasingly relevant as countries move towards malaria elimination, particularly in areas where it may be cost-effective to integrate malaria surveillance with other disease surveys. Figure 1.11[188] illustrates commonly used immunoassay platforms for detection of antibodies against malaria antigens.

Figure 1.11 Schematic of immuno-assay platforms

As described by van den Hoogen and Drakeley in *Encyclopedia of Malaria* 1-8 (Springer New York, 2015)[188], the figure below illustrates several malaria diagnostic platforms used for antibody detection, including the immunofluorescence antibody test (IFAT), enzyme-linked immunosorbent assay (ELISA), the cytometric bead array (CBA), and protein microarray. From left to right, the number of identified antigenic targets increases in relation to the number of individuals per test (i.e., per microscope slide or 96-well plate).

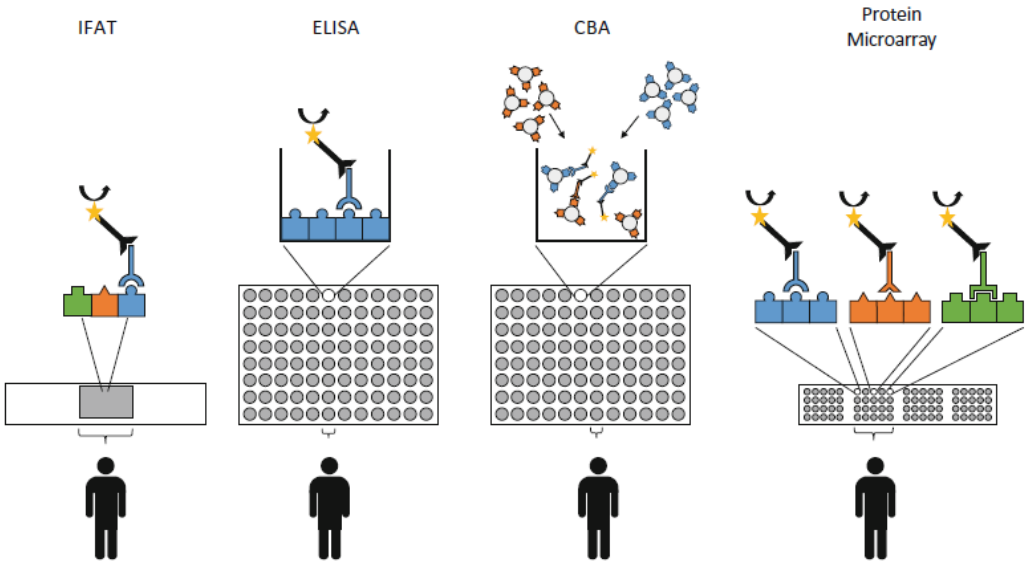

1.8 The history of malaria epidemiology in two pre-elimination settings in sub-Saharan Africa

The two countries explored in the research presented in this thesis are examples of epidemiological settings where elimination may not be easily achieved without intensified efforts, and, hence, where research into tailored strategies is necessary. Most countries that have eliminated are areas with robust surveillance systems and rural public health services, relatively rich and tourism-oriented islands with strong mosquito control programmes, or areas that are not intrinsically malarious or with highly focal endemicity (Table 1.6).[17] Historically, elimination efforts in sub-Saharan regions were limited – by 1964, GMEP activities had only covered 3.2% of the population at-risk in Africa due to concerns about operational and technical challenges.[47,196]

Table 1.6 Countries and regions certified malaria free up to 2010

As described by Najera, J.A. et al in "Some lessons for the future from the Global Malaria Eradication Programme (1955-1969), *PLOS Med*. 8, e1000412 (2011).[17]

Countries and Regions with a Long History of Control	Islands with Tourism-Oriented Economy	Other
North Venezuela (1961), Hungary (1964), Spain (1964), Bulgaria (1965), Taiwan (1965), Cyprus (1967), Poland (1967), Romania (1967), Netherlands (1970), United States (1970), Italy (1970), Puerto Rico (1970), Cuba (1973), Portugal (1973), Yugoslavia (1973), Australia (1980), Turkmenistan (2010)	Grenada & Carriacou (1962), St. Lucia (1962) Trinidad & Tobago (1965), Dominica (1966), Jamaica (1966), U.S. Virgin Islands (1970), Mauritius (1973), Reunion (1979)	Singapore (1982), Brunei Darussalam (1987), United Arab Emirates (2007), Morocco (2010)

doi:10.1371/journal.pmed.1000412.t001

The Gambia

As the smallest country in mainland Africa, The Gambia has contributed more to our understanding of malaria biology and epidemiology than would be expected. It experiences a typical West African savannah climate - an intense and short rainy season between June and October followed by a longer dry season. The majority of malaria transmission occurs during this wet season (and the period immediately after).[197] The predominant malaria parasite is *Pf*, but *Pm* and *Po* are also observed. Prevalence of *Pv*, however, is not high given that the RBC Duffy antigen required for parasite invasion is largely absent from the population. The main mosquito vector is *Anopheles gambiae*,[198] named after their identification by Frederick Theobald and Col. George M. Giles from samples collected in and around the River Gambia,[199,200] where a number of important studies on vector ecology and behaviour and its contribution to variation in malaria transmission would later be conducted.[136,198,201–205]

During an expedition to The Gambia by the Liverpool School of Tropical Medicine and Medical Parasitology in 1902, Dr. J. Everett Dutton was one of the first to observe that the prevalence of spleen enlargement and parasitaemia, as well as parasite density, was lower in older children, suggesting the development of partial immunity to malaria through repeated infections.[206] Fifty years later, studies led by Sir Ian McGregor in Keneba (part of the recently established UK Medical Research Council Unit in The Gambia), demonstrated that gamma globulin prepared from malaria immune adult Gambians given to malaria-infected Gambian children reduced parasite count within days.[129] This provided strong evidence that components of immune serum, likely antibodies, could impede the replication of malaria parasites. Subsequent studies in both The Gambia and Tanzania showed variability in immune responses in children to immune sera from adult Gambians. This was some of the first research to suggest strain specific immune responses to malaria infections due to antigenic variation.[130,207]

Since then, the transmission patterns and seasonality of The Gambia have enabled pivotal research on immunity to malaria, including the correlation of Ab concentrations to protection against clinical malaria (later associated with the blood stage antigen *Pf*EMP1),[208,209] community

cohort studies identifying merozoite antigens as targets of protective Abs,[210,211] and longitudinal studies on the duration of immune response in the absence of re-infection.[212] Later, key epidemiological studies were conducted on the role of gametocytes, asymptomatic infections, and host factors that drive human infectiousness.[213,214] Further work on immune responses to the sexual stages of the parasite focussed on gametocyte antigens as potential vaccine candidates.[215] These studies built a more complete understanding of immunity throughout the parasite life cycle and the dynamics that influence human-to-mosquito transmission at the individual and population level.

The Gambia was also one of the first African countries to document clear declines in malaria burden in recent decades. Between 2003 and 2007, the proportion of malaria positive microscopy slides decreased by 74%, while malaria hospital admissions fell by 81% (Figure 1.12).[153,216] Malaria incidence and mortality continued to decline by 60% between 2010 and 2016.[217] Political and financial investment in malaria control has allowed high coverage of LLINs (>60%), treatment with ACTs and chemoprophylaxis through intermittent prevention therapy in pregnancy (IPTp).[217]

Figure 1.12 Changing epidemiology of malaria incidence and mortality in The Gambia between 2003 and 2007

As described by Ceesay, S.J. et al in "Changes in malaria indices between 1999 and 2007 in The Gambia: a retrospective analysis." *Lancet.* 372, 1545-54 (2008)[216], the figure below illustrates monthly numbers (left panel) and yearly proportions (right panel) of (a) malaria hospital admissions, (b) death, and (c) positive slides in outpatients at the Medical Research Council in Fajara from January 1999 to December 2007. Monthly and yearly rainfall in the Greater Banjul Area over the period is also shown (d).

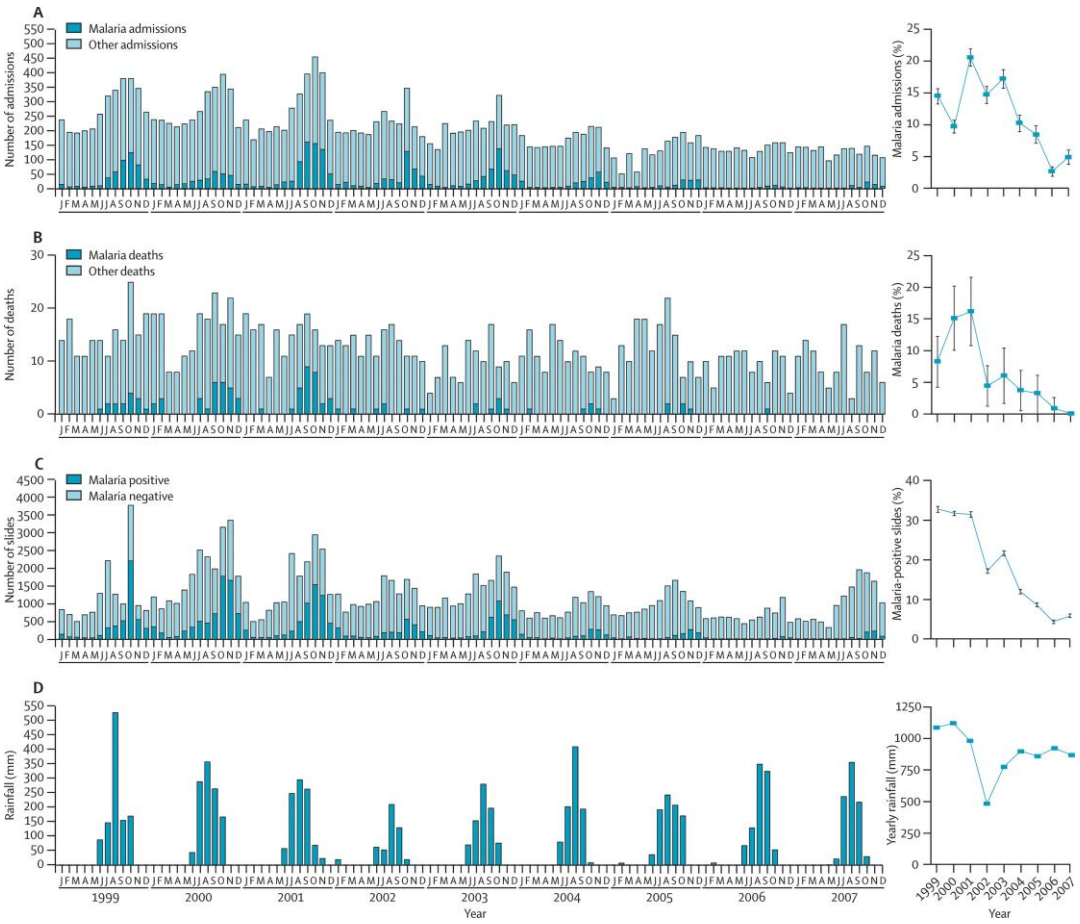

Despite these gains and the potential for elimination, malaria transmission in The Gambia is still on-going across the country and markedly heterogeneous.[218,219] Variations in the proportion of sub-microscopic infections between regions and villages have also been observed.[218] The increasing malaria prevalence documented from west to east may be due lower LLIN usage amongst individuals sleeping outdoors alongside a higher proportion of *Anopheles arabiensis (An. arabiensis)* and *Anopheles coluzzii (An. coluzzii)*, an exophilic outdoor biting mosquito species adapted to semi-arid conditions and potentially more efficient in transmitting infection.[220,221]

Today, The Gambia continues to be an important research site for the evaluation of malaria control strategies given the challenges it still faces to achieve elimination. Ongoing research on vaccines, drugs, and community interventions there will be critical not only for the West African region, but other countries with similarly heterogeneous malaria epidemiology as transmission

declines. The current state of malaria control and elimination in The Gambia will be discussed in more detail in Chapter 6.

Namibia

Namibia is one of a number of southern African countries, including South Africa, Swaziland and Botswana, targeting malaria elimination by 2020, and the Elimination 8 initiative was created in 2009 to support these goals.[217,222] Namibia experienced a remarkable epidemiologic transition between 2001 and 2011, during which clinical cases of malaria fell by 97.4% and malaria-attributable deaths by 98%, owing largely to policies for universal bed-net coverage and IRS in endemic areas, RDT-based case management, and access to ACTs.[223–226]

Overall, climate across this large and sparsely populated country varies considerably from semi-arid to subtropical and temperatures ranging from 5°C and 40°C. The ten northern regions, where 65% of the country's population reside, are categorised as malaria endemic and experience an ecosystem of high temperatures, rainfall and humidity.[227] Malaria risk is driven by rainfall patterns, occurring seasonally with periodic outbreaks in the northwest and more perennially in the northeast.[226] *Pf* accounts for 97% of malaria infections and primary vector is *An. arabiensis*, which are able to breed in "iishanas" or flat, low-lying areas that collect water during the rainy season.[223,226] The Kavango and Zambezi regions have the highest endemicity, while receptivity remains high in Kunene, Omusati, Ohangwena regions. The southern coastal regions of Erongo, Hardap, Khomas and Karas are largely arid and malaria-free (Figure 1.13).[225,228]

Figure 1.13 Map of Namibia and *Plasmodium falciparum* transmission receptivity

As described by Noor, A.M. et al in "Malaria control and the intensity of *Plasmodium falciparum* transmission in Namibia 1969-1992). *PLOS One* 8, e63350 (2013)[225], the figure below illustrates the receptive risks of *P. falciparum* parasite rate for ages 2-10 years (PfPR$_{2-10}$), computed as the maximum mean population adjusted PfPR$_{2-10}$ predicted for years 1969,1974, 1979, 1984 and 1989 for each health district.

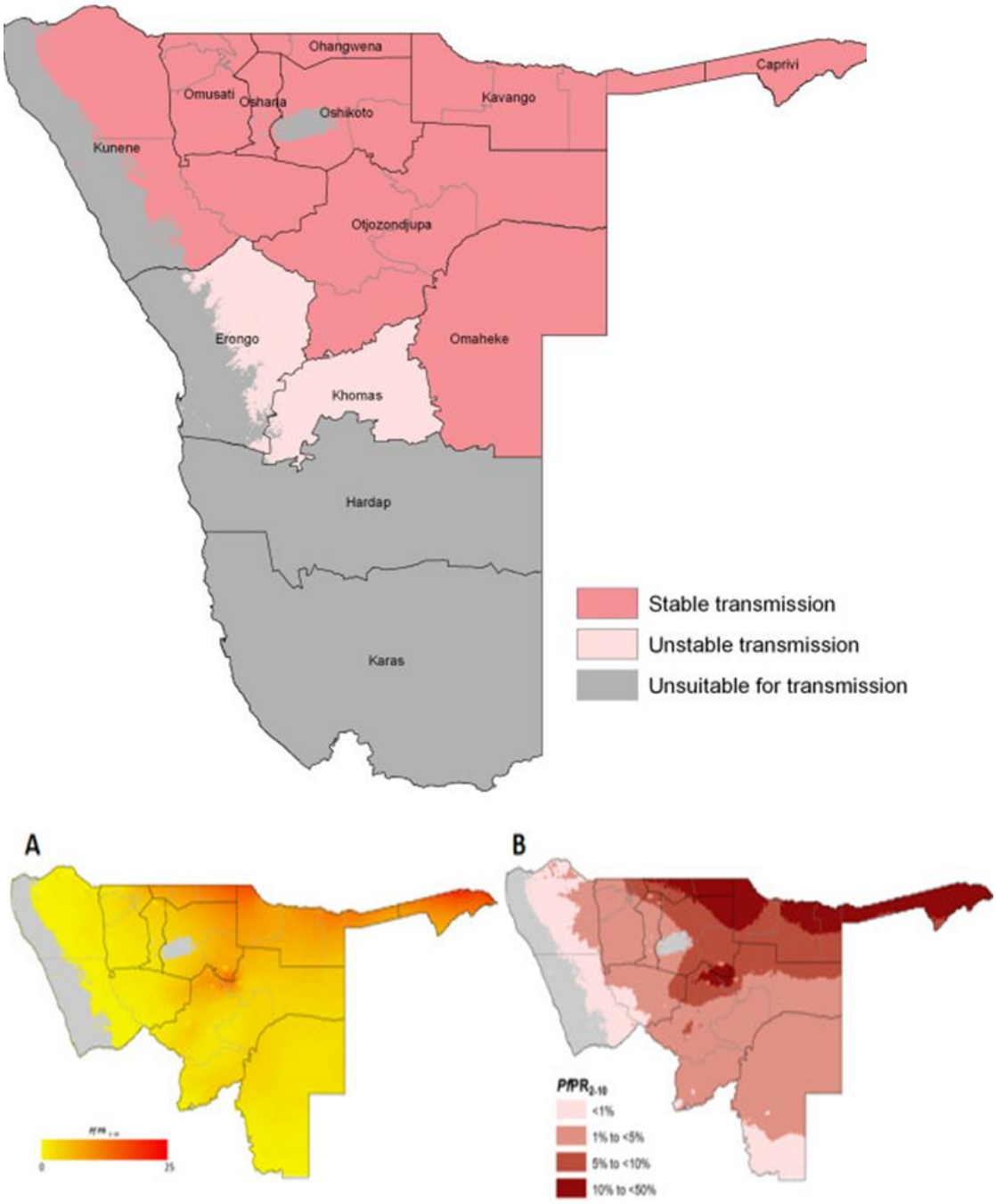

The National Vector-borne Diseases Control Programme (NVDCP) of Namibia launched a campaign for elimination in 2010, with the aim to reduce incidence to less than one case per 1,000 individuals in all districts by 2016 and zero local malaria cases by 2020.[223] DDT-based IRS has been the primary component of the Namibian malaria control programme since the 1960s[229]

and is typically conducted between October to January before the start of the rainy season (November to April). There have been reported coverage issues (falling to as low as 5.0% of the population at risk in the Ohangwena region) due to delayed procurement of insecticides, community acceptance of DDT, and difficulty reaching mobile pastoral populations.[223] IRS has also been periodically supplemented with other vector controls measures. In 2005, the policy of LLIN distribution targeted mainly at-risk groups (children under five years of age and pregnant women), but in 2012, aimed to achieve 95% coverage of the entire population in at risk regions. Free and subsidised LLIN distribution has mainly been supported by the Global Fund and other non-governmental organisations. In 2013, nearly 90 thousand LLINs were distributed, targeting villages with highest malaria burden in Zambezi, Kavango, and Omusati.[223] In 2013, LLIN coverage in the Zambezi region was 17.4% (Namibia Malaria Strategic Plan 2010-2016, Ministry of Health and Social Services).

Due to frequent population movement from neighbouring countries, particularly along the borders with Angola, Zambia and Botswana, low to moderate transmission has been sustained and receptivity remains high. Recent studies in Namibia have found that young male travellers to Angola in particular were disproportionately at risk of malaria, as well as populations living within 15km of the Angolan border, which may be due to mosquito or human movement.[224] The Trans-Kunene Malaria Initiative (TKMI) has aimed to reduce malaria cases in five border regions (Ohangwena, Omusati and Kunene in Namibia and Cunene and Namibe in Angola).[230] The Trans-Zambezi Malaria Initiative (TZMI) also involves Angola, Botswana, Zambia and Zimbabwe.

Historically, Namibia's war for independence from 1975 to approximately 1988 is also an illustration of how easily gains in malaria control can be lost during political instability. Widespread fighting in the areas around Caprivi hampered scale-up and coverage of interventions such as IRS and presumptive treatment. Additionally, large cross-border movements occurred as Namibian fighters engaged South African troops from Angolan bases, which likely blunted the impact of control efforts on the Namibian side. This manifested itself in large malaria rebounds in eastern Kavango and Caprivi by 1989 (increases in *Pf*PR_{2-10} ranging from 4 to 12% compared to levels in 1969).[225]

Today, there have been a limited number of research and capacity building activities Zambezi and neighbouring regions since 2014, in addition to a cluster randomised trial on reactive focal MDA and vector control (the topic of Chapter 7). This includes the Malaria Risk Factor Assessment Tool (MERFAT), developed as part of a case control study that aimed to identify risk factors for malaria in Zambezi by comparing malaria positive and negative cases from the health facility. As part of a 2015 cross-sectional survey, a geographical reconnaissance system was set up that geo-located 8,000 households in the area. This also included a spatial decision support system established via

local health facilities with surveillance data, graphical maps, and tablet-based reporting for use in active case detection and spatially targeted interventions.

Despite progress in reducing malaria burden, outbreaks have been observed in recent years. The areas of northern Namibia have been subject to malaria epidemics in 2004 and 2013, causing high levels of morbidity and mortality (Namibia Malaria Strategic Plan 2010-2016, Ministry of Health and Social Services). In the 2016 malaria season, cases in the country overall were nearly 3-fold higher the annual average in previous years (personal communication Immo Kleinschmidt, Elimination 8). These periodic spikes in incidence have created unexpected challenges for the planning of elimination efforts and case investigations for targeted interventions.

Remaining challenges in malaria elimination and surveillance

The experiences of both The Gambia and Namibia illustrate the many epidemiological and programmatic challenges associated with elimination efforts. In many ways, we are blessed to work on malaria at a time when political commitment is high and there is an arsenal of diverse tools at our disposal with which to target and measure transmission. However, how these tools will be implemented to achieve reductions in transmission and maintain them is still a work in progress. The main challenge addressed in this thesis is the investigation of more sensitive measures of malaria transmission and how they can be applied and standardised for use in surveillance and the evaluation of efficacy trials for elimination.

Chapter 2 Aims and Objectives

The research presented in this thesis seeks to develop improved methods for measuring malaria transmission based on serological endpoints for use in epidemiological surveillance and cluster randomised trials in elimination settings. The work described has the following aims:

Aim 1. To estimate the relative sensitivities of diagnostics currently used to measure malaria infection in humans at the community or cluster level. Specific objectives include:

1. To quantify the comparative sensitivity of existing diagnostics (microscopy, RDTs, PCR, and serology) for the detection of patent and asymptomatic *P.falciparum* infection.
2. To evaluate whether relative diagnostic sensitivities vary by age, geographical region, and transmission intensity.

These objectives are addressed by the work described in Chapters 3 and 4.

Aim 2. To assess the suitability of novel *P.falciparum* recombinant antigens as candidate serological biomarkers of previous malaria infection. Specific objectives include:

1. To estimate the predictive power of candidate biomarkers for measuring previous malaria infection and time since last infection.
2. To evaluate whether the strength of association of novel serological biomarkers varies by age, geographical region, transmission intensity, and other covariates.
3. To select an optimal subset of serological biomarkers for use in measuring short-term changes in malaria transmission at the cluster level.

These objectives are addressed by the work described in Chapter 5.

Aim 3. To investigate the use of novel candidate serological markers of previous malaria infection for use in malaria surveillance and cluster randomised trials. Specific objectives include:

1. To estimate cluster-level antibody responses between transmission seasons and geographical region in The Gambia and between study arms in a cluster randomised trial in Zambezi Region, Namibia.
2. To develop standardised methods for evaluating differences in malaria transmission between clusters or study arms in efficacy trials based on novel serological endpoints.

These objectives are addressed by the work described in Chapters 6 and 7.

Chapter 3 Comparison of diagnostics used to measure cluster-level parasite prevalence

As introduced in Chapter 1, the accurate identification of asymptomatic human infections, which can sustain a large proportion of transmission, is a vital component of control and elimination programmes. This chapter explores the relationship across common diagnostics used to measure malaria prevalence — polymerase chain reaction, rapid diagnostic tests, and microscopy — for the detection of *Plasmodium falciparum* infections in endemic populations based on a pooled analysis of cross-sectional data.

This study was published in 2015 (https://www.nature.com/articles/nature16039) as part of a Nature Supplement on the role of diagnostic tools for infectious disease control and elimination in resource poor settings, and the published version is included here.

London School of Hygiene & Tropical Medicine
Keppel Street, London WC1E 7HT
www.lshtm.ac.uk

Registry
T: +44(0)2072994646
F: +44(0)207299 4656
E: registry@lshtm.ac.uk

RESEARCH PAPER COVER SHEET

PLEASE NOTE THAT A COVER SHEET MUST BE COMPLETED FOR EACH RESEARCH PAPER INCLUDED IN A THESIS

SECTION A – Student Details

Student	**Lindsey Wu**
Principal Supervisor	**Chris Drakeley**
Thesis Title	**Navigating the immuno-epidemiology of malaria: Potential metrics for surveillance and cluster randomised trials**

If the Research Paper has previously been published please complete section B, if not please move to Section C

SECTION B – Paper already published

Where was the work published?	**Nature Supplement**		
When was the work published?	**3 December 2015**		
If the work was published prior to registration for your research degree, give a brief rationale for its inclusion			
Have you retained the copyright for the work?*	**Yes**	Was the work subject to academic peer review?	**Yes**

***If yes, please attach evidence of retention, if no, or if the work is being included in its published format, please attach evidence of permission from the copyright holder (publisher or other author) to include this work.**

SECTION C – Prepared for publication, but not yet published

Where is the work intended to be published	
Please list the paper's authors in the intended authorship order.	
Stage of publication	

SECTION D – Multi-authored work

For multi-authored work, give full details of your role in the research included in the paper and in the preparation of the paper. (Attach a further sheet if necessary)	Co-first-author with Lotus van den Hoogen. Both authors contributed equally to all analysis and writing.

Student Signature: _____ [redacted] **_____ Date: ____12/07/2018_____**

Supervisor Signature: ____ [redacted] **_____ Date: ____12/07/2018_____**

ARTICLE OPEN

Comparison of diagnostics for the detection of asymptomatic *Plasmodium falciparum* infections to inform control and elimination strategies

Lindsey Wu*[1], Lotus L. van den Hoogen*[1], Hannah Slater[2], Patrick G. T. Walker[2], Azra C. Ghani[2], Chris J. Drakeley[1] & Lucy C. Okell[2]

The global burden of malaria has been substantially reduced over the past two decades. Future efforts to reduce malaria further will require moving beyond the treatment of clinical infections to targeting malaria transmission more broadly in the community. As such, the accurate identification of asymptomatic human infections, which can sustain a large proportion of transmission, is becoming a vital component of control and elimination programmes. We determined the relationship across common diagnostics used to measure malaria prevalence — polymerase chain reaction (PCR), rapid diagnostic test and microscopy — for the detection of *Plasmodium falciparum* infections in endemic populations based on a pooled analysis of cross-sectional data. We included data from more than 170,000 individuals comparing the detection by rapid diagnostic test and microscopy, and 30,000 for detection by rapid diagnostic test and PCR. The analysis showed that, on average, rapid diagnostic tests detected 41% (95% confidence interval = 26–66%) of PCR-positive infections. Data for the comparison of rapid diagnostic test to PCR detection at high transmission intensity and in adults were sparse. Prevalence measured by rapid diagnostic test and microscopy was comparable, although rapid diagnostic test detected slightly more infections than microscopy. On average, microscopy captured 87% (95% confidence interval = 74–102%) of rapid diagnostic test-positive infections. The extent to which higher rapid diagnostic test detection reflects increased sensitivity, lack of specificity or both, is unclear. Once the contribution of asymptomatic individuals to the infectious reservoir is better defined, future analyses should ideally establish optimal detection limits of new diagnostics for use in control and elimination strategies.

Nature 528, S86–S93 (3 December 2015), DOI: 10.1038/nature16039

Over the past two decades, considerable progress has been made in reducing the global malaria burden. Between 2000 and 2013 alone, malaria-related mortality decreased by 47% worldwide and 54% in Africa. In addition, more than half of malaria endemic countries are on track to meet global targets to reduce malaria incidence by 75% in 2015 (ref. 1). These achievements are largely due to the widespread use of insecticide-treated nets (ITNs) and highly effective antimalarial treatments. The treatment of symptomatic cases in particular has been enabled by notable advances in the development and deployment of more accurate malaria diagnostics[2,3]. However, efforts to reduce the burden of malaria infections further in the future will require moving beyond the treatment of clinical infections to targeting transmission more broadly in the community. As such, the accurate identification of asymptomatic human infections, which can sustain a large proportion of transmission, is becoming a vital component of control and elimination programmes[2,4].

Community chemotherapy (for example, mass screen and treat (MSAT) or mass drug administration (MDA) programmes) in conjunction with ongoing vector control is an approach under consideration for the interruption of transmission. This is achieved through the direct treatment of potentially infectious individuals. In the case of MSAT strategies, delivering drugs specifically on the basis of positive test results may be considered preferable to presumptive treatment because it provides clear benefit to the recipient and limits excess drug use that may drive antimalarial resistance. However, owing to the insufficient sensitivity of existing field diagnostics used to identify asymptomatic infections, studies have shown that MSAT has limited effect in reducing transmission[5,6].

Measuring parasite infection by microscopy has been the gold standard in malaria research for more than a century and remains relatively widespread as a point-of-care diagnostic in clinical and epidemiological settings. More recently, the advent of rapid diagnostic tests (RDTs), which measure the presence of histidine-rich protein 2 (HRP2) for *Plasmodium falciparum* and/or lactate dehydrogenase for other *Plasmodium* species (pLDH), has expanded the range of diagnostic options. Originally developed to inform clinical treatment, RDTs are increasingly important for epidemiological characterization[7] because of their low cost and field applicability. However, most only have reported detection limits in the range of 100 to 200 parasites per microlitre[8,9] in comparison with around 50 parasites per microlitre by expert microscopy[10].

Over the past three decades, the development of nucleic acid amplification tests has improved the detection limit for malaria infection to less than 1 parasite per microlitre by ultrasensitive quantitative polymerase chain reaction (qPCR)[11,12]. Although these detection thresholds are more appropriate for

*These authors contributed equally. [1]Department of Immunology and Infection, Faculty of Infectious and Tropical Diseases, London School of Hygiene and Tropical Medicine, Keppel Street, London WC1E 7HT, UK. [2]MRC Centre for Outbreak Analysis and Modelling, Department of Infectious Disease Epidemiology, Faculty of Medicine, Imperial College London, Norfolk Place, London W2 1PG, UK. Correspondence should be addressed to: L. W. e-mail lindsey.wu@lshtm.ac.uk.

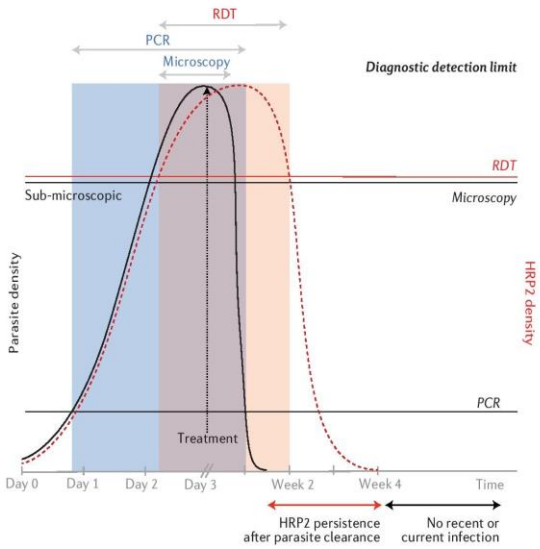

Figure 1 | Schematic of diagnostic detection limits with respect to parasite and HRP2 density. The black curve indicates parasite density and the red curve indicates HRP2 density. Time scale is in days prior to treatment and in weeks after treatment. Horizontal lines are the detection limits of respective diagnostics. The blue shaded area shows detectability of parasites by microscopy and/or polymerase chain reaction (PCR), whereas the red shaded area shows detectability of HRP2 by rapid diagnostic test (RDT).

measuring low-density infections than microscopy and RDTs, most PCR techniques remain impractical for wide-scale use in field surveys owing to cost, processing time and the lack of appropriate laboratory facilities in many endemic countries[10]. Comparative analysis of malaria prevalence, measured by both microscopy and PCR in cross-sectional surveys, has shown that sub-microscopic low-density infections are common across a range of transmission settings[13,14]. These infections may be chronic and asymptomatic, particularly in previously exposed individuals with more mature immune responses. More importantly, even at low parasite densities, they are still capable of infecting mosquitoes and seeding onward transmission[15]. Even though RDTs are becoming more common in areas where these types of infections are prevalent, studies formally evaluating their performance in detecting asymptomatic infections remain scarce.

Recently, there has been an increased focus on developing improved diagnostics to inform malaria elimination strategies. The analysis presented in this paper aims to determine the concordance of current malaria diagnostic methods, forming a baseline to evaluate further how they can be improved to inform malaria control and elimination strategies. It should be noted that, in principle, quantifying the presence of gametocytes is considered the most accurate method for characterizing transmission and the potential infectiousness of individuals. Research in this area is ongoing, but the technical challenges of existing gametocyte assays preclude them from standardized use[16]. Moreover, all malaria infections have the capacity to produce gametocytes[17,18]. Therefore, in the context of community chemotherapy programmes, any individual who tests positive for asexual parasites should be treated to reduce transmission. Given this operational framework, this paper does not address the role of diagnostics that specifically measure gametocytaemia.

So far, no studies have comprehensively evaluated the concordance across PCR, RDT and microscopy detection methods simultaneously in asymptomatic populations. Although microscopy- and PCR-measured prevalences are based on similar biological endpoints (parasite density), diagnostic results based on RDTs are less comparable given that HRP2 and pLDH are indirect measures of parasite biomass[19]. HRP2 can persist in the blood for up to two weeks after parasite clearance[20]. Consequently, results across these diagnostic methods indicate a range of possible infection states, from patent or sub-microscopic infection to recently cleared infection (Fig. 1). A limited number of studies have reviewed the detection capability of RDTs in asymptomatic individuals[8,21], but key research questions still remain. A recent analysis of Demographic and Health Surveys (DHS) across Africa showed a higher prevalence of malaria when measured by RDTs compared with detection by microscopy in 19 out of 22 surveys. This report also highlighted the issue of false positives owing to prolonged presence of HRP2 after parasite clearance[21]. However, studies have not reviewed the detection capability across all three diagnostics. Furthermore, the DHS study only considered children under 5 years of age and did not determine the effect of malaria transmission intensity on diagnostic discordance. This is particularly important given that low-density infections seem to be most common in adults and in low-transmission settings[13,14].

In this study, we determine the relationship across malaria prevalence measures obtained by current diagnostic methods — PCR, RDT and microscopy — for the detection of *P. falciparum* infections in endemic populations based on a pooled analysis of published and unpublished cross-sectional data.

METHODS

Literature review and data collection. We carried out two separate literature reviews to identify studies in which *P. falciparum* prevalence was measured by different diagnostic techniques in the same individuals: first, by RDT and microscopy, and, second, by RDT and PCR. Relevant studies were identified in PubMed and Embase, using MeSH and Map terms when possible. For the RDT and microscopy review, the search terms were: "'rapid diagnostic test' and 'microscopy' [MeSH/Map] and 'malaria falciparum' [MeSH/Map]", and for the RDT and PCR review the search terms were: "'polymerase chain reaction' [MeSH/Map] and 'malaria falciparum' [MeSH/Map]". Searches were limited to English, human and post-2005 (considering the substantial development in RDTs over time[22]). For Embase, the searches were also limited to journal articles. Inclusion criteria were applied as previously described[13]. In short, only studies that were cross-sectional (on populations not selected according to malaria test results or symptoms), that were of populations from a malaria endemic region, that used RDTs targeting *P. falciparum* only or mixed infections (HRP2 and/or pLDH) and that used PCR or loop-mediated isothermal amplification (LAMP) methods were included. For intervention studies, only baseline data were included, except for treatment studies where a sufficient amount of time had passed between last treatment and follow-up. Separate publications that used the same data set or measured 0% prevalence by both methods were removed, as well as data from clusters with fewer than five individuals. RDT and microscopy studies identified in our literature search that also included PCR measurements were included in the RDT and PCR data set, and vice versa for RDT and PCR studies that included microscopy measurements. In addition to the literature review, we sought as many individual-level data sets as possible from studies with the above inclusion criteria.

RDT and microscopy. Where available, information on location, sample size, RDT brand and type (HRP2 or pLDH), age group (15 or younger compared with older than 15) and prevalence estimates were recorded[5,23–42]. Furthermore, data from the DHS online database were extracted[43]. These included individual-level data on location and timing of collection, RDT and microscopy test results, RDT brand[21], age, sex, use of an ITN, fever and antimalarial use in the past two weeks. In addition, individual-level data sets from one unpublished and one published study were included[44], as well as shared data sets of the RDT and PCR comparison that also included microscopy measurements (see below)[45–49].

RDT and PCR. Corresponding authors of the 13 studies identified from the literature search were contacted to request individual-level data in December 2014 and reminders were sent out 4 weeks later. Of the contacted authors, six responded within the timeframe; five data sets were included[45–47,49,50], and one data set had been destroyed for privacy compliance. Prevalence measures and study information (including PCR method) were extracted as described above from the publications in the aforementioned literature search and the non-responders group, as well as included studies from the RDT and microscopy search that also reported PCR proportions[25,27,34,39,40,42,51–55]. Four additional individual-level unpublished and published data sets were included[44,48].

Statistical analyses. We analysed the association between PCR- and RDT-measured prevalence, and microscopy- and RDT-measured prevalence by fitting a linear relationship on the log odds scale[13,56]. Prevalence (on a scale of 0 to 1) was defined as $\frac{e^{(\log odds)}}{1+e^{(\log odds)}}$, where log odds = $\log_e(\frac{prevalence}{1-prevalence})$

$$\Omega_{Ri} = \Omega_{Pi} + \delta_{Ri} \quad (1)$$

$$\delta_{Ri} = \delta'_{Ri} + \beta_0 (\Omega_{Pi} - \bar{\Omega}_P) \quad (2)$$

$$\Omega_{Ri} = \Omega_{Mi} + \delta_{Ri} \quad (3)$$

$$\delta_{Ri} = \delta'_{Ri} + \beta_0 (\Omega_{Mi} - \bar{\Omega}_M) \quad (4)$$

In Equations 1–4, Ω_{Ri} is the log odds of RDT-measured prevalence in trial i, Ω_{Pi} is the log odds of PCR prevalence, Ω_{Mi} is the log odds of microscopy-measured prevalence, δ_{Ri} is the log odds ratio (OR) of RDT- to PCR-measured prevalence (RDT:PCR; Equation 1) or RDT- to microscopy-measured prevalence (RDT:microscopy; Equation 3), δ'_{Ri} is the expected log OR of RDT:PCR prevalence (Equation 2) or RDT:microscopy prevalence (Equation 4) when the log odds of PCR- or microscopy-measured prevalence is equal to the mean across trials, $\bar{\Omega}_P$ and $\bar{\Omega}_M$ are the mean log odds of PCR- and microscopy-measured prevalence, respectively, across trials, and β_0 is the regression coefficient. To allow for varying sample size and sampling variation across the surveys included in our analysis, the model was fitted using Bayesian Markov Chain Monte Carlo methods in JAGS version 3.4.0 and the *rjags* package in R version 3.0.2 (ref. 13). We also explored fitting polynomial relationships, but these provided no substantial improvement in fit to the data over the linear model as assessed by deviance information criterion, nor were these fitted relationships qualitatively different (data not shown). To confirm that the fitted curves at different prevalence ranges were not overly influenced by the high number of data points in lower transmission areas, we fitted separate relationships in three PCR-measured prevalence bands: <5%, 5–20% and >20%. These categories represent approximate cut-offs that have been suggested as thresholds for operational decision-making. Broadly speaking, programmes can begin to consider targeted and focal control strategies when parasite prevalence by microscopy falls below 5% (ref. 57), which translates to a PCR-measured prevalence of 20% (ref. 14), and move towards targeted elimination when it falls below 1% (ref. 58) (5% PCR-measured prevalence[14]).

We also conducted a meta-analysis of the risk ratio between RDT:PCR prevalence or RDT:microscopy prevalence, adjusted for random effects at the study level (for RDT:PCR) or country level (for RDT:microscopy). Studies that reported zero infections by either diagnostic method were assigned a value of 0.01 to allow a risk ratio to be calculated. To evaluate the effect of explanatory factors on discordant test results, individual-level data were analysed by logistic regression, allowing for random effects at the study or country level as noted above. The meta-analysis was done with the *metafor* package in R version 3.0.2, and the logistic regression with the *logit* command in STATA version 13.

We assessed the ability of our models to predict RDT-measured prevalence based on microscopy- or PCR-measured prevalence data. Leave-one-out cross validation was used to evaluate the RDT:PCR and the RDT:microscopy models separately. The data available for direct comparison of malaria detection by RDT and PCR in the same individuals were sparse relative to the quantity of data available for the RDT:microscopy and previous microscopy:PCR comparisons. Therefore, we also triangulated the relationship between RDT- and PCR-measured prevalence by combining the RDT:microscopy relationship calculated in this study with the microscopy:PCR prevalence relationship that has been previously defined[13]. The credible interval of the triangulation line was computed from the posterior distributions of all the parameters from both equations combined. We evaluated whether this triangulated RDT:PCR relationship was significantly different from the observed RDT:PCR relationship using the posterior distributions of the predictions from each model.

RESULTS

Literature search and data collection. The literature search generated 549 results in Pubmed and an additional 37 in Embase for RDT and microscopy, and 2,247 results in PubMed and an additional 426 in Embase for RDT and PCR. In total, 20 RDT: microscopy studies and 13 RDT:PCR studies from the literature search met our inclusion criteria. Combined with additional data sets from DHS and unpublished studies, the pooled data available for evaluation yielded 323 pairs of prevalence estimates for RDT and microscopy[5,23–42,44–49] and 162 pairs for RDT and PCR[25,27,34,39,40,42,45–55]. The extracted proportions together with the main characteristics of the studies from our literature search are provided in the Supplementary Information. The main PCR method used was nested PCR (nPCR; 15 of 20) of which mainly the Snounou method[59] was used (11 of 15). The other methods included LAMP (1 of 20) and qPCR (4 of 20). All of the included RDTs in both comparisons were based on HRP2, with 8 out of 20 studies also including pLDH to measure species other than *P. falciparum*. However, this study only focuses on the detection of *P. falciparum* infections.

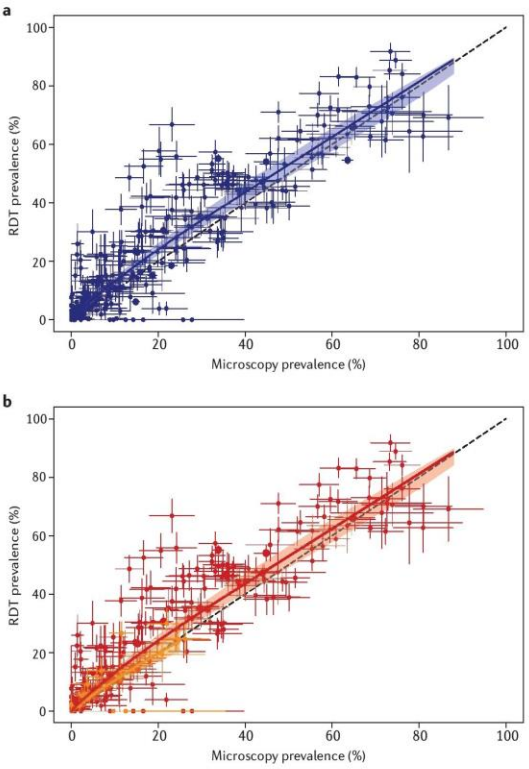

Figure 2 | The relationship between rapid diagnostic tests (RDTs) and microscopy *Plasmodium falciparum* prevalence overall (**a**) and stratified by age group (**b**). In **b** red indicates children (those under 15 years) and yellow indicates adults (those over 15 years). Dashed lines indicate the expected relationship if RDT and microscopy detected equal prevalence. Horizontal and vertical lines indicate 95% confidence intervals around point estimates, whereas coloured solid lines indicate the median of the Bayesian posterior distributions from the fitted model and shaded areas indicate 95% credible intervals. Radius of point estimates indicate cluster size (from small to large: <100, 100–1,000 and >1,000).

Comparison of RDT- and microscopy-measured prevalence. Analysis of RDT- and microscopy-measured prevalence included data from 172,281 individuals who were tested with RDTs (cluster prevalence range = 0–92%) and 186,434 tested with microscopy (cluster prevalence range = 0–87%). The 323 geographical clusters spanned a total of 29 countries (cluster size range = 5–7,664). Overall, prevalence of *P. falciparum* measured by microscopy detected 87% (95% confidence interval (CI) = 74–102%) of RDT-positive infections. Therefore, RDT and microscopy detection was comparable (Fig. 2a, Table 1), with less of a difference between the two diagnostic methods in children under 15 years of age (77%, 95% CI = 71–85%) compared with adults (over 15 years)

Table 1 | Best fit relationships between RDT:microscopy and RDT:PCR prevalence.

RDT:microscopy
OVERALL
log odds RDT prevalence = 0.108 + 0.907 × log odds microscopy prevalence (all ages)
BY AGE CATEGORY
log odds RDT prevalence = 0.109 + 0.908 × log odds microscopy prevalence (under 15 years)
log odds RDT prevalence = −0.168 + 0.890 × log odds microscopy prevalence (over 15 years)
RDT:PCR
OVERALL
log odds RDT prevalence = −0.968 + 1.186 × log odds PCR prevalence (all ages)
BY AGE CATEGORY
log odds RDT prevalence = −0.382 + 1.306 × log odds PCR prevalence (under 5 years)
log odds RDT prevalence = −0.864 + 1.213 × log odds PCR prevalence (6–15 years)
log odds RDT prevalence = −1.378 + 1.300 × log odds PCR prevalence (over 15 years)
BY AGE CATEGORY
log odds RDT prevalence = 1.097 + 1.690 × log odds PCR prevalence (<5% prevalence)
log odds RDT prevalence = 0.211 + 1.754 × log odds PCR prevalence (5–20% prevalence)
log odds RDT prevalence = −0.516 + 1.904 × log odds PCR prevalence (>20% prevalence)
PCR PREVALENCE BASED ON DATA TRIANGULATION
log odds PCR prevalence = 0.108 + 0.907 × [(log odds RDT prevalence − 0.954)/0.868]

PCR, polymerase chain reaction; RDT, rapid diagnostic test.

(60%, 95% CI = 48–86%) (Fig. 2b, Table 1). The lower age-specific risk ratios are due to smaller cluster sizes after stratifying the data by age group. However, regression analysis of individual-level data did not show a significant association between age group and test discordance (Supplementary Table 1).

Effect of individual level covariates on RDT:microscopy discordance. In addition to age, we explored the effect of several other covariates on diagnostic outcomes, and adjusted for transmission intensity as assessed by microscopy-measured prevalence (Supplementary Table 1). A significant association was seen between self-reported antimalarial use in the two weeks before survey testing and RDT positivity in individuals who tested negative by microscopy (OR = 1.71, 95% CI = 1.16–2.51, p = 0.006). The presence of fever at the time of testing (recorded temperature with study-specific cut-off or self-reported) reduced the odds of undetected malaria infection by RDT among microscopy-positive individuals (OR = 0.59, 95% CI = 0.39–0.89, p<0.001). Among individuals testing negative by microscopy, presence of a fever was significantly associated with RDT positivity (OR = 1.84, 95% CI = 1.51–2.24, p<0.001), after adjusting for transmission intensity. There was a borderline significant increased risk of malaria infection being undetectable by RDT among those who used an ITN and were microscopy positive (OR = 1.26, 95% CI = 1.00–1.59, p = 0.053), whereas use of an ITN was associated with decreased RDT positivity (OR = 0.84, 95% CI = 0.73–0.97, p = 0.019) among microscopy-negative individuals. There was no evidence of an association between RDT brand and the risk of an undetected malaria infection by RDT among microscopy-positive individuals. Among microscopy-negative individuals, the proportion testing positive was different between RDT brands, but these results are difficult to interpret, owing to complete correlation between study and RDT brand. The year of the survey was not associated with discordant test results for RDT:microscopy.

Comparison of RDT- and PCR-measured prevalence. Analysis of RDT- and PCR-measured prevalence included 35,887 individuals tested with an RDT (cluster prevalence range = 0–45%) and 31,178 individuals tested with PCR (cluster prevalence range = 0–52%). There were a total of 162 geographical clusters across 17 countries (cluster size range = 5–3,307, Figs 3a,b and Table 1). Pooled meta-analysis across all surveys showed that RDTs detected an average of 41% (95% CI = 26–66%) of PCR-positive infections. This primarily reflects the relationship between RDT and PCR in low-transmission settings, with an average PCR prevalence of 8% across all the clusters included in our analysis.

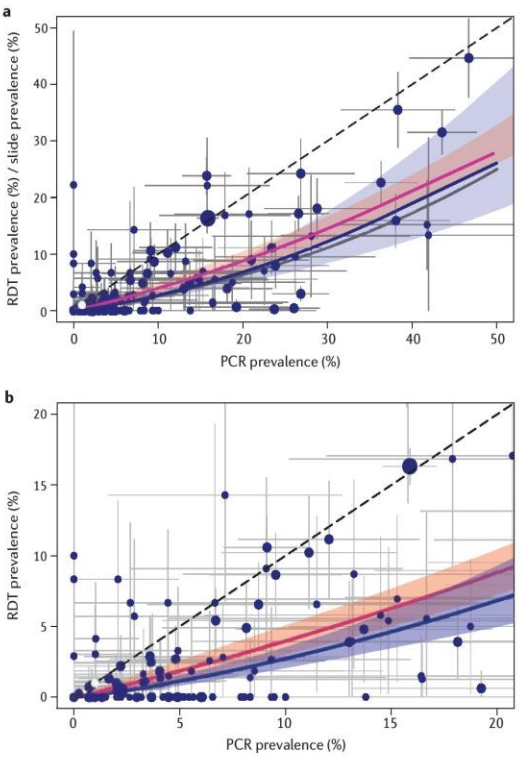

Figure 3 | The relationship between rapid diagnostic test (RDT) and polymerase chain reaction (PCR) prevalence overall (**a**) and zoomed in for <20% PCR prevalence (**b**). Blue, observed RDT:PCR prevalence data and model fit; pink, the triangulated RDT:PCR comparison (see methods); grey, the PCR:microscopy comparison from ref. 13. Dashed lines indicate the expected relationship if RDT (or microscopy) and PCR detected equal prevalence. Horizontal and vertical lines indicate 95% confidence intervals around point estimates, whereas coloured solid lines indicate the median of the Bayesian posterior distributions from the fitted model and shaded areas indicate 95% credible intervals. Radius of point estimates indicate cluster size (from small to large: <100, 100–1,000 and >1,000).

Age, transmission intensity and undetected malaria infection by RDT. As with the relationship between RDT- and microscopy-measured prevalence, stratifying by age group improved the model fit to the data, showing a decrease in detectability by RDT with increasing age (Figs 4a–c). Meta-analysis of the risk ratio between RDT and PCR positivity showed that, for children under 5 years of age, RDTs detected 81% (95% CI = 74–89%) of PCR-positive infections. By comparison, RDTs detected fewer PCR-positive school-aged individuals (6–15 years) (70%, 95% CI = 57–86%), and even fewer among adults over 15 years of age (49%, 95% CI = 31–78%). There was a larger data set available for analysis in the under 5 (140 clusters) and 6–15 (136 clusters) age groups compared with adults (81 clusters), suggesting that additional data in the higher age group could help to improve the accuracy of these estimates.

Previous studies have suggested that the proportion of carriers with sub-microscopic infections decreases in areas of higher transmission intensity, potentially because of an association with re-infection and increased parasite density[13,14]. A similar trend was also observed in the relationship between RDT and PCR detectability. The fit to our data was improved after stratifying by transmission intensity based on PCR-measured prevalence, showing increased RDT sensitivity compared with PCR as transmission increases (Fig. 4d–f). However, meta-analysis of the risk ratio between RDT and PCR positivity did not show a significant difference between the three transmission

ranges, possibly indicating that more data are needed to define a more robust relationship for each transmission setting.

Figure 5 shows RDT detectability as a proportion of PCR-positive individuals, stratified by age and transmission intensity. Irrespective of transmission intensity, adults have the highest percentage of RDT-undetectable infections. By contrast, the percentage of individuals with RDT-detectable infections in all age groups increases as transmission intensity increases. However, since infection rates are greater at high-transmission intensities, RDTs may still miss a larger absolute number of infectious individuals at this level of endemicity. Best-fit model estimates of PCR-measured prevalence based on RDT-measured prevalence are summarized in Figs 3, 4 and Table 1.

Effect of individual-level covariates on RDT:PCR discordance. We evaluated the impact of age and transmission intensity on RDT positivity among PCR-negative individuals as a potential indicator of prolonged HRP2 clearance time. Logistic regression, adjusted for cluster PCR-measured prevalence, showed that among PCR-negative individuals, school-aged children had a significantly higher RDT positivity (OR = 1.53, 95% CI = 1.28–1.82, $p<0.001$) when compared with a baseline of children under 5 years of age. Adults showed similar odds of being RDT positive (OR = 1.00, 95% CI = 0.64–1.58, $p = 0.990$) as those under 5 years. Infections that were undetected by RDT, based on PCR positivity, were highest in adults (OR = 5.04, 95 %CI = 4.14–6.13, $p<0.001$) compared with those under 5 years, with a similar risk in school-aged children and those under 5 years (Supplementary Table 2).

RDT positivity among PCR-negative individuals varied between RDT brands, as did the detection of infection in PCR-positive individuals, but these results were not significant. Patients with a fever were less likely to have undetected infections by RDT if they were PCR positive (OR = 0.14, 95% CI = 0.06–0.32, $p<0.001$), but also more likely to have a RDT-positive result if they were PCR negative (OR = 4.86, 95% CI = 2.29–10.30, $p<0.001$). More recent surveys showed a lower risk of RDT-undetected infections, based on PCR positivity (OR = 0.77 per year, 95% CI = 0.60–0.99, $p = 0.044$), which may indicate an improved performance of RDTs over time. PCR method was associated with test discordance at borderline significance, with RDTs detecting less PCR positive results measured by qPCR than those measured by PCR (OR = 1.92, 95% CI = 0.98–3.74, $p = 0.056$), reflecting higher sensitivity of qPCR, as described previously[15,45].

Model validation. From the leave-one-out analysis, the correlation coefficient between observed and predicted values of RDT-measured prevalence from the RDT:PCR model was 0.67, indicating a moderate agreement. The correlation coefficient between observed and predicted values of RDT-measured prevalence from the RDT:microscopy model was 0.92, indicating a relatively stronger agreement (Fig. 6). The credible interval of this triangulated relationship was narrower than that of the directly observed line, owing to the larger number of data points in the RDT:microscopy and microscopy:PCR data sets (Figs 2, 3, Table 1). There was no significant difference between the triangulated and observed relationships at any transmission intensity.

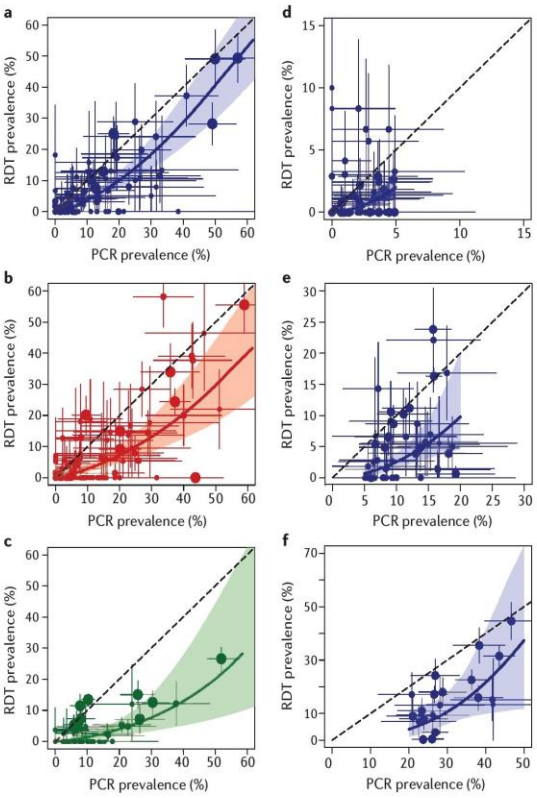

Figure 4 | The relationship between rapid diagnostic test (RDT) and polymerase chain reaction (PCR) prevalence by age group **(a–c)** and PCR prevalence band **(d–f)**. The Bayesian model was fitted separately for each age group or PCR prevalence band. Age groups are younger than 5 years **(a)** 6–15 years **(b)** and older than 15 years **(c)**. PCR prevalence bands are <5% **(d)**, 5–20% **(e)** and >20% **(f)**. Dashed lines indicate the expected relationship if RDT and PCR detected equal prevalence. Horizontal and vertical lines around point estimates indicate 95% confidence intervals, whereas coloured solid lines indicate the median of the Bayesian posterior distributions from the fitted model and shaded areas indicate 95% credible intervals of these fits. Radius of point estimates indicate cluster size (from small to large: <50, 50–100 and >100).

DISCUSSION

As the burden of malaria continues to decline in many regions[1], it is crucial to understand the suitability of diagnostics for use in low-transmission and near-eliminating areas where MSAT and MDA strategies are likely to be applied. More specifically, how will diagnostic accuracy affect the ability of MSAT programmes to detect and treat asymptomatic individuals or determine local malaria prevalence thresholds for the initiation of MDA? Our study results show that the detection capability of RDTs is comparable with, and often greater than, microscopy. On average, microscopy captured 87% of RDT-positive infections, with higher test concordance in children than in adults. The extent to which this higher RDT detection reflects increased sensitivity, lack of specificity, or both, is unclear. Compared with molecular detection methods, however, RDTs still miss a substantial proportion of infections, capturing only 41% of PCR-positive individuals in low-transmission settings. Our analysis included cross-sectional data with paired prevalence measures by either RDT and microscopy or RDT and PCR from more than 180,000 individuals, spanning more than 400 geographical clusters. The detection levels observed differed depending on age and transmission intensity, reflecting complex dynamics at both the ecological and host level that may influence parasite densities and the relative performance of these diagnostics.

Factors correlated with the accuracy of RDTs are varied and likely to be driven by subtleties in the concentration and duration of HRP2 antigens in peripheral circulation. A lower specificity by RDT is expected given that, in addition to current infection, they can detect recent infection owing to residual HRP2 even after parasite clearance. Our analysis found that RDTs had a higher positivity rate than microscopy among those who were more likely to have current or recent high parasite densities — children, those with measured or reported fever and those recently treated with antimalarial drugs. This may indicate that high parasite densities and, therefore, ruptured schizonts (asexual parasites that replicate to form multiple red blood cell invading parasites), lead to increased and/or prolonged HRP2 levels. These levels are likely to vary depending on an individual's clinical status and stage of infection owing to associated fluctuations in parasite density. Because RDTs have been designed for clinical use, it is intuitive that their performance would be optimal in the detection of high-density infections associated with symptomatic disease. A previous analysis evaluating the sensitivity of RDTs and microscopy, specifically in

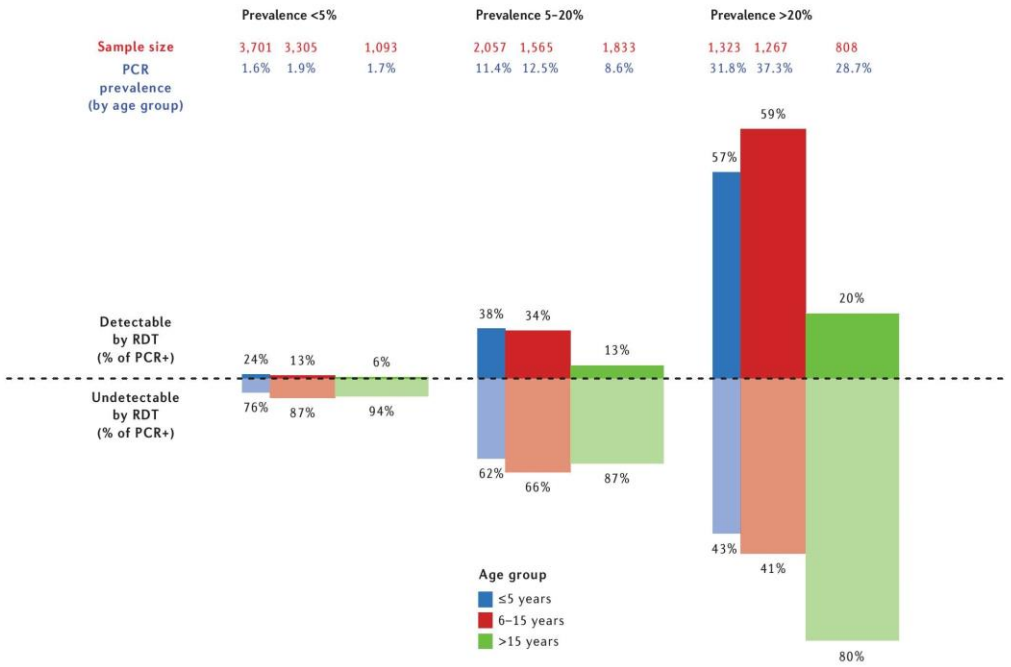

Figure 5 | Rapid diagnostic test (RDT) detectable (darker colours) and undetectable (lighter colours) infections based on polymerase chain reaction positive (PCR+) infections by age (under 5 years, 6–15 years and older than 15 years) and transmission intensity (PCR prevalence <5%, 5–20% and >20%). The height of the bars for RDT detectable and undetectable proportions reflects the total prevalence of infection in that group according to PCR, whereas the width of the bars shows the proportion of the population in each age group in most African settings (younger than 5 years (blue), 15%; 6–15 years (red), 35%; and over 15 years (green), 50% of the total population[79]).

individuals with clinical symptoms, found an association between parasite density and RDT positivity[60]. This study also stressed the issue of false positives and how RDT specificity, in addition to being influenced by parasite density, may be correlated with age and transmission intensity. Further investigation into how RDT accuracy varies between clinical and subclinical populations could help to elucidate the factors that drive these differences. Our analysis also found that using an ITN was associated with better concordance of RDT and microscopy results, most probably due to a lower risk of infection. This distinction is particularly relevant for elimination strategies, because an RDT-positive and microscopy-negative result after parasite clearance may still indicate recent transmission in a population, whereas absence of infection does not. In general, it should be noted that the quality of microscopy is likely to vary more widely than that of RDTs. Microscopy in the context of research surveys is more accurate than those typically encountered during routine surveillance[61]. Therefore, the relative sensitivity of these diagnostics may be more discordant in programmatic settings than the relationship observed in this study.

Our analysis also found a number of factors that correlated with detection by RDT and PCR. Previous studies have demonstrated that the proportion of carriers with sub-microscopic infections decreases in areas of high-transmission intensity, potentially associated with superinfection (new malaria infection in already infected individuals)[13,14]. This trend was also observed in our analysis — the proportion of PCR-measured infections that were detected by RDT increased with higher transmission intensity. Although the interaction between infection, immunity and parasite density in these settings is not fully understood, it has been suggested that only partial cross-immunity is acquired against malaria parasite clones[62]. Greater multiplicity of infection in higher transmission settings could result in higher parasite densities if host immune systems cannot respond to the diversity of parasites or if parasites increase growth rates in the presence of competing clones[14,63]. In addition to transmission intensity, we also observed age-associated variations in RDT detection. Our analysis shows that, after adjusting for transmission intensity, the odds of having an RDT-undetectable infection in adults was fivefold higher compared with under 5 year olds, potentially owing to more enhanced immune responses in adults that suppress parasite proliferation. This finding coincides well with data that show a lower sensitivity of microscopy relative to PCR among adults[13]. In addition, among PCR-positive individuals, the odds of a positive RDT result was seven times higher in patients with a fever. Overall, these results emphasize that fever, superinfections and childhood infections are commonly associated with high parasite densities, which, in turn, may lead to higher HRP2 levels that persist after parasite clearance. A number of studies have shown a relationship between parasite biomass and HRP2 clearance time[64–66]. However, these studies were predominantly in areas of high-density infections; studies in areas of lower parasite densities are less conclusive[61]. Moreover, HRP2 concentrations may be influenced by duration of infection, parasite sequestration and HRP2 antibody responses[67]. Therefore, characterizing HRP2 detection profiles at parasite densities that are more typically found in elimination settings can help to better gauge the accuracy of RDTs in these areas. Our results also showed that risk of an RDT-positive and PCR-negative test result was higher in school-aged children compared with children under 5 and adults. This may be further evidence for an association between age and recent high parasite density (approximately 2–4 weeks), but may also suggest that infections can fall below the detection limit of PCR and still be captured by RDTs. RDT results that are typically presumed to be false positives may be advantageous when the identification of a recent as well as a current infection is needed, such as in elimination settings, or if HRP2 is still measurable during periods of fluctuating parasite density that drop below the molecular detection threshold. An improved understanding of RDT performance relative to PCR methods of various sensitivities, such as qPCR and LAMP, could help to further benchmark the range at which RDTs can optimally operate. Although the impact of the PCR method on test sensitivity has been investigated in previous studies[14], more data are required to evaluate this relative to RDT sensitivity in more detail.

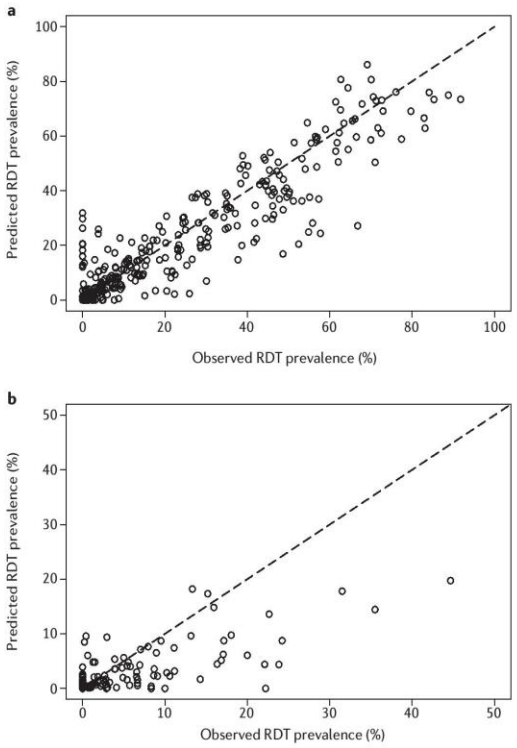

Figure 6 | The relationship between observed and predicted rapid diagnostic test (RDT) prevalence from the RDT:microscopy comparison **(a)**, and the RDT:polymerase chain reaction comparison **(b)**. Predictions were obtained using leave-one-out cross-validation.

We were able to define a more robust model for the relationship between prevalence measured by RDT compared with microscopy, than for the relationship between prevalence measured by RDT compared with PCR. This is because a more comprehensive data set of comparative RDT and microscopy measures was available across a wider range of transmission intensities. Medium- to high-transmission settings were particularly under-represented in the comparison of RDT and PCR measures. With more than half of our data from <5% PCR prevalence settings (57%; 93 of 162 clusters), the RDT:PCR relationship described here primarily reflects RDT performance at low-transmission intensity. However, the relationship between RDT- and PCR-measured prevalence estimated from directly observed paired data was not statistically different from the RDT:PCR relationship estimated by triangulating the RDT:microscopy and microscopy:PCR relationships based on independent data sets, improving confidence in our findings. Additional covariate information in future studies would further explain other factors that influence diagnostic sensitivity. Although we included RDT brand as a covariate in both the RDT:microscopy and RDT:PCR models, studies in this meta-analysis were not collected specifically to evaluate RDT brand so data are not sufficiently representative to draw conclusions on its impact on diagnostic sensitivity.

Overall, this study has established the relative detection capabilities of existing diagnostics for the identification of asymptomatic individuals infected with *P. falciparum*. To inform community chemotherapy programmes, however, further analysis is needed to determine to what extent these individuals contribute to onward transmission. As with detection, the potential infectiousness of asymptomatic individuals is sensitive to fluctuations in parasite density over the course of an infection and by season[15,68]. These are driven by the maturity of the host's immune response, which may vary by age and by local transmission dynamics, such as seasonality, that can influence population-level immunity or within-host parasite behaviour. Therefore, defining infectivity in relation to parasite density is especially important; this is addressed further by Slater and colleagues in a companion paper in this supplement[69]. Once the contribution of asymptomatic individuals to the infectious reservoir is better defined, future analyses should ideally establish optimal detection limits of new diagnostics for use in control and elimination strategies.

1. World Health Organization. *World Malaria Report 2014* (WHO, 2014)
2. The malERA Consultative Group on Diagnoses and Diagnostics. A research agenda for malaria eradication: diagnoses and diagnostics. *PLoS Med* **8,** e1000396 (2011).
3. Anthony, M. P., Burrows, J. N., Duparc, S., Moehrle, J. J. & Wells, T. N. The global pipeline of new medicines for the control and elimination of malaria. *Malar. J.* **11,** 316 (2012).
4. Tietje, K. *et al.* The essential role of infection-detection technologies for malaria elimination and eradication. *Trends Parasitol.* **30,** 259–266 (2014).
5. Tiono, A. B. *et al.* Lessons learned from the use of HRP-2 based rapid diagnostic test in community-wide screening and treatment of asymptomatic carriers of *Plasmodium falciparum* in Burkina Faso. *Malar. J.* **13,** 30 (2014).
6. Cook, J. *et al.* Mass screening and treatment using a falciparum-specific rapid diagnostic test did not reduce malaria incidence in Zanzibar. *J. Infect. Dis.* **211,** jiu655 (2014).
7. Guerra, C. A. *et al.* Assembling a global database of malaria parasite prevalence for the Malaria Atlas Project. *Malar. J.* **6,** 17 (2007).
8. Ochola, L. B., Vounatsou, P., Smith, T., Mabaso, M. L. H. & Newton, C. R. J. C. The reliability of diagnostic techniques in the diagnosis and management of malaria in the absence of a gold standard. *Lancet. Infect. Dis.* **6,** 582–588 (2006).
9. World Health Organization. *Malaria Rapid Diagnostic Test Performance. Results of WHO Product Testing of Malaria RDTs: Round 4 (2012)* (WHO, 2012).
10. Cordray, M. S. & Richards-Kortum, R. R. Emerging nucleic acid–based tests for point-of-care detection of malaria. *Am. J. Trop. Med. Hyg.* **87,** 223–230 (2012).
11. Andrews, L. *et al.* Quantitative real-time polymerase chain reaction for malaria diagnosis and its use in malaria vaccine clinical trials. *Am. J. Trop. Med. Hyg.* **73,** 191–198 (2005).
12. Rockett, R. J. *et al.* A real-time, quantitative PCR method using hydrolysis probes for the monitoring of *Plasmodium falciparum* load in experimentally infected human volunteers. *Malar. J.* **10,** 48 (2011).
13. Okell, L. C., Ghani, A. C., Lyons, E. & Drakeley, C. J. Submicroscopic infection in *Plasmodium falciparum*-endemic populations: a systematic review and meta-analysis. *J. Infect. Dis.* **200,** 1509–1517 (2009).
14. Okell, L. C. *et al.* Factors determining the occurrence of submicroscopic malaria infections and their relevance for control. *Nature Commun.* **3,** 1237 (2012).
15. Bousema, T., Okell, L., Felger, I. & Drakeley, C. Asymptomatic malaria infections: detectability, transmissibility and public health relevance. *Nature Rev. Microbiol.* **12,** 833–840 (2014).
16. Stone, W., Gonçalves, B. P., Bousema, T. & Drakeley, C. Assessing the infectious reservoir of falciparum malaria: past and future. *Trends Parasitol.* **31,** 287–296 (2015)
17. Bousema, T. & Drakeley, C. Epidemiology and infectivity of *Plasmodium falciparum* and *Plasmodium vivax* gametocytes in relation to malaria control and elimination. *Clin. Microbiol. Rev.* **24,** 377–410 (2011).
18. Schneider, P. *et al.* Quantification of *Plasmodium falciparum* gametocytes in differential stages of development by quantitative nucleic acid sequence-based amplification. *Mol. Biochem. Parasitol.* **137,** 35–41 (2004).
19. Dondorp, A. M. *et al.* Estimation of the total parasite biomass in acute falciparum malaria from plasma PfHRP2. *PLoS Med* **2,** e204 (2005).
20. McMorrow, M. L., Aidoo, M. & Kachur, S. P. Malaria rapid diagnostic tests in elimination settings--can they find the last parasite? *Clin. Microbiol. Infect. Off. Publ. Eur. Soc. Clin. Microbiol. Infect. Dis.* **17,** 1624–1631 (2011).
21. Florey, L. *Measures of Malaria Parasitemia Prevalence in National Surveys: Agreement Between Rapid Diagnostic Tests and Microscopy.* DHS Analytical Studies No. 43. (2014).
22. Mouatcho, J. C. & Goldring, J. P. D. Malaria rapid diagnostic tests: challenges and prospects. *J. Med. Microbiol.* **62,** 1491–1505 (2013).
23. Endeshaw, T. *et al.* Evaluation of light microscopy and rapid diagnostic test for the detection of malaria under operational field conditions: a household survey in Ethiopia. *Malar. J.* **7,** 118 (2008).
24. Falade, C. O. *et al.* Blood banking in a malaria-endemic area: evaluating the problem posed by malarial parasitaemias. *Ann. Trop. Med. Parasitol.* **103,** 383–392 (2009).
25. Ganguly, S. *et al.* High prevalence of asymptomatic malaria in a tribal population in Eastern India. *J. Clin. Microbiol.* **51,** 1439–1444 (2013).
26. Gitonga, C. W. *et al.* Use of rapid diagnostic tests in malaria school surveys in Kenya: does their under-performance matter for planning malaria control? *Am. J. Trop. Med. Hyg.* **87,** 1004–1011 (2012).
27. Golassa, L., Enweji, N., Erko, B., Aseffa, A. & Swedberg, G. Detection of a substantial number of sub-microscopic *Plasmodium falciparum* infections by polymerase chain reaction: a potential threat to malaria control and diagnosis in Ethiopia. *Malar. J.* **12,** 352 (2013).
28. Gonçalves, L. *et al.* Bayesian latent class models in malaria diagnosis. *PLoS ONE* **7,** e40633 (2012).
29. Ishengoma, D. S. *et al.* Accuracy of malaria rapid diagnostic tests in community studies and their impact on treatment of malaria in an area with declining malaria burden in north-eastern Tanzania. *Malar. J.* **10,** 176 (2011).
30. Keating, J., Miller, J. M., Bennett, A., Moonga, H. B. & Eisele, T. P. *Plasmodium falciparum* parasite infection prevalence from a household survey in Zambia using microscopy and a rapid diagnostic test: implications for monitoring and evaluation. *Acta Trop.* **112,** 277–282 (2009).

31. Laurent, A. *et al.* Performance of HRP-2 based rapid diagnostic test for malaria and its variation with age in an area of intense malaria transmission in southern Tanzania. *Malar. J.* **9,** 294 (2010).
32. Mboera, L. E. G. *et al.* Comparison of the Paracheck-Pf test with microscopy, for the confirmation of *Plasmodium falciparum* malaria in Tanzania. *Ann. Trop. Med. Parasitol.* **100,** 115–122 (2006).
33. Neumann, C. G. *et al.* Comparison of blood smear microscopy to a rapid diagnostic test for *in-vitro* testing for *P. falciparum* malaria in Kenyan school children. *East Afr. Med. J.* **85,** 544–549 (2008).
34. Satoguina, J. *et al.* Comparison of surveillance methods applied to a situation of low malaria prevalence at rural sites in The Gambia and Guinea Bissau. *Malar. J.* **8,** 274 (2009).
35. Shekalaghe, S. A. *et al.* Submicroscopic *Plasmodium falciparum* gametocyte carriage is common in an area of low and seasonal transmission in Tanzania. *Trop. Med. Int. Heal.* **12,** 547–553 (2007).
36. Sousa-Figueiredo, J. C. *et al.* Investigating portable fluorescent microscopy (CyScope®) as an alternative rapid diagnostic test for malaria in children and women of child-bearing age. *Malar. J.* **9,** 245 (2010).
37. Wanji, S., Kimbi, H. K., Eyong, J. E., Tendongfor, N. & Ndamukong, J. L. Performance and usefulness of the Hexagon rapid diagnostic test in children with asymptomatic malaria living in the Mount Cameroon region. *Malar. J.* **7,** 89 (2008).
38. Ye, Y., Madise, N., Ndugwa, R., Ochola, S. & Snow, R. W. Fever treatment in the absence of malaria transmission in an urban informal settlement in Nairobi, Kenya. *Malar. J.* **8,** 160 (2009).
39. Dal-Bianco, M. P. *et al.* High prevalence of asymptomatic *Plasmodium falciparum* infection in Gabonese adults. *Am. J. Trop. Med. Hyg.* **77,** 939–942 (2007).
40. Fancony, C., Sebastiao, Y., Pires, J., Gamboa, D. & Nery, S. Performance of microscopy and RDTs in the context of a malaria prevalence survey in Angola: a comparison using PCR as the gold standard. *Malar. J.* **12,** 284 (2013).
41. Ouattara, A. *et al. Plasmodium falciparum* infection and clinical indicators in relation to net coverage in central Cote d'Ivoire. *Parasites Vectors* **7,** 306 (2014).
42. Faucher, J.-F. *et al.* What would PCR assessment change in the management of fevers in a malaria endemic area? A school-based study in Benin in children with and without fever. *Malar. J.* **9,** 224 (2010).
43. ICF International, C. M. *Demographic and Health Surveys* (ICF, 2012).
44. Yeka, A. *et al.* Factors associated with malaria parasitemia, anemia and serological responses in a spectrum of epidemiological settings in Uganda. *PLoS ONE* **10,** e0118901 (2015).
45. Mwingira, F., Genton, B., Kabanywanyi, A.-N. M. & Felger, I. Comparison of detection methods to estimate asexual *Plasmodium falciparum* parasite prevalence and gametocyte carriage in a community survey in Tanzania. *Malar. J.* **13,** (2014).
46. Harris, I. *et al.* A large proportion of asymptomatic *Plasmodium* infections with low and sub-microscopic parasite densities in the low transmission setting of Temotu Province, Solomon Islands: challenges for malaria diagnostics in an elimination setting. *Malar. J.* **9,** 254 (2010).
47. Mharakurwa, S. *et al.* Pre-amplification methods for tracking low-grade *Plasmodium falciparum* populations during scaled-up interventions in Southern Zambia. *Malar. J.* **13,** 89 (2014).
48. Tram, T. M. *et al.* An intensive longitudinal cohort study of Malian children and adults reveals no evidence of acquired immunity to *Plasmodium falciparum* infection. *Clin. Infect. Dis.* **57,** 40–47 (2013)
49. Proietti, C. *et al.* Influence of infection on malaria-specific antibody dynamics in a cohort exposed to intense malaria transmission in northern Uganda. *Parasite Immunol.* **35,** 164–173 (2013).
50. Stevenson, J. C. *et al.* Reliability of school surveys in estimating geographic variation in malaria transmission in the Western Kenyan Highlands. *PLoS ONE* **8,** e77641 (2013).
51. Aydin-Schmidt, B. *et al.* Loop mediated isothermal amplification (LAMP) accurately detects malaria DNA from filter paper blood samples of low density parasitaemias. *PLoS One* **9,** e103905 (2014).
52. Brown, T. *et al.* Molecular surveillance for drug-resistant *Plasmodium falciparum* in clinical and subclinical populations from three border regions of Burma/Myanmar: cross-sectional data and a systematic review of resistance studies. *Malar. J.* **11,** 333 (2012).
53. (2008) J. *et al.* Loop-mediated isothermal amplification (LAMP) for point-of-care detection of asymptomatic low-density malaria parasite carriers in Zanzibar. *Malar. J.* **14,** 43 (2015).
54. Stauffer, W. M. *et al.* Evaluation of malaria screening in newly arrived refugees to the United States by microscopy and rapid antigen capture enzyme assay. *Pediatr. Infect. Dis. J.* **25,** 948–950 (2006).
55. Stresman, G. H. *et al.* A method of active case detection to target reservoirs of asymptomatic malaria and gametocyte carriers in a rural area in Southern Province, Zambia. *Malar. J.* **9,** 265 (2010).
56. Sharp, S. J. & Thompson, S. G. Analysing the relationship between treatment effect and underlying risk in meta-analysis: comparison and development of approaches. *Stat. Med.* **19,** 3251–3274 (2000).
57. Hay, S. I., Smith, D. L. & Snow, R. W. Measuring malaria endemicity from intense to interrupted transmission. *Lancet. Infect. Dis.* **8,** 369–378 (2008).
58. World Health Organization. *From Malaria Control to Malaria Elimination. A Manual for Elimination Scenario Planning* (WHO, 2014).
59. Snounou, G. *et al.* High sensitivity of detection of human malaria parasites by the use of nested polymerase chain reaction. *Mol. Biochem. Parasitol.* **61,** 315–320 (1993).
60. Abeku, T. A. *et al.* Determinants of the accuracy of rapid diagnostic tests in malaria case management: evidence from low and moderate transmission settings in the East African highlands. *Malar. J.* **7,** (2008).
61. World Health Organisation. *Parasitological Confirmation of Malaria Diagnosis. Report of a WHO Technical Consultation* (WHO, 2010).
62. Ofosu-Okyere, A. *et al.* Novel *Plasmodium falciparum* clones and rising clone multiplicities are associated with the increase in malaria morbidity in Ghanaian children during the transition into the high transmission season. *Parasitology* **123,** 113–23 (2001).
63. Pollitt, L. C. *et al.* Competition and the evolution of reproductive restraint in malaria parasites. *Am. Nat.* **177,** 358–67 (2011).
64. Kyabayinze, D. J., Tibenderana, J. K., Odong, G. W., Rwakimari, J. B. & Counihan, H. Operational accuracy and comparative persistent antigenicity of HRP2 rapid diagnostic tests for *Plasmodium falciparum* malaria in a hyperendemic region of Uganda. *Malar. J.* **7,** 221 (2008).
65. Swarthout, T. D., Counihan, H., Senga, R. K. & Broek, I. van den. Paracheck-Pf® accuracy and recently treated *Plasmodium falciparum* infections: is there a risk of over-diagnosis? *Malar. J.* **6,** 58 (2007).
66. Houzé, S., Boly, M. D., Bras, J. Le, Deloron, P. & Faucher, J.-F. PfHRP2 and PfLDH antigen detection for monitoring the efficacy of artemisinin-based combination therapy (ACT) in the treatment of uncomplicated falciparum malaria. *Malar. J.* **8,** 211 (2009).
67. Aydin-Schmidt, B. *et al.* Usefulness of *Plasmodium falciparum*-specific rapid diagnostic tests for assessment of parasite clearance and detection of recurrent infections after artemisinin-based combination therapy. *Malar. J.* **12,** 349 (2013).
68. Tusting, L. S., Bousema, T., Smith, D. L. & Drakeley, C. Measuring changes in *Plasmodium falciparum* transmission: precision, accuracy and costs of metrics. *Adv. Parasitol.* **84,** 151–208 (2014).
69. Slater, H. *et al.* Assessing the impact of next-generationrapid diagnostic testson *Plasmodium falciparum* malaria elimination strategies *Nature* **528,** S94–S101 (2015).
70. United Nations, Department of Economic & Social Affairs, Population Division. *World Population Prospects, the 2010 Revision* (UN, 2010).

SUPPLEMENTARY MATERIAL

Is linked to the online version of this paper at: http://dx.doi.org/10.1038/nature16039

ACKNOWLEDGEMENTS

We thank F. Mwingira and I. Felger (Tanzania), I. Harris and Q. Cheng (Solomon Islands), S. Portugal and P. Crompton (Mali), S. Mharakurwa and S. Volkman (Zambia), S. Staedke and G. Dorsey (Uganda), C. Proietti and T. Bousema (Uganda), J. Stevenson, G. Stresman and J. Cox (Kenya), H. Kafy, A. Bashir, E. Malik, A. Mnzava, K. Subramaniam, K. Elmardi, I. Kleinschmidt and M. Donnelly (Sudan), M. Al-Selwei, S. Al-Eryani, A. Mnzava, A. Al-Samei, K. Mustafa, H. Atta, H. Al-Yarie, G. Zamanai and C. Barwa (Yemen) for kindly sharing their data from prevalence surveys, and the Demographic and Health Survey Programme for providing survey data. We would also like to thank L. Grignard, N. Alexander and J. Cook for sharing their expertise on statistical and diagnostic methods. This study was funded by the Bill and Melinda Gates Foundation (BMGF) Diagnostics Modelling Consortium. P.W. and L.O. acknowledge funding from fellowships jointly funded by the UK Medical Research Council (MRC) and the UK Department for International Development (DFID) under the MRC/DFID Concordat Agreement. L.W. acknowledges doctoral training funding from the UK MRC. A.G. acknowledges support from the BMGF, the Medicines for Malaria Venture, the UK MRC and the UK DFID. C.D. is funded by the Wellcome Trust grant number 091924.

COMPETING FINANCIAL INTERESTS

The authors declare no competing financial interests. Financial support for this publication has been provided by the Bill & Melinda Gates Foundation.

ADDITIONAL INFORMATION

Chapter 4 Correlating estimates of malaria sero-prevalence with parasite prevalence

In Chapter 3, the relationship between parasitological measures of malaria infection - rapid diagnostic tests, microscopy, and polymerase chain reaction – was estimated based on cluster-level estimates of prevalence. This chapter aims to extend this cross-metric analysis to serological measures of malaria exposure, using a large dataset of paired cluster-level sero-conversion rates and parasite prevalence estimates.

4.1 Background

Accurate field-deployable diagnostic tools for the characterisation of malaria transmission will be the hallmark of any successful surveillance system in elimination settings. As introduced in Chapters 1 and 3, malaria transmission is typically measured as the prevalence of infection, also known as the parasite rate (PR), based on RDT or microscopy slide positivity, or the entomological inoculation rate (EIR).[80,231] However, as transmission declines and becomes more heterogeneous, classical surveillance tools often fail to fully detect the asymptomatic reservoir or capture fluctuations in population prevalence over time.[232–237] Even nucleic-acid amplification techniques (NAATs) such as quantitative PCR (qPCR), which are sensitive enough to detect low-density parasitaemia[86,238], are limited to measuring current infections at a single point in time.

In areas where transmission is temporally and spatially heterogeneous or where there is a potentially large reservoir of asymptomatic infections, reliance on intermittent cross-sectional surveys[239] or reactive case detection may be inadequate to fully characterise transmission risk.[240,241] On the other hand, large-scale routine monitoring with currently available technologies can be costly or logistically burdensome for most health systems. Mathematical models suggest that R_C, the basic reproduction number under malaria control measures, should be less than 0.5 to interrupt endemic transmission within a reasonable time frame.[242] Given these quantitative thresholds, sensitive laboratory assays or field-based point-of-care tests such as lateral flow assays (LFAs) are needed to define and stratify transmission at a finer-scale to guide operational strategies and track progress towards elimination.

Serology is a potentially more sensitive measure in elimination settings where PR and EIR are less robust.[243] With markers that can detect previously exposed (but not necessarily currently infected) individuals, cross-sectional serology data can be used to characterise exposure history over a longer window of time. Therefore, unlike cross-sectional PR data, it can be more easily used to estimate a force of infection and relate to R_C as a measure of transmission over a relevant time scale. As discussed in Chapter 1, the ability to standardise the use of *Pf* blood-stage antigens *Pf*AMA1 and *Pf*MSP1$_{19}$ (due to their long half-life, moderate levels of immunogenicity, and limited polymorphisms) has allowed the use of immunological assays as practical epidemiological tools. Antibody responses to these antigens are used as a proxy for malaria transmission intensity. More specifically, age-stratified sero-prevalence data are used to fit reverse catalytic models and estimate a population-level force of infection or seroconversion rate (SCR) - the rate at which seronegative individuals become seropositive after exposure to malaria parasites.[122]

Evidence suggests that serology could be a powerful addition to the existing repertoire of surveillance tools.[244] In its infancy, the epidemiological application of malaria serology was

limited to a handful of research studies. With the greater availability of serological data as well as standardised reagents and protocols, it is now possible to compare results across a broader range of settings and antigens.

This chapter aims to harmonise serological estimates of transmission (i.e., force of infection / SCR) through a pooled analysis of datasets with *Pf*MSP1$_{19}$ and *Pf*AMA1 sero-prevalence and parasite prevalence as measured by PCR, RDT or microscopy. It estimates a relationship between SCR and PR, and also compares this against previously measured relationships between PR, EIR and clinical incidence. For use in epidemiological studies, one goal is to determine where (or within which populations), sero-conversion rates are most consistent and aligned with other measures, potentially allowing the selection of sentinel populations where sampling could be more efficient and informative. It is also important to determine if serology can provide a more granular measure in settings where other endpoints are limited in their ability to discriminate between transmission intensities or simply impractical to measure operationally. Finally, it is important to identify settings where data are too sparse (e.g., limited coverage geographically, over time, or across transmission intensities) to understand the relative relationship between serology and other metrics. These may be particularly important where the population dynamics of human immunity are variable.

4.2 Methods

Data

Serology

Data from 102 clusters, representing 15 countries, were compiled from 32 different cross-sectional surveys that had paired measurements of antibody response and parasite rate for *P. falciparum*. Clusters (i.e., sample size and geographical radius) were defined according to study specific protocols, but are commonly done according to enumeration area. This varied according to study design, which included both cross-sectional surveys and efficacy trials. Studies were selected if they i) included concurrent estimates of antibody responses (*Pf*MSP1$_{19}$ and/or *Pf*AMA1) and parasite positivity detected by RDT, microscopy, or PCR and ii) both diagnostic endpoints were measured in the general community and not selected based on clinical symptoms, diagnostic test results, or patient sub-groups.

All surveys were all-age cross-sectional samples, with the exception of three studies: Sudan 2012 clusters were study arms in an intervention trial evaluating the effectiveness of LLINs and IRS; Yemen 2012 clusters included only individuals under the age of 15 years; and Tanzania 2007 clusters were surveys conducted after the implementation of intermittent preventive treatment

infants (IPTi), where participants were recruited based on attendance at district health facilities for any reason including accompanying a patient (Appendix 4.1).

For all studies, antibody response was quantified using enzyme linked immunosorbent assays (ELISA). Final antibody response was measured either as an optical density (OD) or converted to arbitrary antibody titres using a standard curve. Sero-positivity was determined using study- and antigen-specific thresholds. That is, for each study, the distribution of antibody titre values (or normalised optical (OD) values if titre values were not available) was fitted to a two-component Gaussian mixture model using maximum likelihood methods.[245] For each antigen in the study, the sero-positivity threshold was defined as the mean titre (or OD) value of the seronegative population plus 2 (or up to 5) standard deviations, where the number of standard deviations used varied between studies. For the purposes of this pooled analysis, sero-positivity values previously assigned by the original study were used and not re-calculated here.

Data were limited to study clusters with a sample size greater than 100 and where sero-prevalence was greater than zero. Study clusters from Cambodia 2004 and 2007 Malaria Indicator Surveys (MIS), where the majority were less than 100 individuals, were aggregated based on risk zones (based on expert opinion, but approximately defined as proximity to forest areas). A schematic and table of the studies included in the pooled analysis are summarised in Figure 4.1 and Appendix 4.1.

Figure 4.1 Study sites included in serology meta-analysis by country, survey year, sample size, and antigen

Study clusters measuring $MSP1_{19}$ (green) and AMA1 (blue) shown as points along a horizontal axis indicating survey year. Point diameters vary based on cluster size (<500, 500-1000, 1000-2000, >2000) and are jittered so overlapping points are easily viewed.

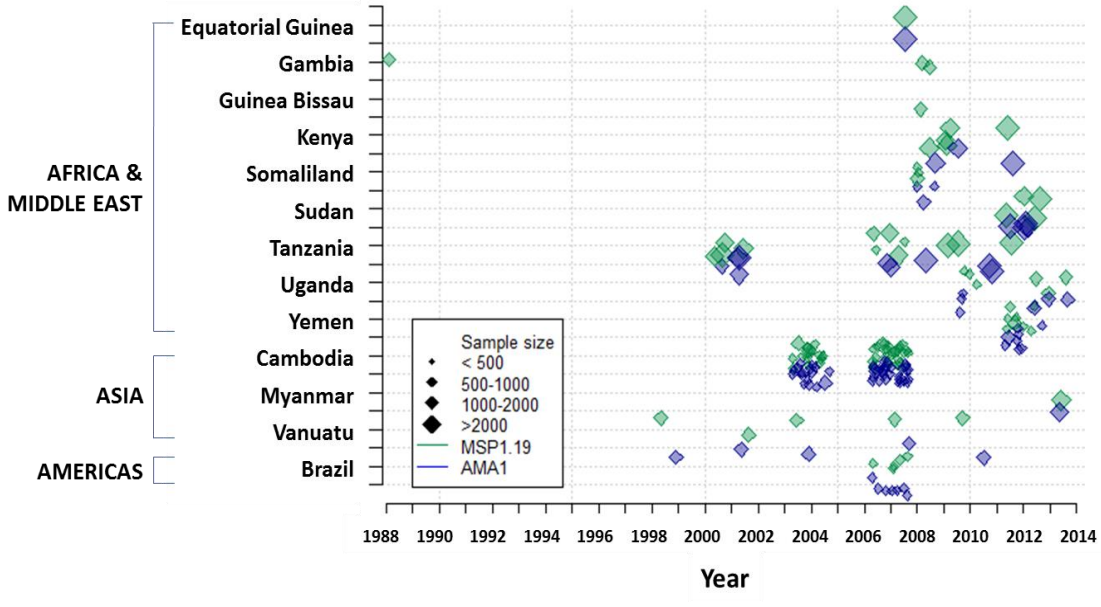

Clinical incidence and entomological inoculation rate

To benchmark the use of serology with other measures of transmission, datasets were compiled from previous studies modelling parasite rate with clinical incidence and EIR.

Studies with concurrent estimates of EIR and PR were taken from Smith et al[246], where the best fit relationship between the two measures is described by $PR = 1 - (1 + 1.89 * EIR)^{4.2}$. However, the credible intervals of the model are not published, and therefore, results presented here only show the empirical point estimates from the study and not their fitted relationship. A total of 127 study clusters were included, covering 15 countries. All studies were from countries in sub-Saharan Africa and in children under 15 years of age.

Concurrent estimates of parasite rate and clinical incidence were taken from Battle et al 2015,[247] excluding studies where empirical estimates of PR were not available or where the PR data were not age matched to clinical incidence data. Modelled or age-adjusted data were excluded as this study aims to analyse the granularity of data that can be collected operationally through routine surveys as a comparison against similarly collected data for serology rather than inferred estimates. After these exclusions, 693 study clusters were included in the analysis of clinical incidence and EIR, covering 30 countries globally with a variety of age ranges across studies. Estimates of the relationship between clinical incidence and PR are inclusive of modelled and age-standardised data and are therefore not included here for analysis.

Statistical analyses

Sero-catalytic models – estimating force of infection from sero-prevalence as a measure of cluster level transmission

We estimated a force of infection (SCR) in each cluster by fitting reverse catalytic models to age-adjusted sero-prevalence data. Infants under 1 year of age were excluded to avoid the influence of maternally derived antibodies. We fit variations of the reverse catalytic model, which has been described in the context of malaria by Corran et al[121], Drakeley et al[248], and Sepulveda et al[122]. Data are first fit assuming no change in malaria transmission over time and no difference in exposure by age. Where cluster sizes and expected value of seroconversion rate ($\boldsymbol{\lambda}$) are too small to accurately estimate sero-reversion rate ($\boldsymbol{\rho}$) (based on sample size estimates previously published by Sepulveda et al),[249] region-specific $\boldsymbol{\rho}$ is used (see regions below). Out of a total of 102 clusters, 55 clusters did not have adequate sample size to estimate a cluster-specific $\boldsymbol{\rho}$ for *Pf*MSP1$_{19}$ and 63 did not have adequate sample size for *Pf*AMA1 (Appendix 4.1). Therefore, a region-specific $\boldsymbol{\rho}$ was used to fit the model for these clusters.

Models that allow for changes in transmission over time or by age were also tested, and the seroconversion rate from the best fit model (based on likelihood ratio tests) is used as the SCR data point included for the final analysis the SCR:PR relationship. It should be noted that it is not possible to determine from the model alone whether changes in sero-conversion rate occur due to the effect of time, age, or both. In settings where differences in transmission are likely due to temporal changes (e.g., following intervention campaigns in most sub-Saharan African countries), the $\boldsymbol{\lambda}$ experienced by children is assumed to reflect the most recent transmission level. In settings where differences in seroconversion rates are hypothesised to be due to behaviour (e.g., adult forest workers in South East Asia and the Americas), the $\boldsymbol{\lambda}$ describing the transmission intensity experienced by the highest-risk population is used in the SCR:PR model fit. For this dataset, this was relevant for any clusters exhibiting a change in SCR in Cambodia (6 clusters for *Pf*MSP1$_{19}$ and 15 clusters for *Pf*AMA1), Myanmar (1 cluster for both *Pf*MSP1$_{19}$ and *Pf*AMA1), and Brazil (1 cluster for both *Pf*MSP1$_{19}$ and *Pf*AMA1) (Appendix 4.1). Similarly, where cluster size is too small to accurately estimate a change in transmission (based on previous analysis by Sepulveda et al[249]), a model with no change in $\boldsymbol{\lambda}$ is used. Out of a total of 102 clusters, 13 had sample sizes adequate to estimate a change in *Pf*MSP1$_{19}$ SCR and 18 for *Pf*AMA1 (Appendix 4.1).

- Reverse Catalytic Model 1: Constant sero-conversion rate $(\boldsymbol{\lambda})$, cluster specific sero-reversion rate $(\boldsymbol{\rho})$

$$p_{S+}(t) = \frac{\lambda}{\lambda+\rho_c}\left(1 - e^{-(\lambda+\rho_c)t}\right) \quad (4.1)$$

Model 1 fits cluster specific sero-reversion and constant sero-conversion rates, where $p_{S+}(t)$ represents the probability of an individual being seropositive at age t, and ρ_c represents the cluster-specific sero-reversion rate.

- Reverse Catalytic Model 2: Constant sero-conversion rate $(\boldsymbol{\lambda})$, region-specific sero-reversion rate $(\boldsymbol{\rho})$

$$p_{S+}(t) = \frac{\lambda}{\lambda+\rho_r}\left(1 - e^{-(\lambda+\rho_r)t}\right) \quad (4.2)$$

Model 2 uses a fixed sero-reversion rate, which is calculated for each geographical region (Africa & Middle East, Asia, and the Americas), where $p_{S+}(t)$ is the probability of an individual being seropositive at age *t* (same as equation 4.1), and ρ_r represents the region specific sero-reversion rate. The regional sero-reversion rate is estimated by running Model 1, but treating all clusters within a geographical region as a single cluster. The rationale behind using a regional ρ_r is that sero-reversion rate (or the rate of antibody decay) is usually governed by population genetics in a broad geographical region and is unlikely to have micro-epidemiological variations at the cluster level.

- Reverse Catalytic Model 3: Change in $\boldsymbol{\lambda}$

$$p_{S+}(t) = \begin{cases} \frac{\lambda_2}{\lambda_2+\rho}\left(1 - e^{-(\lambda_2+\rho)\,t}\right) & : t \leq \tau \\ \frac{\lambda_2}{\lambda_2+\rho}\left(1 - e^{-(\lambda_2+\rho)\,\tau}\right) + \frac{\lambda_1}{\lambda_1+\rho}\left(1 - e^{-(\lambda_1+\rho)\,(t-\tau)}\right) e^{-(\lambda_2+\rho)\,\tau} & : t > \tau \end{cases} \quad (4.3)$$

Model 3, previously described by Sepulveda et al[122], allows for a change in transmission intensity from $\boldsymbol{\lambda_1}$ to $\boldsymbol{\lambda_2}$ at time or age $\boldsymbol{\tau}$. Individuals born after the change in transmission ($\boldsymbol{t \leq \tau}$), will have a probability of being sero-positive under conditions with constant transmission (Models 1 and 2) subject to the most recent seroconversion rate $\boldsymbol{\lambda_2}$. Individuals born before the change in transmission ($\boldsymbol{t > \tau}$) will have a probability of being sero-positive that is a function of both sero-conversion rates. The $\boldsymbol{\rho}$ value included in Model 3 is a fixed value chosen from either Model 1 or Model 2 (based on the model with the highest log likelihood).

Association between seroconversion rate and parasite rate (SCR:PR Model)

Once seroconversion rates are estimated for all clusters, a comparison against other measures of transmission is feasible. To analyse the association between seroconversion rate (λ) and parasite rate (PR), a linear relationship was fitted between the log of seroconversion rate and the log odds of parasite prevalence.

- SCR:PR model unadjusted

$$\theta_{Si} = \alpha_0 + \alpha_1(\theta_{Pi} - \bar{\theta}_P) \quad (4.4)$$

$$\lambda_i \sim \mathcal{N}(e^{\theta_{Si}}, \sigma_i^2) \quad (4.5)$$

θ_{Si} is the log of the seroconversion rate (λ_i) measured in cluster *i*, θ_{Pi} is the log odds of the PCR prevalence in cluster *i*, and $\bar{\theta}_P$ is the mean log odds of PCR prevalence across all clusters. α_0 represents the expected log seroconversion rate when log odds of the PCR prevalence in cluster *i* is equal to the mean across all clusters, and α_1 is the regression coefficient. The model accounts for the influence of sample size and sampling variation across surveys in a few ways. For parasite rate, prevalence (on a scale of 0 to 1) is assumed to be beta distributed (which allows for propensity of infection to change according to variables such as age), and the probability of an individual being parasite-positive is assumed to be binomially distributed based on the number of individuals that were parasite positive out of those tested in each cluster and defined as $\frac{e^{(\log odds)}}{1+e^{\log odds}}$ and log odds = $\log_e(\frac{prevalence}{1-prevalence})$. All clusters observed at least one parasite positive individual by either PCR, RDT, or microscopy, and therefore all could be fit into a logistic model without continuity correction or other methods to adjust for PR values of zero. For SCR, log seroconversion rate is assumed to be normally distributed about a mean of $e^{\theta_{Si}}$ and variance σ_i^2, where σ_i^2 is the cluster-specific variance of the SCR fitted with the reverse catalytic model for

cluster *i*. The models were fitted using Bayesian Markov Chain Monte Carlo methods in JAGS version 3.4.0.

To ensure that the model fit across PR and SCR ranges was not dominated by clusters in a particular transmission setting, separate relationships were fit to clusters with PCR prevalence <20% and >20%. We could not further stratify in the lower transmission settings because the large number of clusters with a parasite prevalence of zero does not allow the model to be fit accurately at this prevalence range.

When measuring PR, sentinel populations such as school-aged children are often used as a convenience sample when all-age surveys are logistically challenging. Therefore, the SCR:PR model was also fit using PR based on different age cohorts: 2-10 year olds and 5-15 year olds. This used only data from Africa given that the at-risk populations in Asia and the Americas are typically adults rather than children[250–253].

To account for geographical variation in population level immune responses, the model was also fit including a covariate for each region (Americas, Africa & Middle East, Asia).

- SCR:PR model by geographical region

$$\theta_{Si} = \alpha_0 + \alpha_1(\theta_{Pi} - \bar{\theta}_P) + \beta_1 + \beta_2 + \beta_3 \quad (4.6)$$

$$\lambda_i \sim \mathcal{N}(e^{\theta_{Si}}, \sigma_i^2) \quad (4.7)$$

β_1, β_2 and β_3 are dummy variables (0/1) for the effects of clusters being located in either Africa & Middle East, Asia, or the Americas respectively. To assess the significance of each region as a covariate, the 95% credible intervals of the β parameters were assessed, with values that did not include zero deemed significant. It should be noted this is not entirely comprehensive as the β specific estimates do not reflect posterior distribution of the entire model fit. A comparison of the 95% credible intervals of the model with and without regional covariates was not done, but can potentially be explored in future adjustments to the analysis. This model by region was also fit separately for different PCR prevalence ranges, as described above.

Data transformations and model validation

Serology is expected to detect differences in transmission at PR ranges below the detectability of RDT and microscopy. Therefore, the model is fit using a prevalence scale based on PCR-measured PR. Studies with PR measured by RDT or microscopy, but no PCR data, were transformed to units on the PCR prevalence scale using previously modelled relationships between RDT and PCR from Wu & van den Hoogen (Chapter 3) and microscopy and PCR from Okell et al[234]. This allows all studies to be combined in a single dataset and fit on the same parasite rate scale. Data used for

paired clinical incidence and PR clusters from Battle et al is comprised primarily of PR measured by microscopy or RDT. Therefore, data from these studies were also transformed to the PCR PR scale as described above. However, information on the specific diagnostic used to measure PR was not reported in the Smith et al study, therefore this adjustment could not be made and PR values are assumed to be based on PCR to avoid extra data transformations.

The ability to accurately predict PR based on the modelled SCR:PR relationships and to evaluate whether any level of data over-influenced the fit of the model, leave-one-out analysis was conducted at the study, country, and cluster level.

4.3 Results

Global estimates of parasite rate and sero-conversion rates by geographical region and country

Sero-conversion rates varied across geographical regions, countries and study clusters (Figure 4.2). Data from the Americas and Asia were sparse, comprising clusters from only one country in the Americas (Brazil) and three countries in Asia (Cambodia, Myanmar, Vanuatu). In Asia, the large majority of clusters were from two Malaria Indicator Surveys (MIS) in Cambodia, so may not be representative of the South East Asian region generally. All clusters in the Asian region had a parasite rate below 40% and all clusters in Brazil were below 20%. Therefore, it was not possible to evaluate a PCR prevalence specific model fit at the higher transmission range for these regions. Clusters in Africa had a more dynamic range of parasite rate values, allowing evaluation of the model fit at PCR prevalence ranging from zero to 75%.

A much larger range of SCRs based on *Pf*AMA1 was observed, with a mean SCR of 0.076 (SD=0.112), compared with *Pf*MSP1$_{19}$ where mean SCR was 0.033 (SD=0.032), due to the stronger immunogenicity of *Pf*AMA1. In Africa and the Middle East, mean SCR for *Pf*MSP1$_{19}$ was 0.047 (SD=0.034), compared to mean SCR of 0.104 for *Pf*AMA1 (SD=0.103). In Asia, mean SCR for *Pf*MSP1$_{19}$ was 0.022 (SD=0.026) and 0.066 (SD=0.120) for *Pf*AMA1. In the Americas, which only included data from Brazil, the mean SCR for *Pf*MSP1$_{19}$ was 0.019 (SD=0.022) and 0.005 (SD=0.005) for *Pf*AMA1.

The range of SCRs observed at the country level indicate areas with consistently low transmission (e.g., Somaliland, Sudan, Vanuatu, Brazil) and others with greater heterogeneity in transmission (e.g., Uganda, Tanzania, Kenya, Yemen, Cambodia). However, datasets in the pooled analysis include surveys conducted in different years with a variety of sampling strategies, in select geographical regions, or before and after roll-out of malaria control programmes. Therefore, they may not be representative of overall country level transmission or the current levels of transmission. The precision of the seroconversion rate estimate varied by cluster as it is

dependent on sample size and age distribution.[249] For all clusters, model fits using the reverse catalytic model to calculate the final seroconversion rate used to estimate the SCR:PR relationship can be found in Appendix 4.2.

Figure 4.2 Seroconversion rate (SCR) estimates by region and study cluster

Listed alphabetically by country, survey/study, and sero-conversion rate in ascending order.

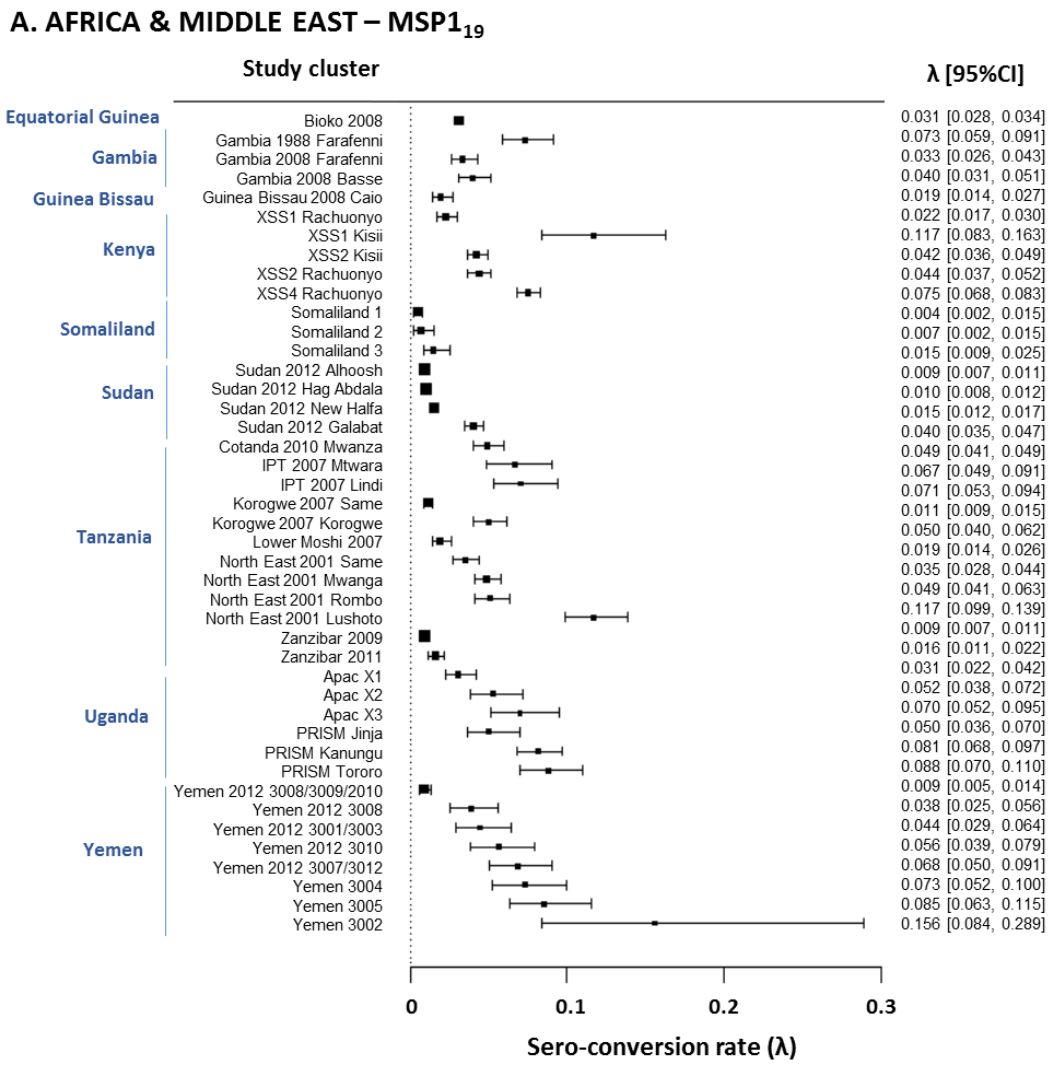

B. AFRICA & MIDDLE EAST – AMA1

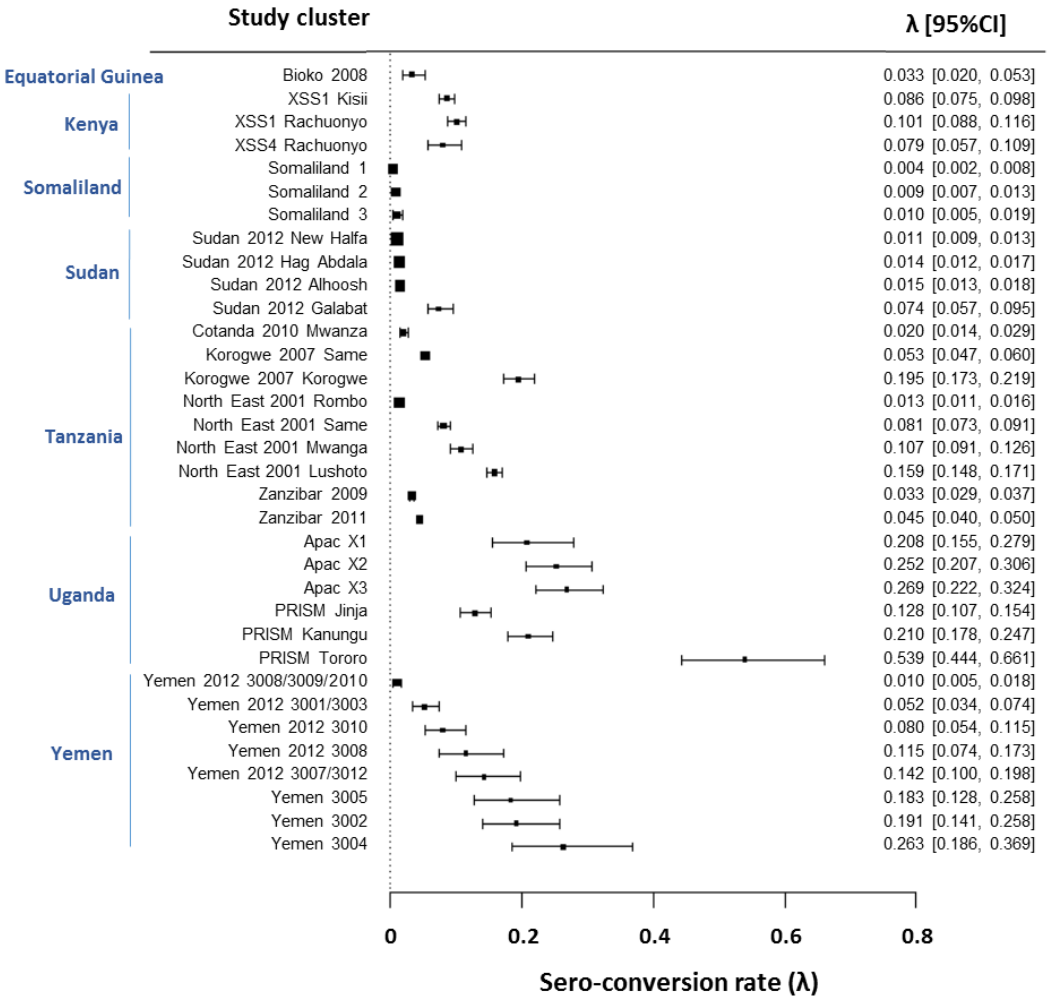

C. ASIA - $MSP1_{19}$

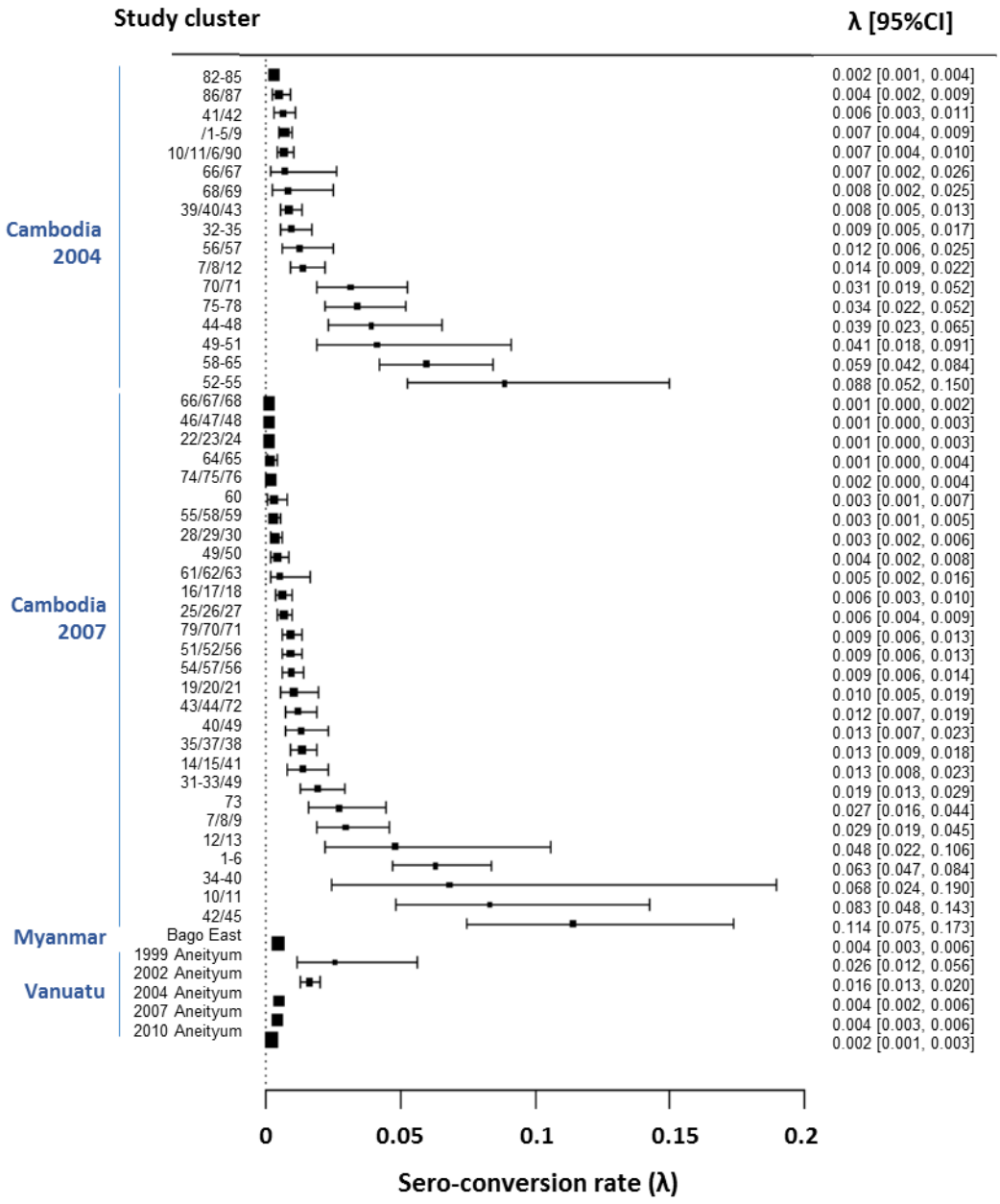

D. ASIA - AMA1

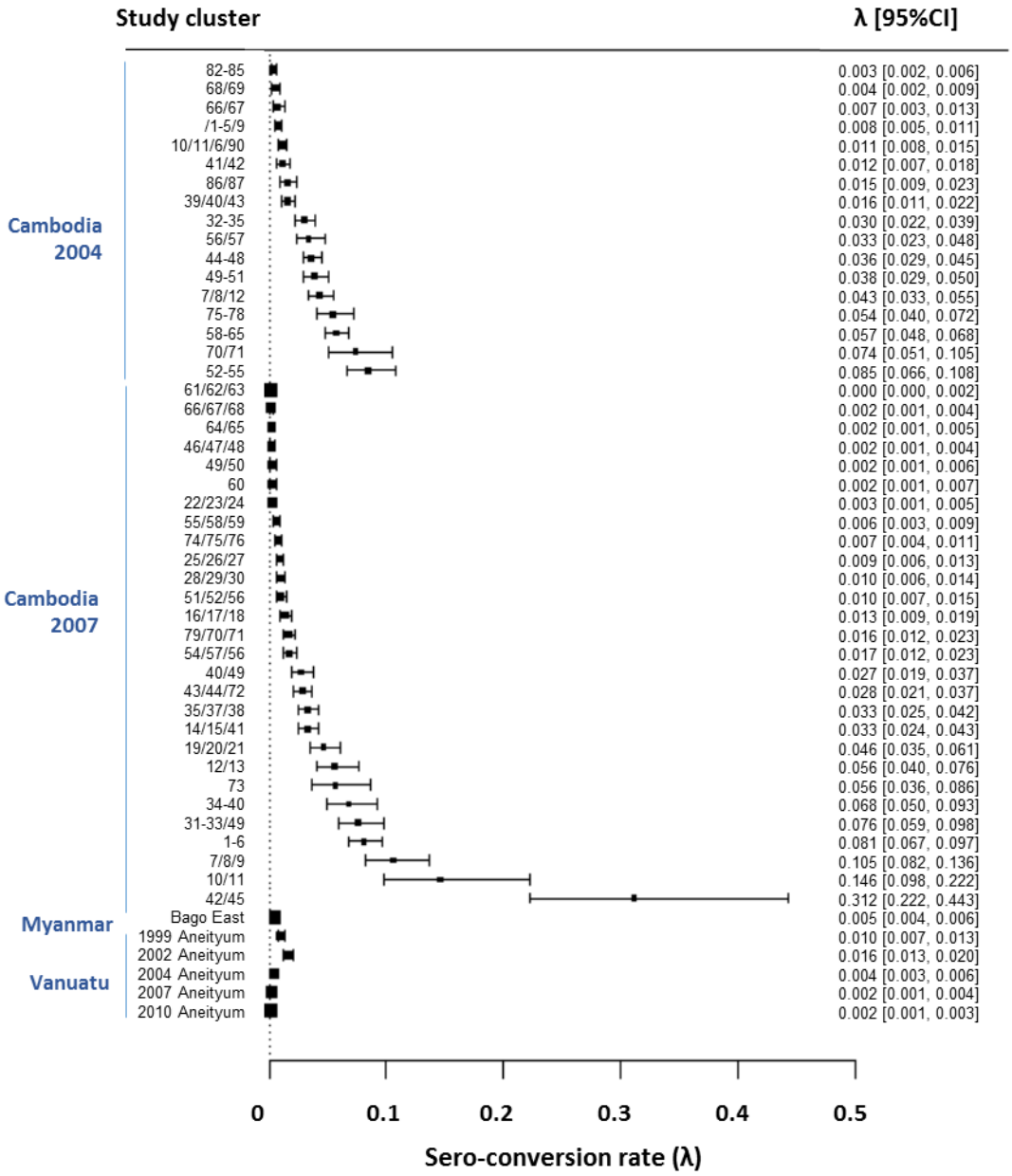
Study cluster
λ [95%CI]
Cambodia 2004
82-85 0.003 [0.002, 0.006]
68/69 0.004 [0.002, 0.009]
66/67 0.007 [0.003, 0.013]
/1-5/9 0.008 [0.005, 0.011]
10/11/6/90 0.011 [0.008, 0.015]
41/42 0.012 [0.007, 0.018]
86/87 0.015 [0.009, 0.023]
39/40/43 0.016 [0.011, 0.022]
32-35 0.030 [0.022, 0.039]
56/57 0.033 [0.023, 0.048]
44-48 0.036 [0.029, 0.045]
49-51 0.038 [0.029, 0.050]
7/8/12 0.043 [0.033, 0.055]
75-78 0.054 [0.040, 0.072]
58-65 0.057 [0.048, 0.068]
70/71 0.074 [0.051, 0.105]
52-55 0.085 [0.066, 0.108]
Cambodia 2007
61/62/63 0.000 [0.000, 0.002]
66/67/68 0.002 [0.001, 0.004]
64/65 0.002 [0.001, 0.005]
46/47/48 0.002 [0.001, 0.004]
49/50 0.002 [0.001, 0.006]
60 0.002 [0.001, 0.007]
22/23/24 0.003 [0.001, 0.005]
55/58/59 0.006 [0.003, 0.009]
74/75/76 0.007 [0.004, 0.011]
25/26/27 0.009 [0.006, 0.013]
28/29/30 0.010 [0.006, 0.014]
51/52/56 0.010 [0.007, 0.015]
16/17/18 0.013 [0.009, 0.019]
79/70/71 0.016 [0.012, 0.023]
54/57/56 0.017 [0.012, 0.023]
40/49 0.027 [0.019, 0.037]
43/44/72 0.028 [0.021, 0.037]
35/37/38 0.033 [0.025, 0.042]
14/15/41 0.033 [0.024, 0.043]
19/20/21 0.046 [0.035, 0.061]
12/13 0.056 [0.040, 0.076]
73 0.056 [0.036, 0.086]
34-40 0.068 [0.050, 0.093]
31-33/49 0.076 [0.059, 0.098]
1-6 0.081 [0.067, 0.097]
7/8/9 0.105 [0.082, 0.136]
10/11 0.146 [0.098, 0.222]
42/45 0.312 [0.222, 0.443]
Myanmar
Bago East 0.005 [0.004, 0.006]
Vanuatu
1999 Aneityum 0.010 [0.007, 0.013]
2002 Aneityum 0.016 [0.013, 0.020]
2004 Aneityum 0.004 [0.003, 0.006]
2007 Aneityum 0.002 [0.001, 0.004]
2010 Aneityum 0.002 [0.001, 0.003]
0
0.1
0.2
0.3
0.4
0.5
Sero-conversion rate (λ)

E. AMERICAS - $MSP1_{19}$

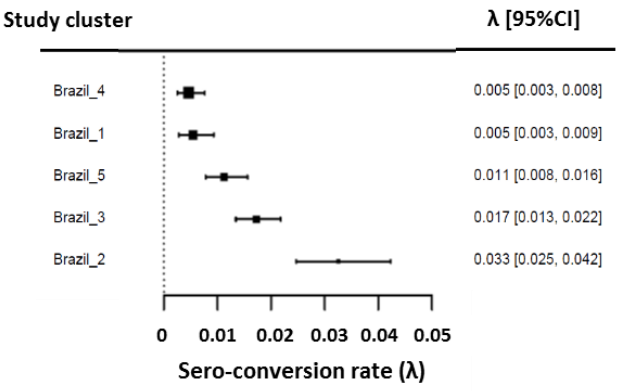

F. AMERICAS - AMA1

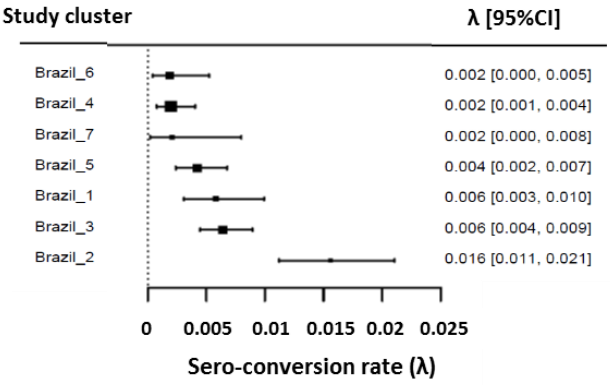

Relationship between seroconversion rate and parasite rate

Overall, SCR was observed to be positively associated with PR for both *Pf*MSP1$_{19}$ and *Pf*AMA1, based on estimates for α_1 (Figure 4.3, Table 4.1). For *Pf*MSP1$_{19}$, statistical evidence for a positive correlation between SCR and PR was weaker at PCR prevalence ranges below 20%, based on the 95% credible intervals of the posterior distributions for α_1 (Appendix 4.3). However, this is likely due to the fact the model is less precise when the model is fit separately for these prevalence ranges. The model was also less precise for *Pf*AMA1 when splitting the dataset by prevalence. This may reflect the large number of clusters with PCR prevalence of zero, but where a large range of SCR values is still measurable.

Overall, SCRs based on *Pf*AMA1 were higher for equivalent PR values than SCRs based on *Pf*MSP1$_{19}$, reflecting the greater immunogenicity of *Pf*AMA1. *Pf*AMA1 SCR also increases at a greater rate as PCR prevalence increases (α_1=0.28 for *Pf*MSP1$_{19}$, α_1=0.71 for *Pf*AMA1), indicating a non-linear increase in population immune response as transmission increases.

Fitting the model separately by PCR prevalence had an influence on the α_1 estimates (Table 4.1, Appendix 4.3). For clusters below 20% PCR prevalence, *Pf*MSP1$_{19}$ SCR values increase at a slower rate with respect to PR [α_1= 0.09 (95%CI -0.02,0.25), Appendix 4.3] compared to clusters with >20% PCR prevalence [α_1 = 0.28 (95%CI 0.13, 0.41)], but 95% credible intervals do not suggest this difference is statistically strong (Figure 4.4a-b). For *Pf*AMA1, on the other hand, SCR values increase faster with respect to PR at PCR prevalence <20% [α_1 = 0.98 (95%CI 0.92, 1.00)] compared to clusters with >20% PCR prevalence [95%CI α_1 = 0.83 (95%CI 0.75, 0.92)] and statistical strength for this difference appears more robust (Figure 4.4c-d, Appendix 4.3). However, after adjusting for region, the difference between the PCR prevalence ranges for *Pf*AMA1 were less statistically different [α_1 = 0.71 (95%CI 0.57, 0.87) at PCR prevalence <20% vs. α_1 = 0.76 (95%CI 0.68, 0.88) at PCR prevalence >20%] (Table 4.1, Appendix 4.3), though this is driven primarily by clusters in Africa (Figure 4.6c-d).

In low transmission settings in Africa, clusters experienced higher than average *Pf*AMA1 SCRs compared to clusters in equivalent PCR prevalence ranges in Asia and the Americas (β_1 = 1.32 95%CI 0.27 – 1.97, Figure 4.6c-d, Appendix 4.3). Statistical evidence for a different relationship in other regions and transmission intensities for *Pf*AMA1 and across all regions and transmission intensities for MSP1$_{19}$ was weak (i.e., based on 95% credible intervals for β values) (Appendix 4.3, Figures 4.5 – 4.6). However, median estimates suggest that for both antigens, clusters in Africa experience higher SCRs, followed next by Asia, and the lowest SCRs observed in the Americas (Table 4.1).

Table 4.1 Best fit relationships between sero-conversion rate (SCR) and parasite rate (PR)

Listed by geographical region and PCR prevalence. Region-specific estimates are based on β values (Appendix 4.3) of models fit separately for clusters <20% vs >20% PCR prevalence.

	Prevalence band (PCR parasite rate)	
Antigen / Region	**< 20 %**	**> 20%**
***Pf*MSP1$_{19}$**		
Overall	log SCR = -2.66 + 0.28 * log odds PR	
Africa & Middle East	log SCR = -3.06 + 0.09 * log odds PR	log SCR = -2.66 + 0.28 * log odds PR
Asia	log SCR = -3.50 + 0.09 * log odds PR	log SCR = -2.18 + 0.28 * log odds PR
Americas †	log SCR = -4.27 + 0.09 * log odds PR	--
***Pf*AMA1**		
Overall	log SCR = -1.50 + 0.71 * log odds PR	
Africa & Middle East	log SCR = -0.18 + 0.71 * log odds PR	log SCR = -1.61 + 0.76 * log odds PR
Asia †	log SCR = -1.43 + 0.71 * log odds PR	--
Americas †	log SCR = -2.90 + 0.71 * log odds PR	--

† Limited study sites (≤ 2 clusters) with >20% PR, so SCR:PR relationship for <20% PR only shown

Figure 4.3 Sero-conversion rate vs. PCR parasite rate overall

Parasite rate measured by PCR, RDT and microscopy on a PCR-prevalence scale (red=empirical PCR prevalence, blue=PCR-prevalence derived from microscopy prevalence, yellow=PCR-prevalence derived from RDT prevalence). Model fit weighted by cluster size and inverse log variance of SCR (95%CI lambda) estimated in reverse catalytic model. Solid line is the best fit line and shaded area is 95% credible interval. Point diameters are relative to increasing cluster size and crosshairs represent 95% confidence intervals for parasite rate (horizontal) and SCR (vertical)

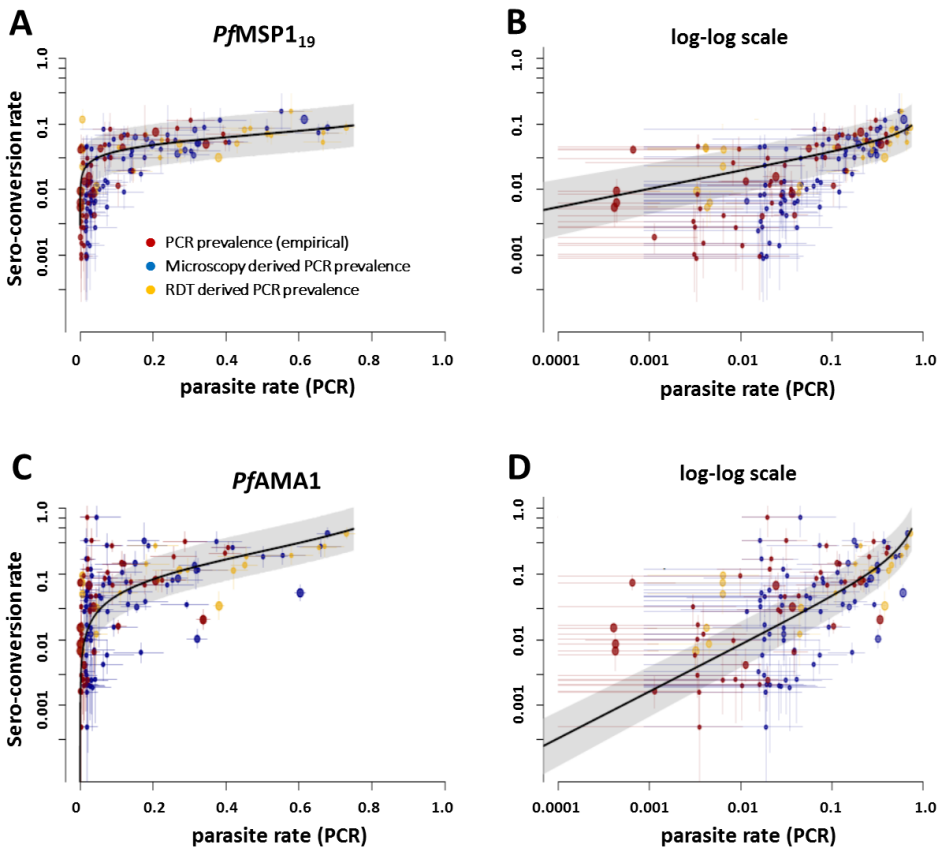

Figure 4.4 Sero-conversion rate vs. PCR parasite rate by PCR prevalence range (<20% and >20%)
Parasite rate measured by PCR, RDT and microscopy on a PCR-prevalence scale (red=empirical PCR prevalence, blue=PCR-prevalence derived from microscopy prevalence, yellow=PCR-prevalence derived from RDT prevalence). Model fit weighted by cluster size and inverse log variance of SCR (95%CI lambda) estimated in reverse catalytic model. Solid line is the best fit line and shaded area is 95% credible interval. Point diameters are relative to increasing cluster size and crosshairs represent 95% confidence intervals for parasite rate (horizontal) and SCR (vertical)

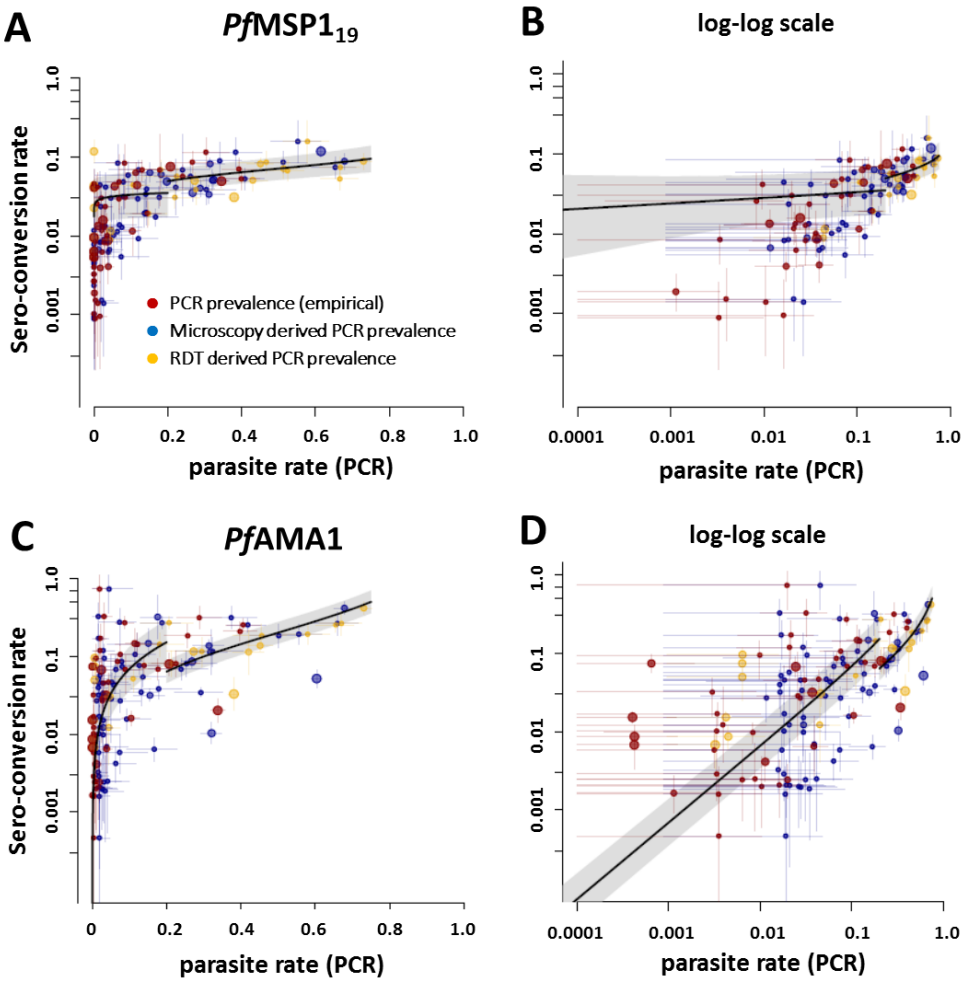

Figure 4.5 *Pf*MSP1$_{19}$ sero-conversion rate vs. parasite rate (PCR prevalence)

By geographical region (Americas - yellow, Africa & Middle East - blue, and Asia - red), and PCR prevalence (<20% and >20%). Solid line is the best fit line and shaded area is 95% credible interval. Point diameters are relative to increasing cluster size and crosshairs represent 95% confidence intervals for parasite rate (horizontal) and SCR (vertical)

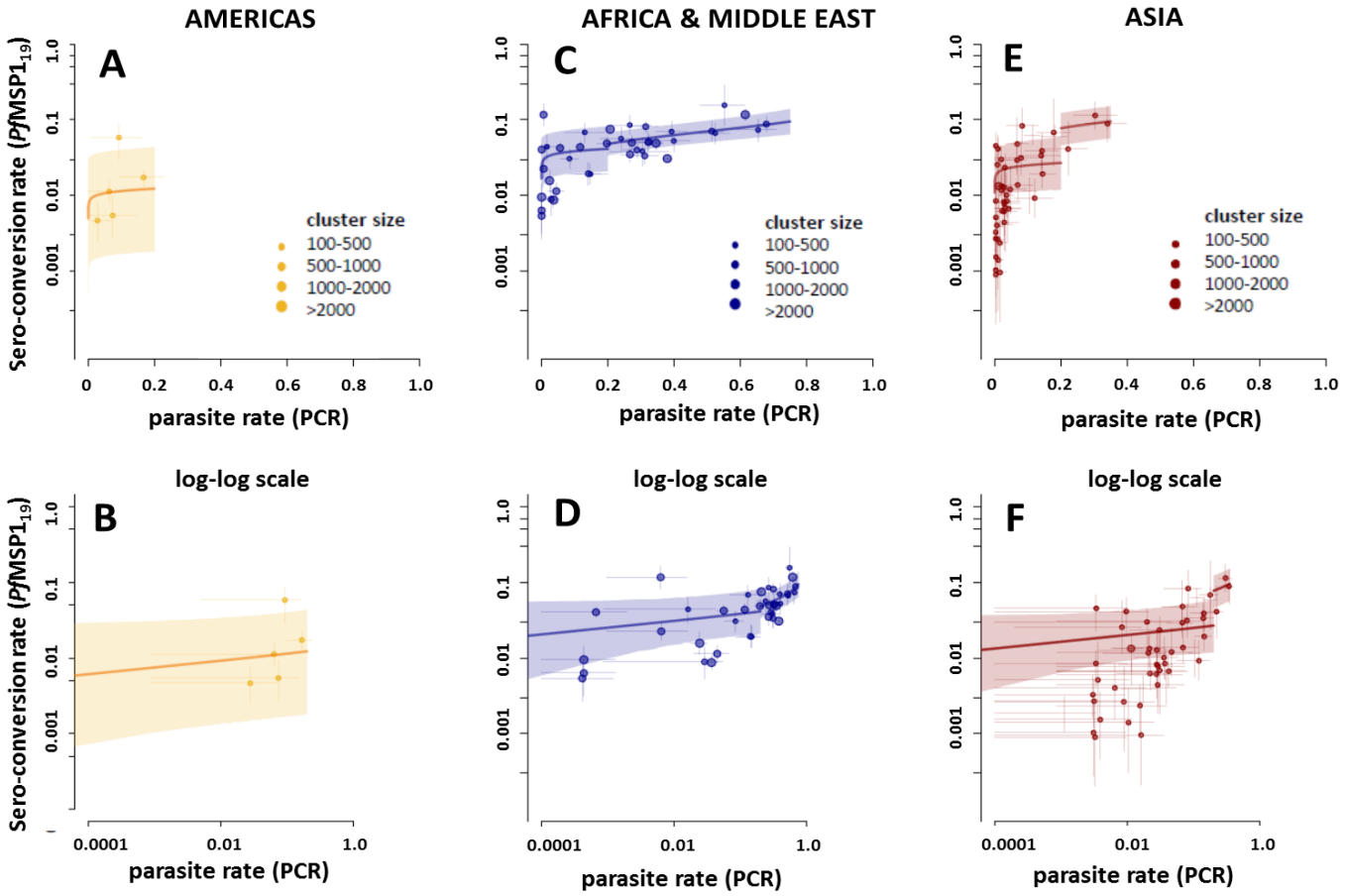

Figure 4.6 *Pf*AMA1 sero-conversion rate vs. parasite rate (PCR prevalence)

By geographical region (Americas - yellow, Africa & Middle East - blue, and Asia - red), and PCR prevalence (<20% and >20%). Solid line is the best fit line and shaded area is 95% credible interval. Point diameters are relative to increasing cluster size and crosshairs represent 95% confidence intervals for parasite rate (horizontal) and SCR (vertical)

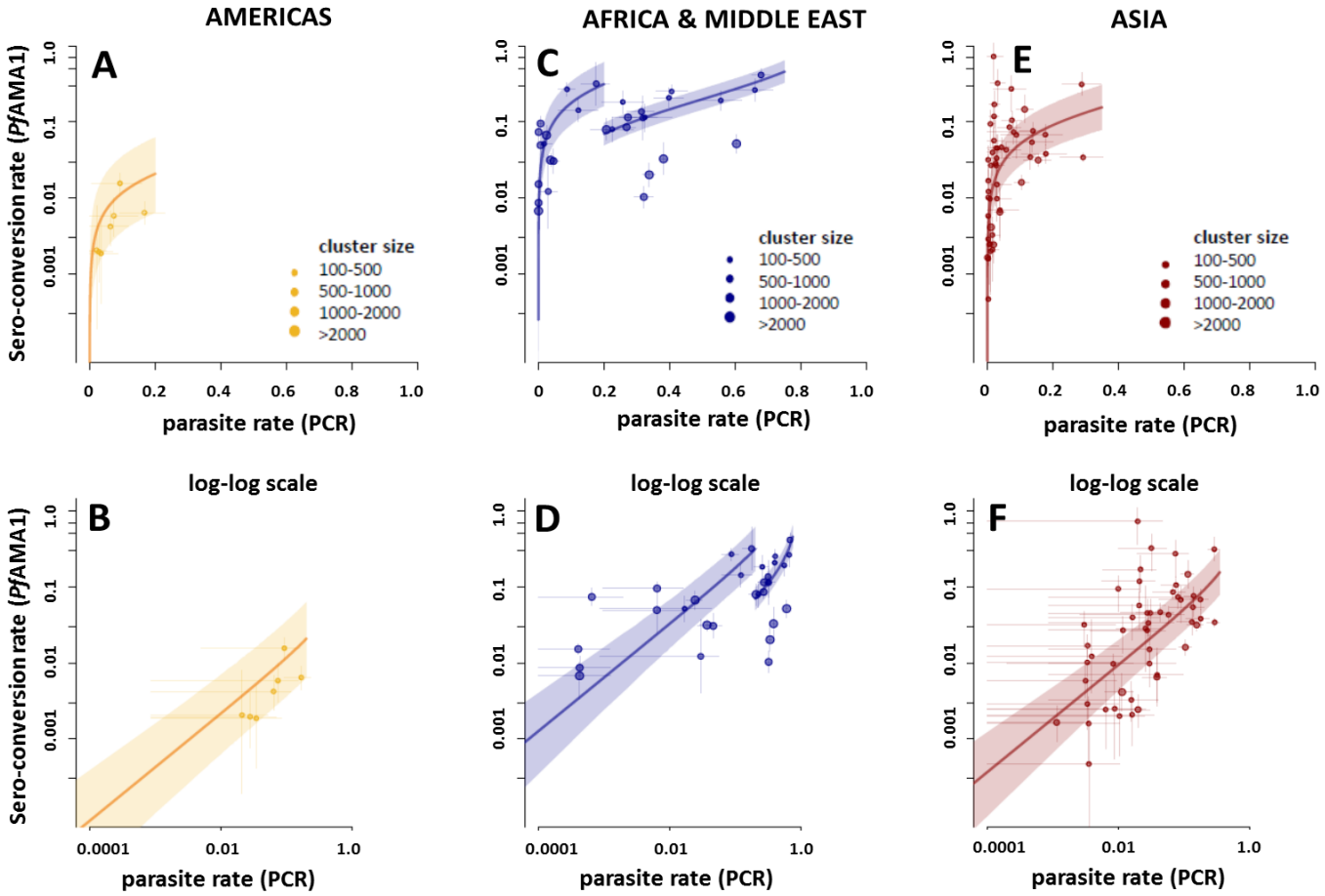

Comparisons against clinical incidence and entomological inoculation rate

A comparison of the SCR:PR relationship to previously explored relationships between EIR vs. PR and clinical incidence vs PR indicate that (Figure 4.7) data for EIR is most widely available at ranges of PCR prevalence above 20%, likely due to the large sample sizes required to measure EIR in low transmission settings. SCR values for both *Pf*MSP1$_{19}$ and *Pf*AMA1, on the other hand, show the most resolution below 10% PCR prevalence and begins to saturate at transmission levels above this.

This suggests that serology may be capable of discriminating fine-scale differences in transmission at levels where PCR prevalence is below 10% and in particular, where estimated PCR prevalence is close to zero (and RDT/microscopy is also likely to be zero), as seen by the wide range of SCR values along the y-axis. However, in the absence of a gold standard, it is not clear whether this range of SCR values at low PR prevalence reflects increased sensitivity of serological measures for current transmission or lack of specificity due to residual immune responses and a longer historical period of malaria transmission. The relationship between clinical incidence and PR is variable, with a large range of clinical incidence values at all levels of PR, suggesting relatively weaker precision of this metric compared to serology. However, it should be noted that these endpoints are not directly comparable due to the different biological endpoints they measure. Here, they are plotted together primarily to show their relative precision across transmission intensities.

Figure 4.7 Relationship of three measures of transmission (sero-conversion rate, clinical incidence, and entomological inoculation rate) with PCR parasite rate

Clinical incidence and SCR are reported as cases or seropositive individuals per 1000 person-years observed (PYO) compared to annual *Pf* EIR (a*PfEIR*) per 1000 PYO or (a*Pf*EIR x 1000)

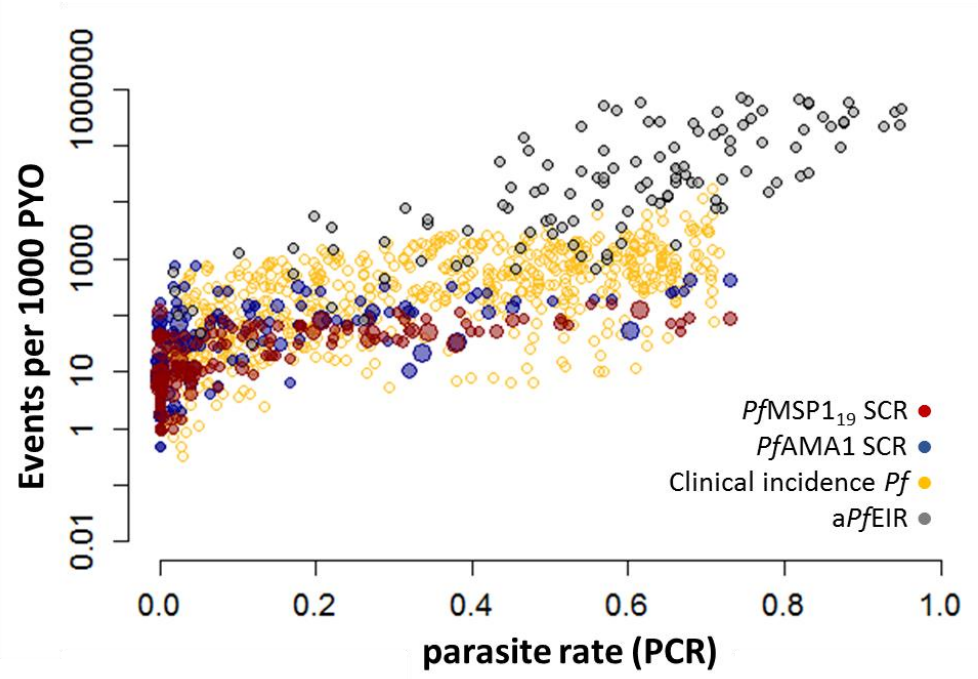

Despite the fact that *Pf*MSP1$_{19}$ and *Pf*AMA1 SCRs show the best resolution below 10% PR, maximum *Pf*MSP1$_{19}$ SCR values are smaller compared to *Pf*AMA1 and saturate at lower levels of transmission, while AMA1 SCR values continue to increase and show discriminatory ranges above 20% PR. This dynamic is most evident amongst clusters in the African and Middle East regions, where the majority of the high PCR prevalence data is from. At the lower PR range, however, clusters in Asia illustrate the tendency for *Pf*AMA1 SCR values to increase rapidly with parasite prevalence. This may be due to the relatively larger size and epitope diversity in the *Pf*AMA1 recombinant antigen fragment used in these assays compared to *Pf*MSP1$_{19}$, allowing measurement of a greater breadth of response in the population.

Influence of age in estimating parasite rate

Model fits using different age groups suggest that PR based on children aged 2-10 years are higher for equivalent *Pf*MSP1$_{19}$ SCR values in the overall population or children ages 5-15, which likely reflects that infections in younger age groups will tend to be more common than the general population. However, for *Pf*AMA1, the opposite is observed, where PR values for children aged 2-10 are actually lower for equivalent SCR values compared to the overall population or children aged 5-15. However, the SCR:PR estimate for *Pf*AMA1 is less precise, making it difficult to draw conclusions on the effect of the PR age cohort. Furthermore, for both antigens, any differences between age cohorts are primarily at prevalence of 1% or lower (though 95% credible intervals suggest these are not statistically different). This may indicate that SCR has the potential to be a robust measure of transmission if it correlates consistently across different age demographics used to measure PR. However, this may simply reflect that, for data clusters included in the analysis, when considering clusters across all prevalence ranges, PR according to different age subsets do not differ substantially from all-age parasite rate, as seen in Figure 4.8.

Figure 4.8 Best fit relationship between sero-conversion rate and parasite rate by age subset
All age seroconversion rate vs. PCR parasite rate based on different age subsets (African clusters only). Grey = all ages, yellow = ages 2-10 year olds, red = 5-15 year olds. Solid line is the best fit line and shaded area is 95% credible interval.

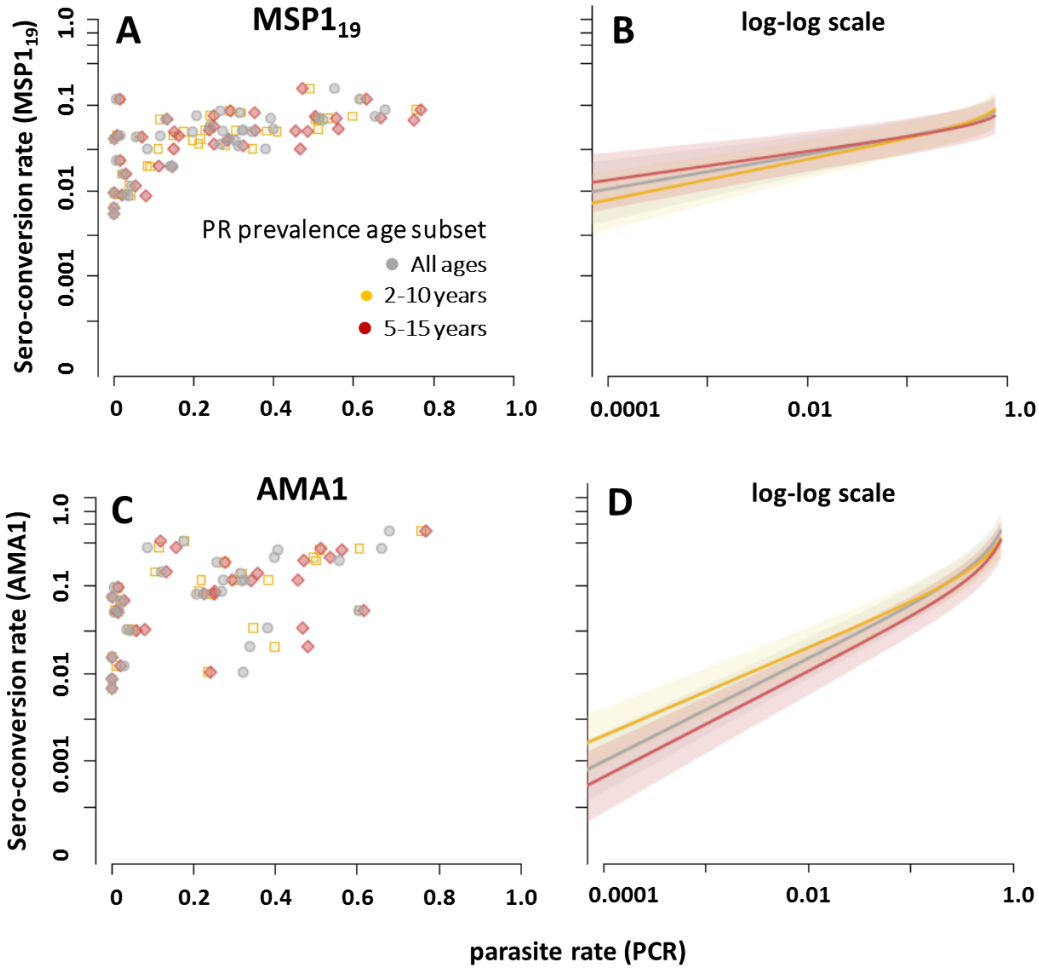

Model validation and predictive power of seroconversion rate

Leave-one-out analysis at the cluster level (i.e., leaving out a single cluster at a time) did not strongly influence the model. However, bootstrapping by country and study showed a tendency for SCR to overestimate PR for all clusters (Figure 4.9). It should be noted that certain countries had a particularly large number of studies and/or clusters (i.e., Cambodia). Separate model validation was not conducted with the region-specific model, so the overestimation at country and study level may be due to differences in the best fit relationships by region.

Figure 4.9 Comparison of observed vs. predicted PCR parasite rate (example of *Pf*MSP1$_{19}$)
Based on best fit model of *Pf*MSP1$_{19}$ SCR:PR overall, using leave-one-out analysis at study, country, and cluster level. Best fit model is based on SCR:PR overall and not by geographical region or PCR prevalence.

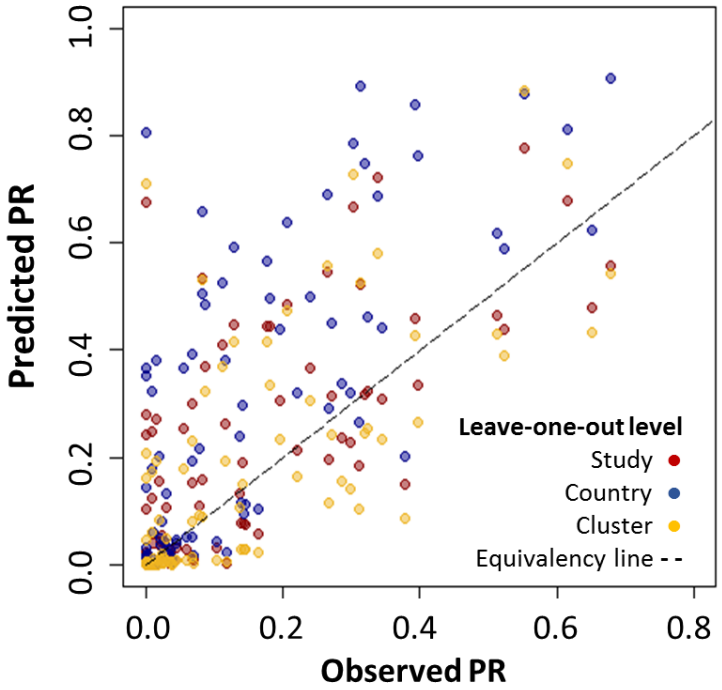

4.4 Discussion

Global patterns in sero-conversion rates

The analysis in this chapter describes a wide range of SCRs within country and region, which may reflect heterogeneities in transmission in these areas. This could be driven by a number of factors, depending on the country. The highest SCRs on average for both *Pf*MSP1$_{19}$ and *Pf*AMA1 were observed in Africa and the Middle east, followed by Asia, with the Americas (i.e., Brazil) having the lowest mean SCRs. However, these values may not be geographically representative of the regions overall, nor are they necessarily based on recent estimates as studies in this analysis range from years 1988 to 2014.

Due to the longevity of antibodies to *Pf*AMA1 and *Pf*MSP1$_{19}$, it may be that, depending on how recently a region has undergone changes in transmission, the impact of malaria control programmes or natural reductions in malaria transmission will be reflected in more immediate reductions in PR while changes in SCR are subject to a time lag. While we aimed to explicitly model this by testing for a change in force of infection over time, the size or age distribution of the sample did not always allow this, which may be the reason for the weakness of the model in some regions or countries. The precision of the fit is often dependent on adequate sampling around the age or time of presumed change in transmission, and profile likelihood plots of estimated change points can often have very large confidence intervals if this is not the case. Due

to the limited number of clusters in this analysis where a change in transmission could be detected, not enough data is available to explore the impact of recent changes in transmission on the SCR:PR relationship.

Relationship between sero-conversion rate and parasite prevalence by geographical region and transmission intensity

While a number of studies have observed that SCR is positively correlated with parasite rate at the study level, the analysis here confirms this association regionally and globally based on a pooled analysis of available serological studies to date. However, the nature of this association was observed to differ slightly by geographical region and by transmission intensity. SCRs were found to increase at a faster rate relative to PR at PCR prevalence less than 20%, while increasing more gradually at PCR prevalence values above 20%. This effect was more distinct for *Pf*AMA1 compared to *Pf*MSP1_{19} (where the SCR:PR relationship at low vs high PCR prevalence were not statistically strong). This is consistent with previous studies that have found that sero-prevalence to *Pf*AMA1 saturates quickly across a range of transmission intensities.[254,255]

Consistent with estimates of average SCR values by region, studies in Africa and the Middle East were observed to have higher SCRs for both antigens compared to clusters with equivalent PR values in Asia and the Americas. The Americas had the lowest SCRs across all transmission intensities. However, statistical evidence that the model including regional covariates differed from the general model was weak (with the exception of higher *Pf*AMA1 SCRs observed in low transmission African settings). This may reflect a lack of enough data to fit the model with precision, and updating these estimates as countries continue to monitor transmission based on serological endpoints will be useful.

However, the higher levels of antibody response in African settings could reflect historical patterns of transmission intensity that are not captured in parasite rate. Residual immune responses in this population may still be measurable if changes in transmission have been very recent, as opposed to the longer period of low *Pf* infection rates in Asia and the Americas that may have resulted in some loss of immunity over time. It is not clear how this might be affected by the relatively higher levels of *P.vivax* infection if there is some degree of cross-reactivity with *Pv*MSP$_{19}$ and *Pv*AMA1.

Differences in range of SCR measured by PfAMA1 and PfMSP1$_{19}$

It is not surprising that in general *Pf*AMA1 SCR values are higher than *Pf*MSP1_{19}, given that it is known to be more immunogenic. This may suggest that it is a more useful measure at lower levels of transmission, where it would have a larger range of values than *Pf*MSP1_{19}. What is surprising is the tendency for *Pf*MSP1_{19} SCR values to saturate at lower levels of parasite prevalence, whereas *Pf*AMA1 SCRs not only increase faster, but continue to increase even at quite high parasite prevalence values. This is contrary to previous studies that have observed that *Pf*AMA1

SCR estimates tend to saturate very quickly,[248] and that antibodies to *Pf*AMA1 and *Pf*MSP1$_{19}$ are both generally very long-lived. While in general, individuals become seronegative to *Pf*AMA1 at a similar (or even slower) rate than *Pf*MSP1$_{19}$, sero-reversion rates and antibody half-lives will vary by age and children often experience faster decay rates.[254]

The increased sensitivity of *Pf*AMA1 to detect transmission differences at higher parasite prevalence may be confounded by the age distribution of clusters in the dataset. If the samples are over-representative of younger age groups, the population could have a high proportion of individuals sero-reverting quickly to *Pf*AMA1 relative to *Pf*MSP1$_{19}$ while experiencing a greater number of repeat infections, particularly in high transmission settings. In this context, *Pf*AMA1 may be better at detecting changes in the sero-conversion / sero-reversion dynamic (i.e., a greater frequency of sero-negative to positive conversion events) even within the same individual, while *Pf*MSP1$_{19}$ sero-prevalence remains at a steady state for longer once it saturates. However, there is not much evidence currently to suggest that the sero-reversion rate differs this dramatically to the two antigens.

Another explanation may be that the relatively larger size of the *Pf*AMA1 recombinant antigen and its inclusion of a greater number of epitopes allows it to measure a higher diversity of human antibody responses in the population. Conversely, the smaller *Pf*MSP1$_{19}$ fragment used may cause saturation at lower SCR values. As transmission intensity increases, the genetic diversity of the parasite population also tends to increase, potentially allowing *Pf*AMA1 to measure higher levels of sero-prevalence and SCR. Variant-specific immune responses have also been observed for other polymorphic antigens such as MSP2, though they are not covered in this analysis specifically.[256]

Overall, it is not clear whether rapid increases in *Pf*AMA1 SCR are due to its strong immunogenicity or a slow rate of sero-reversion. On the other hand, it is also difficult to balance these potential causes with the fact that *Pf*AMA1 measures differences in immune responses at high levels of parasite prevalence, which could be due to its ability to measure a greater breadth of antibody response in the population.

It should be noted that in this dataset, the high immunogenicity of *Pf*AMA1 may also lead to a rapid saturation of sero-prevalence at young ages for clusters in high transmission intensities, such as Tororo, Uganda in the PRISM study, which experiences a*Pf*EIR values as high as 340.[257] This highlights the limited utility of certain serological markers at very high transmission intensities, where either less immunogenic markers such as *Pf*MSP1$_{19}$ or other measures such as clinical incidence and EIR are more suitable. While this single cluster is unlikely to have a large influence on the overall model fit, this can be assessed by investigating the cluster level leave-one-out analysis presented in Figure 4.9 in more detail or by computing a Hat projection matrix to estimate the level of influence this cluster or other outliers have on the regression.

The effect of age on sero-conversion rate, parasite prevalence, and clinical incidence

The influence of age on different measures of malaria transmission is only partially explored in this analysis. Models fitting sero-conversion rate already account for the effect of age to a degree, as force of infection is fit to age-specific sero-prevalence. The effect of age on parasite prevalence is only indirectly explored by fitting the SCR:PR model separately with two different age subsets. This specifically checks for the effect of age on the relationship between two diagnostic measures. Another method would be to define age categories of interest and include them as parameters in the SCR:PR model in the same manner that geographical region has been included as a covariate. If this method suggests that age has an effect, the SCR:PR relationship could be re-calculated based on age standardised PR estimates, for example using the methodology by Smith et al.[258] However, including age as a covariate in the SCR:PR relationship may not be valid if SCR is already an age-derived measure.

The clinical incidence and PR dataset published by Battle et al also includes age standardised estimates using the method by Smith et al. For the purposes of the analysis in this chapter, only the datasets where the empirically collected information of PR and clinical incidence cover the same age range are included. Comparison between SCR:PR against clinical incidence and PR could potentially cover a larger dataset if age-standardised or modelled data points are included. While an argument can be made for including the age-standardised data, including all modelled data points based on the MAP estimates may need more careful consideration. If the goal is to understand the utility of data that can be operationally collected through health facility or household surveys, using modelled data may lead one to falsely assume a better precision for particular diagnostics/metrics than would occur in practice.

Future work should consider overall age standardisation of the data, which could be particularly helpful when comparing against the EIR:PR data by Smith et al, given that this only includes data for ages under 15 years. The fact that this dataset is only based on African settings, however, would still need to be taken into account.

Comparing against EIR and clinical incidence

Our analysis suggests that SCR may be able to reflect a greater range of values at PR values of zero (or close to zero). More specifically, SCR appears to have a greater dynamic range starting at PCR prevalence values of 5% and lower. As noted above, while SCR values estimated for the antigens analysed here tend to saturate in high transmission settings, EIR data is more likely to be available at these higher PR ranges. Meanwhile, estimating PR values based on API or clinical incidence does not appear to be precise at any PR prevalence range.

The point estimates of the different metrics against PR suggest that SCR may have greater precision at moderate transmission intensities or have a greater dynamic range at low transmission intensities. A limitation to this analysis is the lack of information on credible

intervals for the EIR vs. PR or clinical incidence vs. PR best fit relationships. When this is available, future analysis could quantitatively compare the precision of the various measures across transmission intensities. Additional data that could be included in this analysis are datasets with paired estimates of SCR and EIR[259] that could allow triangulation of the relationships between measures.

Overall, it is important to note that there is a lack of a gold standard definition for transmission in this context. Variation in serological responses at very low PR prevalence could reflect heterogeneities in transmission as areas move towards elimination, or, given the longevity of immune responses to *Pf*MSP1$_{19}$ and *Pf*AMA1, lack of specificity due to the historical immune signatures in the population that may or may not reflect current transmission intensity. Therefore, immune responses to malaria antigens that have a shorter antibody half-life may provide more precise estimates of current levels of transmission, combined with information that *Pf*MSP1$_{19}$ and *Pf*AMA1 provide on either historical levels of transmission or current levels of protective immunity.

In order to make serological markers truly operational, their sensitivity and specificity need to be defined for different use-case scenarios, which should no longer be defined based on existing parasites in the blood at time of testing, as the sensitivity and specificity of parasite rate or clinical incidence are assessed. First, what is the window of time during which infection is epidemiologically relevant for assessing risk of malaria infection with regards to asymptomatic infection and its contribution to onwards transmission or the potential for increased clinical malaria if protective immunity has declined. This will vary by antigen and its relative correlation with either exposure of protection. Once these are defined, the next step is to determine the relevance of this information for targeting interventions such as focal MDA, focal vector control or future transmission blocking vaccines over space and time. Nonetheless, the data presented here may help to inform when to incorporate serological measures of transmission to complement other measures of malaria exposure. An investigation into novel serological markers that may be more associated with recent or current transmission is explored in Chapters 5-7.

Other data or model limitations

It should be noted that while parameter values and their 95% credible intervals as well as overall model DIC values and effective number of parameters (pD) were computed for each model in this chapter (Appendix 4.3), these models could also be compared by structuring them as nested models and comparing them using likelihood ratio tests or assessing whether the 95% confidence intervals of covariates are significantly different from zero. Alternative criterion, such as the Akaike information criterion (AIC) could also be considered given that the models assessed here are not overly complex and do not necessarily require effective number of parameters to be estimated, as the DIC does. For assessing the effect of transmission intensity, rather than

separate models at different PR ranges, non-log-linear relationships could also be tested or models that combine all the data but allow for segmented regression or smoothed piece-wise fits (i.e., splines at ranges of transmission intensity where there SCR-PR relationship may not be clear). All these models could be compared using DIC values or developed as nested models and likelihood compared as described above.

The analysis in this chapter combines PR data as measured using three different diagnostics (RDT, microscopy, and PCR). While the modelled relationship between these diagnostics (detailed in Chapter 3) can be used for transforming these units so that a combined analysis can be explored, it also introduces potential biases in interpretation, given the uncertainty in the RDT/microscopy – PCR modelled fit that is not accounted for in the data transformation in Chapter 4. The analysis would be improved by incorporating this uncertainty into the model. Alternatively, models could be fit for the different diagnostic datasets separately to determine if the regression coefficients vary between models. As a combined model, the diagnostic test used can also be included as a variable, which would also allow nested model comparison to test for improvements in fit or to verify that a bias is not introduced due to data transformation.

Validation of the model using leave-one-out analysis indicate that the model does not accurately predict PR based on the SCR:PR relationship at the country or study level. This is likely due to the fact that some countries have a very large number of clusters (e.g., Cambodia) with a wide range of SCR values and this may over-influence the model fit. It may also reflect the fact that the SCR:PR relationship differs by region. The model validation could be adjusted to check the effect of leave-one-out analysis by study or cluster, but using the best fit relationships by geographical region instead. Similarly, it could be tested for different PCR prevalence ranges. It may also be worth checking how to aggregate clusters for the Cambodia dataset so that they do not comprise such a large proportion of point estimates in the model.

The analysis in here treats *Pf*AMA1 and *Pf*MSP1$_{19}$ separately, but precision could potentially be gained by combining these datasets and fitting models based on sero-positivity to either antigen. However, assessing the correlation between SCRs for the two antigens separately would also be useful to determine precisely at which transmission intensities antibody responses between them will differ.

Other adjustments that could be made are a better estimation of prevalence for clusters measuring no parasite positive infections, rather than simply assuming a fixed value close to zero as is done in this analysis. This could be done by taking advantage of Bayesian spatial fitting methods and the large number of clusters compiled in this study, where a more informative prior could be included based on clusters in similar geographical regions with low (but non-zero) prevalence values and the influence of sample size on the precision of the estimates.

Also, while most serology models define sero-prevalence using a binary threshold for sero-positivity, some models account for boosting of immunity upon repeat infection by including additional sero-positive compartments[122,260] or using magnitude of change in antibody titres.[123,124] These are most relevant in hyper-endemic settings where sero-prevalence may saturate at earlier ages. For surveillance purposes in high transmission settings, however, it is possible to rely accurately on EIR and PR estimates of prevalence, and serology can serve as a validation of these estimates rather than as a primary measure of transmission.

Applications for surveillance and cluster randomised trial design

As the relationship between different measures of malaria transmission are refined, the use of serology is likely to have a number of distinct operational applications. This includes its use as a measure of baseline transmission at the community or cluster level for trial stratification, identifying geographic or demographic foci of transmission risk or receptivity, as a secondary endpoint in cluster randomised trials, or as part of routine surveillance to monitor progress towards elimination and to prevent re-introduction after local elimination.

Once prevalence measures based on PCR, microscopy or RDT approach levels close to zero, it can be difficult to achieve statistical power to measure changes in transmission.[239] Some alternatives have been suggested to deal with these measurement issues in low transmission settings, such as a greater emphasis on the basic reproduction number R_0 to certify elimination, but this is difficult to measure empirically without modelling.[261] SCR measures transmission by estimating a force of infection, and this relationship with R_0 makes it a powerful quantitative metric. It is also relatively easier to implement operationally in resource-limited settings compared to other equivalently sensitive molecular methods.

Future surveillance does not have to be limited to one or two antigens, and a multiplexed serological platform that can measure the combined response across a number of markers, including those more associated with recent or current transmission, could increase the utility of malaria serology for a wider range of transmission intensities. This is discussed further in Chapter 5. Additional studies comparing clonal diversity or the multiplicity of infection and its impact on antigen-specific SCR dynamics would be useful analysis to explore this hypothesis and to optimise future assay development.

Appendix 4.1 List of surveys included in serology meta-analysis

A. Africa

Region	Country	Survey year	Sampling strategy	Site/Cluster	Serology sample size		Parasite rate sample size			Regional SCR*		Change in SCR†	
					*Pf*MSP1$_{19}$	*Pf*AMA1	PCR	RDT	Slide	*Pf*MSP1$_{19}$	*Pf*AMA1	*Pf*MSP1$_{19}$	*Pf*AMA1
AFRICA	Kenya	2009	All-age XS survey	XSS1 Kisii	1076	1056	--	1071	--				
				XSS1 Rachuonyo	1047	1045	--	1046	--				
		2009	All-age XS survey	XSS2 Kisii	1743	--	1715	1743	--				
				XSS2 Rachuonyo	1761	--	1733	1761	--				
		2011	All-age XS survey	XSS4 Rachuonyo	16627	16627	12229	--	--				
	Somaliland	2008	All-age XS survey	Gebiley1	241	240	241	--	--	✓	✓		
				Gebiley2	99	131	105	--	--	✓	✓	✓	
				Gebiley3	616	635	616	--	--				
	Sudan	2012	LLIN and IRS trial arms, all ages	Alhoosh	2517	2562	2427	1682	--		✓	✓	
				Hag Abdala	2345	2403	2296	1555	--			✓	✓
				Galabat	1601	1632	1509	1025	--				
				New Halfa	2302	2369	2298	2298	--			✓	
	Equatorial Guinea	2008	All-age XS survey	Bioko	6466	6436	--	5586	--				
	Gambia	1988	All-age XS survey	Farafenni	742	--	--	--	7				
		2008	All-age XS survey	Basse	859	--	--	--	848				
			All-age XS survey	Farafenni	670	--	--	--	662				
	Guinea Bissau	2008	All-age XS survey	Caio	769	--	--	--	750				

Region	Country	Survey year	Sampling strategy	Site/Cluster	Serology sample size		Parasite rate sample size			Regional SCR*		Change in SCR†	
					*Pf*MSP1$_{19}$	*Pf*AMA1	PCR	RDT	Slide	*Pf*MSP1$_{19}$	*Pf*AMA1	*Pf*MSP1$_{19}$	*Pf*AMA1
AFRICA	**Tanzania**	2010	All-age XS survey	Mwanza Cotanda	2496	2382	2496	--	--				
		2007	Post-IPTi survey	Mtwara IPTi	393	--	--	392	--				
			Post-IPTi survey	Lindi IPTi	619	--	--	617	--				
		2007	Health-facility patients/attendees, post-IPTi	Korogwe	1746	1746	--	1746	--				
				Same	1670	1713	--	1006	--				
		2007		Lower Moshi	331	--	--	331	--				
		2001	All-age XS survey	Rombo	1637	1672	--	--	1636				
				Mwanga	1628	705	--	--	1580				
				Same	1670	1678	--	--	1643				
				Lushoto	3747	3820	--	--	3722				
		2009	All-age XS survey	Zanzibar	2185	2170	2181	--	--				
		2011		Zanzibar	2014	2010	2014	--	--				
	Uganda	2010	All-age XS survey	Apac X1	436	463	436	--	--		✓		
				Apac X2	426	448	401	212	392		✓		
				Apac X3	432	475	427	219	392		✓		
		2014	All-age XS survey	Jinja	552	592	--	552	552				
				Kanungu	753	755	--	753	753				
				Tororo	781	777	--	780	781				

B. Asia

Region	Country	Survey year	Sampling strategy	Site/Cluster	Serology sample size		Parasite rate sample size			Regional SCR*		Change in SCR†	
					*Pf*MSP1$_{19}$	*Pf*AMA1	PCR	RDT	Slide	*Pf*MSP1$_{19}$	*Pf*AMA1	*Pf*MSP1$_{19}$	*Pf*AMA1
ASIA	**Myanmar†**	2013	All-age XS survey	Bago East	1576	1586	1576	--	--			✓	✓
	Vanuatu	1999	All-age XS survey	Aneityum	618	619	493	--	--		✓		
		2002		Aneityum	712	719	711	--	--		✓	✓	
		2004		Aneityum	590	598	590	--	--	✓			
		2007		Aneityum	755	755	755	--	--	✓	✓		
		2010		Aneityum	883	876	883	--	--	✓	✓		
	Cambodia†	2004	All-age XS survey Clusters combined based on risk zones (proximity to forest)	1-5, 9	500	499	--	--	500	✓	✓		✓
				10,11,6,90	332	338	--	--	332	✓	✓		✓
				7,8,12	305	303	--	--	305		✓		
				32-25	307	340	--	--	307	✓	✓		✓
				39,40,43	260	257	--	--	260	✓	✓		✓
				41,42	184	184	--	--	184	✓	✓		✓
				44-48	445	439	--	--	445				
				49-51	317	276	--	--	317	✓	✓		
				52-55	327	317	--	--	327				
				56,57	197	176	--	--	197	✓	✓		
				58-65	737	686	--	--	737				
				66,67	161	122	--	--	161	✓	✓		
				68,69	172	168	--	--	172	✓	✓		
				70,71	155	152	--	--	155	✓	✓		
				75-78	278	236	--	--	278		✓		
				82-85	358	354	--	--	358	✓	✓		
				86,87	175	168	--	--	175	✓	✓		

Region	Country	Survey year	Sampling strategy	Site/Cluster	Serology sample size		Parasite rate sample size			Regional SCR*		Change in SCR†	
					*Pf*MSP1$_{19}$	*Pf*AMA1	PCR	RDT	Slide	*Pf*MSP1$_{19}$	*Pf*AMA1	*Pf*MSP1$_{19}$	*Pf*AMA1
ASIA (continued)	**Cambodia†**	2007	All-age XS survey Clusters combined based on risk zones (proximity to forest)	1-6	617	620	610	--	617				
				7,8,9	281	292	281	--	281		✓		
				10,11	133	135	133	--	133	✓	✓		
				12,13	206	207	206	--	206	✓	✓		
				14,15,41	330	341	325	--	330	✓	✓		✓
				16,17,18	295	295	295	--	295	✓	✓	✓	✓
				19,20,21	253	255	252	--	253	✓	✓		
				22,23,24	325	300	323	--	325	✓	✓		
				25,26,27	365	350	364	--	365	✓			
				28,29,30	332	335	330	--	332	✓	✓		✓
				31-33,49	314	288	312	--	314		✓		
				34-40	210	211	208	--	210	✓	✓		
				35,37,38	337	339	252	--	337		✓	✓	✓
				40,39	219	220	180	--	219	✓	✓		✓
				42,45	198	219	198	--	198	✓	✓		
				43,44,72	290	324	289	--	290	✓	✓		✓
				46,47,48	279	279	186	--	279	✓	✓		
				49,50	155	158	154	--	155	✓	✓		
				51,52,53	298	299	298	--	298	✓	✓	✓	✓
				54,56,57	295	296	294	--	295	✓	✓	✓	✓
				55,58,59	317	317	317	--	317	✓	✓		✓
				60	113	114	113	--	113	✓	✓		
				61,62,63	279	284	278	--	279	✓	✓		
				64,65	192	193	192	--	192	✓	✓		
				66,67,68	308	287	306	--	308	✓	✓		
				79,70,71	312	303	312	--	312	✓	✓	✓	✓
				73	101	102	101	--	101	✓	✓	✓	
				74,75,76	256	256	256	--	256	✓			

C. Middle East

Region	Country	Survey year	Sampling strategy	Site/Cluster	Serology sample size		Parasite rate sample size			Regional SCR*		Change in SCR†	
					*Pf*MSP1$_{19}$	*Pf*AMA1	PCR	RDT	Slide	*Pf*MSP1$_{19}$	*Pf*AMA1	*Pf*MSP1$_{19}$	*Pf*AMA1
MIDDLE EAST	**Yemen**	2012	Only age < 15 years	3001/3003	340	325	--	340	340		✓		
				3002	195	186	--	194	195	✓	✓		
				3004	181	173	--	181	181	✓	✓		
				3005	188	187	184	188	188	✓	✓		
				3006,3009,3011	523	505	--	523	521	✓			
				3007,3012	219	218	115	219	214	✓	✓		
				3008	167	160	--	167	167	✓	✓		
				3010	175	160	175	175	175	✓	✓		

D. Americas

Region	Country	Survey year	Sampling strategy	Site/Cluster	Serology sample size		Parasite rate sample size			Regional SCR*		Change in SCR†	
					*Pf*MSP1$_{19}$	*Pf*AMA1	PCR	RDT	Slide	*Pf*MSP1$_{19}$	*Pf*AMA1	*Pf*MSP1$_{19}$	*Pf*AMA1
AMERICAS	**Brazil†**	2007	All-age XS survey	1	113	113	--	--	113	✓	✓		
				2	171	171	--	--	171	✓	✓	✓	✓
				3	262	262	--	--	262	✓	✓		
				4	182	182	--	--	182	✓	✓		
				5	204	204	--	--	204	✓	✓		
				6	--	141	--	--	253	✓	✓		
				7	--	253	--	--	499	✓	✓		

*For clusters that do not have adequate sample size to estimate a cluster-specific sero-reversion rate (SRR), a region-specific SRR is used in the model.
† Clusters where differences in sero-conversion rate (SCR) by age represent occupational risk (e.g., forest workers), and the SCR experienced by this higher-risk group is used for inclusion in the SCR-parasite rate model. For all other clusters, SCR experienced by the younger age groups is assumed to reflect most recent malaria transmission.

Appendix 4.2 Sero-conversion rate model fits by study cluster

Modelled seroconversion rates (SCR) for *Pf*MSP1$_{19}$ are shown in blue (single SCR for all ages) and green (change in SCR between age groups) and for *Pf*AMA1 in red (single SCR) and yellow (change in SCR), with shaded area indicating the 95% confidence interval (CI) of the SCR model fit. Observed sero-prevalence for each age group (split by deciles based on maximum age in study) are shown as black points and 95% CI as vertical lines.

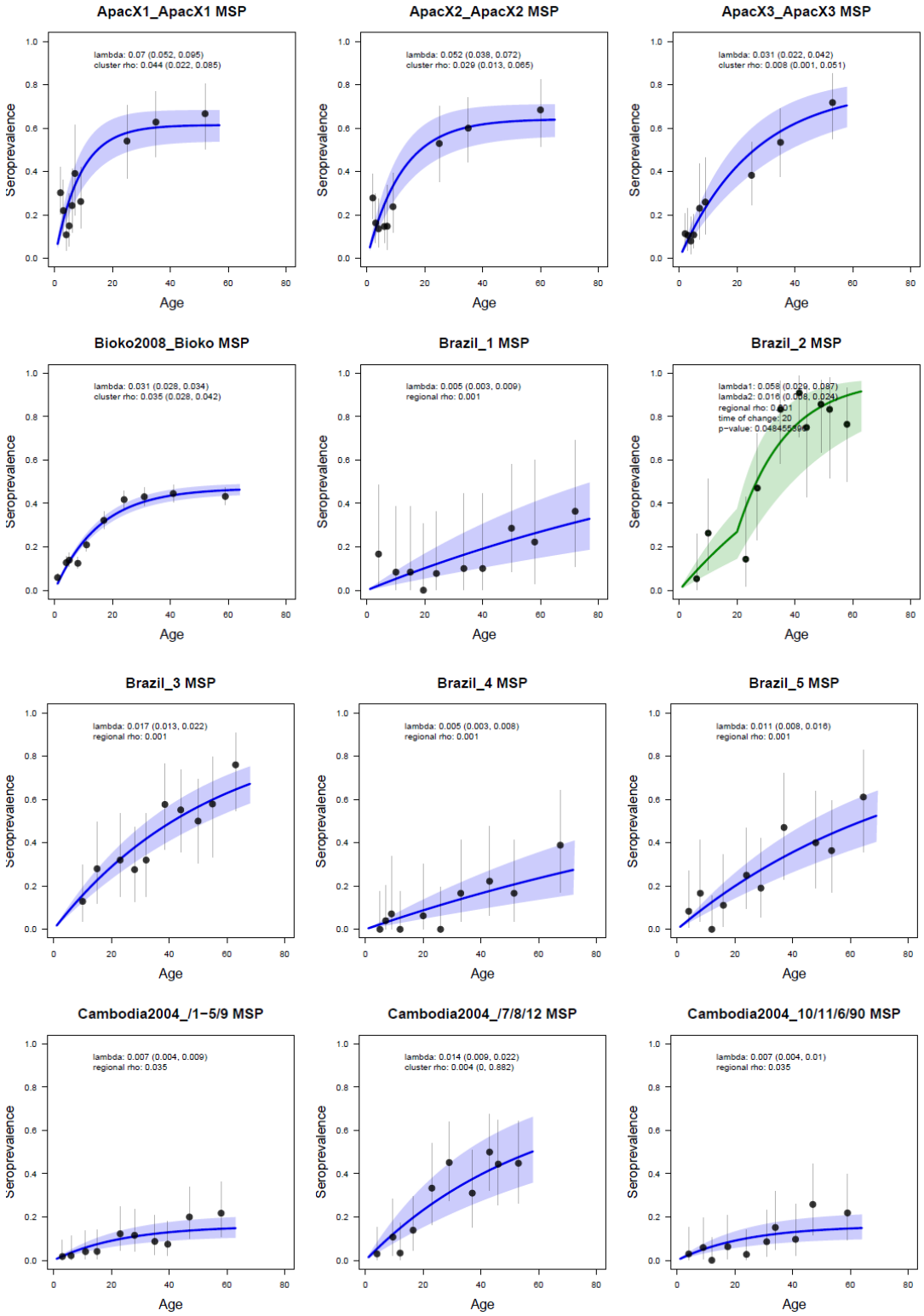

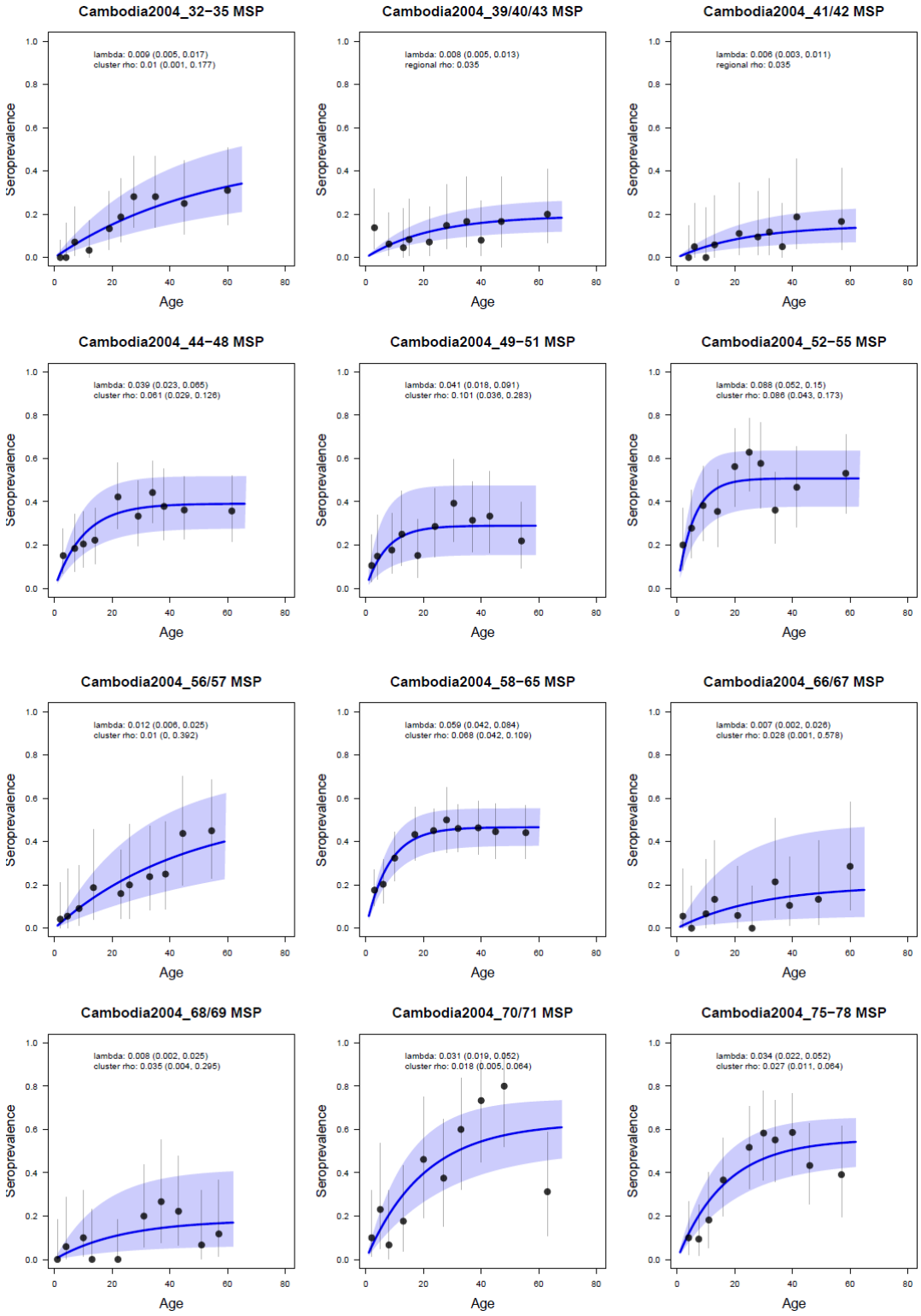
Cambodia2004_32−35 MSP
lambda: 0.009 (0.005, 0.017)
cluster rho: 0.01 (0.001, 0.177)
Cambodia2004_39/40/43 MSP
lambda: 0.008 (0.005, 0.013)
regional rho: 0.035
Cambodia2004_41/42 MSP
lambda: 0.006 (0.003, 0.011)
regional rho: 0.035
Cambodia2004_44−48 MSP
lambda: 0.039 (0.023, 0.065)
cluster rho: 0.061 (0.029, 0.126)
Cambodia2004_49−51 MSP
lambda: 0.041 (0.018, 0.091)
cluster rho: 0.101 (0.036, 0.283)
Cambodia2004_52−55 MSP
lambda: 0.088 (0.052, 0.15)
cluster rho: 0.086 (0.043, 0.173)
Cambodia2004_56/57 MSP
lambda: 0.012 (0.006, 0.025)
cluster rho: 0.01 (0, 0.392)
Cambodia2004_58−65 MSP
lambda: 0.059 (0.042, 0.084)
cluster rho: 0.068 (0.042, 0.109)
Cambodia2004_66/67 MSP
lambda: 0.007 (0.002, 0.026)
cluster rho: 0.028 (0.001, 0.578)
Cambodia2004_68/69 MSP
lambda: 0.008 (0.002, 0.025)
cluster rho: 0.035 (0.004, 0.295)
Cambodia2004_70/71 MSP
lambda: 0.031 (0.019, 0.052)
cluster rho: 0.018 (0.005, 0.064)
Cambodia2004_75−78 MSP
lambda: 0.034 (0.022, 0.052)
cluster rho: 0.027 (0.011, 0.064)
Seroprevalence
Age

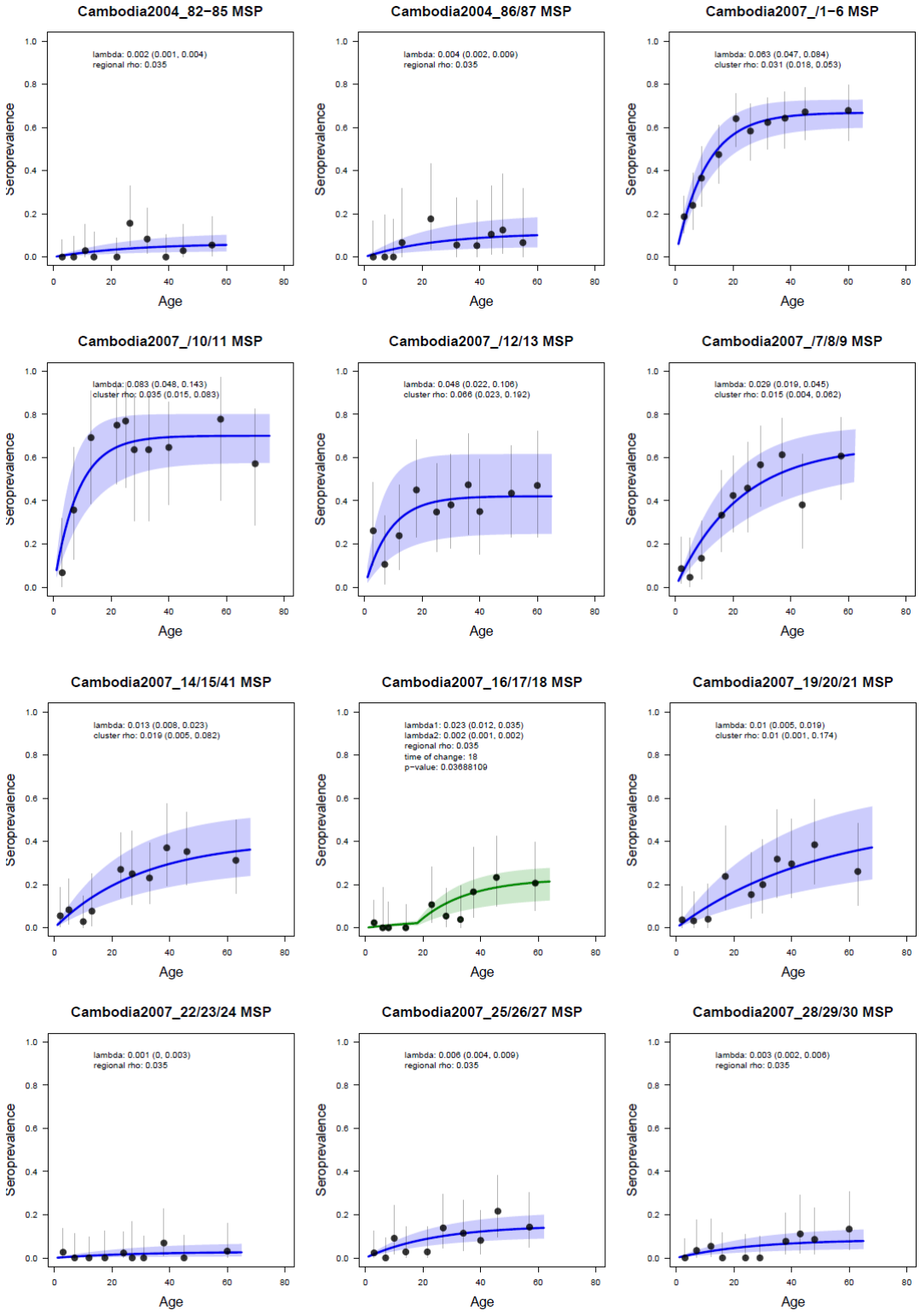
Cambodia2004_82−85 MSP
lambda: 0.002 (0.001, 0.004)
regional rho: 0.035
Cambodia2004_86/87 MSP
lambda: 0.004 (0.002, 0.009)
regional rho: 0.035
Cambodia2007_/1−6 MSP
lambda: 0.063 (0.047, 0.084)
cluster rho: 0.031 (0.018, 0.053)
Cambodia2007_/10/11 MSP
lambda: 0.083 (0.048, 0.143)
cluster rho: 0.035 (0.015, 0.083)
Cambodia2007_/12/13 MSP
lambda: 0.048 (0.022, 0.106)
cluster rho: 0.066 (0.023, 0.192)
Cambodia2007_/7/8/9 MSP
lambda: 0.029 (0.019, 0.045)
cluster rho: 0.015 (0.004, 0.062)
Cambodia2007_14/15/41 MSP
lambda: 0.013 (0.008, 0.023)
cluster rho: 0.019 (0.005, 0.082)
Cambodia2007_16/17/18 MSP
lambda1: 0.023 (0.012, 0.035)
lambda2: 0.002 (0.001, 0.002)
regional rho: 0.035
time of change: 18
p−value: 0.03688109
Cambodia2007_19/20/21 MSP
lambda: 0.01 (0.005, 0.019)
cluster rho: 0.01 (0.001, 0.174)
Cambodia2007_22/23/24 MSP
lambda: 0.001 (0, 0.003)
regional rho: 0.035
Cambodia2007_25/26/27 MSP
lambda: 0.006 (0.004, 0.009)
regional rho: 0.035
Cambodia2007_28/29/30 MSP
lambda: 0.003 (0.002, 0.006)
regional rho: 0.035
Seroprevalence
Age

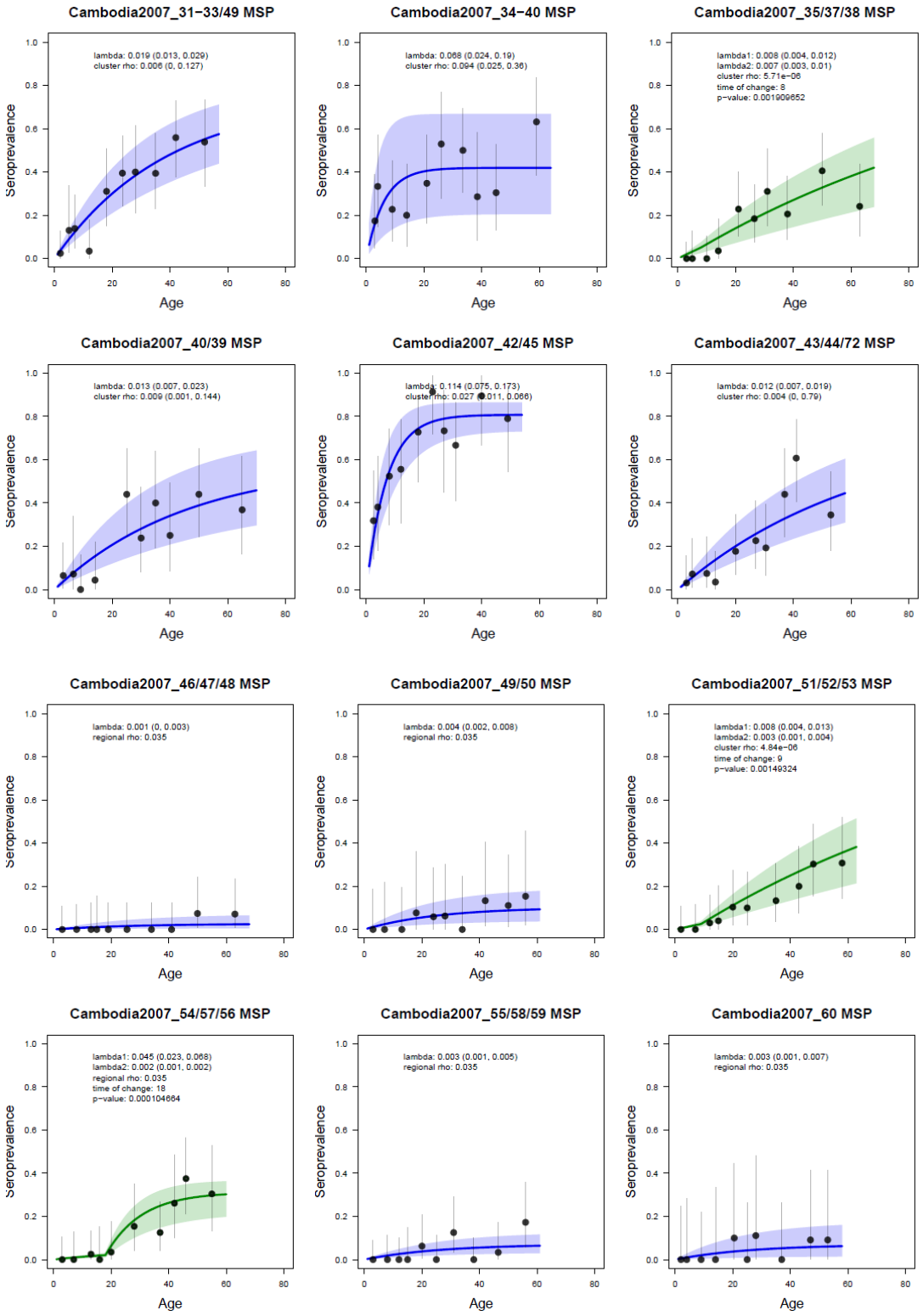
Cambodia2007_31−33/49 MSP
lambda: 0.019 (0.013, 0.029)
cluster rho: 0.006 (0, 0.127)
Cambodia2007_34−40 MSP
lambda: 0.068 (0.024, 0.19)
cluster rho: 0.094 (0.025, 0.36)
Cambodia2007_35/37/38 MSP
lambda1: 0.008 (0.004, 0.012)
lambda2: 0.007 (0.003, 0.01)
cluster rho: 5.71e−06
time of change: 8
p−value: 0.001909652
Cambodia2007_40/39 MSP
lambda: 0.013 (0.007, 0.023)
cluster rho: 0.009 (0.001, 0.144)
Cambodia2007_42/45 MSP
lambda: 0.114 (0.075, 0.173)
cluster rho: 0.027 (0.011, 0.066)
Cambodia2007_43/44/72 MSP
lambda: 0.012 (0.007, 0.019)
cluster rho: 0.004 (0, 0.79)
Cambodia2007_46/47/48 MSP
lambda: 0.001 (0, 0.003)
regional rho: 0.035
Cambodia2007_49/50 MSP
lambda: 0.004 (0.002, 0.008)
regional rho: 0.035
Cambodia2007_51/52/53 MSP
lambda1: 0.008 (0.004, 0.013)
lambda2: 0.003 (0.001, 0.004)
cluster rho: 4.84e−06
time of change: 9
p−value: 0.00149324
Cambodia2007_54/57/56 MSP
lambda1: 0.045 (0.023, 0.068)
lambda2: 0.002 (0.001, 0.002)
regional rho: 0.035
time of change: 18
p−value: 0.000104664
Cambodia2007_55/58/59 MSP
lambda: 0.003 (0.001, 0.005)
regional rho: 0.035
Cambodia2007_60 MSP
lambda: 0.003 (0.001, 0.007)
regional rho: 0.035
Seroprevalence
Age

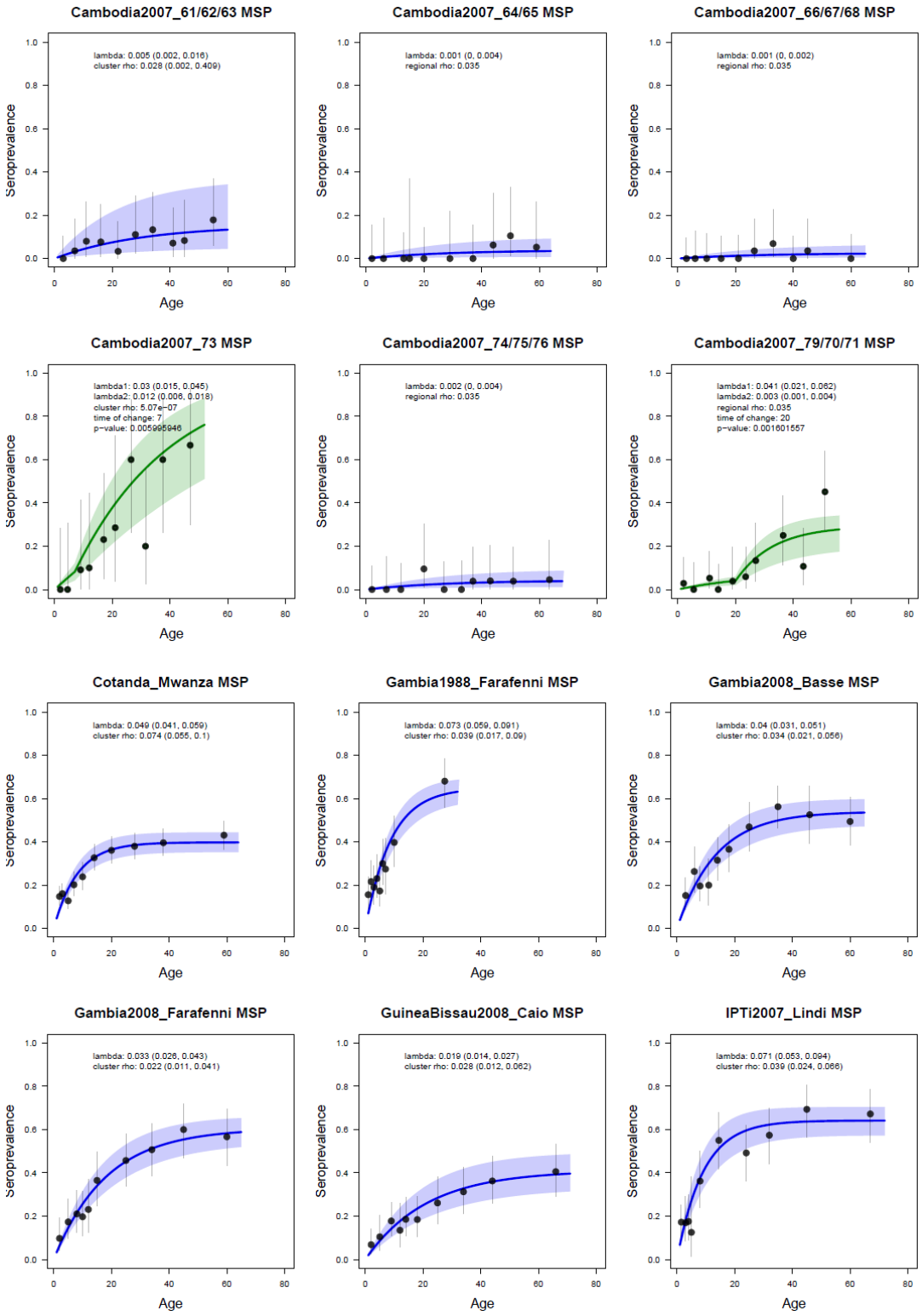
Cambodia2007_61/62/63 MSP
lambda: 0.005 (0.002, 0.016)
cluster rho: 0.028 (0.002, 0.409)
Cambodia2007_64/65 MSP
lambda: 0.001 (0, 0.004)
regional rho: 0.035
Cambodia2007_66/67/68 MSP
lambda: 0.001 (0, 0.002)
regional rho: 0.035
Cambodia2007_73 MSP
lambda1: 0.03 (0.015, 0.045)
lambda2: 0.012 (0.006, 0.018)
cluster rho: 5.07e-07
time of change: 7
p-value: 0.005995946
Cambodia2007_74/75/76 MSP
lambda: 0.002 (0, 0.004)
regional rho: 0.035
Cambodia2007_79/70/71 MSP
lambda1: 0.041 (0.021, 0.062)
lambda2: 0.003 (0.001, 0.004)
regional rho: 0.035
time of change: 20
p-value: 0.001601557
Cotanda_Mwanza MSP
lambda: 0.049 (0.041, 0.059)
cluster rho: 0.074 (0.055, 0.1)
Gambia1988_Farafenni MSP
lambda: 0.073 (0.059, 0.091)
cluster rho: 0.039 (0.017, 0.09)
Gambia2008_Basse MSP
lambda: 0.04 (0.031, 0.051)
cluster rho: 0.034 (0.021, 0.056)
Gambia2008_Farafenni MSP
lambda: 0.033 (0.026, 0.043)
cluster rho: 0.022 (0.011, 0.041)
GuineaBissau2008_Caio MSP
lambda: 0.019 (0.014, 0.027)
cluster rho: 0.028 (0.012, 0.062)
IPTi2007_Lindi MSP
lambda: 0.071 (0.053, 0.094)
cluster rho: 0.039 (0.024, 0.066)
Seroprevalence
Age

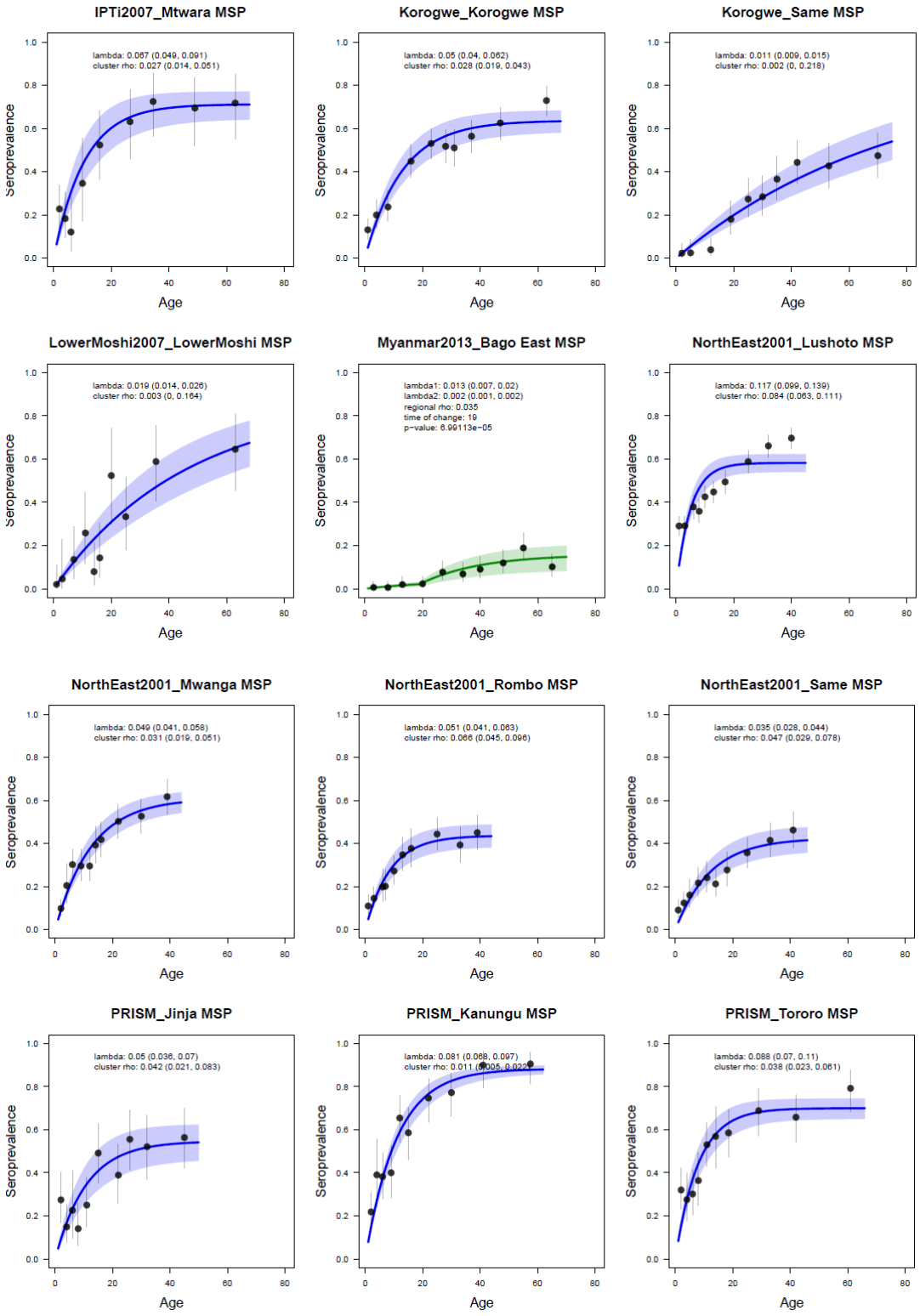
IPTi2007_Mtwara MSP
lambda: 0.067 (0.049, 0.091)
cluster rho: 0.027 (0.014, 0.051)
Korogwe_Korogwe MSP
lambda: 0.05 (0.04, 0.062)
cluster rho: 0.028 (0.019, 0.043)
Korogwe_Same MSP
lambda: 0.011 (0.009, 0.015)
cluster rho: 0.002 (0, 0.218)
LowerMoshi2007_LowerMoshi MSP
lambda: 0.019 (0.014, 0.026)
cluster rho: 0.003 (0, 0.164)
Myanmar2013_Bago East MSP
lambda1: 0.013 (0.007, 0.02)
lambda2: 0.002 (0.001, 0.002)
regional rho: 0.035
time of change: 19
p-value: 6.99113e-05
NorthEast2001_Lushoto MSP
lambda: 0.117 (0.099, 0.139)
cluster rho: 0.084 (0.063, 0.111)
NorthEast2001_Mwanga MSP
lambda: 0.049 (0.041, 0.058)
cluster rho: 0.031 (0.019, 0.051)
NorthEast2001_Rombo MSP
lambda: 0.051 (0.041, 0.063)
cluster rho: 0.066 (0.045, 0.096)
NorthEast2001_Same MSP
lambda: 0.035 (0.028, 0.044)
cluster rho: 0.047 (0.029, 0.078)
PRISM_Jinja MSP
lambda: 0.05 (0.036, 0.07)
cluster rho: 0.042 (0.021, 0.083)
PRISM_Kanungu MSP
lambda: 0.081 (0.068, 0.097)
PRISM_Tororo MSP
lambda: 0.088 (0.07, 0.11)
cluster rho: 0.038 (0.023, 0.061)
Seroprevalence
Age

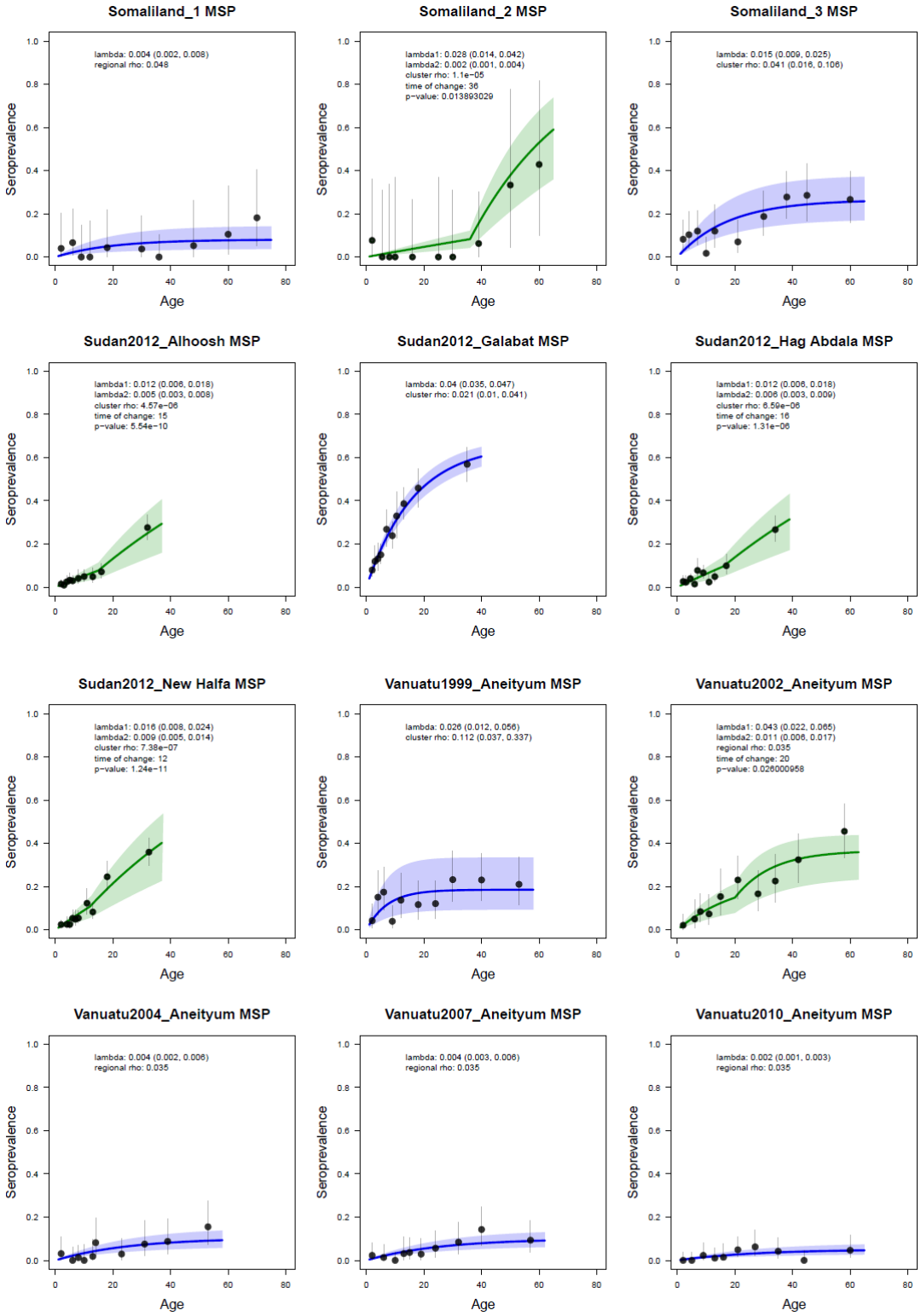
Somaliland_1 MSP
lambda: 0.004 (0.002, 0.008)
regional rho: 0.048
Somaliland_2 MSP
lambda1: 0.028 (0.014, 0.042)
lambda2: 0.002 (0.001, 0.004)
cluster rho: 1.1e−05
time of change: 36
p−value: 0.013893029
Somaliland_3 MSP
lambda: 0.015 (0.009, 0.025)
cluster rho: 0.041 (0.016, 0.106)
Sudan2012_Alhoosh MSP
lambda1: 0.012 (0.006, 0.018)
lambda2: 0.005 (0.003, 0.008)
cluster rho: 4.57e−06
time of change: 15
p−value: 5.54e−10
Sudan2012_Galabat MSP
lambda: 0.04 (0.035, 0.047)
cluster rho: 0.021 (0.01, 0.041)
Sudan2012_Hag Abdala MSP
lambda1: 0.012 (0.006, 0.018)
lambda2: 0.006 (0.003, 0.009)
cluster rho: 6.59e−06
time of change: 16
p−value: 1.31e−06
Sudan2012_New Halfa MSP
lambda1: 0.016 (0.008, 0.024)
lambda2: 0.009 (0.005, 0.014)
cluster rho: 7.38e−07
time of change: 12
p−value: 1.24e−11
Vanuatu1999_Aneityum MSP
lambda: 0.026 (0.012, 0.056)
cluster rho: 0.112 (0.037, 0.337)
Vanuatu2002_Aneityum MSP
lambda1: 0.043 (0.022, 0.065)
lambda2: 0.011 (0.006, 0.017)
regional rho: 0.035
time of change: 20
p−value: 0.026000958
Vanuatu2004_Aneityum MSP
lambda: 0.004 (0.002, 0.006)
regional rho: 0.035
Vanuatu2007_Aneityum MSP
lambda: 0.004 (0.003, 0.006)
regional rho: 0.035
Vanuatu2010_Aneityum MSP
lambda: 0.002 (0.001, 0.003)
regional rho: 0.035
Seroprevalence
Age

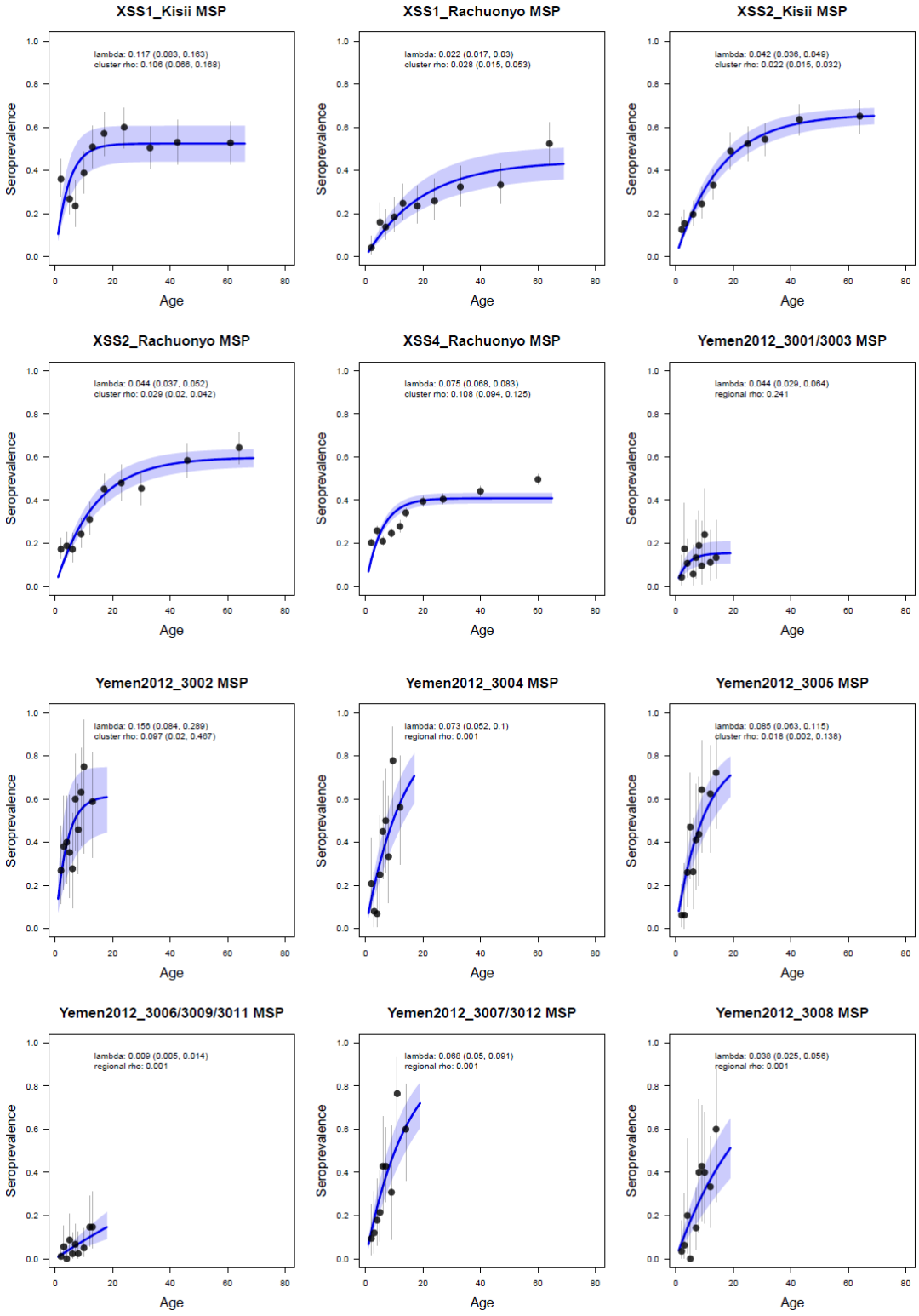
XSS1_Kisii MSP
lambda: 0.117 (0.083, 0.163)
cluster rho: 0.106 (0.066, 0.168)
XSS1_Rachuonyo MSP
lambda: 0.022 (0.017, 0.03)
cluster rho: 0.028 (0.015, 0.053)
XSS2_Kisii MSP
lambda: 0.042 (0.036, 0.049)
cluster rho: 0.022 (0.015, 0.032)
XSS2_Rachuonyo MSP
lambda: 0.044 (0.037, 0.052)
cluster rho: 0.029 (0.02, 0.042)
XSS4_Rachuonyo MSP
lambda: 0.075 (0.068, 0.083)
cluster rho: 0.108 (0.094, 0.125)
Yemen2012_3001/3003 MSP
lambda: 0.044 (0.029, 0.064)
regional rho: 0.241
Yemen2012_3002 MSP
lambda: 0.156 (0.084, 0.289)
cluster rho: 0.097 (0.02, 0.467)
Yemen2012_3004 MSP
lambda: 0.073 (0.052, 0.1)
regional rho: 0.001
Yemen2012_3005 MSP
lambda: 0.085 (0.063, 0.115)
cluster rho: 0.018 (0.002, 0.138)
Yemen2012_3006/3009/3011 MSP
lambda: 0.009 (0.005, 0.014)
regional rho: 0.001
Yemen2012_3007/3012 MSP
lambda: 0.068 (0.05, 0.091)
regional rho: 0.001
Yemen2012_3008 MSP
lambda: 0.038 (0.025, 0.056)
regional rho: 0.001
Seroprevalence
Age

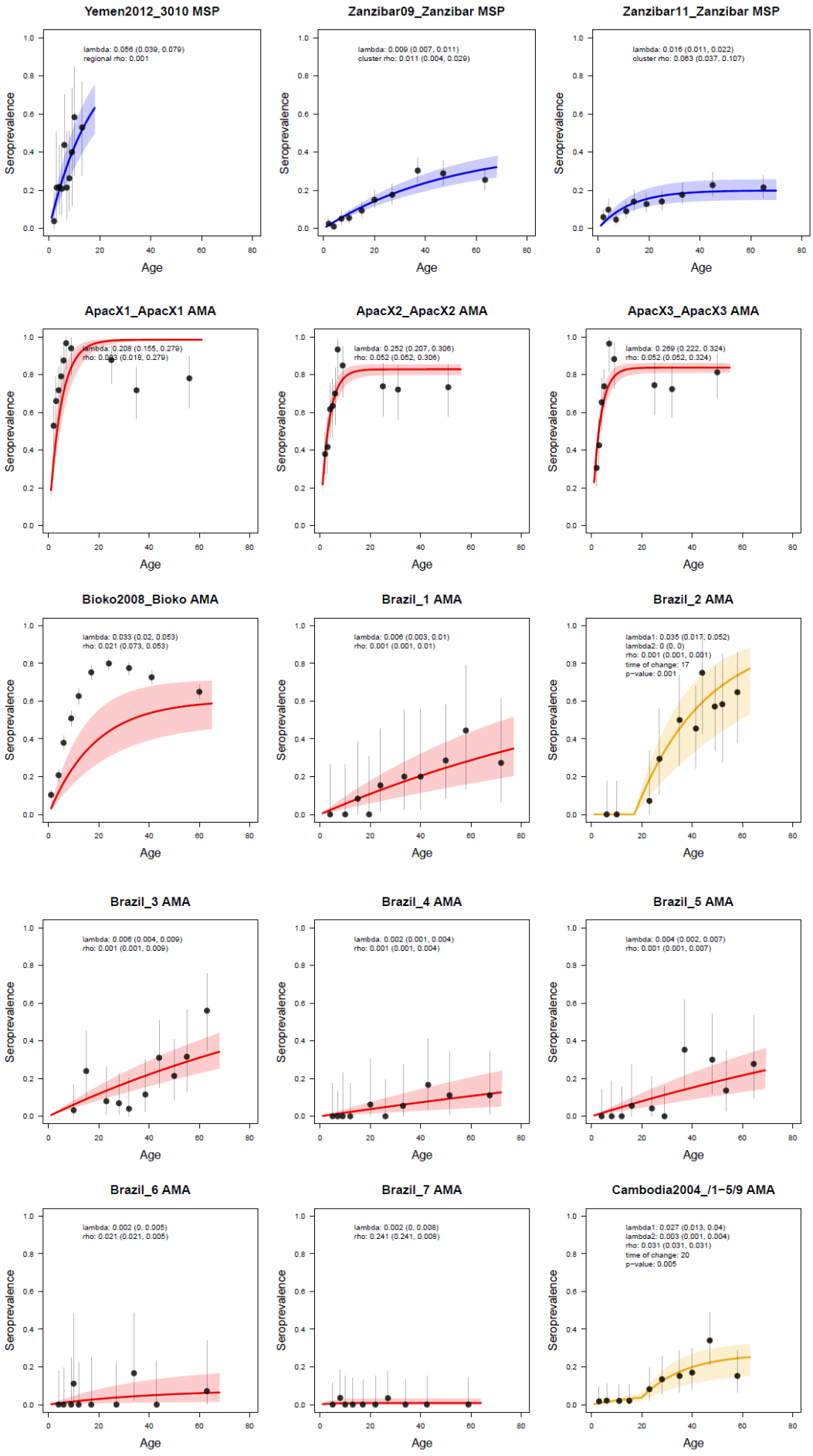
Yemen2012_3010 MSP
lambda: 0.056 (0.039, 0.079)
regional rho: 0.001
Zanzibar09_Zanzibar MSP
lambda: 0.009 (0.007, 0.011)
cluster rho: 0.011 (0.004, 0.029)
Zanzibar11_Zanzibar MSP
lambda: 0.016 (0.011, 0.022)
cluster rho: 0.063 (0.037, 0.107)
ApacX1_ApacX1 AMA
lambda: 0.208 (0.155, 0.279)
rho: 0.083 (0.018, 0.279)
ApacX2_ApacX2 AMA
lambda: 0.252 (0.207, 0.306)
rho: 0.052 (0.052, 0.306)
ApacX3_ApacX3 AMA
lambda: 0.269 (0.222, 0.324)
rho: 0.052 (0.052, 0.324)
Bioko2008_Bioko AMA
lambda: 0.033 (0.02, 0.053)
rho: 0.021 (0.073, 0.053)
Brazil_1 AMA
lambda: 0.006 (0.003, 0.01)
rho: 0.001 (0.001, 0.01)
Brazil_2 AMA
lambda1: 0.035 (0.017, 0.052)
lambda2: 0 (0, 0)
rho: 0.001 (0.001, 0.001)
time of change: 17
p-value: 0.001
Brazil_3 AMA
lambda: 0.006 (0.004, 0.009)
rho: 0.001 (0.001, 0.009)
Brazil_4 AMA
lambda: 0.002 (0.001, 0.004)
rho: 0.001 (0.001, 0.004)
Brazil_5 AMA
lambda: 0.004 (0.002, 0.007)
rho: 0.001 (0.001, 0.007)
Brazil_6 AMA
lambda: 0.002 (0, 0.005)
rho: 0.021 (0.021, 0.005)
Brazil_7 AMA
lambda: 0.002 (0, 0.008)
rho: 0.241 (0.241, 0.008)
Cambodia2004_/1−5/9 AMA
lambda1: 0.027 (0.013, 0.04)
lambda2: 0.003 (0.001, 0.004)
rho: 0.031 (0.031, 0.031)
time of change: 20
p-value: 0.005
Seroprevalence
Age

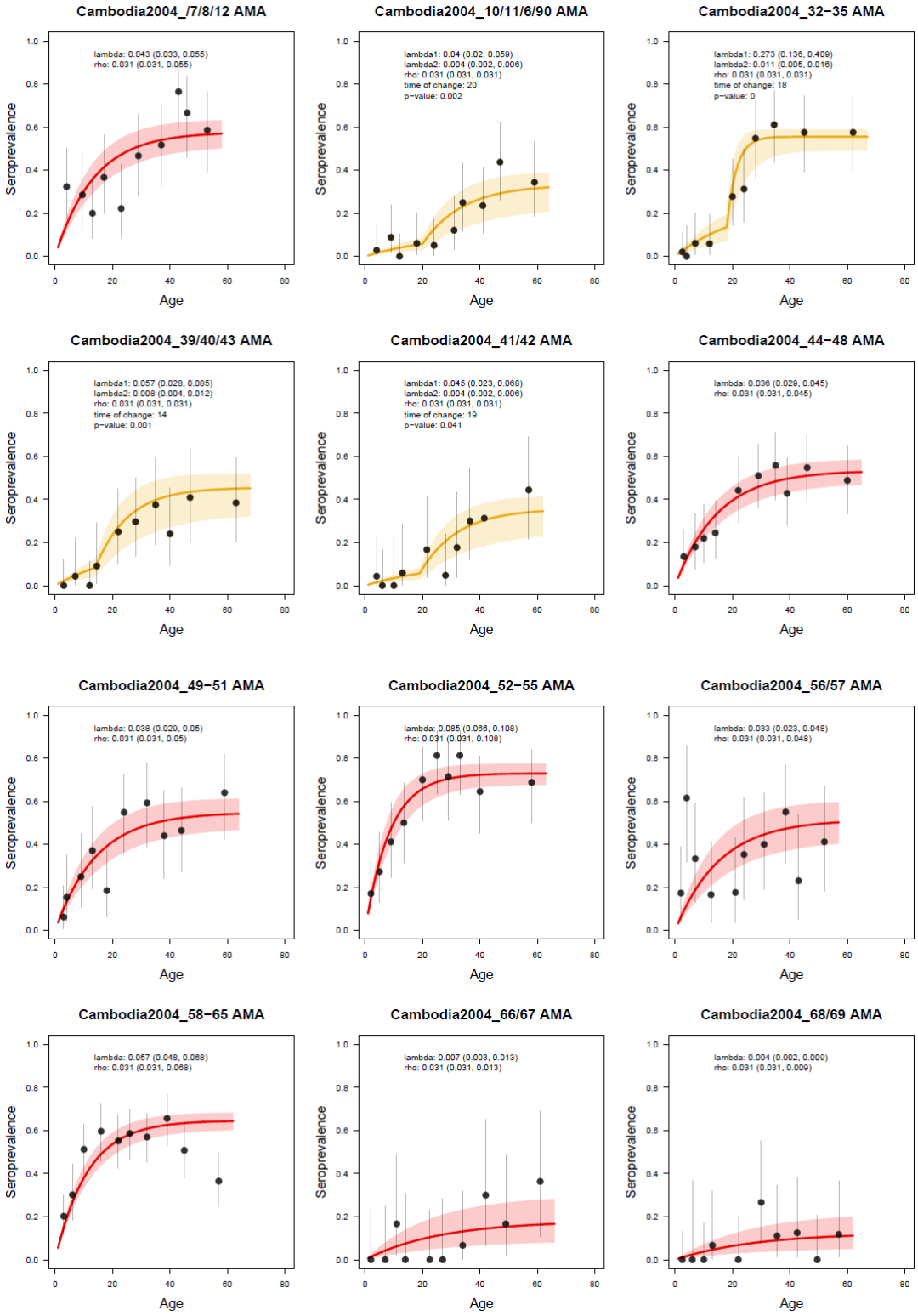
Cambodia2004_/7/8/12 AMA
lambda: 0.043 (0.033, 0.055)
rho: 0.031 (0.031, 0.055)
Cambodia2004_10/11/6/90 AMA
lambda1: 0.04 (0.02, 0.059)
lambda2: 0.004 (0.002, 0.006)
rho: 0.031 (0.031, 0.031)
time of change: 20
p-value: 0.002
Cambodia2004_32−35 AMA
lambda1: 0.273 (0.136, 0.409)
lambda2: 0.011 (0.005, 0.016)
rho: 0.031 (0.031, 0.031)
time of change: 18
p-value: 0
Cambodia2004_39/40/43 AMA
lambda1: 0.057 (0.028, 0.085)
lambda2: 0.008 (0.004, 0.012)
rho: 0.031 (0.031, 0.031)
time of change: 14
p-value: 0.001
Cambodia2004_41/42 AMA
lambda1: 0.045 (0.023, 0.068)
lambda2: 0.004 (0.002, 0.006)
rho: 0.031 (0.031, 0.031)
time of change: 19
p-value: 0.041
Cambodia2004_44−48 AMA
lambda: 0.036 (0.029, 0.045)
rho: 0.031 (0.031, 0.045)
Cambodia2004_49−51 AMA
lambda: 0.038 (0.029, 0.05)
rho: 0.031 (0.031, 0.05)
Cambodia2004_52−55 AMA
lambda: 0.085 (0.066, 0.108)
rho: 0.031 (0.031, 0.108)
Cambodia2004_56/57 AMA
lambda: 0.033 (0.023, 0.048)
rho: 0.031 (0.031, 0.048)
Cambodia2004_58−65 AMA
lambda: 0.057 (0.048, 0.068)
rho: 0.031 (0.031, 0.068)
Cambodia2004_66/67 AMA
lambda: 0.007 (0.003, 0.013)
rho: 0.031 (0.031, 0.013)
Cambodia2004_68/69 AMA
lambda: 0.004 (0.002, 0.009)
rho: 0.031 (0.031, 0.009)
Seroprevalence
Age

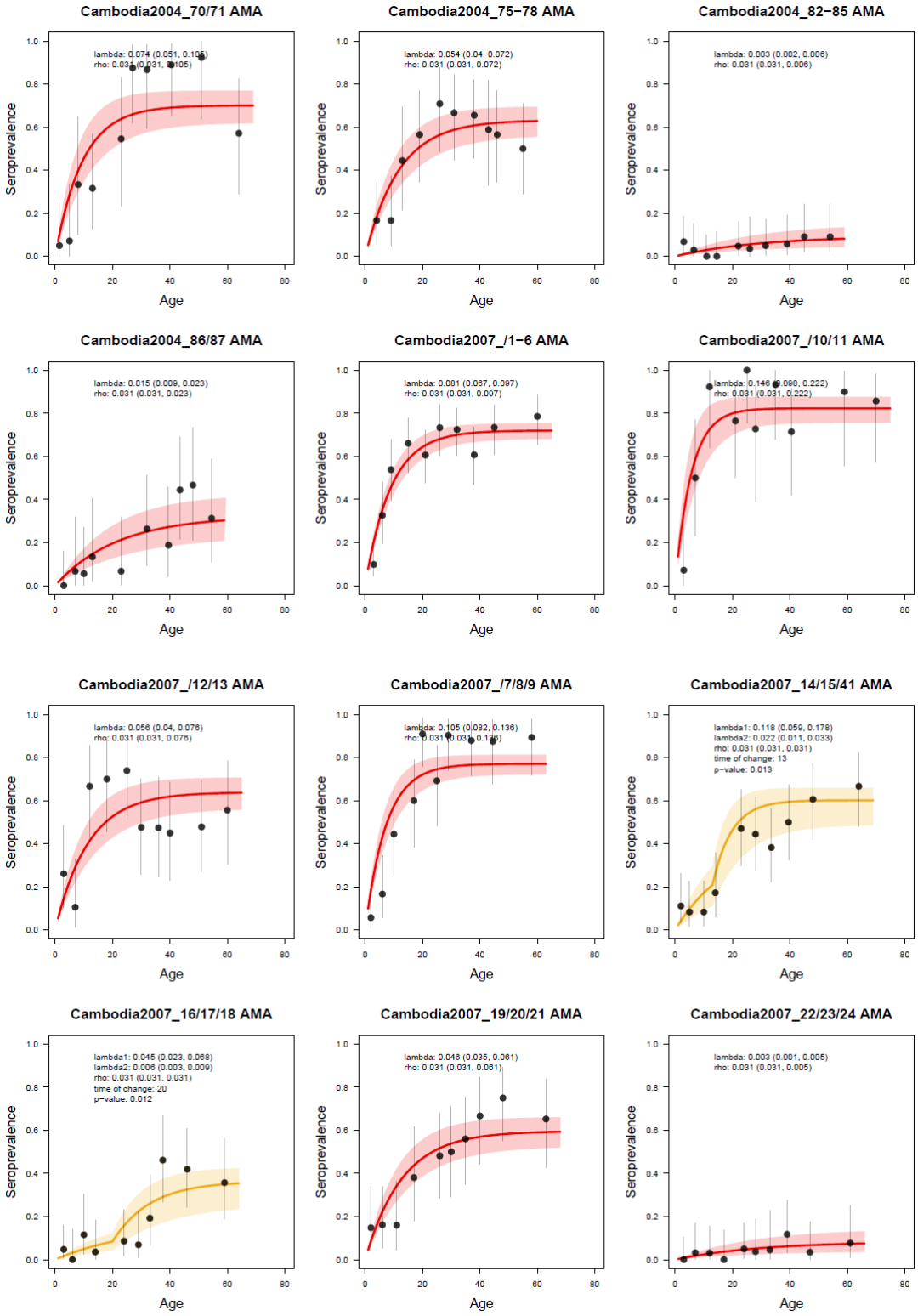
Cambodia2004_70/71 AMA
lambda: 0.074 (0.051, 0.105)
rho: 0.031 (0.031, 0.105)
Cambodia2004_75−78 AMA
lambda: 0.054 (0.04, 0.072)
rho: 0.031 (0.031, 0.072)
Cambodia2004_82−85 AMA
lambda: 0.003 (0.002, 0.006)
rho: 0.031 (0.031, 0.006)
Cambodia2004_86/87 AMA
lambda: 0.015 (0.009, 0.023)
rho: 0.031 (0.031, 0.023)
Cambodia2007_/1−6 AMA
lambda: 0.081 (0.067, 0.097)
rho: 0.031 (0.031, 0.097)
Cambodia2007_/10/11 AMA
lambda: 0.146 (0.098, 0.222)
rho: 0.031 (0.031, 0.222)
Cambodia2007_/12/13 AMA
lambda: 0.056 (0.04, 0.076)
rho: 0.031 (0.031, 0.076)
Cambodia2007_/7/8/9 AMA
lambda: 0.105 (0.082, 0.136)
rho: 0.031 (0.031, 0.136)
Cambodia2007_14/15/41 AMA
lambda1: 0.118 (0.059, 0.178)
lambda2: 0.022 (0.011, 0.033)
rho: 0.031 (0.031, 0.031)
time of change: 13
p−value: 0.013
Cambodia2007_16/17/18 AMA
lambda1: 0.045 (0.023, 0.068)
lambda2: 0.006 (0.003, 0.009)
rho: 0.031 (0.031, 0.031)
time of change: 20
p−value: 0.012
Cambodia2007_19/20/21 AMA
lambda: 0.046 (0.035, 0.061)
rho: 0.031 (0.031, 0.061)
Cambodia2007_22/23/24 AMA
lambda: 0.003 (0.001, 0.005)
rho: 0.031 (0.031, 0.005)
Seroprevalence
Age

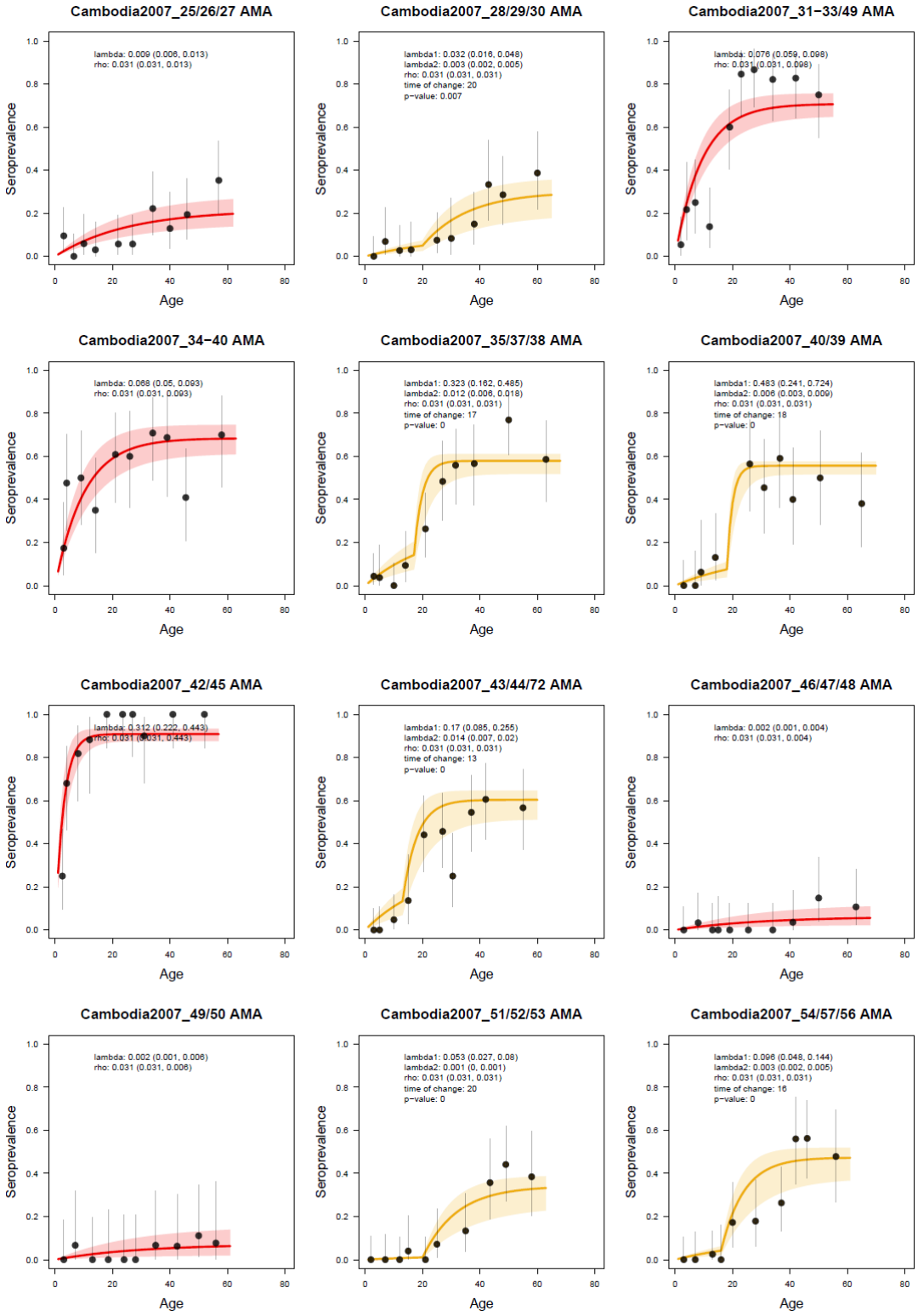
Cambodia2007_25/26/27 AMA
lambda: 0.009 (0.006, 0.013)
rho: 0.031 (0.031, 0.013)
Cambodia2007_28/29/30 AMA
lambda1: 0.032 (0.016, 0.048)
lambda2: 0.003 (0.002, 0.005)
rho: 0.031 (0.031, 0.031)
time of change: 20
p-value: 0.007
Cambodia2007_31−33/49 AMA
lambda: 0.076 (0.059, 0.098)
rho: 0.031 (0.031, 0.098)
Cambodia2007_34−40 AMA
lambda: 0.068 (0.05, 0.093)
rho: 0.031 (0.031, 0.093)
Cambodia2007_35/37/38 AMA
lambda1: 0.323 (0.162, 0.485)
lambda2: 0.012 (0.006, 0.018)
rho: 0.031 (0.031, 0.031)
time of change: 17
p-value: 0
Cambodia2007_40/39 AMA
lambda1: 0.483 (0.241, 0.724)
lambda2: 0.006 (0.003, 0.009)
rho: 0.031 (0.031, 0.031)
time of change: 18
p-value: 0
Cambodia2007_42/45 AMA
lambda: 0.312 (0.222, 0.443)
rho: 0.031 (0.031, 0.443)
Cambodia2007_43/44/72 AMA
lambda1: 0.17 (0.085, 0.255)
lambda2: 0.014 (0.007, 0.02)
rho: 0.031 (0.031, 0.031)
time of change: 13
p-value: 0
Cambodia2007_46/47/48 AMA
lambda: 0.002 (0.001, 0.004)
rho: 0.031 (0.031, 0.004)
Cambodia2007_49/50 AMA
lambda: 0.002 (0.001, 0.006)
rho: 0.031 (0.031, 0.006)
Cambodia2007_51/52/53 AMA
lambda1: 0.053 (0.027, 0.08)
lambda2: 0.001 (0, 0.001)
rho: 0.031 (0.031, 0.031)
time of change: 20
p-value: 0
Cambodia2007_54/57/56 AMA
lambda1: 0.096 (0.048, 0.144)
lambda2: 0.003 (0.002, 0.005)
rho: 0.031 (0.031, 0.031)
time of change: 16
p-value: 0
Seroprevalence
Age

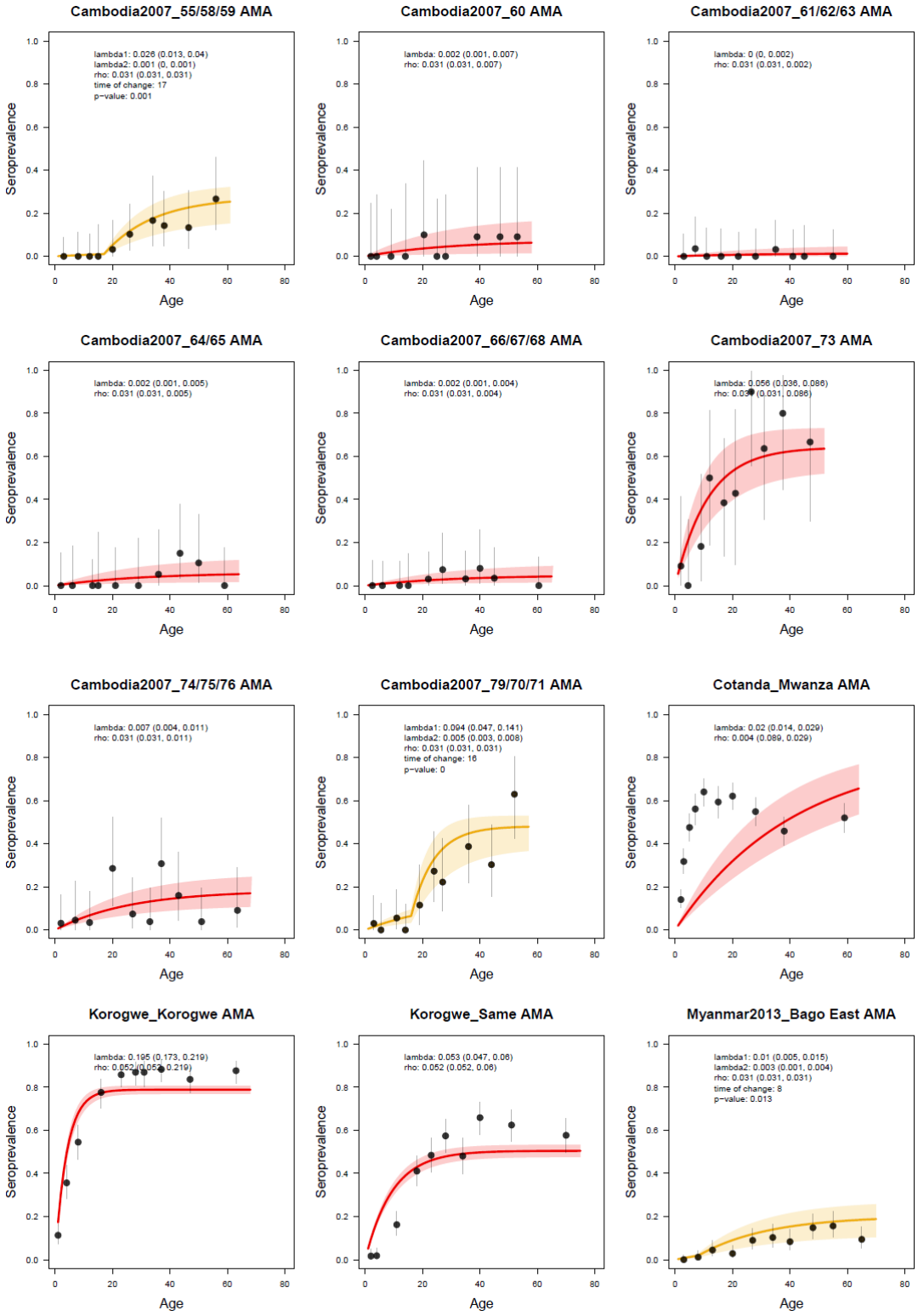
Cambodia2007_55/58/59 AMA
lambda1: 0.026 (0.013, 0.04)
lambda2: 0.001 (0, 0.001)
rho: 0.031 (0.031, 0.031)
time of change: 17
p−value: 0.001
Cambodia2007_60 AMA
lambda: 0.002 (0.001, 0.007)
rho: 0.031 (0.031, 0.007)
Cambodia2007_61/62/63 AMA
lambda: 0 (0, 0.002)
rho: 0.031 (0.031, 0.002)
Cambodia2007_64/65 AMA
lambda: 0.002 (0.001, 0.005)
rho: 0.031 (0.031, 0.005)
Cambodia2007_66/67/68 AMA
lambda: 0.002 (0.001, 0.004)
rho: 0.031 (0.031, 0.004)
Cambodia2007_73 AMA
lambda: 0.056 (0.036, 0.086)
Cambodia2007_74/75/76 AMA
lambda: 0.007 (0.004, 0.011)
rho: 0.031 (0.031, 0.011)
Cambodia2007_79/70/71 AMA
lambda1: 0.094 (0.047, 0.141)
lambda2: 0.005 (0.003, 0.008)
rho: 0.031 (0.031, 0.031)
time of change: 16
p−value: 0
Cotanda_Mwanza AMA
lambda: 0.02 (0.014, 0.029)
rho: 0.004 (0.089, 0.029)
Korogwe_Korogwe AMA
lambda: 0.195 (0.173, 0.219)
Korogwe_Same AMA
lambda: 0.053 (0.047, 0.06)
rho: 0.052 (0.052, 0.06)
Myanmar2013_Bago East AMA
lambda1: 0.01 (0.005, 0.015)
lambda2: 0.003 (0.001, 0.004)
rho: 0.031 (0.031, 0.031)
time of change: 8
p−value: 0.013
Seroprevalence
Age

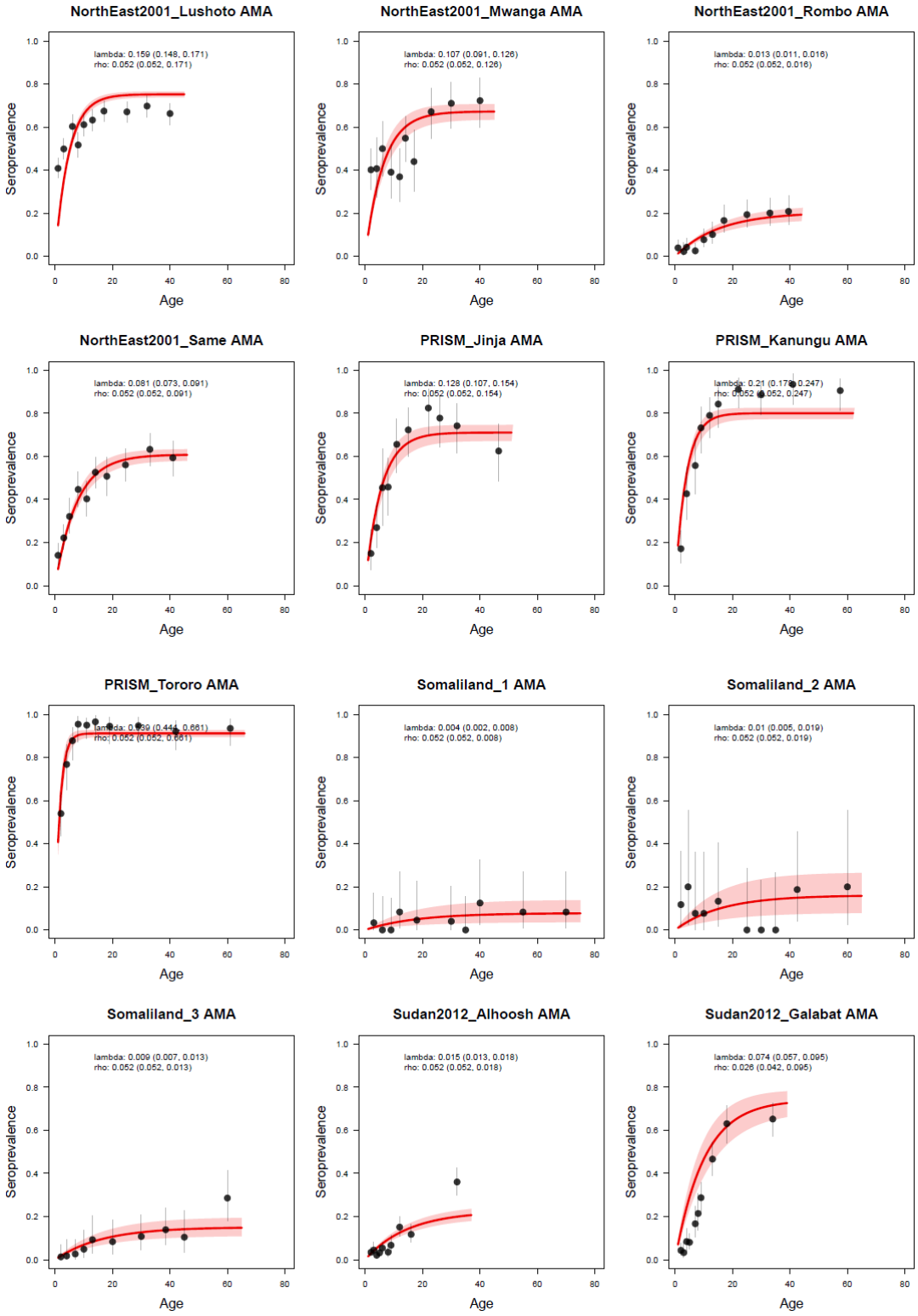
NorthEast2001_Lushoto AMA
lambda: 0.159 (0.148, 0.171)
rho: 0.052 (0.052, 0.171)
NorthEast2001_Mwanga AMA
lambda: 0.107 (0.091, 0.126)
rho: 0.052 (0.052, 0.126)
NorthEast2001_Rombo AMA
lambda: 0.013 (0.011, 0.016)
rho: 0.052 (0.052, 0.016)
NorthEast2001_Same AMA
lambda: 0.081 (0.073, 0.091)
rho: 0.052 (0.052, 0.091)
PRISM_Jinja AMA
lambda: 0.128 (0.107, 0.154)
rho: 0.052 (0.052, 0.154)
PRISM_Kanungu AMA
lambda: 0.21 (0.178, 0.247)
rho: 0.052 (0.052, 0.247)
PRISM_Tororo AMA
lambda: 0.539 (0.444, 0.661)
rho: 0.052 (0.052, 0.661)
Somaliland_1 AMA
lambda: 0.004 (0.002, 0.008)
rho: 0.052 (0.052, 0.008)
Somaliland_2 AMA
lambda: 0.01 (0.005, 0.019)
rho: 0.052 (0.052, 0.019)
Somaliland_3 AMA
lambda: 0.009 (0.007, 0.013)
rho: 0.052 (0.052, 0.013)
Sudan2012_Alhoosh AMA
lambda: 0.015 (0.013, 0.018)
rho: 0.052 (0.052, 0.018)
Sudan2012_Galabat AMA
lambda: 0.074 (0.057, 0.095)
rho: 0.026 (0.042, 0.095)
Seroprevalence
Age

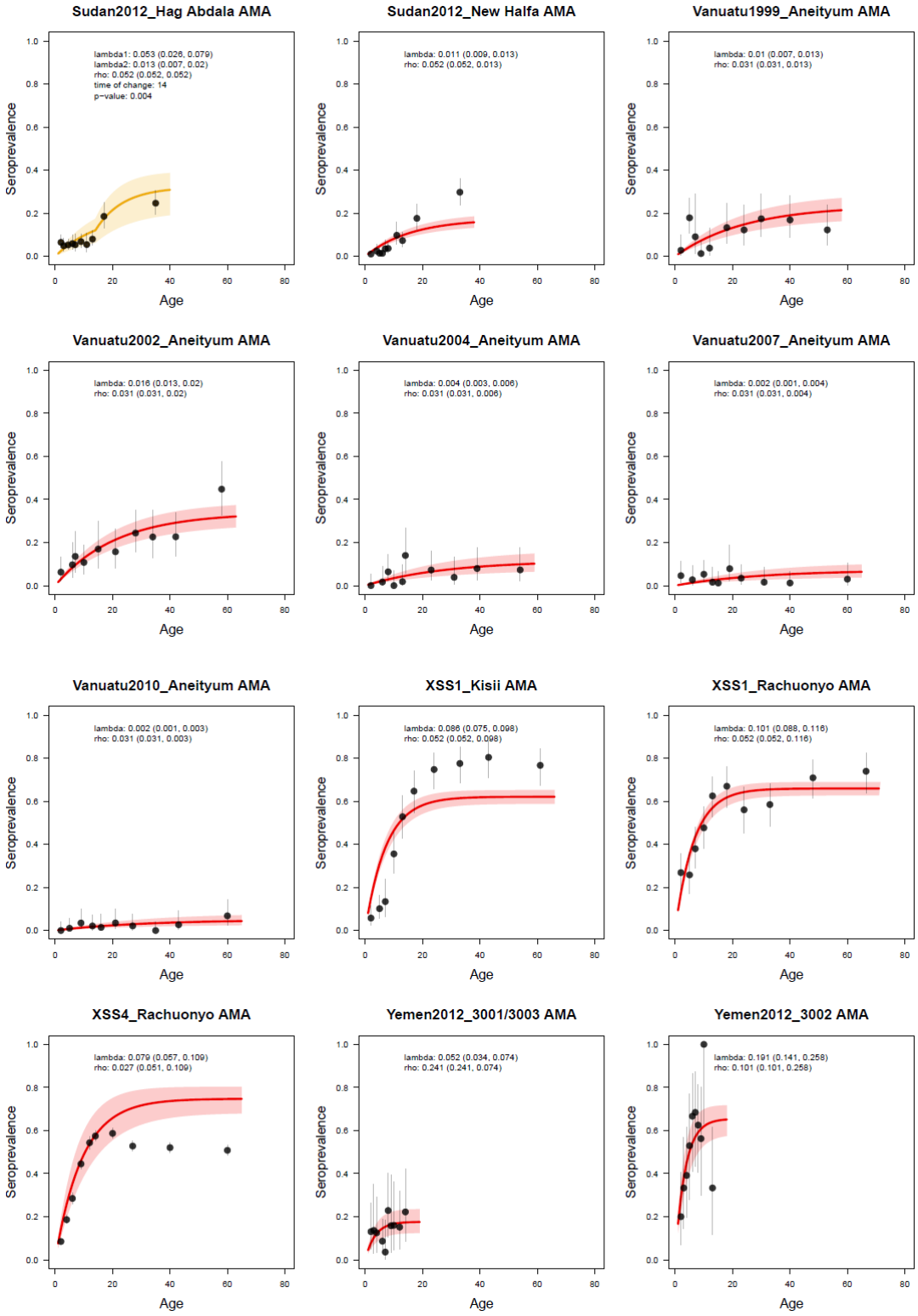
Sudan2012_Hag Abdala AMA
lambda1: 0.053 (0.026, 0.079)
lambda2: 0.013 (0.007, 0.02)
rho: 0.052 (0.052, 0.052)
time of change: 14
p−value: 0.004
Sudan2012_New Halfa AMA
lambda: 0.011 (0.009, 0.013)
rho: 0.052 (0.052, 0.013)
Vanuatu1999_Aneityum AMA
lambda: 0.01 (0.007, 0.013)
rho: 0.031 (0.031, 0.013)
Vanuatu2002_Aneityum AMA
lambda: 0.016 (0.013, 0.02)
rho: 0.031 (0.031, 0.02)
Vanuatu2004_Aneityum AMA
lambda: 0.004 (0.003, 0.006)
rho: 0.031 (0.031, 0.006)
Vanuatu2007_Aneityum AMA
lambda: 0.002 (0.001, 0.004)
rho: 0.031 (0.031, 0.004)
Vanuatu2010_Aneityum AMA
lambda: 0.002 (0.001, 0.003)
rho: 0.031 (0.031, 0.003)
XSS1_Kisii AMA
lambda: 0.086 (0.075, 0.098)
rho: 0.052 (0.052, 0.098)
XSS1_Rachuonyo AMA
lambda: 0.101 (0.088, 0.116)
rho: 0.052 (0.052, 0.116)
XSS4_Rachuonyo AMA
lambda: 0.079 (0.057, 0.109)
rho: 0.027 (0.051, 0.109)
Yemen2012_3001/3003 AMA
lambda: 0.052 (0.034, 0.074)
rho: 0.241 (0.241, 0.074)
Yemen2012_3002 AMA
lambda: 0.191 (0.141, 0.258)
rho: 0.101 (0.101, 0.258)
Seroprevalence
Age

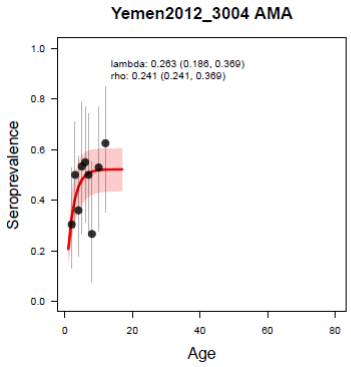
Yemen2012_3004 AMA
lambda: 0.263 (0.186, 0.369)
rho: 0.241 (0.241, 0.369)
Seroprevalence
Age

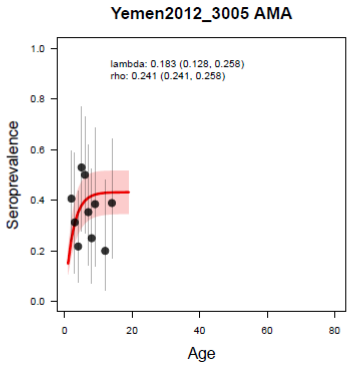
Yemen2012_3005 AMA
lambda: 0.183 (0.128, 0.258)
rho: 0.241 (0.241, 0.258)
Seroprevalence
Age

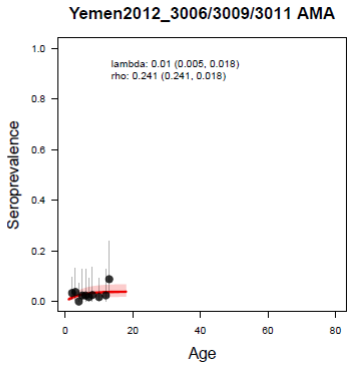
Yemen2012_3006/3009/3011 AMA
lambda: 0.01 (0.005, 0.018)
rho: 0.241 (0.241, 0.018)
Seroprevalence
Age

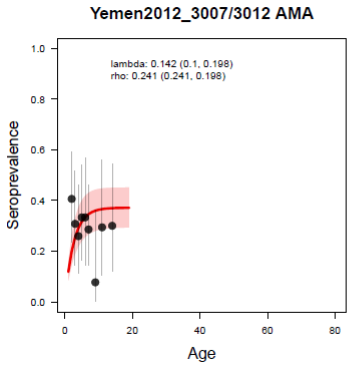
Yemen2012_3007/3012 AMA
lambda: 0.142 (0.1, 0.198)
rho: 0.241 (0.241, 0.198)
Seroprevalence
Age

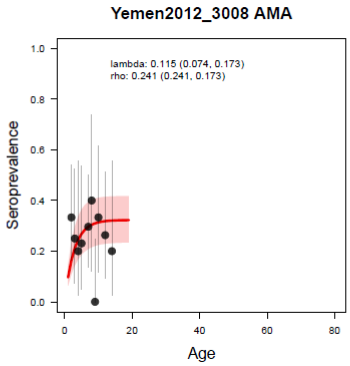
Yemen2012_3008 AMA
lambda: 0.115 (0.074, 0.173)
rho: 0.241 (0.241, 0.173)
Seroprevalence
Age

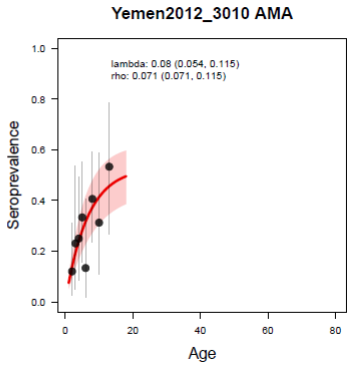
Yemen2012_3010 AMA
lambda: 0.08 (0.054, 0.115)
rho: 0.071 (0.071, 0.115)
Seroprevalence
Age

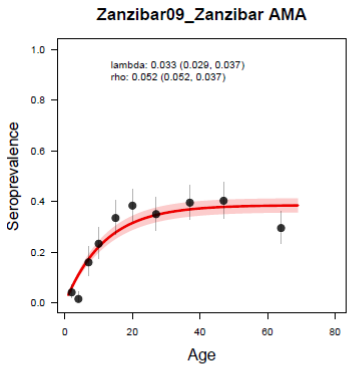
Zanzibar09_Zanzibar AMA
lambda: 0.033 (0.029, 0.037)
rho: 0.052 (0.052, 0.037)
Seroprevalence
Age

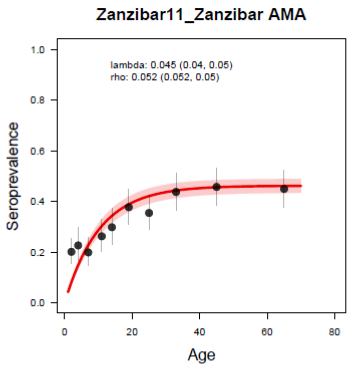
Zanzibar11_Zanzibar AMA
lambda: 0.045 (0.04, 0.05)
rho: 0.052 (0.052, 0.05)
Seroprevalence
Age

Appendix 4.3 Parameter estimates for sero-conversion rate vs. parasite rate relationships

A. Overall model - precision of model fit inverse weighted by log variance of SCR estimate from reverse catalytic model
B. Age subsets - same as model A, but PCR prevalence based on different age subsets (2-10 year olds, 5-15 year olds)
C. Adjusted for geographical region - Africa & Middle East (β1) , Asia (β2), Americas (β3)

***Pf*MSP1$_{19}$**

	Description	Parameter estimates (95% credible interval)					DIC values		
	***Pf*MSP 1$_{19}$**	α_0	α_1	β_1	β_2	β_3	**DIC**	**Mean Deviance**	**pD**
A	**Overall**	-2.66 (-2.75, -2.57)	0.28 (0.21, 0.36)	--	--	--	-332.6	-342.1	9.543
	PCR prevalence <20% only	-3.26 (-3.71, -2.79)	0.07 (-0.05, 0.24)	--	--	--	-289.6	-298.5	8.884
	PCR prevalence >20% only	-2.65 (-2.75, -2.56)	0.26 (0.12, 0.40)	--	--	--	-41.92	-45.08	3.161
B	**PCR prevalence based on all ages (Africa only)**	-2.70 (-2.81, -2.61)	0.20 (0.13, 0.29)	--	--	--	-99.92	-103.5	3.605
	PCR prevalence based on 2-10 year olds only	-2.67 (-2.77, -2.59)	0.23 (0.16, 0.31)	--	--	--	-115.5	-119.3	3.829
	PCR prevalence based on 5-15 year olds only	-2.78 (-2.89, -2.70)	0.16 (0.10, 0.24)	--	--	--	-95.06	-98.69	3.63
C	**By geographical region**	-3.34 (-4.59, -1.49)	0.26 (0.17, 0.34)	0.67 (-1.17, 1.92)	0.58 (-1.29, 1.87)	-0.58 (-1.94, 1.17)	-336.9	-347.7	11.49
	By geographical region (PCR prevalence <20% only)	-3.67 (-5.11, -1.88)	0.09 (-0.02, 0.25)	0.61 (-1.15, 1.94)	0.17 (-1.62, 1.63)	-0.60 (-1.94, 1.23)	-295.2	-305.5	10.37
	By geographical region (PCR prevalence >20% only)	-2.36 (-4.11, -0.74)	0.28 (0.13, 0.41)	-0.30 (-1.92, 1.45)	0.18 (-1.49, 1.89)	-0.006 (-1.90, 1.89)	-45.3	-49.56	4.259

***Pf*AMA1**

	Description	Parameter estimates (95% credible interval)					DIC values		
	***Pf*AMA1**	α_0	α_1	β_1	β_2	β_3	**DIC**	**Mean Deviance**	**pD**
A	**Overall**	-1.50 (-1.57, -1.44)	0.71 (0.65, 0.78)	--	--	--	100.4	74.17	26.21
	PCR prevalence <20% only	-0.54 (-0.69, -0.40)	0.98 (0.92, 1.00)	--	--	--	-81.23	-100.9	19.71
	PCR prevalence >20% only	-1.61 (-1.68, -1.54)	0.83 (0.75, 0.92)	--	--	--	108.9	99.45	9.495
B	**PCR prevalence based on all ages (Africa only)**	-1.52 (-1.57, -1.46)	0.59 (0.52, 0.66)	--	--	--	193.6	182.9	10.64
	PCR prevalence based on 2-10 year olds only	-1.62 (-1.68, -1.56)	0.50 (0.44, 0.57)	--	--	--	140.2	129.3	10.87
	PCR prevalence based on 5-15 year olds only	-1.78 (-1.85, -1.71)	0.60 (0.53, 0.69)	--	--	--	67.96	57.12	10.84
C	**By geographical region**	-2.59 (-4.48, -0.94)	0.57 (0.50, 066)	1.07 (-0.59, 1.96)	0.72 (-0.92, 1.66)	-0.99 (-1.96, 0.54)	126.5	102.1	24.48
	By geographical region (PCR prevalence <20% only)	-1.50 (-2.29, -0.41)	0.71 (0.57, 0.87)	1.32 (0.27, 1.97)	0.07 (-0.99, 0.79)	-1.40 (-1.98, -0.36)	-149.1	-168.2	19.08
	By geographical region (PCR prevalence >20% only)	-1.88 (-3.49, -0.31)	0.76 (0.68, 0.88)	0.27 (-1.30, 1.87)	-0.40 (-1.91, 1.31)	0.002 (-1.89, 1.91)	113.7	102.1	11.55

Chapter 5 Validating serological markers of malaria infection using a multiplex immunoassay

Serology is a potentially promising new tool for use in malaria surveillance, but the correlation of candidate biomarkers with existing measures of malaria incidence requires validation. Chapter 5a presents work to standardise laboratory data from the Luminex multiplex immunoassay specifically for use in epidemiological evaluation. Chapter 5b assesses the accuracy and precision of serological biomarkers in estimating recent *P. falciparum* infection in endemic settings.

5.1 Background

As introduced in Chapters 3 and 4, serology may be a promising diagnostic tool in low-transmission settings, where clinical and molecular measures of infection have limited sensitivity.[248] However, currently used assays and serological markers are not optimised to measure individual-level or recent infections. Improving serological platforms to address this gap could have potential utility in both routine surveillance and cluster-randomised trials.

P. falciparum presents a diverse array of antigens to the human immune system throughout the parasite life cycle, all eliciting antibody responses with varying magnitudes and kinetics. This provides a large and diverse set of potential markers for malaria infection from which to select.[262] Correlating existing measures of malaria infection with antibody responses from a variety of *Pf* antigens can guide the selection of biomarkers for use in multiplexed sero-surveillance tools.

Previous studies based on protein microarray have investigated antibody responses for up to thousands of *Pf* antigens, evaluating their association with malaria infection.[262,263] However, studies on post-infection antibody kinetics in endemic settings are limited.[264] Most describe long-lived antibody responses to small subsets of antigens or focus on children and pregnant women.[166,170,212,265–267] These are practical easy-access groups to target for sentinel surveillance, but demographic-wide biomarkers of infection may also still have utility, particularly in regions where transmission is associated with older ages or other high-risk groups (e.g., forest, mining, or fishing industries; displaced or migrant populations)[62,268].

Current estimates of antibody dynamics remain imprecise because kinetics models require frequently sampled longitudinal data, reliable data on previous infection, and population representative sample sizes.[262,265] For the better part of the last 10 years, cost-effectively doing so with immunoassays has been limited by the state of the art. The majority of sero-epidemiological studies measure antibody response by enzyme-linked immunosorbent assay (ELISA). While cost-effective for high-throughput analysis of a single antigen (or combined response to multiple antigens), the processing time and relatively large sample volumes make it less efficient for the evaluation of multiple analyte-specific responses. Conversely, protein microarray allows high throughput analysis of thousands of analytes at a time,[269,270] but is still a prohibitively expensive technology and limited by sample processing time.

Quantitative suspension array technologies (qSAT), such as the Luminex MAGPIX© (Luminex Corp, Austin TX), are now available as affordable mid-high throughput multiplexing platforms. They offer several advantages over ELISA and microarray for large-scale epidemiological screening, including the simultaneous quantification of 50-500 proteins in a single well and the use of standard 96-well plates with as little as 5µl of plasma or serum.[271–273] The Luminex assay has also

been shown to measure a larger dynamic range of antibody response compared to ELISA,[274,275] though this has yet to be validated for the specific analytes in the work presented here.

In this study, human antibody responses to 24 *Pf* antigens were quantified using the Luminex platform based on samples from an all-age longitudinal cohort study in The Gambia. The first section discusses assay procedures and methods to standardise Luminex data for epidemiological analysis based on samples from The Gambia and Namibia. The second section aims to estimate the rate of antibody decay after malaria infection and to evaluate how *Pf* antibody responses can be used as estimators of time since previous malaria infection. Subsequent chapters will describe the use of these biomarkers to measure cluster-level differences in transmission in The Gambia and Namibia.

Chapter 5a. Optimisation of Luminex assay procedures and data standardisation

5.2 Methods

Laboratory methods

Antigen panel and microsphere coupling

A multiplex panel was developed for the Luminex MAGPIX© suspension bead array containing 24 *Pf* recombinant proteins (1 sporozoite surface, 23 erythrocytic) (Table 5.1). Antigens were selected from an initial screen of 856 candidates on the protein microarray assay based on their correlation with previous malaria infection in children.[262] Four antigens were excluded from final analysis either due to universally low signals below 500 mean fluorescence intensity (MFI) units (H101, EPFv1) or because they were redundant fragments of antigens already included in the panel (Etramp5.Ag2, Etramp4.Ag1 were non-immunogenic fragments of Etramp5.Ag1 and Etramp4.Ag2 respectively). Recombinant antigens were coupled to MagPlex© COOH-microspheres or 'beads' (Luminex Corp., Austin TX) following the protocol described by Luminex Corparation.[276] Optimal coupling concentration for each antigen was based on the mid-point of the dose-response curve (EC_{50}) of a 6-dilution serial titration of the antigen. Glutathione S-transferase (GST) coupled beads were included as a control to test for GST-specific immunoglobulin (IgG) response against GST-tagged fusion proteins (Table 5.1). Beads coupled with tetanus toxoid vaccine protein were also included as controls.

Sample preparation and assay procedures

Gambian blood samples were eluted from a 6mm dried blood spot (DBS) punch, corresponding to 4 µl of whole blood, and shaken overnight at room temperature in 200 µl of protein elution buffer containing phosphate buffered saline (PBS) (pH 7.2), 0.05% sodium azide and 0.05% Tween-20, yielding an initial 1:50 sample dilution. At least one day prior to assay processing, samples were further diluted to a final 1:500 dilution using 10 µl of the 1:50 pre-dilution sample and 90 µl of blocking Buffer B to prevent non-specific binding (1xPBS, 0.05% Tween, 0.5% bovine serum albumin (BSA), 0.02% sodium azide, 0.1% casein, 0.5% polyvinyl alcohol (PVA), 0.5% polyvinyl pyrrolidone (PVP) and 1,500 µg/ml *E.coli* extract). Negative and positive controls were also incubated one day prior in Buffer B, with negative controls prepared at a 1:500 dilution and Gambian pooled positive controls in a 6-point 5-fold serial dilution (1:10 – 1:31,250). Two wells on each plate containing only antigen-coupled beads and Buffer B, but absent of any human serum, were included to measure background signal. For analysis of individual-level antibody kinetics, all samples from the same individual were processed on a single plate to remove the influence of plate variation when quantifying antibody response over time. The positive control was based on a pool of 22 serum samples from malaria hyper-immune individuals in The Gambia,

and ten individual plasma samples from European malaria-naive adults were used as negative controls.

For Namibian samples, a 1:50 pre-dilution was made using plasma samples, isolated from 250 µl of whole blood collected in BD Microtainer tubes with EDTA additive, and diluted to a final 1:400 sample dilution as described above. A pool of sera samples from 100 hyper-immune Tanzanian individuals as well as a WHO malaria reference lyophilised serum reagent (NIBSC 10-198)[277] were used as a positive controls with a 6-point 5-fold serial dilution standard curve. European malaria-naïve adults were used as negative controls, as described above.

General assay procedures were as follows. First, an initial mixture containing 8 µl of each antigen-coupled microsphere set and 5 ml of Buffer A (1xPBS, 0.05% Tween, 0.5% bovine serum albumin (BSA), 0.02% sodium azide) was prepared, yielding approximately 1,000 beads per region per well. Next, 50 µl of this combined microsphere mixture was added to a 96-well flat bottom plate (BioPlex Pro™, Bio-Rad Laboratories, UK) and washed once with 100 µl of PBS-Tween (1xPBS, 0.05% Tween-20) on a magnetic washer (Bio-Plex Pro for Gambian samples and BioPlex Magnetic Hand Washer for Namibian samples). 50 µl of samples and controls were added to the plate and incubated in the dark at room temperature (RT) on a microplate shaker at 500 rpm for 90 minutes. Following three washes, 50 µl of fluorescent secondary antibody (Jackson Immuno 109-116-098: Goat Anti-human Fcy-fragment specific IgG conjugated to R-Phycoerythrin (R-PE)), diluted to a 1:200 dilution with Buffer A, was added to all wells and incubated for 90 minutes in the dark at RT at 500 rpm. After a further three washes, the plate was incubated in 50 µl of Buffer A for 30 minutes. Plates had an additional wash and, after a final addition of 100 µl 1xPBS, were read using the Luminex MAGPIX© analyser. At least 50 beads per analyte were acquired per sample and median fluorescent intensity (MFI) data were used for analysis.

Table 5.1 Summary of antigens in multiplex Luminex panel

Antigens that were included in the assay, but not in the final analysis due to low signal (Etramp5.Ag2, Etramp4.Ag1, EPFv1, H101), are not listed.

Gene ID	Antigen name	Allele	Antigen concentration (ng/5000 beads)	Expression	Location	Description	Reference
PF3D7_0930300	*Pf* MSP1.19	Wellcome	16.924	GST	Merozoite surface	19kDa fragment of MSP1 molecule	[278]
PF3D7_1133400	*Pf* AMA1	FVO	1.56	His_{x6}	Sporozoite / Merozoite	Apical membrane antigen 1	[279]
PF3D7_1035300	*Pf* GLURP.R2	F32	3.688	N/A	Merozoite	Glutamate rich protein R2	[280]
PF3D7_0731500	EBA175 RIII-V	3D7	163.328	GST	Merozoite	Erythrocyte binding antigen-175	[281]
PF3D7_0102500	EBA181 RIII-V	3D7	97.76	GST	Merozoite	Erythrocyte binding antigen-181	[281]
PF3D7_1301600	EBA140 RIII-V	3D7	97.62	GST	Merozoite	Erythrocyte binding antigen-140	[281]
PF3D7_0424100	Rh5	3D7	5.48	C-tag	Merozoite	Reticulocyte binding protein homologue 5	[282]
PF3D7_1335400	Rh2.2030	D10	97.72	GST	Merozoite	Reticulocyte binding protein homologue 2	[283]
PF3D7_0424200	Rh4.2	3D7	1.744	His_{x6}	Merozoite	Reticulocyte binding protein homologue 4	[284]
PF3D7_0532100	Etramp5.Ag1	3D7	13.972	GST	iRBC/PVM	Early transcribed membrane protein 5	[285]
PF3D7_0423700	Etramp4.Ag2	3D7	72.004	GST	iRBC/PVM	Early transcribed membrane protein 4	[285]
PF3D7_0402400	GexP18	3D7	250	GST	Gametocytes	Gametocyte exported protein 18	[262]
PF3D7_0501100.1	HSP40.Ag1	3D7	17.016	GST	iRBC / Gametocytes	Heat shock protein 40, type II	[262]
PF3D7_1021800	*Pf* SEA-1	3D7	8.68	GST	Schizont / Maurer's cleft	Schizont egress antigen 1	[286]
PF3D7_1002000	Hyp2	3D7	250	GST	iRBC / PVM	Plasmodium exported protein	[262]
PF3D7_0206800	*Pf* MSP2.Dd2	Dd2	0.116	GST	Merozoite surface	Merozoite surface protein 2, Dd2 allele	[287]
PF3D7_0206800	*Pf* MSP2.Ch150	Ch150/9	0.076	GST	Merozoite surface	Merozoite surface protein 2, Ch150/9 allele	[287]
PF3D7_1036000	*Pf* MSP11/H103	3D7	46.88	GST	Merozoite	Merozoite surface protein 11/H101/MSP3.7	[288]
PF3D&_0501300	SBP1	3D7	97.776	GST	Schizont / Maurer's cleft	Skeleton-binding protein 1	[289]
PF3D7_0304600	*Pf* CSP	3D7	107.776	--	Sporozoite surface	Circumsporozoite (CS) protein	[290]
--	GST	--	34.396	--	--	GST expression tag	
--	TT	--	24.608	--	--	Tetanus Toxoid	

*infected red blood cell – iRBC; parasitophorous vacuole membrane – PVM, glutathione S –transferase - GST

Quality control

Levey-Jennings charts[291] were used to plot the mean MFI values of three concentrations from the positive control standard curve (high - 1:10, medium - 1:50, and low - 1:250) as well as the background values for each plate (Figure 5.2). The acceptable range of MFI values for inclusion in the study was defined as the mean +/- two standard deviations of a subset of ten reference plates (selected based on the quality and consistency of their standard curve values). Plates with MFI values outside this range for at least two standard curve dilutions and at least three antigens were rejected and repeated. Points on the Levey-Jennings plots were ordered by date of plate processing to monitor bead stability over time.

Statistical analyses

Immunoassay data normalisation

Analysis of continuous antibody response was conducted in normalised MFI. Standard curves of antibody concentrations versus MFIs were fitted using a 4-parameter logistic equation[292–294]:

$$MFI = MFI_{max} + \frac{(MFI_{min} - MFI_{max})}{\left[1+\left(\frac{conc}{MFI_{50}}\right)^{slope}\right]} \quad (5.1)$$

where MFI_{max} is the upper asymptote or maximum MFI response of the standard curve, MFI_{min} is the lower asymptote or minimum MFI response of the standard curve, MFI_{50} is 50% of MFI_{max}, *conc* is the sample concentration from the serial dilution, and *slope* is Hill coefficient or slope factor of the dose-response curve (Figure 5.1). EC_{50} is the concentration or dilution that corresponds to MFI_{50}.

Figure 5.1 Four-parameter dose-response curve

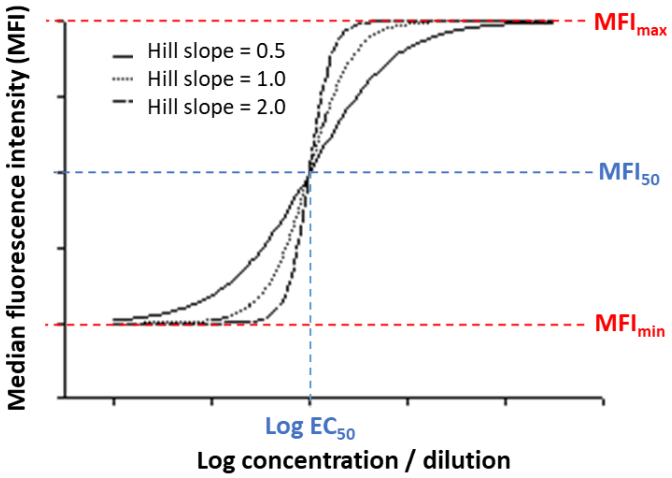

Data were normalised to adjust for between plate variation using a loess normalisation method.[295] This involved the selection of ten reference plates based on the quality and consistency of their standard curve fits from equation 5.1. For each antigen, a composite standard

curve was computed by calculating the mean MFI values for the reference plates for 100 concentrations between the highest and lowest concentration on the standard curve. For each plate, the plate-to-reference standard curve MFI difference (ΔMFI) was calculated for these 100 concentration points and a loess regression fit to ΔMFI as a function of mean MFI. The raw MFI data for all samples on the plate were then adjusted by the predicted ΔMFI based on the loess regression fit. Data were not corrected for background signal given that the between plate variation was already accounted for in the loess normalisation and all background MFIs were below 30 and therefore negligible.

Binary antibody responses were based on antigen-specific sero-positivity thresholds calculated using one of two methods. A two-component finite mixture model (FMM) (using the *normalmixEM* command in the *mixtools* R package) was fitted to log MFI of all cross-sectional serology samples from The Gambia (West Coast and Upper River Region, June 2013 and December 2013), with the cut-off defined as the mean log MFI plus two standard deviations of the 'sero-negative' component. Alternatively, for antigens where distinct 'sero-negative' and 'sero-positive' components could not be distinguished using the mixture model, sero-positivity threshold was based on the mean MFI plus three standard deviations of 71 European malaria-naïve negative controls (Figure 5.6, Table 5.2).

Estimating antigen-specific limits of quantification

Lower and upper limits of quantification (LLOQ and HLOQ respectively) were estimated for each plate and antigen using standard curves fit with equation 5.1. The LLOQ MFI was defined as the MFI value where the upper 95%CI of the MFI_{min} parameter estimate equals the lower 95%CI of the standard curve estimate, and the HLOQ MFI where the lower 95%CI of the MFI_{max} parameter estimate equals the upper 95%CI of the standard curve estimate.[293] The mean LLOQ and HLOQ values were then calculated across all plates as overall LOQ values for the whole batch.

5.3 Results

Quality control. For samples from The Gambia, a total of 7,868 field blood samples were analysed across 96 96-well plates. After quality control assessment based on standard curves, three plates fell outside the acceptable range of MFI values and were repeated. Visual inspection of Levey-Jennings charts suggest there was no clear change in positive control MFI values over time, indicating negligible degradation of bead quality after shipment of reagents from the United Kingdom to The Gambia and stability of the Luminex MAGPIX© machine during the two months of sample processing.

For samples from Namibia, a total of 4,125 plasma samples were analysed across 52 96-well plates. After quality control assessment, seven plates fell outside the acceptable range of MFI values and were repeated. Data for five samples could not be matched to relevant epidemiological data and were excluded, yielding a total of 4,120 samples for analysis. Positive control MFI values over time appeared consistent based on Levey-Jennings charts and therefore, similar to The Gambia data, did not warrant a more formal statistical test (e.g., segmented regression) to check for significant changes in MFI signal.

The response to GST-coupled beads across the entire sampled population was generally low (median MFI 163, interquartile range (IQR) 89 – 274 MFI), indicating that non-specific background reactivity to GST was extremely low. Therefore, no adjustment for GST signal was conducted, as these values were in a range of MFI that are negligible. The use of tetanus toxoid as a positive control also showed that there was a standard distribution of antibody responses to TT-coupled beads, with a median MFI of 4,161 across the sampled population (IQR 372 – 12,647). The variability in MFI response likely reflects both variation in vaccination coverage and/or additional booster vaccinations given to women of child-bearing age, according to national policy in The Gambia for the prevention of maternal and neonatal tetanus.

Data normalisation. Proportional differences in plate-specific MFI values compared with mean MFI values of reference plates were dependent on the MFI range (Figure 5.3). In other words, MFIs in the higher end of responses could show larger between plate variations than MFIs in the lower end of responses (or vice versa) and may not be easily adjusted for using one proportional factor across the full range of MFI values. These extent of these variations differed by plate and antigen. The loess normalisation methods allowed for raw data to be adjusted and weighted according to MFI range-specific differences (Figure 5.3).

Limits of quantification. The MFI and antibody concentration range within the limits of quantification (LOQ) varied by antigen (Figure 5.4). For all antigens, the LLOQ was distinguishable from the upper limit of blank (LOB), as determined by the mean MFI value of background controls across plates (Figure 5.5). However, the range of LOQ for some antigens was small (e.g., Etramp5.Ag1 and $MSP1_{19}$), invalidating its practical use for setting sample exclusion criteria as more than half of the data would be excluded. Therefore, no LOQs were used to set data exclusion criteria for the data in this study.

Sero-positivity thresholds. Using the FMM method, sero-negative and sero-positive populations could not be distinguished for a number of antigens in both The Gambian and Namibian datasets (Figure 5.6). Additionally, for some antigens, while a sero-negative population could be estimated, the cut-off value based on the mean plus three standard deviations of non malaria-exposed negative controls was higher than the sero-negative component estimated with the

FMM, suggesting either that endemic and non-endemic individuals have similar sero-negative thresholds or the FMM model is not an accurate method for determining sero-negative populations. Therefore, for these antigens, negative controls were used as a more conservative estimate of sero-negativity. The final cut-off values used in analysis for all Luminex serology presented are listed in Table 5.2 for The Gambia and Namibia respectively.

Figure 5.2 Levey Jennings charts for quality control

Solid points represent the MFI values of positive controls, ordered left to right by date of plate processing. Solid horizontal lines represent mean positive control MFI of the reference plates and the dotted lines represent MFI values of either one or two standard deviations from the mean.

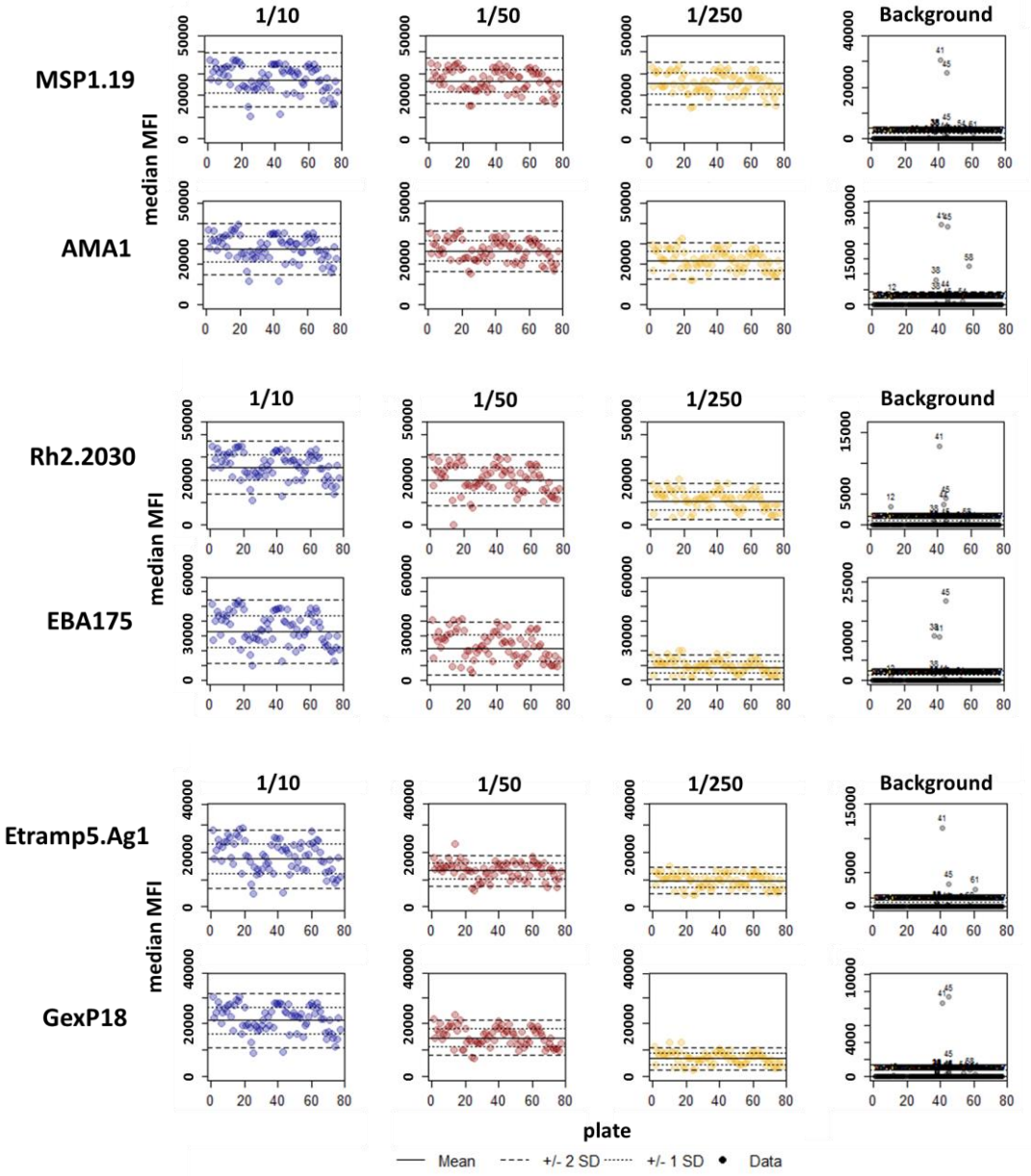

Figure 5.3 Example of loess regression normalisation methods

Loess regression fit to difference between plate MFI and mean MFI of reference standard curves (left) and raw vs. normalised MFI values (right). On the left, black points represent the observed MFI difference between plate-specific standard curve values and mean standard curve values of the reference plates, red line is the loess fit of ΔMFI as a function of reference mean MFIs, and blue line is a linear regression fit of ΔMFI as a function of reference mean MFIs. On the right, red diagonal line represent points where the raw and normalised MFI values are equal and black points represent the raw MFI value on the x-axis and the normalised MFI value on the y-axis for all samples on a plate.

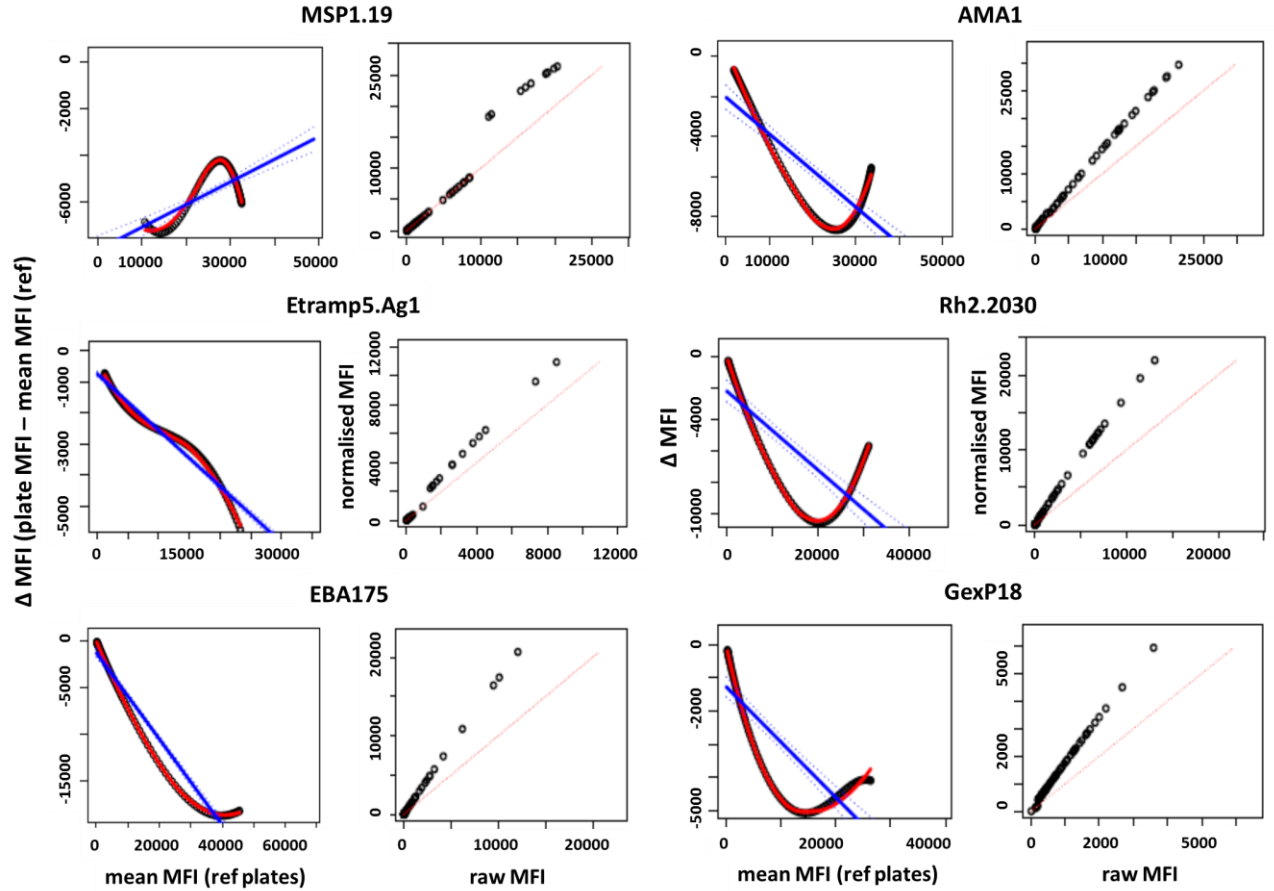

Figure 5.4 Examples of standard curve and limits of quantification estimation

Black points represent the observed MFI values for serial dilutions of the positive control, black solid line represents the standard curve fit, grey shaded area represents the 95%CI of the standard curve fit, blue solid and dotted horizontal lines are the mean and 95%CI estimates MFI_{min} and MFI_{max}, red vertical lines are the estimated LLOQ and HLOQ, and green horizontal lines are the background MFI.

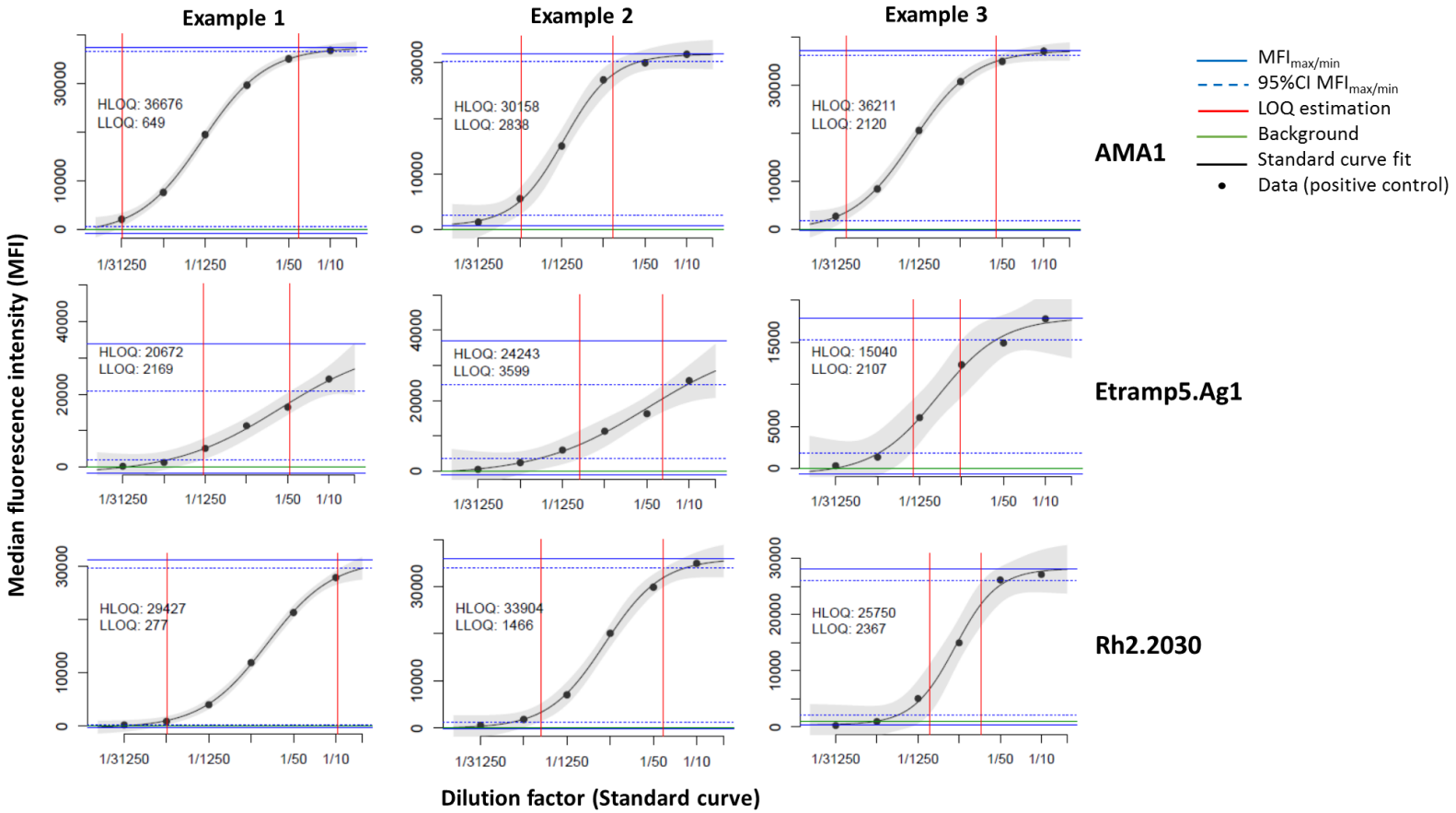

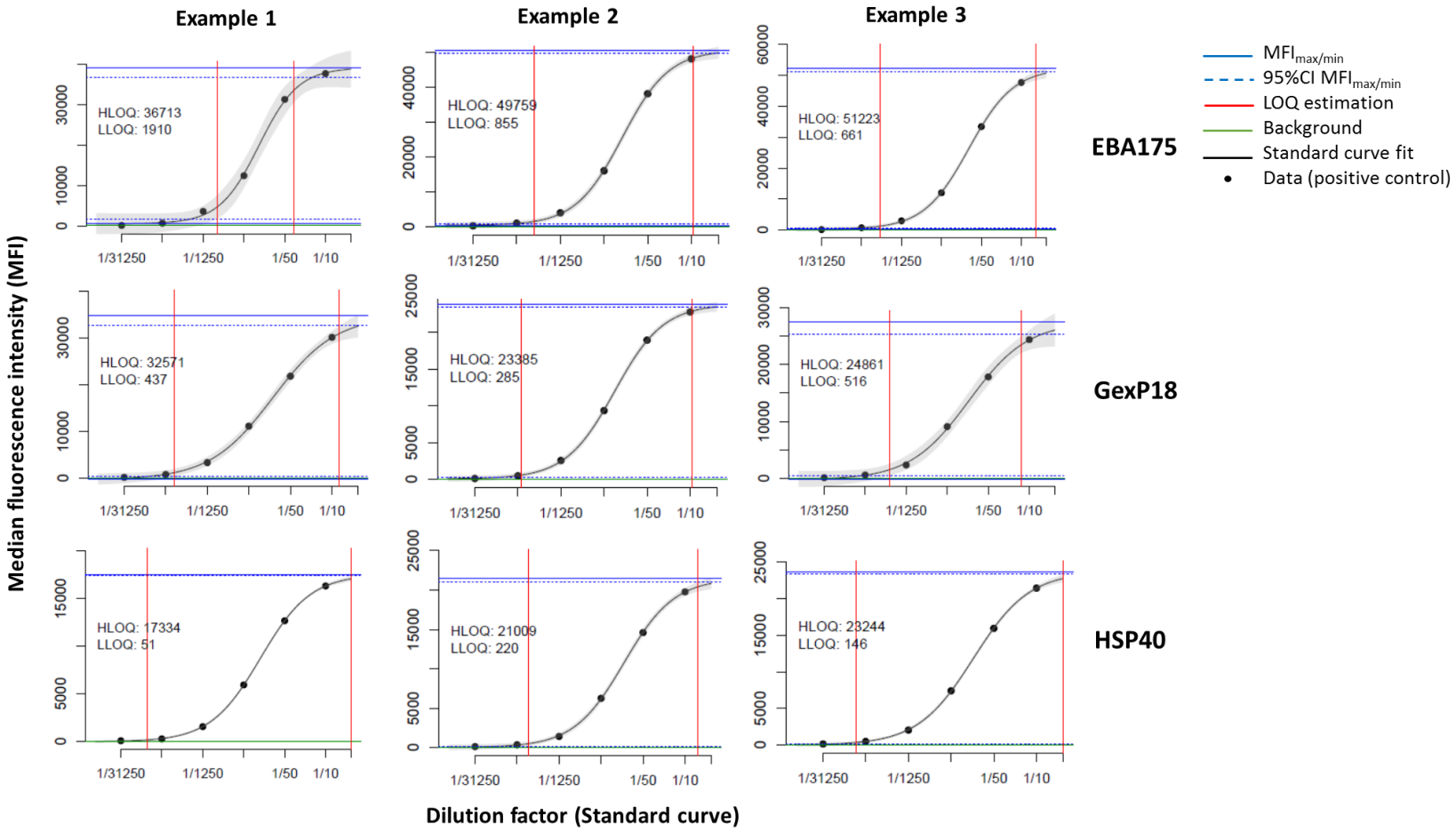
Example 1
Example 2
Example 3
Median fluorescence intensity (MFI)
Dilution factor (Standard curve)
HLOQ: 36713
LLOQ: 1910
HLOQ: 49759
LLOQ: 855
HLOQ: 51223
LLOQ: 661
HLOQ: 32571
LLOQ: 437
HLOQ: 23385
LLOQ: 285
HLOQ: 24861
LLOQ: 516
HLOQ: 17334
LLOQ: 51
HLOQ: 21009
LLOQ: 220
HLOQ: 23244
LLOQ: 146
1/31250
1/1250
1/50
1/10
EBA175
GexP18
HSP40
MFImax/min
95%CI MFImax/min
LOQ estimation
Background
Standard curve fit
Data (positive control)

Figure 5.5 Example of mean limits of quantification across all reference plates

Solid points are plate-specific LLOQ and HLOQ values, horizontal solid and dotted lines are the mean LOQ values and 95%CI across all plates (red = LLOQ, blue = HLOQ, green = background signal).

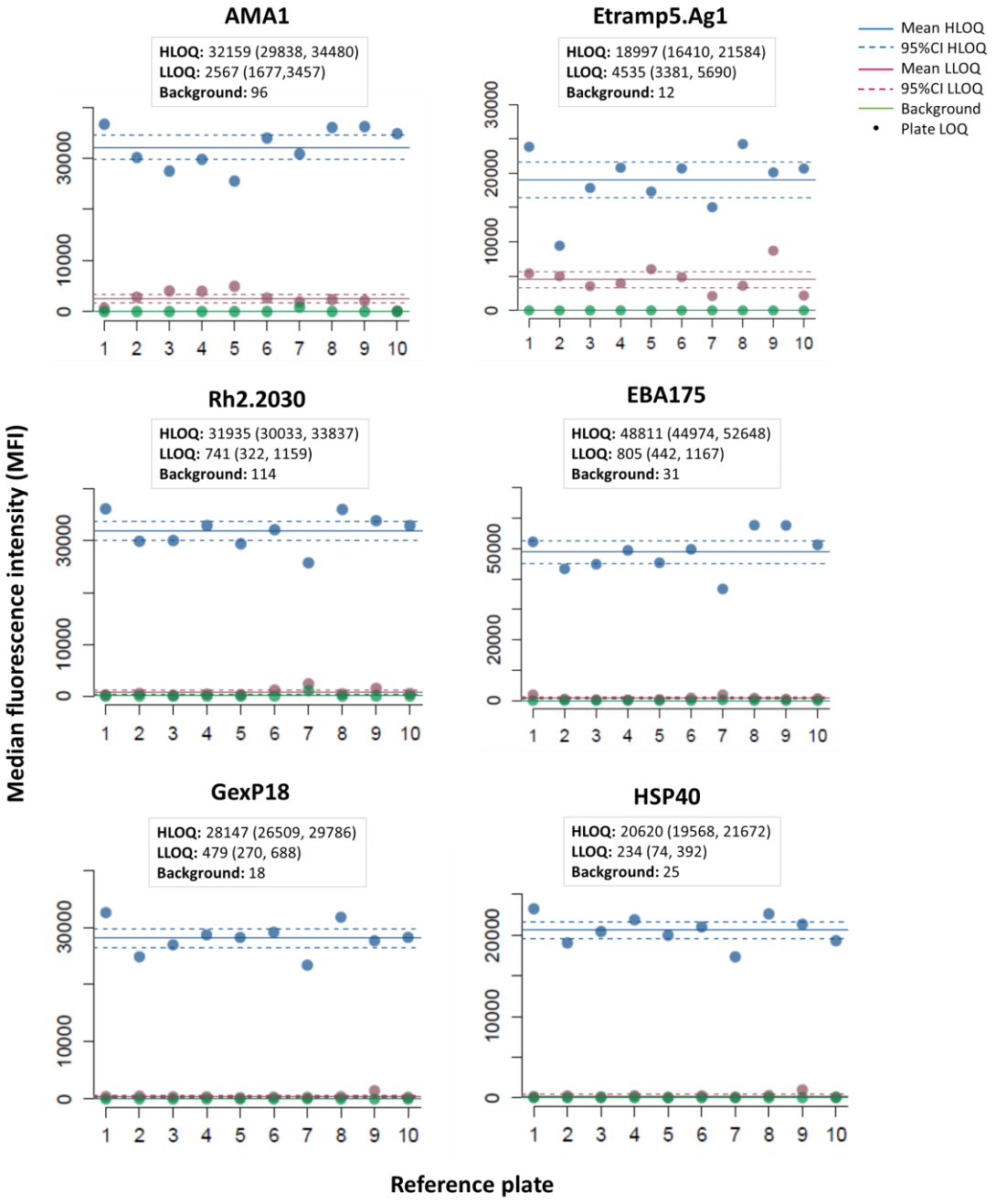

Table 5.2 Sero-positivity thresholds by antigen

Thresholds determined using either a 2-component finite mixture model (FMM) to identify sero-negative and positive populations or mean plus three standard deviations of non malaria-exposed European negative controls.

A. GAMBIA

Antigen	FMM	Malaria naïve cutoff	Method used
***Pf*MSP1$_{19}$**	**6982**	311	FMM
***Pf*AMA1**	**2791**	260	FMM
***Pf*GLURP.R2**	513	**677**	Malaria naïve controls
EBA175	201	**898**	Malaria naïve controls
EBA181	185	**652**	Malaria naïve controls
EBA140	219	**2576**	Malaria naïve controls
Rh5	6082	**1935**	Malaria naïve controls
Rh2.2030	1007	**945**	Malaria naïve controls
Rh4.2	181	**1425**	Malaria naïve controls
Etramp5.Ag1	724	**224**	Malaria naïve controls
Etramp4.Ag2	1034	**1170**	Malaria naïve controls
GexP18	4949	**435**	Malaria naïve controls
HSP40.Ag1	2958	**277**	Malaria naïve controls
Hyp2	2354	**345**	Malaria naïve controls
SEA-1	3719	**949**	Malaria naïve controls
***Pf*MSP2.Ch150**	392	**138**	Malaria naïve controls
***Pf*MSP2.Dd2**	266	**1357**	Malaria naïve controls
H103	1453	**3223**	Malaria naïve controls
SBP1	524	**1206**	Malaria naïve controls
***Pf*CSP**	237	**283**	Malaria naïve controls

B. NAMIBIA

Antigen	FMM	Malaria naïve cutoff	Method used
***Pf*MSP1$_{19}$**	**1351**	311	FMM
***Pf*AMA1**	**856**	260	FMM
***Pf*GLURP.R2**	1748	**677**	Malaria naïve controls
EBA175	908	**898**	Malaria naïve controls
EBA181	715	**652**	Malaria naïve controls
EBA140	1066	**2576**	Malaria naïve controls
Rh5	1443	**1935**	Malaria naïve controls
Rh2.2030	5391	**945**	Malaria naïve controls
Rh4.2	774	**1425**	Malaria naïve controls
Etramp5.Ag1	1664	**224**	Malaria naïve controls
Etramp4.Ag2	3155	**1170**	Malaria naïve controls
GexP18	2453	**435**	Malaria naïve controls
HSP40.Ag1	1089	**277**	Malaria naïve controls
Hyp2	1348	**345**	Malaria naïve controls
SEA-1	2036	**949**	Malaria naïve controls
***Pf*MSP2.Ch150**	185	**138**	Malaria naïve controls
***Pf*MSP2.Dd2**	760	**1357**	Malaria naïve controls
H103	2494	**3223**	Malaria naïve controls
SBP1	1648	**1206**	Malaria naïve controls
CSP	8195	**283**	Malaria naïve controls

Figure 5.6 Sero-positivity threshold estimation compared between methods and regions

Determined by two-component finite mixture model (FMM) (left) or mean plus three standard deviations of non-malaria-exposed European negative controls (right).

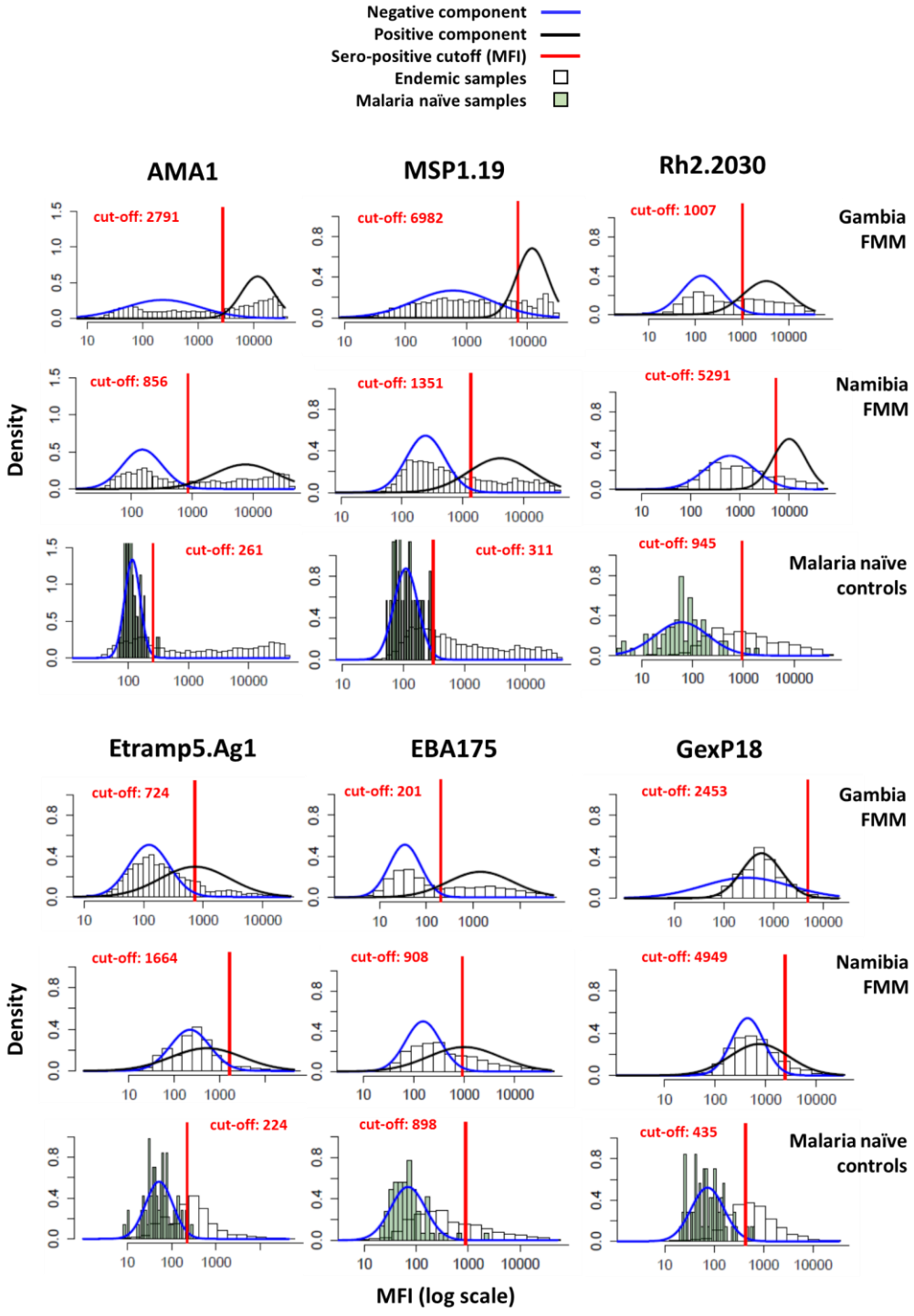

5.4 Discussion

qSAT platforms have been used for a number of diseases to measure multiple analyte-specific responses simultaneously for cytokines[293,296] nucleic acids[297], and antibodies[108,111,273]. It is now being used increasingly to measure antibody responses across a range of *Plasmodium* antigens[106,109,168,243,272,274,275,298–302] and may be a promising addition or replacement to ELISA-based screening[303]. Previous studies based on Luminex data and the results from this chapter suggest that there are still standardisation issues to be addressed to improve the efficiency and comparability of the data for routine epidemiological analysis.

Nonetheless, the data presented here adds to the growing body of evidence supporting the use of Luminex to assess the immuno-epidemiology of malaria. Additionally, it is the first in-country implementation of a multiplex serological assay for malaria in The Gambia and one of two known malaria serology studies using qSAT in Namibia (though Namibian samples were processed in London).

From an operational standpoint, this study has demonstrated that high-throughput and cost-efficient screening of field DBS samples using a Luminex protocol developed in London is feasible in a West African laboratory setting. This specific protocol has previously been used in East Africa (Uganda), Hispaniola (Haiti), and South East Asia (Indonesia, Malaysia, Philippines), though these data are not yet published. This study also builds on previous work conducted by Helb et al[304] using protein microarray, but extends similar research questions to the Luminex platform based on a rationally down-selected subset of antigens identified as potential markers of recent *Pf* infection. The utility of this will be discussed in more detail in Chapter 5b. An additional advantage over existing studies exploring markers of recent infection is the use of recombinant antigens, which typically allows better immunogenicity by preserving a protein's conformational structure compared to synthetic peptides.

Laboratory considerations

Laboratory experiments to optimise the Luminex protocol was not an objective of this study. However, the inclusion of this chapter was motivated by the lessons learned during assay set-up in The Gambia and secondary observations made during data cleaning and analysis.

In The Gambia, high throughput sample processing was efficient and reliable, with approximately 8,500 samples screened in three months. The main time-limiting step was preparation and quality control of eluting serum from DBS related to variability in the number and quality of DBS rather than the elution protocol itself. Care was taken here due to the potential for Luminex to be more sensitive to differences in serum concentration than ELISA, and previous studies using this Luminex protocol were based on plasma.[305] Comparing the use of DBS and plasma was not an

aim of this study, but previous research suggests that DBS is a suitable alternative to plasma in serological studies if there is quality control. The key issue is operational – balancing the potentially superior consistency in sample concentration whole-blood derived serum/plasma with the ease of DBS field collection and storage.

Other challenges included the need for quality testing of beads before and during processing to monitor the potential impact of interruption to cold-chain during transport. While the assay was previously optimised at LSHTM for bead coupling concentration, sample dilution, and positive and negative controls, initial tests were run prior to sample processing to ensure the same optimisation would produce a similar range of MFI values in The Gambia and for the specific study samples being screened.

As discussed by Vidal et al, the selection of appropriate sample dilutions rests on a number of factors such as the demographic and clinical characteristics of the study population (age, level of malaria infection, pregnancy, and treatment).[168] Optimal sample dilutions for the protocol used were chosen based on testing of pooled sera from hyper-immune individuals in Uganda, Tanzania and The Gambia. This study confirmed that similar sample dilutions and coupling concentrations can be used across different endemic populations and produce measurable results, though this was not experimentally tested.

The immunogenicity of the antigens is also critical, and, therefore, sample dilution and bead coupling concentration needs to be well balanced. Several antigens had universally low signals across all samples and were excluded from final analysis. This could be the result of sub-optimal bead coupling concentration or the construct of the recombinant protein (e.g., native conformational structure required to elicit strong immune response). Therefore, while not explored in this study, a titration of sample dilutions for different bead coupling concentrations that are region specific for The Gambia and Namibia could be beneficial for future studies in these countries or to confirm generalisability of results across regions.

Constraints on time and cost meant that samples and standard curves could not be processed in duplicate. Nor were the samples validated against an alternative immunoassay. Though limited, several studies have found that antibody responses measured by Luminex correlate well with those measured by standard ELISA and often measure a range of antibody responses where duplicate samples on ELISA saturate.[274,275] Validating the correlation of this data with ELISA and/or microarray was outside the scope of this study, but can be explored in future work.

Sero-positivity thresholds

Many ELISA-based malaria epidemiology studies have used the FMM approach to determine sero-positive threshold values,[115,116,219,306] which has also been used in tuberculosis,[307]

measles,[308] rubella,[309] and trachoma,[310] while the majority of commercial ELISA kits will include in-built controls.

The distribution of antibody responses in both The Gambia and Namibia show that - with the exception of *Pf*MSP1$_{19}$ and *Pf*AMA1 - defining sero-positivity thresholds with previously used methods for ELISA data may not be suitable. For *Pf*MSP1$_{19}$ and *Pf*AMA1, use of FMM has been preferred because individuals in endemic settings often retain a higher level of antibodies relative to non-endemic controls, even in the absence of being immunologically challenged with a recent infection. However, short-lived antibody responses to many antigens investigated in this study may drop to the same level as malaria naïve negative controls. This is confirmed by 1) the low mean MFI response for the first FMM component relative to the mean MFI of European negatives observed across many antigens or 2) the lack of two distinct components at all. For this reason, recent Luminex-based malaria studies have tended to use non-endemic negative controls for defining seropositive thresholds, which is also common for other disease areas.

It should also be noted that if antibody responses wane rapidly after infection, as has been hypothesised, the FMM model would be highly affected by sampling season or demographic (if not representative of overall population structure). Neither are the case in this study where the data for cut-offs were based on cross-sectional surveys during transmission season.

Interestingly, the use of FMM for *Pf*AMA1 and *Pf*MSP1$_{19}$ led to different cut-off values between The Gambia and Namibia, which may reflect different baseline levels of immunogenicity between the regions or inter-lab variation (which can potentially be confirmed by comparing positive standard curve values between the studies). This is one argument for using the FMM rather than non-endemic controls, allowing for regionally specific cut-off values to be determined. However, this may simply be an artefact of the cross-sectional study in Namibia being conducted at the latter end of the transmission season when overall antibody levels may begin to wane slightly, even for antigens associated with longer-lived immune responses.

There are a number of other methods that can be used to determine sero-positivity thresholds not yet explored in this dataset. Firstly, the FMM models fitted to this data only assumed normal distributed components, but combinations of gamma or other non-Gaussian distributions may be appropriate if the data is highly skewed. However, the fact the multiple distributions in the data are not visually obvious suggests that searching for distinct components would be more of a statistical exercise rather than biologically motivated. Latent class models have also been suggested as one method to overcome assumptions about underlying distributions or dichotomous cut-off values.

Irion et al discuss several reasons why thresholds based on mixture models or standard deviations may be sub-optimal, particularly for immune-epidemiological data in malaria, regardless of

whether the negative controls are an endemic population or not.[311] These are illustrated in Figure 5.7, where 1) the average difference between negative and positive samples can be very small (a-c), 2) variability in the difference between negative and positive populations is high, so not all positive samples can be distinguished, or 3) the negative control measurements are highly variable (high standard deviation) so that even if separation of the populations is clear, many positive samples will have measurements below the cut-off.

Figure 5.7 Examples of hypothetical distributions of sero-positive and negative populations

Comprising a mixture of 80% positive and 20% negative samples. The unshaded peak is the distribution of controls, the dark grey corresponds to true negatives samples and the light grey to true positives. The arrow indicates the mean + 2 SD cut-off and P is the proportion of test samples with measurements greater than the cut-off.

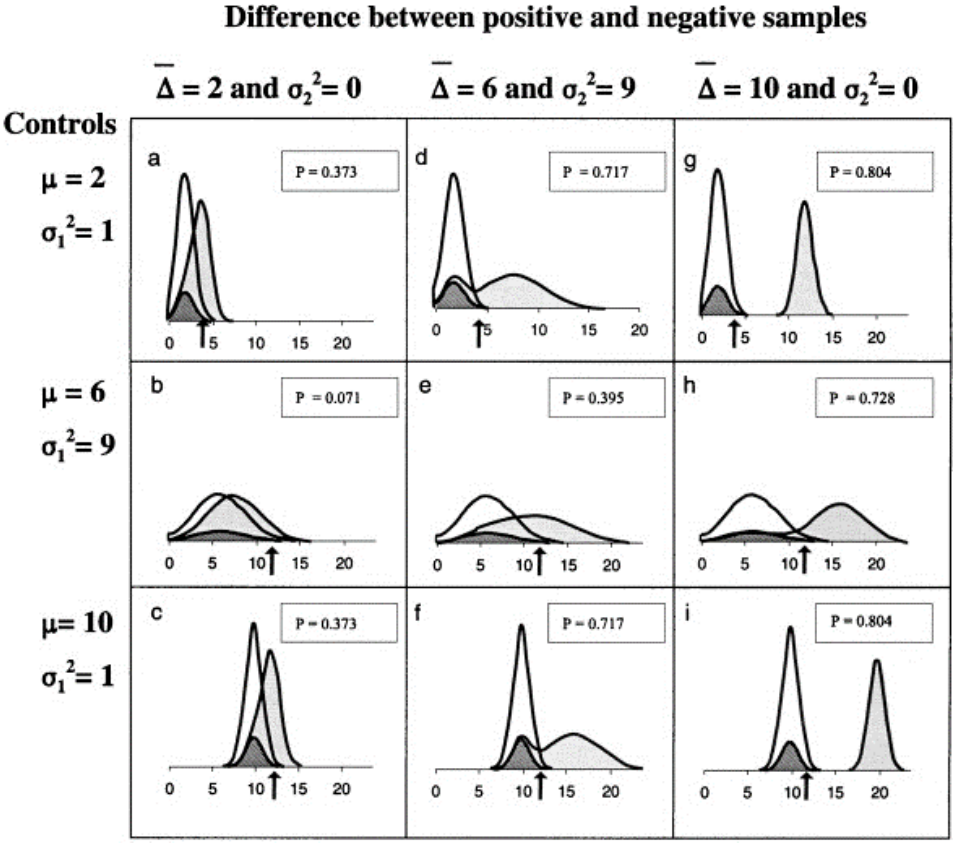

The main reasons for these challenges is the absence of a clear gold standard. This could allow the use of receiver operating characteristic (ROC) curves to determine cut-off values based on a desired level of sensitivity/specificity, which has been explored in studies on trachoma.[310] Another method is measuring fold-change from a known negative baseline used commonly to determine post-vaccination sero-conversion for diseases such as influenza[312] and rotavirus[313]. The latter assumes that an individual begins from a sero-negative antibody level in the case of longitudinal sampling or that there is consistent and known baseline antibody level that can be

used across studies. For malaria, this will face the same issues as both the FMM model (confirming the sub-population is sero-negative for a given antigen in an endemic sample) and the use of non-endemic populations (cut-offs may be too conservative if baseline antibodies level in endemic populations are higher even in the absence of reinfection due to either lack of exposure or genotypic variations in immune responses compared to Europeans).

Rather than using statistical approaches that assume that data distributions correlate with particular phenotypes in the populations, more directed selection of negative controls could be used, such as the selection of individuals from the arid western regions of Namibia that has historically experienced little to no malaria transmission. In The Gambia, where reductions in malaria transmission have been more recent, identification of a negative population may be more challenging. Options may include young children from the urban west coast region, an area of recently low transmission. However, instability of immune responses in children may also result in large standard deviations and over-estimated sero-positive thresholds. Ultimately, what is required is a sensitivity analysis of whether these thresholds affect analysis at the population level, depending on the outcomes of interest.

Data normalisation

The analysis in this study adapts the loess normalisation method to Luminex data, which has been previously used for cDNA microarray data.[295] This was motivated by the observation that between plate variation was dependent on the range of MFI values, and linear adjustments of the data based on a mid-point of the standard curve, as is typically done for *Pf*AMA1 and *Pf*MSP1$_{19}$ ELISA data, may tend to over- or under-adjust the data. These inter-plate differences at extremes of the standard curve has also been observed in other qSAT based studies.[314] The data adjustments in this study demonstrate that it can more accurately adjust raw data when differences in MFI values between plates vary at extreme values of the standard curve. This is particularly important if a large proportion of your dataset falls in this range and analysis is based on continuous rather than dichotomous antibody responses.

The most commonly used for method normalisation is conversion to antibody titre concentration. However, this is not yet feasible for most antigens analysed as it requires the availability of monoclonal antibodies (mAbs) specific to each antigen to determine exact titres. In the absence of mAbs, the standardisation is usually to arbitrary antibody concentration units using a standard curve. Without consistency between positive controls, however, this makes comparisons between studies difficult.[314] Developing mAbs for a panel of malaria antigens of interest would therefore be very useful for comparability across labs, study sites, and protocols. Future work may be useful to compare loess normalisation methods with transformation of data

to arbitrary antibody units using concentration in positive control standard curves to understand which epidemiological analyses it will influence the most.

While also not formally tested during this study, better monitoring of temperature and laboratory conditions during each incubation step in the protocol can help to explain why variation in standard curves observed in The Gambia were larger than those typically observed in assays conducted in London, despite stable temperature readings on the MAGPIX machine itself. This may be due to the use of machine rather than manual plate washing, which has shown to have an effect on ELISA signals as well.

Another data normalisation issue not addressed in these data is the influence of non malaria-specific responses to GST-tagged proteins. This may be important in regions such as The Gambia, where schistosomiasis remains prevalent and high GST-signals could be high due to the cross-reactivity of *S.haematobium* antibodies with the *S.japonicum* protein used in the GST-tag. GST-coupled beads were included in the assay to adjust MFI values if needed.

While the data shows that GST responses in the population are generally low and may not require correction for this background, some methods were explored for future data normalisation. Initial adjustments made to the data were based on estimating the log-linear relationship between GST-tagged antigen MFIs and GST-only bead MFIs (Figure 5.8). However, this resulted in very large shifts in the adjusted sample data, which is likely due to the difference in GST-specific bead coupling concentration relative to both the size of the GST-tag in the recombinant protein construct and the antigen-specific bead coupling concentration. Therefore, data in this chapter have not adjusted for GST, though it is likely that based on a weighted adjustment for MFI values using relative coupling concentration, adjustments will be small.

Another option may be to exclude the GST-tag to avoid the need for data adjustment, but this will likely result in poor solubility and recombinant protein yields[315] or to reduce the coupling concentration of the GST-beads to be more aligned with the relative size and concentration of the recombinant protein coupled beads.

Figure 5.8 Examples of GST-control adjustment to antigen-specific MFI values

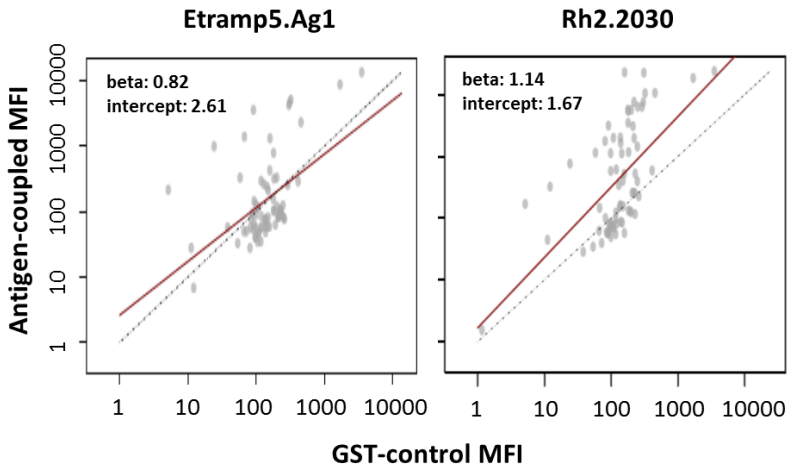

The use of standard curves have many advantages over a single positive-control dilution. Ideally, optimal sample and bead coupling concentrations should selected closest to the EC_{50} point on the standard curve for several reasons. First, this reflect the point at which the dose-response is linear, avoiding the MFI dependent between-plate variations observed in these datasets. However, from an operational standpoint, these data-driven considerations need to be balanced against the need to use cost-efficient amounts of recombinant antigens and reagents – critical for the application of this technology for high-volume epidemiological studies and developing country use.

Limits of quantification

Defining LOQs for the antigens in this study were explored, but not used as thresholds for data exclusion. While only data from The Gambia were used so far to determine LOQs as exploratory analysis, preliminary results indicate that defining the LLOQ was more important because most MFI values were on the lower extremes of the standard curve.

Overall, accurately quantifying both the lower and upper thresholds by antigen would be useful to define which samples MFIs to exclude from future analysis. When the majority of samples in cross-sectional studies have MFI signals that fall below or above the LOQs, it may indicate either 1) these antigens are not suitable for detecting population variation in antibody responses, 2) adjustment should be made to the sample dilution, or 3) bead coupling concentrations are not optimal. This data also demonstrates that developing a suitable standard curve can be challenging for some antigens. This has knock-on effects for accurately estimating the EC_{50} point, especially if data is to be transformed to arbitrary Ab concentration units, potentially impacting final data analysis.

As mentioned above, laboratory-optimisation of the Luminex protocol was not an objective of this research. However, a number of experimental investigations that could be explored in the

future. First, additional dilutions on positive control standard curves could allow better estimation of LOQs, though caution with high concentrations is required to avoid prozone or hook effect.[316] Other methods for determining LOQ could also be explored. For example, where a percent change in MFI of 1% does not lead to a more than 5% change in dilution antibody concentration, as used by Ubillos et al.[314]

Immunogenicity may also be compromised due to antibody competition of blocking if antigens sharing similar epitopes are included on the same panel.[274] Balancing the optimisation of sample- and antigen-specific conditions without sacrificing the utility of a multiplexed platform is one of the key challenges for Luminex-based studies. Future work to improve on the immunogenicity signal detected for certain antigens is to explore the use of multiple sandwich assays, though previous work indicates that this also required the testing of multiple titration, leading to a potentially length optimisation process.[168]

Developing Luminex-based tools for capacity building

For use in sero-surveillence, developing new malaria biomarkers for use on lateral flow assays (LFA) or ELISA-based kits may be the final goal. However, Luminex is becoming more affordable for use in some endemic countries and may have potential as a standardised platform in endemic country laboratories. If so, future work that can help to enable this may include:

- Developing standardised methods for bead stability testing after transport and the researching the impact of interruptions to cold chain[317]
- Between lab standardisation of positive and negative controls[317]
- Establishing assay LOQs between labs
- User-friendly computer packages for data cleaning and analysis
- Comparability against ELISA and microarray data, as discordance has been observed in some studies comparing Luminex and ELISA[272,300]

Appendix 5.1 R functions for Luminex data processing

Function name	Description
Reading in data and merging files	
read.batch	Reads multiple plate csv files into R – only keep the median MFI values, trims the rest of the luminex file for each plate. Option to include date of plate and/or plate number as variables. Saves each plate as a cleaned file.
read.batch.beads	Reads multiple plate csv files into R – only keep the bead count values, trims the rest of the luminex file for each plate. Option to include date of plate and/or plate number as variables. Saves each plate as a cleaned file.
read.plate	Reads in a single plate csv file into R – only keep the median MFI values, trims the rest of the luminex file. Option to include date of plate as a variable. Saves as a cleaned file
read.plate.beads	Reads in a single plate csv file into R – only keeps the bead count values, trims the rest of the luminex file. Option to include date of plate as a variable. Saves as a cleaned file
join.plates	After using "read.batch" function to import multiple plate csv files, this function will merge all plates into a single file. • Note: before merging the files, user can (and should) check that all the antigen column headings are the same and spelled uniformly – see functions "ag.match.check" and "ag.column.add" below
ag.col.print	For each plate in a data batch, prints the column names (i.e., the antigen names)
ag.column.add	For a batch of plates, checks if any antigen names (i.e., columns) are missing in any plate. Adds this antigen column if it is missing and records the MFI values as NA. Allows the file to be merged with other plates that contain values for this antigen. Requires function "ag.match.check" below
ag.match.check	For a batch of plates, checks which antigen names are common across all plates and which are different or are contained in some plates but not in others (e.g., if different runs have different antigens or if there are different spellings). Allows the user to make edits so they are uniform
exclude	Removes sample rows for Background, Negative controls and/or Positive controls
Quality control	
plot.std.curve1	Plots the standard curve for a single plate and antigen. Requires the object returned by "get.standard" function below. Option to include a reference curve for comparison.
plot.std.curve2	Plots the standard curve for multiple antigens from a single plate. Option to include a reference curve for comparison. Requires the object returned by "get.standard" function below
plot.std.curve3	Plots the standard curve for multiple plates (up to 5 on one plot) and multiple antigens. Requires the objects returned by "get.standard" function below
get.standard	Saves the rows that contain the standard curve values for a plate, for all antigens
bead.check	User specifies a minimum bead count. For each antigen on a plate, indicates which wells have bead count below the minimum. For each antigen, prints a table of inadequate bead count samples: • Well number • Sample ID • Bead count
levy.jennings	Displays Levy Jennings plots for a batch of plates. User can specify which dilutions on the standard curve they want plotted. Plots display for 4 controls: • 3 dilutions on the standard curve • Background values User can specify if points should be ordered according to plate number or date. (see option in "read.batch" function)
view.plate.data	Displays data for a single plate and antigen in a 96-well format to view in the R console. Variables that can be displayed are: • MFI values • Sample IDs • Bead counts
plot.plate	Plots a single plate and antigen as a heatmap in a 96-well format

LOQ	Determines plate and antigen specific lower and upper limits of quantification (LOQ) based on the 95%CI range of the fitted standard curve and the 95%CI of the parameters estimates for the lower and upper asymptotes of the standard curve. Computes and average LOQ across all plates in a study batch for each antigen.
Data cleaning and normalisation	
blank.adjust	Calculates the median MFI values for each antigen on a single plate and subtracts this value from the sample MFI values. Does not substract from the blank/background values
blank.adjust.batch	Same as "blank.adjust" function but does this for a batch of plates (using the data object that is returned from the "read.batch" function)
norm.conc	Converts MFI data into arbitrary antibody (Ab) concentration units based on plate specific standard curve values.

norm.frac	Normalises MFI data using two methods using the midpoint (3rd most concentrated dilution) of the standard curve.
	• Fractional proportion
	  ○ Samples MFI values adjusted by log (plate midpoint MFI) / log (average midpoint MFI all plates). Final values are in MFI
	• Percent proportion
	  ○ Sample MFI values divided by plate's standard midpoint MFI value. Final values are in proportion (arbitrary units)

norm.loess	Normalises MFI data by calculating the difference in MFI between each dilution on a plate's standard curve and the average MFI value for the same dilution across all plates in a batch. Fits a regression of difference in MFI vs. average MFI and uses this regression fit to adjust all sample MFI values in the plate. • Regression is fit using either linear regression (lm) or loess. For loess fit, MFI values that fall outside the MFI values of the standard curve cannot be fit and are adjusted based on the lm fit instead. • Function checks for outliers (if a standard curve point falls outside 2 standard errors from the regression), excludes these points and recalculates the regression.
FMM, cutoffs and sero-positivity	
cutoff	Calculates sero-positivity cutoff for all antigens based on FMM using raw MFI and log transformed MFI. User can specify number of standard deviations desired to set cutoff
sero-pos	Assigns sero-positivity based on thresholds calculated in "cutoff" function above (requires object returned from this function, which has cutoffs stored). • Saves new datafile with sero-positivity variables for all antigens based on MFI and logMFI FMM
MagPIX file prep	
plate2list	Using Excel/csv file with plate plans and sample ids recorded in 96-well format, reformats to a vertical list of sample IDs for import into xPonent software. csv file can contain as many plate plans as desired and each plan will be saved as an independent import list for MAGPIX This allows us to use QR/barcode scanner straight into plate plan during deep well preparation, and not have to manually enter sample IDs after Luminex plate run.

Chapter 5b. Validating serological biomarkers for the detection of recent malaria infection

Previously, work by Helb et al aimed to identify novel serological biomarkers of previous malaria infection amongst a panel of 856 *Pf* antigens on protein microarray. This analysis was based on a cohort of 186 Ugandan and 94 Malian children with confirmed *Pf* infection and identified novel antigens that were able to classify individuals infected in the last 30, 90 and 365 days and to estimate an individuals' malaria incidence in the prior year with a high degree of accuracy.[304]

The analysis presented here extends the evaluation of these identified markers using the Luminex assay, but aims to validate them across all ages and in different geographical regions to determine the generalisability of previous study results. Amongst the antigens in the protein microarray study included in this study are four of the top ten markers able to classify time since previous infection (Hyp2, GexP18, HSP40, Etramp4) and five of the top ten markers highly associated with incidence in the prior year (Hyp2, Etramp5, Etramp4, CSP and MSP2). It should be noted that the overall panel, in addition to the potential markers of recent infection, includes antigens associated with long-lived antibody response as well. The analysis in this chapter does not evaluate them separately, but is an initial investigation across all to identify their association with previous infection.

5.5 Methods

Samples

Serological data for this study were based on a subset of samples from a larger prospective cohort study on malaria transmission dynamics and mass drug administration (MDA) carried out in six pairs of villages in The Gambia between June 2013 and April 2014, as described by Mwesigwa et al.[220] Study sites were located in five of seven administrative regions - West Coast (WCR), North Bank (NBR), Lower River (LRR), Central River (CRR) and Upper River (URR) Regions (Figure 5.7). In the baseline year, surveys were conducted in the last two weeks of each month during transmission season (June-December 2013) and an additional dry season survey conducted in April 2014 (Figure 5.9). All consenting village residents more than six months of age and present at the time of the survey (4,194 individuals) were enrolled. MDA was administered in all study villages in 2014 and 2015 between June and August, with monthly surveys conducted from June to December and April, as in the baseline year (Figure 5.10).

Blood samples were collected by finger prick for haemoglobin measurement, malaria diagnosis by microscopy, and molecular and serological analysis on dry blood spot (DBS) filter paper (Whatman 3 Corporation, Florham Park, NJ, USA). Clinical malaria cases were identified through

passive case detection (PCD) at local health facilities or in villages by study nurses and defined as history of fever in the previous 24 hours or auxillary temperature ≥ 37.5^{o}C and confirmed by a positive Rapid Diagnostic Test (RDT) result (Paracheck *Pf*, Orchid Biomedical System, India).

A subset of samples collected during the cohort study were selected for serological analysis (Figure 5.10) to 1) characterise individual level antibody kinetics over time before and after malaria infection and 2) evaluate changes in population antibody responses at the village level pre- and post-transmission season and pre- and post-MDA. The analysis in this chapter focuses on antibody kinetics, and cluster level analysis using cross-sectional time points will be addressed in Chapters 6.

To quantify individual level kinetics of antibody responses, samples were selected for 200 individuals with a positive PCR or RDT result during any survey between June – December 2013. All available samples for these individuals were included in the study for laboratory processing, resulting in 1,747 samples in total. For analysis of antibody decay, samples were included if they were a) after the first recorded infection b) less than 150 days after the first recorded infection and c) prior to second infection. This resulted in 192 individuals total included in the analysis. Table 5.3 summarises the sample size by age group, RDT- or PCR-positivity, and number of post-infection samples per individual.

Figure 5.9 Map of The Gambia and Malaria Transmission Dynamics study villages

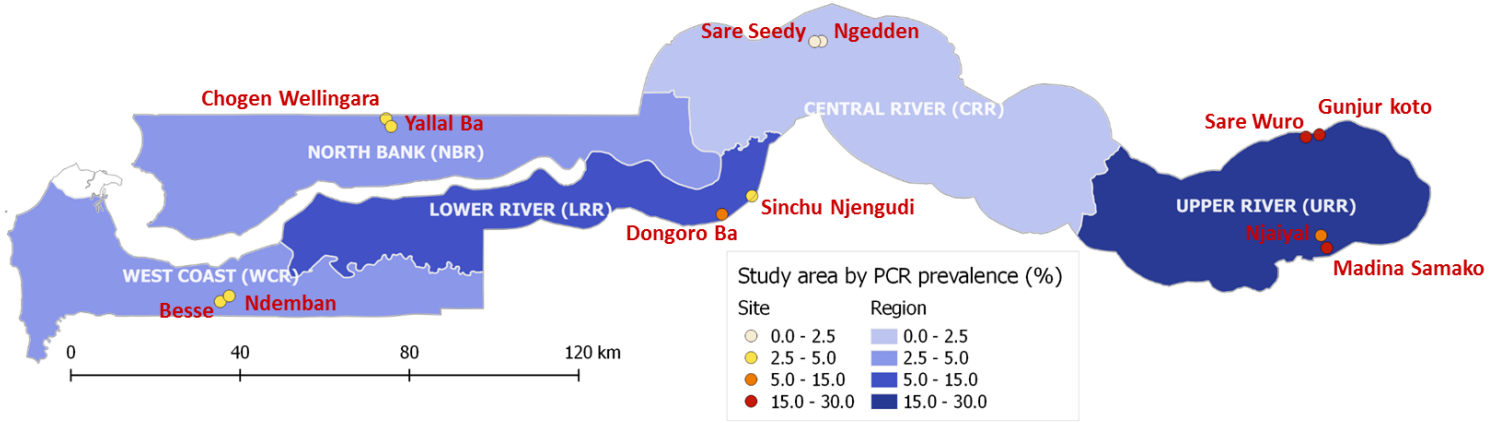

Figure 5.10 Sampling timeline of Malaria Transmission Dynamics study

Monthly samples selected for analysis in Chapters 5 and 6 are indicated in blue (kinetics) and green (cross-sectional cluster analysis).

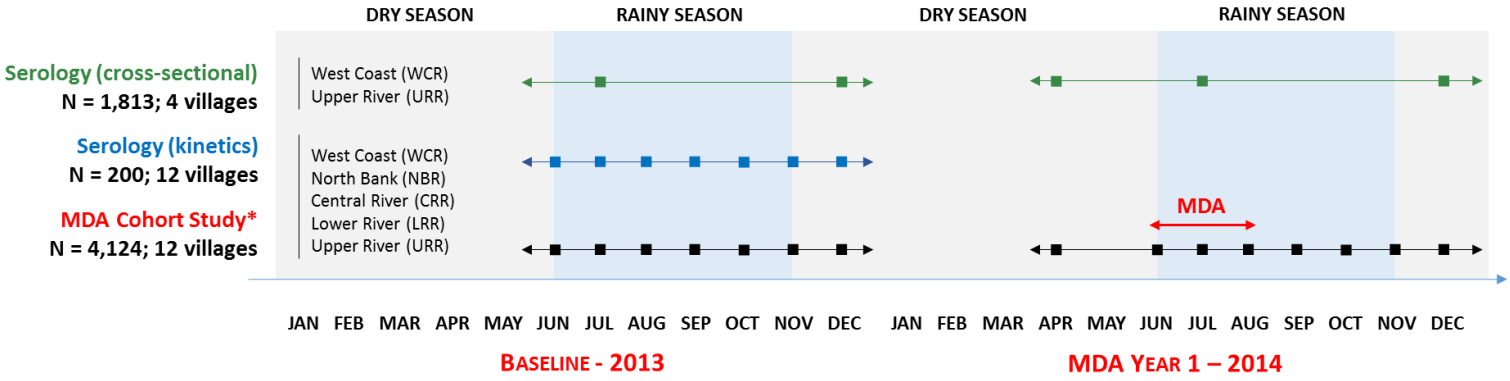

* MDA cohort study was also conducted in 2015, but is not shown on this timeline as no samples from this year were used for serological analysis.

Table 5.3 Sample size by age category and number of samples per individual

Age	RDT positive (% of age group)	PCR positive (% of age group)	No. samples per individual (post-infection samples only)				Total (%)
			2	3	4	5+	
1-5 years	17 (36.2)	46 (97.9)	3	11	20	13	47 (24.5)
6-15 years	43 (52.4)	79 (96.3)	10	22	32	18	82 (42.7)
>15 years	23 (36.5)	63 (100.0)	7	16	22	18	63 (32.8)

Statistical analyses

This chapter has two primary aims and multiple analyses are used for each. Approaches are briefly outlined here, but detailed further in the text below.

1. *Antibody dynamics after infection.* This was characterised to ultimately quantify the rate of antibody decay, with the hypothesis that antigens associated with shorter-lived antibodies responses will have the strongest sensitivity and specificity for detecting recent infection.[244,318] Methods include:

    a. Unadjusted antibody intensity over time is visualised to confirm whether dynamics of boost and decay post-infection are observed generally
    b. Breadth of antibody response by age group and time since infection
    c. Antibody decay rate estimated using
        i. Linear regression
        ii. Cox proportional hazard functions

2. *Predictive power of antigens to detect previous malaria infection*. The aim was to identify the strongest markers of recent *Pf* infection to be used in surveillance or efficacy trial evaluation. Methods include:

    a. Identifying a subset of antigens most associated with previous *Pf* infection overall using:
        i. Logistic regression
        ii. Random forest variable importance scores
    b. Receiver operating characteristic (ROC) curves and their Area Under the Curve (AUC) values based on logistic regression prediction models using the top 5 antigens selected from 2a.

All samples were categorised into six 'time since infection' categories (pre-infection, <30, 30-60, 60-90, 90-120 and 120-150 days since infection). Categories were also defined for transmission intensities based on village-level PCR prevalence (less than or greater than 10%) and age group (1-5 years, 6-15 years, and >15 years).

Unadjusted antibody intensity over time

Antibody intensity data is plotted in several ways to visualise the dynamics of antibody response at the individual and population level. First, heatmaps are used to plot Ab intensity over time (as a continuous variable) and ordered by antigen according to the mean Ab intensity across all time points overall. Next, trajectories of Ab intensity to each antigen over time (continuous) are plotted for each individual. Finally, boxplots of mean Ab intensity over time (categorical) by age group

Breadth of antibody response

Breadth of response was calculated to evaluate whether the number of antigens an individual immunologically responds to changes during the course of an infection. Samples were assigned a score of 1-4 (increasing intensity) based on the quartiles of MFI antibody response across all individuals for each antigen. An antibody breadth score was calculated for each sample by adding all antigen-specific intensity scores.[319] Breadth of response was also assessed based on binary sero-positive responses as a comparison.

Estimating rate of antibody decay

Linear regression. First, to assess whether there was evidence of antibody decay over time, mixed effects linear regression models were used to fit log MFI against time since infection as a categorical variable. Next, to estimate the rate of post-infection antibody decay for each antigen based on the slope of the linear regression, time since infection was included as a continuous variable to make full use of available data. All models were adjusted for age and transmission intensity (PCR prevalence) and allowed for individual-level random effects (intercept-only). Models were not adjusted for RDT-positivity given that, in a longitudinal dataset, some individuals had both RDT+ and RDT- infections over the course of 6 months that may have been due to fluctuating parasitaemia during the course of a single infection. Without parasite genotyping, it is not possible to determine if a PCR-positive / RDT-negative result for time points following an RDT-positive result is detecting parasite density due to a previous or new infection. However, this could be potentially ruled out for individuals confirmed to have received treatment. Data for samples on or after a second RDT- or PCR-positive result in the same individual were excluded from the kinetics analysis.

Antigen-specific antibody half-lives can be estimated using the formula:

$$t_{0.5} = \frac{-LN(2)}{slope} \quad (5.2)$$

Where $t_{0.5}$ is the estimated half-life and *slope* is the coefficient of time since infection from the regression model. Time to reaching peak antibody response post-infection varies by antigen and

individual. To allow for a lag time during which antibodies are still boosting, average time to peak MFI was calculated for each antigen and age group (1-5 years, 6-15 years, and >15 years) and data points taken prior to this time point were excluded. Models were fit using the *lmer* function in the 'lme4' R package.

Cox proportional hazard models. Antibody half-life estimates based on linear regression had large confidence intervals, therefore Cox proportional hazard models were also explored as an alternative method. Models were used to estimate time to sero-negative antibody levels after infection and were adjusted for age group. Hazard rates were also used to calculate the half-life for each antigen (using equation 5.2, replacing slope with hazard rate). This could then be compared against half-life estimates based on decay rates (slope) from linear regression analysis. Crude and adjusted survival functions were fit using the *survreg* function in the 'survival' R package and *coxph* function in the 'OIsurv' R package. These methods are compared in Table 5.4 below.

Table 5.4 Comparison of half-life estimated by linear regression vs. Cox proportional hazard models

	Linear regression	**Cox proportional hazard model**
Dependent variable	Time since infection, days	Time since infection, days
Outcome variable	Antibody intensity (continuous) MFI	Time to event (days until sero-negative based on antibody thresholds defined in Chapter 5a)
Half-life derivation	Slope of linear regression	Hazard rate
Data censoring to exclude antibody boost period	Excludes data points prior to mean time to peak MFI	Only visit dates after first recorded RDT/PCR + infection included

Evaluating predictive power of antibody response for recent malaria infection

It is hypothesised that antigens with shorter antibody half-lives will be most associated with recent *Pf* infection. However, it will also be highly dependent on the level of immunogenicity, which, as discussed Chapter 1, may vary by age and transmission intensity but also on antigen-specific factors (e.g., role in infection and pathogenesis, *in vivo* location and presentation to the immune system, and conformational structure of the recombinant antigen construct).

To assess these factors, the strength of individual level antibody responses to predict days since last infection was evaluated using both continuous (normalised median MFI) and binary (sero-positive or sero-negative) antibody responses. For infected individuals, samples after first reported infection based on a positive RDT or PCR result were categorised into 'time since infection' categories as described above. For individuals with no reported infection for the duration of the cohort study that comprised the 'non recently infected' population, only samples after two months of negative RDT and PCR results were included to exclude the possibility of recent malaria infection prior to the start of the study. The importance of each antigen in predicting previous infection were evaluated using two methods.

Logistic regression to estimate association of each antigen with previous Pf infection.

A separate logistic regression model was fit for each 'time since infection' window to calculate the association of each antigen with log odds of infection during that period. Regression models also included current RDT/PCR test result, age, and transmission intensity as covariates. Antigens that were associated increased odds of previous infection were then ranked according to 1) having a p-value less than 0.1 and 2) the strength of the association with odds of previous infection in the specified 'time since infection' window.

Random forest variable importance of each antigen in predicting previous Pf infection

Random forest prediction models have been used in large-scale bioinformatics association studies for selecting subsets of genetic markers relevant for disease prediction and prioritising them for further study.[320,321] Their main advantage is their efficiency in selecting large numbers of predictors that may be associated with each other and the disease/outcome of interest in a non-linear way.[322]

Here, we used a cross-validated random forest model for each time since infection window, age category, and infection severity (RDT+ or RDT-), and antigens were ranked based on their variable importance score (i.e., a measure of a marker's contribution to the accuracy of the model prediction). Each model was cross-validated, where 30% of dataset was used as a training set and bootstrapped over 50 iterations.

To determine the optimal number of antigens to include in a predictive panel, sensitivity analysis was also conducted using random forest models to assess the relationship between the number of antigens used and predictive accuracy. The *mtry* value (i.e., the number of prediction features to include in the random forest) was varied between 1 and 21 antigens, and the out-of-bag error of the random forest was plotted for each *mtry* value. Overall, inclusion of more than five antigens did not lead to notable reduction in prediction error and was chosen as the optimal number of markers to include in a predictive panel (Appendix 5.2, Figure 5.31).

ROC analysis using cross-validated logistic regression. Cross-validated logistic regression models (bootstrapped and iterated as described above) with the top five ranked antigens from the logistic regression above were then used to calculate predictive power of these combined antibody responses. Models were adjusted for current RDT/PCR test result, age, and transmission intensity. Prediction accuracy for these combined antigen panels were evaluated using Receiver Operating Characteristic (ROC) curves and Area Under the Curve (AUC) values.

A correlation matrix was used to assess whether any antigens had highly correlated antibody responses, which may need to be taken into consideration when selecting or excluding potential markers in a combined panel.[323]

5.6 Results

Antibody dynamics post-infection by age and transmission intensity

Unadjusted antibody intensity. The age distribution of samples included in the analysis ranged from six months to 80 years (Figure 5.11) in line with overall population age distribution in The Gambia.[324] Samples were also uniformly representative of a range of post-infection time points from zero to 150 days (Figure 5.11). Reporting peaks at approximately thirty days are due to monthly survey sampling schedule. Passive case detection (PCD) samples are also included in the dataset, which may have visit dates outside the monthly sampling schedule.

Based on unadjusted MFI data visualised in the heat map in Figure 5.12, antibody response tends to increase upon infection and decay over time across the entire sample population overall. Antigens with the highest antibody intensity across all post-infection samples were *Pf*AMA1, *Pf*GLURP, *Pf*MSP1$_{19}$ Rh2.2030 and EBA175, while those with the lowest antibody intensity were HSP40.Ag1, H103, SBP1, and Hyp2.

Clear dynamics of boost and decay are also observed at the individual level at different ages, geographical regions and infection severity, illustrated with samples of individual level antibody trajectories in Figure 5.13.

Figure 5.11 Distribution of age and days since last malaria infection distribution of sampled individuals

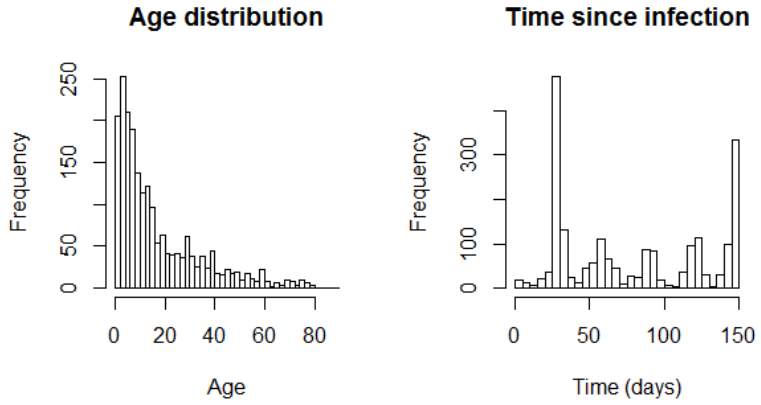

Figure 5.12 Heat map of antibody intensity by antigen and time since infection

Antigens listed vertically in order of decreasing mean MFI across all samples and post-infection time points, and horizontally by increasing time since first recorded PCR- or RDT-positive result.

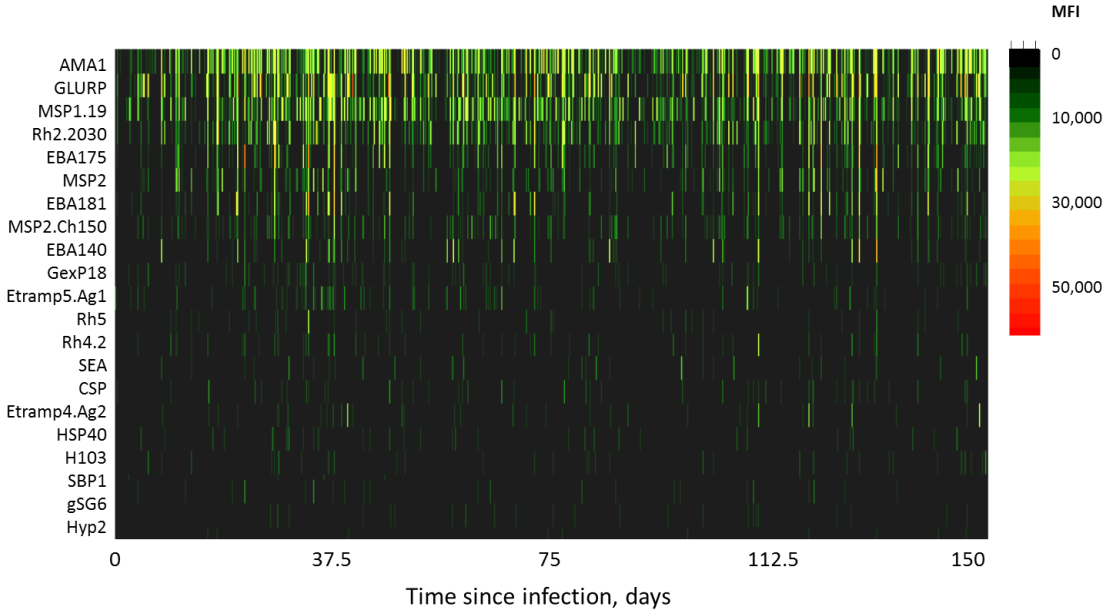

Figure 5.13 Example trajectories of individual antibody dynamics before and after infection

The data point associated with the first recorded RDT- or PCR-positive test result is set at time since infection = 0 days. Data are presented in three panels: antigens with maximum antibody responses above MFI 5,000 (left), MFI 1,000 – 5,000 (middle), and less than 1,000 MFI (right). Filled blue circles represent a concurrent positive RDT test result and filled green triangles a positive PCR test result.

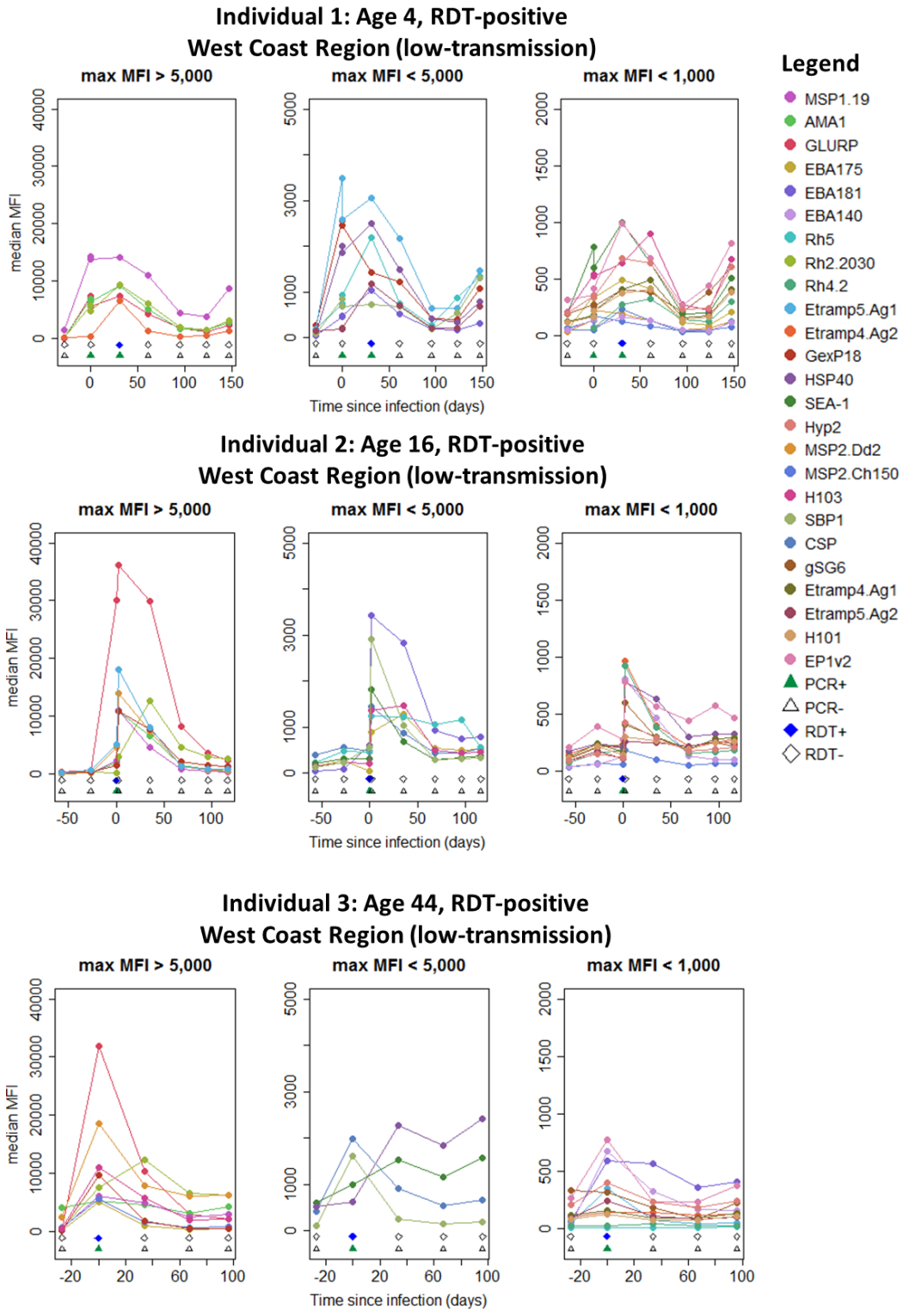

Individual 4: Age 1, RDT-negative / PCR positive
West Coast Region (low-transmission)

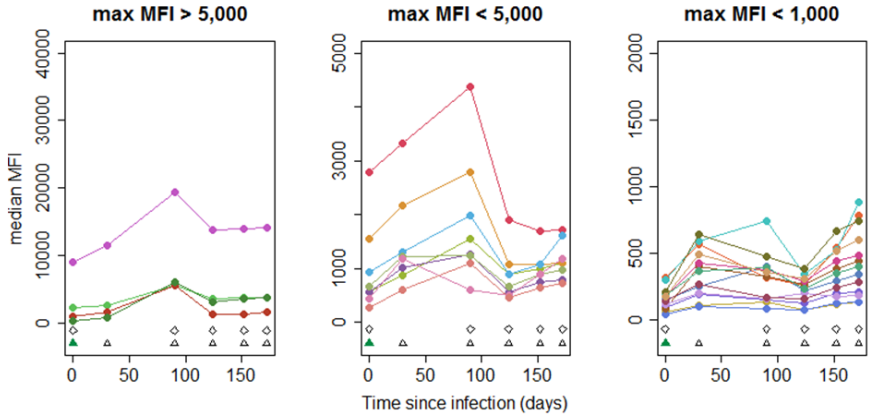

Individual 5: Age 13, RDT-negative / PCR-positive
North Bank Region (low-transmission)

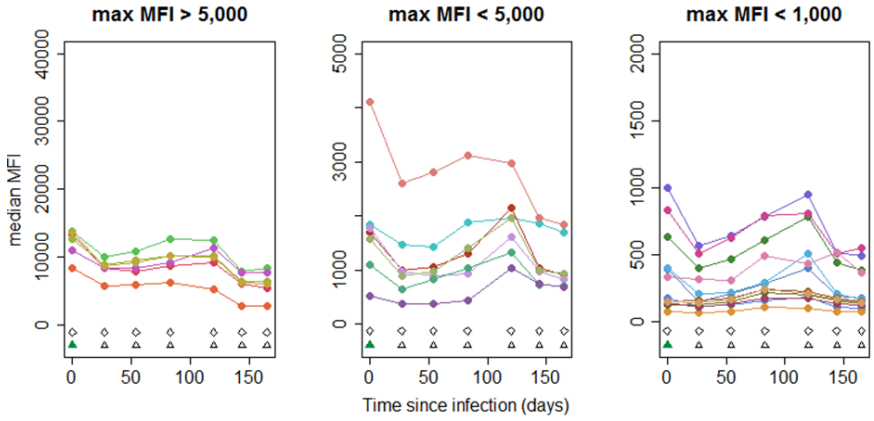

Individual 6: Age 31, RDT-negative / PCR-positive
Upper River Region (low-transmission)

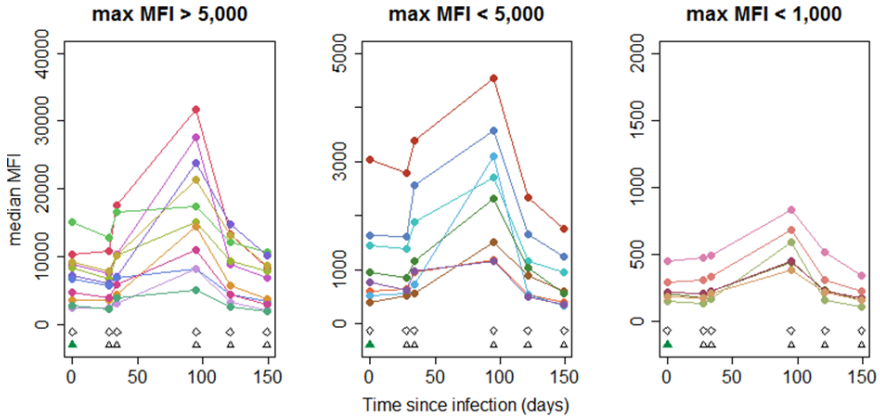

Figure 5.14 Boxplots of unadjusted MFI by time since infection and age group

For each age group and time since infection category, solid horizontal lines represent median MFI, shaded boxes represent interquartile range (IQR), dashed vertical lines represent the 95%CI and filled circles represent data points outside the 95%CI.

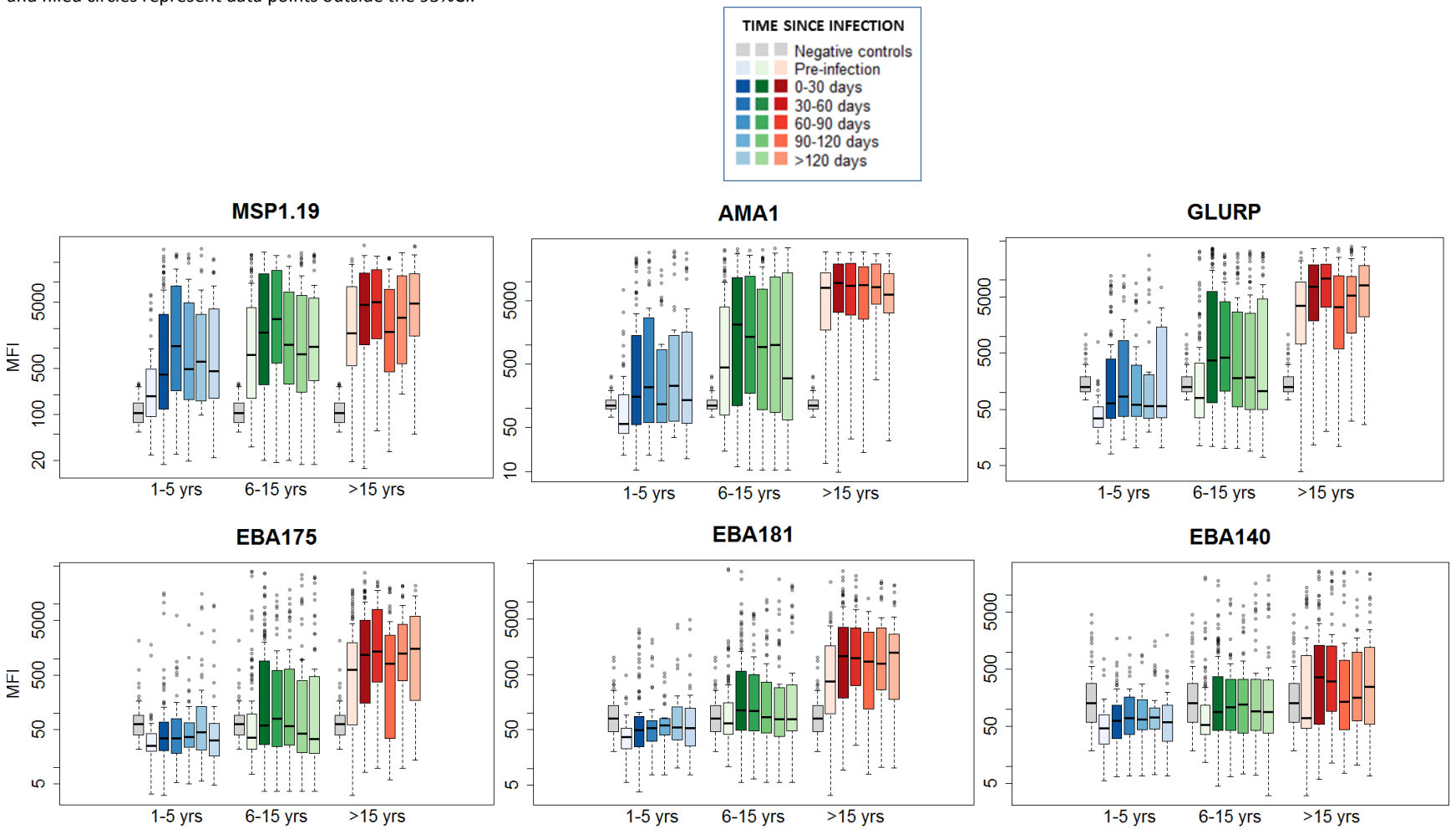

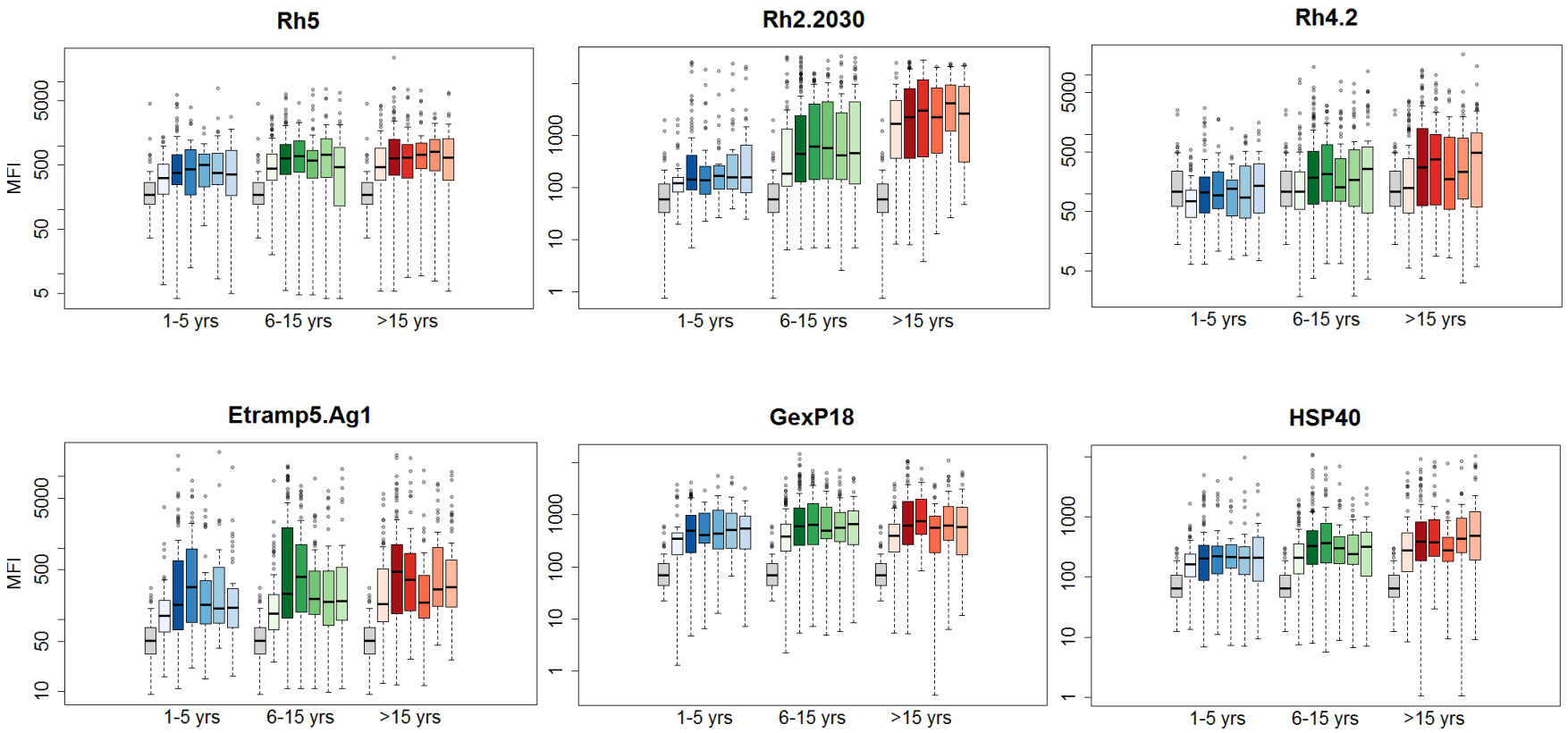
Rh5
Rh2.2030
Rh4.2
Etramp5.Ag1
GexP18
HSP40
MFI
5
50
500
5000
1
10
100
1000
1-5 yrs
6-15 yrs
>15 yrs

Breadth of antibody response

Mean breadth of antibody response based on both MFI and sero-positivity increased with each age group (Figure 5.15). Across all post-infection time points, mean antibody breadth score based on binary sero-positivity values was 5.9 (95%CI 5.3 – 6.5) for young children, 8.9 (95%CI 8.4 – 9.4) for older children, and 12.0 (95%CI 11.5 – 12.5) for adults. Based on continuous MFI values, which better reflects a combination of breadth and antibody intensity, mean antibody breadth score was 45.3 (95%CI 43.6 – 47.0) amongst young children, 53.9 (95%CI 52.5 – 55.3) amongst older children, and 61.4 (95%CI 60.0 – 62.7) amongst adults. However, linear regression of breadth of response with respect to time within each age group did not suggest that breadth of response changed significantly within 150 days after infection (analysis not shown).

Figure 5.15 Breadth of antibody response by time since infection and age group
Breadth score for continuous antibody responses is based antigen-specific quartiles of MFI values (lowest quartile =1, highest quartile =4) and for sero-positivity based on binary values (sero-positive = 1, sero-negative = 0).

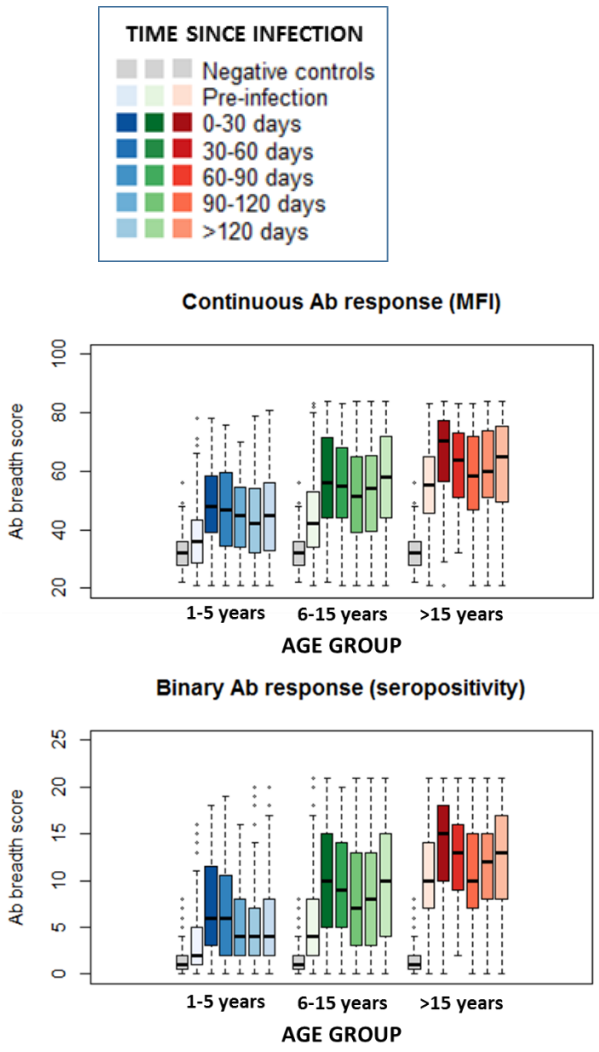

Period of antibody acquisition after infection

Mean time to peak antibody response differed by age and antigen, but there was no consistent trend between age and time to peak antibody response across antigens (Figure 5.14, Appendix 5.2 Figure 5.29). However, time to peak antibody response appeared to be longer amongst individuals who were RDT-positive (Appendix 5.2 Figure 5.30).

Figure 5.16 Time to peak antibody response, overall and by age

Mean number of days post-infection to reach maximum MFI before antibody levels begin to decay. Average number of days post-infection to reach maximum MFI before antibody levels begin to decay for all ages (blue), 1-5 years (orange), 6-15 years (grey) and >15 years (yellow). Data excludes individuals with no antibody decay during time period of observation.

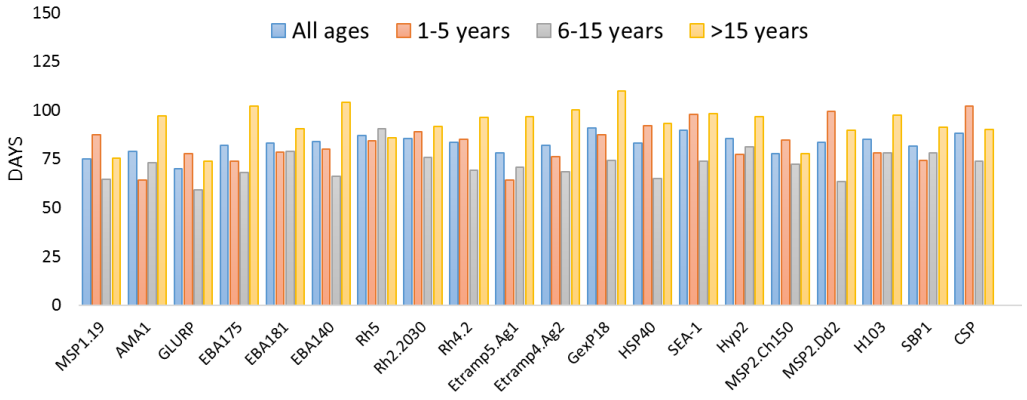

Antibody decay based on linear regression

Unadjusted linear regression of log MFI versus time since infection as a categorical variable suggests that antibody intensity for most antigens decrease within 6 months after infection, based on negative slope coefficient values (Appendix 5.2, Table 5.16). However, the magnitude of antibody decay is estimated to be small and p-values were less than 0.05 for only three antigens (Etramp5.Ag1, Rh5, and SBP1). After adjusting for age group and village-level PCR prevalence, however, thirteen antigens showed decreasing antibody response over time and but p-values were all greater than 0.1 (Appendix 5.2, Table 5.17).

Results suggest that for most antigens, antibody response differs between age groups, which is consistent with most existing studies that have observed immune responses modulated by age. The largest differences in antibody responses were observed between adults (>15 years) and young children (1-5 years) for antigens *Pf*GLURP.R2, *Pf*AMA1, EBA175, EBA181, Rh2.2030, EBA140, *Pf*MSP1$_{19}$, and Rh4.2 (Figure 5.12, Appendix 5.2 Table 5.11). However, there were a number of antigens eliciting more consistent immune responses between age groups. Antibody

intensities were not significantly different between 6-15 year olds and 1-5 year olds against antigens Rh5 (p=0.207), Etramp5.Ag1 (p=0.330), Etramp4.Ag1 (p=0.190), GexP18 (p=0.800), HSP40.Ag1 (p=0.139), Hyp2 (p=0.145), and SBP1 (p=0.305). Transmission intensity based on village-level PCR prevalence was associated with differences in antibody response for all antigens (Appendix 5.2, Table 5.11).

Overall, the precision of antibody decay rates estimated using linear regression was weak given that the 95%CI of the decay rate estimate often included negative values (i.e., converting decay rate to half-life translated to infinity values, indicating there was no evidence of antibody decay) (Table 5.6). This was true for all antigens except for Etramp5.Ag1 but only for ages 6-15 (Figure 5.17). Nonetheless, the lower 95%CI estimate of antibody half-life in children aged 1-5 years was equal to or less than one year for Etramp5.Ag1, SEA-1 and H103 and between 1-2 years for Rh5. In children aged 6-15 years, Etramp5.Ag1 had an estimated mean antibody half-life of less than 6 months, while *Pf*GLURP.R2, Rh5, Rh4.2, Etramp4.Ag2 had estimated mean antibody half-lives of less than 2 years. In adults, Etramp5.Ag1 had an estimated mean antibody half-life of between 1-2 years with a lower 95%CI estimated half-life of less than 6 months. All other antigens had an estimated mean antibody half-life of greater than 2 years.

Figure 5.17 Antibody decay rates estimated with linear regression

Decay rate is the slope coefficient estimated with the linear regression model, and can be expressed as an antibody half-life using the formula $t_{0.5} = LN(2)/\text{decay rate}$. Decay rates were estimated per antigen for A) All ages, B) Ages 1-5 years, C) Ages 6-15 years, and D) Ages >15 years. The all-age model adjusted for age group and village-level PCR prevalence, and age-stratified models adjusted for village-level PCR prevalence. Vertical lines represent 95%CI of decay rate (slope coefficient) estimate. Horizontal lines represent values where decay rates above the line correspond to a half-life equal to or shorter than the time indicated in the legend. Antigens ranked left to right in order of decreasing decay rate.

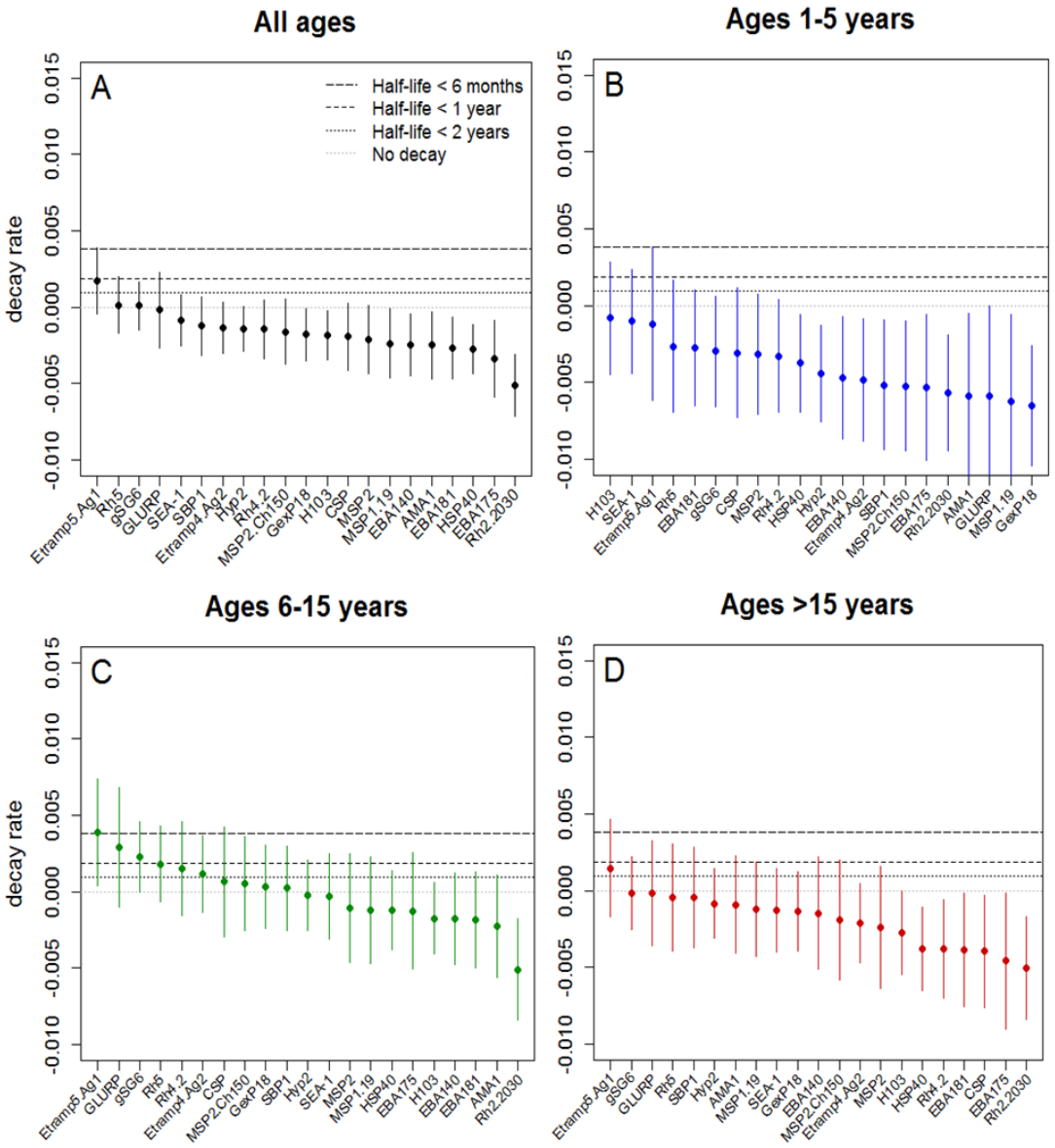

Figure 5.18 Estimated population antibody decay

Solid lines represent antibody decay over time based on mean slope coefficient from linear regression and shaded areas represent 95%CI. Post-infection antibody dynamics for two example individuals in black.

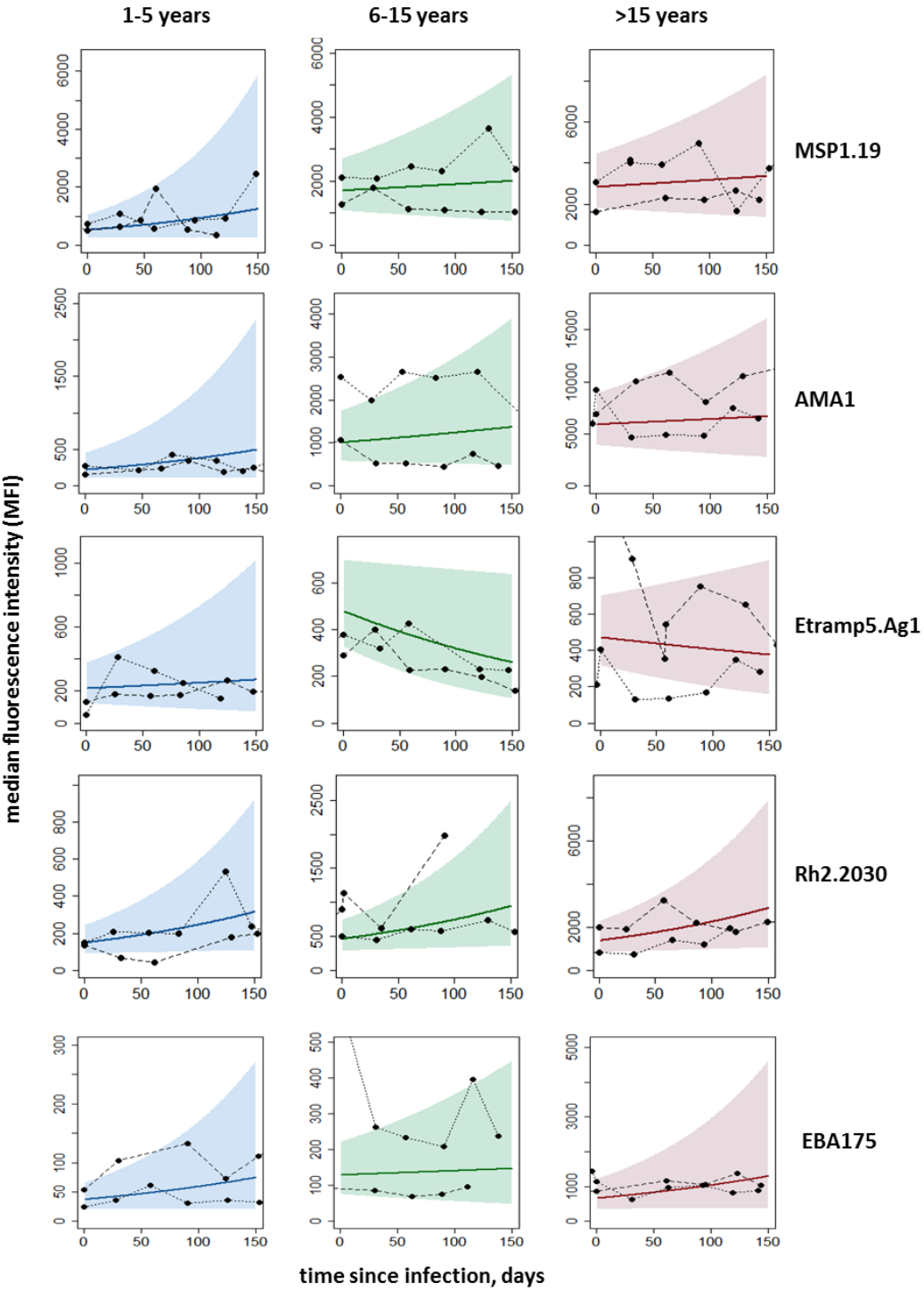

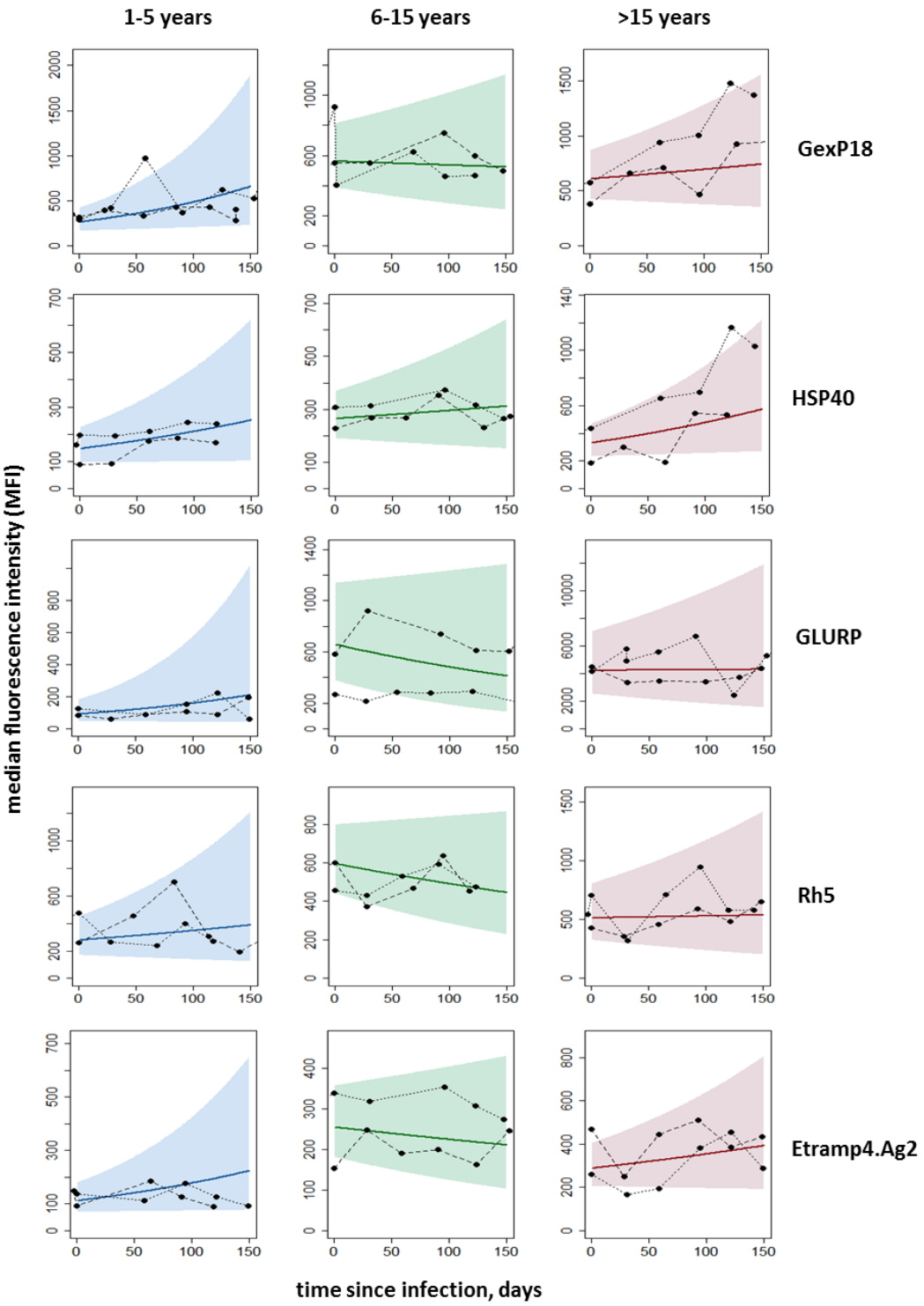
1-5 years
6-15 years
>15 years
GexP18
HSP40
GLURP
Rh5
Etramp4.Ag2
median fluorescence intensity (MFI)
time since infection, days

Antibody decay based on Cox proportional hazard functions

Compared to linear regression, antibody half-life estimates based on Cox proportional hazard models were shorter for the majority of antigens (Figure 5.20, Table 5.6). In young children, nearly all antigens had an estimated half-life between 30 and 60 days (H103, Rh4.2, EBA140, SBP1, SEA-1, Rh5, EBA181, Hyp2, Etramp4.Ag2, CSP, EBA175, *Pf*MSP2, Rh2.2030, *Pf*MSP2.Ch150 and HSP40.Ag1), while the remaining antigens had an estimated half-life between 60 and 90 days (*Pf*MSP1$_{19}$, *Pf*AMA1, *Pf*GLURP.R2, Etramp5.Ag1 and GexP18).

In older children, half-life estimates were slightly longer. Eight antigens had half-lives less than 60 days (H103, Rh4.2, Rh5, EBA140, SBP1, Etramp4.Ag2, and SEA-1), five antigens had half-lives between 60 and 90 days (EBA181, Hyp2, MSP2.Dd2, HSP40.Ag1) and either antigens had half-lives approximately between 90 and 120 days (Rh2.2030, *Pf*MSP1$_{19}$, *Pf*CSP, Etramp5.Ag1, GexP18, *Pf*GLURP.R2, *Pf*AMA1, and *Pf*MSP2.Ch150).

Half-life estimates were longest in adults. Only five antigens had half-lives of less than 60 days (SBP1, H103, Etramp4.Ag2, and SEA-1), four antigens had half-lives between 60 and 90 days (Rh5, Rh4.2, EBA140, Hyp2), eight antigens had half-lives between 120 days and 6 months (Etramp5.Ag1, HSP40.Ag1, *Pf*MSP1$_{19}$, GexP18, *Pf*MSP2.Dd2, Rh2.2030, EBA181, and EBA175), while four antigens had half-lives longer than 6 months (*Pf*AMA1, *Pf*MSP2.Ch150, *Pf*CSP, and *Pf*GLURP.R2)

Surprisingly, antigens most associated with a faster time to sero-reversion based on Cox regression analysis were not necessarily the same antigens with the fastest antibody decay rates based on linear regression (Etramp5.Ag1, *Pf*GLURP.R2, Rh5) (Table 5.6).

Age was an important factor in post-infection time to sero-reversion for several antigens (Figure 5.19, Table 5.5). In adults (age >15 years), the hazard ratio of time to sero-reversion compared to young children (age 1-5 years) was 0.18 (95%CI 0.10 – 0.32, p<0.001) for *Pf*GLURP.R2, 0.27 (0.17-0.44, p<0.001) for *Pf*AMA1, 0.36 (0.23-0.55, p<0.001) for EBA181, 0.36 (0.24-0.56, p<0.001) for EBA175, 0.40 (0.26-0.62, p<0.001) for Rh2.2030, 0.57 (0.37-0.87, p=0.009) for *Pf*MSP1$_{19}$, and 0.59 (0.39-0.89, p=0.12) for HSP40.Ag1. However, time to sero-reversion for older children (age 6-15 years) compared to young children did not differ for as many antigens. Hazard ratios were 0.67 (0.45-1.00, 0.49) for GLURP and 0.67 (0.46-0.98, p=0.039) for Rh2.2030.

Figure 5.19 Cox proportional hazard functions and Kaplan-Meier curves by antigen and age

Hazard function represents the probability of being sero-positive as a function of days post-infection. Hazard functions were estimated per antigen and adjusted for age categories 1-5 years (blue), 6-15 years (green) and >15 years (red). Black lines are the Kaplan-Meier survival curves and coloured lines are hazard functions estimated with cox proportion model.

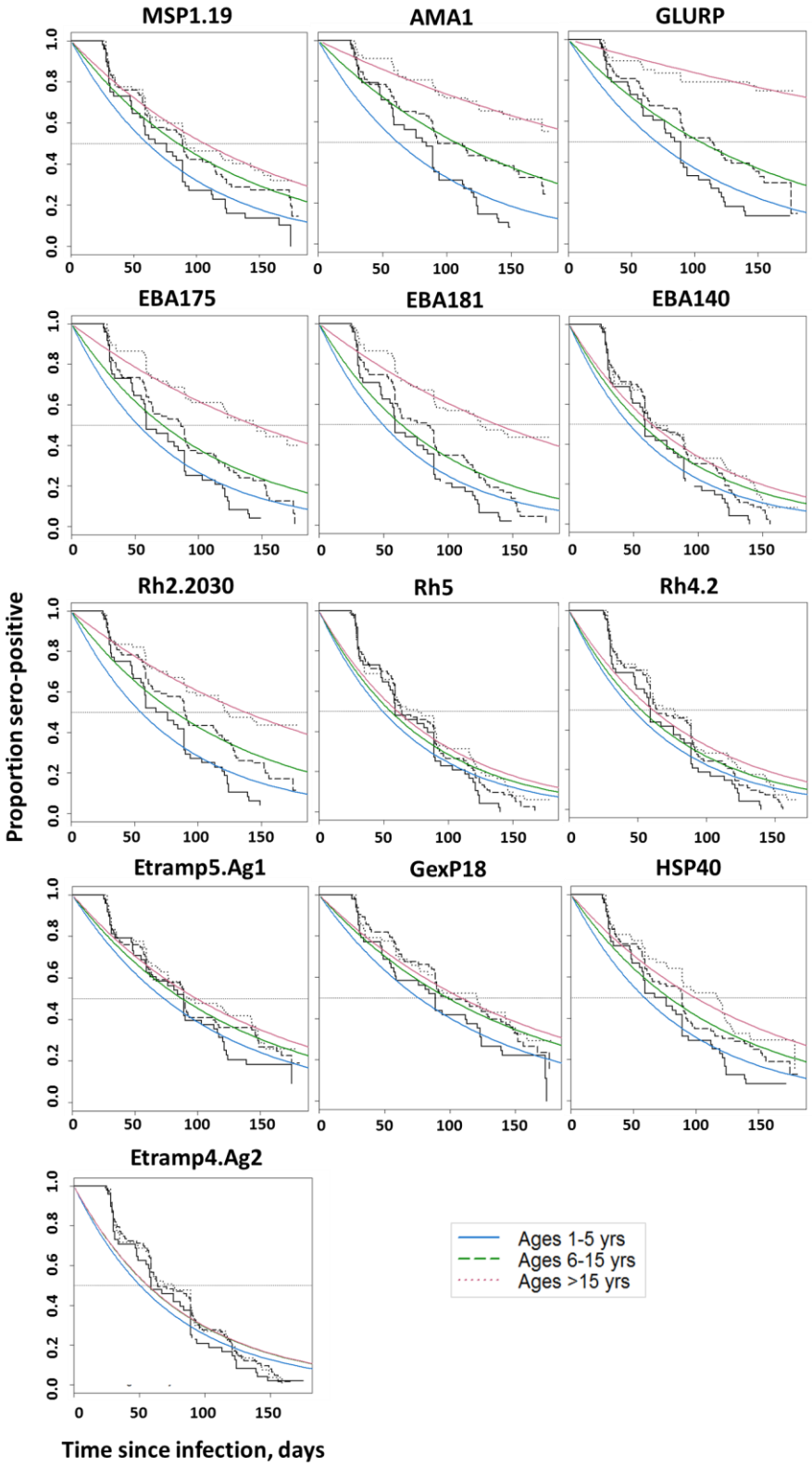

Figure 5.20 Hazard rates estimated by Cox proportional hazard model

Hazard rates (to reach sero-negative antibody threshold) estimated per antigen for A) All ages, unadjusted and adjusted for age categories B) 1-5 years, C) 6-15 years, and D) >15 years. Antigens ranked left to right in order of decreasing hazard rate. Vertical lines represent 95%CI of hazard rate estimate. Horizontal lines represent corresponding half-life, with estimates above the line representing half-life equal to or less than the days indicated in the legend.

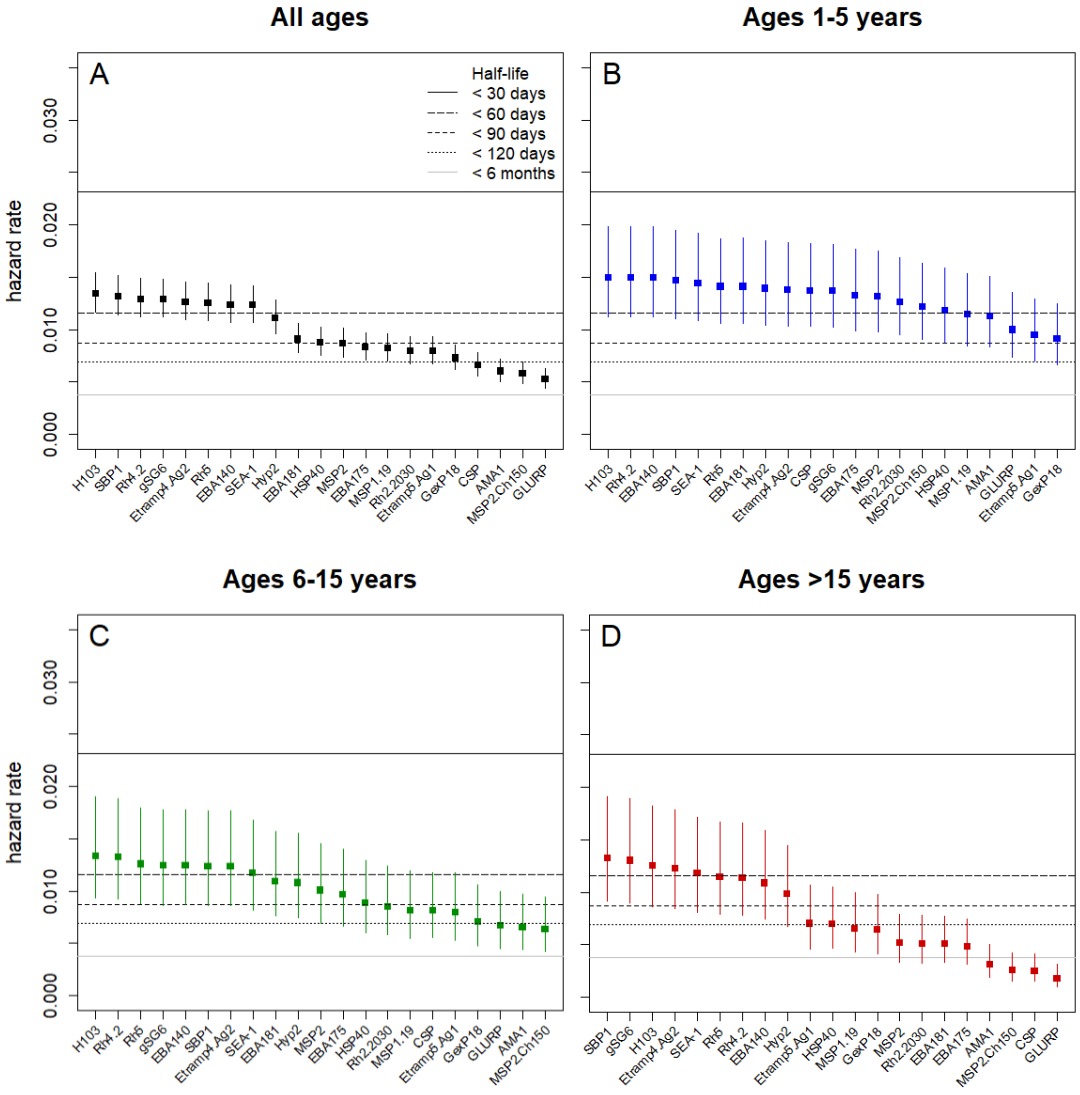

Table 5.5 Hazard ratios of antibody decay based on Cox proportional hazard functions, by antigen and age category

Reference is hazard rate for individuals aged 1-5 years.

	Hazard ratio (95%CI)	
	6-15 years	**>15 years**
***Pf*MSP1$_{19}$**	0.71 (0.48 - 1.05)	0.57 (0.37 - 0.87)
***Pf*AMA1**	0.58 (0.39 - 0.86)	0.27 (0.17 - 0.44)
***Pf*GLURP.R2**	0.67 (0.45 - 1.00)	0.18 (0.10 - 0.32)
EBA175	0.73 (0.50 - 1.06)	0.36 (0.24 - 0.56)
EBA181	0.77 (0.54 - 1.11)	0.36 (0.23 - 0.55)
EBA140	0.83 (0.58 - 1.19)	0.73 (0.50 - 1.06)
Rh5	0.89 (0.62 - 1.28)	0.81 (0.56 - 1.19)
Rh2.2030	0.67 (0.46 - 0.98)	0.40 (0.26 - 0.62)
Rh4.2	0.89 (0.62 - 1.26)	0.76 (0.52 - 1.11)
Etramp5.Ag1	0.83 (0.56 - 1.24)	0.74 (0.48 - 1.12)
Etramp4.Ag2	0.90 (0.63 - 1.29)	0.89 (0.61 - 1.30)
GexP18	0.78 (0.52 - 1.16)	0.70 (0.45 - 1.08)
HSP40.Ag1	0.75 (0.51 - 1.10)	0.59 (0.39 - 0.89)
SEA-1	0.81 (0.57 - 1.17)	0.82 (0.56 - 1.19)
Hyp2	0.77 (0.54 - 1.11)	0.71 (0.48 - 1.04)
***Pf*MSP2.Dd2**	0.77 (0.53 - 1.11)	0.39 (0.25 - 0.60)
***Pf*MSP2.Ch150**	0.52 (0.35 - 0.77)	0.21 (0.12 - 0.35)
H103	0.89 (0.63 - 1.27)	0.84 (0.58 - 1.22)
SBP1	0.84 (0.59 - 1.20)	0.90 (0.62 - 1.31)
***Pf*CSP**	0.59 (0.41 - 0.86)	0.18 (0.11 - 0.30)

Table 5.6 Antibody half-life estimates based on Cox proportional hazard rate and linear regression

Cox proportional hazard rate (by antigen and age category) and linear regression (all ages adjusted for age and PCR prevalence). Event in Cox proportional hazard model was defined as having a sero-negative antibody level, with cut-off values are based on 2-component finite mixture model (FMM) or mean plus three standard deviations of European malaria naïve controls, as described in Chapter 5a.

	Cox proportional hazard rate (95% CI)				Linear regression slope (95% CI)
	All ages	**1-5 years**	**6 -15 years**	**>15 years**	**All ages**
***Pf*MSP1$_{19}$**	85 (72 - 99)	61 (45 - 81)	85 (58 - 126)	106 (70 - 162)	∞
***Pf*AMA1**	115 (97 - 138)	62 (46 - 83)	106 (72 - 158)	226 (139 - 367)	∞
***Pf*GLURP.R2**	132 (110 - 158)	70 (51 - 95)	104 (70 - 156)	390 (219 - 695)	∞ (301 - ∞)
EBA175	84 (71 - 98)	52 (39 - 70)	72 (50 - 104)	144 (94 - 222)	∞
EBA181	76 (66 - 89)	49 (37 - 66)	64 (44 - 91)	138 (90 - 212)	∞
EBA140	56 (49 - 65)	46 (35 - 62)	56 (39 - 80)	64 (44 - 93)	∞
Rh5	55 (48 - 64)	49 (37 - 65)	55 (39 - 79)	61 (42 - 88)	4,743 (345 - ∞)
Rh2.2030	87 (74 - 102)	55 (41 - 73)	82 (56 - 119)	13 (89 - 212)	∞
Rh4.2	54 (47 - 62)	46 (35 - 62)	52 (37 - 75)	61 (42 - 89)	∞ (1,470 - ∞)
Etramp5.Ag1	87 (74 - 103)	73 (54 - 100)	88 (59 - 130)	99 (65 - 151)	406 (179 - ∞)
Etramp4.Ag2	55 (48 - 63)	50 (38 - 67)	56 (39 - 81)	57 (39 - 82)	∞ (2,233 - ∞)
GexP18	95 (81 - 112)	76 (56 - 104)	98 (66 - 147)	109 (71 - 167)	∞
HSP40.Ag1	79 (68 - 93)	59 (44 - 79)	78 (54 - 115)	99 (66 - 149)	∞
SEA-1	56 (49 - 65)	48 (36 - 64)	59 (41 - 85)	59 (40 - 86)	∞ (839 - ∞)
Hyp2	63 (54 - 72)	50 (37 - 66)	64 (45 - 93)	70 (48 - 104)	∞ (9,654 - ∞)
***Pf*MSP2.Dd2**	80 (69 - 94)	53 (40 - 71)	69 (48 - 100)	135 (88 - 208)	∞ (7,642 - ∞)
***Pf*MSP2.Ch150**	120 (100 - 143)	57 (42 - 76)	110 (74 - 163)	274 (164 - 456)	∞ (1,306 - ∞)
H103	52 (45 - 60)	46 (35 - 62)	52 (36 - 74)	55 (38 - 80)	∞
SBP1	53 (46 - 61)	47 (36 - 63)	56 (39 - 80)	52 (36 - 76)	∞ (978 - ∞)
***Pf*CSP**	105 (89 - 124)	51 (38 - 67)	86 (59 - 125)	277 (167 - 460)	∞ (2,348 - ∞)

Evaluating predictive power of antibody response for recent malaria infection

Linear regression to estimate association of each antigen with previous Pf infection

Antigens most correlated with previous malaria infection based on logistic regression were Etramp5.Ag1, GexP18, EBA140, Rh2.2030, *Pf*GLURP.R2, *Pf*MSP1$_{19}$, Rh5, Etramp4.Ag2, HSP40.Ag1, and SEA-1 (Figure 5.21), based on ranking of odds ratios for antigens with p-values less than 0.1 (a less conservative p-value cut-off of 0.1 is used purely as a reporting threshold here in order to report the effect size for a larger range of antigens, even if not significant according to standard cut-off values). Odds ratios ranged from below 1 to greater than 2 (GexP18) based on both continuous MFI responses and binary sero-positivity values, but amongst ORs with p-values less than 0.05, Etramp5.Ag1 had the largest ORs of approximately 1.75.

Figure 5.21 Effect size of each antigen based on linear regression testing association with previous infection

Separate logistic regression models were fit for each time since infection window, overall (all ages and infection severities) and by age category and infection severity (RDT+ vs. PCR+ / RDT -), with all antigens, current RDT/PCR test result, age category and transmission intensity (region) included as covariates in all models. Each point represents the antigen-specific effect size for a particular model. Only odds ratios greater than 1 (i.e., positive correlation with log odds of infection in the last 6 months) are shown. Red and blue data points represent effect sizes with p-value < 0.05 for continuous and binary antibody responses respectively.

Continuous antibody response (MFI)

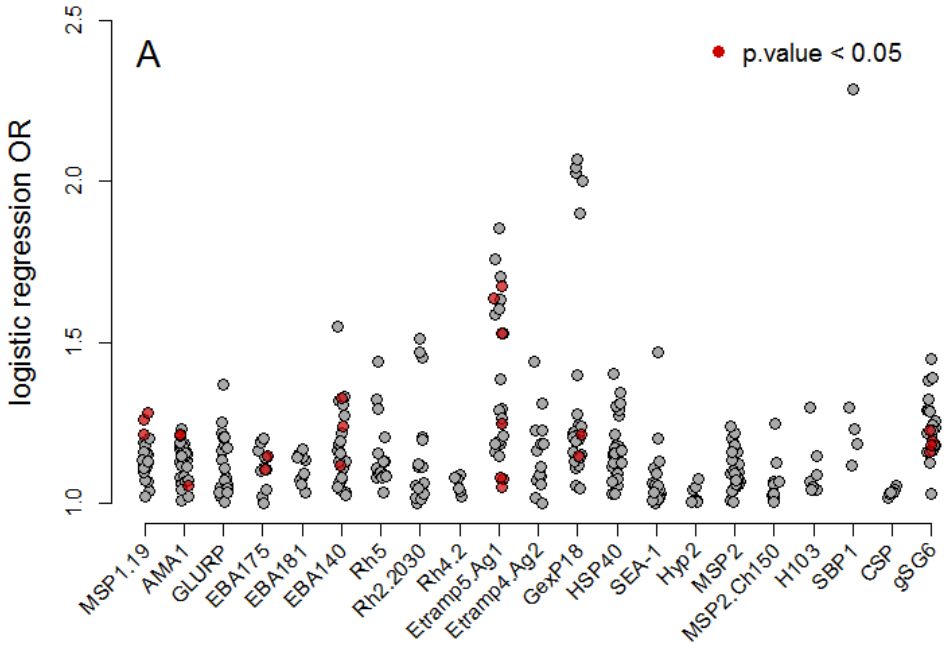

Binary antibody response (sero-positivity)

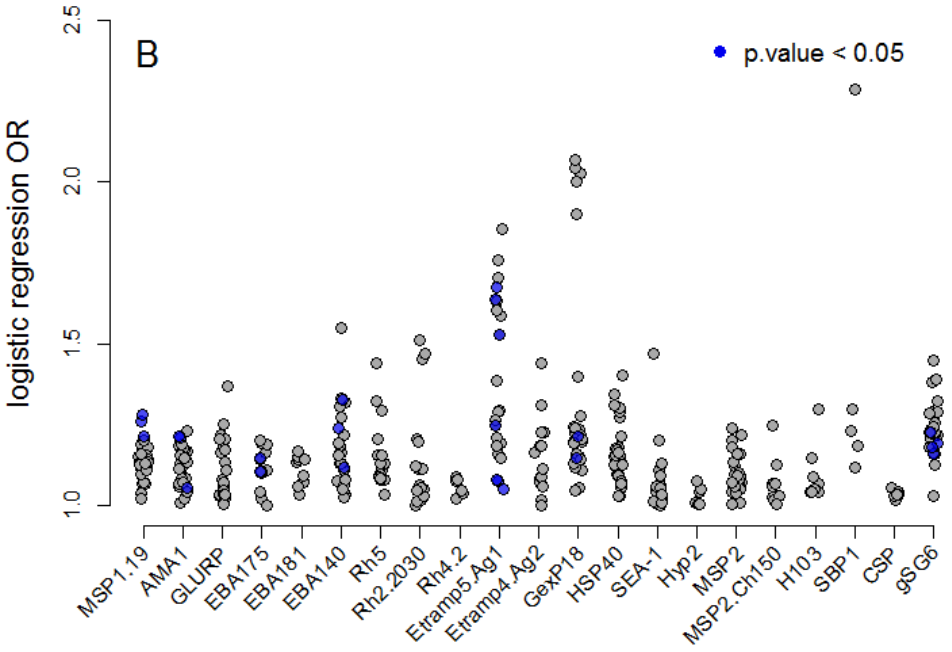

Random forest variable importance of each antigen in predicting previous Pf infection

When using random forest models, the antigens that were the strongest in predicting previous infection (based in variable importance z-scores) were Etramp5.Ag1, AMA1, GLURP, Rh2.2030, $MSP1_{19}$, HSP40, Rh2.2030, and EBA181 (Figure 5.22). RDT/PCR test result and transmission intensity were still stronger predictors of previous infection than antibody response. However, the variable importance score of the antigens identified above tended to increase relative to RDT/PCR result and transmission intensity for infections that occurred in the last 90 or 150 days compared to the last 30 days (Figure 5.22). In other words, as the time since infection period becomes longer, transmission intensity and PCR- or RDT-positivity become weaker predictors and serological markers become relatively more important predictors.

Figure 5.22 Random forest z-scores for predictors of time since last infection

Random forest z-scores (scale 0 - 100) for all potential predictors – each antigen, current RDT/PCR test result, age and transmission intensity. Values represent relative variable importance or each potential predictor in the accuracy of the model. Separate models were fit for each time since infection category, overall (all ages and infection severities) and by age category and infection severity (RDT+ vs. PCR+ / RDT-).

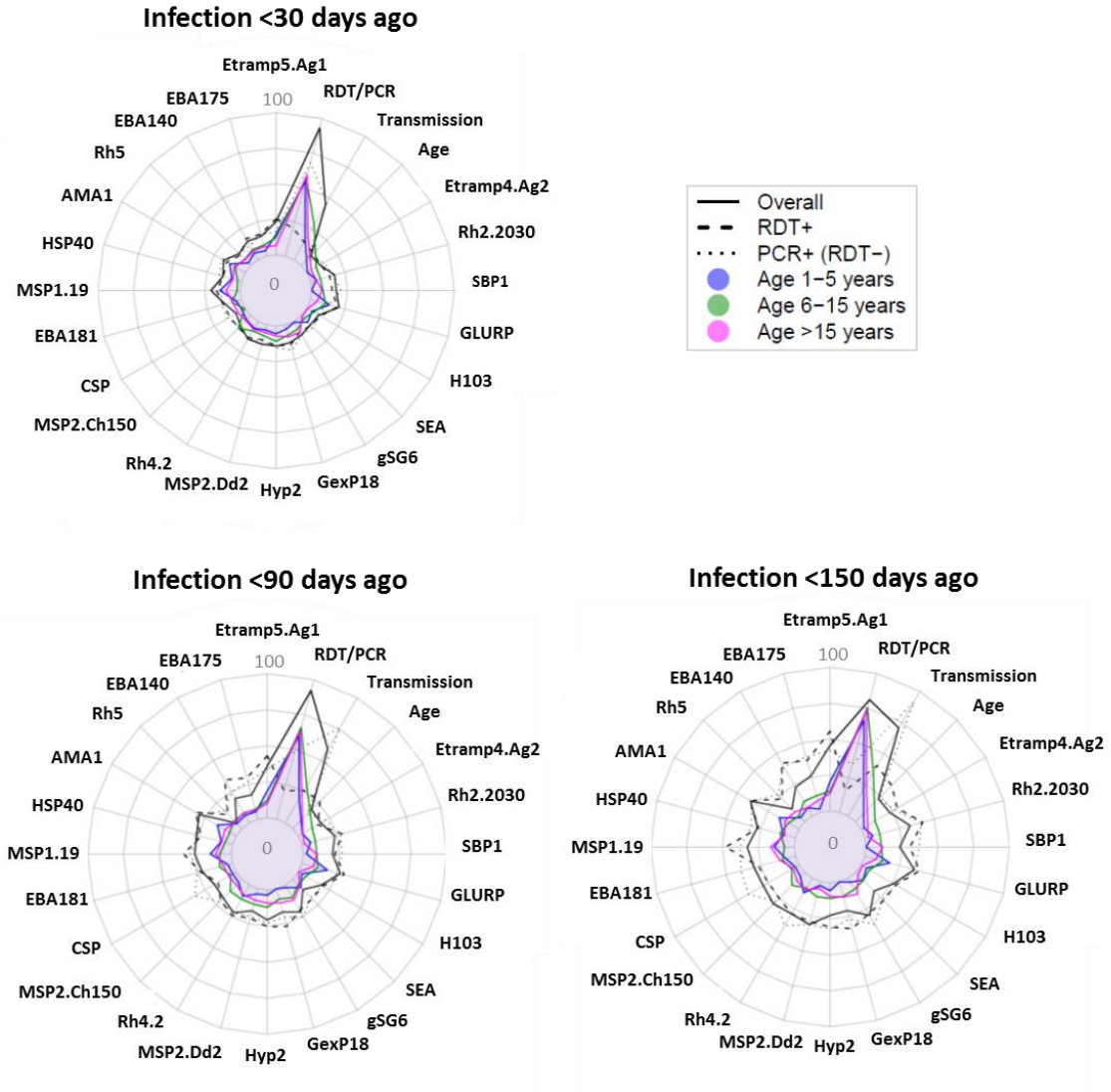

ROC analysis using cross-validated logistic regression

ROC curves representing the prediction accuracy for the top five antigens (listed in Table 5.7 and 5.8), selected based on their effect size in logistic regression, are shown in Figures 5.24 and 5.25 for each time since infection category. Models were fit using data overall for all ages and infection severities, as well as separately by age category and infection severity (RDT+ vs PCR+ / RDT-).

For all time since infection categories, AUC values were higher in children compared to adults (Figure 5.23, Tables 5.7 and 5.8). For children aged 1-5 years, antibody responses had consistent AUC values when predicting infection in the last 30 days, AUC 0.85 (95%CI 0.72 – 0.93), the last 90 days, AUC 0.85 (95%CI 0.77 – 0.92), and the last 150 days, AUC 0.84 (95%CI 0.72 – 0.91). For older children, predictive power was highest for infections in the last 30 days, AUC 0.85 (95%CI

0.77 - 0.92), and begins to decrease when predicting infection in the last 90 days, AUC 0.80 (0.74 – 0.88) and the last 150 days, AUC 0.79 (95%CI 0.73 - 0.84). For adults, predictive power also decreased over time, from AUC 0.72 (95%CI 0.62 – 0.82) for infection in the last 30 days to AUC 0.68 (95%CI 0.56 – 0.77) for infections in the last 150 days.

Predictive power when including current RDT/PCR test result as a predictor were consistently higher than models excluding this variable, though AUC values differed most when predicting previous infection in adults compared to children (Table 5.7). Antibody responses had higher AUC values when predicting RDT-positive infection, AUC 0.83 (95%CI 0.78 – 0.91) when including current RDT/PCR test result and AUC 0.84 (95%CI 0.72 – 0.89) when excluding RDT/PCR test result, compared to RDT-negative (PCR-positive) infection in the last 30 days, AUC 0.76 (95%CI 0.67 – 0.84) with current RDT/PCR test result and AUC 0.73 (95%CI 0.65 – 0.80) excluding RDT/PCR test result. However, predictive power between the two infection severities were similar when infection was greater than 30 days ago.

AUCs values based on binary antibody response were similar to models using continuous antibody responses (Table 5.8). However, antigens included at the top five predictors were different (Tables 5.7 and 5.8, Figure 5.26).

Figure 5.23 Area Under the ROC Curve values by age and time since infection

AUC values by age group and time since infection category. Solid horizontal lines represent median MFI, shaded boxes represent interquartile range (IQR), and dashed vertical lines represent the 95%CI.

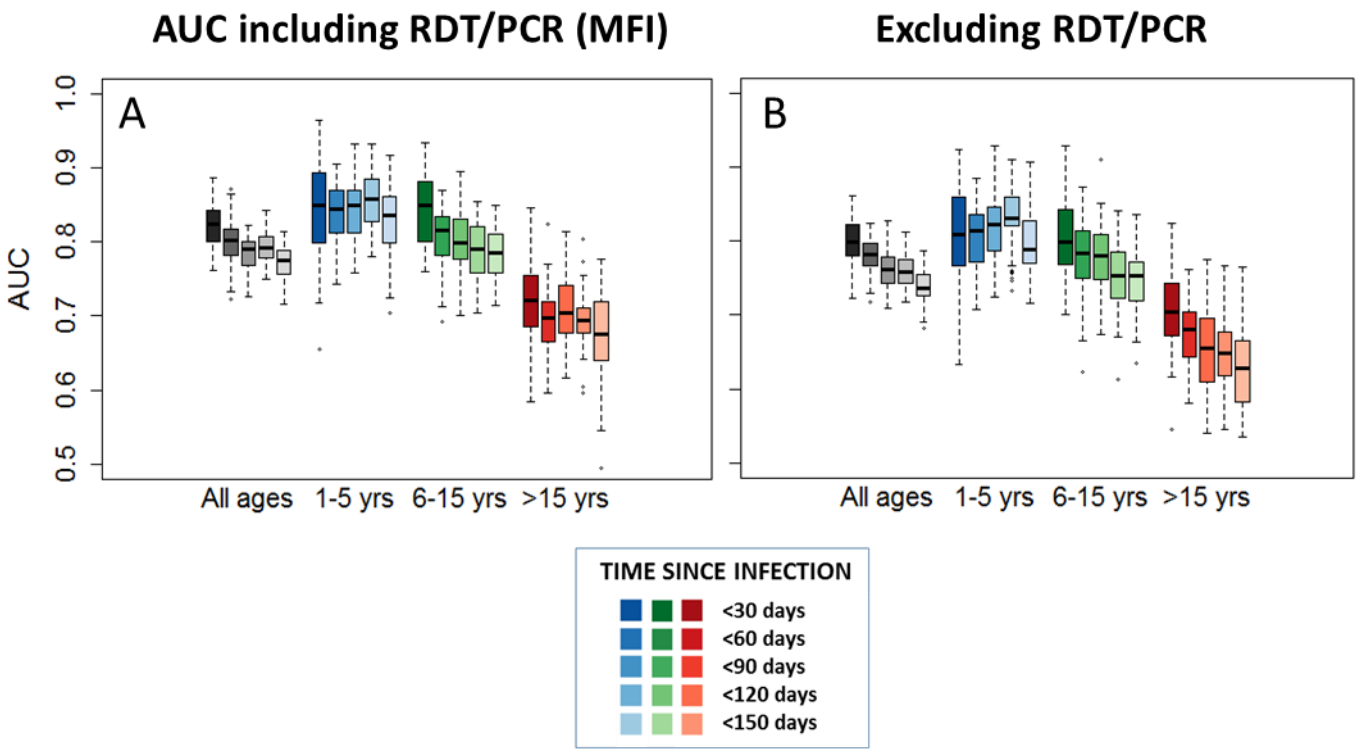

Figure 5.24 ROC curves predicting infection with continuous antibody response

ROC curves predicting infection with continuous Ab response - MFI (overall, by infection severity and age category). Predictive models were based on current RDT/PCR test result, transmission intensity (region), antibody response (MFI) to the top 5 antigens based on effect size and p-value from logistic regression model and age category (for non-age stratified models only). ROCs based on models excluding current RDT/PCR test result shown on the right.

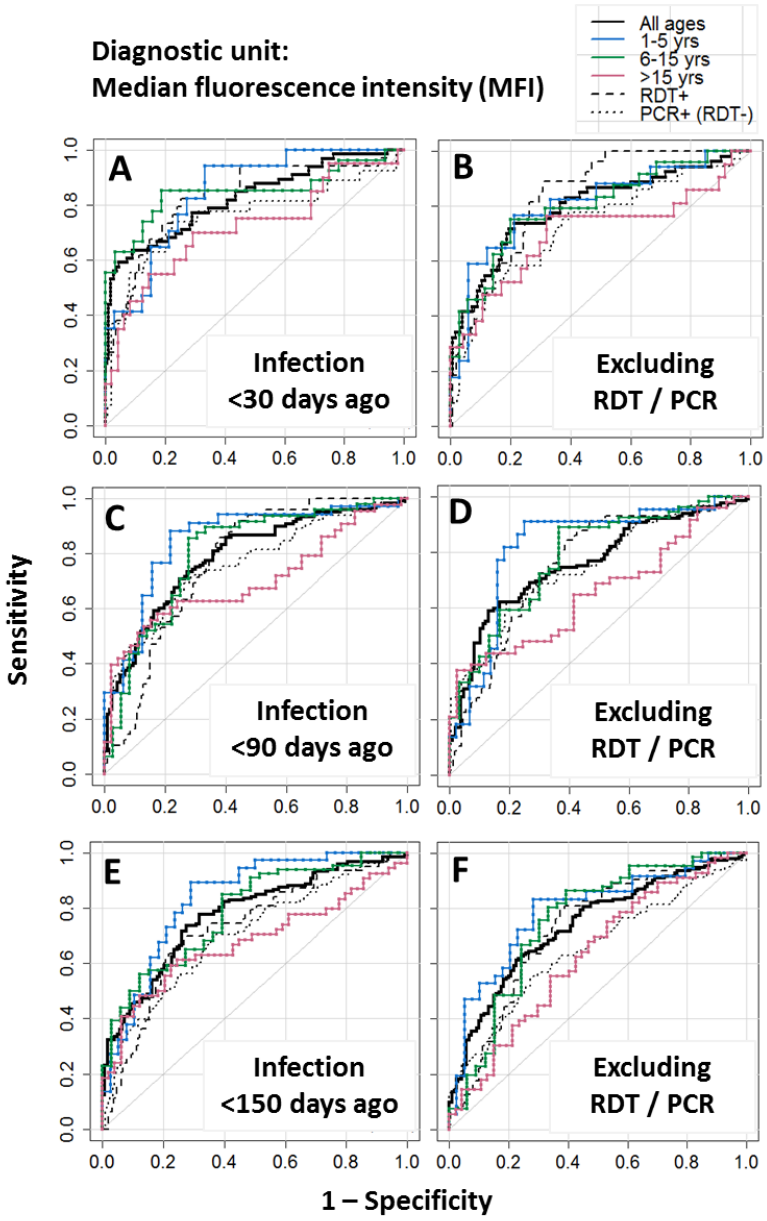

Table 5.7 AUC values and antigens used in ROC models, continuous antibody response (MFI)

Sample size, AUC values and antigens used for prediction for each ROC model, based on continuous MFI antibody response. Antigens are listed from left to right in order of strength of association with previous infection from logistic regression.

Time since infection		AUC	AUC	Antigens included in predictive panel				
Infection & age category		RDT/PCR included	RDT/PCR excluded	Ranked by effect size in logistic regression				
<30 days ago	N (% pos)	**mean (95%CI)**	**mean (95%CI)**	**1**	**2**	**3**	**4**	**5**
Overall	681 (32.0%)	0.82 (0.78 - 0.88)	0.80 (0.74 - 0.86)	GexP18	HSP40.Ag1	Etramp5.Ag1	*Pf*AMA1	--
RDT+	681 (15.3%)	0.83 (0.78 - 0.91)	0.84 (0.72 - 0.89)	Etramp5.Ag1	*Pf*MSP2.Ch150	*Pf*GLURP.R2	*Pf*AMA1	GexP18
PCR+ (RDT-)	681 (15.3%)	0.76 (0.67 - 0.84)	0.73 (0.65 - 0.80)	*Pf*AMA1	HSP40.Ag1	H103	EBA140	--
Age 1-5 years	199 (24.1%)	0.85 (0.72 - 0.93)	0.81 (0.67 - 0.91)	SBP1	GexP18	Rh5	Etramp5.Ag1	EBA175
Age 6-15 years	229 (40.6%)	0.85 (0.77 - 0.92)	0.80 (0.70 - 0.90)	Rh5	HSP40.Ag1	GexP18	*Pf*AMA1	--
Age >15 years	253 (30.4%)	0.72 (0.62 - 0.82)	0.70 (0.62 - 0.81)	GexP18	HSP40.Ag1	*Pf*AMA1	*Pf*MSP2.Ch150	--
<90 days ago	N (% pos)	**mean (95%CI)**	**mean (95%CI)**	**1**	**2**	**3**	**4**	**5**
Overall	1125 (58.8%)	0.79 (0.74 - 0.82)	0.76 (0.72 - 0.82)	*Pf*AMA1	HSP40.Ag1	Etramp5.Ag1	GexP18	--
RDT+	1125 (26.5%0	0.77 (0.72 - 0.83)	0.76 (0.72 - 0.82)	Etramp5.Ag1	*Pf*AMA1	Rh2.2030	GexP18	HSP40.Ag1
PCR+ (RDT-)	1125 (29.0%)	0.76 (0.70 - 0.83)	0.75 (0.70 - 0.80)	EBA140	*Pf*AMA1	HSP40.Ag1	EBA175	--
Age 1-5 years	310 (51.3%)	0.85 (0.77 - 0.92)	0.82 (0.73 - 0.92)	GexP18	HSP40.Ag1	Etramp5.Ag1	Rh5	*Pf*AMA1
Age 6-15 years	419 (67.5%)	0.80 (0.74 - 0.88)	0.78 (0.69 - 0.85)	HSP40.Ag1	EBA175	Rh5	*Pf*MSP1$_{19}$	GexP18
Age >15 years	396 (55.6%)	0.70 (0.64 - 0.79)	0.66 (0.56 - 0.74)	*Pf*AMA1	EBA181	HSP40.Ag1	GexP18	--
<150 days ago	N (% pos)	**mean (95%CI)**	**mean (95%CI)**	**1**	**2**	**3**	**4**	**5**
Overall	1538 (69.9%)	0.78 (0.73 - 0.81)	0.74 (0.69 - 0.78)	*Pf*AMA1	HSP40.Ag1	Etramp5.Ag1	GexP18	--
RDT+	1538 (26.5%)	0.73 (0.66 - 0.78)	0.73 (0.68 - 0.78)	Etramp5.Ag1	Rh2.2030	GexP18	*Pf*AMA1	*Pf*MSP1$_{19}$
PCR+ (RDT-)	1538 (40.6%)	0.70 (0.66 - 0.77)	0.65 (0.59 - 0.71)	EBA140	Hyp2	EBA175	HSP40.Ag1	--
Age 1-5 years	411 (63.3%)	0.84 (0.72 - 0.91)	0.79 (0.72 - 0.87)	GexP18	EBA175	AMA1	Etramp5.Ag1	*Pf*MSP1$_{19}$
Age 6-15 years	577 (76.4%)	0.79 (0.73 - 0.84)	0.75 (0.66 - 0.83)	EBA175	HSP40.Ag1	GexP18	Rh5	*Pf*GLURP.R2
Age >15 years	550 (68.0%)	0.68 (0.56 - 0.77)	0.62 (0.55 - 0.73)	GexP18	*Pf*AMA1	*Pf*MSP2.Dd2	HSP40.Ag1	--

Figure 5.25 ROC curves predicting infection with binary antibody response

ROC curves predicting infection with binary Ab response - sero-positivity (overall, by infection severity and age category). Predictive models were based on current RDT/PCR test result, transmission intensity (region), antibody response (MFI) to the top 5 antigens and age category (for non-age stratified models only). ROCs based on models excluding current RDT/PCR test result shown on the right.

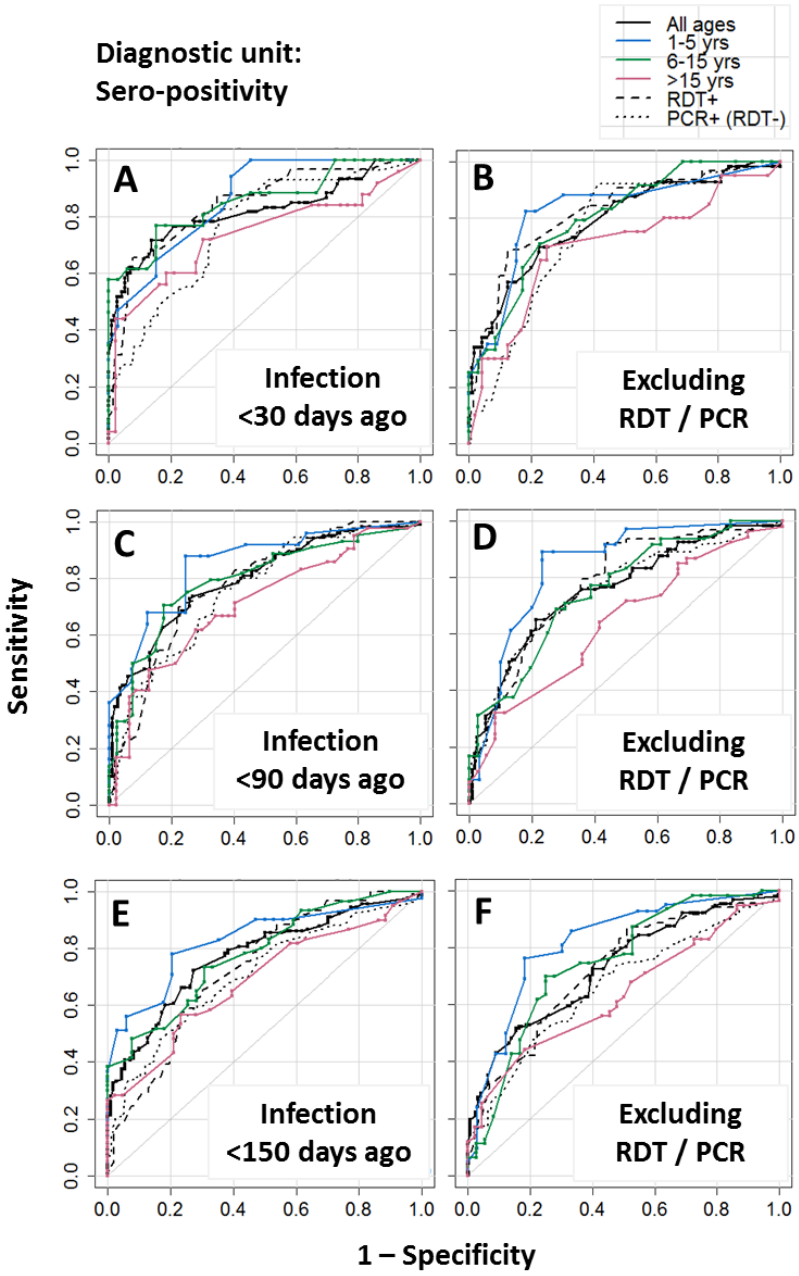

Table 5.8 AUC values and antigens in each ROC model, based on binary antibody response.

Sample size, AUC values and antigens used for prediction for each ROC model, based on binary antibody response (sero-positivity). Antigens are listed from left to right in order of strength of association with previous infection from logistic regression.

Time since infection		**AUC**	**AUC**	**Antigens included in predictive panel**				
Infection & age category		**RDT/PCR included**	**RDT/PCR excluded**	**Ranked by effect size in logistic regression**				
<30 days ago	N (% pos)	**mean (95%CI)**	**mean (95%CI)**	**1**	**2**	**3**	**4**	**5**
Overall	681 (32.0%)	0.81 (0.75 - 0.87)	0.78 (0.72 - 0.84)	Etramp5.Ag1	*Pf*MSP1$_{19}$	*Pf*AMA1	HSP40.Ag1	--
RDT+	681 (15.3%)	0.83 (0.76 - 0.88)	0.81 (0.73 - 0.88)	Etramp5.Ag1	*Pf*GLURP.R2	*Pf*CSP	Rh5	HSP40.Ag1
PCR+ (RDT-)	681 (15.3%)	0.76 (0.68 - 0.82)	0.76 (0.68 - 0.84)	H103	*Pf*AMA1	EBA140	HSP40.Ag1	Hyp2
Age 1-5 years	199 (24.1%)	0.87 (0.69 - 0.93)	0.82 (0.64 - 0.92)	Rh5	*Pf*MSP1$_{19}$	*Pf*AMA1	Etramp5.Ag1	H103
Age 6-15 years	229 (40.6%)	0.84 (0.78 - 0.92)	0.82 (0.71 - 0.89)	Etramp5.Ag1	Rh2.2030	*Pf*MSP1$_{19}$	HSP40	
Age >15 years	253 (30.4%)	0.74 (0.66 - 0.82)	0.70 (0.57 - 0.80)	Etramp5.Ag1	*Pf*AMA1	Hyp2	EBA181	
<90 days ago	N (% pos)	**mean (95%CI)**	**mean (95%CI)**	**1**	**2**	**3**	**4**	**5**
Overall	1125 (58.8%)	0.79 (0.73 - 0.83)	0.76 (0.68 - 0.81)	Etramp5.Ag1	*Pf*AMA1	*Pf*MSP1.19	Rh2.2030	--
RDT+	1125 (26.5%0	0.76 (0.71 - 0.84)	0.76 (0.70 - 0.82)	Etramp5.Ag1	*Pf*GLURP.R2	Rh2.2030	GexP18	HSP40.Ag1
PCR+ (RDT-)	1125 (29.0%)	0.76 (0.71 - 0.81)	0.75 (0.69 - 0.80)	EBA140	*Pf*AMA1	H103	Hyp2	--
Age 1-5 years	310 (51.3%)	0.82 (0.75 - 0.88)	0.82 (0.72 - 0.89)	*Pf*MSP1.19	Rh2.2030	Etramp5.Ag1	*Pf*GLURP.R2	Rh5
Age 6-15 years	419 (67.5%)	0.81 (0.71 - 0.86)	0.77 (0.70 - 0.84)	Etramp5.Ag1	*Pf*MSP1$_{19}$	GexP18	Rh2.2030	--
Age >15 years	396 (55.6%)	0.70 (0.63 - 0.78)	0.66 (0.57 - 0.74)	*Pf*AMA1	EBA181	Etramp5.Ag1	*Pf*MSP2.Dd2	--
<150 days ago	N (% pos)	**mean (95%CI)**	**mean (95%CI)**	**1**	**2**	**3**	**4**	**5**
Overall	1538 (69.9%)	0.76 (0.71 - 0.80)	0.73 (0.68 - 0.78)	Etramp5.Ag1	*Pf*AMA1	HSP40.Ag1	EBA140.Ag1	--
RDT+	1538 (26.5%)	0.72 (0.67 - 0.78)	0.72 (0.65 - 0.77)	Etramp5.Ag1	*Pf*GLURP.R2	Rh2.2030	GexP18	Etramp5.Ag2
PCR+ (RDT-)	1538 (40.6%)	0.71 (0.65 - 0.76)	0.66 (0.60 - 0.73)	*Pf*AMA1	Rh5	EBA140	EBA175	--
Age 1-5 years	411 (63.3%)	0.81 (0.72 - 0.88)	0.79 (0.69 - 0.85)	Rh2.2030	*Pf*MSP1.19	Etramp5.Ag1	Rh5	EBA175
Age 6-15 years	577 (76.4%)	0.78 (0.69 - 0.85)	0.75 (0.64 - 0.82)	Etramp5.Ag1	EBA175	GexP18	*Pf*MSP2.Dd2	Rh5
Age >15 years	550 (68.0%)	0.69 (0.60 - 0.77)	0.65 (0.57 - 0.73)	*Pf*AMA1	Etramp5.Ag1	EBA181	*Pf*MSP2.Dd2	--

Out of 42 models based on seven time since infection categories, three age groups and two infection severity categories, antigens were included as top 5 predictors in varying frequencies (Figure 5.26). Which antigens were included as top predictors differed depending on whether continuous (MFI) or binary (sero-positivity) antibody response was used as the prediction value. Based on continuous response, HSP40.Ag1, *Pf*AMA1, GexP18, Etramp5.Ag1, and EBA175 are each strong predictors in over 25% models. Based on binary response, Etramp5.Ag1, *Pf*AMA1, *Pf*MSP1$_{19}$, Rh2.2030, HSP40.Ag1, GexP18, Rh5, EBA175 appear in at least 25% models.

Figure 5.26 Antigen frequency as top 5 biomarker associated with previous malaria infection

Frequency is expressed a percent of all logistic regression models run for each time since infection category, age group and infection severity.

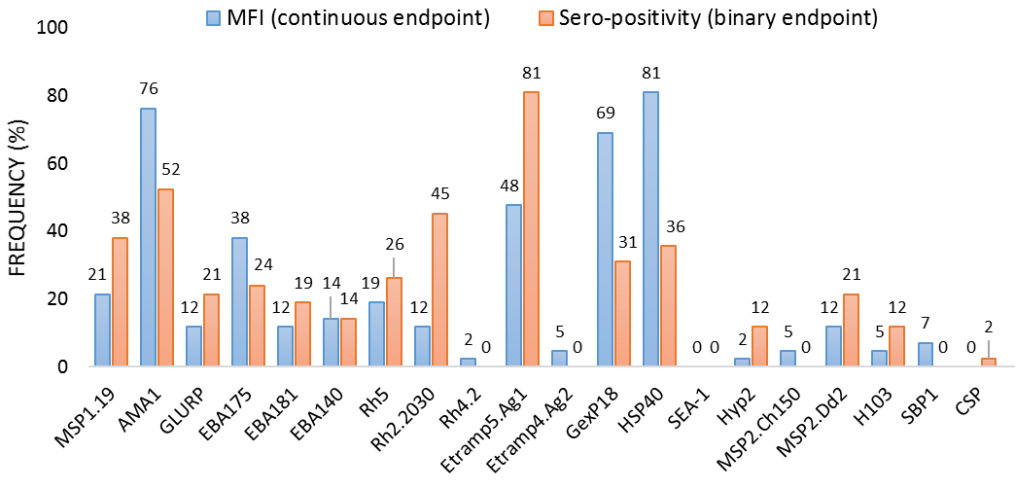

Antibody responses were moderately correlated for several groups of antigens (Figure 5.27). Generally, merozoite surface protein antigens were highly correlated, particularly EBA and Rh antigens. *Pf*AMA1 showed high correlation with *Pf*GLURP.R2, *Pf*MSP, and EBA antigens, as well as Rh2.2030. *Pf*GLURP.R2 was also highly correlated with MSP and EBA antigens, and Rh2.2030 and Rh4.2, but also showed correlation with GexP and Hyp2. Etramp5.Ag1 showed high correlation with *Pf*MSP1$_{19}$.

Figure 5.27 Correlation of antibody responses across antigens

Antigen grouped according to factors likely to influence correlation: longevity of antibody responses (long-lived - *Pf*AMA1, *Pf*GLURP.R2, *Pf*CSP, *Pf*MSP1$_{19}$, short-lived – Etramp5.Ag1, Etramp4.Ag2, HSP40.Ag1, GexP18, SEA, Hyp2, H103, SBP1), location/function of antigen in *Pf* life-cycle (erythrocyte-binding – EBA, reticulocyte-binding – Rh, merozoite-surface proteins – MSP).

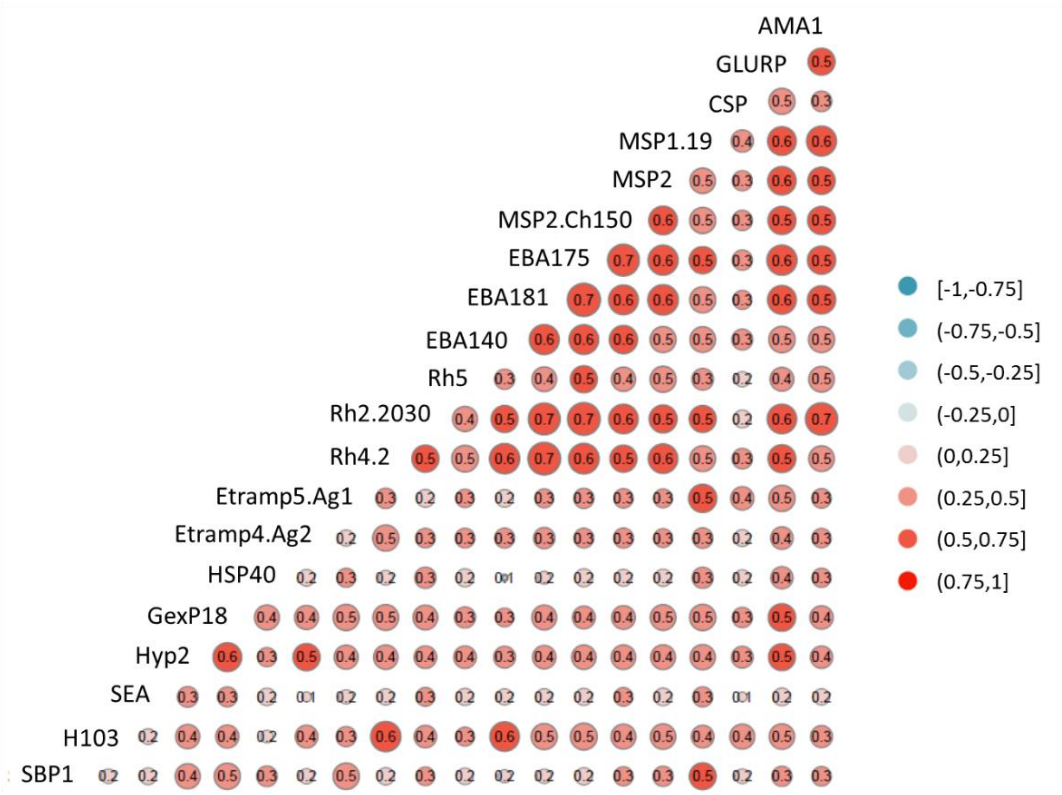

5.7 Discussion

In the context of epidemiological surveillance, there are several characteristics that may be important in a serological biomarker of recent infection. This includes sufficient immunogenicity (i.e., measurable antibody boost upon infection) coupled with rapid antibody decay. Also important may be consistency of response across age groups and transmission intensities. However, particular markers might be strong measures of population susceptibility to clinical disease if they are more associated with protective immunity. These could potentially be used to

monitor the risk of reintroduction in areas that have recently eliminated. Antigens investigated in this study have exhibited varying degrees of all these characteristics.

Dynamics of antibody acquisition, age, and transmission intensity

While most antigens were associated with a boost in antibody levels upon infection, the relative intensity of the signal varied, with *Pf*AMA1, *Pf*GLURP.R2, *Pf*MSP1$_{19}$, Rh2.2030, and EBA175 showing the highest mean antibody intensities and HSP40.Ag1, H103, SBP1, and Hyp2 showing the lowest. These differences in immunogenicity could be due to biological characteristics of the protein or how the assay has been developed (e.g., antigen coupling concentration) as discussed in Chapter 5a.

Age and transmission intensity were both found to be important factors in antibody intensity and breadth of antibody response. As discussed in Chapter 1, this is consistent with our current and historical understanding of immune responses to *Pf* and the acquisition of clinical protection across multiple endemic settings.[1,9,120,141,164,166,325–327] Protective humoral immunity is also believed to be dependent on a larger antibody repertoire across multiple antigens.[170,318,328–330]

However, the extent to which these factors influenced antibody response varied by antigen, with the largest differences between age groups observed for *Pf*AMA1, *Pf*MSP1$_{19}$, *Pf*GLURP.R2, EBA family of antigens, Rh2.2030 and Rh4.2. It is not surprising that these antigens are those thought to be most reflective of protective immunity or cumulative exposure[318], where chronic infection is associated the acquisition of sustained antibody levels. On the other hand, most antigens with more consistent responses across age groups (Etramp5.Ag1, Etramp4.Ag2, GexP18, Hyp2, HSP40.Ag1) have been previously identified by Helb et al as potential markers of recent infection. For these antigens, cumulative exposure may not play as large a role in developing immunological memory.

Rh5 also showed consistent responses across age groups, despite the fact that it has been considered as potential blood-stage vaccine candidate. While some studies have found this antigen to be associated with clinical immunity[331], others suggests that antibody levels in naturally immune individuals may be too low to confer protection, and it may need to be combined with other targets to be a viable vaccine.[332] If not, the consistency of response across ages may render it a relatively strong marker of recent infection instead.

Transmission intensity was associated with higher antibody responses for all antigens. The influence of this on serological responses at the population level will be discussed in more detail in Chapters 6 and 7, addressing cluster levels differences in The Gambia and Namibia.

Estimating the rate of antibody decay

Overall, assessing antibody kinetics in endemic populations is extremely challenging, not only because of confounding by age and transmission intensity. It may also be inaccurate due to unknown or incomplete information on the history of previous infection in older individuals and recurring infection during longitudinal studies that will lead to fluctuating antibody levels.

In this study, antibody half-life estimates varied depending on the method of estimation. Assuming a monophasic exponential decay (with linear regression), very few antigens were found to have a half-life shorter than six months. The only exception was Etramp5.Ag1, where a half-life of less than 6 months was estimated, but in ages 6-15 years only, while in young children and adults, it was only the lower 95%CI estimate that was less than 6 months. Other antigens with relatively shorter half-lives (approximately 1 year) for all ages overall were *Pf*GLURP and Rh5. On the other hand, half-lives based on Cox proportional hazard models were estimated to be less than 6 months for all antigens in children under 15 years of age and for nearly all antigens in adults except for *Pf*AMA1, *Pf*CSP and *Pf*GLURP.R2. The reasons this might be will be discussed further in the section below on methodological limitations.

Previous estimates of antibody decay

Previous half-life estimates of *Pf*-specific antibodies vary across studies. Some estimate very rapid declines in antibody levels, while others estimate a much longer duration after infection (Table 5.9). The shortest decay rates are based on a cohort of 41 Kenyan children under 10 years of age, where IgG1 and IgG3 antibody reactivity to *Pf*AMA1, *Pf*MSP1$_{19}$, two *Pf*MSP2 allelic types, and EBA175 was estimated over a 12-week period after clinical malaria infection.[333] The mean half-life of IgG1 responses for the five antigens combined was 9.8 days, while mean half-life of IgG3 was 6.1 days. This analysis was restricted to individuals who showed consistent decline of antibody levels over four consecutive periods only, excluding any individuals with evidence of antibody boosting.

In The Gambia, a longitudinal analysis of IgG1 and IgG3 responses to *Pf*AMA1, *Pf*MSP1, *Pf*MSP2 and EBA175 was also conducted in children, but only up to age six and followed during the dry season after malaria transmission. This study also found that most antibodies were lost within four months in the absence of reinfection. Based on Kaplan Meier survival analysis, the mean time to reach 50% of initial antibody levels was 16 days in children ages 1-3 years, and slightly longer in children aged 4-6 years (52 days for IgG1 and 47 days for IgG3).[212] Declines in antibody responses to *Pf*AMA1 and EBA175 also showed large differences between age groups, with levels declining more rapidly in younger children.

Amongst studies assessing antibody kinetics across all ages, a longitudinal study in Nigeria with individuals ranging from 5 to 70 years old observed slightly longer duration of antibodies to EBA175 and Rh2.[267] Based on linear regression, decay of antibodies to EBA175 was estimated to be 98 days for parasite positive individuals (by microscopy) and 64 days for parasite negative individuals. For Rh2, half-life was estimated to be 120 days for parasite positive individuals and 82 days for parasite negative. Higher antibody levels (total IgG3 and IgG3) to EBA175 were associated with older ages, but not for IgG2 and IgG4. However, no age differences were observed for antibodies to Rh2. Additionally, differences in EBA175 antibody half-lives were observed between IgG subtypes, with shorter half-lives for IgG2 and IgG4 compared to IgG1, IgG3 and total IgG. Subtype-specific antibody responses to Rh2, on the other hand, showed shorter half-lives of IgG1, IgG2 and IgG4 compared to total IgG.

In an all-age longitudinal study based on PCR-positive individuals in Cambodia, the 95%CI half-life estimates for *Pf*MSP1$_{19}$ and *Pf*GLURP were much longer, ranging from just under 7.5 months to 1.5 years, while for CSP the estimates ranged from less than 7.5 months to over 2 years. This is one of the few studies to estimate antibody half-lives using the Luminex platform, though the majority of the antigens evaluated were for *P.vivax* and did not include any the *Pf*-specific markers of recent infection investigated in this chapter.

The influence of age and acute clinical infection on antibody decay

These studies highlight several considerations. First, that antibody decay may be more rapid in children and following acute infections, especially if they are quickly treated with anti-malarials. This is likely manifested as intense initial boosting of antibodies, followed by a subsequently fast reduction after the parasitic stimulus is cleared. This emphasises the need for studies to include both symptomatic and asymptomatic individuals to assess the utility of biomarkers in surveillance across all types of infection, particularly those that are sub-patent and more likely to have subtle antibody dynamics.

Second, the role of IgG subclasses may also be important. IgG3 antibodies thought to be shorter lived due to their rapid clearance from circulation.[212,334,335] However, based on the subtype-specific analysis in the Nigerian study described above, these dynamics may differ depending on the antigen. Generally, IgG2 and IgG4 are believed to bind more weakly than IgG1 and IgG3.[336] This may have implications not only for the estimation of antibody half-life, but the differential specificity of subclasses as markers of recent malaria infection. Our current understanding of IgG subclasses and their association with antigen, age, and protective immunity remains mixed.[255,299] Therefore, further investigation into the effect of subclasses for the antigens in this study might help to fine-tune the type of response that should be measured for maximum specificity as a diagnostic marker.

The role of memory B cells - models estimating the half-life of short vs. long-lived plasma cells

A number of studies have also tried to quantify the longevity of memory B cells (MBCs) and its contribution to protective immunity. For instance, a study in adults in Thailand estimated the half-lives of antibodies and MBCs to *Pf*AMA1 and *Pf*MSP1$_{19}$ after clinical infection and did not observe decay rates significantly different from zero. This suggested stable maintenance of antibodies over a long period, even in the absence of reinfection.[337]

As described in Chapter 1, antibody-secreting plasma cells (ASCs) can be short-lived or long-lived. Naïve B cells will differentiate into short-lived plasma cells to control initial infection or into long-lived plasma cells (LLPCs) and MBCs for sustained antibody-based immunity. While short-lived plasma cells need to be replenished from a MBC population, LLPCs survive and can secret antibody for extended periods independently.[212,338,339] It is believed that repeated infection is required to build up LLPCs to a steady-state antibody level. *Pf*-specific MBC prevalence appears to be low in adults (~30-50%), even in those with a history of *Pf* infection. However, once acquired, they appear to be long lived and persist in the absence of chronic infection.[127,340]

Using longitudinal data on immune responses in Ghanaian and Gambian children, White et al developed a model to estimate the half-life of both short and long-lived ASCs.[265] This model assumes that both ASC types produce antibodies, but decay at different rates. They hypothesised that the differentiation of naïve B cells and MBCs into ASCs may generate rapid boosts in antibody titres as well as less discrete waves of antibodies, and that this underlying biphasic decay is not always easily distinguished if observing total IgG overall. For short-lived ASCs, the model estimates half-lives in the order of approximately 10-20 days, while LLPCs are estimated to have half-lives of 2-4 years or more (Table 5.9).

Generally, models such as the one described above are difficult to validate biologically. Long-lived ASCs and MBCs are located primarily in lymphoid organs and only detectable in peripheral blood mononuclear cells (PMBCs) in the short period between differentiation and migration to the bone marrow.[341] While mouse models indicate there is a correlation between ASCs in tissue and serum antibody concentrations,[342] they are still poorly studied in humans due the experimental limitations described here. Even if the long half-lives estimated based on total IgG in the study presented in this chapter could be explained by parameterising short and long-lived ASCs, models make large assumptions about their relative proportions. Furthermore, existing estimates based on these models have still shown to be imprecise. More importantly, challenges related to measuring these dynamics with a cost-effective assay design are likely to make it impractical for surveillance purposes.

Table 5.9 Studies estimating *Pf*-specific antibody half-life

STUDY	ASSAY / ANTIGENS*	STUDY POPULATION	STATISTICAL METHOD	HALF-LIFE ESTIMATES
KINYANJUI ET AL 2007 [333]	**ELISA** Antigens: *Pf*MSP1$_{19}$, *Pf*AMA1, *Pf*MSP2 type A and B, EBA175 region II Subclasses: IgG1 and IgG3	**Kenya** 32 children diagnosed with clinical malaria (Kilifi District Hospital) Clinical infections (treated)	**Linear regression** – monophasic exponential decay Only individuals with antibody decline over 4 consecutive time points, excludes individuals with antibody boosting	**All antigens combined** IgG1 (n = 23 children): 9.8 days IgG3 (n= 9 children): 6.1 days
AKPOGHENETA ET AL 2008 [212]	**ELISA** Antigens: *Pf*MSP1$_{19}$, *Pf*AMA1, *Pf*MSP2 type A and B, EBA175 region II Subclasses: IgG2 and IgG3	**Gambia** 35 children ages 1-6 years Follow-up during dry season	**Kaplan Meier survival analysis** – mean days to reach 50% of day 0 antibody levels Only individuals with marked declines in IgG antibodies to either or both *Pf*AMA1 and *Pf*MSP2	***Pf*AMA1 and *Pf*MSP2** combined Ages 1-3 years (IgG1 and IgG3): 16 days Ages 4-6 years (IgG1): 52 days Ages 4-6 years (IgG3): 47 days
ISMAIL ET AL 2014 [267]	**ELISA** Antigens: EBA175, Rh2 Subclasses: Total IgG, IgG1, IgG2, IgG3, IgG4	**Nigeria** 40 individuals ages 5 – 70 years Clinical infections (treated)	**Linear regression** – exponential decay Only individuals with decreasing antibody levels over 3 consecutive time points	Total IgG **EBA175** (parasite positive): 98 days **EBA175** (parasite negative): 64 days **Rh2** (parasite positive): 120 days **Rh2** (parasite negative): 82 days Shorter half-lives for IgG2 and IgG4
KERKHOF ET AL 2016 [301]	**Luminex** Antigens: *Pf*MSP1$_{19}$, *Pf*GLURP, *Pf*CSP Total IgG	**Cambodia** PCR positive samples from individuals ages 2- 50	**Linear regression** adjusted for age group	***Pf*MSP1$_{19}$:** 225 days (171 – 329) ***Pf*GLURP:** 207 days (130 – 512) ***Pf*CSP:** 277 days (165 – 866)

Table 5.9 (continued) Studies estimating *Pf*-specific antibody half-life

STUDY	ASSAY / ANTIGENS*	STUDY POPULATION	STATISTICAL METHOD	HALF-LIFE ESTIMATES
WIPASA ET AL 2010 [337]	**ELISA, ELISPOT** Antigens: *Pf*AMA1, *Pf*MSP1$_{19}$ Antibody (total IgG) and memory B cells	**Thailand** 17 adults aged 23 – 48 with history of clinical malaria	**Mixed effects linear regression**	**Antibodies** ***Pf*AMA1**: 10.36 years (3.45, ∞) ***Pf*MSP1$_{19}$: 7.56 (3.54, ∞) ***Pf*MSP1 + *Pf*AMA1:** 16.27 years (4.15, ∞) **Memory B cells** ***Pf*AMA1:** ∞ (1.8, ∞) ***Pf*MSP1$_{19}$:** 10.6 years (1.18, ∞) ***Pf*MSP1 + *Pf*AMA1:** 7.47 years (1.75, ∞)
WHITE ET AL 2014 [265]	**ELISA** Antigens: *Pf*AMA1, *Pf*MSP1, *Pf*CSP, EBA175 Total IgG	**Ghana** 151 children followed from birth to 2 years **Gambia** 123 children ages 1-6 years, followed for 3 months in dry season following previous malaria infection in transmission season	**Bi-phasic exponential boost and decay model** Model estimates half-life for: Total IgG antibodies Short-lived antibody secreting plasma cells (ASC) Long-lived ASCs	**Ghana** ***Pf*AMA1** IgG: 17 days; short-lived ASC: 2.5 days Long-lived ASC: 2,956 days ***Pf*MSP1** IgG: 19 days; short-lived ASC: 2.4 days Long-lived ASC: 1,901 days ***PfCSP*** IgG: 14 days; short-lived ASC: 3.0 days Long-lived ASC: 2,881 days **Gambia** ***Pf*AMA1** IgG: 7 days; short-lived ASC: 4 days Long-lived ASC: 1,050 days ***Pf*MSP1** IgG: 7 days; short-lived ASC: 10 days Long-lived ASC: 859 days **EBA175** IgG: 11 days; short-lived ASC: 10 days Long-lived ASC: 1,607 days

*some studies include additional antigens, but only those antigens for comparison against this study are listed here

The influence of genetic diversity and antigenic variation on immunogenicity

Additional explanations for the varying antibody dynamics observed in this dataset may be the genetic diversity of the parasite population or antigenic variation. As mentioned above, studies have shown that protection from clinical malaria requires a repertoire of antibody responses across antigens. It is believed that inefficient acquisition of antibodies may be associated with the parasite's ability to clonally vary protein expression on the surface of infected red blood cells as a means of immune evasion. Individuals may only generate a protective repertoire of antibodies after years in endemic areas and infection by multiple parasite clones.[343–345] For example, the high level of within-population polymorphism in the MSP2 antigen is thought to result in slower acquisition of memory B and T-cell responses and more transient antibody production (though, this might also be overcome by cross-reactivity between variants).[346] Ultimately, investigating the role of antigenic variation for more novel antigens in this study may be useful in case multiple variants or chimeric antigen constructs[347] need to be developed or included in future assay platforms. These and other factors influencing serological detection of previous and current malaria infection are illustrated in Figure 5.28.

Methodological limitations

Half-life estimation

The large variation of antibody kinetics estimated (Table 5.9) highlights the lack of a standardised approach in both study design and half-life estimation methods. Studies estimate half-life with linear regression[267,301,333,337], survival analysis[212] or estimate additional factors such as MBCs and ASCs[265,337]. Other factors that varied across studies include the age range of the study population, type of malaria infection (clinical episode vs. PCR-positive), and whether individuals or samples with antibody boosting post infection were excluded.

In this study, estimating antibody decay rate using linear regression resulted in very large confidence intervals, most of which included negative values (i.e., no antibody decay). Using Cox proportional hazard models to estimate time sero-negative antibody levels resulted in shorter and more precise half-life estimates. This may be a more accurate way to define decay in the context of surveillance, given that decay is highly dependent on the magnitude of the boost. If this is not very strong, half-life could be estimated to be very long, even if they reach a sero-negative antibody levels quickly. The baseline population antibody level for some antigens may also be higher. Studies that have used survival analysis[212] define time to event as reaching 50% of baseline antibody levels. One option for the data presented in this chapter is to use antibody levels of individuals without recorded malaria infection during the study. However, caution

should be taken as their infection history prior to the study may still influence antibody levels, potentially resulting in overestimated baseline levels.

Survival analysis does not estimate the individual-level rate of decay, but rather the rate at which a certain proportion of the population reverts to sero-negative antibody levels after infection. This can be compared to the use of reverse-catalytic models that estimate population-level sero-reversion rate.[291] Linear regression and the use of continuous antibody data has some advantages over the use of binary data in survival analysis,[123] but it also introduces more variation and potentially non-informative noise to the estimates.

Data censoring

A number of studies exclude individuals or time points where antibodies are still boosting, and this could lead to biases. For linear regression analysis, this may over fit the data and underestimate half-life, but including time points during which an individual may still be acquiring antibodies would overestimate. For survival analysis, time to event can be defined as either the first time point at which an individual has a sero-negative antibody level or two consecutive sero-negative readings. It is not clear which would best allow for fluctuations in antibody levels that occur even in the absence of re-infection. Analysing the difference in results for this dataset would be useful, but would require a longer period of follow-up.

Antibody acquisition

So far, this study focuses only on estimating antibody decay, and not the rate of antibody acquisition. However, potential methods to estimate this include segmented regression analysis, where both boost and decay parameters are estimated as an interrupted time series. These parameters could also be estimated with Bayesian Markov Chain Monte Carlo (MCMC) methods, which may be better suited to situations where individuals vary in their time to boost, such as in this dataset (Figure 5.16). Antibody acquisition models applied at the cluster level will be described in more detail in Chapter 6. However, future work could involve using these models to estimate antibody acquisition at the individual-level, as has been used by White et al.

Biomarkers for detecting previous malaria infection – predictive accuracy

While quantifying the dynamics of antibody response aids in our understanding of immune responses, the study presented here is ultimately interested in how these antigens serve as biomarkers of recent malaria infection. Antigens evaluated by Helb et al in Ugandan children estimated AUC values ranging from 0.87 (HSP40) to 0.91 (Hyp2, GexP18) for detecting infections in the last 30 days and AUC values from 0.86 (GexP18) to 0.92 (HSP40) for detecting infection in the last year. This study included current microscopy result as a predictor in their ROC analysis.

The data presented in this chapter also estimated similar AUC values in young children when including RDT or PCR test results in ROC analysis (AUC 0.72 – 0.93 for infection < 30 days ago, and 0.72 -0.91 for infection <150 days ago). However, predictive accuracy was slightly lower when RDT/PCR results are not used, particularly for less recent infections (mean AUC 0.81 for infection <30 days vs mean AUC 0.79 for infections <150 days). While the predictive accuracy for infections in older children was similar for recent infections (<30 days), AUC values began to fall for detecting infections occurring more than 3 months ago. Overall, the predictive accuracy in adults was low compared to children, regardless of time since last infection. The predictive accuracy was also stronger in RDT-positive compared to RDT-negative / PCR-positive individuals.

For the biomarkers investigated here, children may be a better target for sero-surveillance of malaria incidence because they experience more differentiating antibody responses upon infection relative to adults. However, lower AUC values in adults may also reflect limitations in the dataset because they may be more likely to experience infection prior to the start of the study and be misclassified as negative for recent infection in the predictive model. For particular markers more associated with protective immunity, they may also have higher antibody levels even in the absence of recent infection, decreasing the ability of these markers to identify recent infection. Additionally, they are also more likely to experience asymptomatic infection, whereas children will be more likely to have RDT-positive infections due to higher parasite densities. Therefore, AUC values might reflect imprecision in the data and/or model as opposed to a weakness in the serological markers. Identifying serological markers specifically for adults, therefore, should aim to use datasets where a longer history of infection is known (up to one year or more).

A number of antigens in this study were found to have highly correlated antibody responses (Figure 5.27). This included associations within the EBA and Rh antigen families, while AMA1 was correlated with GLURP, MSP, EBA antigens and Rh2.2030. GLURP was correlated with MSP and EBA antigens, Rh2.2030, Rh4.2, GexP18 and Hyp2. Additionally, Etramp5.Ag1 was highly correlated with $MSP1_{19}$. This is expected given that these are all blood-stage antigens and many share similar functions for parasite invasion or red blood cell attachment (as discussed in Chapter 1).

While many of these antigens have not been widely studied previously (Etramp5.Ag1, GexP18, Hyp2), associations between other merozoite antigens have been observed before. In a cohort of 206 Papua New Guinean children, the combination of antibody responses to EBA, Rh2 and Rh4 antigens were found to have an additive effect, where high responses to all three antigens were strongly associated with protective immunity against symptomatic malaria. Rh5 also showed additive protective effects when combined with EBA175, AMA1 and $MSP1_{19}$. Conversely,

combinations of different MSP antigens, or MSPs with micronemal antigens ($MSP1_{19}$/AMA1, $MSP1_{19}$/EBA175RII) did not show stronger protective effects compared to single-antigen responses.[170] The association with EBA and Rh antigens may suggest that there is an additional benefit to the host in mounting an immune response to blocking ligands in a variety of invasion pathways.[173]

Understanding these associations may aid in biomarker selection in a multiplex panel to determine which antigens may be redundant or add to the comprehensiveness of capturing total antibody responses in the population. It would be useful to further assess whether these correlations are the same for different age groups. Final ROC analysis was based on combined biomarker panels chosen with logistic regression because random forest models do not always account well for correlations between variables used in prediction.[323] Random forest models could be used for sensitivity analysis to test the variable importance of antigens when combined with other correlated antigens based on Figure 5.27 and when included in models without other correlated antigens.

Additionally, estimates of the predictive power of single antigens suggest they may be just as robust as combined biomarker panels for detecting previous infection (AUC range 0.69–0.82 across top 5 antigens and time since infection categories; Appendix 5.2, Table 5.19). Linear regression was used to select the antigen most correlated with previous infection, but the predictive power was then assessed for the top antigens combined. It should be noted that the association of individual antigens with previous infection was not necessarily strong based on linear regression, but still used to prioritise which antigens amongst the full panel should be selected for further ROC analysis. Further analysis should further quantify the additional predictive power that is gained by combining particular antigens. Specifically, panels that separate antigens associated with short-lived vs. long-lived antibody responses should be assessed using ROC analysis for their predictive power as single antigens and combined. Additionally, this can be investigated for antigens shown to be highly correlated, as mentioned above.

In this study, individuals who are RDT-positive were treated with artemether-lumefantrine, clearing the parasitaemia that would stimulate antibody levels for detection. Additionally, while this study aims to account for parasite density by distinguishing between RDT- and PCR-positive infections, without genotyping to determine whether these are due to the same infection or a new infection, it is difficult to draw conclusions on the association of antibody responses between patent and sub-patent infections. Other adjustments or analyses that could be made include correcting p-values to account for multiple testing (Bonferroni), sensitivity analysis using data normalised to arbitrary antibody concentration units rather than loess normalised MFI values (as

discussed in Chapter 5a), and testing the influence of sero-positivity thresholds for ROC analysis based on binary outcomes.

Overall, results presented here indicate that several antigens are consistently top predictors of recent infection across ages, time since infection and infection severities (Figure 5.26), including Etramp5.Ag1, GexP18, HSP40, and certain Rh and EBA antigens (e.g., Rh2.2030, EBA175). These could be potentially promising tools for surveillance. However, antigens associated with long-lived antibody responses (MSP1.19 and AMA1) are also correlated with recent infection, and may still have utility for surveillance over longer periods of time.

Future work for developing sero-surveillance tools – study design, sampling frames, and use-case scenarios

As mentioned above, studies similar to the one presented in this chapter are limited because longitudinal data often faces sampling challenges such as variability in previous infection, as well as reinfection during prospective follow-up. Additionally, these studies are primarily concerned with validating markers of protective immunity, as opposed to previous infection. This is one reason why controlled human malaria infection (CHMI) studies in malaria-naïve subjects are becoming increasingly common. While extremely useful, these are not ideal for understanding antibody dynamics in endemic populations due to differences in naturally acquired immunity that may not lead to similar outcomes. For instance, results from the RTS,S trials showed that vaccination conferred sterile protection in approximately half of malaria-naïve adults[348], but only 30-50% protective efficacy in African infants and children[349,350]. Similar vaccines studies for candidates targeting the liver stage antigen thrombospondin related adhesion protein (TRAP) also showed partial efficacy in malaria naïve adults, but no efficacy in African children or adults.[351–353] This could be due to important genetic factors, such as differences in major histocompatibility complex (MHC) HLA alleles.[354] Another possibility is that factors such as nutritional status[355] and co-infections with other pathogens common in malaria endemic areas may modulate the development of *Plasmodium*-specific immunity[356]

Endemic settings with intensely seasonal transmission (e.g., West African, Sahelian) can allow useful designs for field-based immunological studies. As described by Crompton et al[127,357], cohorts can be enrolled during the dry season where there is little to no malaria and followed through the malaria season, or vice versa (similar to the study by Akpogheneta et al[212]). The predictable timing of transmission could allow multi-year cohort studies where infections and clinical episodes are monitored through active parasitological and clinical surveillance, with samples collected at time points before, during, and after asymptomatic and symptomatic infection. These study designs can also allow participants to serve as their own healthy pre-

infection controls. Future studies designed in this fashion could allow better investigation of how acute and chronic *Pf* infections modulate the human immune response.

Antigens that tend to be more associated with protective immunity could be a means of post—elimination surveillance to understand population susceptibility to clinical disease in the event of reintroduction. In areas of low or rapidly declining transmission intensity, it is likely that the level of parasite exposure will affect the dynamics of the immune response measured in the population[358] and the ability of serology platforms to have a stable signal. Therefore, careful selection of biomarkers at different stages of elimination will be important.

Figure 5.28 Factors influencing serological detection of malaria infection

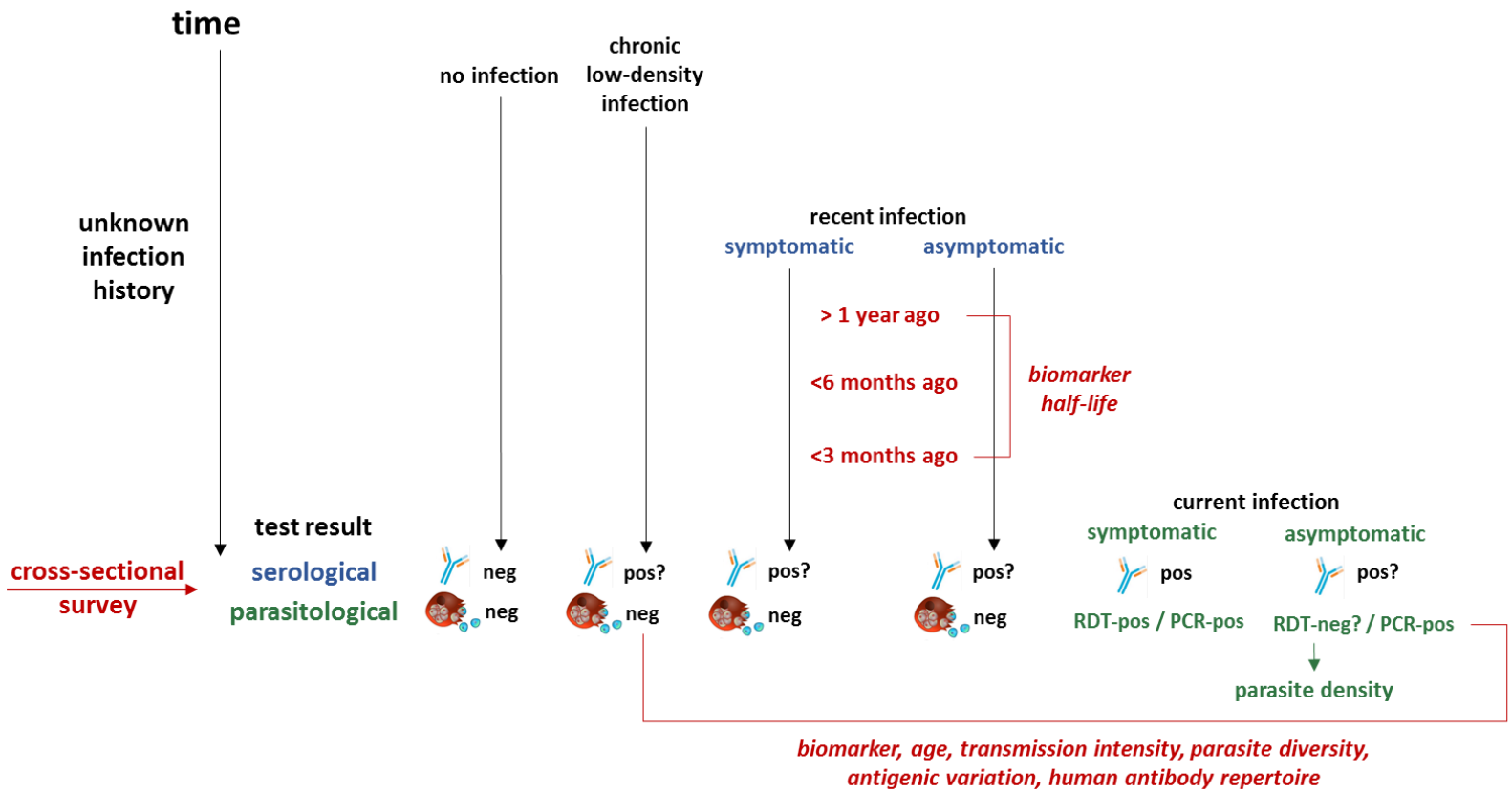

The results presented in this chapter have made first steps in assessing which antigens could be included in sero-surveillance tools. However, there is a sizeable amount of future work that is required to determine how they will be used. This includes:

- Separate assessment of antigens eliciting long vs. short-lived antibody responses and by extension, distinguishing between markers of recent infection and markers of protective immunity
- Determining for which antigens there is differential antibody kinetics between subclasses that may be more specific to recent infection (IgG and IgM responses) and optimising assay according to capture these responses
- Identifying which allelic variants (if any) are relevant for capturing infection by all circulating parasites in environments with a high degree of genetic diversity. This will likely require a revisit to micro-array platforms that are able to assess reactivity to a larger number of analytes and has been done previously exploring v*ar* genes and sero-reactivity to *Pf*EMP1[158]. Future down-selected surveillance platforms could include all variants or chimeric antigen constructs.[347]
- Classifying antigens according to demographic groups (age, history of infection, transmission intensity) and determining whether they are best used as population-wide biomarkers or only useful for convenience sampling (school children, expanded program on immunization (EPI), pregnant women and antenatal clinics, or occupational risk (e.g., male adult forest /mine workers)
- Setting desired sensitivity/specificity thresholds depending on diagnostic use by:
    - Defining what constitutes a false-positive or false-negative in different elimination strategies or trials
    - Quantifying the magnitude of false-positive or negative results across transmission settings and what the potential impact on intervention decisions would be

Appendix 5.2. Additional graphs and tables assessing antibody dynamics

Figure 5.29 Distribution of time to decay, by antigen and age

Vertical lines along the x-axis show individual data points. Individuals with no antibody decay during time period of observation are recorded as having time to decay of 180 days.

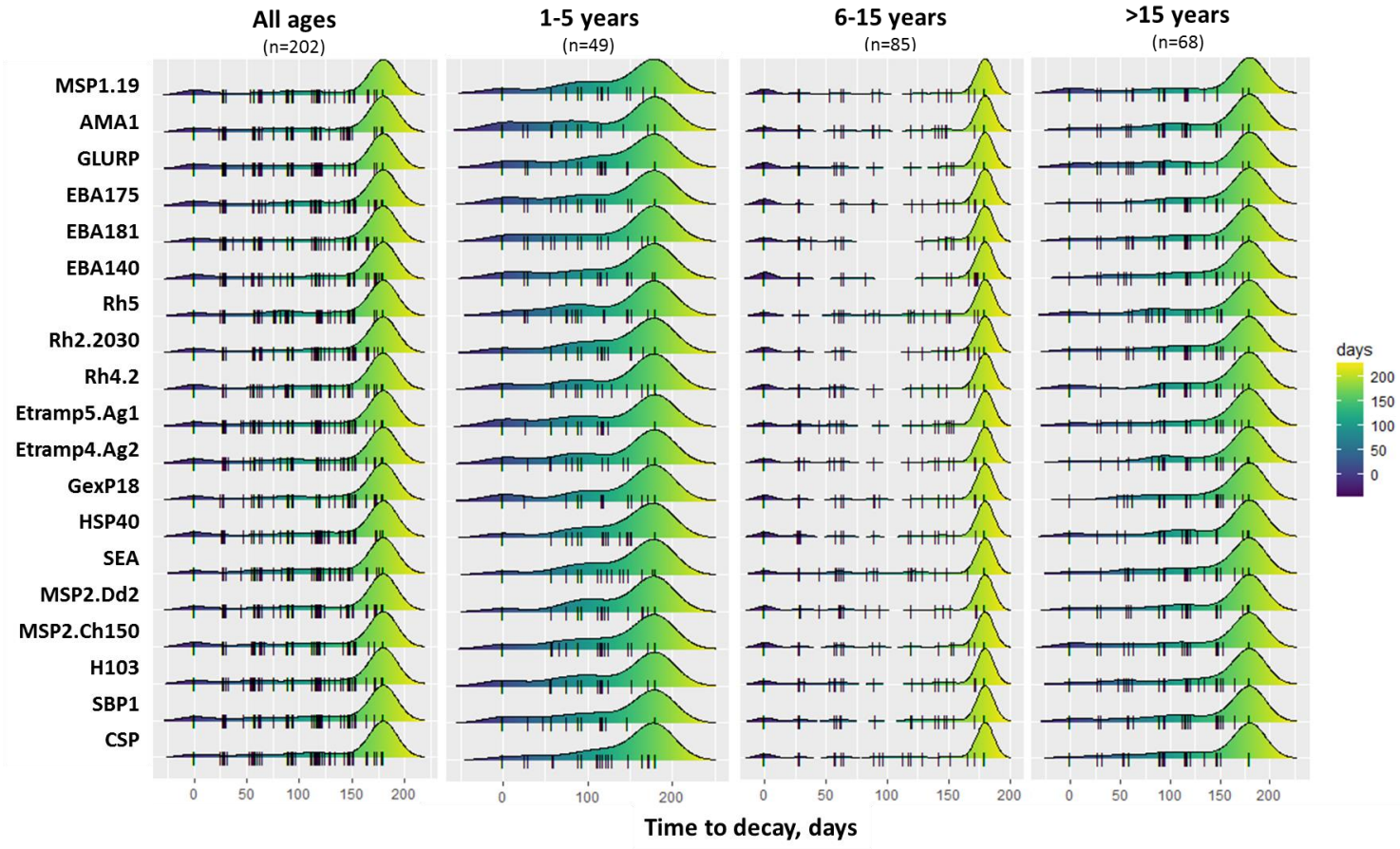

Figure 5.30 Distribution of time to decay, by antigen and RDT-positivity

Vertical lines along the x-axis show individual data points. Individuals with no antibody decay during time period of observation are recorded as having time to decay of 180 days.

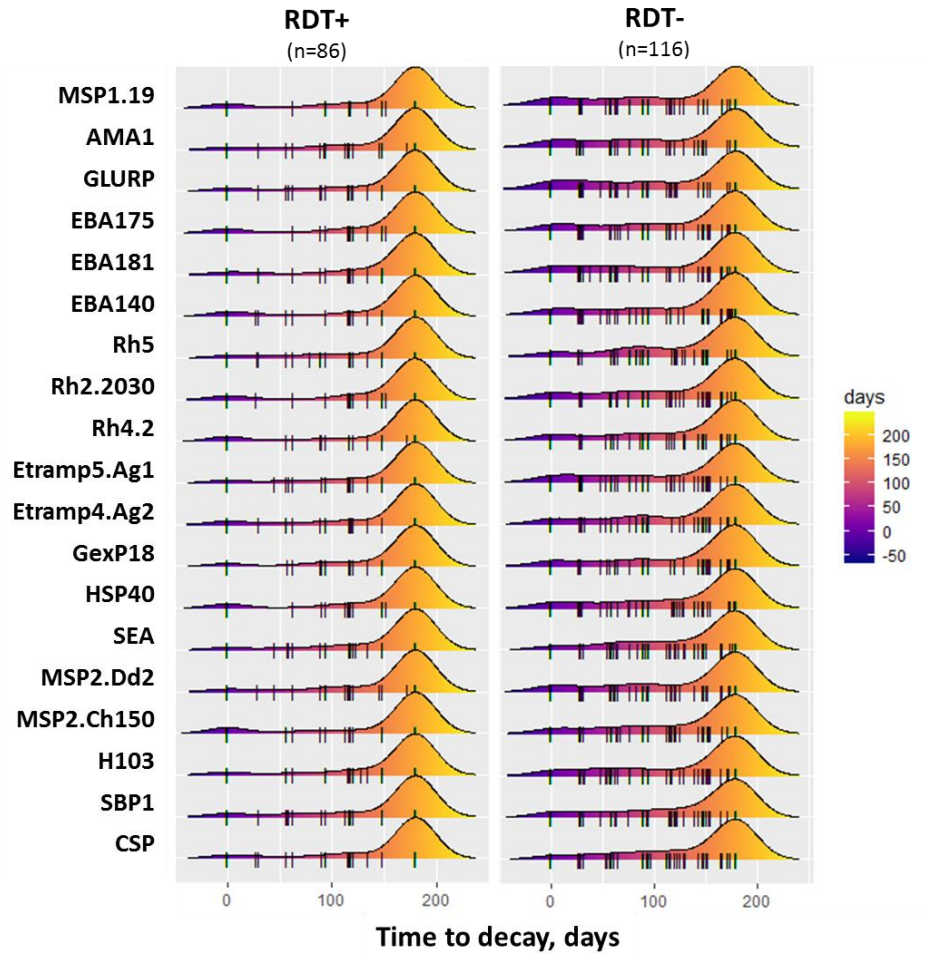

Table 5.10 Antibody intensity and days since infection (continuous), unadjusted

Antigen	baseline log MFI	Δ log MFI time	95%CI lower	95%CI upper	p-value Δ log MFI
MSP1.19	7.33	0.0022	0.0000	0.0045	0.054
AMA1	7.16	0.0023	0.0001	0.0046	0.043
GLURP	6.65	0.0001	-0.0024	0.0027	0.926
EBA175	5.10	0.0031	0.0006	0.0057	0.015
EBA181	5.27	0.0026	0.0005	0.0046	0.016
EBA140	4.91	0.0023	0.0002	0.0043	0.028
Rh5	6.18	-0.0003	-0.0022	0.0015	0.719
Rh2.2030	6.22	0.0049	0.0028	0.0069	0.000
Rh4.2	5.16	0.0012	-0.0007	0.0031	0.214
Etramp5.Ag1	5.98	-0.0019	-0.0040	0.0003	0.097
Etramp4.Ag2	5.39	0.0012	-0.0004	0.0029	0.145
GexP18	6.19	0.0016	-0.0001	0.0034	0.066
HSP40	5.51	0.0027	0.0010	0.0043	0.001
SEA-1	5.75	0.0007	-0.0009	0.0024	0.391
Hyp2	5.55	0.0013	-0.0002	0.0027	0.091
MSP2.Dd2	5.74	0.0022	-0.0001	0.0044	0.057
MSP2.Ch150	5.53	0.0013	-0.0009	0.0034	0.257
H103	5.49	0.0017	0.0001	0.0033	0.039
SBP1	5.61	0.0011	-0.0009	0.0030	0.282
CSP	5.03	0.0018	-0.0005	0.0040	0.119

Table 5.11 Antibody intensity and days since infection (continuous), adjusted for age and transmission intensity

Linear regression of log MFI by days since infection, adjusted for age and village-level PCR prevalence (<10% and >10%)

Antigen	baseline (log MFI)	Δ log MFI time	95%CI lower	95%CI upper	p-value Δ log MFI	age	p-value age	PCR prevalence	p-value prevalence
MSP1.19	4.298	0.0024	0.0001	0.0046	0.040	0.69	0.000	1.21	0.000
AMA1	1.359	0.0025	0.0003	0.0047	0.028	1.54	0.000	1.96	0.000
GLURP	1.160	0.0002	-0.0023	0.0027	0.883	1.77	0.000	1.37	0.000
EBA175	-0.306	0.0033	0.0009	0.0058	0.009	1.52	0.000	1.71	0.000
EBA181	0.685	0.0027	0.0006	0.0047	0.010	1.39	0.000	1.29	0.000
EBA140	2.124	0.0025	0.0004	0.0045	0.018	0.82	0.000	0.81	0.001
Rh5	4.746	-0.0001	-0.0020	0.0017	0.878	0.24	0.042	0.70	0.000
Rh2.2030	1.883	0.0051	0.0031	0.0071	0.000	1.16	0.000	1.46	0.000
Rh4.2	2.718	0.0014	-0.0005	0.0033	0.140	0.57	0.000	0.94	0.000
Etramp5.Ag1	4.035	-0.0017	-0.0039	0.0005	0.123	0.30	0.012	1.01	0.000
Etramp4.Ag2	3.994	0.0014	-0.0003	0.0030	0.111	0.38	0.001	0.45	0.020
GexP18	4.505	0.0018	0.0001	0.0035	0.042	0.25	0.034	0.88	0.000
HSP40	3.671	0.0028	0.0011	0.0044	0.001	0.43	0.000	0.71	0.000
SEA-1	4.265	0.0009	-0.0008	0.0025	0.319	0.33	0.015	0.61	0.005
Hyp2	4.096	0.0014	-0.0001	0.0028	0.062	0.31	0.002	0.61	0.000
MSP2.Dd2	1.617	0.0021	-0.0001	0.0043	0.060	1.31	0.000	1.07	0.000
MSP2.Ch150	0.921	0.0016	-0.0005	0.0037	0.142	1.15	0.000	1.68	0.000
H103	3.352	0.0018	0.0002	0.0034	0.023	0.60	0.000	0.66	0.001
SBP1	4.588	0.0012	-0.0007	0.0031	0.215	0.09	0.380	0.63	0.000
CSP	1.058	0.0019	-0.0003	0.0041	0.090	1.24	0.000	1.06	0.000

Table 5.12 Antibody intensity and days since infection (continuous), ages 1-5 years (unadjusted)

Antigen	baseline (log MFI)	Δ log MFI time	95%CI lower	95%CI upper	p-value Δ log MFI
MSP1.19	6.24	0.0059	0.0002	0.0116	0.042
AMA1	5.40	0.0054	-0.0001	0.0109	0.055
GLURP	4.51	0.0056	-0.0004	0.0115	0.065
EBA175	3.61	0.0047	-0.0002	0.0096	0.061
EBA181	3.97	0.0024	-0.0015	0.0062	0.226
EBA140	3.90	0.0045	0.0006	0.0085	0.025
Rh5	5.63	0.0022	-0.0021	0.0066	0.315
Rh2.2030	4.99	0.0051	0.0012	0.0089	0.010
Rh4.2	4.30	0.0031	-0.0005	0.0068	0.095
Etramp5.Ag1	5.38	0.0015	-0.0036	0.0066	0.567
Etramp4.Ag2	4.71	0.0047	0.0007	0.0086	0.021
GexP18	5.58	0.0061	0.0021	0.0101	0.003
HSP40	4.99	0.0036	0.0004	0.0068	0.027
SEA-1	5.32	0.0009	-0.0025	0.0043	0.599
Hyp2	4.97	0.0042	0.0011	0.0074	0.009
MSP2	4.44	0.0029	-0.0010	0.0069	0.149
MSP2.Ch150	4.21	0.0046	0.0002	0.0090	0.039
H103	4.88	0.0006	-0.0031	0.0043	0.744
SBP1	5.13	0.0050	0.0007	0.0093	0.024
CSP	3.58	0.0029	-0.0014	0.0071	0.184

Table 5.13 Antibody intensity and days since infection (continuous), ages 1-5 years (adjusted for village-level PCR prevalence)

Antigen	baseline (log MFI)	Δ log MFI time	95%CI lower	95%CI upper	p-value Δ log MFI	PCR prevalence	p-value prevalence
MSP1.19	4.04	0.0062	0.0006	0.0118	0.030	1.65	0.002
AMA1	1.68	0.0058	0.0005	0.0112	0.031	2.80	0.000
GLURP	2.65	0.0059	0.0000	0.0118	0.050	1.40	0.005
EBA175	1.22	0.0053	0.0006	0.0100	0.028	1.78	0.000
EBA181	2.25	0.0027	-0.0010	0.0065	0.152	1.29	0.000
EBA140	3.43	0.0047	0.0007	0.0087	0.020	0.34	0.269
Rh5	4.31	0.0027	-0.0016	0.0069	0.225	0.97	0.004
Rh2.2030	2.87	0.0057	0.0019	0.0094	0.003	1.58	0.000
Rh4.2	3.58	0.0033	-0.0004	0.0069	0.080	0.54	0.145
Etramp5.Ag1	3.34	0.0012	-0.0037	0.0062	0.626	1.57	0.000
Etramp4.Ag2	3.88	0.0048	0.0009	0.0088	0.017	0.62	0.100
GexP18	4.13	0.0065	0.0026	0.0104	0.001	1.08	0.001
HSP40	3.44	0.0037	0.0006	0.0069	0.020	1.17	0.001
SEA-1	4.38	0.0010	-0.0024	0.0044	0.558	0.71	0.128
Hyp2	4.05	0.0044	0.0013	0.0076	0.006	0.69	0.015
MSP2.Dd2	2.58	0.0031	-0.0008	0.0070	0.117	1.40	0.000
MSP2.Ch150	1.91	0.0052	0.0010	0.0094	0.015	1.72	0.000
H103	4.09	0.0008	-0.0029	0.0045	0.668	0.59	0.069
SBP1	3.74	0.0052	0.0009	0.0094	0.016	1.04	0.000
CSP	2.15	0.0031	-0.0012	0.0073	0.154	1.07	0.006

Table 5.14 Antibody intensity and days since infection (continuous), ages 6-15 years (unadjusted)

Antigen	baseline (log MFI)	Δ log MFI time	95%CI lower	95%CI upper	p-value Δ log MFI
MSP1.19	7.44	0.0011	-0.0024	0.0046	0.541
AMA1	6.91	0.0021	-0.0013	0.0054	0.227
GLURP	6.49	-0.0031	-0.0071	0.0008	0.120
EBA175	4.86	0.0009	-0.0030	0.0047	0.659
EBA181	5.04	0.0016	-0.0016	0.0047	0.333
EBA140	4.85	0.0016	-0.0014	0.0045	0.303
Rh5	6.39	-0.0019	-0.0044	0.0005	0.127
Rh2.2030	6.13	0.0048	0.0015	0.0082	0.005
Rh4.2	5.44	-0.0017	-0.0048	0.0013	0.265
Etramp5.Ag1	6.17	-0.0041	-0.0076	-0.0006	0.021
Etramp4.Ag2	5.54	-0.0013	-0.0038	0.0012	0.321
GexP18	6.33	-0.0005	-0.0032	0.0023	0.732
HSP40	5.58	0.0011	-0.0015	0.0037	0.410
SEA-1	5.86	0.0002	-0.0026	0.0030	0.898
Hyp2	5.62	0.0001	-0.0022	0.0024	0.924
MSP2.Dd2	5.53	0.0009	-0.0027	0.0044	0.636
MSP2.Ch150	5.40	-0.0009	-0.0040	0.0022	0.588
H103	5.50	0.0016	-0.0007	0.0039	0.169
SBP1	5.82	-0.0004	-0.0032	0.0023	0.762
CSP	5.17	-0.0010	-0.0046	0.0026	0.581

Table 5.15 Antibody intensity and days since infection (continuous), ages 6-15 years (adjusted for village-level PCR prevalence)

Antigen	baseline (log MFI)	Δ log MFI time	95%CI lower	95%CI upper	p-value Δ log MFI	PCR prevalence	p-value prevalence
MSP1.19	5.46	0.0012	-0.0023	0.0047	0.499	1.49	0.000
AMA1	3.84	0.0023	-0.0011	0.0056	0.183	2.32	0.000
GLURP	4.02	-0.0029	-0.0068	0.0010	0.143	1.86	0.000
EBA175	1.79	0.0012	-0.0026	0.0051	0.523	2.30	0.000
EBA181	2.89	0.0018	-0.0013	0.0049	0.256	1.61	0.000
EBA140	3.55	0.0018	-0.0012	0.0047	0.247	0.97	0.007
Rh5	5.66	-0.0018	-0.0043	0.0007	0.153	0.54	0.035
Rh2.2030	3.66	0.0051	0.0017	0.0084	0.003	1.85	0.000
Rh4.2	4.48	-0.0015	-0.0046	0.0015	0.323	0.71	0.039
Etramp5.Ag1	5.01	-0.0039	-0.0073	-0.0004	0.029	0.87	0.004
Etramp4.Ag2	4.91	-0.0012	-0.0037	0.0013	0.360	0.47	0.136
GexP18	5.11	-0.0003	-0.0030	0.0024	0.819	0.91	0.006
HSP40	4.76	0.0012	-0.0014	0.0038	0.367	0.61	0.040
SEA-1	5.09	0.0003	-0.0025	0.0031	0.831	0.58	0.100
Hyp2	4.82	0.0002	-0.0021	0.0025	0.851	0.59	0.038
MSP2.Dd2	4.01	0.0010	-0.0025	0.0046	0.564	1.14	0.002
MSP2.Ch150	2.75	-0.0005	-0.0036	0.0025	0.740	1.98	0.000
H103	4.61	0.0017	-0.0006	0.0040	0.142	0.66	0.029
SBP1	4.66	-0.0003	-0.0030	0.0025	0.859	0.86	0.002
CSP	3.76	-0.0007	-0.0042	0.0029	0.716	1.05	0.002

Table 5.16 Linear regression of log MFI and days since infection (categorical), unadjusted

Antigen	Unadjusted		
	baseline (log MFI)	Δ log MFI time	p-value time
MSP1.19	7.88	-0.1175	0.072
AMA1	7.60	-0.0916	0.259
GLURP	6.79	-0.0679	0.428
EBA175	5.41	-0.0408	0.624
EBA181	5.39	-0.0037	0.957
EBA140	5.21	-0.0468	0.449
Rh5	6.56	-0.1085	0.032
Rh2.2030	6.59	-0.0030	0.966
Rh4.2	5.28	-0.0208	0.719
Etramp5.Ag1	6.11	-0.1024	0.038
Etramp4.Ag2	5.58	-0.0347	0.467
GexP18	6.54	-0.0712	0.152
HSP40	5.87	-0.0524	0.270
SEA	5.93	-0.0372	0.498
Hyp2	5.68	-0.0226	0.593
MSP2.Dd2	6.32	-0.1230	0.064
MSP2.Ch150	5.64	-0.0275	0.686
H103	5.64	-0.0134	0.792
SBP1	6.03	-0.0909	0.039
CSP	5.07	0.0043	0.948

Table 5.17 Linear regression of log MFI and days since infection (categorical), adjusted for age and village-level PCR prevalence

Antigen		Δ log MFI time		Age 6-15 years		Age >15 years		PCR prevalence > 10%	
	baseline (log MFI)	coef	p-value	coef	p-value	coef	p-value	coef	p-value
MSP1.19	5.22	-0.0603	0.317	0.47	0.006	1.19	0.000	1.43	0.000
AMA1	2.97	-0.0065	0.919	0.95	0.000	2.88	0.000	2.28	0.000
GLURP	2.81	-0.0061	0.929	0.95	0.000	3.26	0.000	1.76	0.000
EBA175	1.36	0.0268	0.692	0.73	0.000	2.86	0.000	1.96	0.000
EBA181	1.98	0.0516	0.343	0.82	0.000	2.58	0.000	1.54	0.000
EBA140	3.18	-0.0105	0.856	0.57	0.001	1.39	0.000	0.92	0.000
Rh5	5.14	-0.0741	0.132	0.18	0.207	0.37	0.012	0.85	0.000
Rh2.2030	2.91	0.0675	0.255	0.99	0.000	2.24	0.000	1.74	0.000
Rh4.2	3.16	0.0251	0.645	0.59	0.000	1.00	0.000	1.05	0.000
Etramp5.Ag1	3.89	-0.0478	0.285	0.13	0.330	0.50	0.000	1.39	0.000
Etramp4.Ag2	4.35	-0.0100	0.829	0.17	0.190	0.61	0.000	0.66	0.000
GexP18	4.87	-0.0291	0.538	0.03	0.800	0.27	0.058	1.09	0.000
HSP40	4.26	-0.0189	0.673	0.19	0.139	0.75	0.000	0.89	0.000
SEA	4.51	-0.0043	0.937	0.35	0.025	0.54	0.001	0.75	0.000
Hyp2	4.36	0.0074	0.856	0.17	0.145	0.47	0.000	0.75	0.000
MSP2.Dd2	3.28	-0.0748	0.169	0.72	0.000	2.42	0.000	1.35	0.000
MSP2.Ch150	1.82	0.0448	0.404	0.58	0.000	2.18	0.000	2.00	0.000
H103	3.77	0.0228	0.631	0.59	0.000	1.17	0.000	0.85	0.000
SBP1	4.75	-0.0567	0.183	0.13	0.305	0.13	0.303	0.81	0.000
CSP	1.95	0.0564	0.306	1.14	0.000	2.46	0.000	1.26	0.000

Table 5.18 Cox proportional hazard rates by antigen and age

	Hazard rate (95%CI)			
	All ages	**1-5 years**	**6-15 years**	**>15 years**
MSP1.19	0.008 (0.007 - 0.010)	0.011 (0.008 - 0.015)	0.008 (0.006 - 0.012)	0.007 (0.004 - 0.010)
AMA1	0.006 (0.005 - 0.007)	0.011 (0.008 - 0.015)	0.007 (0.004 - 0.010)	0.003 (0.002 - 0.005)
GLURP	0.005 (0.004 - 0.006)	0.001 (0.007 - 0.014)	0.007 (0.004 - 0.010)	0.002 (0.001 - 0.003)
EBA175	0.008 (0.007 - 0.010)	0.013 (0.010 - 0.018)	0.010 (0.007 - 0.014)	0.005 (0.003 - 0.007)
EBA181	0.009 (0.008 - 0.011)	0.014 (0.011 - 0.019)	0.011 (0.008 - 0.016)	0.005 (0.003 - 0.008)
EBA140	0.012 (0.011 - 0.014)	0.015 (0.011 - 0.020)	0.012 (0.009 - 0.018)	0.011 (0.007 - 0.016)
Rh5	0.013 (0.011 - 0.014)	0.014 (0.011 - 0.019)	0.013 (0.009 - 0.018)	0.011 (0.008 - 0.017)
Rh2.2030	0.008 (0.007 - 0.009)	0.013 (0.009 - 0.017)	0.008 (0.006 - 0.012)	0.005 (0.003 - 0.008)
Rh4.2	0.013 (0.011 - 0.015)	0.015 (0.011 - 0.020)	0.013 (0.009 - 0.019)	0.011 (0.008 - 0.017)
Etramp5.Ag1	0.008 (0.007 - 0.009)	0.009 (0.007 - 0.013)	0.008 (0.005 - 0.012)	0.007 (0.005 - 0.011)
Etramp4.Ag2	0.013 (0.011 - 0.015)	0.014 (0.010 - 0.018)	0.012 (0.009 - 0.018)	0.012 (0.008 - 0.018)
GexP18	0.007 (0.006 - 0.009)	0.009 (0.007 - 0.012)	0.007 (0.005 - 0.011)	0.006 (0.004 - 0.010)
HSP40	0.009 (0.007 - 0.010)	0.012 (0.009 - 0.016)	0.009 (0.006 - 0.013)	0.007 (0.005 - 0.011)
SEA-1	0.012 (0.011 - 0.014)	0.014 (0.011 - 0.019)	0.012 (0.008 - 0.017)	0.012 (0.008 - 0.017)
Hyp2	0.011 (0.010 - 0.013)	0.014 (0.010 - 0.018)	0.011 (0.007 - 0.015)	0.010 (0.007 - 0.014)
MSP2.Dd2	0.009 (0.007 - 0.010)	0.013 (0.010 - 0.017)	0.010 (0.007 - 0.015)	0.005 (0.003 - 0.008)
MSP2.Ch150	0.006 (0.005 - 0.007)	0.012 (0.009 - 0.016)	0.006 (0.004 - 0.009)	0.003 (0.002 - 0.004)
H103	0.013 (0.012 - 0.015)	0.015 (0.011 - 0.020)	0.013 (0.009 - 0.019)	0.013 (0.009 - 0.018)
SBP1	0.013 (0.011 - 0.015)	0.015 (0.011 - 0.019)	0.012 (0.009 - 0.018)	0.013 (0.009 - 0.019)
CSP	0.007 (0.006 - 0.008)	0.014 (0.010 - 0.018)	0.008 (0.006 - 0.012)	0.002 (0.002 - 0.004)

Figure 5.31 Random forest sensitivity analysis, number of predictors and out-of-bag prediction error

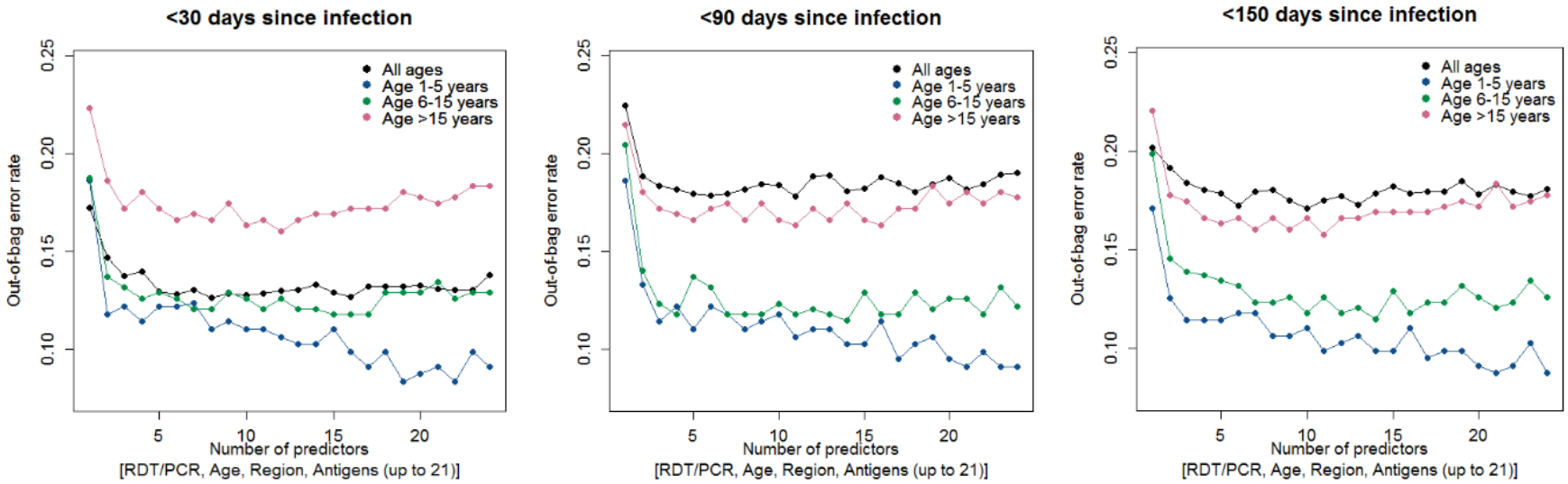

Figure 5.32 Mean MFI by days since infection and age

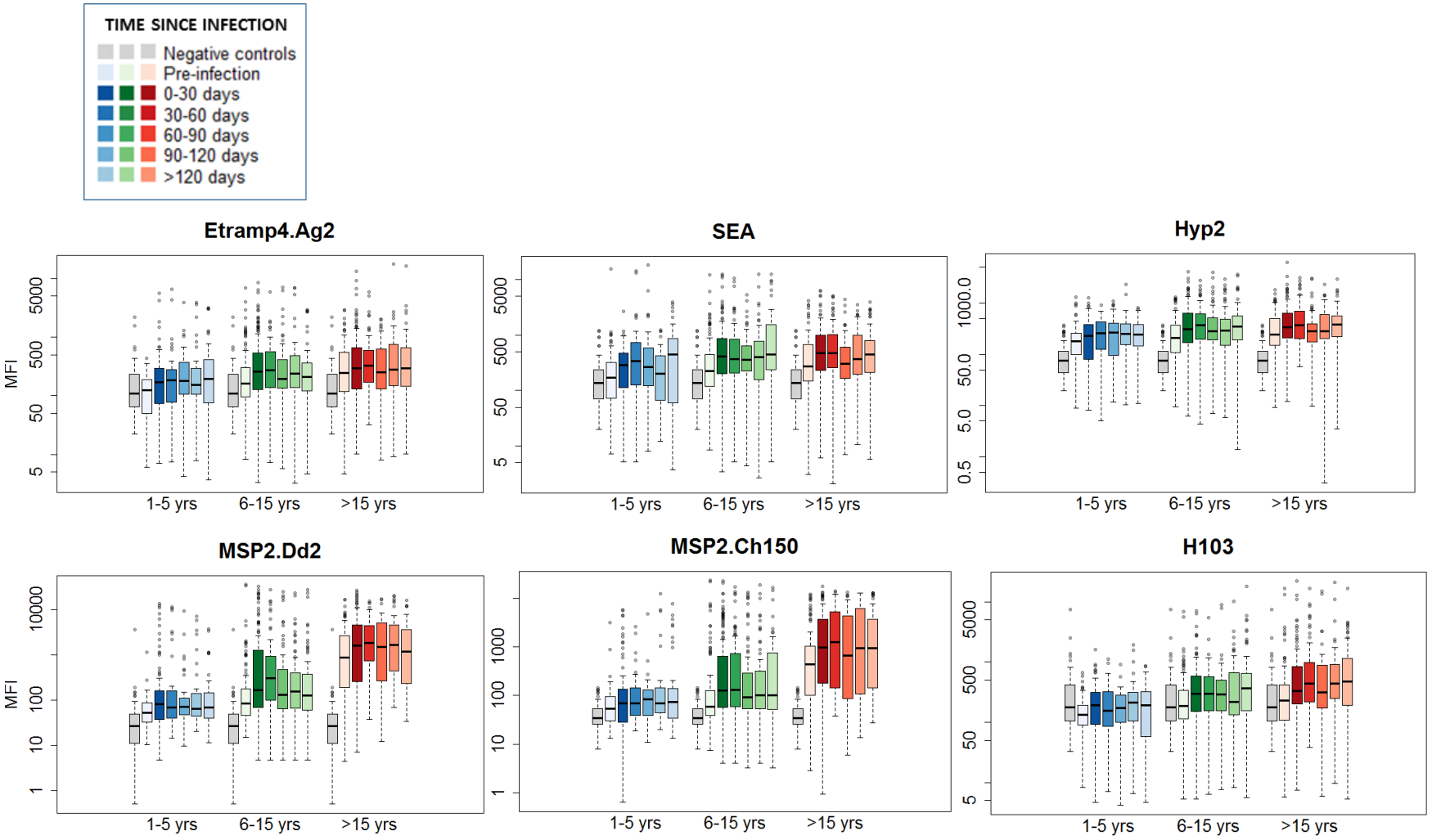

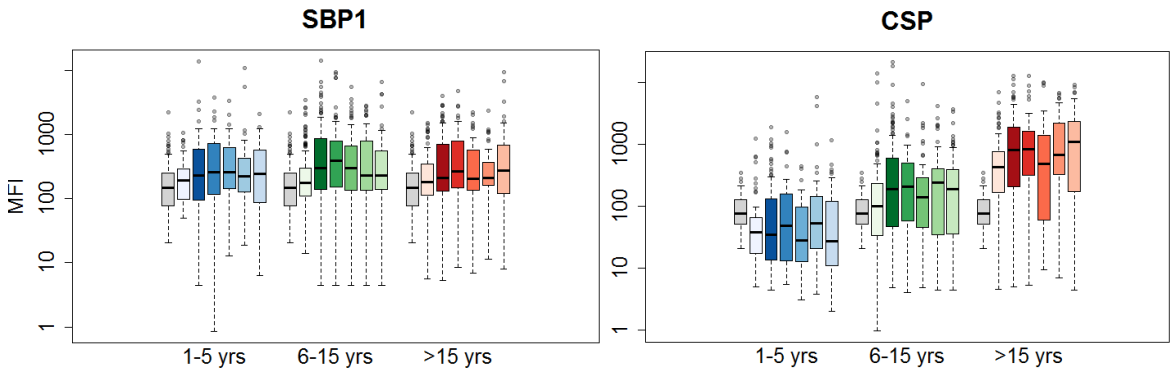
SBP1
CSP
MFI
1
10
100
1000
1-5 yrs
6-15 yrs
>15 yrs

Table 5.19 Cross-validated AUC values predicting infection based on Ab response to a single antigen

AUCs based on predictive model including current RDT/PCR test result shown on left, and excluding RDT/PCR test results shown on right.

AUC (single antigen)		Excluding RDT/PCR	
Top 5 antigens	**Median AUC (95%CI)**	**Top 5 antigens**	**Median AUC (95%CI)**
		<30 days ago	
MSP1.19	0.82 (0.77-0.86)	**Etramp5.Ag1**	0.78 (0.71-0.84)
Etramp5.Ag1	0.82 (0.77-0.88)	**AMA1**	0.78 (0.73-0.82)
AMA1	0.81 (0.76-0.87)	**MSP1.19**	0.77 (0.72-0.84)
MSP2.Dd2	0.81 (0.75-0.86)	**GLURP**	0.77 (0.69-0.84)
MSP2.Ch150	0.81 (0.76-0.85)	**Rh2.2030**	0.76 (0.71-0.80)
		<90 days ago	
AMA1	0.80 (0.74-0.83)	**AMA1**	0.76 (0.71-0.79)
MSP1.19	0.78 (0.74-0.83)	**MSP1.19**	0.74 (0.68-0.80)
Etramp5.Ag1	0.77 (0.73-0.82)	**Etramp5.Ag1**	0.73 (0.68-0.79)
GLURP	0.77 (0.71-0.80)	**GLURP**	0.72 (0.69-0.77)
Rh2.2030	0.76 (0.73-0.81)	**Rh2.2030**	0.72 (0.67-0.77)
		<150 days ago	
MSP1.19	0.77 (0.71-0.81)	**AMA1**	0.72 (0.67-0.77)
AMA1	0.76 (0.73-0.80)	**MSP1.19**	0.71 (0.68-0.76)
Etramp5.Ag1	0.75 (0.71-0.78)	**Etramp5.Ag1**	0.70 (0.65-0.75)
Rh2.2030	0.74 (0.69-0.78)	**GLURP**	0.70 (0.65-0.75)
GLURP	0.74 (0.67-0.78)	**Rh2.2030**	0.69 (0.65-0.74)

Chapter 6 Measuring seasonal and geographical variation in malaria transmission in The Gambia with novel serological biomarkers

In Chapter 5, antibody responses a panel of *P.falciparum* antigens were investigated to identify the strongest biomarkers for recent malaria infection. These were validated using individual-level longitudinal data. This chapter describes antibody responses to a subset of these antigens at the cluster-level by comparing areas of low and high transmission intensity and between dry and wet season in four villages in The Gambia to assess how serological markers can be used to measure short-term changes in transmission.

6.1 Background

For decades, the geographical size and pronounced seasonality of The Gambia has led to numerous studies on the heterogeneity of malaria. The country is characterised by marked variations in clinical incidence, parasite prevalence, and parasitaemia, even over small distances with similar infection risk. Studies as early as the 1980s observed local-scale variation in malaria infection within 2 kilometres of mosquito breeding sites that are unexplained by bed-net usage or entomological inoculation rate (EIR).[136] At that time, researchers hypothesised that this was due to variations in protective immunity, leading to reductions in parasite prevalence in children experiencing the more intense malaria challenge.

This epidemiological landscape has also enabled pivotal studies evaluating the effectiveness of cluster-level interventions to reduce malaria transmission. Amongst the first community-based studies in The Gambia were randomised controlled trials to determine the efficacy of insecticide treated bed nets (ITNs). Significant reductions were observed in villages where all nets in a village were treated (as opposed to individual nets), suggesting a potential herd effect for individuals sleeping in proximity to households using ITNs.[359–361] Larger-scale studies following this also included chemoprophylaxis for children under 6 years of age together with ITNs and found significant reductions in clinical incidence in children.[362] These findings led to WHO support for additional multi-country studies in Africa confirming the efficacy of ITNs in reducing child mortality as well as WHO support in The Gambia for free national provision of insecticide.[363] Bed-net usage across the country remains high today (71.5% ownership of LLINs in 2013).[220] In 2012, seasonal malaria chemoprevention (SMC) in children under age five was recommended by the WHO for use in the Sahel and sub-Sahel where malaria transmission is seasonal and sufficiently intense.

Today, micro-epidemiological variations in malaria transmission still remain. These are even more relevant now as the country aims to achieve elimination for the monitoring and evaluation of community-based interventions.[364] The Malaria Transmission Dynamics study conducted in 2013 (and described in Chapter 5) has observed ongoing variation across the country in EIR, clinical incidence, and *Pf* infection measured by PCR.[220] The latter of these also had varying proportions of patent, sub-patent, and gametocyte-positive infections (Figure 6.1 and Table 6.1).

Table 6.1 Malaria Transmission Dynamics study, clinical and infection incidence June - December 2013

A. Clinical incidence by month

Month	Clinical malaria episodes	Person-years (PYAR)	Incidence rates	Incidence rate ratio	p value
July	8	206.76	0.04 (0.02–0.08)	1	
August	29	320.71	0.09 (0.06–0.13)	2.34 (1.05–5.94)	0.003
September	60	312.19	0.19 (0.15–0.25)	4.98 (0.37–12.05)	<0.01
October	180	316.11	0.57 (0.49–0.66)	14.74 (7.32–34.66)	<0.01
November	308	282.48	1.09 (0.98–1.20)	28.26 (14.16–66.05)	<0.01
December	45	121.41	0.37 (0.28–0.49)	9.62 (4.49–23.64)	<0.01

* Incidence rate ratios comparing incidence rates in July to other months during the transmission season

B. *P. falciparum* infection

Month	*P. falciparum* episodes	Person-years (PYAR)	Incidence rates	Incidence rate ratio	p value
July	151	206.76	0.73 (0.62–0.86)	1	
August	156	320.71	0.49 (0.42–0.57)	0.67 (0.53–0.84)	<0.01
September	121	312.19	0.39 (0.32–0.46)	0.53 (0.42–0.68)	<0.01
October	314	316.11	0.99 (0.89–1.11)	1.36 (1.12–1.67)	0.01
November	453	282.48	1.60 (1.46–1.76)	2.20 (1.83–2.67)	<0.01
December	300	121.41	2.47 (2.21–2.77)	3.39 (2.79–4.16)	<0.01

* Incidence rate ratios comparing incidence in July with the other months during the transmission season

Figure 6.1 Malaria Transmission Dynamics study, overall malaria prevalence and incidence by month

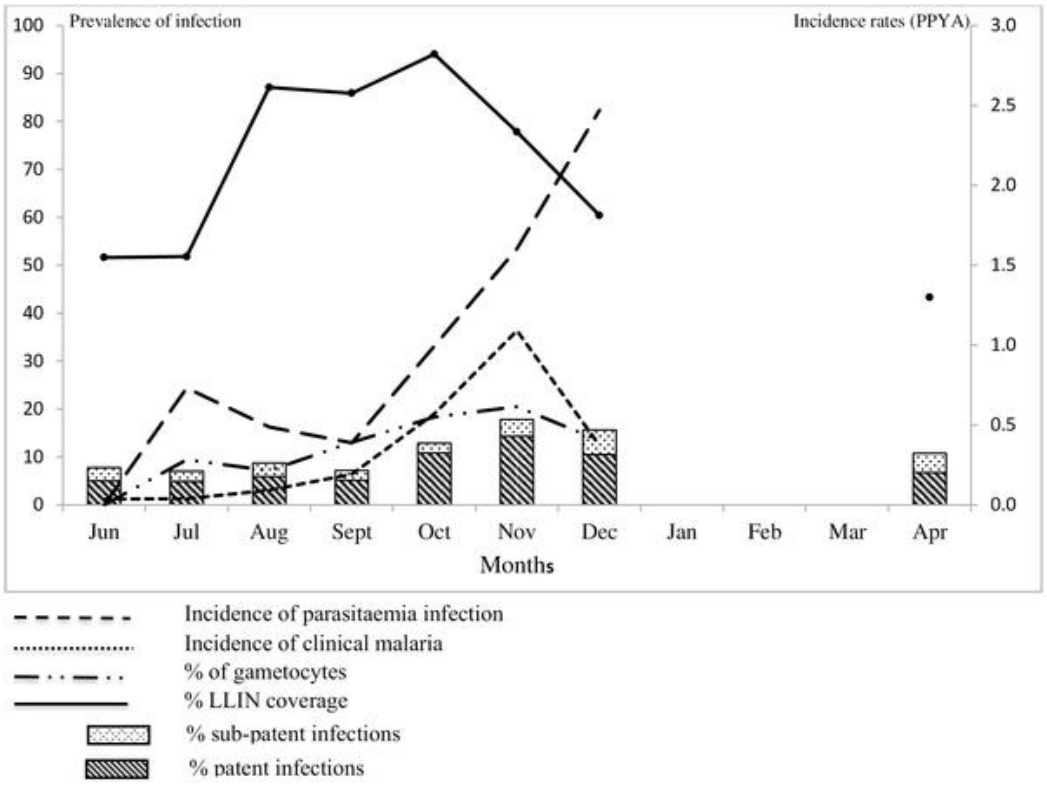

Serological surveys based on $MSP1_{19}$ in Farafenni on the North Bank Region of The Gambia have shown rapid declines in transmission between 1988 and 2011, correlating with declines in under-5 parasite prevalence and all-cause mortality over the same period.[260] In 2012, school-based serological surveys based on $MSP1_{19}$ also showed countrywide variation in transmission, with the highest levels of sero-prevalence in the Upper River Region compared to the West Coast Region.

This study also found a strong association between parasite and sero-prevalence (sero-positive children had a 3-fold increased odds of parasitaemia detectable by microscopy).[219]

Using an expanded panel of serological markers of malaria infection - selected based on their predictive power in Chapter 5b - this chapter aims to evaluate differences in antibody responses at the cluster-level between regions of low transmission intensity (West Coast Region) and high transmission intensity (Upper River Region). It also assesses short-term changes in antibody response within the same region before and after malaria transmission season (July vs. December). An additional cross-sectional survey in April for the Upper River Region is also included to assess whether there are significant declines in antibody responses several months after transmission season.

6.2 Methods

Laboratory procedures and data normalisation

Human plasma from whole blood samples were prepared and tested on the Luminex assay platform using the procedures described in Chapter 5a. Data were normalised to adjust for between plate variation using a loess normalisation method[295] and sero-positivity defined according to methods described in Chapter 5a. Analyses of Ab intensity are based on either median fluorescence intensity (MFI) as a measure of continuous Ab response or sero-positivity as a binary Ab response.

Statistical analyses

Antigen selection

A total of 20 antigens were included in the Luminex multiplex assay for sample processing, but data from only a subset of the most informative markers are included here for brevity. Antigen selection was based on the results summarised in Chapter 5b and includes two markers of long-lived antibody response ($MSP1_{19}$ and AMA1) and five markers of recent infection that demonstrated the highest frequencies as predictors of malaria infection in the last six months across all age categories, "time since infection" windows and infection severity (Etramp5.Ag1, Rh2.2030, EBA175, GexP18, and HSP40).

Sero-prevalence in children

Sero-prevalence in children was estimated for three age ranges - 1-15 years, 2-10 years, and 1-5 years - and sero-positivity values were assigned according to thresholds defined in Chapter 5a. While it has been suggested that sero-prevalence in children age 1-5 years is most correlated with parasite prevalence[260], estimates of clinical incidence and parasite prevalence are routinely standardised to ages 2-10 years[247,258,365] because it has historically been used to classify regions

into hypoendemic (<10%), mesoendemic (10–50%), and hyperendemic (50–75%) transmission categories[366].

Sero-prevalence based on children aged 1-15 may have most relevance for school-based convenience surveys[219,367]. As discussed in Chapter 1 and 5b, it also reflects the age range where individuals may not have fully acquired long lived antibodies to most malaria antigens. Therefore, measuring antibodies in these ages is more likely to correlate with other measures of malaria incidence.

Seroconversion rate

Age-adjusted sero-conversion rates (using Reverse Catalytic Model 1 described in Chapter 4) were estimated for antigens associated with long-lived antibody response ($MSP1_{19}$, AMA1). A fixed sero-reversion rate for each antigen was used across all clusters, which was estimated based on fitting a single sero-catalytic model to all individuals in the sample and setting sero-reversion rate to this value in all subsequent cluster-specific model fits. Models were fit for each antigen and SCRs estimated separately for each cluster and survey month.

Antibody acquisition

The reverse catalytic model is most suitable for long-lived antibody responses due to assumptions about cumulative sero-prevalence by age. However, this is not an accurate assumption for antigens eliciting short-lived antibody response and SCR models are not appropriate. Therefore, for short-term markers, population-level serological responses can be characterised with Ab acquisition models, which use antibody levels as a continuous variable, based on mean MFI as a function of age, rather than dichotomising individuals into sero-positive and sero-negative status.[124] An Ab acquisition model that assumes constant transmission across all ages can be described as:

$$A(a) = \alpha_0 + \frac{\alpha}{r}\,(1 - e^{-r*a}) \tag{6.1}$$

Where $A(a)$ is the geometric mean MFI at age a, α_0 is the baseline antibody intensity, α is the rate of Ab acquisition, and r is the rate of Ab decay in a given population. The model is derived from the differential equation:

$$\frac{dA}{dt} = \alpha(a) - rA \tag{6.2}$$

Acquisition and decay rates are estimated by assuming that antibody intensity at a given age, $Y(a)$, is log-normally distributed:

$$Y(a)|\,\alpha_0, \alpha, r, a \sim \text{LogNormal}\,(\log\big(A(a)\big),\ \sigma^2\,) \tag{6.3}$$

Similar to reverse catalytic models used to estimate sero-conversion and sero-reversion rates, Ab acquisition models can be extended to estimate different Ab acquisition rates depending on age, which can be described as:

$$A(a) = \begin{cases} \alpha_0 + \frac{\alpha_2}{r}\,(1 - e^{-r*a_c}) & : a \leq a_c \\ \alpha_0 + \frac{\alpha_2}{r}\,(1 - e^{-r*a_c}) + \frac{\alpha_1}{r}\left(1 - e^{-r*(a - a_c)}\right)e^{-r*a_c} & : a > a_c \end{cases} \quad (6.4)$$

Where a_c is the age at which there is a change in Ab acquisition rate, α_2 is the Ab acquisition rate for individuals aged less than or equal to a_c, α_1 is the Ab acquisition rate for individuals aged greater than a_c, and Ab decay rate r is assumed to be constant across all ages. The best fit model for each antigen and study arm or intervention was chosen based on deviance information criterion (DIC) values.

Some short-term markers (Etramp5.Ag1, GexP19, and HSP40) had very small Ab decay rates with respect age, and models excluding this parameter fit the data better (as assessed by DIC values).

The simplified model can be expressed as follows:

$$A(a) = \alpha_0 + \alpha * a \quad (6.5)$$

$$A(a) = \begin{cases} \alpha_0 + \alpha_2 * a_c & : a \leq a_c \\ \alpha_0 + \alpha_2 * a_c + \alpha_1(a - a_c) & : a > a_c \end{cases} \quad (6.6)$$

All models were fit using Bayesian Monte Carlo Markov Chain (MCMC) estimation with the *rjags* package in R version 3.3.2.

Area under the Ab acquisition curve (AUC) values[109] were calculated based on the Ab acquisition model fit for each cluster and survey month, with 95% credible intervals based on the distribution of estimated Ab intensity for covariate values sampled in the MCMC. This gives an estimate of the cumulative antibody intensity across all ages in the population. (Note: this is different to the AUC values computed in Chapter 5b, which refers to the Area Under the Receiver Operating Characteristic (ROC) curve to define the sensitivity and specificity of a diagnostic test).

6.3 Results

Sero-prevalence in children by geographical region and transmission season

Changes in sero-prevalence between geographical region and transmission season differed by antigen and age range (Figure 6.2 and Table 6.2). Overall, differences across most antigens were most pronounced in children under age 15 and less apparent in children aged 2-10 years. In

children under 5, small differences are still observed between region and season, but p-values suggest that none of these differences are statistically significant.

In the West Coast Region, seasonal differences in under-15 sero-prevalence observed for $MSP1_{19}$, with 2.0% (95%CI 1.0 – 3.1) prevalence in July and 4.9% (95%CI 3.4 – 6.4) in December. Differences were also seen for Etramp5.Ag1 – seroprevalence was 3.5% (95%CI 2.2 – 4.9) in July compared to 8.2% (95%CI 6.3 – 10.1) in December. Statistical evidence for differences in sero-prevalence for all other antigens in this age range was weak. On the other hand, sero-prevalence in ages 2-10 between July and December on the West Coast showed no statistically significant differences.

In the Upper River Region, all antigens showed differences in under-15 sero-prevalence between July and December. Between December 2013 and April 2014, there were also slight decreases in under-15 sero-prevalence for $MSP1_{19}$ (12.8% 95%CI 10.8 – 14.9 vs. 9.0% 95%CI 7.4 – 10.5), AMA1 (22.6% 95%CI 29.1 – 25.2 vs. 19.5% 95%CI 17.3 – 21.6), and Etramp5.Ag1 (18.7% 95%CI 16.3 – 21.1 vs. 14.6% 95%CI 12.7 – 16.5). However, none of these decreases were as large as the change between July and December 2013.

Figure 6.2 Sero-prevalence by antigen, geographical region, and transmission season

A. Ages < 15 years

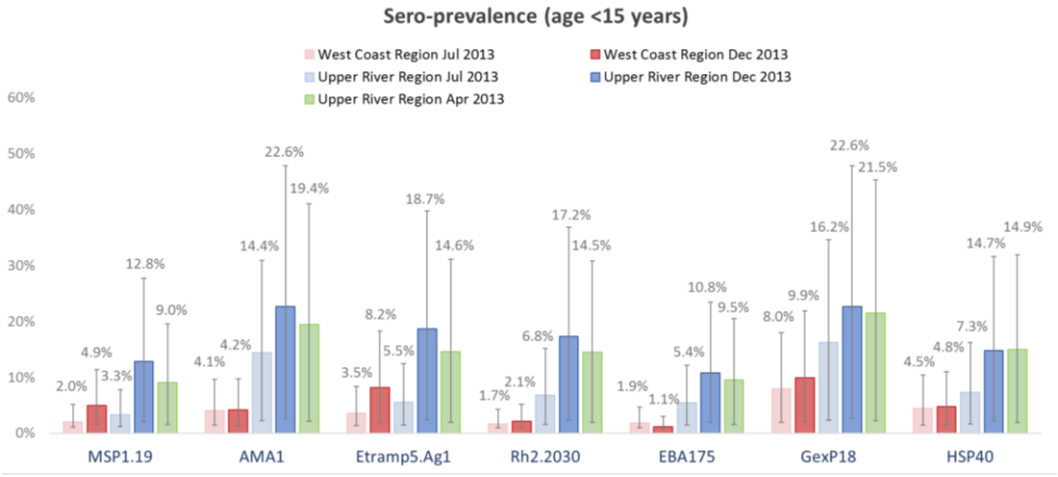

B. Ages 2-10 years

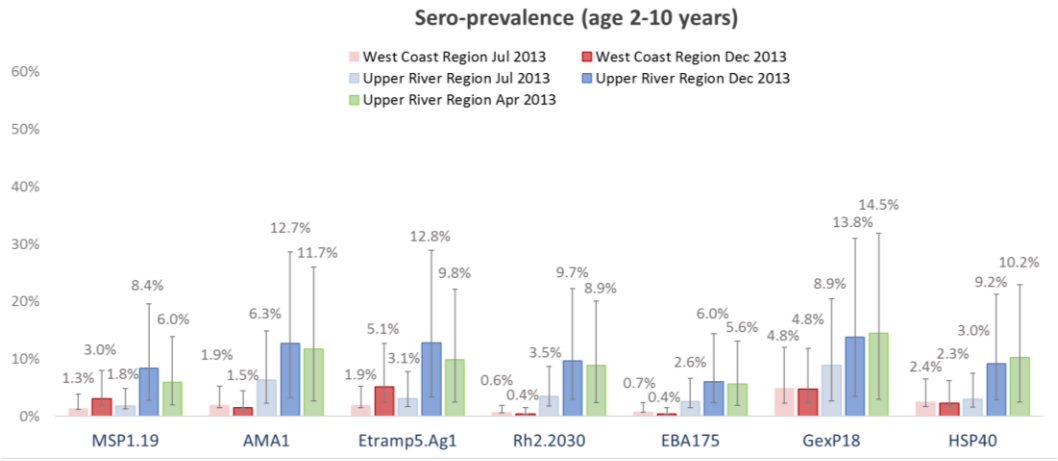

C. Ages < 5 years

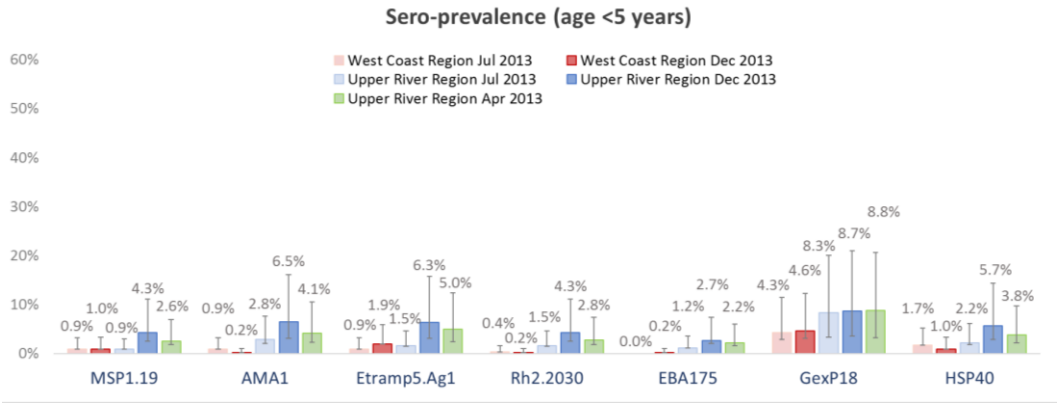

Table 6.2 Sero-prevalence by antigen, geographical region, and transmission season

A. Ages < 15 years (95%CI)

	$MSP1_{19}$	AMA1	Etramp5.Ag1	Rh2.2030	EBA175	GexP18	HSP40
West Coast Region							
July 2013 (n=314)	2.0% (1.0 - 3.1)	4.1% (2.7 - 5.5)	3.5% (2.2 - 4.9)	1.7% (0.8 - 2.6)	1.9% (0.9 - 2.8)	8.0% (6.1 - 9.9)	4.5% (3.0 - 5.9)
Dec 2013 (n=317)	4.9% (3.4 - 6.4)	4.2% (2.8 - 5.6)	8.2% (6.3 - 10.1)	2.1% (1.1 - 3.1)	1.1% (0.4 - 1.9)	9.9% (7.8 - 12.0)	4.8% (3.3 - 6.2)
Upper River Region							
July 2013 (n=437)	3.3% (2.2 - 4.5)	14.4% (12.2 - 16.6)	5.5% (4.1 - 6.9)	6.8% (5.2 - 8.4)	5.4% (4.0 - 6.8)	16.2% (13.9 - 18.5)	7.3% (5.7 - 8.9)
Dec 2013 (n=390)	12.8% (10.8 - 14.9)	22.6% (20.1 - 25.2)	18.7% (16.3 - 21.1)	17.2% (14.9 - 19.6)	10.8% (8.9 - 12.7)	22.6% (20.1 - 25.2)	14.7% (12.5 - 16.9)
Apr 2014 (n=504)	9.0% (7.4 - 10.5)	19.4% (17.3 - 21.6)	14.6% (12.7 - 16.5)	14.5% (12.5 - 16.4)	9.5% (7.9 - 11.1)	21.5% (19.3 - 23.7)	14.9% (13.0 - 16.9)

B. Ages 2-10 years (95%CI)

	$MSP1_{19}$	AMA1	Etramp5.Ag1	Rh2.2030	EBA175	GexP18	HSP40
West Coast Region							
July 2013 (n=207)	1.3% (0.1 - 2.5)	1.9% (0.4 - 3.3)	1.9% (0.4 - 3.3)	0.6% (0.0 - 1.4)	0.7% (0.0 - 1.7)	4.8% (2.5 - 7.1)	2.4% (0.8 - 4.1)
Dec 2013 (n=197)	3.0% (1.1 - 4.9)	1.5% (0.2 - 2.9)	5.1% (2.7 - 7.6)	0.4% (0.0 - 1.1)	0.4% (0.0 - 1.1)	4.8% (2.4 - 7.1)	2.3% (0.6 - 3.9)
Upper River Region							
July 2013 (n=275)	1.8% (0.5 - 3.1)	6.3% (4.0- 8.6)	3.1% (1.4 - 4.7)	3.5% (1.7 - 5.2)	2.6% (1.1 - 4.1)	8.9% (6.2 - 11.6)	3.0% (1.3 - 4.6)
Dec 2013 (n=241)	8.4% (5.6 – 11.1)	12.7% (9.4 - 16.0)	12.8% (9.5 - 16.1)	9.7% (6.7 - 12.6)	6.0% (3.7 - 8.4)	13.8% (10.3 - 17.7)	9.2% (6.3 - 12.0)
Apr 2014 (n=334)	6.0% (4.0 - 7.9)	11.7% (9.0 - 14.3)	9.8% (7.4 - 12.3)	8.9% (6.5 – 11.2)	5.6% (3.7 - 7.5)	17.0% (13.6 - 17.4)	10.2% (7.7 - 12.7)

C. Ages <5 years (95%CI)

	$MSP1_{19}$	AMA1	Etramp5.Ag1	Rh2.2030	EBA175	GexP18	HSP40
West Coast Region							
July 2013 (n=138)	0.9% (0.0 - 2.3)	0.9% (0.0 - 2.3)	0.9% (0.0 - 2.3)	0.4% (0.0 - 1.2)	0.0% (0.0 - 0.0)	4.3% (1.4 - 7.2)	1.7% (0.0 - 3.5)
Dec 2013 (n=131)	1.0% (0.0 - 2.4)	0.2% (0.0 - 0.8)	1.9% (0.0 - 3.9)	0.2% (0.0 - 0.8)	0.2% (0.0 – 0.8)	4.6% (1.5 - 7.7)	1.0% (0.0 - 2.4)
Upper River Region							
July 2013 (n=193)	0.9% (0.0 - 2.1)	2.8% (0.8- 4.9)	1.5% (0.0 - 3.0)	1.5% (0.0 – 3.0)	1.2% (0.0 - 2.5)	8.3% (5.0 - 11.7)	2.2% (0.4 - 4.0)
Dec 2013 (n=175)	4.3% (1.7 – 6.8)	6.5% (3.4 - 9.6)	6.3% (3.3 - 9.4)	4.3% (1.7 – 6.8)	2.7% (0.7 – 4.7)	8.7% (5.2 - 12.3)	5.7% (2.8 - 8.6)
Apr 2014 (n=223)	2.6% (0.8 - 4.3)	4.1% (1.9 – 6.4)	5.0% (2.5 - 7.4)	2.8% (0.9 – 4.6)	2.2% (0.5 - 3.8)	8.7% (5.6 - 11.9)	3.8% (1.6 - 5.9)

Sero-conversion rate between geographical region and transmission season.

Differences in SCR between geographical region and transmission season varied by antigen (Table 6.3, Figure 6.3). In the West Coast Region, changes in antibody responses between transmission seasons were larger for $MSP1_{19}$ (difference in SCR between July and December was 0.0147) compared to AMA1 (difference in SCR of 0.0007), though with weak statistical evidence for difference. In the Upper River, differences in antibody response between season was similar for both antigens but both were larger than seasonal differences observed on the West Coast. Change in $MSP1_{19}$ SCR between July and December was 0.0405 and 0.0301 for AMA1 SCR. Additionally, decreases in antibody responses between December 2013 and April 2014 were observed for both antigens ($MSP1_{19}$SCR declined by 0.0213 and AMA1 SCR by 0.0138), but p-values do not suggest these differences are statistically significant.

In the dry season (July), $MSP1_{19}$SCR between the West Coast Region and Upper River Region were 0.0067 (95%CI 0.0037 – 0.0123) and 0.0130 (95%CI 0.0088 – 0.0194) respectively. However, just after peak malaria season, this difference was more pronounced, with $MSP1_{19}$ SCR 0.0214 (95%CI 0.0087 – 0.0530) in the West Coast compared to 0.0535 (95%CI 0.0344 – 0.0831) in the Upper River. On the other hand, AMA1 SCR differed between regions in both the dry and wet season. In July, AMA1 SCR for the West Coast Region was 0.0159 (95%CI 0.0080 – 0.0239) and 0.0614 (95%CI 0.0509 – 0.0740) in the Upper River Region. This difference was more pronounced in the December, where AMA1 SCR in West Coast was 0.0166 (95%CI 0.0124 – 0.0224) and 0.0915 (95%CI 0.0738 – 0.1135) in Upper River.

Table 6.3 Sero-conversion rates for $MSP1_{19}$and AMA1 by transmission season and geographical region

	$MSP1_{19}$ SCR (95%CI)	AMA1 SCR (95%CI)	
	SCR overall	**SCR overall / SCR children***	**SCR adults**
West Coast Region			
July 2013	0.0067 (0.0037 – 0.0123)	0.0159 (0.0080 – 0.0239)	0.0877 (0.0438 – 0.1315)
December 2013	0.0214 (0.0087 – 0.0530)	0.0166 (0.0124 – 0.0224)	
Upper River Region			
July 2013	0.0130 (0.0088 – 0.0194)	0.0614 (0.0509 – 0.0740)	
December 2013	0.0535 (0.0344 – 0.0831)	0.0915 (0.0738 – 0.1135)	
April 2014	0.0322 (0.0241 – 0.0431)	0.0777 (0.0389 – 0.1166)	0.0815 (0.0408 – 0.1223)

*For clusters with an age-dependent change in sero-conversion rate for AMA1, SCR for younger ages is listed on left and older ages listed on right. No change in transmission for $MSP1_{19}$ was significant for any clusters or month. Therefore, all $MSP1_{19}$ SCRs are listed are for all ages.

Figure 6.3 $MSP1_{19}$ and AMA1 sero-conversion rates by transmission season and geographical region
Cluster level sero-conversion rates are compared between a) West Coast Region July vs. December 2013 (low endemicity pre- vs. post-transmission season) b) Upper River Region South July vs. December 2013 (moderate endemicity pre- vs. post-transmission season) c) West Coast Region vs. Upper River Region July 2013 (low vs. moderate endemicity pre-transmission season) and d) West Coast Region vs. Upper River Region December 2013 (low vs. moderate endemicity post-transmission season).

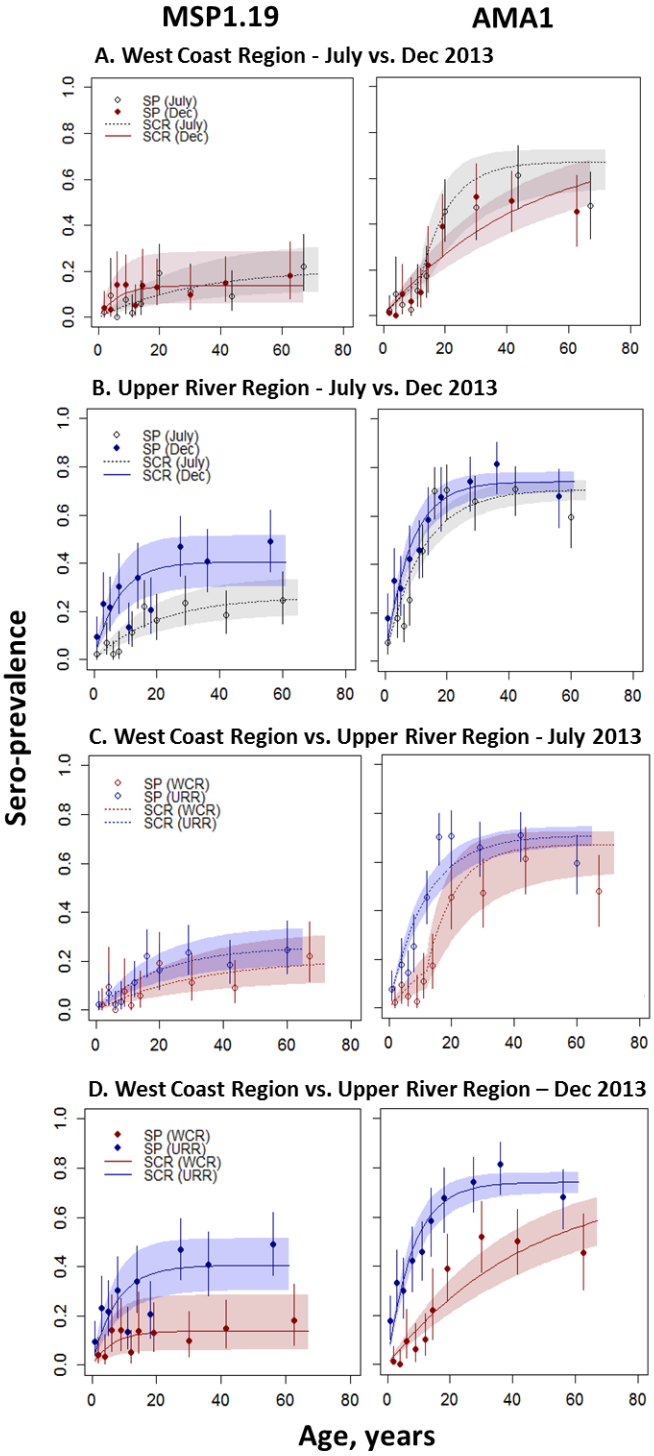

Age-adjusted antibody acquisition by geographical region and transmission season

Based on antigens associated with long-lived antibody responses ($MSP1_{19}$ and AMA1), AUC values of antibody acquisition (age-adjusted mean MFI) across all ages did not show statistically strong differences between region or season (Tables 6.4 and 6.5, Figures 6.4A-B, 6.5A-B and 6.6A-D). However, in children under 15, AUC values for $MSP1_{19}$ showed differences between the West Coast Region and the Upper River Region, but only in December at the end of peak malaria season ($p = 0.008$) (Table 6.4, Figure 6.6A-B). AUC values for AMA1 showed differences between geographical regions in both the dry season ($p = 0.069$) and peak season ($p<0.001$) (Table 6.5, Figure 6.6C-D). However, no differences AUC values were observed in children under 15 between seasons in either region (Tables 6.4 and 6.5, Figures 6.4A-B and 6.5A-B).

Based on antigens associated with shorter-lived antibody responses, nearly all showed differences in AUC values in December between regions across all age ranges (Figure 6.6E-N, Tables 6.6 – 6.10). The exceptions were Etramp5.Ag1 (Table 6.6) and GexP18 (Table 6.9), where differences between regions were only observed in children under 15 ($p=0.009$ and $p=0.004$ respectively), but not across all ages ($p = 0.359$ and $0=0.098$ respectively).

However, some of these antigens did show differences in AUC values between seasons or between regions in the dry season. In the Upper River Region, Etramp5.Ag1 showed differences in antibody acquisition between July and December in children under 15 ($p=0.001$) (Figure 6.5C). While GexP18 did not show differences between seasons, there were differences between regions in the dry season ($p=0.029$) (Figure 6.6L). Additionally, AUC values based on antibody acquisition to HSP40 showed seasonal differences in the West Coast Region in all ages ($p=0.055$) and in children under 15 ($p=0.002$) (Figure 6.4G, Table 6.10).

Antibody acquisition to Rh2.2030 and EBA175 did not show statistically strong seasonal differences for either region nor did it show differences between the West Coast and Upper River Regions in the dry season (Tables 6.7 and 6.8). Between December 2013 and April 2014, there did not appear to be any changes in antibody acquisition to any antigens, regardless of whether there were changes between July and December 2013 for the same antigen (Figure 6.7, Tables 6.5 – 6.10).

Figure 6.4 Antibody acquisition, West Coast Region July - December 2013
Ab acquisition for the West Coast Region (Besse and Ndemban) between July 2013 (pre-transmission season) and December 2013 (post-transmission season). P-values for difference in AUC values between seasons are shown for all ages and for under-15 year olds.

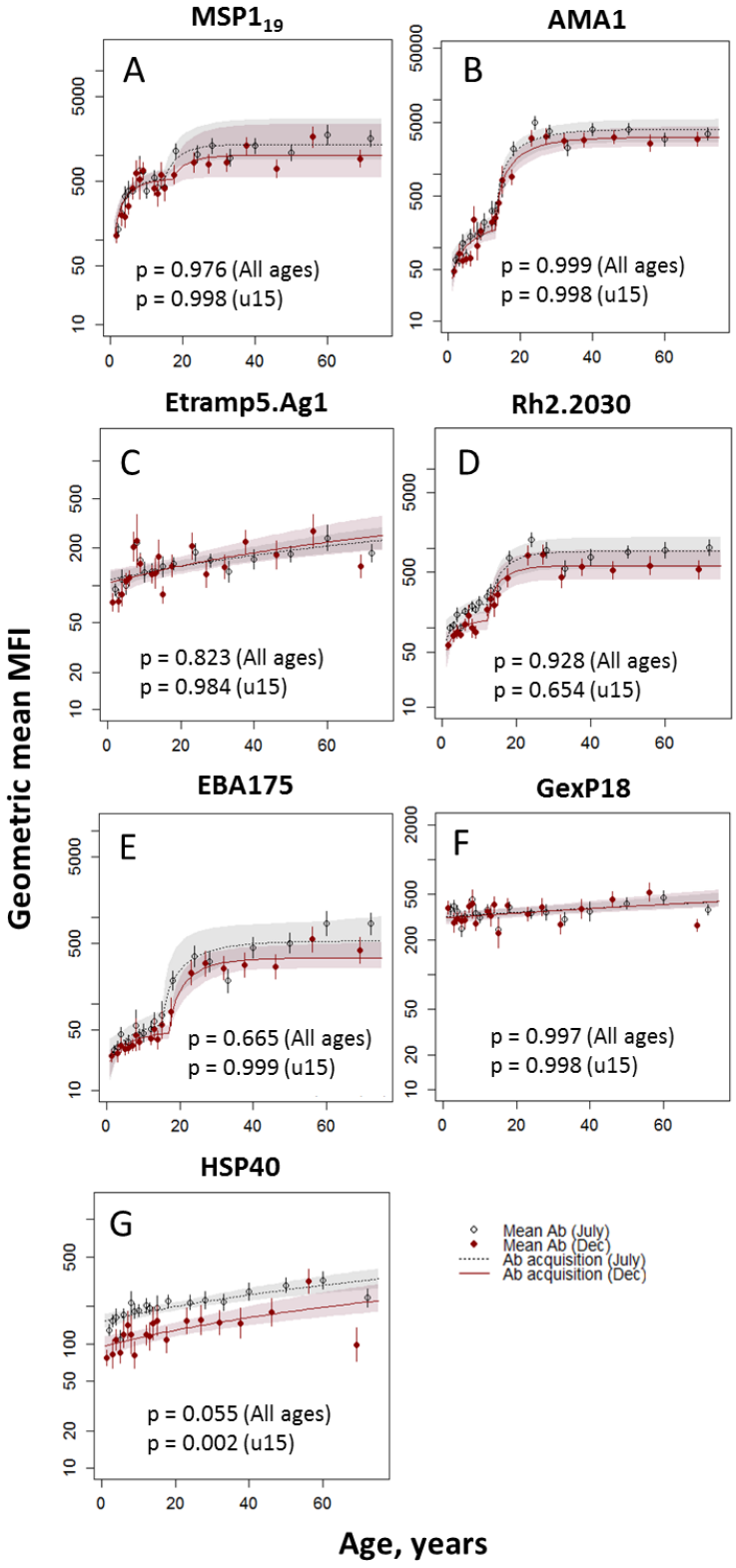

Figure 6.5 Antibody acquisition, Upper River Region South July - December 2013
Ab acquisition for the Upper River Region South (Madina Samako and Njaiyal) between July 2013 (pre-transmission season) and December 2013 (post-transmission season). P-values for difference in AUC values between seasons are shown for all ages and for under-15 year olds.

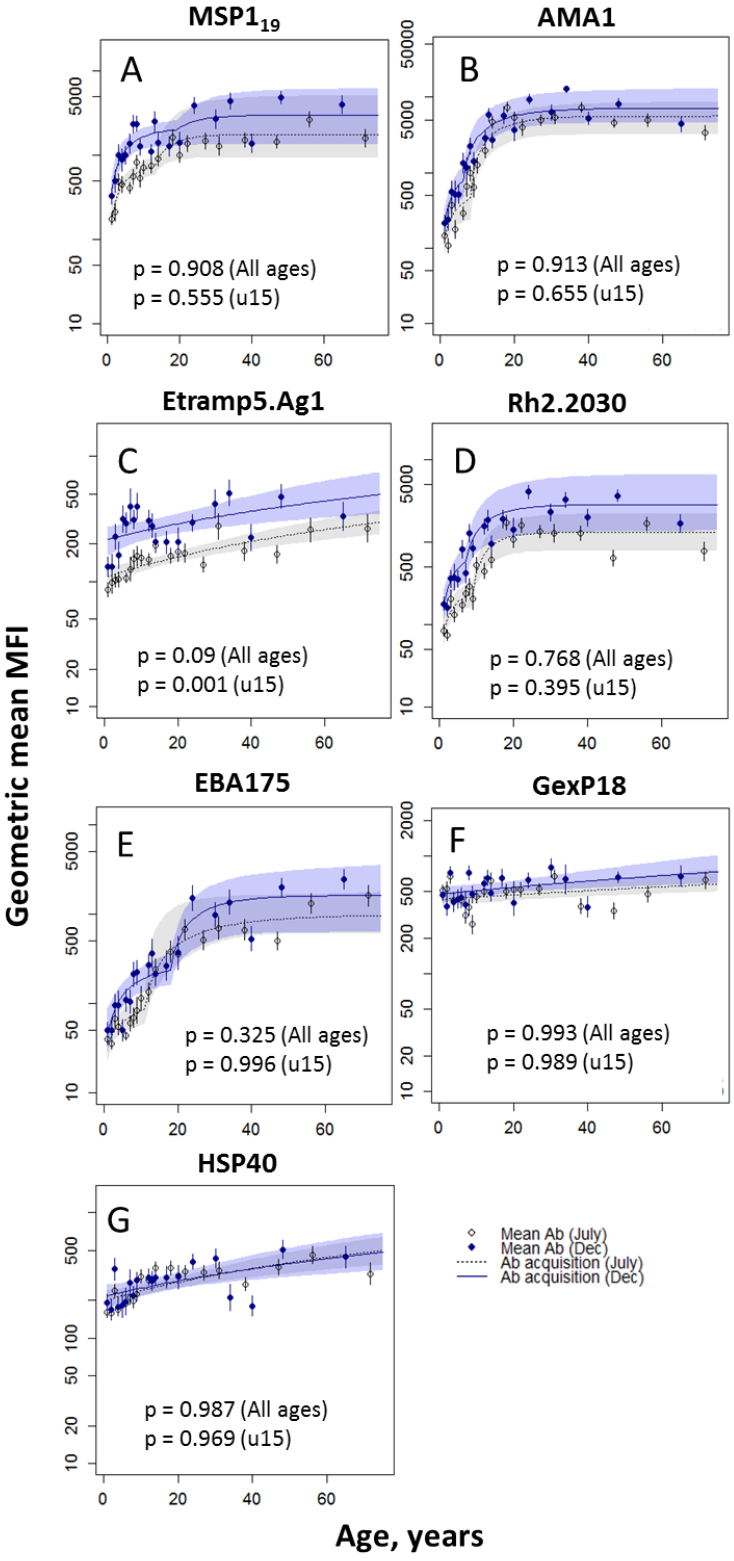

Figure 6.6 Antibody acquisition, West Coast Region cs. Upper River Region July - December 2013
Ab acquisition for West Coast Region (WCR) vs. Upper River Region South (URR) between July 2013 (left) and December 2013 (right). P-values for difference in AUC values between seasons are shown for all ages and for under-15 year olds.

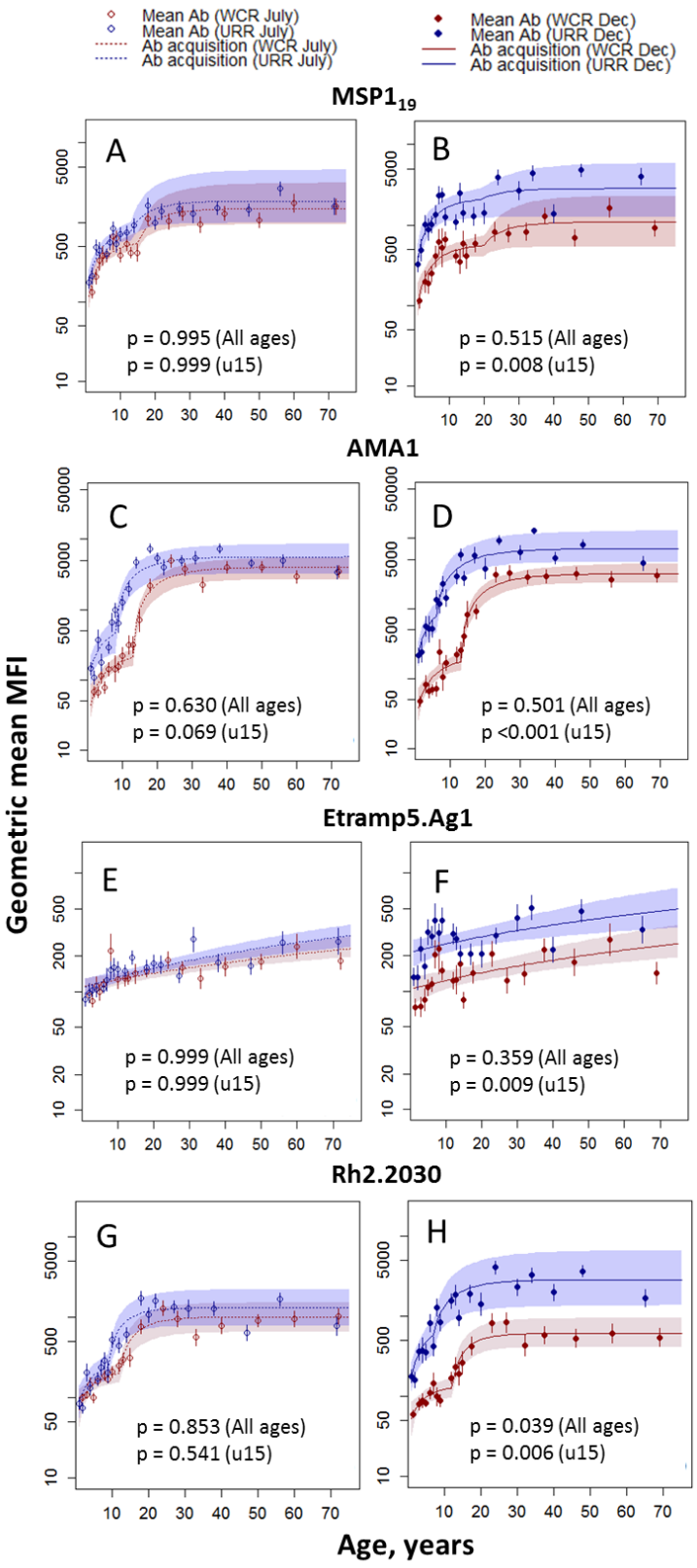

Figure 6.6 continued

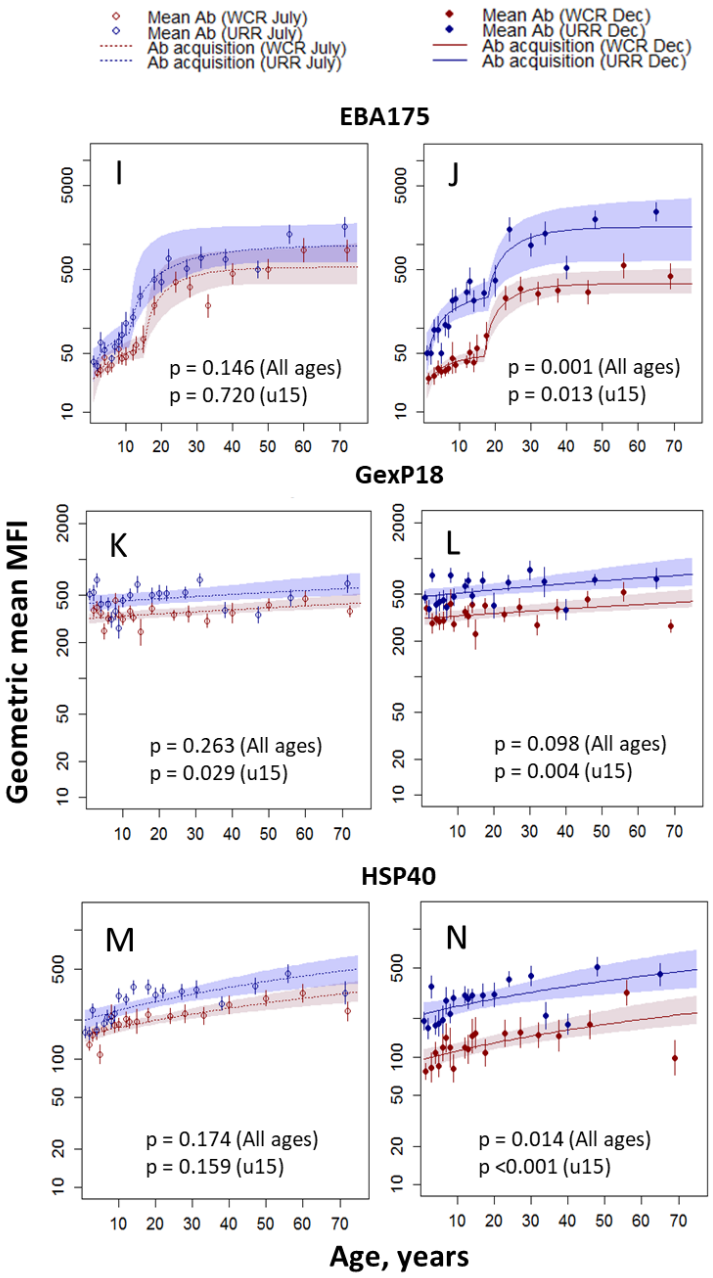

Figure 6.7 Antibody acquisition, Upper River Region before and after peak transmission season
Before peak transmission season (July 2013 in black), immediately after transmission season (December 2013 in blue), and several months after peak transmission season (April 2014 in green).

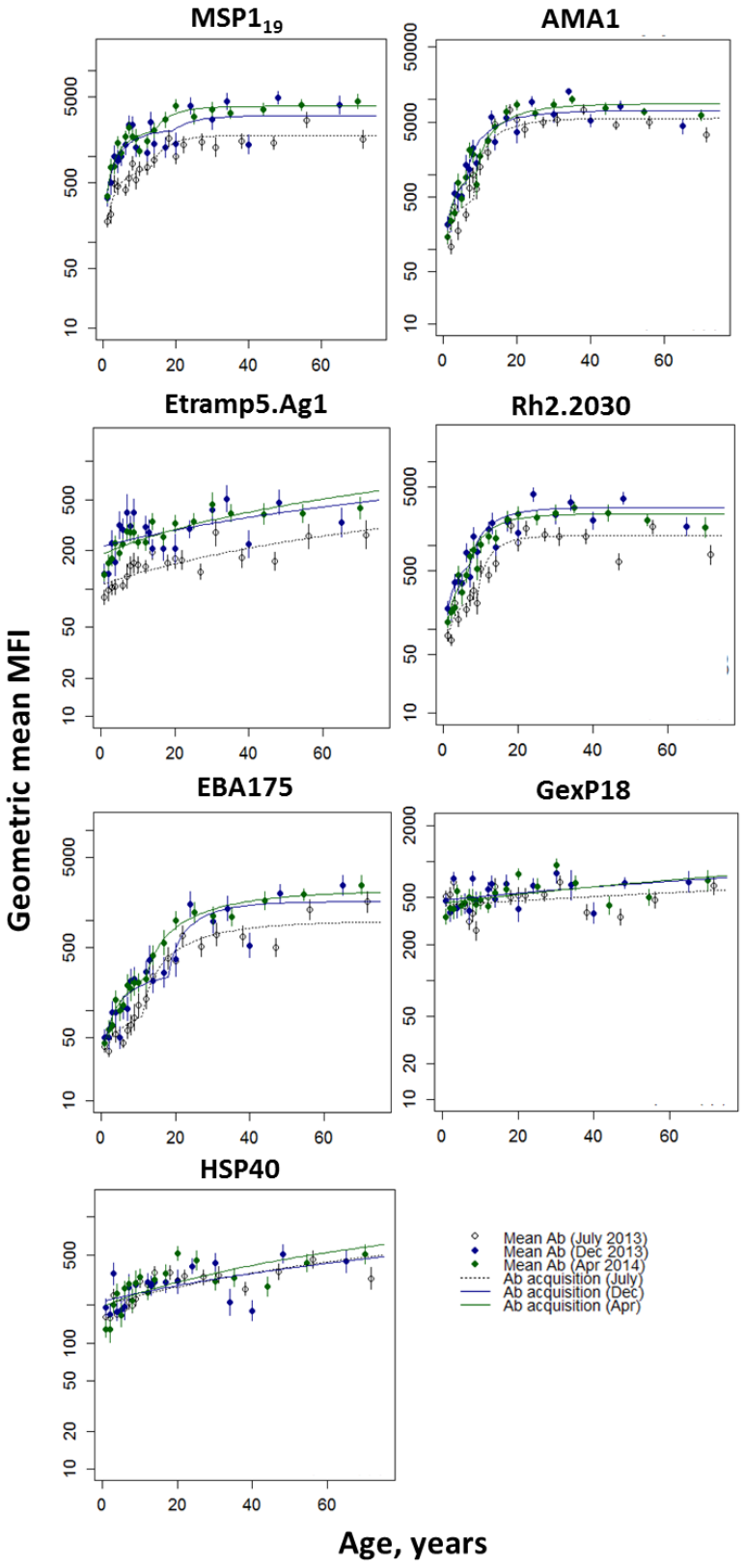

Table 6.4 $MSP1_{19}$ AUC values by geographical region and transmission season

All ages	AUC (95% CI)	p-value July/Dec 2013 WCR	p-value July/Dec 2013 URR	p-value WCR/URR July 2013	p-value WCR/URR Dec 2013
West Coast Region (WCR)					
July 2013	88,717 (57,837 – 176,435)	--	--	--	--
Dec 2013	65,739 (35,931 – 121,350)	0.976	--	--	--
Upper River Region (URR)					
July 2013	110,271 (62,775 – 244,436)	--	--	0.995	--
Dec 2013	183,300 (89,459 – 326,546)	--	0.908	--	0.515
Apr 2014	243,843 (176,640 – 415,626)	--	--	--	--

Ages <15 years only	AUC (95% CI)	p-value July/Dec 2013 WCR	p-value July/Dec 2013 URR	p-value WCR/URR July 2013	p-value WCR/URR Dec 2013
West Coast Region (WCR)					
July 2013	5,741 (5,146 – 7,275)	--	--	--	--
Dec 2013	5,580 (4,719 – 7,089)	0.998	--	--	--
Upper River Region (URR)					
July 2013	8,319 (6,790 – 11,191)	--	--	0.999	--
Dec 2013	19,412 (14,357 – 25,252)	--	0.555	--	0.008
Apr 2014	20,821 (19,088 – 28,570)	--	--	--	--

Table 6.5 AMA1 AUC values by geographical region and transmission season

All ages	AUC (95% CI)	p-value July/Dec 2013 WCR	p-value July/Dec 2013 URR	p-value WCR/URR July 2013	p-value WCR/URR Dec 2013
West Coast Region (WCR)					
July 2013	219,039 (145,845 – 289,917)	--	--	--	--
Dec 2013	169,068 (122,449 – 224,763)	0.999	--	--	--
Upper River Region (URR)					
July 2013	336,028 (197,768 – 493,597)	--	--	0.630	--
Dec 2013	436,288 (283,089 – 762,328)	--	0.913	--	0.501
Apr 2014	508,273 (266,363 – 740,284)	--	--	--	--

Ages <15 years only	AUC (95% CI)	p-value July/Dec 2013 WCR	p-value July/Dec 2013 URR	p-value WCR/URR July 2013	p-value WCR/URR Dec 2013
West Coast Region (WCR)					
July 2013	7,006 (4,879 – 12,464)	--	--	--	--
Dec 2013	6,219 (4,142 – 11,835)	0.998	--	--	--
Upper River Region (URR)					
July 2013	17,167 (12,153 – 23,123)	--	--	0.069	--
Dec 2013	27,228 (17,878 – 46,864)	--	0.655	--	<0.001
Apr 2014	25,364 (15,162 – 34,686)	--	--	--	--

Table 6.6 Etramp5.Ag1 AUC values by geographical region and transmission season

All ages	AUC (95% CI)	p-value July/Dec 2013 WCR	p-value July/Dec 2013 URR	p-value WCR/URR July 2013	p-value WCR/URR Dec 2013
West Coast Region (WCR)					
July 2013	12,721 (11,196 – 15,075)	--	--	--	--
Dec 2013	13,254 (10,809 – 17,351)	0.823	--	--	--
Upper River Region (URR)					
July 2013	15,081 (12,916 – 17,666)	--	--	0.998	--
Dec 2013	26,377 (20,400 – 35,645)	--	0.09	--	0.359
Apr 2014	28,769 (24,524 – 33,842)	--	--	--	--

Ages <15 years only	AUC (95% CI)	p-value July/Dec 2013 WCR	p-value July/Dec 2013 URR	p-value WCR/URR July 2013	p-value WCR/URR Dec 2013
West Coast Region (WCR)					
July 2013	1,728 (1,526 – 1,960)	--	--	--	--
Dec 2013	1,673 (1,382 – 2,013)	0.984	--	--	--
Upper River Region (URR)					
July 2013	1,785 (1,595 – 2,011)	--	--	0.999	--
Dec 2013	3,391 (2,810 – 4,123)	--	0.001	--	0.009
Apr 2014	3,190 (3,508 – 4,406)	--	--	--	--

Table 6.7 Rh2.2030 AUC values by geographical region and transmission season

All ages	AUC (95% CI)	p-value July/Dec 2013 WCR	p-value July/Dec 2013 URR	p-value WCR/URR July 2013	p-value WCR/URR Dec 2013
West Coast Region (WCR)					
July 2013	54,819 (34,196 – 81,653)	--	--	--	--
Dec 2013	37,413 (24,815 – 57,649)	0.928	--	--	--
Upper River Region (URR)					
July 2013	84,691 (50,407 – 144,936)	--	--	0.853	--
Dec 2013	183,443 (82,844 – 450,577)	--	0.768	--	0.039
Apr 2014	153,004 (105,268 – 285,397)	--	--	--	--

Ages <15 years only	AUC (95% CI)	p-value July/Dec 2013 WCR	p-value July/Dec 2013 URR	p-value WCR/URR July 2013	p-value WCR/URR Dec 2013
West Coast Region (WCR)					
July 2013	2,845 (2,138 – 3,668)	--	--	--	--
Dec 2013	1,838 (1,404 – 2,442)	0.654	--	--	--
Upper River Region (URR)					
July 2013	5,434 (3,536 – 8,021)	--	--	0.541	--
Dec 2013	13,895 (7,381 – 24,865)	--	0.395	--	0.006
Apr 2014	12,233 (7,724 – 21,278)	--	--	--	--

Table 6.8 EBA175 AUC values by geographical region and transmission season

All ages	AUC (95% CI)	p-value July/Dec 2013 WCR	p-value July/Dec 2013 URR	p-value WCR/URR July 2013	p-value WCR/URR Dec 2013
West Coast Region (WCR)					
July 2013	28,955 (17,123 – 48,401)	--	--	--	--
Dec 2013	18,718 (13,458 – 26,138)	0.665	--	--	--
Upper River Region (URR)					
July 2013	47,335 (32,625 – 82,388)	--	--	0.146	--
Dec 2013	79,607 (36,561 – 158,344)	--	0.325	--	0.001
Apr 2014	99,205 (79,983 – 124,841)	--	--	--	--

Ages <15 years only	AUC (95% CI)	p-value July/Dec 2013 WCR	p-value July/Dec 2013 URR	p-value WCR/URR July 2013	p-value WCR/URR Dec 2013
West Coast Region (WCR)					
July 2013	663 (516 – 888)	--	--	--	--
Dec 2013	512 (450 – 613)	0.999	--	--	--
Upper River Region (URR)					
July 2013	1,335 (915 – 2,415)	--	--	0.720	--
Dec 2013	2,141 (1,538 – 3,035)	--	0.996	--	0.013
Apr 2014	2,691 (2,287 – 3,319)	--	--	--	--

Table 6.9 GexP18 AUC values by geographical region and transmission season

All ages	AUC (95% CI)	p-value July/Dec 2013 WCR	p-value July/Dec 2013 URR	p-value WCR/URR July 2013	p-value WCR/URR Dec 2013
West Coast Region (WCR)					
July 2013	27,830 (25,627 – 31,218)	--	--	--	--
Dec 2013	27,636 (24,974 – 32,314)	0.997	--	--	--
Upper River Region (URR)					
July 2013	37,428 (32,984 – 45,333)	--	--	0.263	--
Dec 2013	44,968 (38,378 – 55,513)	--	0.993	--	0.098
Apr 2014	44,954 (52,676 – 66,419)	--	--	--	--

Ages <15 years only	AUC (95% CI)	p-value July/Dec 2013 WCR	p-value July/Dec 2013 URR	p-value WCR/URR July 2013	p-value WCR/URR Dec 2013
West Coast Region (WCR)					
July 2013	4,461 (4,259 – 5,058)	--	--	--	--
Dec 2013	4,544 (4,078 – 5,044)	0.998	--	--	--
Upper River Region (URR)					
July 2013	6,244 (5,426 – 7,111)	--	--	0.029	--
Dec 2013	7,031 (6,150 – 8,016)	--	0.989	--	0.004
Apr 2014	6,705 (5,933 – 7,575)	--	--	--	--

Table 6.10 HSP40 AUC values by geographical region and transmission season

All ages	AUC (95% CI)	p-value July/Dec 2013 WCR	p-value July/Dec 2013 URR	p-value WCR/URR July 2013	p-value WCR/URR Dec 2013
West Coast Region (WCR)					
July 2013	17,944 (15,882 – 20,542)	--	--	--	--
Dec 2013	11,785 (10,038 – 14,717)	0.055	--	--	--
Upper River Region (URR)					
July 2013	25,948 (21,711 – 30,965)	--	--	0.174	--
Dec 2013	25,841 (20,639 – 33,565)	--	0.987	--	0.014
Apr 2014	29,716 (23,513 – 38,341)	--	--	--	--

Ages <15 years only	AUC (95% CI)	p-value July/Dec 2013 WCR	p-value July/Dec 2013 URR	p-value WCR/URR July 2013	p-value WCR/URR Dec 2013
West Coast Region (WCR)					
July 2013	17,944 (15,882 – 20,542)	--	--	--	--
Dec 2013	11,785 (10,038 – 14,717)	0.002	--	--	--
Upper River Region (URR)					
July 2013	25,948 (21,711 – 30,965)	--	--	0.159	--
Dec 2013	25,841 (20,639 – 33,565)	--	0.969	--	<0.001
Apr 2014	29,716 (23,513 – 38,341)	--	--	--	--

6.4 Discussion

The analysis in this chapter explores methods for measuring short-term changes in antibody responses at the population-level. As discussed in Chapters 1 and 4, sero-epidemiology in malaria has focused on the use of markers of previous infection associated with long-lived antibody responses. New serological markers evaluated here highlight the limitations of existing sero-epidemiological models, but shows the potential of new methods for measuring cluster-level antibody responses.

Sero-prevalence and sero-conversion rates in low transmission settings

Based on sero-prevalence in children under 15, differences between geographical region and transmission season were observed for nearly all antigens in the Upper River Region, while only $MSP1_{19}$ and Etramp5.Ag1 detected seasonal differences in the West Coast Region. The extent to which these differences reflect short-term changes in infection incidence as opposed to cumulative historical infection is not clear. Differences in sero-prevalence in children aged 2-10 were only observed in the Upper River Region, while in children under five, there were no statistically significant differences in sero-prevalence to any antigen by region or season. However, given that differences are observed between a span of only six months in the Upper

River Region in the same cohort suggests that these changes do reflect short-term incidence to some degree. Inability to detect differences in the West Coast Region may reflect the challenge of measuring fine-scale differences at low transmission intensity.

Models estimating population level force of infection (sero-conversion rate) are predicated on the assumption that sero-prevalence will increase predictably with age. While this may still be true for newer antigens evaluated in this thesis, as transmission declines, increases in cumulative sero-prevalence with age will become more subtle. As with clinical incidence at low transmission, changes over time or between clusters derived from sero-prevalence may become undetectable. Alternatively, they may require larger samples sizes for accurate measures of prevalence from a single cross-sectional survey or to statistically test for differences over time and in space. These factors become more critical as countries deploy a variety of community-based interventions (Chapter 1 Table 1.1) to accelerate towards elimination that will require surveillance monitoring or testing in efficacy trials.

Another limitation of these approaches is that sero-prevalence is potentially influenced by the sero-positivity threshold, as discussed in Chapter 5a. Therefore, future analysis could include sensitivity testing to understand the impact on outcomes if alternative cut-offs are used. The use of antibody acquisition models also introduces challenges in significance testing, which are less routinely used in the manner introduced in this chapter for Bayesian fitting methods. However, it has been used here for better interpretation of model outputs. Alternatively, antibody acquisition models can also be fit using maximum likelihood methods, where likelihood ratio tests are more amenable to frequentist significance testing.

The use of antibody acquisition models is also amenable to analysis that may combine continuous antibody responses to multiple antigens in a single model. For example, investigation of which antigens exhibit a change in antibody acquisition rate with age compared to those that do not may help to distinguish long versus short-term markers of previous exposure. With the use of continuous instead of dichotomous serology data, it can also help to highlight those antigens that may be associated with medium-term exposure, such as the Rh and EBA families of antigens, where either the magnitude of change between age groups is less pronounced, or the age at which a change in antibody acquisition rate occurs differs from longer-lived antibody responses to antigens such as MSP1.19 and AMA1.

Comparison of serological, clinical and parasitological endpoints

Comparisons between geographical regions and transmission season based on serological endpoints align generally with trends in clinical and parasitological endpoints previously assessed by Mwesigwa et al (Figure 6.8, Table 6.10).

In the West Coast Region, there were no significant differences in clinical incidence between July and December (Figure 6.8, Table 6.11), which is also reflected in cluster-level antibody responses for all antigens assessed. However, parasite prevalence in December was slightly higher than in July. In the Upper River Region, however, while clinical incidence was not shown to be significantly different between July and December, serological responses did not differ for some antigens and age ranges, while differences were observed for Etramp5.Ag1 and GexP18.

On the West Coast, sero-prevalence only showed differences between July and December for $MSP1_{19}$ and Etramp5.Ag1, while all antigens showed increases in sero-positivity in December in the Upper River Region. It may be possible that serological responses are better correlated with clinical incidence and parasite prevalence two months prior given the time required to build an antibody response upon infection. In this context, antibody boost and decay estimates for each antigen can help to determine what period of lag time to account for when considering correlation with other measures of infection. Generally, however, trying to correlate the temporal dynamics of parasite density, clinical symptoms, and serological responses would be challenging and likely requires frequent sampling to account for fluctuations in both parasite density and antibody levels, while also factoring in reinfection and the impact of treatment.

In Chapter 5b, logistic regression was used to evaluate the association between and odds of RDT or PCR positive infections based on time since infection windows. However, this was not tested based on the subset of cross-sectional data here. Chapter 5b analysis also adjusted for individual level covariates that could be further explored with the cluster/population-level data here. Household risk of infection can also be investigated using data on bednet usage or EIR. Antibody acquisition models have been developed that can adjust for a number of covariates and future analysis can update the results in this chapter to account for these factors.

Figure 6.8 Incidence of clinical malaria and *P.falciparum* infection by region and month

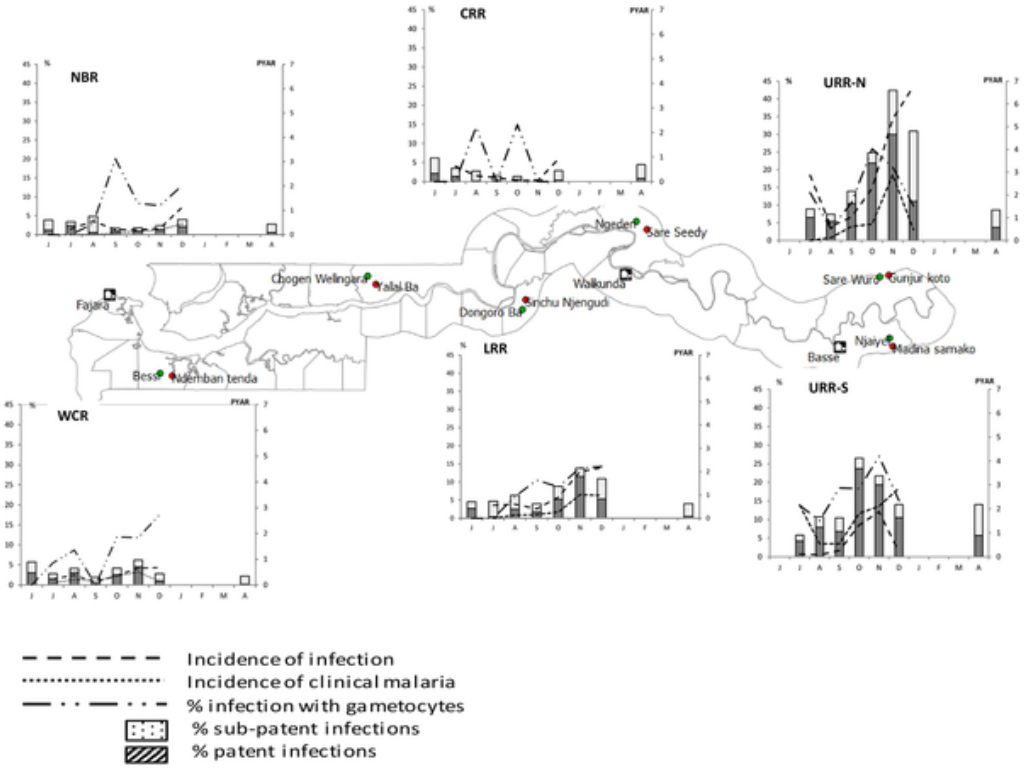

Table 6.11 Incidence of clinical malaria and *P.falciparum* infection by region and month

***P. falciparum* infection**						
Regions	**WCR**	**NBR**	**LRR**	**CRR**	**URR-S**	**URR-N**
July	0.23	0.24	0.56	0.62	-	-
	(0.13–0.39)	(0.13–0.42)	(0.37–0.85)	(0.39–1.01)		
August	0.38	0.55	0.60	0.24	0.56	0.62
	(0.25–0.57)	(0.38–0.80)	(0.41–0.89)	(0.13–0.43)	(0.42–0.74)	(0.44–0.96)
September	0.11	0.21	0.41	0.16	0.54	1.03
	(0.05–0.24)	(0.11–0.38)	(0.26–0.67)	(0.13–0.43)	(0.40–0.72)	(0.74–1.44)
October	0.37	0.20	0.91	0.04	1.81	2.30
	(0.24–0.57)	(0.11–0.38)	(0.66–1.26)	(0.01–0.18)	(1.55–2.12)	(1.85–2.87)
November	0.65	0.26	2.0	0.05	2.11	5.35
	(0.47–0.92)	(0.15–0.46)	(1.58–2.53)	(0.01–0.21)	(1.81–2.47)	(4.61–6.22)
December	0.67	1.13	2.17	0.93	2.87	6.77
	(0.40–1.13)	(0.73–1.76)	(1.59–2.96)	(0.51–1.67)	(2.36–3.50)	(5.63–8.14)
IRR compared to WCR		0.4	0.6	2.1	0.4	0.2
		(0.3–0.5)	(0.5–0.7)	(1.7–2.7)	(0.3–0.5)	(0.15–0.24)
		p<0.01	p<0.01	p<0.01	p<0.01	p<0.01
Clinical malaria						
July	0.08	0	0	0	0.13	-
	(0.04–0.21)				(0.04–0.39)	
August	0.21	0	0.14	0	0.08	0.12
	(0.11–0.36)		(0.02–0.22)		(0.04–1.65)	(0.05–0.33)
September	0.16	0.06	0.15	0	0.26	0.61
	(0.08–0.31)	(0.02–0.18)	(0.07–0.33)		(0.16–0.38)	(0.37–0.92)
October	0.35	0.14	0.27	0	1.32	0.72
	(0.23–0.55)	(0.07–0.29)	(0.13–0.47)		(1.11–1.62)	(0.42–0.98)
November	0.50	0.19	1.01	0	1.89	2.88
	(0.34–0.73)	(0.09–0.35)	(0.67–1.36)		(1.42–2.07)	(2.36–3.68)
December	0.14	0.45	0.98	0	0.21	0.47
	(0.04–0.44)	(0.27–0.99)	(0.61–1.64)		(0.10–0.51)	(0.23–1.14)
IRR compared to WCR		2.3	0.7	0	0.4	0.25
		(1.8–3.0)	(0.5–0.7)		(0.3–0.5)	(0.2–0.3)
		p<0.01	p = 0.002		p<0.01	p<0.01

https://doi.org/10.1371/journal.pone.0187059.t006

As discussed in Chapter 5b, acute clinical infection and its subsequent treatment may have a strong effect on an individual's serological response. The degree to which this varies by antigen would be useful further investigation. This could be done by stratifying the analysis by infection severity – clinical infections identified through passive case detection, asymptomatic patent infections positive by RDT, and asymptomatic sub-patent cases negative by RDT but PCR positive. However, it is likely that these factors would have strong collinearity with age and other risk factors (such as bednet usage), and this would need to be accounted for in the analysis.

Assessing the impact of mass drug administration with serological endpoints

While not explored in this analysis, as the full epidemiological data is not yet available, what naturally follows is an evaluation of the impact of MDA on antibody responses. A comparison of antibody acquisition between December 2013 (prior to MDA) and December 2014 (after one year of MDA) for the Upper River Region is illustrated in Appendix 6. However, this cohort study was not based on a cluster randomised trial design, as all villages received MDA. However, villages located close to MDA study villages, but not receiving the intervention, could serve as suitable controls. As part of this serology study, cross-sectional samples were processed on Luminex for one such village (Gambisera) from the International Centers of Excellence for Malaria Research (ICEMR) longitudinal study. Only sample for two time points (dry season June 2014 and post-transmission season January 2015) were selected for comparison against the dry and wet season cross-sectional surveys in the year that MDA was administration in the Malaria Transmission Dynamics study. According to national policy, the "control" cluster received SMC for children under age five. Therefore, comparisons would be testing for differences between two types of a population wide drug-based interventions. In light of recent research in Senegal supporting the efficacy of administering SMC in children up to age ten[32], this comparison of under-5 SMC against all-age MDA could be informative, particularly in Sahelian settings.

Future study designs

As introduced in Chapters 1 and 5b and in the background of this chapter, The Gambia's seasonal transmission patterns provide ample opportunity for unique study designs assessing serological responses in the absence of reinfection. The data used in this chapter was not collected with this type of analysis in mind, with the exception of a monthly survey conducted in April. However, the results presented here suggest that between December and April, serological responses for the antigens of interest do not decline significantly at any age range, despite the observation that differences in population responses are measurable between July and December. This suggests that in this setting, antibody decay occurs over a period longer than four months.

As described in Chapter 5b (Table 5.10), several longitudinal studies in The Gambia have observed measurable decay in antibody responses in the dry season in children, even for antigens believed to be more associated with protective immunity.[212,265] Similarly, other West African studies in Mali assessed antibody responses to over 2,000 *Pf* antigens on protein microarray before and after the malaria season found levels declined rapidly in children under 10 within six months after transmission season.[263] Therefore, there is precedent for further research to determine more precisely the longevity of population-level antibody responses across all ages and to determine if these are influenced by current and historical transmission intensity. These studies may help to clarify the sampling timeframe (and population) for future surveillance activities incorporating serological endpoints.

Given previous evidence of heterogeneity and spatial clustering in The Gambia, future analyses should also investigate whether this is also true for serological endpoints. This may include logistic regression of odds of sero-positivity based on distance from households of infected individuals identified with passive or active case detection. Descriptive mapping of household level antibody levels would also be informative, which could be compared with other maps of clinical incidence and parasite prevalence from the same study.

Overall, the results in this chapter indicate that cluster-level serological responses to several antigen correlate with known differences in malaria transmission between geographical regions and transmission seasons. However, the number of clusters in this study are small. The following chapter will extend on this analysis to determine how these serological measures can be used as trial efficacy endpoints in a study with a larger number of clusters.

Appendix 6

Figure 6.9 Serological responses in the Upper River Region pre- and post-MDA

Pre-MDA (April 2014, black) and post-MDA (December 2014, green)

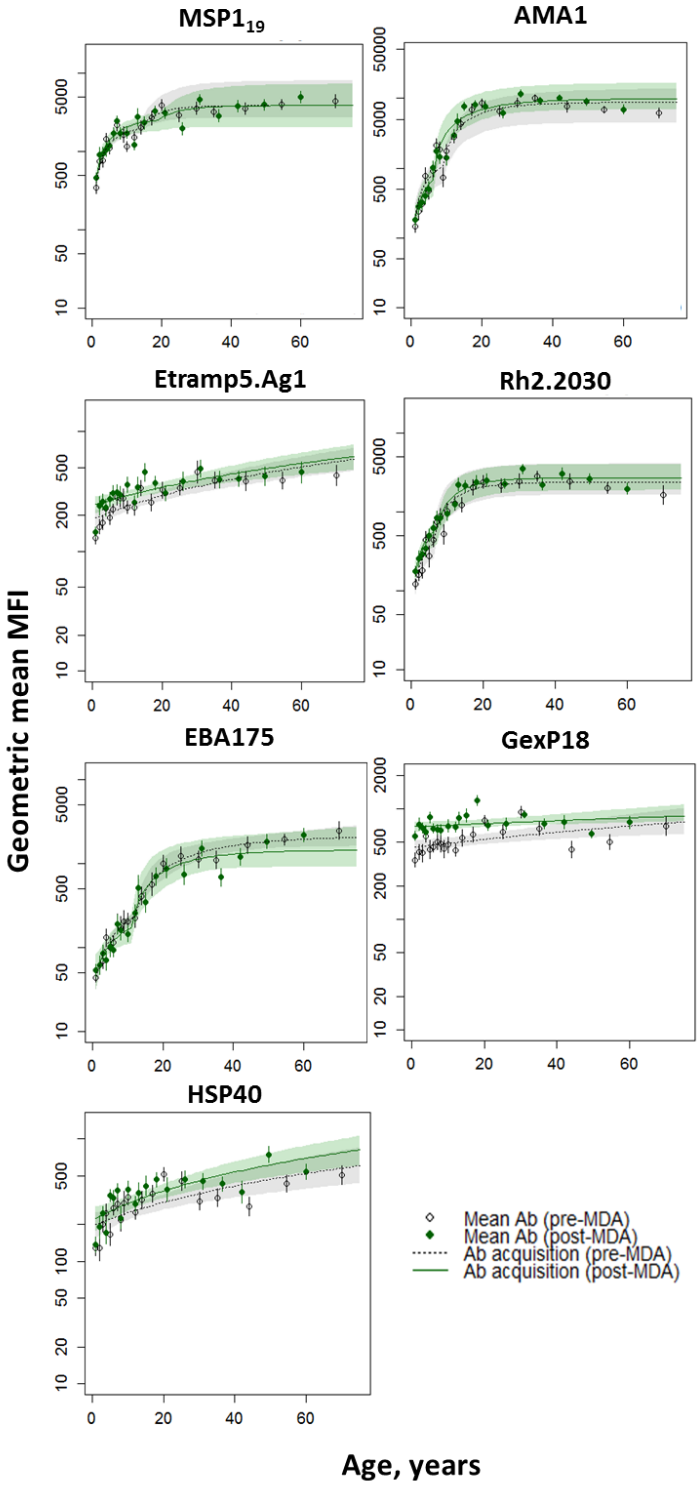

Chapter 7 Evaluating the effectiveness of reactive focal mass drug administration and reactive vector control in Zambezi Region, Namibia, using serological endpoints

In Chapter 6, serological endpoints were used to measure cluster-level differences in antibody response between areas of low and high transmission intensity and between dry and wet season in four villages in The Gambia. In this chapter, cluster-level serological analysis is extended to evaluate differences between study arms of a cluster-randomised trial in Namibia testing the effectiveness of reactive focal mass drug administration and reactive vector control.

7.1 Background

The identification of infected, but asymptomatic, individuals remains a key challenge in low-transmission settings. More importantly, failure to treat asymptomatic individuals that do not present at the health facility can delay country or regional progress toward elimination if they contribute significantly to onward transmission.[368] As described in Chapter 1, reactive case detection (RACD) is widely used for actively targeting asymptomatic residents in the neighbourhood of passively identified index cases from the clinic.[369] However, the limited sensitivity of current field diagnostics for the detection of asymptomatic individuals[232,370] has been suggested as one reason RACD has not demonstrated effectiveness in low transmission settings.[236,371]

The WHO recently endorsed the use of mass drug administration (MDA) for elimination in regions with a very high potential for interrupting transmission, defined as high treatment access, strong vector control and surveillance, and minimal risk of re-introduction.[372] This is driven by the fact that MDA often faces a dual challenge – the need for high coverage to impact transmission coupled with low adherence and acceptability in communities where clinical cases are rare. In addition to the safety risks of treating uninfected populations, failure to eliminate after the implementation of MDA can create an environment suitable for selection pressure and the emergence of drug resistance.[74]

Reactive focal MDA (rfMDA) is a potential alternative, where the aim is to target the infectious human reservoir. In this strategy, chemoprophylaxis is only administered to individuals with increased risk of infection based on proximity to a passively-detected index case.[369] As with MDA, vector control measures such as indoor residual spraying (IRS) face spray quality and coverage challenges and the risk of resistance if insecticides are not rotated.[373] Therefore, reactive focal IRS or reactive vector control (RAVC) is a strategy akin to rfMDA, but specifically targeting the infectious mosquito reservoir in elimination settings.[374]

Limited studies have investigated these strategies in low-transmission settings in sub-Saharan Africa. In order to evaluate the effectiveness and feasibility of rfMDA and RAVC compared to RACD and standard IRS campaigns, a cluster randomised control trial was conducted in Zambezi Region, Namibia. Zambezi is an area of moderately low transmission targeting malaria elimination by 2020.[375,376] However, it still has sufficiently high incidence to provide study power for a randomised controlled trial. This trial was part of the Namibia Malaria Elimination Research Programme (NAMEP).

Primary endpoints of the trial were cumulative clinical incidence and infection prevalence based on rapid diagnostic test (RDT) and quantitative polymerase chain reaction (qPCR). The evaluation of serological outcomes as secondary endpoints using both long- and short-lived antibody responses can help to determine whether serological markers can be useful measures of transmission specifically in the context of cluster-randomised trials. This chapter assesses cluster-level antibody responses to a panel of 20 serological markers, measured using the Luminex multiplex assay and based on samples from the end line cross-sectional survey of the RACD/rfMDA/RAVC trial. The aim is to evaluate the effectiveness of two interventions, independently and combined, using novel serological biomarkers of recent malaria infection.

7.2 Methods

Study design

The study was an open label cluster randomised controlled trial with a 2x2 factorial study design (Table 7.1) with three interventions:

- **RACD:** rapid diagnostic testing and treatment using artemether-lumefantrine (AL) of individuals residing within a 500m radius of a recent passively detected index case
- **rfMDA:** presumptive treatment with artemether-lumefantrine (AL)
- **RAVC:** IRS using pirimiphos-methyl, administered to household of individuals residing within a 500m radius of a recent passively detected index case. Note: this is in addition to routine annual IRS conducted as part of standard malaria control by the Ministry of Health.

The trial was conducted in Zambezi Region, Namibia from January to November 2017 (Figure 7.1), which covers catchment areas for 11 health facilities. Of the 102 EAs in the study area, 56 EAs were selected and randomly allocated to one of four arms. The primary outcome was cumulative incidence of passively detected, locally acquired malaria. Secondary outcomes included infection prevalence, intervention coverage, refusal rates, adverse events, and adherence. Further details of the study are reported on ClinicalTrials.gov: NCT02610400[377] and described in Medzihradsky et al, 2018.[378]

Table 7.1 Study arms in 2x2 factorial design trial

		Strategies targeting the human reservoir	
		RACD* *28 clusters*	**rfMDA†** *28 clusters*
Strategies targeting the mosquito reservoir	**No RAVC** *28 clusters*	**RACD only** *14 clusters*	**rfMDA only** *14 clusters*
	RAVC‡ *28 clusters*	**RACD + RAVC** *14 clusters*	**rfMDA + RAVC** *14 clusters*

Reactive case detection (RACD): RDT testing of individuals residing within a 500m radius of a recent passively detected index case; treating positive with artemether-lumenfrantrine (AL).

Reactive focal mass drug administration (rfMDA): presumptively treating individuals living in a 500m radius around an index case using artemether-lumefantrine, without RDT testing.

Reactive vector control (RAVC): spraying long-acting insecticide Actellic 300CS to interior walls of living structures of individuals residing within a 500m radius of a recent passively detected index case.

The cross-sectional end line survey was conducted at the end of the malaria season from May to August 2017 to measure infection- and sero-prevalance. Within each of the 56 EAs of the cluster RCT study, 25 households were randomly sampled for inclusion in the cross-sectional survey. All participants greater than six months of age and slept in the household at least three nights per week in the previous four weeks were eligible for inclusion in the study. Blood samples were collected by finger prick for molecular and serological analysis on dry blood spot (DBS) filter paper (Whatman 3 Corporation, Florham Park, NJ, USA) and 250 μl of whole blood in BD Microtainer tubes with EDTA additive. Participants were tested with two different rapid diagnostic tests - CareStart™ Malaria Pf/PAN (HRP2/pLDH) and a highly-sensitive RDT (HSRDT) developed by Standard Diagnostics. Individuals, both symptomatic and asymptomatic, with positive CareStart™ RDT results were treated with AL according to national guidelines.[379]

Figure 7.1 Study area in western Zambezi Region, Namibia

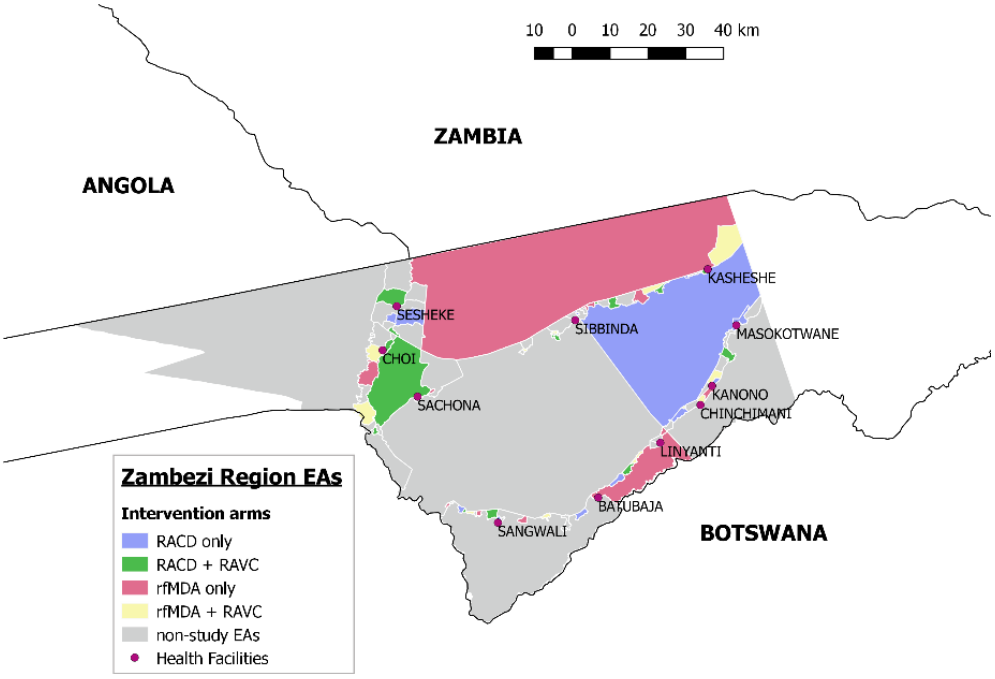

Laboratory procedures and data normalisation

Human plasma from whole blood samples were prepared and tested on the Luminex assay platform using the procedures described in Chapter 5a. Data were normalised to adjust for between plate variation using a loess normalisation method[295] and sero-positivity defined according to methods described in Chapter 5a. Analyses of Ab intensity are based on ether median fluorescence intensity (MFI) as a measure of continuous Ab response or sero-positivity as a binary Ab response.

Statistical analyses

Antigen selection. A total of 20 antigens were included in the Luminex multiplex assay for sample processing, but data from only a subset of the most informative markers are included here for brevity. Antigen selection was based on the results summarised in Chapter 5b and includes two markers of long-lived antibody response ($MSP1_{19}$, AMA1) and five markers of recent infection that demonstrated the highest frequencies as predictors of malaria infection in the last six months across all age categories, "time since infection" windows and infection severity (Etramp5.Ag1, Rh2.2030, EBA175, GexP18, and HSP40).

Sero-positivity. The odds of sero-positivity to each antigen were calculated based on logistic regression with generalised estimating equations (GEE), which allows for clustering at the EA-level, and assessed by study arm and intervention:

1. **Study arm:** RACD only, RACD + RAVC, rfMDA only, rfMDA + RAVC
2. **Intervention strategy**
    a. RACD vs. rfMDA (with or without RAVC aggregated)
    b. No RAVC vs. RAVC (with either RACD or rfMDA aggregated)

Analyses were adjusted for age category, trial intervention coverage, visit day (to account for effect of declining transmission during the cross-sectional survey period), fever, and gender. Trial intervention coverage was defined as the proportion of target households correctly receiving the intervention for their study arm (greater than or less than 75%). This was calculated as the proportion of index cases where the RACD or rfMDA intervention was implemented in households covering at least 25 individuals within 5 weeks of case identification. For the RAVC intervention, it was defined as the proportion of index cases where at least 7 households were sprayed within 5 weeks of case identification.

Separate regression analysis was also conducted to test if the interaction of rfMDA and RAVC as a combined intervention has a multiplicative effect on the odds of sero-positivity. Responses to a subset of short-term markers which showed the greatest effect with study arm were combined for analysis of odds of sero-positivity to any short-term marker.

Outcomes were also adjusted for travel in the last 8 weeks, receiving IRS in the last 12 months, and sleeping under a bed net, but none of these covariates were found to be significant confounders and were therefore excluded from final regression analysis.

Seroconversion rate. Age-adjusted sero-conversion rates (using Reverse Catalytic Model 1 described in Chapter 4) were estimated for antigens associated with long-lived antibody response ($MSP1_{19}$, AMA1). A fixed sero-reversion rate for each antigen was used across all clusters, which was estimated based on fitting a single sero-catalytic model to all individuals in the sample and setting sero-reversion rate to this value in all subsequent cluster-specific model fits. SCRs were fit for each EA independently and the mean SCR across all EAs within a study arm or intervention estimated.

Sero-prevalence in children. All-age sero-prevalence for most antigens will include adults who may be sero-positive due to long-lived antibody responses from repeated infection. Therefore, sero-prevalence in individuals less than 15 years of age may be more useful for assessing recent infections. These were calculated for each antigen and cluster separately. Combined sero-

prevalence was also assessed for a subset of short-term markers based on whether individuals were sero-positive to any antigen.

Antibody acquisition. For all antigens, Ab acquisition and decay were estimated for each study cluster (based on equations 6.1-6.6 as described in Chapter 6), and an Area under the Ab acquisition curve (AUC) value[109] calculated based on the mean and 95% credible intervals of the model fit. Differences in mean AUC values between study arms were assessed using linear regression of cluster-level AUC adjusted for study arm and trial intervention coverage and inverse weighted by the 95%CI of the cluster-level AUC.

Ab acquisition was also estimated for each study arm overall, allowing for random effects at the cluster level (Appendix 7, Figure 7.17), but this was not used for final analysis as independently fitting the model for each cluster was considered to be a more accurate reflection of cluster level variation, and also allowed for more standard evaluation of differences between study arms using linear regression or mean AUC.

Assessing the effect of study arm and intervention. The effect of study arm and intervention on sero-prevalence, sero-conversion rate and antibody acquisition were assessed based on linear regression of cluster-level effect by study arm. Analysis was adjusted for trial intervention coverage and inverse-weighted by the 95%CI of the cluster-specific SCR.

Regression analyses tested the effect of each study arm and intervention independently as well with an interaction between rfMDA and RAVC. This allows assessment of the effect of each intervention singly (rfMDA only or RACD + RAVC) or in combination (rfMDA + RAVC). This allows one to interpret whether outcomes in the rfMDA + RAVC arm were due entirely to one intervention and whether there were any synergistic or adverse effects when the interventions are combined.

Interpreting interaction terms. For outcomes based on logistic regression, interpretation of the interaction effect is multiplicative (i.e., the effect of the interventions combined is the multiplication of the ORs for rfMDA only, RACD+RAVC, and rfMDA:RAVC). For outcomes based on linear regression, the interpretation of the interaction effect is additive (i.e., the effect of the interventions combined is expressed as the difference from the mean baseline value and is the sum of the rfMDA only, RACD + RAVC, and rfMDA:RAVC coefficients).

In some instances, the effect of a single intervention could be harmful (OR of sero-positivity greater than 1 or increase in mean antibody response), but if the combined effect of the intervention is synergistic, it may counteract this effect, resulting in the rfMDA + RAVC arm having a neutral effect compared to the control/reference arm.

Comparison of trial endpoints. To compare the relative utility of serological endpoints, clinical incidence rate ratio (IRR) (intention-to-treat and per-protocol) is compared against mean SCR by study arm or intervention, and using RACD only, RACD (with or without RAVC) and No RAVC (with RACD or rfMDA) as reference. Additionally, odds ratios of sero-positivity of each antigen are compared to the odds ratio of HSRDT positivity by study arm and intervention. Finally, the AUC values of Ab acquisition for each antigen are compared by study arm and intervention.

7.3 Results

Population demographics, baseline transmission intensity, and intervention coverage

In total, 4,212 samples from the study were analysed for antibody responses. Of these individuals, 1,117 were from study clusters receiving RACD, 1,119 receiving RAVC, 1,030 receiving RACD + rfMDA, and 898 receiving RAVC + rfMDA (Table 7.2). The majority of individuals in all study arms were >15 years of age. Less than 1% of individuals in all study arms had fever based on temperature greater than 37.5^{o}C. There were similar proportions of females and males in all study arms. Less than 10% of individuals in all study arms reported sleeping outdoors in the previous two weeks, while between 18.7 – 28.3% of individuals reported sleeping under a bednet the previous night. Only 13.4 – 28.3% of individuals received IRS in the previous 12 months.

Trial intervention coverage also varied across study arms. Amongst EAs randomised to either RACD only, rfMDA only or rfMDA + RAVC interventions, 35.7% of EAs within the study arm received less than 75% trial intervention coverage, while 42.9% of EAs randomised to the RACD + RAVC arm received less than 75% trial intervention coverage (Table 7.3).

Table 7.2 Demographics of study population by study arm

	RACD only	RACD + RAVC	rfMDA only	rfMDA + RAVC
Individuals	**n = 1117 (%)**	**n = 1119 (%)**	**n = 1030 (%)**	**n = 898 (%)**
Age				
6 months - 5 years	195 (17.5)	199 (17.8)	166 (16.1)	164 (18.3)
6-15 years	309 (27.7)	307 (27.4)	297 (28.8)	260 (29.0)
> 15 years	613 (54.9)	613 (54.8)	567 (55.0)	474 (52.8)
Fever (≥ 37.5^{o}C)	1 (0.1)	4 (0.4)	2 (0.2)	3 (0.3)
Sex				
Female	634 (56.8)	634 (56.7)	558 (54.2)	482 (53.7)
Male	483 (43.2)	485 (43.3)	472 (45.8)	416 (46.3)
Slept outdoors in past 2 weeks	69 (6.2)	58 (5.2)	74 (7.2)	61 (6.8)
Slept under bednet previous night	266 (23.8)	219 (19.6)	193 (18.7)	254 (28.3)
Recent IRS in past 12 months	256 (22.9)	317 (28.3)	161 (15.6)	120 (13.4)
Recent travel in past 8 weeks	119 (10.6)	126 (11.3)	128 (12.4)	146 (16.3)

Table 7.3 Enumeration area level intervention coverage by study arm

	RACD only	RACD + RAVC	rfMDA only	rfMDA + RAVC
EAs	**n (EAs) = 14 (%)**	**n (EAs) = 14 (%)**	**n (EAs) = 14 (%)**	**n (EAs) = 14 (%)**
Intervention coverage				
< 75%	5 (35.7)	6 (42.9)	5 (35.7)	5 (35.7)
> 75%	8 (57.1)	8 (57.1)	9 (64.3)	9 (64.3)
Missing	1 (7.2)	0 (0.0)	0 (0.0)	0 (0.0)

Non-serological study outcomes – clinical incidence and parasite prevalence by highly sensitive rapid diagnostic test

The primary aim of this chapter is to assess serological endpoints. However, clinical incidence from the intervention trial (Table 7.4) and HSRDT positivity results from the end-line cross-sectional survey (Table 7.5) are summarised here as background. These are later used as a comparison against serological endpoints in analysis detailed in following sections.

Based on clinical incidence rate ratio (IRR), there was no statistically strong evidence of differences between study arms based on both intention-to-treat and per-protocol analysis (adjusted for 2016 incidence, intervention coverage, and median time to intervention) (Tables 7.4a and 7.4b). Lower IRR values are observed in rfMDA compared to RACD arms (with or without RAVC), RAVC arms compared to No RAVC (with either rfMDA or RACD), and in rfMDA + RAVC arms compared to RACD only. However, p-values for all IRRs were large.

The only study arm to show an effect on HSRDT positivity was the rfMDA + RAVC study arm (OR 0.72 95%CI 0.41 – 1.26, p=0.255), suggesting a synergistic effect of the interventions combined compared to no effect when they are implemented separately (Table 7.5). However, statistical evidence for these effects was weak. Odds of HSRDT positivity was higher in older children and adults, febrile individuals, and females. Intervention coverage did not have an effect on odds of HSRDT positivity, while visit day had a very small effect (OR 0.98 95%CI 0.97 – 0.99, p<0.001).

Table 7.4 Cumulative incidence of locally acquired passively detected malaria cases

A. IRR = incidence rate ratio. Data are mean (95%CI)

		Incidence		Modified Intention-to-treat	
	n		**p-value**	**IRR**	**p-value**
RACD	27	30.6 (18.7-42.5)	0.21	ref	0.67
rfMDA	28	23.3 (9.7-37.0)		0.86 (0.44-1.70)	
No RAVC	27	29.9 (15.9-43.8)	0.25	ref	0.52
RAVC	28	24.0 (12.2-35.7)		0.80 (0.41-1.56)	
RACD only	13	32.3 (16.5-48.1)	0.10	ref	0.38
rfMDA+RAVC	14	19.0 (3.8-34.2)		0.67 (0.27-1.65)	

B. aIRR = adjusted incidence rate ratio. Data are mean (95%CI)

		Per-protocol			
	n	**aIRR***	**p-value**	**aIRR****	**p-value**
RACD	27	Ref	0.49	ref	0.47
rfMDA	28	0.77 (0.38-1.60)		0.67 (0.22-2.03)***	
No RAVC	27	Ref	0.41	ref	0.07
RAVC	28	0.75 (0.38-1.48)		0.58 (0.33-1.04)	
RACD only	13	Ref	0.33	ref	0.12
rfMDA+RAVC	14	0.61 (0.23-1.63)		0.48 (0.20-1.19)	

*adjusted for 2016 incidence of local cases only

** adjusted for 2016 incidence of local cases, intervention coverage, median time to intervention, and co-interventions by Ministry of Health and Social Services

*** additionally adjusted for RAVC intervention coverage

Table 7.5 HSRDT positivity by study arm and intervention

A. By study arm. Logistic regression unadjusted and adjusted (GEE model with clustering at EA-level)

Outcome: HSRDT positivity	**Unadjusted**			**Adjusted**		
	OR	**95% CI**	**p-value**	**OR**	**95% CI**	**p-value**
RACD only	1.00	1.00		1.00	1.00	
RACD + RAVC	1.30	0.83 – 2.03	0.259	1.09	0.65 – 1.82	0.743
rfMDA	0.99	0.61 – 1.61	0.963	1.04	0.57 – 1.90	0.891
rfMDA + RAVC	0.72	0.41 – 1.26	0.255	0.73	0.40 – 1.31	0.292
Age category						
1-5 years	--	--	--	1.00	1.00	
6-15 years	--	--	--	2.28	1.20 – 4.31	0.012
>15 years	--	--	--	2.11	1.18 – 3.76	0.012
Intervention coverage > 75%	--	--	--	1.03	0.68 – 1.57	0.878
Visit day	--	--	--	0.98	0.97 – 0.99	<0.001
Fever	--	--	--	4.74	1.59 – 14.09	0.005
Gender (Female)	--	--	--	0.62	0.44 – 0.88	0.008

B. By intervention (with rfMDA and RAVC interaction effect)

Outcome: HSRDT positivity	**Unadjusted**			**Adjusted**		
	OR	**95% CI**	**p-value**	**OR**	**95% CI**	**p-value**
rfMDA*	0.99	0.61 – 1.61	0.963	1.04	0.57 – 1.90	0.891
RAVC†	1.30	0.83 – 2.03	0.259	1.09	0.65 – 1.82	0.743
rfMDA:RAVC	0.57	0.27 – 1.16	0.122	0.64	0.29 – 1.43	0.276
1-5 years	--	--	--	1.00	1.00	
6-15 years	--	--	--	2.28	1.20 – 4.31	0.012
>15 years	--	--	--	2.11	1.18 – 3.76	0.012
Intervention coverage > 75%	--	--	--	1.03	0.68 – 1.57	0.898
Visit day	--	--	--	0.98	0.97 – 0.99	<0.001
Fever	--	--	--	4.74	1.59 – 14.09	0.005
Gender (Female)	--	--	--	0.62	0.44 – 0.88	0.008

* With or without RAVC † With either RACD or rfMDA

Sero-positivity to antigens associated with long-lived antibody response ($MSP1_{19}$ and AMA1)

After adjusting for age, intervention coverage, visit day, fever, and gender, odds of sero-positivity to antigens associated with long-lived antibodies ($MSP1_{19}$ and AMA1) did not show strong differences between the four study arms (Tables 7.6 and 7.7). In fact, analysis of the interaction of the interventions for both antigens suggests that RAVC is actually associated with increased odds of sero-positivity, but when combined with rfMDA, reduces the odds of being sero-positivity such that there is no net effect on the OR. However, p-values for all these effects were large.

When aggregating study arms to compare EAs receiving RACD (with or without RAVC) with EAs receiving rfMDA (with or without RAVC), there was of a decreased odds of sero-positivity for individuals in EAs receiving rfMDA for $MSP1_{19}$ (OR 0.80 95%CI 0.62 – 1.02, p = 0.075) specifically for clusters receiving more than 75% intervention coverage, but statistical evidence was not strong. There was no difference between interventions based on intention-to-treat analysis. Similarly, specifically for clusters receiving high intervention coverage, sero-positivity to AMA1 was lower in rfMDA EAs (OR 0.78 95%CI 0.60 – 1.01, p=0.061), again without strong statistical evidence. No differences in odds of sero-positivity to either antigen were observed between individuals in EAs receiving RAVC and those that did not.

For both antigens, odds of sero-positivity increased with age (Tables 7.6 and 7.7). Compared to young children (ages 1-5 years), odds of sero-positivity to $MSP1_{19}$ for older children (ages 6-15 years) was 3.44 (95%CI 2.50 – 4.74, p < 0.001) and adults (>15 years) had an OR of 10.77 (95%CI 7.91 – 14.57, p < 0.001). Age effect was even stronger for AMA1, where older children had an OR of 3.03 (95%CI 2.24 – 4.11, p < 0.001) and adults had an OR of 37.66 (95%CI 28.22 – 50.25, p<0.001). Females also showed decreased odds of sero-positivity to both antigens compared to males for $MSP1_{19}$ (OR 0.79, 0.69 – 0.91; p=0.001), while for AMA1, the OR was 0.87 (95%CI 0.74 – 1.02, p=0.099), but statistical evidence was not strong.

An effect of intervention coverage on the odds of sero-positivity to both antigens was observed, with individuals in EAs that received greater than 75% trial coverage having an OR of sero-positivity to $MSP1_{19}$ of 0.85 (95%CI 0.71 – 1.01, p=0.072) and OR 0.86 to AMA1 (95%CI 0.73 – 1.01, p=0.157), but p-values were above 0.05. Visit day did not appear to have an effect on sero-positivity, suggesting that the impact of changing seasonality during the course of the survey was minimal on this endpoint (Tables 7.6 and 7.7). By comparison, visit day had a small effect on the odds of HSRDT positivity (OR 0.98 95%CI 0.97 – 0.99, p<0.001) (Table 7.5).

Table 7.6 $MSP1_{19}$ sero-positivity by study arm and intervention

A. **By study arm.** Logistic regression unadjusted and adjusted (GEE model with clustering at EA-level)

Outcome: sero-positivity	Unadjusted			Adjusted		
	OR	95% CI	p-value	OR	95% CI	p-value
RACD only	1.00	1.00		1.00	1.00	
RACD + RAVC	1.16	0.97 – 1.39	0.102	1.17	0.95 – 1.45	0.148
rfMDA	1.01	0.84 – 1.21	0.903	1.02	0.81 – 1.30	0.843
rfMDA + RAVC	0.94	0.78 – 1.14	0.537	0.98	0.75 – 1.27	0.865
Age category						
1-5 years	--	--	--	1.00	1.00	
6-15 years	--	--	--	3.44	2.50 – 4.74	0.000
>15 years	--	--	--	10.77	7.91 – 14.67	0.000
Intervention coverage > 75%	--	--	--	0.85	0.71 – 1.01	0.072
Visit day	--	--	--	1.00	0.99 – 1.00	0.128
Fever	--	--	--	1.04	0.26 – 4.07	0.960
Gender (Female)	--	--	--	0.79	0.69 – 0.91	0.001

B. **By intervention (with rfMDA and RAVC interaction effect).** Logistic regression unadjusted and adjusted (GEE model with clustering at EA-level)

Outcome: sero-positivity	Unadjusted			Adjusted		
	OR	95% CI	p-value	OR	95% CI	p-value
rfMDA*	1.04	0.86 – 1.24	0.707	1.03	0.81 – 1.32	0.786
RAVC†	1.18	0.99 – 1.41	0.060	1.18	0.95 – 1.46	0.137
rfMDA:RAVC	0.77	0.59 – 1.00	0.047	0.81	0.57 – 1.15	0.244
1-5 years	--	--	--	1.00	1.00	
6-15 years	--	--	--	3.47	2.52 – 4.77	<0.001
>15 years	--	--	--	10.84	7.97 – 14.76	<0.001
Intervention coverage > 75%	--	--	--	0.85	0.71 – 1.01	0.070
Visit day	--	--	--	1.00	0.99 – 1.00	0.123
Fever	--	--	--	1.16	0.46 – 2.97	0.751
Gender (Female)	--	--	--	0.79	0.69 – 0.91	0.001

* With or without RAVC † With either RACD or rfMDA

Table 7.7 AMA1 sero-positivity by study arm and intervention

A. **By study arm.** Logistic regression unadjusted and adjusted (GEE model with clustering at EA-level)

Outcome: sero-positivity	Unadjusted			Adjusted		
	OR	95% CI	p-value	OR	95% CI	p-value
RACD only	1.00	1.00		1.00	1.00	
RACD + RAVC	1.08	0.91 – 1.28	0.384	1.12	0.91 – 1.39	0.390
rfMDA	1.05	0.88 – 1.25	0.572	1.09	0.87 – 1.35	0.551
rfMDA + RAVC	0.95	0.79 – 1.14	0.571	1.01	0.80 – 1.26	0.966
Age category						
1-5 years	--	--	--	1.00	1.00	
6-15 years	--	--	--	3.03	2.24 – 4.11	0.000
>15 years	--	--	--	37.66	28.22 – 50.25	0.000
Intervention coverage > 75%	--	--	--	0.86	0.73 – 1.01	0.157
Visit day	--	--	--	1.00	0.99 – 1.00	0.313
Fever	--	--	--	1.06	0.22 – 5.05	0.947
Gender (Female)	--	--	--	0.87	0.74 – 1.02	0.099

B. **By intervention (with rfMDA and RAVC interaction effect).** Logistic regression unadjusted and adjusted (GEE model with clustering at EA-level)

Outcome: sero-positivity	Unadjusted			Adjusted		
	OR	95% CI	p-value	OR	95% CI	p-value
rfMDA*	1.06	0.89 – 1.25	0.525	1.09	0.83 – 1.43	0.547
RAVC†	1.09	0.92 – 1.29	0.310	1.13	0.87 – 1.47	0.353
rfMDA:RAVC	0.80	0.63 – 1.02	0.076	0.82	0.54 – 1.26	0.368
1-5 years	--	--	--	1.00	1.00	
6-15 years	--	--	--	3.04	2.21 – 4.19	<0.001
>15 years	--	--	--	37.77	27.87 – 51.20	<0.001
Intervention coverage > 75%	--	--	--	0.86	0.69 – 1.06	0.157
Visit day	--	--	--	1.00	0.99 – 1.00	0.275
Fever	--	--	--	1.19	0.36 – 3.95	0.775
Gender (Female)	--	--	--	0.87	0.73 – 1.03	0.102

* With or without RAVC † With either RACD or rfMDA

Seroconversion rate to $MSP1_{19}$ and AMA1

Across all clusters irrespective of trial intervention coverage, there were no differences between study arms for either $MSP1_{19}$ SCR (Table 7.8a) or AMA1 (Table 7.9a). Similar to the outcomes for sero-positivity, RAVC is associated with an increase in mean $MSP1_{19}$ sero-conversion rate. While the combination of the interventions is synergistic (Table 7.9b), it is not enough to counteract the harmful effect of RAVC, and the net effect is slightly higher mean sero-conversion rates in the rfMDA + RAVC compared with the RACD only reference arm. For AMA1, both rfMDA only and RAVC were associated with higher mean sero-conversion rates, but the combination had a net effect of slightly lower mean sero-conversion rates in the rfMDA + RAVC arm compared to the reference arm. However, p-values for all results were large, suggesting that statistical evidence for any study arm differences is weak.

This is likely due to the large variations in SCR estimates between clusters causing a lack of precision when evaluating differences between study arms. The largest inter-cluster variations in $MSP1_{19}$ SCR were seen in the RACD + RAVC arm, which had an mean SCR standard error (SE) of 0.020 across all clusters and 0.034 for clusters with >75% trial coverage (data not shown). With the exception of this study arm, analysis based on clusters with >75% trial coverage had smaller SCR standard errors (0.007 compared to 0.017 for rfMDA only, 0.005 vs. 0.015 for rfMDA + RAVC and 0.004 v. 0.011 for rfMDA with or without RAVC) (data not shown). For AMA1, the largest variations in SCR were in the rfMDA + RAVC study arm, but the SE is reduced when analysis is restricted to high intervention coverage clusters (data not shown).

Figure 7.2 $MSP1_{19}$ sero-conversion rate overall, by intervention coverage and study arm

A. Overall and by intervention coverage

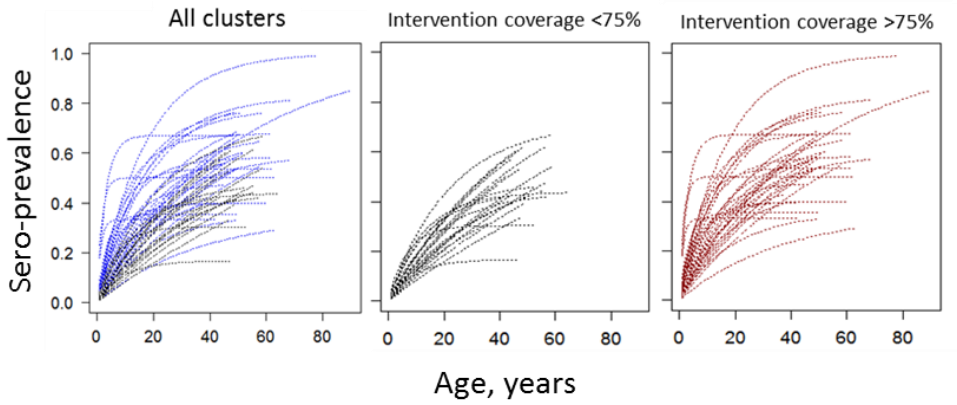

B. By study arm

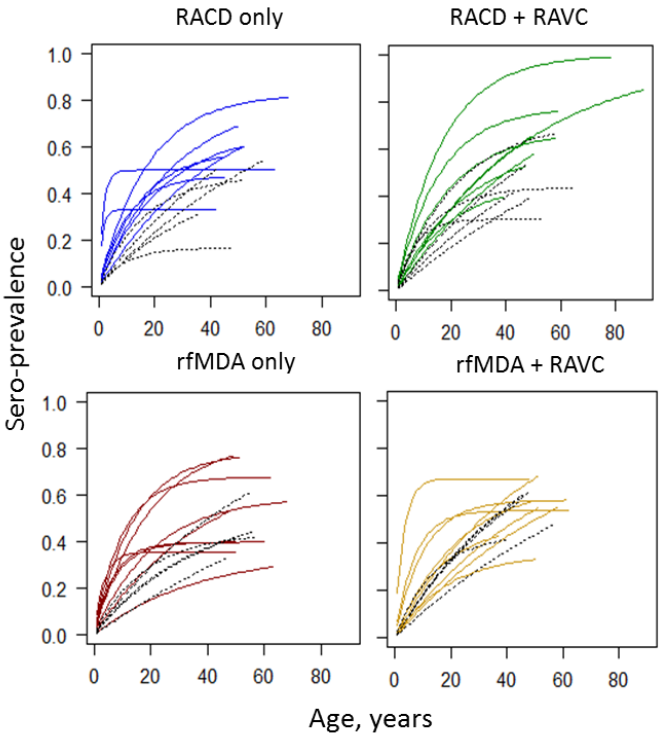

Table 7.8 $MSP1_{19}$ sero-conversion rate by study arm and intervention

A. **By study arm.** Reference (intercept) is the mean SCR of clusters in the RACD only arm, and difference in mean SCR is listed for all other study arms based on linear regression unadjusted and adjusted for intervention coverage (>75%).

	Unadjusted		Adjusted	
Study arm	**Difference in SCR (95%CI)**	**p-value**	**Difference in SCR (95%CI)**	**p-value**
RACD only mean SCR (intercept)	0.0251 (0.0110; 0.0393)	--	0.0287 (0.0118; 0.0457)	--
RACD + RAVC	0.0053 (-0.0145; 0.0250)	0.603	0.0047 (-0.0152; 0.0246)	0.644
rfMDA only	-0.0002 (-0.0200; 0.0195)	0.983	0.0004 (-0.0195; 0.0203)	0.968
rfMDA + RAVC	0.0018 (-0.0186; 0.0222)	0.864	0.0029 (-0.0178; 0.0235)	0.785
Intervention coverage	--	--	-0.0059 (-0.0211; 0.0094)	0.452

B. By intervention. Reference (intercept) is the mean SCR of clusters in the RACD only arm, and difference in mean SCR is listed for rfMDA only and RACD + RAVC based on linear regression unadjusted and adjusted for intervention coverage (>75%). rfMDA:RAVC is the additional SCR difference of the two interventions combined (included as an interaction effect in the linear regression).

	Unadjusted		Adjusted	
Intervention	**Difference in SCR (95%CI)**	**p-value**	**Difference in SCR (95%CI)**	**p-value**
RACD only mean SCR (intercept)	0.0251 (0.0110; 0.0393)	--	0.0287 (0.0118; 0.0457)	--
rfMDA	-0.0002 (-0.0200; 0.0195)	0.983	0.0004 (-0.0195; 0.0203)	0.968
RAVC	0.0053 (-0.0145; 0.0250)	0.603	0.0047 (-0.0152; 0.0246)	0.644
rfMDA:RAVC	-0.0033 (-0.0315; 0.0250)	0.822	-0.0022 (-0.0307; 0.0262)	0.878
Intervention coverage	--	--	-0.0059 (-0.0211; 0.0094)	0.452

Figure 7.3 AMA1 sero-conversion rate overall, by intervention coverage and study arm

A. Overall and by intervention coverage

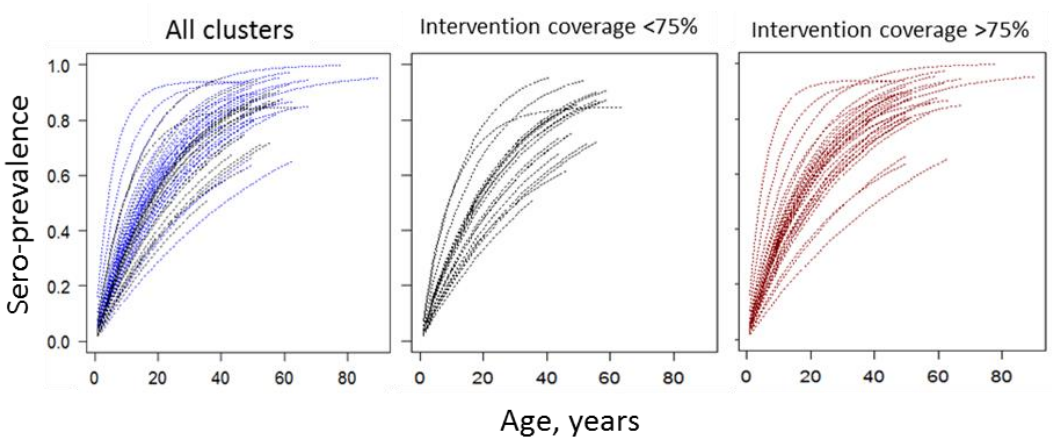

B. By study arm

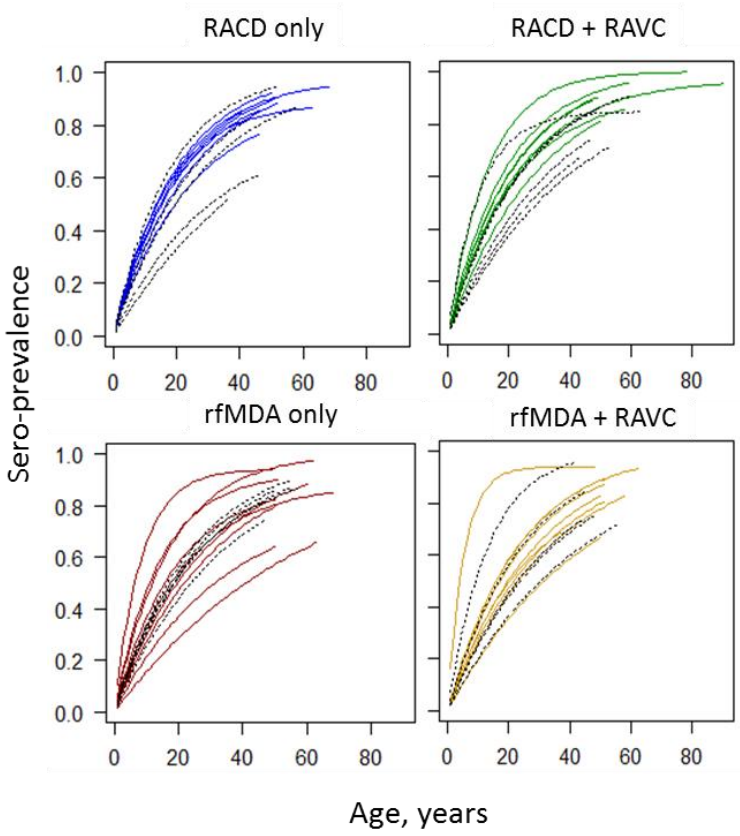

Table 7.9 AMA1 sero-conversion rate by study arm and intervention

A. **By study arm.** Reference (intercept) is the mean SCR of clusters in the RACD only arm, and difference in mean SCR is listed for all other study arms based on linear regression unadjusted and adjusted for intervention coverage (>75%).

	Unadjusted		Adjusted	
Study arm	**Difference in SCR (95%CI)**	**p-value**	**Difference in SCR (95%CI)**	**p-value**
RACD only mean SCR (Intercept)	0.0384 (0.0285; 0.0484)	--	0.0396 (0.0278; 0.0514)	--
RACD + RAVC	0.0043 (-0.0097; 0.0184)	0.549	0.0043 (-0.0099; 0.0185)	0.557
rfMDA only	0.0047 (-0.0094; 0.0187)	0.517	0.0049 (-0.0093; 0.0191)	0.501
rfMDA + RAVC	-0.0017 (-0.0158; 0.0124)	0.817	-0.0015 (-0.0157; 0.0128)	0.842
Intervention coverage	--	--	-0.0020 (-0.0125; 0.0085)	0.706

B. By intervention. Reference is the mean SCR of clusters in the RACD only arm, and difference in mean SCR is listed for rfMDA only and RACD + RAVC based on linear regression unadjusted and adjusted for intervention coverage (>75%). rfMDA:RAVC is the additional SCR difference of the two interventions combined (included as an interaction effect in the linear regression).

	Unadjusted		Adjusted	
Intervention	**Difference in SCR (95%CI)**	**p-value**	**Difference in SCR (95%CI)**	**p-value**
RACD only mean SCR (Intercept)	0.0384 (0.0285; 0.0484)	--	0.0396 (0.0278; 0.0514)	--
rfMDA	0.0047 (-0.0094; 0.0187)	0.517	0.0049 (-0.0093; 0.0191)	0.501
RAVC	0.0043 (-0.0097; 0.0184)	0.549	0.0043 (-0.0099; 0.0185)	0.557
rfMDA:RAVC	-0.0107 (-0.0306; 0.0092)	0.297	-0.0107 (-0.0307; 0.0094)	0.303
Intervention coverage	--	--	-0.0020 (-0.0125; 0.0085)	0.706

Sero-prevalence to $MSP1_{19}$ and AMA1 in children

Sero-prevalence to $MSP1_{19}$ in children was slightly lower in the RACD + RAVC study arm by 1.4% (95%CI 0.0-2.8, p=0.057) and in the rfMDA + RAVC study arm by 2.0% (95%CI 0.6 – 3.5, p=0.007) (Table 7.10). However, sero-prevalence in the rfMDA only arm did not appear to be significantly lower than the RACD only arm. Regression analysis comparing the interventions (Table 7.10b) suggest that the decrease in sero-prevalence is entirely due to the RAVC intervention, contributing to a decrease of 1.4% (95%CI 0.0 – 2.9, p=0.057). This was also observed for AMA1, where sero-prevalence in the RACD + RAVC arm was lower by 0.7% (95%CI 0.0 – 1.5%, p=0.053) and in the rfMDA + RAVC arm was lower by 1.1% (95%CI 0.4 – 1.8, p=0.005). Contrary to the effects on sero-positivity and sero-conversion rates, the effect on sero-prevalence appears to be driven by the RAVC intervention, while the interaction of the interventions combined results in a slight increase in sero-prevalence. However, results for the interaction effect have large p-values (Table 7.11b). Intervention coverage did not have an effect on sero-prevalence to either antigen.

Table 7.10 $MSP1_{19}$ under-15 sero-prevalence by study arm and intervention

A. **By study arm**. Reference (intercept) is the mean sero-prevalence for ages <15 years amongst of clusters in the RACD only arm, and difference in mean sero-prevalence is listed for all other study arms based on linear regression unadjusted and adjusted for intervention coverage (>75%).

	Unadjusted		Adjusted	
Study arm	**Difference in SP (95%CI)**	**p-value**	**Difference in SP (95%CI)**	**p-value**
RACD only mean SP (Intercept)	6.0% (5.0 - 7.0)	--	6.2% (5.0 – 7.4)	--
RACD + RAVC	-1.3% (-2.7; 0.1)	0.085	-1.4% (-2.9; 0.0)	0.057
rfMDA only	-0.9% (-2.3; 0.5)	0.194	-1.1% (-2.5; 0.3)	0.137
rfMDA + RAVC	-1.9% (-3.3; -0.5)	0.011	-2.0% (-3.5; -0.6)	0.007
Intervention coverage	--	--	-0.1% (-1.1; 1.0)	0.880

B. **By intervention.** Reference (intercept) is the mean sero-prevalence of ages <15 years of clusters in the RACD only arm, and difference in mean sero-prevalence is listed for rfMDA only and RACD + RAVC based on linear regression unadjusted and adjusted for intervention coverage (>75%). rfMDA:RAVC is the additional sero-prevalence difference of the two interventions combined (included as an interaction effect in the linear regression).

	Unadjusted		Adjusted	
Intervention	**Difference in SP (95%CI)**	**p-value**	**Difference in SP (95%CI)**	**p-value**
RACD only mean SP (Intercept)	6.0% (5.0 - 7.0)	--	6.2% (5.0 – 7.4)	--
rfMDA	-0.9% (-2.3; 0.5)	0.194	-1.1% (-2.5; 0.3)	0.137
RAVC	-1.3% (-2.7; 0.1)	0.085	-1.4% (-2.9; 0.0)	0.057
rfMDA:RAVC	0.3% (-1.7; 2.3)	0.758	0.5% (-1.5; 2.5)	0.638
Intervention coverage	--	--	-0.1% (-1.1; 1.0)	0.880

Table 7.11 AMA1 under-15 sero-prevalence by study arm and intervention

A. **By study arm.** Reference (intercept) is the mean sero-prevalence for ages <15 years amongst of clusters in the RACD only arm, and difference in mean sero-prevalence is listed for all other study arms based on linear regression unadjusted and adjusted for intervention coverage (>75%).

	Unadjusted		Adjusted	
Study arm	**Difference in SP (95%CI)**	**p-value**	**Difference in SP (95%CI)**	**p-value**
RACD only mean SP (Intercept)	6.3% (5.8 - 6.8)	<0.001	6.4% (5.8 – 7.0)	<0.001
RACD + RAVC	-0.7% (-1.4; 0.1)	0.079	-0.7% (-1.5; 0.0)	0.053
rfMDA only	-0.5% (-1.2; 0.2)	0.190	-0.6% (-1.3; 0.2)	0.135
rfMDA + RAVC	-1.0% (-1.8; -0.3)	0.008	-1.1% (-1.8; -0.4)	0.005
Intervention coverage	--	--	-0.04% (-0.6; 0.5)	0.893

B. **By intervention.** Reference (intercept) is the mean sero-prevalence of ages <15 years of clusters in the RACD only arm, and difference in mean sero-prevalence is listed for rfMDA only and RACD + RAVC based on linear regression unadjusted and adjusted for intervention coverage (>75%). rfMDA:RAVC is the additional sero-prevalence difference of the two interventions combined (included as an interaction effect in the linear regression).

	Unadjusted		Adjusted	
Intervention	**Difference in SP (95%CI)**	**p-value**	**Difference in SP (95%CI)**	**p-value**
RACD only mean SP (Intercept)	6.3% (5.8 - 7.8)	<0.001	6.4% (5.8 – 7.0)	<0.001
rfMDA	-0.5% (-1.2; 0.2)	0.190	-0.6% (-1.3; 0.2)	0.135
RAVC	-0.7% (-1.4; 0.1)	0.079	-0.7% (-1.5; 0.0)	0.053
rfMDA:RAVC	0.1% (-0.9; 1.2)	0.808	0.2% (-0.8; 1.3)	0.690
Intervention coverage	--	--	-0.04% (-0.6; 0.5)	0.893

Antibody acquisition to $MSP1_{19}$ and AMA1

Based on antibody acquisition to $MSP1_{19}$, there were no statistically strong differences in AUC values between study arms (Figure 7.4b, Table 7.12). For AMA1, antibody acquisition AUC values were slightly higher in the rfMDA only compared to the RACD only arm (p=0.025) (Figure 7.5b, Table 7.13). Intervention coverage did not have an effect on AUC values for either antigen (Figures 7.4a and 7.5a, Tables 7.12 and 7.13).

Figure 7.4 $MSP1_{19}$ Antibody acquisition overall, by trial coverage and study arm

A. **Overall and by trial coverage**. Ab acquisition fit for all clusters (top), points are age-adjusted MFI, black dotted lines are clusters with <75% intervention coverage, blue dotted lines are clusters with >75% intervention coverage, and shaded areas are the 95% credible intervals of the Ab acquisition fit. Clusters with <75% intervention coverage shown in black (bottom left) and >75% intervention coverage in red (bottom right).

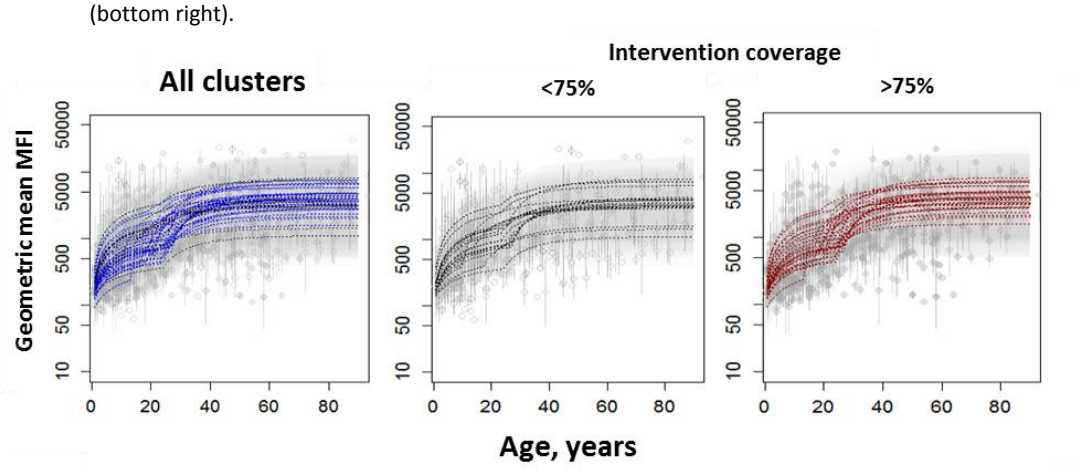

B. By study arm. RACD only in blue (top left), RACD + RACD in green (top right), rfMDA only in red (bottom left), and rfMDA + RAVC in yellow (bottom right). Dotted lines show clusters with <75% intervention coverage and solid lines clusters with >75% intervention coverage.

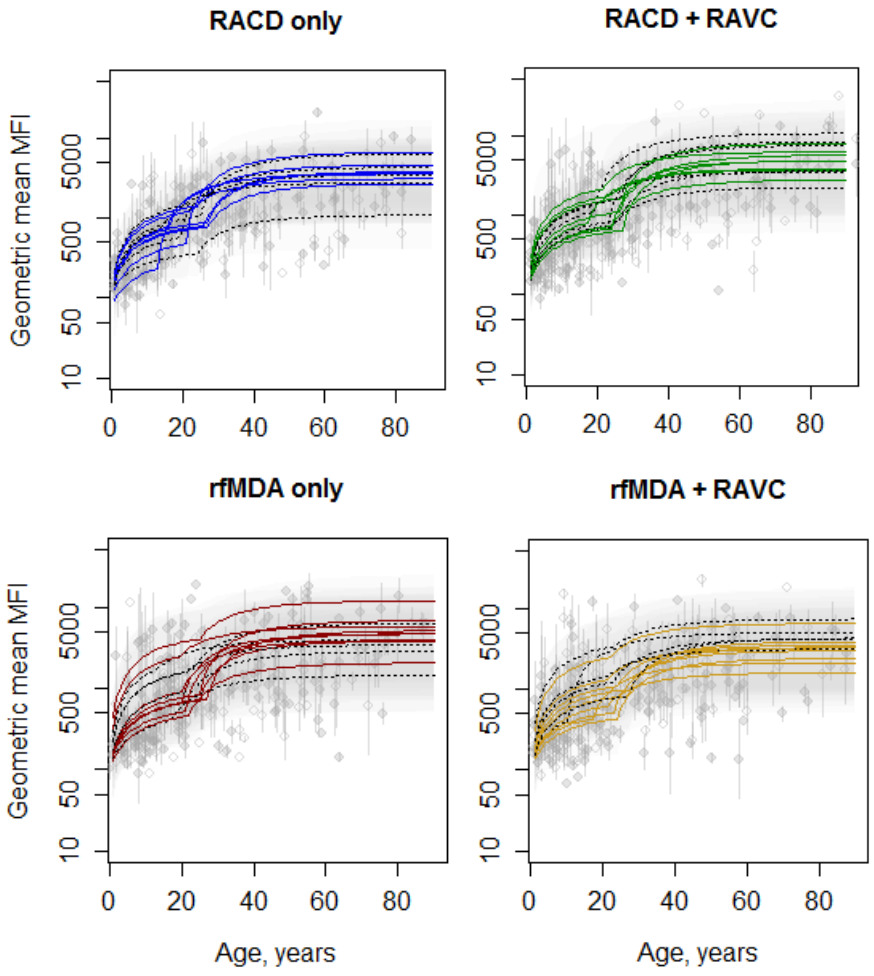

Table 7.12 $MSP1_{19}$ Area under the antibody acquisition curve by study arm and intervention

A. **By study arm.** Reference (intercept) is the mean AUC of clusters in the RACD only arm, and difference in mean AUC is listed for all other study arms based on linear regression unadjusted and adjusted for intervention coverage (>75%).

	Unadjusted		Adjusted	
Study arm	**Difference in AUC (95%CI)**	**p-value**	**Difference in AUC (95%CI)**	**p-value**
RACD only mean AUC (Intercept)	187,724 (139,267; 236,181)	--	175,252 (116,591; 233,913)	--
RACD + RAVC	69,504 (-5,891; 144,899)	0.077	71,147 (-6,270; 148,564)	0.078
rfMDA only	39,999 (-34,809; 114,806)	0.299	42,085 (-34,679; 118,849)	0.288
rfMDA + RAVC	14,255 (-57,592; 86,102)	0.699	13,253 (-61,571; 88,078)	0.730
Intervention coverage	--	--	18,081 (-38,994; 75,155)	0.537

B. By intervention. Reference (intercept) is the mean AUC of clusters in the RACD only arm, and difference in mean AUC is listed for rfMDA only and RACD + RAVC based on linear regression unadjusted and adjusted for intervention coverage (>75%). rfMDA:RAVC is the additional AUC difference of the two interventions combined (included as an interaction effect in the linear regression).

	Unadjusted		Adjusted	
Intervention	**Difference in AUC (95%CI)**	**p-value**	**Difference in AUC (95%CI)**	**p-value**
RACD only mean AUC (Intercept)	187,724 (139,267; 236,181)	<0.001	175,252 (116,591; 233,913)	<0.001
rfMDA	39,999 (-34,809; 114,806)	0.299	42,085 (-34,679; 118,849)	0.288
RAVC	69,504 (-5,891; 144,899)	0.077	71,147 (-6,270; 148,564)	0.078
rfMDA:RAVC	-95,248 (-203,629; 13,133)	0.091	-99,979 (-210,566; 10,608)	0.082
Intervention coverage	--	--	18,081 (-38,994; 75,155)	0.537

Figure 7.5 AMA1 antibody acquisition overall, by trial coverage and study arm

A. **Overall and by trial coverage**. Ab acquisition fit for all clusters (top), points are age-adjusted MFI, black dotted lines are clusters with <75% intervention coverage, blue dotted lines are clusters with >75% intervention coverage, and shaded areas are the 95% credible intervals of the Ab acquisition fit. Clusters with <75% intervention coverage shown in black (bottom left) and >75% intervention coverage in red (bottom right).

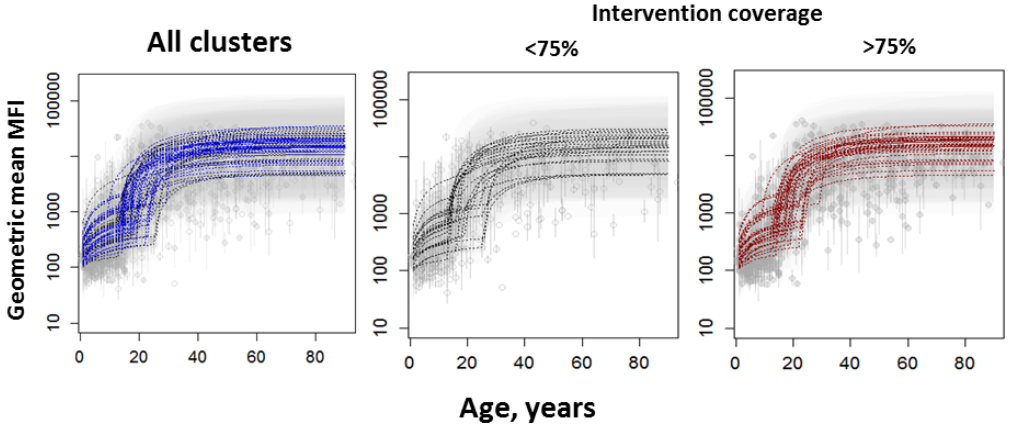

B. **By study arm.** RACD only in blue (top left), RACD + RACD in green (top right), rfMDA only in red (bottom left), and rfMDA + RAVC in yellow (bottom right). Dotted lines show clusters with <75% intervention coverage and solid lines clusters with >75% intervention coverage.

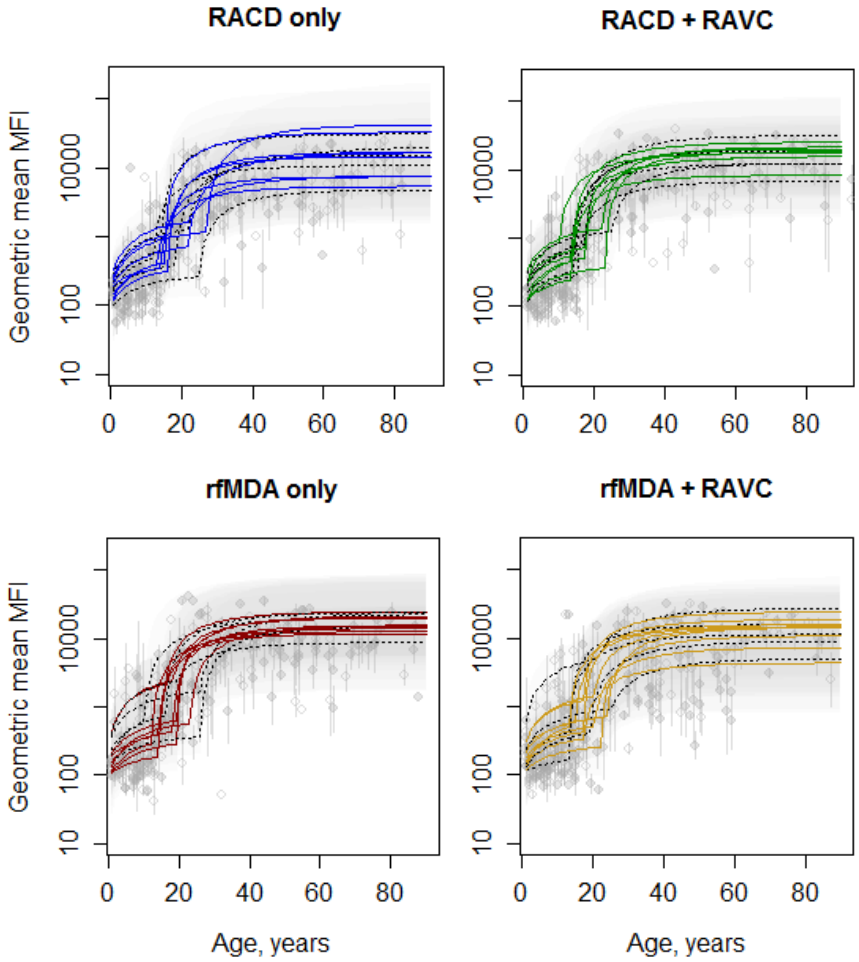

Table 7.13 AMA1 Area under the antibody acquisition curve by study arm and intervention

A. **By study arm.** Reference (intercept) is the mean AUC of clusters in the RACD only arm, and difference in mean AUC is listed for all other study arms based on linear regression unadjusted and adjusted for intervention coverage (>75%).

	Unadjusted		Adjusted	
Study arm	**Difference in AUC (95%CI)**	**p-value**	**Difference in AUC (95%CI)**	**p-value**
RACD only mean AUC (Intercept)	594,657 (436,953; 752,362)	--	549,029 (351,354; 746,704)	--
RACD + RAVC	200,921 (-46,831; 448,674)	0.118	217,282 (-37,179; 471,743)	0.100
rfMDA only	309,240 (49,211; 569,270)	0.024	314,481 (47,041; 581,920)	0.025
rfMDA + RAVC	67,671 (0176,396; 311,738)	0.589	82,077 (-168,454; 332,607)	0.524
Intervention coverage	--	--	58,021 (-132,654; 248,696)	0.554

B. **By intervention.** Reference (intercept) is the mean AUC of clusters in the RACD only arm, and difference in mean AUC is listed for rfMDA only and RACD + RAVC based on linear regression unadjusted and adjusted for intervention coverage (>75%). rfMDA:RAVC is the additional AUC difference of the two interventions combined (included as an interaction effect in the linear regression).

	Unadjusted		Adjusted	
Intervention	**Difference in AUC (95%CI)**	**p-value**	**Difference in AUC (95%CI)**	**p-value**
RACD only mean AUC (Intercept)	594,657 (436,953; 752,362)	--	549,029 (351,354; 746,704)	--
rfMDA	309,240 (49,211; 569,270)	0.024	314,481 (47,041; 581,920)	0.025
RAVC	200,921 (-46,831; 448,674)	0.118	217,282 (-37,179; 471,743)	0.100
rfMDA:RAVC	-442,490 (-815,081; -69,900)	0.024	-449,686 (-829,524; -69,848)	0.024
Intervention coverage	--	--	58,021 (-132,654; 248,696)	0.554

Antigens associated with short-lived antibody responses

Sero-positivity to Etramp5.Ag1, Rh2.2030 and EBA175

Compared with antigens associated with long-lived antibody responses, differences in odds of sero-positivity for Etramp5.Ag1 and Rh2.2030 between study arms were more apparent, though not statistically strong.

Based on unadjusted logistic regression, individuals in the rfMDA + RAVC arm had a reduced odds of Etramp5.Ag1 sero-positivity (OR 0.76 95%CI 0.63 – 0.93, p=0.008) compared to the RACD only arm (Table 7.14a). Individuals receiving rfMDA only had an OR of 0.86 (95%CI 0.71 – 1.03, p=0.107), and individuals receiving RACD + RAVC had an OR of 0.94 (95%CI 0.79 – 1.13, p=0.521). After adjusting for demographic covariates and intervention coverage, odds of sero-positivity to Etramp5.Ag1 was lowest in the rfMDA + RAVC study arm (OR 0.78, 95%CI 0.60 – 1.02, p = 0.071), but statistical evidence for this difference was weak. A similar effect was observed when aggregating rfMDA arms (OR 0.87 95%CI 0.72 – 1.05, p = 0.153), but the effect of RAVC was not strong (OR 0.95, 95%CI 0.80 – 1.14, p = 0.586) based on intention-to-treat analysis, suggesting

that the differences in the rfMDA + RAVC arm compared to RACD only are driven primarily by the rfMDA intervention.

Table 7.14 Etramp5.Ag1 sero-positivity by study arm and intervention

A. **By study arm.** Unadjusted and adjusted (GEE with clustering at EA-level) logistic regression, odds of sero-positivity by study arm.

Outcome: Sero-positivity	Unadjusted			Adjusted‡		
	OR	95% CI	p-value	OR	95% CI	p-value
RACD only	1.00	1.00		1.00	1.00	
RACD + RAVC	0.94	0.79 – 1.13	0.521	0.90	0.69 – 1.18	0.458
rfMDA	0.86	0.71 – 1.03	0.107	0.90	0.68 – 1.18	0.441
rfMDA + RAVC	0.76	0.63 – 0.93	0.008	0.78	0.60 – 1.02	0.071
Age category						
1-5 years	--	--	--	1.00	1.00	
6-15 years	--	--	--	1.65	1.32 – 2.06	0.000
>15 years	--	--	--	1.80	1.46 – 2.22	0.000
Intervention coverage > 75%	--	--	--	0.84	0.70 – 1.01	0.063
Visit day	--	--	--	0.99	0.99 – 1.00	0.000
Fever	--	--	--	1.65	0.48 – 5.70	0.431
Gender (Female)	--	--	--	0.82	0.71 – 0.94	0.005

B. By intervention. Logistic regression unadjusted and adjusted (GEE model with clustering at EA-level)

Outcome: sero-positivity	Unadjusted			Adjusted		
	OR	95% CI	p-value	OR	95% CI	p-value
rfMDA*	0.87	0.72 – 1.05	0.140	0.89	0.68 – 1.17	0.406
RAVC†	0.95	0.80 – 1.14	0.586	0.90	0.69 – 1.17	0.422
rfMDA:RAVC	0.91	0.70 – 1.20	0.511	0.97	0.67 – 1.40	0.880
1-5 years	--	--	--	1.00	1.00	
6-15 years	--	--	--	1.65	1.32 – 2.05	<0.001
>15 years	--	--	--	1.80	1.46 – 2.22	<0.001
Intervention coverage > 75%	--	--	--	0.84	0.70 – 1.01	0.062
Visit day	--	--	--	0.99	0.99 – 1.00	<0.001
Fever	--	--	--	1.74	0.80 – 3.78	0.161
Gender (Female)	--	--	--	0.81	0.71 – 0.94	0.004

* With or without RAVC † With either RACD or rfMDA

Unadjusted odds of Rh2.2030 sero-positivity was lower in all study arms compared to the RACD only arm, but statistical evidence was weak. However, adjusted odds of sero-positivity to Rh2.2030 (Table 7.15) was only observed to be lower in the RACD + RAVC and rfMDA only arms (OR 0.83 95%CI 0.67 – 1.03, p=0.096 and 0.87 95%CI 0.68 – 1.11, p=0.268 respectively). There were no statistically strong differences when aggregating rfMDA arms or RAVC arms for Rh2.2030.

The effect of age on sero-positivity was less pronounced for Etramp5.Ag1 compared with $MSP1_{19}$ and AMA1, where older children had an OR of 1.65 (95%CI 1.32 – 2.06, p<0.001) compared to young children and adults only had an OR of 1.80 (95%CI 1.46 – 2.22, p<0.001). However, the age

effect for Rh2.2030 was similar to long-term antibody markers, with older children having an OR of 2.92 (95%CI 1.95 – 4.36, p<0.001) and adults an OR of 22.29 (95%CI 15.38 – 32.30), p<0.001).

Table 7.15 Rh2.2030 sero-positivity by study arm and intervention

A. **By study arm.** Unadjusted and adjusted (GEE with clustering at EA-level) logistic regression, odds of sero-positivity by study arm.

Outcome: Sero-positivity	Unadjusted			Adjusted‡		
	OR	95% CI	p-value	OR	95% CI	p-value
RACD only	1.00	1.00		1.00	1.00	
RACD + RAVC	0.83	0.72 – 1.04	0.129	0.83	0.67 – 1.03	0.096
rfMDA	0.87	0.74 – 1.07	0.209	0.87	0.68 – 1.11	0.268
rfMDA + RAVC	0.95	0.79 – 1.15	0.623	1.00	0.77 – 1.31	0.988
Age category						
1-5 years	--	--	--	1.00	1.00	
6-15 years	--	--	--	2.92	1.95 – 4.36	0.000
>15 years	--	--	--	22.29	15.38 – 32.30	0.000
Intervention coverage > 75%	--	--	--	0.79	0.66 – 0.95	0.012
Visit day	--	--	--	1.00	0.99 – 1.00	0.270
Fever	--	--	--	1.67	0.64 – 4.39	0.297
Gender (Female)	--	--	--	0.73	0.63 – 0.84	0.000

B. **By intervention.** Logistic regression unadjusted and adjusted (GEE model with clustering at EA-level)

Outcome: sero-positivity	Unadjusted			Adjusted		
	OR	95% CI	p-value	OR	95% CI	p-value
rfMDA*	0.89	0.74 – 1.07	0.204	0.87	0.68 – 1.11	0.268
RAVC†	0.87	0.73 – 1.04	0.123	0.83	0.67 – 1.03	0.096
rfMDA:RAVC	1.21	0.93 – 1.58	0.149	1.39	0.97 – 1.98	0.074
1-5 years	--	--	--	1.00	1.00	
6-15 years	--	--	--	2.92	1.95 – 4.36	<0.001
>15 years	--	--	--	22.29	15.38 – 32.30	<0.001
Intervention coverage > 75%	--	--	--	0.79	0.66 – 0.95	0.012
Visit day	--	--	--	1.00	0.99 – 1.00	0.270
Fever	--	--	--	1.67	0.64 – 4.39	0.297
Gender (Female)	--	--	--	0.73	0.63 – 0.84	<0.001

* With or without RAVC † With either RACD or rfMDA

For EBA175, no differences in odds of sero-positivity were observed between study arms or interventions, nor was there an effect of intervention coverage (Table 7.16). However, there was an effect of age, primarily in adults who had an OR of 7.23 (95%CI 5.23 – 9.31, p<0.001) compared to young children, while older children only had an OR of 1.78 (95%CI 1.33 – 2.39, p<0.001).

Table 7.16 EBA175 sero-positivity by study arm and intervention

A. **By study arm**. Unadjusted and adjusted (GEE with clustering at EA-level) logistic regression, odds of sero-positivity by study arm.

Outcome: sero-positivity	Unadjusted			Adjusted		
	OR	95% CI	p-value	OR	95% CI	p-value
RACD only	1.00	1.00		1.00	1.00	
RACD + RAVC	1.17	0.98 – 1.39	0.088	1.17	0.94 – 1.45	0.162
rfMDA	1.06	0.89 – 1.28	0.502	1.07	0.85 – 1.34	0.562
rfMDA + RAVC	1.03	0.85 – 1.24	0.782	1.06	0.81 – 1.37	0.679
Age category						
1-5 years	--	--	--	1.00	1.00	
6-15 years	--	--	--	1.78	1.33 – 2.39	<0.001
>15 years	--	--	--	7.23	5.23 – 9.31	<0.001
Intervention coverage > 75%	--	--	--	0.98	0.83 – 1.17	0.840
Visit day	--	--	--	1.00	0.99 – 1.00	0.073
Fever	--	--	--	0.76	0.27 – 2.10	0.594
Gender (Female)	--	--	--	0.78	0.68 – 0.91	0.001

B. **By intervention.** Logistic regression unadjusted and adjusted (GEE model with clustering at EA-level)

Outcome: sero-positivity	Unadjusted			Adjusted		
	OR	95% CI	p-value	OR	95% CI	p-value
rfMDA*	1.06	0.89 – 1.28	0.502	1.07	0.85 – 1.34	0.562
RAVC†	1.17	0.98 – 1.39	0.088	1.17	0.94 – 1.45	0.162
rfMDA:RAVC	0.83	0.64 – 1.07	0.155	0.85	0.60 – 1.19	0.332
1-5 years	--	--	--	1.00	1.00	
6-15 years	--	--	--	1.78	1.33 – 2.39	<0.001
>15 years	--	--	--	7.23	5.62 – 9.31	<0.001
Intervention coverage > 75%	--	--	--	0.98	0.83 – 1.17	0.840
Visit day	--	--	--	1.00	0.99 – 1.00	0.073
Fever	--	--	--	0.76	0.27 – 2.10	0.594
Gender (Female)	--	--	--	0.78	0.68 – 0.91	0.001

* With or without RAVC † With either RACD or rfMDA

Similar to long-term markers, clusters with trial intervention coverage greater than 75% had a reduced the odds of sero-positivity to both Etramp5.Ag1 (OR 0.84 95%CI 0.70 – 1.01, p=0.063) and Rh2.2030 (OR 0.079 95%CI 0.66 – 0.95, p=0.012). Females also had a lower odds of sero-positivity compared to males for both Etramp5.Ag1 (OR 0.82 95%CI 0.71 – 0.94, p=0.005) and Rh2.2030 (OR 0.80 95%CI 0.70 – 0.92, p=0.002).

Sero-prevalence in children to Etramp5.Ag1, Rh2.2030 and EBA175

Similar to $MSP1_{19}$, under-15 sero-prevalence to Etramp5.Ag1 was lower in the RACD + RAVC arm by 2.7% (95%CI 0.0 – 5.4, p=0.55) and in the rfMDA + RAVC arm by 3.9% (95%CI 1.2 – 6.6, p=0.006) when adjusted for intervention coverage (Table 7.17a). For Rh2.2030, only the rfMDA + RAVC arm was statistically different, with an adjusted sero-prevalence lower by 1.7% (95%CI 0.4 – 3.0, p=0.013) (Table 7.18a). Similar to Etramp5.Ag1, adjusted sero-prevalence to EBA175 (Table 7.19a) was only slightly lower in the RACD + RAVC arm by 0.7% (95%CI 0.0 – 1.3, p=0.55). In the rfMDA + RAVC arm, adjusted sero-prevalence was lower by 1.0% (95%CI 0.3 - 1.6, p=0.006). Based

on regression analysis comparing the interventions, the differences in the rfMDA + RAVC arm appear to be driven primarily by the effect of the RAVC intervention (Tables 7.17b, 7.18b and 7.19b).

Table 7.17 Etramp5.Ag1 under-15 sero-prevalence by study arm and intervention

A. **By study arm.** Reference (intercept) is the mean sero-prevalence for ages <15 years amongst of clusters in the RACD only arm, and difference in mean sero-prevalence is listed for all other study arms based on linear regression unadjusted and adjusted for intervention coverage (>75%).

	Unadjusted		Adjusted	
Study arm	**Difference in SP (95%CI)**	**p-value**	**Difference in SP (95%CI)**	**p-value**
RACD only mean SP (Intercept)	14.4% (12.6 – 16.2)	--	14.8% (12.5 – 17.0)	--
RACD + RAVC	-2.4% (-5.0; 0.2)	0.081	-2.7% (-5.4; 0.0)	0.055
rfMDA only	-1.8% (-4.4; 0.8)	0.191	-2.1% (-4.7; 0.6)	0.135
rfMDA + RAVC	-3.6% (-6.2; -1.0)	0.009	-3.9% (-6.6; -1.2)	0.006
Intervention coverage	--	--	-0.1% (-2.1; 1.8)	0.888

B. By intervention. Reference (intercept) is the mean sero-prevalence of ages <15 years of clusters in the RACD only arm, and difference in mean sero-prevalence is listed for rfMDA only and RACD + RAVC based on linear regression unadjusted and adjusted for intervention coverage (>75%). rfMDA:RAVC is the additional sero-prevalence difference of the two interventions combined (included as an interaction effect in the linear regression).

	Unadjusted		Adjusted	
Intervention	**Difference in SP (95%CI)**	**p-value**	**Difference in SP (95%CI)**	**p-value**
RACD only mean SP (Intercept)	14.4% (12.6 – 16.2)	--	14.4% (12.6 – 16.2)	--
rfMDA	-1.8% (-4.4; 0.8)	0.191	-2.1% (-4.7; 0.6)	0.135
RAVC	-2.4% (-5.0; 0.2)	0.081	-2.7% (-5.4; 0.0)	0.055
rfMDA:RAVC	0.5% (-3.2; 4.2)	0.787	0.8% (-2.9; 4.6)	0.668
Intervention coverage	--	--	-0.1% (-2.1; 1.8)	0.888

Table 7.18 Rh2.2030 under-15 sero-prevalence by study arm and intervention

A. **By study arm**. Reference (intercept) is the mean sero-prevalence for ages <15 years amongst of clusters in the RACD only arm, and difference in mean sero-prevalence is listed for all other study arms based on linear regression unadjusted and adjusted for intervention coverage (>75%).

	Unadjusted		Adjusted	
Study arm	**Difference in SP (95%CI)**	**p-value**	**Difference in SP (95%CI)**	**p-value**
RACD only mean SP (Intercept)	3.0% (2.1 – 3.9)	--	3.2% (2.1 – 4.3)	--
RACD + RAVC	-1.1% (-2.3; 0.2)	0.104	-1.2% (-2.5; 0.1)	0.070
rfMDA only	-0.8% (-2.1; 0.4)	0.212	-1.0% (-2.3; 0.3)	0.150
rfMDA + RAVC	-1.5% (-2.8; -0.3)	0.020	-1.7% (-3.0; -0.4)	0.013
Intervention coverage	--	--	-0.1% (-1.0; 0.8)	0.865

B. By intervention. Reference (intercept) is the mean sero-prevalence of ages <15 years of clusters in the RACD only arm, and difference in mean sero-prevalence is listed for rfMDA only and RACD + RAVC based on linear regression unadjusted and adjusted for intervention coverage (>75%). rfMDA:RAVC is the additional sero-prevalence difference of the two interventions combined (included as an interaction effect in the linear regression).

	Unadjusted		Adjusted	
Intervention	**Difference in SP (95%CI)**	**p-value**	**Difference in SP (95%CI)**	**p-value**
RACD only mean SP (Intercept)	3.0% (2.1 – 3.9)	--	3.2% (2.1 – 4.3)	--
rfMDA	-0.8% (-2.1; 0.4)	0.212	-1.0% (-2.3; 0.3)	0.150
RAVC	-1.1% (-2.3; 0.2)	0.104	-1.2% (-2.5; 0.1)	0.070
rfMDA:RAVC	0.4% (-1.4; 2.1)	0.695	0.5% (-1.3; 2.3)	0.575
Intervention coverage	--	--	-0.1% (-1.0; 0.8)	0.865

Table 7.19 EBA175 under-15 sero-prevalence by study arm and intervention

A. **By study arm.** Reference (intercept) is the mean sero-prevalence for ages <15 years amongst of clusters in the RACD only arm, and difference in mean sero-prevalence is listed for all other study arms based on linear regression unadjusted and adjusted for intervention coverage (>75%).

	Unadjusted		Adjusted	
Study arm	**Difference in SP (95%CI)**	**p-value**	**Difference in SP (95%CI)**	**p-value**
RACD only mean SP (Intercept)	3.6% (3.1 – 4.0)	--	3.7% (3.1 – 4.2)	--
RACD + RAVC	-0.6% (-1.2; 0.1)	0.082	-0.7% (-1.3; 0.0)	0.055
rfMDA only	-0.4% (-1.1; 0.2)	0.192	-0.5% (-1.2; 0.1)	0.135
rfMDA + RAVC	-0.9% (-1.5; -0.2)	0.010	-1.0% (-1.6; -0.3)	0.006
Intervention coverage	--	--	0.0% (-0.5; 0.4)	0.885

B. By intervention. Reference (intercept) is the mean sero-prevalence of ages <15 years of clusters in the RACD only arm, and difference in mean sero-prevalence is listed for rfMDA only and RACD + RAVC based on linear regression unadjusted and adjusted for intervention coverage (>75%). rfMDA:RAVC is the additional sero-prevalence difference of the two interventions combined (included as an interaction effect in the linear regression).

	Unadjusted		Adjusted	
Intervention	**Difference in SP (95%CI)**	**p-value**	**Difference in SP (95%CI)**	**p-value**
RACD only mean SP (Intercept)	3.6% (3.1 – 4.0)	--	3.7% (3.1 – 4.2)	--
rfMDA	-0.4% (-1.1; 0.2)	0.192	-0.5% (-1.2; 0.1)	0.135
RAVC	-0.6% (-1.2; 0.1)	0.082	-0.7% (-1.3; 0.0)	0.055
rfMDA:RAVC	0.1% (-0.8; 1.1)	0.777	0.2% (-0.7; 1.1)	0.658
Intervention coverage	--	--	0.0% (-0.5; 0.4)	0.885

Sero-positivity and sero-prevalence to any short-term marker or HSRDT combined

When assessing the odds of sero-positivity to any of the three short-term serological markers or HSRDT positivity, differences between study arms were not statistically strong. However, both unadjusted and adjusted regression analysis showed a lower OR in the rfMDA and rfMDA + RAVC study arms (Table 7.20). There was a slightly increased odds of positivity in older children (1.87 95%CI 1.53-2.30, p<0.001), and an even larger increased odds in adults (6.07 95%CI 4.98 – 7.40, p<0.001).

Similar to sero-prevalence to individual antigens, the combined under-15 seroprevalence to all three short-term markers was lower in the RACD + RAVC arm by 3.6% (95%CI 0.0 – 7.1, p=0.056) when adjusted for intervention coverage (Table 7.21a). Sero-prevalence in the rfMDA + RAVC arm was lower by 5.2% (95%CI 1.6 – 8.7, p=0.007). Overall, these differences are larger than those observed for the markers individually. Again, the effect appears to be primarily due to the RAVC intervention, which is associated with a sero-prevalence lower by 3.6% (95%CI 0.09 – 7.1, p=0.056) compared to interventions without RAVC, while rfMDA arms are only associated with a reduction of sero-prevalence of 2.7% compared to RACD arms, but the p-value indicates that statistical evidence for this difference is weak (Table 7.21b).

Table 7.20 Combined sero-positivity (Etramp5.Ag1, Rh2.2030, EBA175) and HSRDT-positivity by study arm

Unadjusted and adjusted (GEE with clustering at EA-level) logistic regression, odds of sero-positivity by study arm.

Outcome: Positive to short-term sero-marker or HSRDT	Unadjusted			Adjusted‡		
	OR	95% CI	p-value	OR	95% CI	p-value
RACD only	1.00	1.00		1.00	1.00	
RACD + RAVC	1.08	0.91 – 1.28	0.53761	1.06	0.84 – 1.33	0.622
rfMDA	0.89	0.75 – 1.05	0.164	0.88	0.69 – 1.12	0.290
rfMDA + RAVC	0.92	0.77 – 1.09	0.329	0.90	0.69 – 1.18	0.452
Age category						
1-5 years	--	--	--	1.00	1.00	
6-15 years	--	--	--	1.87	1.53 – 2.30	<0.001
>15 years	--	--	--	6.07	4.98 – 7.40	<0.001
Intervention coverage > 75%	--	--	--	0.89	0.74 – 1.06	0.177
Visit day	--	--	--	1.00	0.99 – 1.00	0.006
Fever	--	--	--	1.90	0.77 – 4.69	0.166
Gender (Female)	--	--	--	0.75	0.66 – 0.86	<0.001

‡ Adjusted for age category, intervention coverage, visit day, fever, gender and clustering at EA-level, but not shown in table.

Table 7.21 Combined sero-prevalence (Etramp5.Ag1, Rh2.2030, EBA175) by study arm and intervention

A. **By study arm.** Reference (intercept) is the mean sero-prevalence for ages <15 years amongst of clusters in the RACD only arm, and difference in mean sero-prevalence is listed for all other study arms based on linear regression unadjusted and adjusted for intervention coverage (>75%).

	Unadjusted		Adjusted	
Study arm	**Difference in SP (95%CI)**	**p-value**	**Difference in SP (95%CI)**	**p-value**
RACD only mean SP (Intercept)	15.7% (13.2 –18.1)	--	16.2% (13.2 –19.2)	--
RACD + RAVC	-3.1% (-6.6; 0.3)	0.083	-3.6% (-7.1; 0.0)	0.056
rfMDA only	-2.3% (-5.8; 1.1)	0.192	-2.7% (-6.3; 0.8)	0.136
rfMDA + RAVC	-4.7% (-8.2; -1.3)	0.010	-5.2% (-8.7; -1.6)	0.007
Intervention coverage	--	--	-0.2% (-2.8; 2.4)	0.884

B. By intervention. Reference (intercept) is the mean sero-prevalence of ages <15 years of clusters in the RACD only arm, and difference in mean sero-prevalence is listed for rfMDA only and RACD + RAVC based on linear regression unadjusted and adjusted for intervention coverage (>75%). rfMDA:RAVC is the additional sero-prevalence difference of the two interventions combined (included as an interaction effect in the linear regression).

	Unadjusted		Adjusted	
Intervention	**Difference in SP (95%CI)**	**p-value**	**Difference in SP (95%CI)**	**p-value**
RACD only mean SP (Intercept)	15.7% (13.2 –18.1)	--	16.2% (13.2 –19.2)	--
rfMDA	-2.3% (-5.8; 1.1)	0.192	-2.7% (-6.3; 0.8)	0.136
RAVC	-3.1% (-6.6; 0.3)	0.083	-3.6% (-7.1; 0.0)	0.056
rfMDA:RAVC	0.7% (-4.2; 5.7)	0.773	1.2% (-3.8; 6.1)	0.654
Intervention coverage	--	--	-0.2% (-2.8; 2.4)	0.884

Antibody acquisition to Etramp5.Ag1, Rh2.2030, EBA175

Based on Ab acquisition models unadjusted and adjusted for intervention coverage, lower Etramp5.Ag1 antibody responses were observed in all study arms compared to the RACD only arm (Table 7.22, Figure 7.6b). However, these differences were only statistical strong for the rfMDA only arm (p=0.027 unadjusted and p=0.037 adjusted), while there is some weak evidence that differences in rfMDA + RAVC arms are significant (p=0.078 unadjusted and p=0.085 adjusted). Intervention coverage was shown to have a strong effect on differences between study arms, with a lower mean AUC value of 7,013 (95%CI 1,733 – 12,292, p=0.012) in clusters receiving greater than 75% intervention coverage (Table 7.22, Figures 7.6a-b).

On the other hand, antibody acquisition to Rh2.2030 did not appear to be different between study arms (Table 7.23, Figure 7.7b). Study arms with high intervention coverage had mean AUC values lower by 12,737, but p-values suggest that this difference statistically weak (Table 7.23,

Figures 7.7a-b). While this was not tested for each study arm, Figure 7.7b suggests that the effect of intervention coverage may be primarily in the rfMDA + RAVC arm, where high intervention coverage clusters appear to consistently have lower antibody acquisition compared to lower coverage clusters. There were no differences between study arms in antibody acquisition AUC values for EBA175 (Table 7.24), nor was there an effect of intervention coverage observed (Figures 7.8a-b). However, similar to Rh2.2030, Figure 7.8b suggests that the effect may only be apparent in the rfMDA + RAVC arm, but the effect of intervention coverage was not statistically tested by study arm in this analysis.

For a majority of clusters, changes in Ab acquisition rate to both Rh2.2030 (Figures 7.7a-b) and EBA175 (Figures 7.8a-b) appear to occur between ages 15-20, while age-related differences are not observed in the Ab acquisition rates to Etramp5.Ag1 (Figures 7.6a-b). This is consistent with the higher odds of sero-positivity to Rh2.2030 in adults. A higher odds of sero-positivity to EBA175 is also observed in adults, but is not as pronounced relative to Rh2.2030.

Figure 7.6 Etramp5.Ag1 antibody acquisition overall, by intervention coverage and study arm

A. **Overall and by intervention coverage.** Ab acquisition fit for all clusters (top), points are age-adjusted MFI, black dotted lines are clusters with <75% intervention coverage, blue dotted lines are clusters with >75% intervention coverage, and shaded areas are the 95% credible intervals of the Ab acquisition fit. Clusters with <75% intervention coverage shown in black (bottom left) and >75% intervention coverage in red (bottom right).

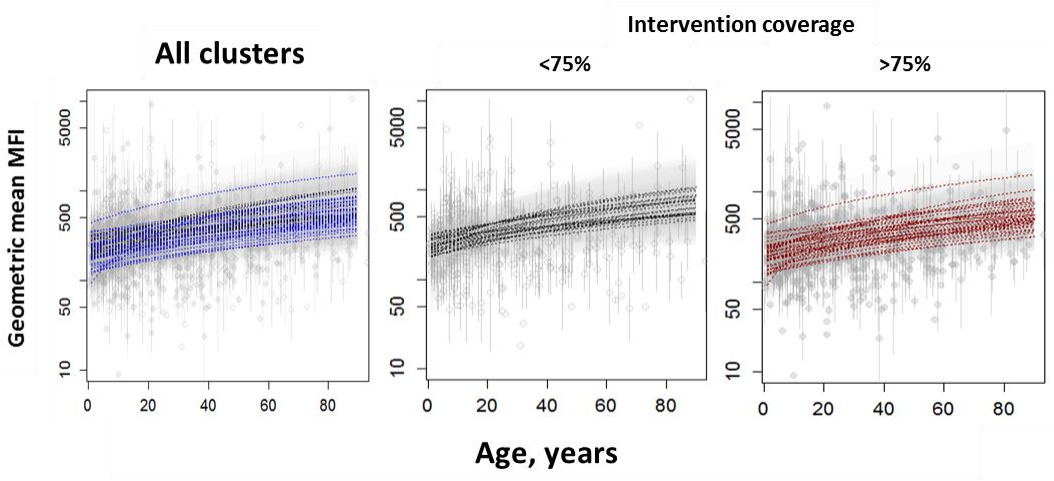

B. **B study arm.** RACD only in blue (top left), RACD + RACD in green (top right), rfMDA only in red (bottom left), and rfMDA + RAVC in yellow (bottom right). Dotted lines show clusters with <75% intervention coverage and solid lines clusters with >75% intervention coverage.

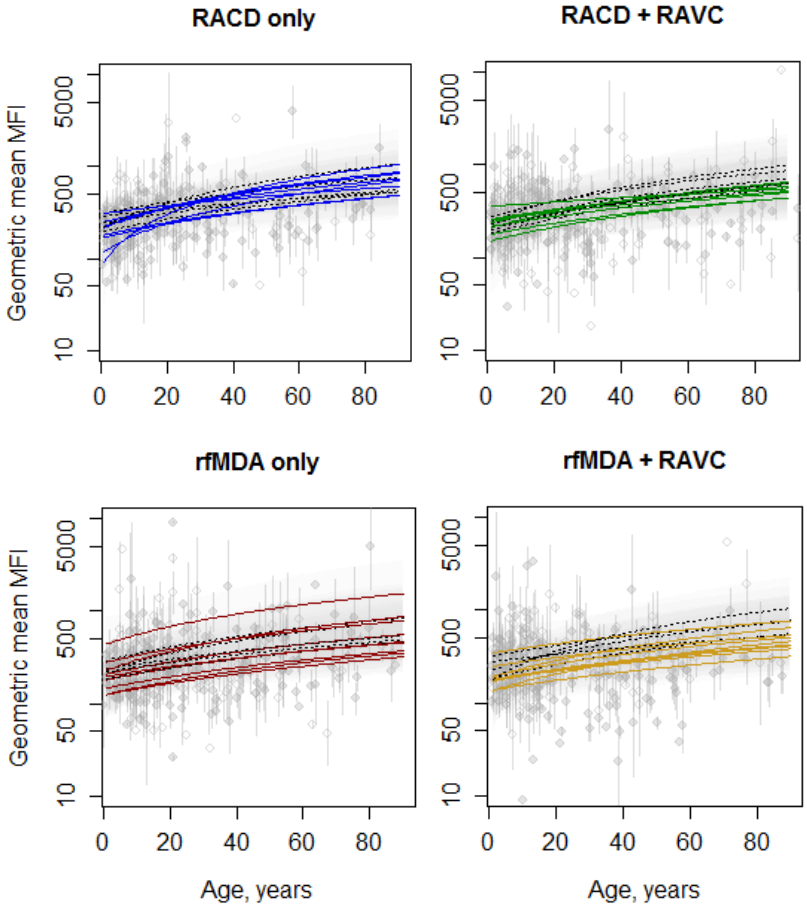

Table 7.22 Etramp5.Ag1 Area under the antibody acquisition curve by study arm and intervention

A. **By study arm.** Reference (intercept) is the mean AUC of clusters in the RACD only arm, and difference in mean AUC is listed for all other study arms based on linear regression unadjusted and adjusted for intervention coverage (>75%).

	Unadjusted		Adjusted	
Study arm	**Difference in AUC (95%CI)**	**p-value**	**Difference in AUC (95%CI)**	**p-value**
RACD only mean AUC (Intercept)	38,843 (33,762; 43,923)	--	43,476 (37,494; 49,458)	--
RACD + RAVC	-3,172 (-10,354; 4,009)	0.391	-2,782 (-9,770; 4,206)	0.439
rfMDA only	-8,118 (-15,101; -1,125)	0.027	-7,453 (-14,273; -632)	0.037
rfMDA + RAVC	-6,546 (-13,682; 589)	0.078	-6,211 (-13,153; 731)	0.086
Intervention coverage	--	--	-7,013 (-12,292; -1,733)	0.012

B. By intervention. Reference (intercept) is the mean AUC of clusters in the RACD only arm, and difference in mean AUC is listed for rfMDA only and RACD + RAVC based on linear regression unadjusted and adjusted for intervention coverage (>75%). rfMDA:RAVC is the additional AUC difference of the two interventions combined (included as an interaction effect in the linear regression).

	Unadjusted		Adjusted	
Intervention	**Difference in AUC (95%CI)**	**p-value**	**Difference in AUC (95%CI)**	**p-value**
RACD only mean AUC (Intercept)	38,843 (33,762; 43,923)	--	43,476 (37,494; 49,458)	--
rfMDA	-8,118 (-15,101; -1,125)	0.027	-7,453 (-14,273; -632)	0.037
RAVC	-3,172 (-10,354; 4,009)	0.391	-2,782 (-9,770; 4,206)	0.439
rfMDA:RAVC	4,744 (-5,238; 14,726)	0.356	4,024 (-5,620; 13,668)	0.417
Intervention coverage	--	--	-7,013 (-12,292; -1,733)	0.012

Figure 7.7 Rh2.2030 Antibody acquisition overall, by trial intervention coverage and study arm

A. **Overall and by intervention coverage.** Ab acquisition fit for all clusters (top), points are age-adjusted MFI, black dotted lines are clusters with <75% intervention coverage, blue dotted lines are clusters with >75% intervention coverage, and shaded areas are the 95% credible intervals of the Ab acquisition fit. Clusters with <75% intervention coverage shown in black (bottom left) and >75% intervention coverage in red (bottom right).

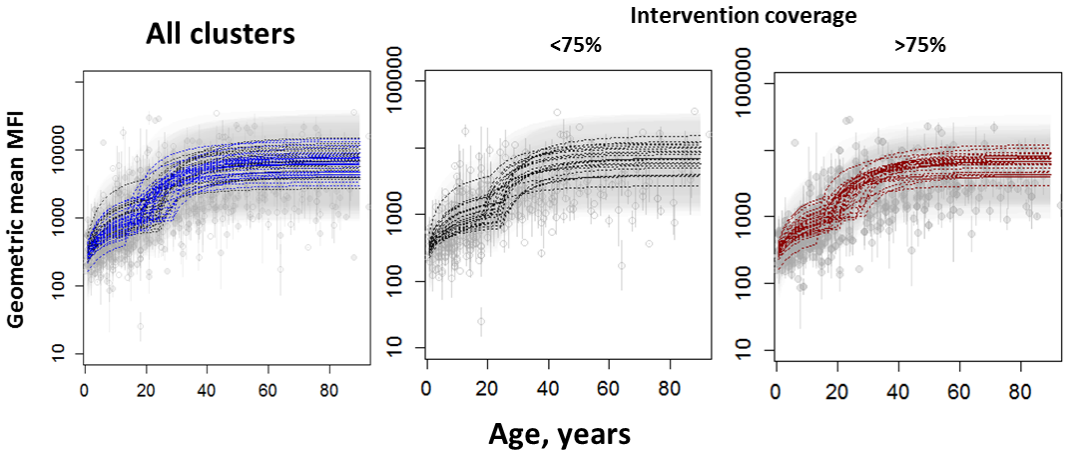

B. **By study arm.** RACD only in blue (top left), RACD + RACD in green (top right), rfMDA only in red (bottom left), and rfMDA + RAVC in yellow (bottom right). Dotted lines show clusters with <75% intervention coverage and solid lines clusters with >75% intervention coverage.

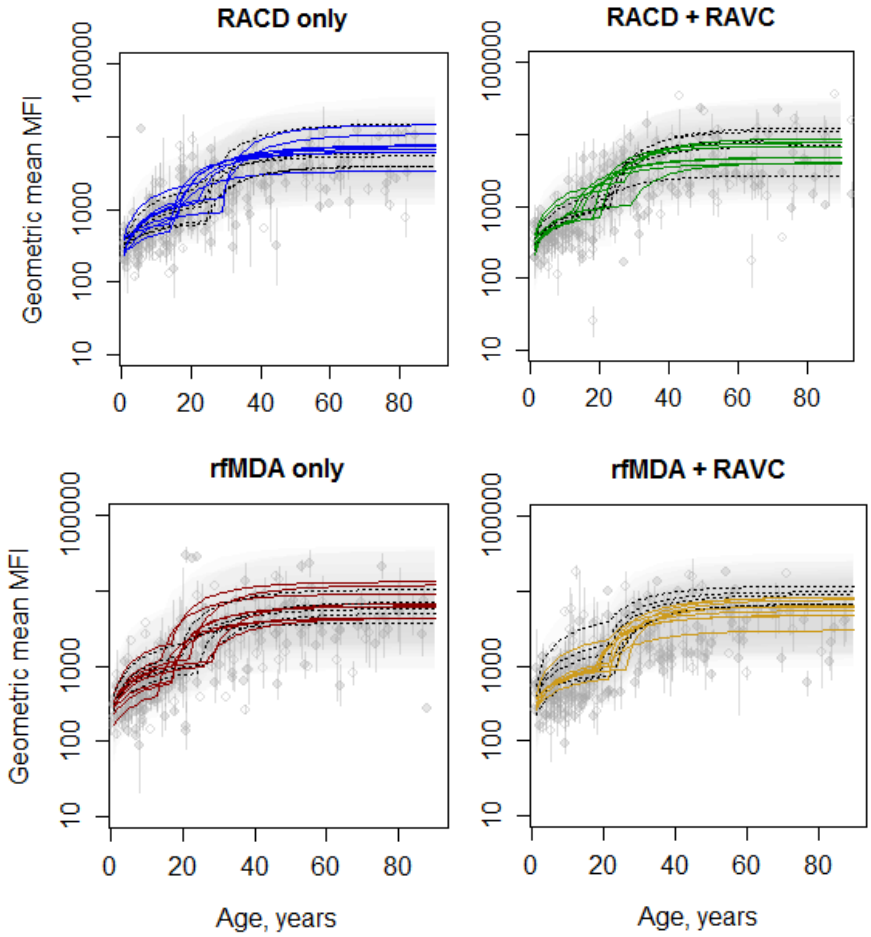

Table 7.23 Rh2.2030 Area under the antibody acquisition curve by study arm and intervention

A. **By study arm.** Reference (intercept) is the mean AUC of clusters in the RACD only arm, and difference in mean AUC is listed for all other study arms based on linear regression unadjusted and adjusted for intervention coverage (>75%).

	Unadjusted		Adjusted	
Study arm	**Difference in AUC (95%CI)**	**p-value**	**Difference in AUC (95%CI)**	**p-value**
RACD only mean AUC (Intercept)	338,528 (271,875; 405,180)	--	353,514 (270,152; 436,876)	--
RACD + RAVC	10,875 (-88,397; 110,147)	0.831	3,760 (-98,728; 106,247)	0.943
rfMDA only	24,379 (-77,119; 125,877)	0.640	17,731 (-87,130; 122,593)	0.742
rfMDA + RAVC	42,591 (-62,181; 147,362)	0.429	37,226 (-71,721; 146,173)	0.506
Intervention coverage	--	--	-12,737 (-92,396; 66,922)	0.755

B. **By intervention.** Reference (intercept) is the mean AUC of clusters in the RACD only arm, and difference in mean AUC is listed for rfMDA only and RACD + RAVC based on linear regression unadjusted and adjusted for intervention coverage (>75%). rfMDA:RAVC is the additional AUC difference of the two interventions combined (included as an interaction effect in the linear regression).

	Unadjusted		Adjusted	
Intervention	**Difference in AUC (95%CI)**	**p-value**	**Difference in AUC (95%CI)**	**p-value**
RACD only mean AUC (Intercept)	338,528 (271,875; 405,180)	--	353,514 (270,152; 436,876)	--
rfMDA	24,379 (-77,119; 125,877)	0.640	17,731 (-87,130; 122,593)	0.742
RAVC	10,875 (-88,397; 110,147)	0.831	3,760 (-98,728; 106,247)	0.943
rfMDA:RAVC	7,337 (-141,823; 156,497)	0.924	15,735 (-136,601; 168,071)	0.840
Intervention coverage	--	--	-12,737 (-92,396; 66,922)	0.755

Figure 7.8 EBA175 Antibody acquisition overall, by trial intervention coverage and study arm

A. **Overall and by intervention coverage.** Ab acquisition fit for all clusters (top), points are age-adjusted MFI, black dotted lines are clusters with <75% intervention coverage, blue dotted lines are clusters with >75% intervention coverage, and shaded areas are the 95% credible intervals of the Ab acquisition fit. Clusters with <75% intervention coverage shown in black (bottom left) and >75% intervention coverage in red (bottom right).

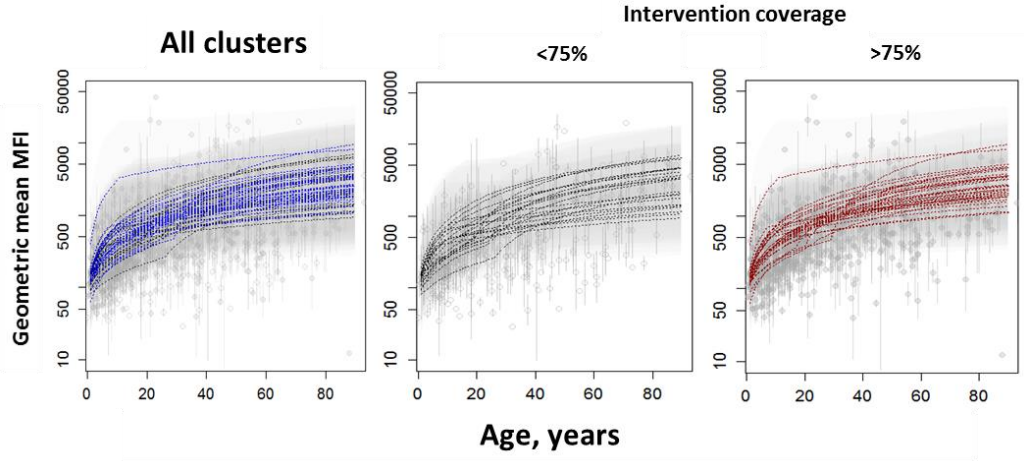

B. **By study arm.** RACD only in blue (top left), RACD + RACD in green (top right), rfMDA only in red (bottom left), and rfMDA + RAVC in yellow (bottom right). Dotted lines show clusters with <75% intervention coverage and solid lines clusters with >75% intervention coverage.

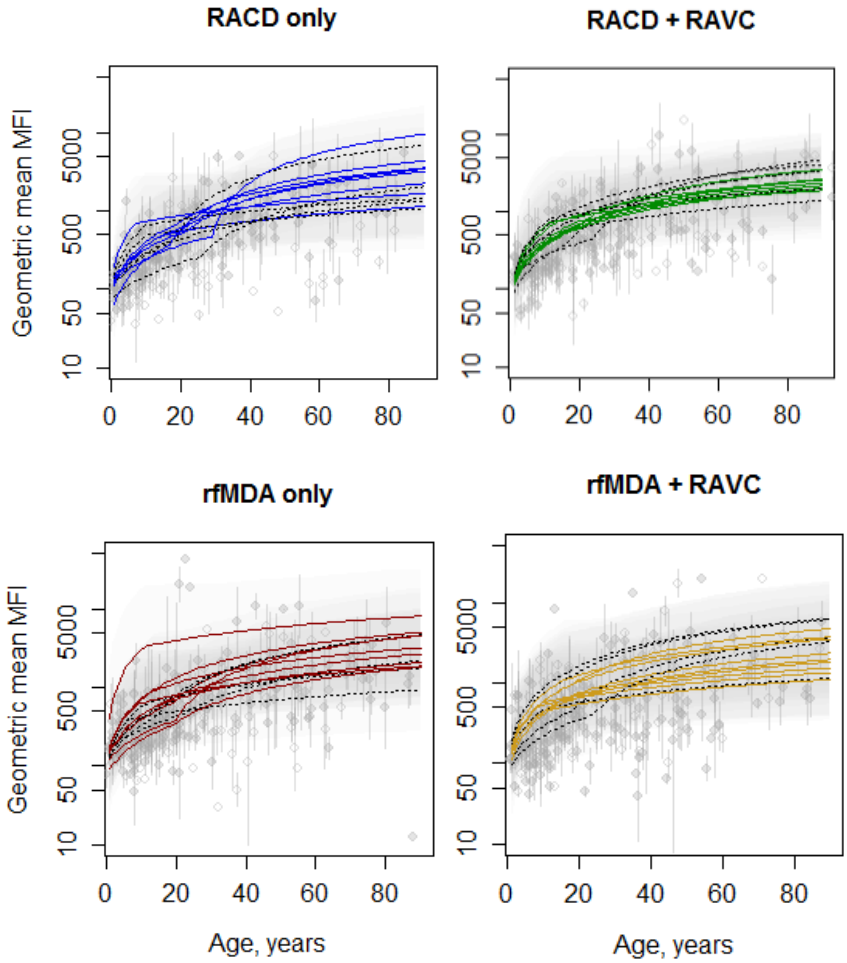

Table 7.24 EBA175 Area under the antibody acquisition curve by study arm and intervention

A. **By study arm.** Reference (intercept) is the mean AUC of clusters in the RACD only arm, and difference in mean AUC is listed for all other study arms based on linear regression unadjusted and adjusted for intervention coverage (>75%).

	Unadjusted		Adjusted	
Study arm	**Difference in AUC (95%CI)**	**p-value**	**Difference in AUC (95%CI)**	**p-value**
RACD only mean AUC (Intercept)	109,604 (82,503; 136,704)	--	108,131 (74,974; 141,289)	--
RACD + RAVC	18,439 (-20,992; 57,871)	0.364	15,142 (-25,708; 55,993)	0.471
rfMDA only	19,304 (-21,622; 60,229)	0.360	16,240 (-26,045; 58,524)	0.455
rfMDA + RAVC	10,461 (-31,009; 51,930)	0.623	6,581 (-36,501; 49,662)	0.766
Intervention coverage	--	--	7,645 (-23,376; 38,666)	0.631

B. **By intervention**. Reference (intercept) is the mean AUC of clusters in the RACD only arm, and difference in mean AUC is listed for rfMDA only and RACD + RAVC based on linear regression unadjusted and adjusted for intervention coverage (>75%). rfMDA:RAVC is the additional AUC difference of the two interventions combined (included as an interaction effect in the linear regression).

	Unadjusted		Adjusted	
Intervention	**Difference in AUC (95%CI)**	**p-value**	**Difference in AUC (95%CI)**	**p-value**
RACD only mean AUC (Intercept)	109,604 (82,503; 136,704)	--	108,131 (74,974; 141,289)	--
rfMDA	19,304 (-21,622; 60,229)	0.360	16,240 (-26,045; 58,524)	0.455
RAVC	18,439 (-20,992; 57,871)	0.364	15,142 (-25,708; 55,993)	0.471
rfMDA:RAVC	-27,282 (-86,279; 31,715)	0.369	-24,801 (-85,130; 35,528)	0.424
Intervention coverage	--	--	7,645 (-23,376; 38,666)	0.631

Comparison of trial endpoints

A comparison of serological, clinical, and HSRDT endpoints are illustrated in Figures 7.9 – 7.11. Overall, confidence intervals appeared large for all endpoints and study arms, making it difficult to draw statistical conclusions from the results according to any endpoint.

Clinical endpoints show a decreased mean IRR in rfMDA and RAVC intervention arms, individually and combined (Figure 7.9c). Smaller confidence intervals were observed for AMA1 SCRs compared to $MSP1_{19}$ SCRs, but remain large for both antigens (Figure 7.9a-b). For most serological endpoints, differences were more apparent between study arms when restricting analysis to clusters with high intervention coverage. Intention-to-treat analysis suggests that SCR values do not differ between study arms for either antigen, while per-protocol analysis suggest that SCR may be lower in the rfMDA only and rfMDA + RAVC arms. However, strong statistical conclusions still cannot be drawn due to the large confidence intervals. SCR and IRR are not directly comparable here, as they are expressed as rates and rate ratios respectively.

Based on HSRDT results, a lower odds of positive test result compared to RACD only was observed only in the rfMDA + RAVC arm, while rfMDA clusters (with or without RAVC) showed lower odds of HSRDT positivity compared to RACD (with or without RAVC) arms (Figure 7.10a and 7.10c). A lower odds of HSRDT positivity was only observed in RAVC compared to No RAVC arms based on per-protocol analysis (Figure 7.10d). For Etramp5.Ag1, lower odds of sero-positivity were observed in all study arms compared to the RACD only arm based on both intention-to-treat and per-protocol analysis. For Rh2.2030, decreased odds of sero-positivity were observed in the RACD + RAVC and rfMDA only arms based on both intention-to-treat and per-protocol analysis.

When comparing interventions, sero-positivity to Rh2.2030 based on per-protocol analysis was lower in rfMDA arms (with or without RAVC) compared to RACD arms. It was also lower in RAVC arms (with either rfMDA or RACD) compared to arms without RAVC (Figure 7.10d). However, these differences were no longer apparent based on intention-to-treat analysis (Figure 7.10b). For $MSP1_{19}$, AMA1 and EBA175, odds of sero-positivity was not lower in any of the study arms compared to the RACD only reference arm based on both intention-to-treat and per-protocol analysis. When comparing interventions, rfMDA study arms (with or without RAVC) showed lower odds of sero-positivity based on per-protocol analysis. However, similar to Rh2.2030, these differences were also no longer apparent based on intention-to-treat analysis. Overall, confidence intervals for the ORs of all serological endpoints were smaller than HSRDT.

Based on Ab acquisition AUC values (Figure 7.11), lower antibody levels to $MSP1_{19}$ or AMA1 were not observed in any study arms compared to the RACD only arm (Figure 7.11a). For both Rh2.2030 and EBA175, AUC values were lower in the RACD + RAVC and the rfMDA + RAVC study arms based on per-protocol analysis, but no differences were observed based on intention-to-treat analysis. On the other hand, AUC values for Etramp5.Ag1 were lower in all study arms compared to the RACD only arm based on both intention-to-treat and per-protocol analysis.

Figure 7.9 Sero-conversion rate and clinical incidence rate ratio by study arm and intervention
Mean SCR by each study arm (left). Mean SCR by intervention (middle) and clinical IRR by intervention (right), where reference arms are RACD only, RACD (with or without RAVC) and No RAVC respectively. Intention-to-treat (ITT) includes all clusters and per-protocol (PP) only includes clusters receiving >75% trial intervention coverage.

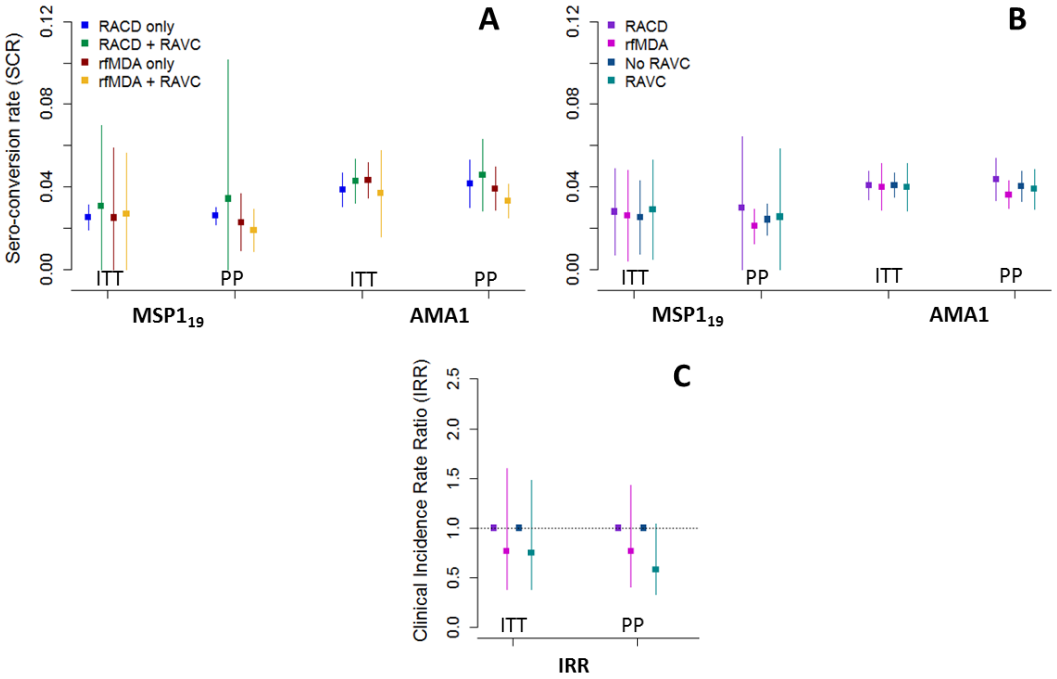

Figure 7.10 Sero-positivity vs. HSRDT positivity odds ratio by study arm and intervention
Reference arms are RACD only, RACD (with or without RAVC) and No RAVC respectively. Intention-to-treat (ITT) includes all clusters and per-protocol (PP) only includes clusters receiving >75% trial intervention coverage.

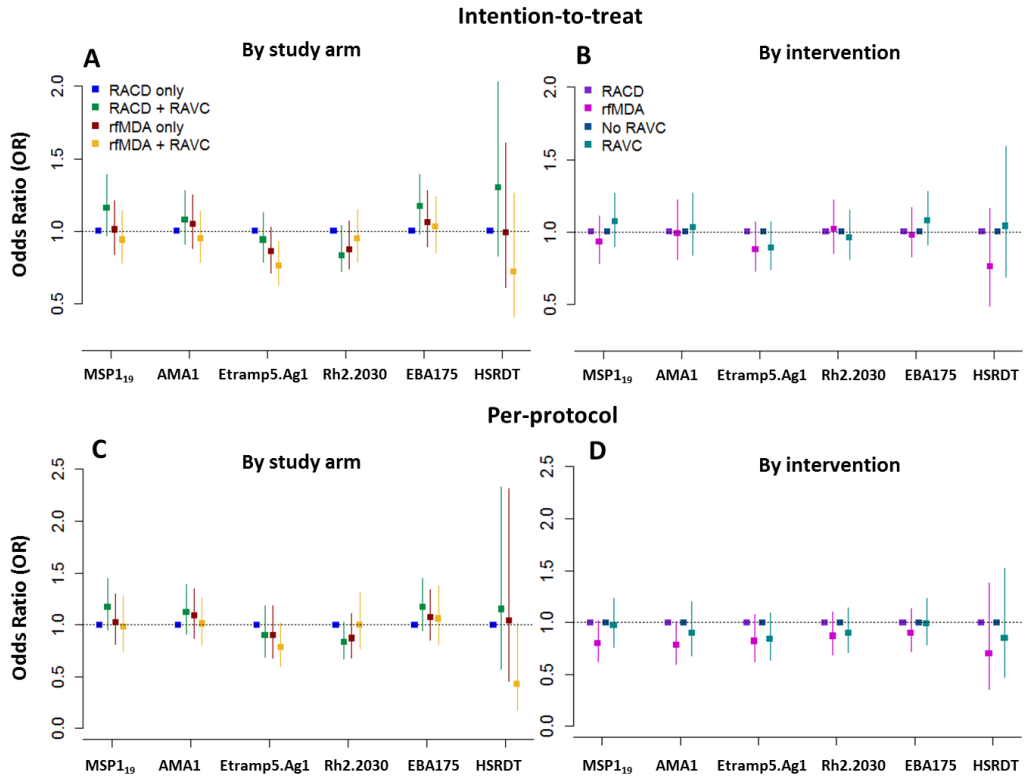

Figure 7.11 Area under the antibody acquisition curve by study arm and intervention

Reference arms are RACD only, RACD (with or without RAVC) and No RAVC respectively. Intention-to-treat (ITT) refers to Ab acquisition model fit overall and per-protocol (PP) refers to Ab acquisition model fit adjusted for intervention coverage.

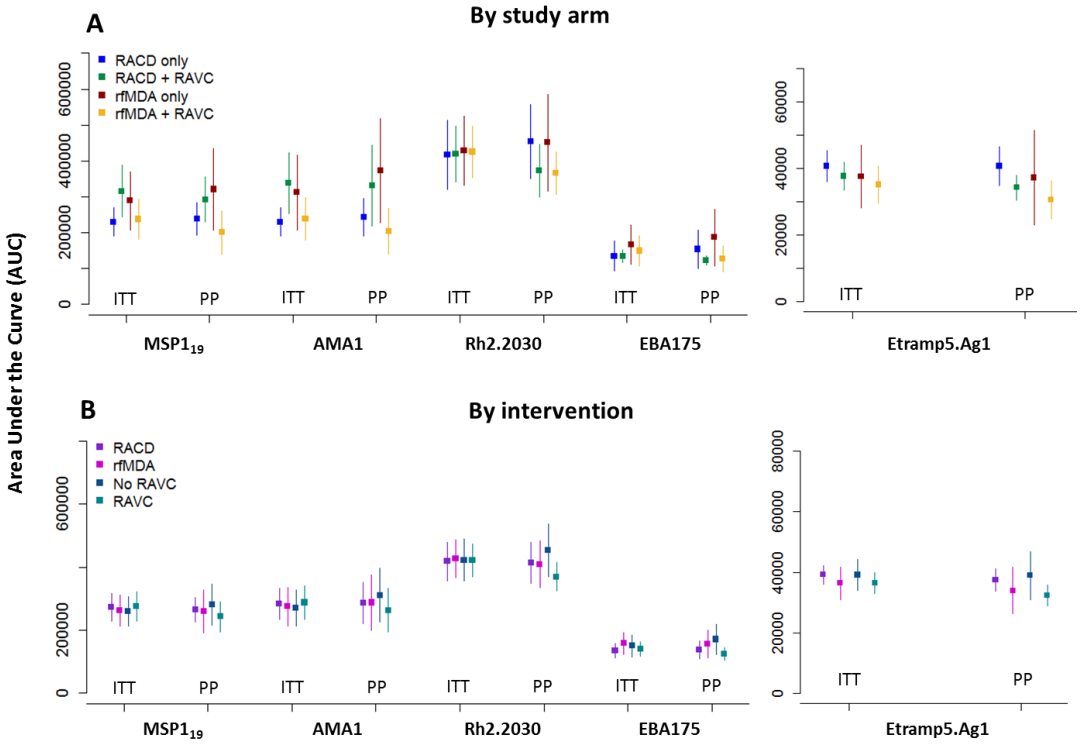

7.4 Discussion

While serological measures have been used widely to monitor medium to long-term trends in malaria transmission, they have almost never been used as endpoints in efficacy trials, which the analysis in this chapter attempts to do using biomarkers of recent malaria infection. Serological results overall are consistent with the primary outcomes of the intervention trial based on clinical and HSRDT endpoints, which also did not show statistical strong evidence for an intervention effect. This may provide some indication that serological endpoints are well correlated with other short-term measures of malaria infection. Potential reasons for why this trial did not show an intervention effect overall are discussed in following sections.

Assessing trial effect with serological endpoints

When assessing differences in antibody responses between study arms, results were varied by antigen and method / unit used to analyse serological endpoints. There was also inconsistency between which intervention (RAVC or rfMDA) was most associated with reduced antibody levels. Overall, analysis to determine if the combination of the interventions had a synergistic effect

were not conclusive, but p-values for the interaction terms were generally large, providing weak statistical evidence for any effects observed.

No differences were observed between study arms in sero-conversion rates or antibody acquisition to $MSP1_{19}$ and AMA1, but slightly lower under-15 sero-prevalence to both antigens in study arms receiving RAVC. However, antibody responses to these antigens reflect high inter-cluster variation, even within study arms. It is unclear if this reflects variation in the study outcomes or in the underlying antibody levels prior to the study. The latter is highly probable given that these antigens are associated with longer-lived antibody responses.

On the other hand, antibody responses to Etramp5.Ag1 showed lower odds of sero-positivity, under-15 sero-prevalence, and antibody acquisition for most study arms compared to the reference arms, but whether differences were due to the RAVC intervention (based on sero-prevalence analysis) or the rfMDA intervention (based on antibody acquisition) were not consistent. Antibody responses to Rh2.2030 based on sero-positivity and sero-prevalence suggest an effect of RAVC on reducing transmission, while antibody acquisition to this antigen was not informative. Assessing the combined antibody response to Etramp5.Ag1, Rh2.2030, EBA175 and HSRDT result did not improve the statistical power of the results compared to Etramp5.Ag1 alone, but the magnitude of the differences measured were larger.

Assessing outcomes based on sero-positivity has the advantage of allowing adjustment by individual level covariates, including age and gender, while sero-prevalence does not. Sero-conversion rate has utility as a measure of force of infection, which can be used as a strong proxy for age-dependent transmission risk. However, the reverse catalytic model is only appropriate for antigens where antibody responses are relatively long-lived. The use of antibody acquisition models allows the estimation of population-level and age-adjusted antibody responses. However, the effects between study arms is not easily interpretable in the context of efficacy trials. For both sero-conversion rates and antibody acquisition models, it is important to consider the inter-cluster coefficient of variation (ICC) within each study arm. Another method for assessing differences between study arms is the breadth of antibody response, which could be included in future analyses of this data.

The relationship between serological outcomes and age, geographical or population, parasite prevalence and clinical outcomes

Strong age-dependency in antibody responses was observed for $MSP1_{19}$, AMA1, Rh2.2030, and EBA175, but not for Etramp5.Ag1. This is consistent with the previous results on age-dependent antibody responses in individuals from The Gambia, as well as the known effects of age on immune responses to many of these antigens, previously discussed in Chapters 1 and 5b.

Antibody responses between study arms to Etramp5.Ag1 were most consistent with clinical incidence outcomes, and were even more aligned with clinical outcomes than HSRDT results. Confidence intervals for HSRDT positivity were much larger than those for sero-positivity. Similarly, clinical IRR had large confidence intervals, but it is not possible to assess these in relation to serological markers of recent infection because the units of analysis are not directly comparable. Due to the weak statistical strength of the clinical and HSRDT results, it is difficult to interpret whether the limited differences observed between study arms reflects inadequate sensitivity and specificity of the serological markers or the absence of an intervention effect in the trial overall.

Indeed, a major challenge with using serological endpoints in trials is how to directly translate differences in antibody responses to clinical and/or parasitological outcomes as they are measuring immunological responses to infection rather than infection itself. These correlations will differ depending on the serological markers used. The analysis in Chapter 4 comparing sero-conversion rates to parasite prevalence and clinical incidence are steps in the right direction. However, as illustrated here and in Chapter 6, reverse catalytic models can only be used for antigens eliciting stable and long-lived antibody responses. Therefore, additional research will need to correlate antibody responses to newer short-lived biomarkers to more established trial endpoints.

qPCR results from the cross-sectional end-line survey were not available at the time of this analysis. Therefore, future work will need to correlate serological endpoints with PCR prevalence, as it will likely be a better measure of low-density infections than the HSRDT, which was not found to be significantly more sensitive than conventional RDTs in this study (analysis not shown).

Impact of intervention coverage and duration on trial outcomes

Intervention coverage did not appear to have an effect on HSRDT positivity or antibody responses to $MSP1_{19}$ and AMA1. On the other hand, it did appear to have an impact on antibody responses to Etramp5.Ag1 (sero-positivity, antibody acquisition AUC) and Rh2.2030 (sero-positivity). There may also be some effect of intervention coverage on antibody acquisition to Rh2.2030 and EBA175 in particular study arms (rfMDA + RAVC), but this was not formally tested in this analysis.

The importance of persistent high coverage in community-based interventions has been highlighted in both modelling studies[380–382] and field trials[74,383]. While other factors (such as the choice of chemo-prophylactic drug used and combination with vector control or other interventions), these studies also emphasise the importance of intervention duration. Modelling studies suggest that multiple MDA rounds over at least 2 years are likely to result in the greatest

reduction in parasite prevalence (Figure 7.12). The fact that this trial only had one year of intervention is likely to be a major reason why an effect is difficult to observe according to any endpoint, not just serological ones.

Figure 7.12 Modelling-based estimates of impact of MDA coverage and frequency on reduction in parasite prevalence

Percentage reduction in mean annual all-age PCR prevalence of Plasmodium falciparum in the third year after mass drug administration.[380]

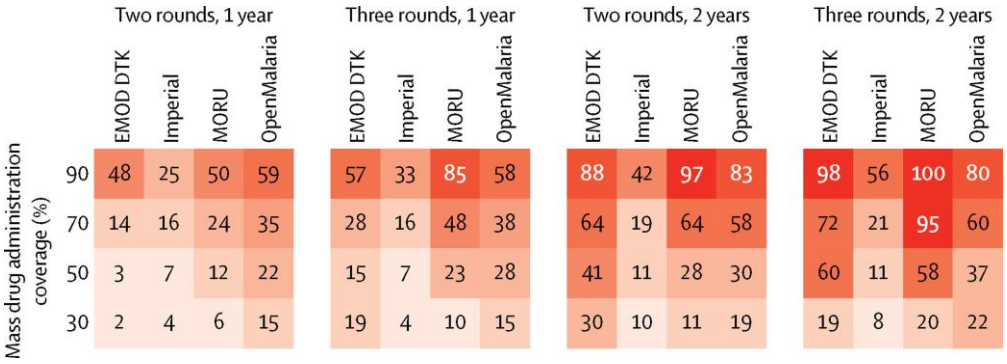

Validating selection of optimal serological biomarkers in Namibia populations

Results from Chapter 6 suggest that Etramp5.Ag1, Rh2.2030, and EBA175 are robust measures of short-term changes in transmission. However, there may be several reasons why these markers are not applicable in the Namibian context. If there are underlying population differences in immune response to these markers, the same endpoints used in Gambia may not be effective in Namibia. While the selection of markers in Chapter 5b was based on longitudinal data from The Gambia, extending this analysis to similar datasets in Namibia will help to validate whether the same markers have similar correlations to previous infection. Data is currently available from a cohort study conducted in the Zambezi region using the same serological markers discussed here, but analysis is not yet complete for inclusion in this chapter.

Spatial clustering and effect of population movement

The impact of spatial clustering of infection and population movement on transmission was not explored in this chapter, but would be useful follow-on analysis. As discussed in Chapter 1, previous research by Smith et al in and near the Zambezi region have made several important observations. A case-control study in Ohangwena and Omusati (north central Namibia) between 2013 and 2014[36] found evidence of spatial clustering of malaria infections around passively detected cases. They found a ten-fold increase the odds of infection (as determined by loop-mediate isothermal amplification (LAMP) methods) within households of index cases from the

health facility and a five-fold increase in odds of infection in the neighbours of index case households compared to randomly selected control households. It also found that the majority of these infections were asymptomatic and at densities below the detection limit of standard RDTs, raising important implications for the success of RACD strategies in these settings.

Health facility data from the same region between 2012 and 2014 also observed excessive risk of malaria in males travelling to Angola (OR 43.58 95%CI 2.12 – 896) with no corresponding risk associated with travel by females.[224] Additionally, individuals living within 15 km of the Angolan border were found to have a nearly three-fold increase in odds of malaria infection, after adjusting for individual and environmental covariates. While these studies were conducted in a region with particularly high cross-border travel to Angola, the study assessed in this chapter is also in a region of travel to Angola (though to a lesser degree), Zambia and Botswana. These countries may represent locations of relatively less malaria compared to Angola, but spatial analysis can help to confirm whether importation is a potential risk.

As discussed in Chapter 1, the spatial distribution of transmission is of particular importance in cluster randomised trials. If there is a large degree of mobility, the risk of contamination between study arms may be high, leading to a reduction in the ability to measure intervention effects accurately. Several study designs have been proposed that can account for these factors (Figure 7.13), in the context of a hypothetical transmission-blocking vaccine (TBV) CRT. Some suggest the inclusion of buffer zones (e.g., “fried egg” design) around a sentinel population that is monitored to measure the intervention effect. More complex is a gradient design with a buffer zone that allows measurement in a central sentinel group for intervention effect as well as individuals in the buffer zone to assess the intervention effect at the edges of the cluster that may be impacted by contamination.

Figure 7.13 Study designs accounting for spill-over and contamination in cluster randomised trials

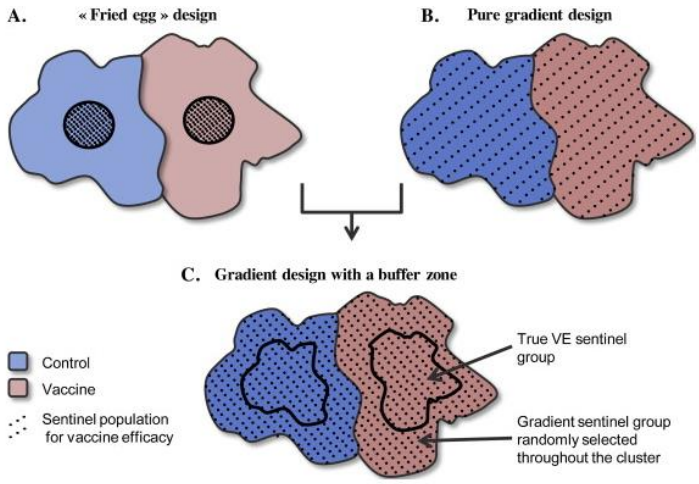

Study design and sample size for serological endpoints in cluster randomised trials

It was observed in Chapter 6 that the sensitivity of these markers were slightly diminished in lower transmission settings in The Gambia. If differences in this trial are too small, than serological markers may still not be sensitive enough to detect differences. This raises considerations with regard to designing cluster trials with serological endpoints in mind. The ability to power a study based on these endpoints will need to use a sampling frame with sufficient cluster size and age distribution in order to fit antibody acquisition (or sero-conversion rates) with precision.

As reflected in the large variation in sero-conversion rates, future study designs based on serological endpoints may need to account for baseline population immune responses. Antibody responses to $MSP1_{19}$ and AMA1 may have several uses. First, they could be used for baseline stratification of study clusters, whereas trial outcomes could be measured with serological markers more associated with recent infection, such as Etramp5.Ag1. This would have the effect of reducing the between-cluster variation within a strata and the design effect, potentially improving study power and precision[77].

There is still the possibility that $MSP1_{19}$ or AMA1 could be used as endpoints if baseline levels are taken into account, or if restricted to particular age groups. Results in this chapter suggest that $MSP1_{19}$ may have the potential be detect some short-term changes in transmission relatively better than AMA1.

To determine optimal sampling frames for trials in the future, a simulation study can be designed that estimates sample size and age distribution requirements, by addressing the following:

- Precision in cluster-level antibody acquisition or sero-conversion rate estimates
- Number of clusters to detect a minimum intervention effect size
- Improving balance between study arms by accounting for antibody levels in restricted randomisation
- Comparison of sample sizes based on different CRT designs (can include two-arm or 2x2 factorial design if there are more than two interventions)
- Impact of intervention coverage or mobility / contamination between clusters

Sample size requirements to estimate precise sero-conversion rates have previously been explored by Sepulveda et al[249] and similar methods should be extended to antibody acquisition models.

The frequency of sampling may also vary depending on the kinetics of the serological marker used and consideration of whether serological endpoints are robust enough to determine

intervention efficacy based on repeated cross-sectional samples (and how many) or if cohort or longitudinal data is needed. A proposed sampling strategy for a hypothetical transmission blocking vaccine (TBV) trial is illustrated in Figure 7.14, where serological endpoints are collected in addition to parasitological endpoints such as PCR and microscopy. This raises factors to consider in future trials with the serological biomarkers assessed in this chapter, such as the frequency of sampling depending on the longevity of antibodies, the serological unit that will be used for evaluation (odds of sero-positivity, sero-prevalence, change magnitude of antibody levels), and whether serological endpoints will only be measures in certain sentinel populations (e.g., children vs. adults).

Overall, there are numerous studies being implemented or planned assessing the impact of community-based interventions to reduce transmission in elimination and pre-elimination settings. Serological endpoints could potentially be considered in any of these studies, which would be useful for correlating with other trial endpoints across various transmission settings. These are discussed in more detail in Chapter 8.

Figure 7.14 Proposed sampling frame for a cluster randomised trial measuring the impact of a transmission reducing intervention (transmission block vaccine) using multiple endpoints

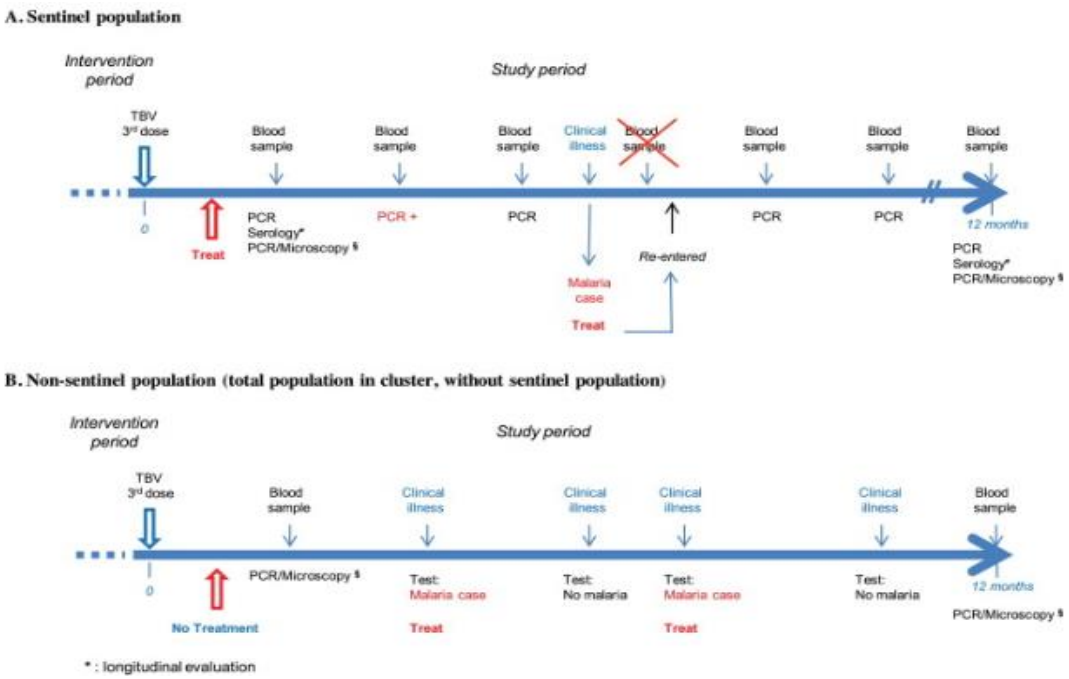

Appendix 7

FIGURE 7.15 EXAMPLE OF SERO-CONVERSION RATES FIT INDEPENDENTLY FOR EACH CLUSTER

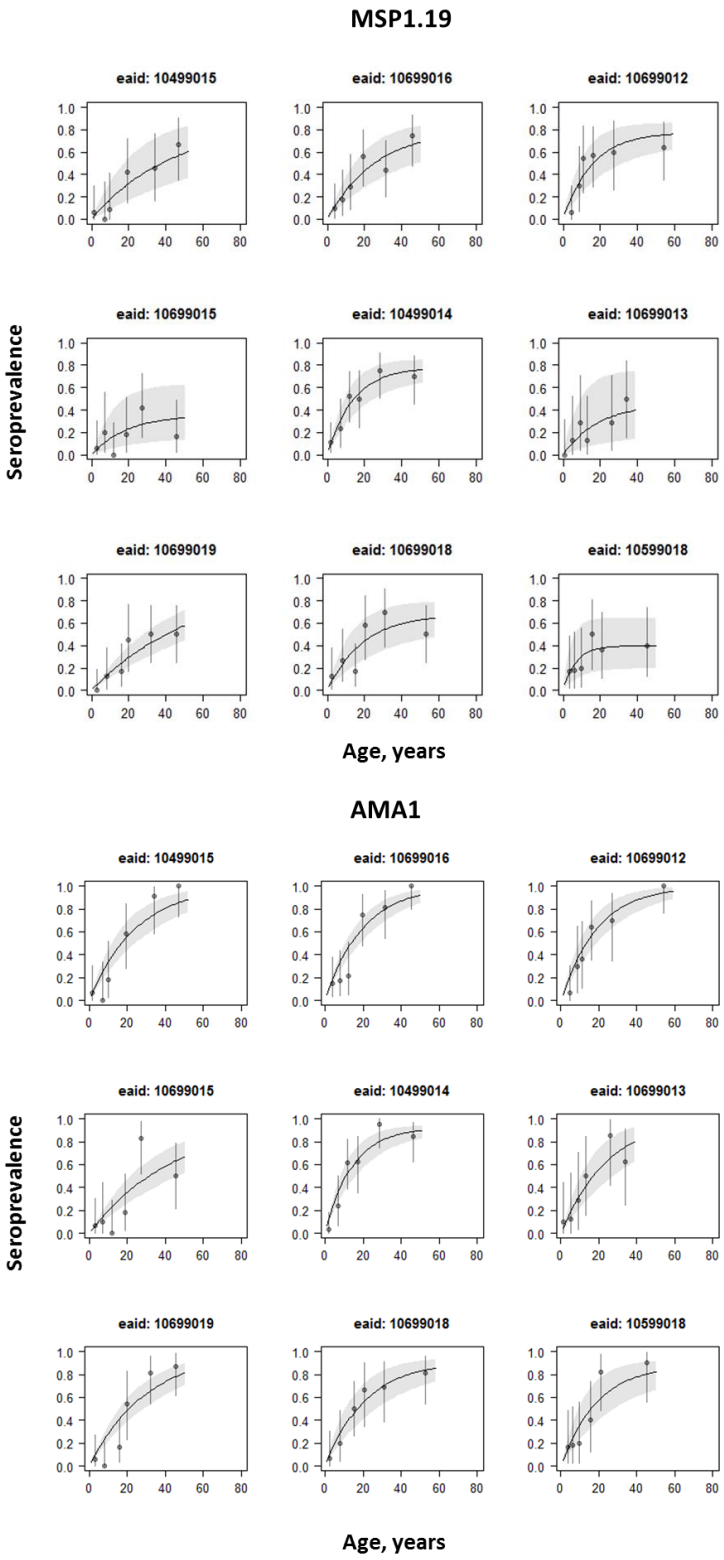

FIGURE 7.16 EXAMPLE OF ANTIBODY ACQUISITION MODELS FIT INDEPENDENTLY FOR EACH CLUSTER

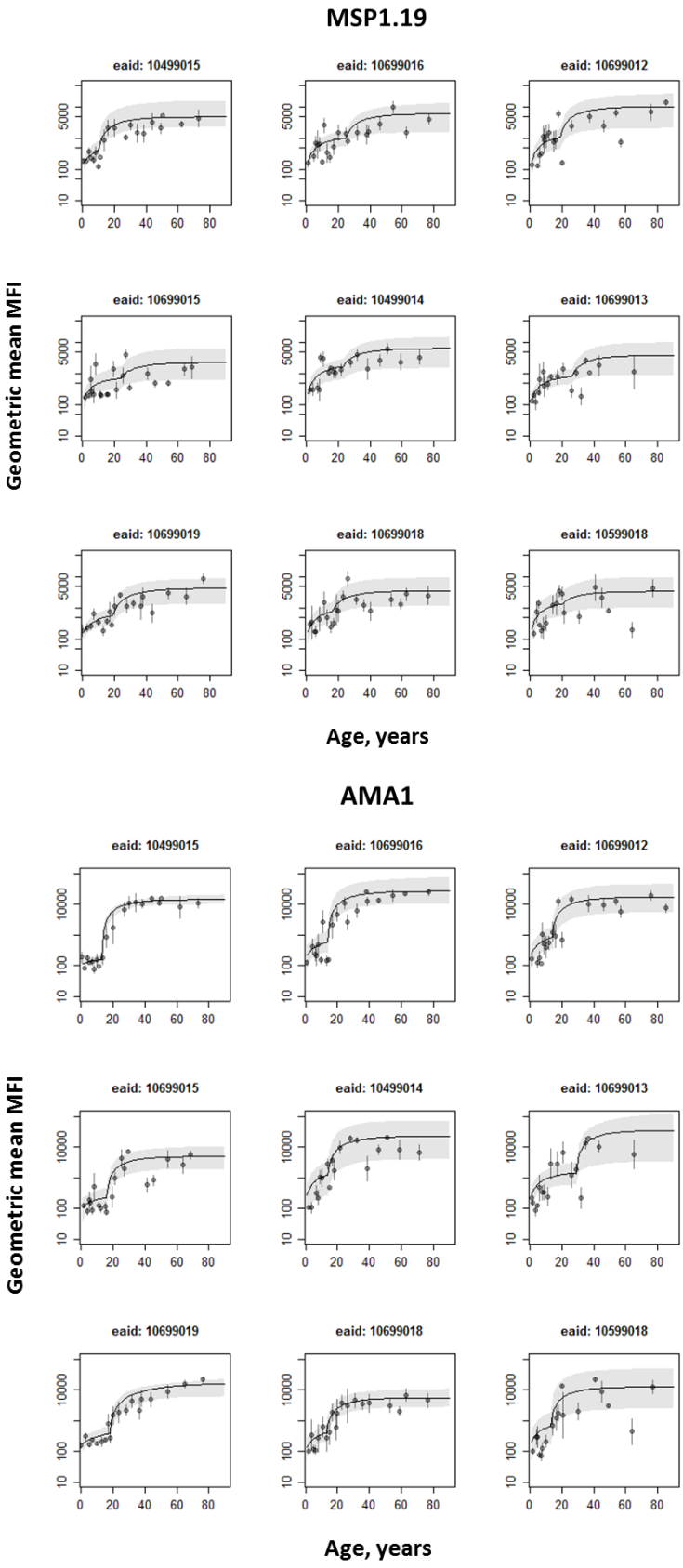

Etramp5.Ag1

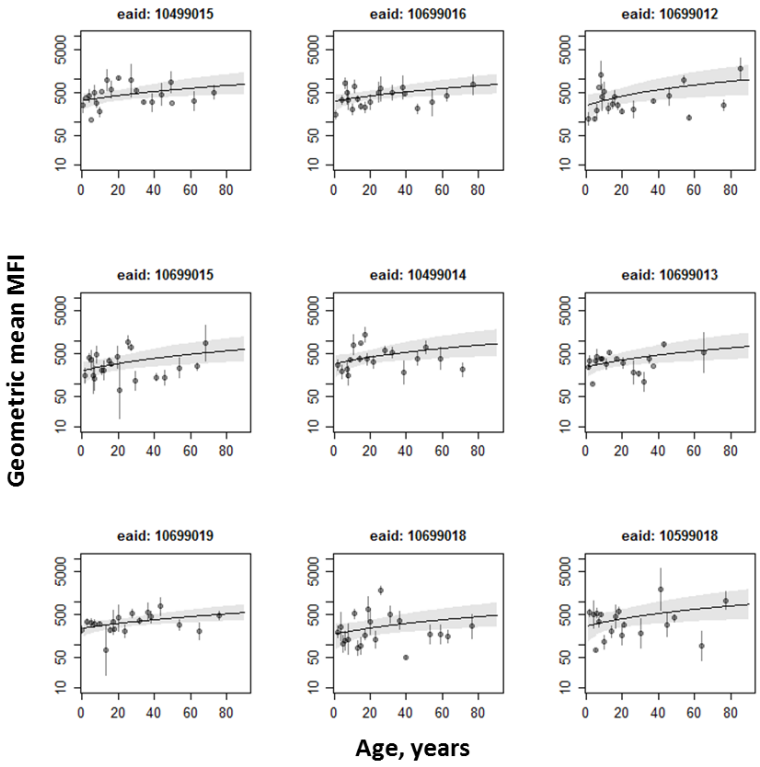

Rh2.2030

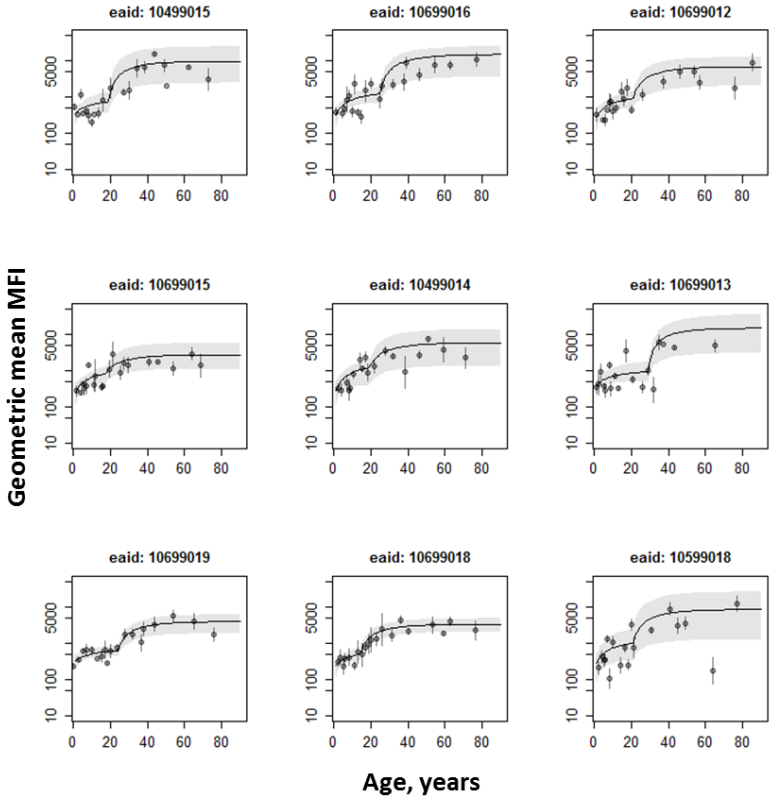

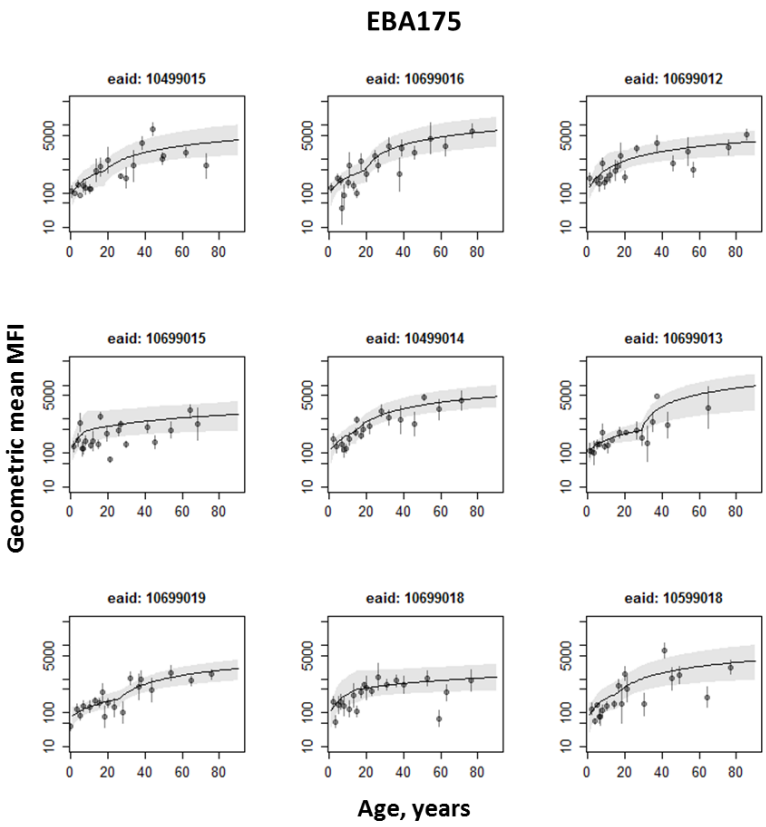
EBA175
eaid: 10499015
eaid: 10699016
eaid: 10699012
eaid: 10699015
eaid: 10499014
eaid: 10699013
eaid: 10699019
eaid: 10699018
eaid: 10599018
Geometric mean MFI
10
100
5000
0
20
40
60
80
Age, years

FIGURE 7.17 ANTIBODY ACQUISITION MODELS FIT BY STUDY ARM WITH CLUSTER-LEVEL RANDOM EFFECTS

MSP1$_{19}$ Ab acquisition by study arm. Study arms are RACD only = blue (top left), RACD + RAVC = green (top right), rfMDA only = red (bottom left), and rfMDA + RAVC = yellow (bottom right). Filled circles are EA-specific mean MFI for clusters with >75% intervention coverage and empty circles for clusters with <75% coverage. Vertical dashes indicate the 95% confidence interval of the age-adjusted mean MFI by EA. Shaded areas and solid lines show the 95% credible interval and mean of the Ab acquisition model fit overall with cluster-level random effects; dotted line is mean of model fit adjusted for intervention coverage.

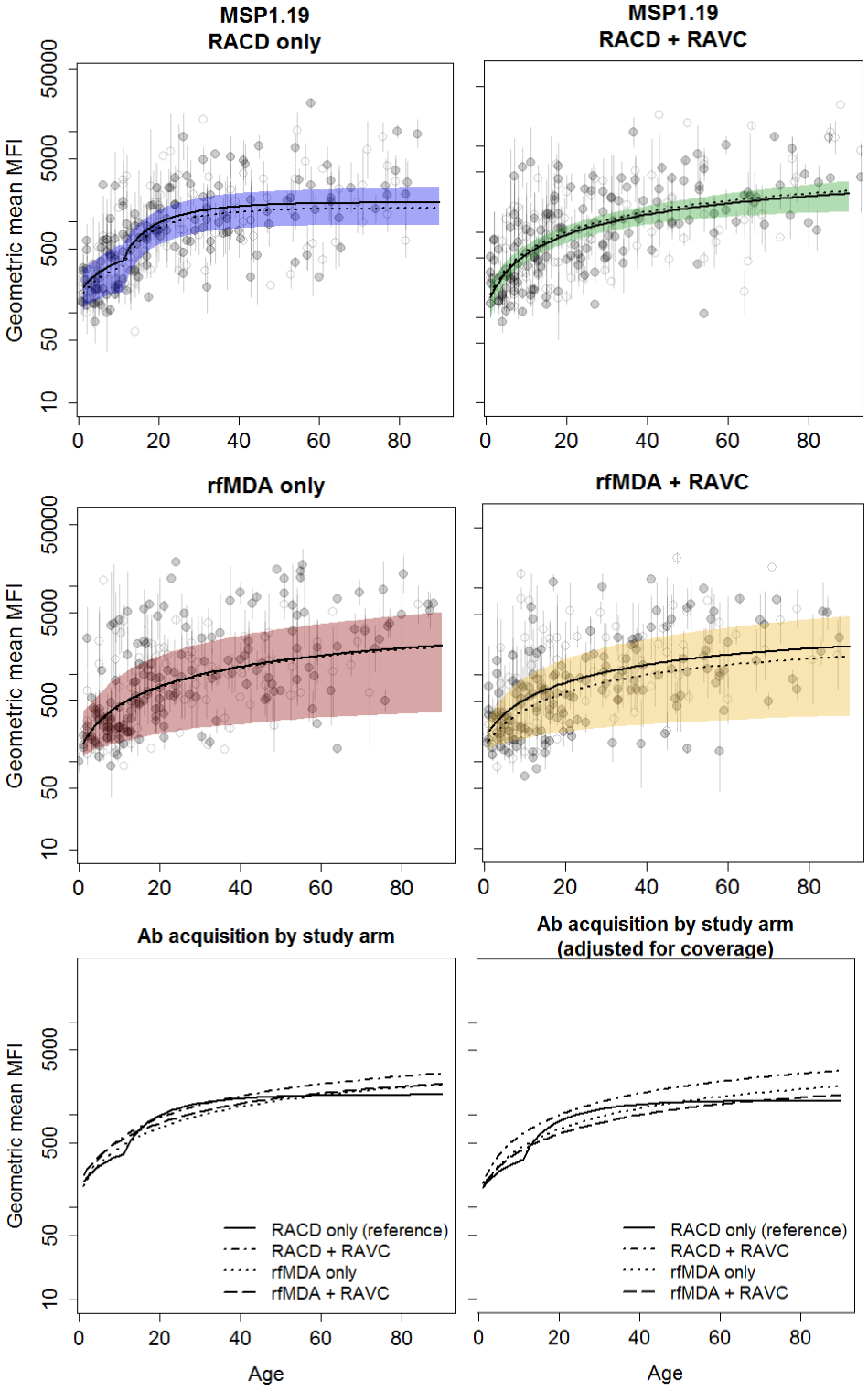

AMA1 Ab acquisition by study arm

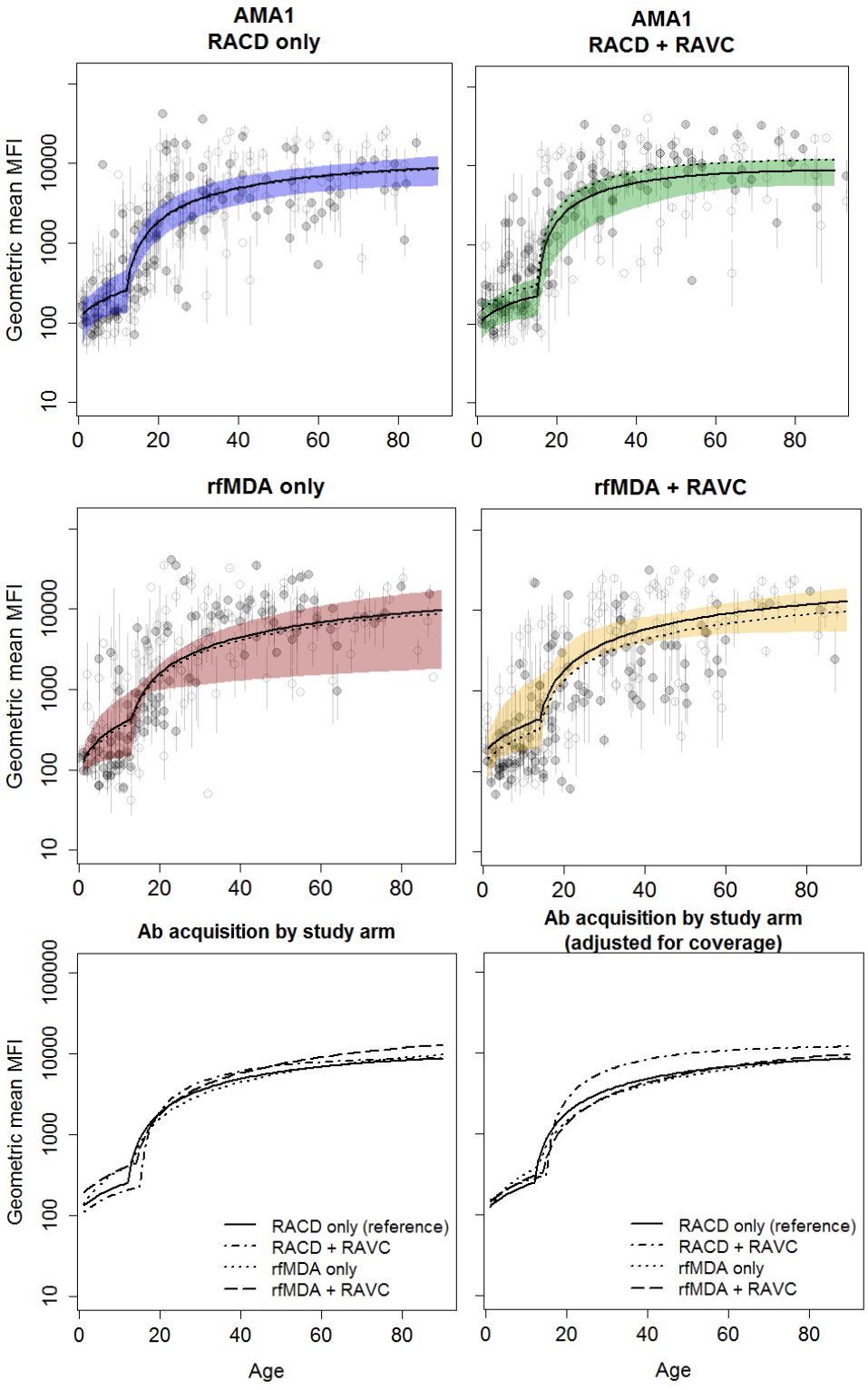

Etramp5.Ag1 Ab acquisition by study arm

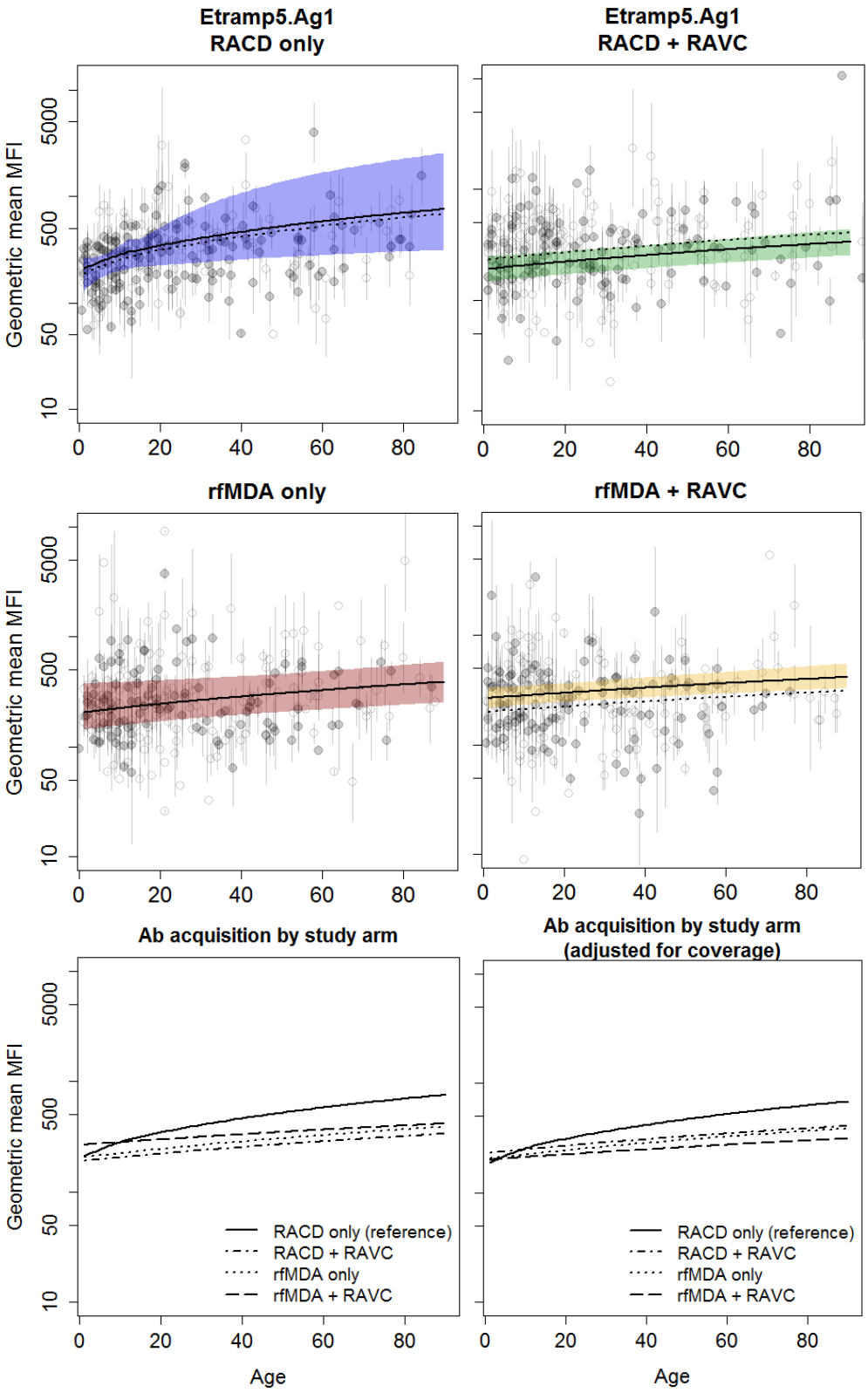

Rh2.2030 Ab acquisition by study arm

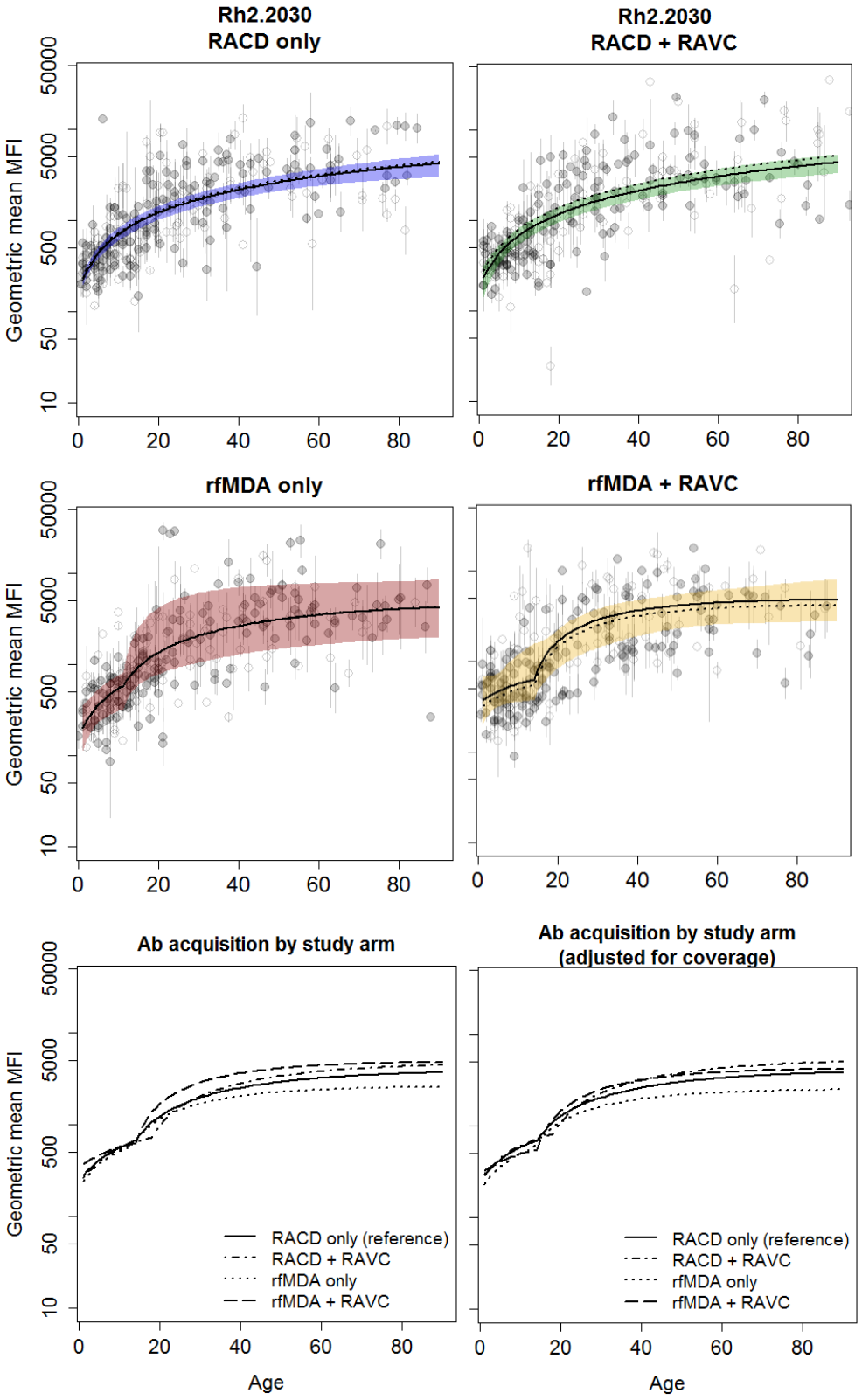

EBA175 Ab acquisition by study arm

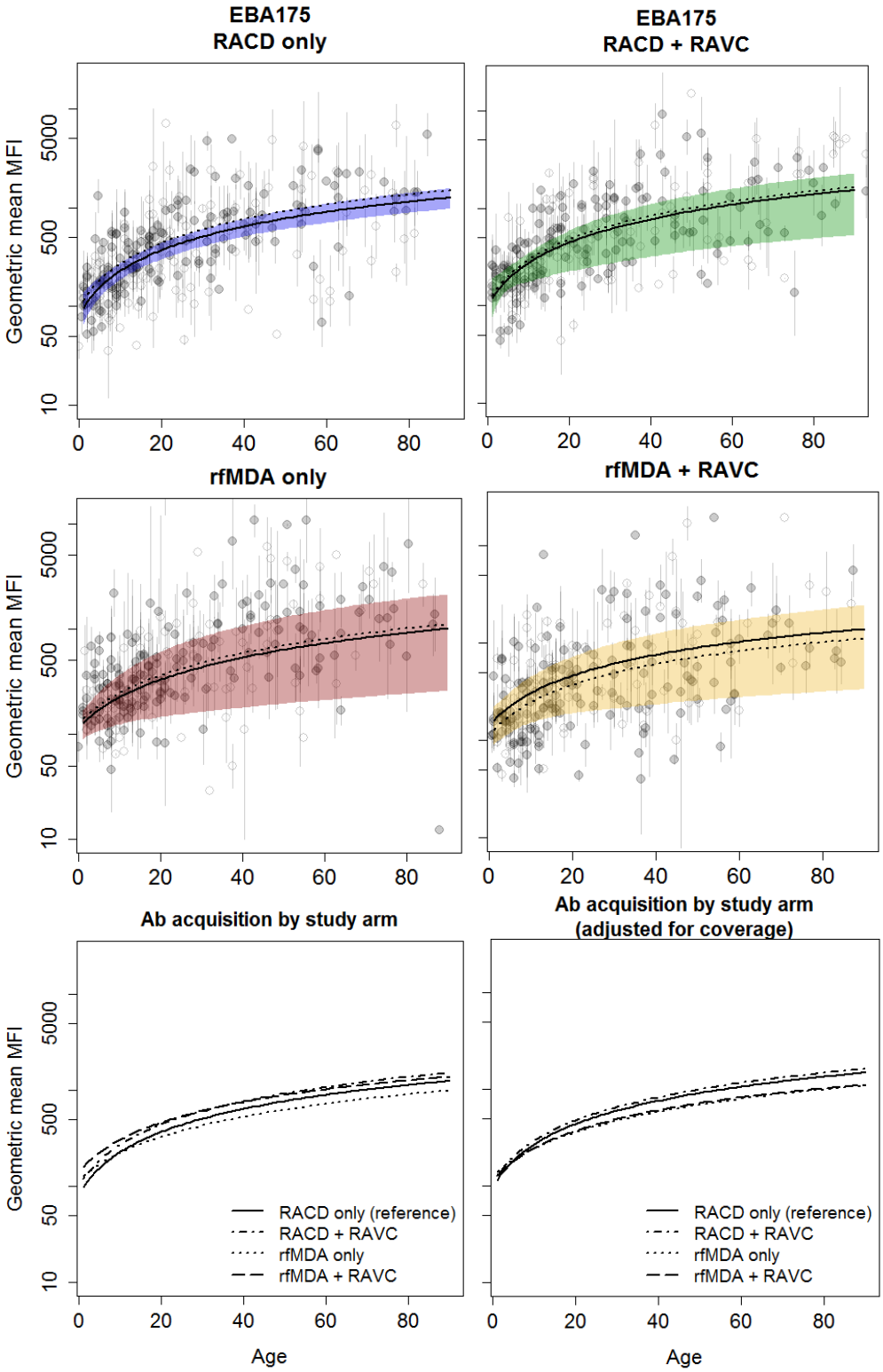

Chapter 8 Discussion

The research presented in this thesis has sought to address current challenges facing the standardised and accurate measurement of malaria infection in low transmission settings, particularly in the context of cluster-level surveillance and efficacy trials. The relative sensitivity of RDTs and microscopy compared to PCR for measuring population parasite prevalence globally has been quantified and found to vary by age and transmission intensity (Chapter 3). The relationship of these parasitological endpoints with commonly used sero-epidemiological markers - $MSP1_{19}$ and AMA1 - has also been characterised across a large range of cross-sectional studies and transmission intensities (Chapter 4), investigating the potential utility of malaria serology at the macro-scale for the first time.

In Chapter 5, the use of a much larger panel of *P.falciparum* serological markers was explored. The association of *Pf*-specific Ab responses with recent malaria infection was estimated and identified several antigens highly predictive of infection in the previous six months. These findings suggest that a number of new serological markers could provide estimates of time since last infection in future diagnostic assays. The use of these markers to monitor changes in malaria transmission at the cluster-level was applied to disease surveillance in The Gambia in Chapter 6 and to cluster randomised trials in Namibia in Chapter 7 and were found to align overall with other measures of malaria infection and transmission. However, results differed by antigen, age, and transmission intensity and suggest the need for further research. Overall, the findings in this thesis contribute to the evidence base that serology has the potential to be used not only to quantify historical trends in malaria transmission, but as a standardised measure of short-term changes in infection in routine surveillance or in efficacy trials.

This chapter discusses implications for current malaria control and elimination efforts as well as potential areas for further research. The application of serological measures of malaria can be thought of in several stages. First, do serological measures offer added value (i.e., sensitivity / specificity) over existing measures of infection at the individual or population level and in which contexts (Chapter 3-5)? Second, as addressed in Chapters 6 and 7, what are the use-case scenarios in which serological metrics should be applied and how can they be standardised for routine use across a range of epidemiological settings. A more challenging question, beyond the scope of the research in this thesis, is what the public health impact of serological measures of transmission may be when deployed in control and elimination strategies.

8.1 Implications in the context of current malaria control and elimination

Standardising sero-diagnostics for routine use in surveillance cluster randomised trials

While the analysis in Chapters 5-7 of novel serological biomarkers for monitoring malaria infection suggest that several antigens could be used in surveillance and cluster randomised trials, the details of how they will be integrated into diagnostic platforms and the interpretation of what they indicate about transmission need to be refined. What has not been explored at length in this thesis is the potential for markers to differentiate between recent infection (Etramp5.Ag1, GexP18) vs. historical transmission or population-level of protective immunity ($MSP1_{19}$, AMA1), the latter of which could have strong application in monitoring risk of reintroduction (e.g., loss of population protective immunity) after local elimination.

A range of factors influencing the suitability and application of serological markers based on their relative characteristics are illustrated in Figures 8.1 and 8.2.

Figure 8.1 Classes of suitability of serological markers for surveillance and cluster randomised trials

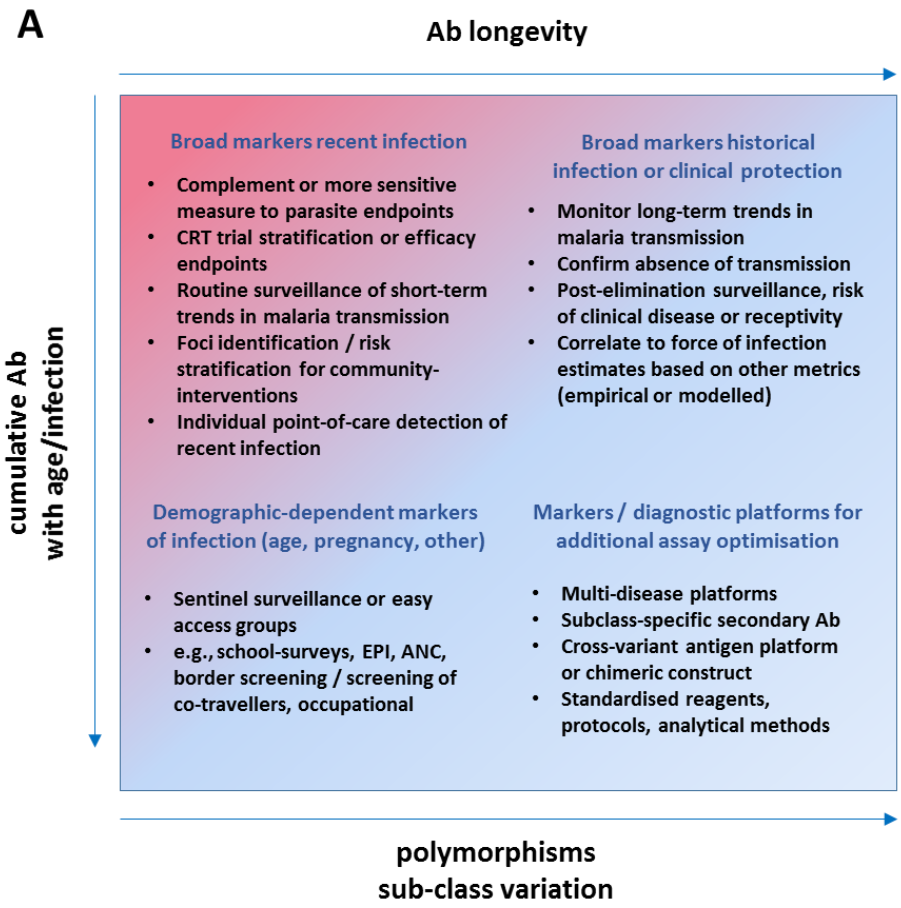

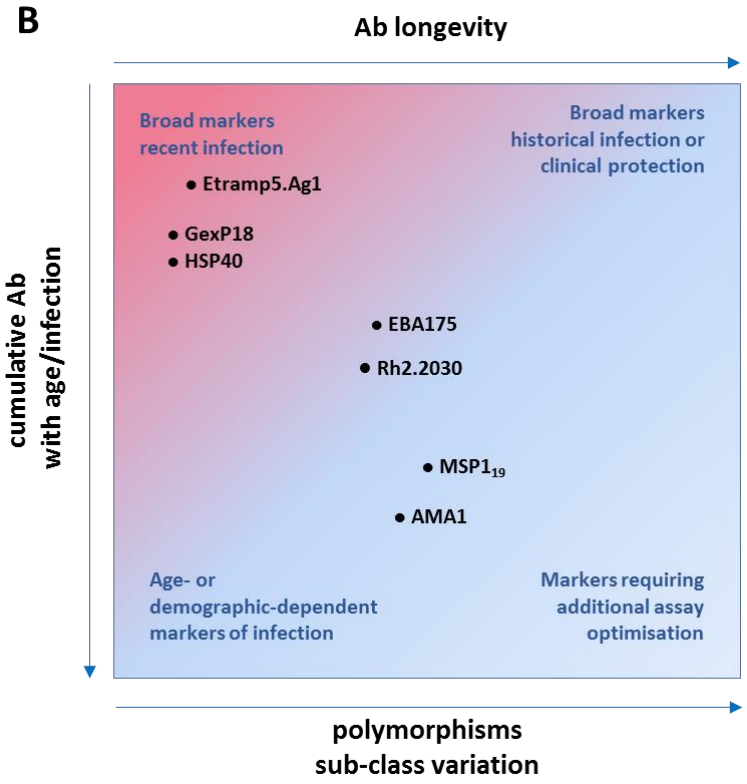
B
Ab longevity
cumulative Ab with age/infection
Broad markers recent infection
Broad markers historical infection or clinical protection
Etramp5.Ag1
GexP18
HSP40
EBA175
Rh2.2030
MSP1$_{19}$
AMA1
Age- or demographic-dependent markers of infection
Markers requiring additional assay optimisation
polymorphisms sub-class variation

Figure 8.2 Factors influencing the suitability of serological markers for surveillance and cluster randomised trials

Antigen	Immunogenicity	Ab longevity	Cumulative Ab response with age / infection	Variation in IgG sub-class response	Polymorphisms	Use scenario
$MSP1_{19}$						• Monitor loss of clinical immunity • Marker of recent infection in children
AMA1						• Monitor loss of clinical immunity
Etramp5.Ag1				?	?	• Marker of recent infection
Rh2.2030						• Marker of recent infection , may require sentinel age population • Potential sub-class variation requires further assay optimisation
EBA175						• Marker of recent infection , may require sentinel age population • Potential sub-class variation requires further assay optimisation
GexP18				?	?	• Marker of recent infection Low immunogenicity, may require combination with other markers
HSP40				?	?	• Marker of recent infection Low immunogenicity, may require combination with other markers

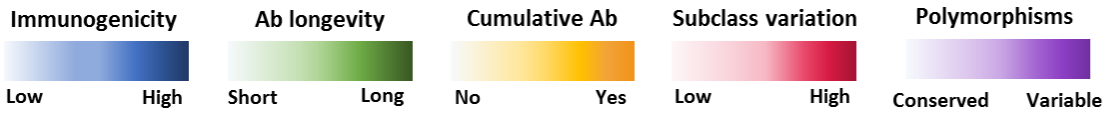

Use in current and future community-based interventions

As discussed in Chapter 7, the use of serological endpoints may have utility in a number of future trials assessing community-based interventions, including ivermectin, primaquine, and transmission-blocking vaccines. They could also serve as a secondary endpoints to measure herd effects in individually randomised trials for pre-erythrocytic or blood stage vaccines. Additionally, as opposed to a use as a specific trial endpoint, serology may have very strong application for baseline stratification to balance clusters between trial study arms or for risk stratification in elimination strategies (i.e., identification of transmission foci to be targeted for response).

For example, in eastern Myanmar, targeted MDA efforts have used cross-sectional surveys to estimate village level prevalence of *P.falciparum* and *P.vivax* by RDT, microscopy, and qPCR. This data was used to classify villages as malaria hotspots above a 40% prevalence threshold and targeted for MDA[384,385]. The use of ultra-sensitive qPCR as the most sensitive measure of prevalence in these studies faces blood volume and technical constraints. Here, the introduction of serological methods of detection could serve as a more rapid and cost-effective alternative. Responses could potentially be triggered based on a threshold of sero-prevalence or antibody intensity at the cluster level if well validated biomarkers for a suitable window of recent infection can be defined. For example, in the central highlands of Madagascar, school-based serological surveys were used as a reference for malaria incidence as part of a focal IRS strategy based on health facility-based cases.[386]

For surveillance, the most immediate application of serology is to monitor longitudinal changes in transmission before and after the scale-up of interventions, as illustrated by IFA antibody titre data from the Garki Project.[109] However, the use of serological surveillance has been largely confined to research settings. In order to integrate its use into routine monitoring programmes, it will be necessary to consider where along the continuum of transmission it will be most useful, from activities to achieve elimination to confirming the absence of transmission. The WHO reference manual on malaria surveillance, monitoring and evaluation highlights the granularity and frequency of data required as countries progress towards elimination (Figure 8.3).[60] As discussed above, the serological markers used may potentially vary depending on the application, as indicated by these surveillance guidelines, and the ideal populations and frequency for sampling will need to be determined. Alternatively, a combined panel of markers optimised across multiple use-case scenarios could be considered. In parallel, strong analytical methods need to be developed, depending on the marker and unit being used. Chapters 6 and 7 highlight the analytical challenges introduced by new serological markers of recent infection, but also develops potential quantitative methods for their use in efficacy trials.

Figure 8.3 Surveillance system processes and requirements along the continuum of malaria transmission settings

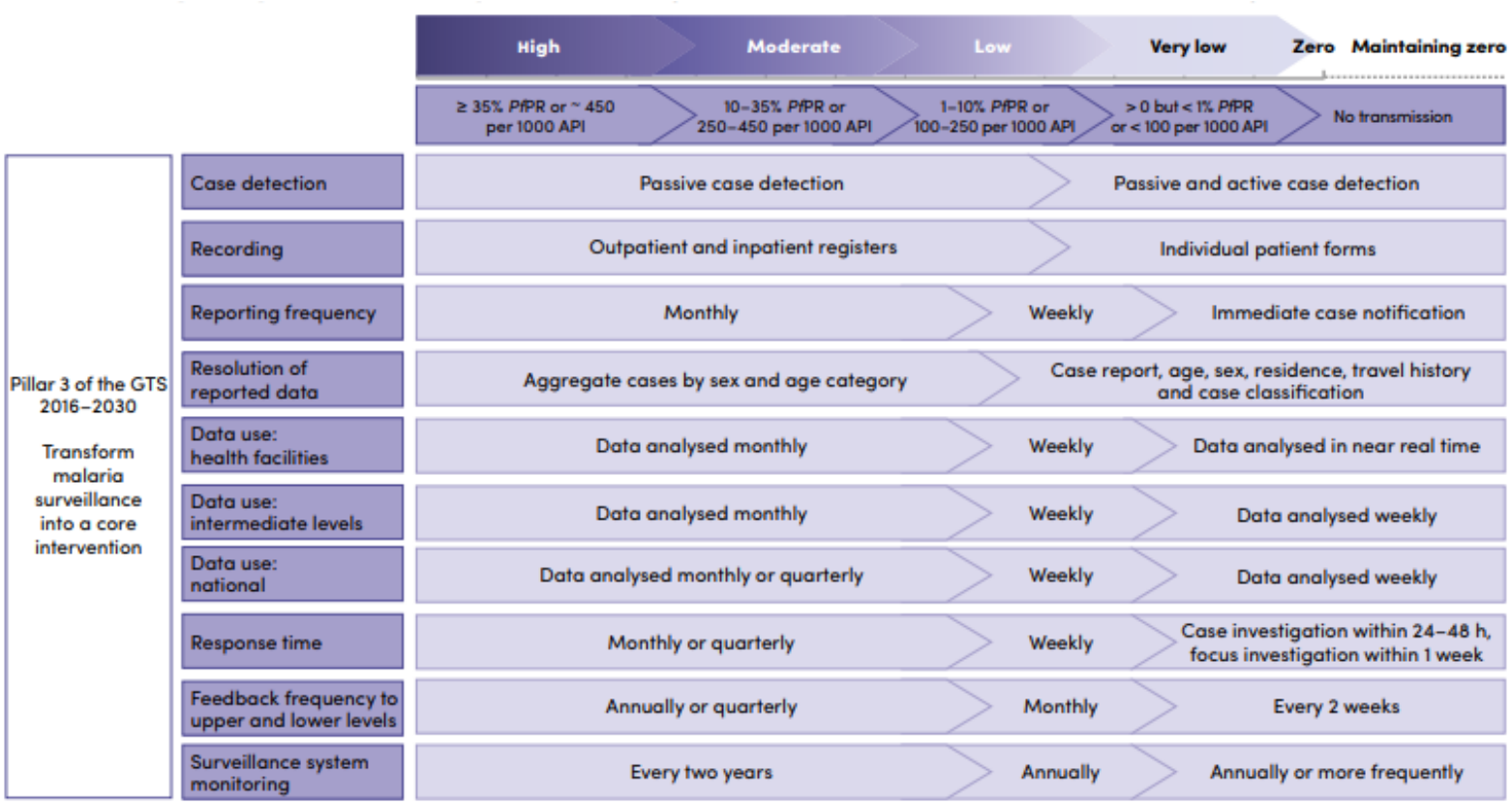

GTS, *Global technical strategy for malaria 2016–2030*; PR, parasite rate; API, annual parasite incidence
Active case detection includes both reactive case detection (RACD) triggered by an index case and proactive case detection (PACD) (see **section 3.2**).

8.2 Applications for future work

Solutions for in-country analysis of immuno-epidemiological malaria data

In Chapter 5, a number of methods were explored for the standardisation and epidemiological analysis of serological data based on new multiplex immunoassays. The initial work here would be most useful if they can be translated into user-friendly platforms for laboratories in country. In particular, the development of cloud-based solutions could enable twinning of data sharing and analysis in regions with mid-level infrastructure.

Similar platforms have been developed for analysis of both clinical and epidemiological surveillance data. For example, Epi Info developed by the US Centers for Disease and Control provided tablet/smart phone or web/cloud-based solutions for data collection, analysis and visualisation. These platforms have been used for outbreak investigation and small- to mid-sized disease surveillance systems[387]. ClinEpiDB is a similar data access and visualisation platform for epidemiological studies.[388]

Cloud-based analytics in genomics represent a more advanced example of potential platforms. These have built open source and web-based applications for users without programming or informatics knowledge to download tools and/or upload and analyse their own data[389]. With relatively smaller datasets and a more focused set of analytical requirements, these platforms could easily be adapted for Luminex serological data.

Multi-disease diagnostic platforms for surveillance and outbreak response

Multiplexing platforms, such as the Luminex or other qSAT platforms, provide an opportunity to collect data on a large number of diseases using a single serum sample or dried blood spot.[243,291] Several studies have begun to investigate the use of this platform for the combined detection of malaria and other pathogens.[108,390] This will become increasingly important in areas where malaria transmission declines to near zero levels and it is no longer cost-effective to conduct malaria-specific surveys or surveillance platforms for identifying asymptomatic cases or resolving non-malaria febrile illnesses.

The benefits of multi-disease platforms has been raised particularly in neglected tropical diseases, where cross-disease surveillance has been suggested for simultaneous mapping of human and zoonotic infections, guiding and monitoring control interventions, assessing vaccine coverage, and post-MDA surveillance.[106]

Another potential application of multi-disease diagnostic platforms is for surveillance during outbreak response. While the 2014-2015 West African Ebola outbreak is estimated to have caused over 11,000 deaths[391], declines in health facility attendance and disruptions in community-based malaria control programmes are also estimated to have caused up to an 88% increase in untreated malaria cases in Sierra Leone alone.[392,393] Increases in individuals presenting with fever-like symptoms led to further complications in the identification and treatment of suspected Ebola cases (33-54% of patients admitted to treatment units during the outbreak did not have Ebola virus disease[394]). These challenges emphasise the need for malaria and other infectious disease control efforts to be sustained or heightened during epidemics as well as the importance of differential diagnosis amongst febrile illnesses.

The WHO Guidance on temporary malaria control measures in Ebola-affected countries recommends community chemotherapy through MDA in areas of high malaria transmission and low treatment access.[395] However, when faced with financial and logistical constraints during outbreak response, achieving adequate intervention coverage can be challenging. Targeting interventions where they will be most cost-effective requires sensitive field diagnostics and accurate epidemiological data on the demographic or geographical locations most susceptible to outbreaks.[244] Additionally, in situations where the co-circulation of multiple infectious pathogens is high, malaria can also serve as a pathfinder or sentinel sample through which to screen for other diseases of public health importance.

The eventual development of a field-deployable multi-disease diagnostic platform could provide Ministries of Health with information on the distribution and prevalence of multiple infectious diseases can help to inform future geographical reconnaissance for targeted infectious disease control efforts in resource-limited scenarios, such as the roll-out of focal mass drug administration, indoor residual spraying or other interventions. A multiplexed diagnostic platform would minimise the number of tests and volume of blood required for testing, enabling efficient and rapid assessment in these outbreak scenarios.

8.3 Conclusions

The research presented in these thesis has aimed to develop new methods for measuring malaria transmission in elimination settings. It has shown that in numerous contexts, serological measures of transmission may have utility above currently used diagnostics, particularly in low transmission settings. Additionally, it has established the use of an in-country multiplex immunoassay for malaria in a sub-Saharan African setting, which has helped to build the platform for future operational and analytical solutions for routine or high throughput sample processing

and epidemiological analysis. It has also found that a number of new candidate serological markers have the potential to improve the measurement of recent malaria infection at both the individual and population level. More importantly, the application of these new markers can be used at the cluster or village level to monitor changes in transmission, which correlate with known differences in malaria prevalence between transmission seasons and geographical regions. For the first time, serological endpoints have been used to assess the effectiveness of community-based interventions between study arms of a cluster randomised trial. The methodologies developed here provide a strong foundation for the use of serological metrics as trial endpoints, risk stratification or routine surveillance that can interpreted in a manner that is similar to currently used clinical or parasitological metrics, allowing for easier comparability across studies and endpoints. While a number of methodological issues still require refinement, serology shows strong promise as an additional tool in our current efforts to achieve malaria elimination globally.

References

1. Doolan, D. L., Dobaño, C. & Baird, J. K. Acquired immunity to malaria. *Clin. Microbiol. Rev.* **22,** 13–36 (2009).

2. Mu, J. *et al.* Chromosome-wide SNPs reveal an ancient origin for Plasmodium falciparum. *Nature* **418,** 323–6 (2002).

3. Roberts, L. & Enserink, M. Malaria. Did they really say ... eradication? *Science* **318,** 1544–5 (2007).

4. WHO Global Malaria Programme. *A framework for malaria elimination*. (World Health Organization, 2017).

5. Tatem, A. J. *et al.* Ranking of elimination feasibility between malaria-endemic countries. *Lancet (London, England)* **376,** 1579–91 (2010).

6. Malaria Indicator Surveys. Available at: http://www.malariasurveys.org/. (Accessed: 1st November 2017)

7. Reiner, R. C., Geary, M., Atkinson, P. M., Smith, D. L. & Gething, P. W. Seasonality of Plasmodium falciparum transmission: a systematic review. *Malar. J.* **14,** 343 (2015).

8. Carneiro, I. *et al.* Age-Patterns of Malaria Vary with Severity, Transmission Intensity and Seasonality in Sub-Saharan Africa: A Systematic Review and Pooled Analysis. *PLoS One* **5,** e8988 (2010).

9. Roca-Feltrer, A. *et al.* The age patterns of severe malaria syndromes in sub-Saharan Africa across a range of transmission intensities and seasonality settings. *Malar. J.* **9,** 282 (2010).

10. Blanford, J. I. *et al.* Implications of temperature variation for malaria parasite development across Africa. *Sci. Rep.* **3,** 1300 (2013).

11. Smith, D. L. *et al.* A sticky situation: the unexpected stability of malaria elimination. *Philos. Trans. R. Soc. Lond. B. Biol. Sci.* **368,** 20120145 (2013).

12. Rabinovich, R. N. *et al.* malERA: An updated research agenda for malaria elimination and eradication. *PLOS Med.* **14,** e1002456 (2017).

13. Pampana, E. *A textbook of malaria eradication*. *2nd edition* (London: Oxford University Press., 1969).

14. Livadas, G. W. E. C. on M. *Is it necessary to continue indefinitely DDT residual spraying programmes: : relevant observations made in Greece*. (1952).

15. Smith, D. L. *et al.* Ross, Macdonald, and a Theory for the Dynamics and Control of Mosquito-Transmitted Pathogens. *PLoS Pathog.* **8,** e1002588 (2012).

16. MacDonald, G. Epidemiological basis of malaria control. *Bull. World Health Organ.* **15,** 613–26 (1956).

17. Nájera, J. A., González-Silva, M. & Alonso, P. L. Some Lessons for the Future from the Global Malaria Eradication Programme (1955–1969). *PLoS Med.* **8,** e1000412 (2011).

18. Hay, S. I., Guerra, C. A., Tatem, A. J., Noor, A. M. & Snow, R. W. The global distribution and population at risk of malaria: past, present, and future. *Lancet Infect. Dis.* **4,** 327–336 (2004).

19. World Health Organization (WHO). *Re-examination of the global strategy of malaria eradication, World Health Assembly 22.* (1969).

20. World Health Organization (WHO). *Malaria. Handbook of resolutions and decisions of the World Health Assembly and the Executive Board. Volume I, 1948–1972, 1st to 25th WHA and 1st to 50th EB.* (1973).

21. Bhatt, S. *et al.* The effect of malaria control on Plasmodium falciparum in Africa between 2000 and 2015. *Nature* **526,** 207–211 (2015).

22. Killeen, G. F. *et al.* Developing an expanded vector control toolbox for malaria elimination. *BMJ Glob. Heal.* **2,** e000211 (2017).

23. Smit, M. R. *et al.* Safety and mosquitocidal efficacy of high-dose ivermectin when co-administered with dihydroartemisinin-piperaquine in Kenyan adults with uncomplicated malaria (IVERMAL): a randomised, double-blind, placebo-controlled trial. *Lancet. Infect. Dis.* **18,** 615–626 (2018).

24. Kobylinski, K. C. *et al.* Ivermectin susceptibility and sporontocidal effect in Greater Mekong Subregion Anopheles. *Malar. J.* **16,** 280 (2017).

25. Cook, J. *et al.* Mass screening and treatment using a falciparum-specific rapid diagnostic test did not reduce malaria incidence in Zanzibar. *J. Infect. Dis.* (2014). doi:10.1093/infdis/jiu655

26. Tiono, A. B. *et al.* Lessons learned from the use of HRP-2 based rapid diagnostic test in community-wide screening and treatment of asymptomatic carriers of Plasmodium falciparum in Burkina Faso. *Malar. J.* **13,** 30 (2014).

27. Hemingway, J. *et al.* Tools and Strategies for Malaria Control and Elimination: What Do We Need to Achieve a Grand Convergence in Malaria? *PLOS Biol.* **14,** e1002380 (2016).

28. Dicko, A. *et al.* Intermittent Preventive Treatment of Malaria Provides Substantial Protection against Malaria in Children Already Protected by an Insecticide-Treated Bednet in Mali: A Randomised, Double-Blind, Placebo-Controlled Trial. *PLoS Med.* **8,** e1000407 (2011).

29. Konaté, A. T. *et al.* Intermittent Preventive Treatment of Malaria Provides Substantial Protection against Malaria in Children Already Protected by an Insecticide-Treated Bednet in Burkina Faso: A Randomised, Double-Blind, Placebo-Controlled Trial. *PLoS Med.* **8,** e1000408 (2011).

30. Cissé, B. *et al.* Seasonal intermittent preventive treatment with artesunate and sulfadoxine-pyrimethamine for prevention of malaria in Senegalese children: a randomised, placebo-controlled, double-blind trial. *Lancet (London, England)* **367,** 659–67 (2006).

31. WHO | WHO policy recommendation: Seasonal malaria chemoprevention (SMC) for Plasmodium falciparum malaria control in highly seasonal transmission areas of the Sahel sub-region in Africa. *WHO* (2015).

32. Cissé, B. *et al.* Effectiveness of Seasonal Malaria Chemoprevention in Children under Ten Years of Age in Senegal: A Stepped-Wedge Cluster-Randomised Trial. *PLOS Med.* **13,** e1002175 (2016).

33. WHO | Seasonal malaria chemoprevention with sulfadoxine-pyrimethamine plus amodiaquine in children: A field guide. *WHO* (2014).

34. Sanders, K., Gueye, C. S., Phillips, A. A. & Gosling, R. Active Case Detection for Malaria Elimination: a Confusion of Acronyms and Definitions. *Ashdin Publ. Malar. Chemother. Control Elimin.* **1,** (2012).

35. Ernst, K. C., Adoka, S. O., Kowuor, D. O., Wilson, M. L. & John, C. C. Malaria hotspot areas in a highland Kenya site are consistent in epidemic and non-epidemic years and are associated with ecological factors. *Malar. J.* **5,** 78 (2006).

36. Smith, J. L. *et al.* Spatial clustering of patent and sub-patent malaria infections in northern Namibia: Implications for surveillance and response strategies for elimination. *PLoS One* **12,** e0180845 (2017).

37. Gaudart, J. *et al.* Space-time clustering of childhood malaria at the household level: a dynamic cohort in a Mali village. *BMC Public Health* **6,** 286 (2006).

38. Carter, R., Mendis, K. N. & Roberts, D. Spatial targeting of interventions against malaria. *Bull. World Health Organ.* **78,** 1401–11 (2000).

39. Mosha, J. F. *et al.* Hot spot or not: a comparison of spatial statistical methods to predict prospective malaria infections. *Malar. J.* **13,** 53 (2014).

40. WHO Malaria Policy Advisory Committee. *WHO Evidence Review Group: Tthe Safety and Effectiveness of Single Dose Primaquine as a P. falciparum gametocytocide.* (2012).

41. Graves, P. M., Choi, L., Gelband, H. & Garner, P. Primaquine or other 8-aminoquinolines for reducing *Plasmodium falciparum* transmission. *Cochrane Database Syst. Rev.* (2018). doi:10.1002/14651858.CD008152.pub5

42. The malERA Consultative Group on Vaccines. A research agenda for malaria eradication: vaccines. *PLoS Med.* **8,** e1000398 (2011).

43. Targett, G. A. T., Moorthy, V. S. & Brown, G. V. Malaria vaccine research and development: the role of the WHO MALVAC committee. *Malar. J.* **12,** 362 (2013).

44. Wu, Y., Sinden, R. E., Churcher, T. S., Tsuboi, T. & Yusibov, V. Development of malaria transmission-blocking vaccines: from concept to product. *Adv. Parasitol.* **89,** 109–52 (2015).

45. Shimp, R. L. *et al.* Development of a Pfs25-EPA malaria transmission blocking vaccine as a chemically conjugated nanoparticle. *Vaccine* **31,** 2954–2962 (2013).

46. Farrance, C. E. *et al.* A plant-produced Pfs230 vaccine candidate blocks transmission of Plasmodium falciparum. *Clin. Vaccine Immunol.* **18,** 1351–7 (2011).

47. Cohen, J. M., Moonen, B., Snow, R. W. & Smith, D. L. How absolute is zero? An evaluation of historical and current definitions of malaria elimination. *Malar. J.* **9,** 213 (2010).

48. Milner, D. A. Malaria Pathogenesis. *Cold Spring Harb. Perspect. Med.* **8,** a025569 (2018).

49. Bousema, T. & Drakeley, C. Determinants of Malaria Transmission at the Population Level. *Cold Spring Harb. Perspect. Med.* **7,** a025510 (2017).

50. Gething, P. W. *et al.* A new world malaria map: Plasmodium falciparum endemicity in 2010. *Malar. J.* **10,** 378 (2011).

51. Noor, A. M. *et al.* The changing risk of Plasmodium falciparum malaria infection in Africa: 2000–10: a spatial and temporal analysis of transmission intensity. *Lancet* **383,** 1739–1747 (2014).

52. Cohen, J. M. *et al.* Malaria resurgence: a systematic review and assessment of its causes. *Malar. J.* **11,** 122 (2012).

53. Oesterholt, M. J. A. M. *et al.* Spatial and temporal variation in malaria transmission in a low endemicity area in northern Tanzania. *Malar. J.* **5,** 98 (2006).

54. Clark, T. D. *et al.* Factors determining the heterogeneity of malaria incidence in children in Kampala, Uganda. *J. Infect. Dis.* **198,** 393–400 (2008).

55. Bousema, T. *et al.* Identification of hot spots of malaria transmission for targeted malaria control. *J. Infect. Dis.* **201,** 1764–74 (2010).

56. Bousema, T. *et al.* Hitting Hotspots: Spatial Targeting of Malaria for Control and Elimination. *PLoS Med.* **9,** e1001165 (2012).

57. Woolhouse, M. E. J. *et al.* Heterogeneities in the transmission of infectious agents: Implications for the design of control programs. *Proc. Natl. Acad. Sci.* **94,** 338–342 (1997).

58. Bejon, P. *et al.* Stable and unstable malaria hotspots in longitudinal cohort studies in Kenya. *PLoS Med.* **7,** e1000304 (2010).

59. Smith, D. L., McKenzie, F. E., Snow, R. W. & Hay, S. I. Revisiting the basic reproductive number for malaria and its implications for malaria control. *PLoS Biol.* **5,** e42 (2007).

60. WHO Global Malaria Programme. *Malaria surveillance, monitoring & evaluation: a reference manual*. (World Health Organization, 2018).

61. Moonen, B. *et al.* Operational strategies to achieve and maintain malaria elimination. *Lancet* **376,** 1592–1603 (2010).

62. Cotter, C. *et al.* The changing epidemiology of malaria elimination: new strategies for new challenges. *Lancet* **382,** 900–911 (2013).

63. Landier, J. *et al.* Safety and effectiveness of mass drug administration to accelerate elimination of artemisinin-resistant falciparum malaria: A pilot trial in four villages of Eastern Myanmar. *Wellcome Open Res.* **2,** 81 (2017).

64. Lemoine, J. F. *et al.* Haiti's Commitment to Malaria Elimination: Progress in the Face of Challenges, 2010-2016. *Am. J. Trop. Med. Hyg.* **97,** 43–48 (2017).

65. Delrieu, I., Leboulleux, D., Ivinson, K. & Gessner, B. D. Design of a Phase III cluster randomized trial to assess the efficacy and safety of a malaria transmission blocking vaccine. *Vaccine* **33,** 1518–26 (2015).

66. Dicko, A. *et al.* The implementation of malaria intermittent preventive trialtreatment with sulphadoxine-pyrimethamine in infants reduced all-cause mortality in the district of Kolokani, Mali: results from a cluster randomized control. *Malar. J.* **11,** 73 (2012).

67. Meremikwu, M. M., Donegan, S., Sinclair, D., Esu, E. & Oringanje, C. Intermittent preventive treatment for malaria in children living in areas with seasonal transmission. *Cochrane database Syst. Rev.* **2,** CD003756 (2012).

68. Schellenberg, J. R. M. A. *et al.* Cluster-randomized study of intermittent preventive treatment for malaria in infants (IPTi) in southern Tanzania: evaluation of impact on survival. *Malar. J.* **10,** 387 (2011).

69. Chandramohan, D. *et al.* Cluster randomised trial of intermittent preventive treatment for malaria in infants in area of high, seasonal transmission in Ghana. *BMJ* **331,** 727–33 (2005).

70. Sochantha, T. *et al.* Insecticide-treated bednets for the prevention of Plasmodium falciparum malaria in Cambodia: a cluster-randomized trial. *Trop. Med. Int. Health* **11,** 1166–77 (2006).

71. Gamble, C., Ekwaru, P. J., Garner, P. & ter Kuile, F. O. Insecticide-treated nets for the prevention of malaria in pregnancy: a systematic review of randomised controlled trials. *PLoS Med.* **4,** e107 (2007).

72. Hawley, W. A. *et al.* Community-wide effects of permethrin-treated bed nets on child mortality and malaria morbidity in western Kenya. *Am. J. Trop. Med. Hyg.* **68,** 121–7 (2003).

73. Browne, E. N., Maude, G. H. & Binka, F. N. The impact of insecticide-treated bednets on malaria and anaemia in pregnancy in Kassena-Nankana district, Ghana: a randomized controlled trial. *Trop. Med. Int. Health* **6,** 667–76 (2001).

74. Poirot, E. *et al.* Mass drug administration for malaria. *Cochrane database Syst. Rev.* **12,** CD008846 (2013).

75. Shekalaghe, S. A. *et al.* A cluster-randomized trial of mass drug administration with a gametocytocidal drug combination to interrupt malaria transmission in a low endemic area in Tanzania. *Malar. J.* **10,** 247 (2011).

76. Pagel, C. *et al.* Intracluster correlation coefficients and coefficients of variation for perinatal outcomes from five cluster-randomised controlled trials in low and middle-income countries: results and methodological implications. *Trials* **12,** 151 (2011).

77. Hayes, R. & Moulton, L. *Cluster Randomised Trials*. (Chapman & Hall/CRC Press, 2009).

78. Bousema, T. *et al.* The impact of hotspot-targeted interventions on malaria transmission: study protocol for a cluster-randomized controlled trial. *Trials* **14,** 36 (2013).

79. Bautista, C. T. *et al.* Epidemiology and spatial analysis of malaria in the northern Peruvian Amazon. *Am J Trop Med Hyg* **75,** 1216–1222 (2006).

80. Tusting, L. S., Bousema, T., Smith, D. L. & Drakeley, C. Measuring changes in Plasmodium falciparum transmission: precision, accuracy and costs of metrics. *Adv. Parasitol.* **84,** 151–208 (2014).

81. Hay, S. I., Smith, D. L. & Snow, R. W. Measuring malaria endemicity from intense to interrupted transmission. *Lancet. Infect. Dis.* **8,** 369–78 (2008).

82. Neumann, C. G. *et al.* Comparison of blood smear microscopy to a rapid diagnostic test for in-vitro testing for P. falciparum malaria in Kenyan school children. *East Afr. Med. J.* **85,** 544–549 (2008).

83. WHO. *Malaria Rapid Diagnostic Test Performance. Results of WHO product testing of malaria RDTs: Round 4 (2012).* (2012).

84. Fancony, C., Sebastiao, Y. ., Pires, J. ., Gamboa, D. & Nery, S. . Performance of microscopy and RDTs in the context of a malaria prevalence survey in Angola: a comparison using PCR as the gold standard. *Malar. J.* (2013). doi:10.1186/1475-2875-12-284

85. Andrews, L. *et al.* Quantitative real-time polymerase chain reaction for malaria diagnosis and its use in malaria vaccine clinical trials. *Am. J. Trop. Med. Hyg.* **73,** 191–8 (2005).

86. Rockett, R. J. *et al.* A real-time, quantitative PCR method using hydrolysis probes for the monitoring of Plasmodium falciparum load in experimentally infected human volunteers. *Malar. J.* **10,** 48 (2011).

87. Cordray, M. S. & Richards-Kortum, R. R. Emerging Nucleic Acid–Based Tests for Point-of-Care Detection of Malaria. *Am. J. Trop. Med. Hyg.* **87,** 223–230 (2012).

88. The malERA Refresh Consultative Panel on Characterising the Reservoir and Measuring Transmission. malERA: An updated research agenda for characterising the reservoir and measuring transmission in malaria elimination and eradication. *PLOS Med.* **14,** e1002452 (2017).

89. Mueller, I. *et al.* Force of infection is key to understanding the epidemiology of Plasmodium falciparum malaria in Papua New Guinean children. *Proc. Natl. Acad. Sci. U. S. A.* **109,** 10030–5 (2012).

90. Sama, W., Owusu-Agyei, S., Felger, I., Dietz, K. & Smith, T. Age and seasonal variation in the transition rates and detectability of Plasmodium falciparum malaria. *Parasitology* **132,** 13–21 (2006).

91. Falk, N. *et al.* Comparison of PCR-RFLP and Genescan-based genotyping for analyzing infection dynamics of Plasmodium falciparum. *Am. J. Trop. Med. Hyg.* **74,** 944–50 (2006).

92. Felger, I., Genton, B., Smith, T., Tanner, M. & Beck, H. P. Molecular monitoring in malaria vaccine trials. *Trends Parasitol.* **19,** 60–3 (2003).

93. Genton, B. *et al.* A recombinant blood-stage malaria vaccine reduces Plasmodium falciparum density and exerts selective pressure on parasite populations in a phase 1-2b trial in Papua New Guinea. *J. Infect. Dis.* **185,** 820–7 (2002).

94. Daniels, R. *et al.* Genetic surveillance detects both clonal and epidemic transmission of malaria following enhanced intervention in Senegal. *PLoS One* **8,** e60780 (2013).

95. Daniels, R. F. *et al.* Modeling malaria genomics reveals transmission decline and rebound in Senegal. *Proc. Natl. Acad. Sci. U. S. A.* **112,** 7067–72 (2015).

96. Okell, L. C. *et al.* Factors determining the occurrence of submicroscopic malaria infections and their relevance for control. *Nat. Commun.* **3,** 1237 (2012).

97. Okell, L. C., Ghani, A. C., Lyons, E. & Drakeley, C. J. Submicroscopic infection in Plasmodium falciparum-endemic populations: a systematic review and meta-analysis. *J. Infect. Dis.* **200,** 1509–1517 (2009).

98. Cutts, F. T. & Hanson, M. Seroepidemiology: an underused tool for designing and monitoring vaccination programmes in low- and middle-income countries. *Trop. Med. Int. Heal.* **21,** 1086–1098 (2016).

99. Iliyasu, Z. *et al.* Survey of poliovirus antibodies in Kano, Northern Nigeria. *Vaccine* **32,** 1414–1420 (2014).

100. Deshpande, J. M. *et al.* Assessing population immunity in a persistently high-risk area for wild poliovirus transmission in India: a serological study in Moradabad, Western Uttar Pradesh. *J. Infect. Dis.* **210 Suppl 1,** S225-33 (2014).

101. Andrews, N. *et al.* Towards elimination: measles susceptibility in Australia and 17 European countries. *Bull. World Health Organ.* **8686,** 197–204 (2008).

102. Nardone, A. *et al.* Comparison of rubella seroepidemiology in 17 countries: progress towards international disease control targets. *Bull. World Health Organ.* **86,** 118–25 (2008).

103. Di Giovine, P. *et al.* Comparative seroepidemiology of diphtheria in six European countries and Israel. *Epidemiol. Infect.* **141,** 132–142 (2013).

104. Ladhani, S. *et al.* Haemophilus influenzae serotype B (Hib) seroprevalence in England and Wales in 2009. *Euro Surveill.* **17,** (2012).

105. Barkoff, A.-M., Gröndahl-Yli-Hannuksela, K. & He, Q. Seroprevalence studies of pertussis: what have we learned from different immunized populations. *Pathog. Dis.* **73,** ftv050 (2015).

106. Lammie, P. J. *et al.* Development of a new platform for neglected tropical disease surveillance. *Int. J. Parasitol.* **42,** 797–800 (2012).

107. Ngwe Tun, M. M. *et al.* Retrospective seroepidemiological study of chikungunya infection in South Asia, Southeast Asia and the Pacific region. *Epidemiol. Infect.* **144,** 2268–2275 (2016).

108. Poirier, M. J. *et al.* Measuring Haitian children's exposure to chikungunya, dengue and malaria. *Bull. World Health Organ.* **94,** 817–825A (2016).

109. Arnold, B. F. *et al.* Measuring changes in transmission of neglected tropical diseases, malaria, and enteric pathogens from quantitative antibody levels. *PLoS Negl. Trop. Dis.* **11,** e0005616 (2017).

110. Egger, J. Reconstructing historical changes in the force of infection of dengue fever in Singapore: implications for surveillance and control. *Bull. World Health Organ.* **86,** 187–196 (2008).

111. Migchelsen, S. J. *et al.* Serology reflects a decline in the prevalence of trachoma in two regions of The Gambia. *Sci. Rep.* **7,** 15040 (2017).

112. Grenfell, B. T. & Anderson, R. M. The estimation of age-related rates of infection from case notifications and serological data. *J. Hyg. (Lond).* **95,** 419–36 (1985).

113. Pan, C. Q. & Zhang, J. X. Natural History and Clinical Consequences of Hepatitis B Virus Infection. *Int. J. Med. Sci.* **2,** 36–40 (2005).

114. Ondigo, B. N. *et al.* Estimation of recent and long-term malaria transmission in a population by antibody testing to multiple Plasmodium falciparum antigens. *J. Infect. Dis.* **210,** 1123–32 (2014).

115. Stewart, L. *et al.* Rapid assessment of malaria transmission using age-specific sero-conversion rates. *PLoS One* **4,** e6083 (2009).

116. Cook, J. *et al.* Using serological measures to monitor changes in malaria transmission in Vanuatu. *Malar. J.* **9,** 169 (2010).

117. Cook, J. *et al.* Serological markers suggest heterogeneity of effectiveness of malaria control interventions on Bioko Island, equatorial Guinea. *PLoS One* **6,** e25137 (2011).

118. Wong, J. *et al.* Serological markers for monitoring historical changes in malaria transmission intensity in a highly endemic region of Western Kenya, 1994-2009. *Malar. J.* **13,** 451 (2014).

119. Drakeley, C. & Cook, J. Chapter 5. Potential contribution of sero-epidemiological analysis for monitoring malaria control and elimination: historical and current perspectives. *Adv. Parasitol.* **69,** 299–352 (2009).

120. Drakeley, C. J. *et al.* Estimating medium- and long-term trends in malaria transmission by using serological markers of malaria exposure. *Proc. Natl. Acad. Sci. U. S. A.* **102,** 5108–13 (2005).

121. Corran, P., Coleman, P., Riley, E. & Drakeley, C. Serology: a robust indicator of malaria transmission intensity? *Trends Parasitol.* **23,** 575–82 (2007).

122. Sepúlveda, N., Stresman, G., White, M. T. & Drakeley, C. J. Current Mathematical Models for Analyzing Anti-Malarial Antibody Data with an Eye to Malaria Elimination and Eradication. *J. Immunol. Res.* **2015,** 1–21 (2015).

123. Pothin, E., Ferguson, N. M., Drakeley, C. J. & Ghani, A. C. Estimating malaria transmission intensity from Plasmodium falciparum serological data using antibody density models. *Malar. J.* **15,** 79 (2016).

124. Yman, V. *et al.* Antibody acquisition models: A new tool for serological surveillance of malaria transmission intensity. *Sci. Rep.* **6,** 19472 (2016).

125. Weiss, G. E. *et al.* The Plasmodium falciparum-Specific Human Memory B Cell Compartment Expands Gradually with Repeated Malaria Infections. *PLoS Pathog.* **6,** e1000912 (2010).

126. Plotkin, S. A. & Plotkin, S. A. Vaccines: Correlates of Vaccine-Induced Immunity. *Clin. Infect. Dis.* **47,** 401–409 (2008).

127. Crompton, P. D. *et al.* Malaria Immunity in Man and Mosquito: Insights into Unsolved Mysteries of a Deadly Infectious Disease. *Annu. Rev. Immunol.* **32,** 157–187 (2014).

128. Snounou, G. & Pérignon, J.-L. Malariotherapy – Insanity at the Service of Malariology. *Adv.*

Parasitol. **81,** 223–255 (2013).

129. Cohen, S., McGregor, I. A. & Carrington, S. Gamma-Globulin and Acquired Immunity to Human Malaria. *Nature* **192,** 733–737 (1961).

130. McGregor, I. ., Carrington, S. . & Cohen, S. Treatment of east african P. falciparum malaria with west african human γ-globulin. *Trans. R. Soc. Trop. Med. Hyg.* **57,** 170–175 (1963).

131. Mwangi, T. W., Ross, A., Snow, R. W. & Marsh, K. Case Definitions of Clinical Malaria under Different Transmission Conditions in Kilifi District, Kenya. *J. Infect. Dis.* **191,** 1932–1939 (2005).

132. Griffin, J. T., Ferguson, N. M. & Ghani, A. C. Estimates of the changing age-burden of Plasmodium falciparum malaria disease in sub-Saharan Africa. *Nat. Commun.* **5,** 3136 (2014).

133. Snow, R. W. *et al.* Relation between severe malaria morbidity in children and level of Plasmodium falciparum transmission in Africa. *Lancet* **349,** 1650–1654 (1997).

134. McElroy, P. D. *et al.* Predicting outcome in malaria: correlation between rate of exposure to infected mosquitoes and level of Plasmodium falciparum parasitemia. *Am. J. Trop. Med. Hyg.* **51,** 523–32 (1994).

135. McElroy, P. D. *et al.* Dose- and time-dependent relations between infective Anopheles inoculation and outcomes of Plasmodium falciparum parasitemia among children in western Kenya. *Am. J. Epidemiol.* **145,** 945–56 (1997).

136. Thomas, C. J. & Lindsay, S. W. Local-scale variation in malaria infection amongst rural Gambian children estimated by satellite remote sensing. *Trans. R. Soc. Trop. Med. Hyg.* **94,** 159–63

137. Bejon, P. *et al.* Analysis of immunity to febrile malaria in children that distinguishes immunity from lack of exposure. *Infect. Immun.* **77,** 1917–23 (2009).

138. Bejon, P. *et al.* A micro-epidemiological analysis of febrile malaria in Coastal Kenya showing hotspots within hotspots. *Elife* **3,** e02130 (2014).

139. Mosha, J. F. *et al.* Epidemiology of subpatent Plasmodium falciparum infection: implications for detection of hotspots with imperfect diagnostics. *Malar. J.* **12,** 221 (2013).

140. Ndungu, F. M. *et al.* Identifying children with excess malaria episodes after adjusting for variation in exposure: identification from a longitudinal study using statistical count models. *BMC Med.* **13,** 183 (2015).

141. Reyburn, H. *et al.* Association of Transmission Intensity and Age With Clinical Manifestations and Case Fatality of Severe Plasmodium falciparum Malaria. *JAMA* **293,** 1461 (2005).

142. Creasey, A. *et al.* Eleven years of malaria surveillance in a Sudanese village highlights unexpected variation in individual disease susceptibility and outbreak severity. *Parasitology* **129,** 263–71 (2004).

143. Smith, T., Felger, I., Tanner, M. & Beck, H.-P. 11. Premunition in Plasmodium falciparum infection: insights from the epidemiology of multiple infections. *Trans. R. Soc. Trop. Med. Hyg.* **93,** 59–64 (1999).

144. Shekalaghe, S. *et al.* Low density parasitaemia, red blood cell polymorphisms and Plasmodium falciparumspecific immune responses in a low endemic area in northern Tanzania. *BMC Infect. Dis.* **9,** 69 (2009).

145. Fowkes, F. J. *et al.* New Insights into Acquisition, Boosting, and Longevity of Immunity to Malaria in Pregnant Women. *J. Infect. Dis.* **206,** 1612–1621 (2012).

146. Ibison, F. *et al.* Lack of Avidity Maturation of Merozoite Antigen-Specific Antibodies with

Increasing Exposure to Plasmodium falciparum amongst Children and Adults Exposed to Endemic Malaria in Kenya. *PLoS One* **7,** e52939 (2012).

147. Daou, M. *et al.* Protection of Malian children from clinical malaria is associated with recognition of multiple antigens. *Malar. J.* **14,** 56 (2015).

148. Rono, J. *et al.* Multiple clinical episodes of Plasmodium falciparum malaria in a low transmission intensity setting: exposure versus immunity. *BMC Med.* **13,** 114 (2015).

149. Färnert, A., Rooth, I., Svensson, Å., Snounou, G. & Björkman, A. Complexity of *Plasmodium falciparum* Infections Is Consistent over Time and Protects against Clinical Disease in Tanzanian Children. *J. Infect. Dis.* **179,** 989–995 (1999).

150. Proietti, C. *et al.* Influence of infection on malaria-specific antibody dynamics in a cohort exposed to intense malaria transmission in northern Uganda. *Parasite Immunol.* **35,** 164–173 (2013).

151. Deloron, P. & Chougnet, C. Is Immunity to malaria really short-lived? *Parasitol. Today* **8,** 375–378 (1992).

152. Brasseur, P. *et al.* Changing patterns of malaria during 1996-2010 in an area of moderate transmission in Southern Senegal. *Malar. J.* **10,** 203 (2011).

153. Ceesay, S. J. *et al.* Changes in malaria indices between 1999 and 2007 in The Gambia: a retrospective analysis. *Lancet (London, England)* **372,** 1545–54 (2008).

154. Gray, J. C. *et al.* Profiling the antibody immune response against blood stage malaria vaccine candidates. *Clin. Chem.* **53,** 1244–53 (2007).

155. Kaneko, A. *et al.* Characteristic age distribution of Plasmodium vivax infections after malaria elimination on Aneityum Island, Vanuatu. *Infect. Immun.* **82,** 243–52 (2014).

156. Farnert, A., Snounou, G., Rooth, I. & Bjorkman, A. Daily dynamics of Plasmodium falciparum subpopulations in asymptomatic children in a holoendemic area. *Am. J. Trop. Med. Hyg.* **56,** 538–47 (1997).

157. Claessens, A. *et al.* Generation of antigenic diversity in Plasmodium falciparum by structured rearrangement of Var genes during mitosis. *PLoS Genet.* **10,** e1004812 (2014).

158. Travassos, M. A. *et al.* Seroreactivity to Plasmodium falciparum erythrocyte membrane protein 1 intracellular domain in malaria-exposed children and adults. *J. Infect. Dis.* **208,** 1514–9 (2013).

159. Kraemer, S. M. & Smith, J. D. A family affair: var genes, PfEMP1 binding, and malaria disease. *Curr. Opin. Microbiol.* **9,** 374–380 (2006).

160. Jones, T. R. *et al.* Age-Dependent Acquired Protection against Plasmodium Falciparum in People Having Two Years Exposure to Hyperendemic Malaria. *Am. J. Trop. Med. Hyg.* **45,** 65–76 (1991).

161. Masbar, S. *et al.* Age-Specific Prevalence of Plasmodium falciparum Among Six Populations with Limited Histories of Exposure to Endemic Malaria. *Am. J. Trop. Med. Hyg.* **49,** 707–719 (1993).

162. Schellenberg, D. *et al.* Intermittent treatment for malaria and anaemia control at time of routine vaccinations in Tanzanian infants: a randomised, placebo-controlled trial. *Lancet* **357,** 1471–1477 (2001).

163. Alonso, P. L. *et al.* Randomised trial of efficacy of SPf66 vaccine against Plasmodium falciparum malaria in children in southern Tanzania. *Lancet (London, England)* **344,** 1175–81

(1994).

164. Griffin, J. T. *et al.* Gradual acquisition of immunity to severe malaria with increasing exposure. *Proceedings. Biol. Sci.* **282,** 20142657 (2015).

165. Riley, E. M., Wahl, S., Perkins, D. J. & Schofield, L. Regulating immunity to malaria. *Parasite Immunol.* **28,** 35–49 (2006).

166. Stanisic, D. I. *et al.* Acquisition of antibodies against Plasmodium falciparum merozoites and malaria immunity in young children and the influence of age, force of infection, and magnitude of response. *Infect. Immun.* **83,** 646–60 (2015).

167. Langhorne, J., Ndungu, F. M., Sponaas, A.-M. & Marsh, K. Immunity to malaria: more questions than answers. *Nat. Immunol.* **9,** 725–732 (2008).

168. Vidal, M., Aguilar, R., Campo, J. J. & Dobaño, C. Development of quantitative suspension array assays for six immunoglobulin isotypes and subclasses to multiple Plasmodium falciparum antigens. *J. Immunol. Methods* **455,** 41–54 (2018).

169. Richards, J. S. & Beeson, J. G. The future for blood-stage vaccines against malaria. *Immunol. Cell Biol.* **87,** 377–390 (2009).

170. Richards, J. S. *et al.* Identification and prioritization of merozoite antigens as targets of protective human immunity to Plasmodium falciparum malaria for vaccine and biomarker development. *J. Immunol.* **191,** 795–809 (2013).

171. Cowman, A. F. & Crabb, B. S. Invasion of Red Blood Cells by Malaria Parasites. *Cell* **124,** 755–766 (2006).

172. Blackman, M. J., Scott-Finnigan, T. J., Shai, S. & Holder, A. A. Antibodies inhibit the protease-mediated processing of a malaria merozoite surface protein. *J. Exp. Med.* **180,** 389–93 (1994).

173. Persson, K. E. M. *et al.* Variation in use of erythrocyte invasion pathways by Plasmodium falciparum mediates evasion of human inhibitory antibodies. *J. Clin. Invest.* **118,** 342–51 (2008).

174. Jiang, L. *et al.* Evidence for erythrocyte-binding antigen 175 as a component of a ligand-blocking blood-stage malaria vaccine. *Proc. Natl. Acad. Sci. U. S. A.* **108,** 7553–8 (2011).

175. Adams, J. H. *et al.* A family of erythrocyte binding proteins of malaria parasites. *Proc. Natl. Acad. Sci. U. S. A.* **89,** 7085–9 (1992).

176. Osier, F. H. *et al.* Opsonic phagocytosis of Plasmodium falciparummerozoites: mechanism in human immunity and a correlate of protection against malaria. *BMC Med.* **12,** 108 (2014).

177. McCallum, F. J. *et al.* Acquisition of Growth-Inhibitory Antibodies against Blood-Stage Plasmodium falciparum. *PLoS One* **3,** e3571 (2008).

178. Bouharoun-Tayoun, H., Oeuvray, C., Lunel, F. & Druilhe, P. Mechanisms underlying the monocyte-mediated antibody-dependent killing of Plasmodium falciparum asexual blood stages. *J. Exp. Med.* **182,** 409–18 (1995).

179. Coppel, R. L. Vaccinating with the genome: a Sisyphean task? *Trends Parasitol.* **25,** 205–212 (2009).

180. Draper, S. J. *et al.* Recent advances in recombinant protein-based malaria vaccines. *Vaccine* **33,** 7433–43 (2015).

181. Scholzen, A. & Sauerwein, R. W. How malaria modulates memory: activation and dysregulation of B cells in Plasmodium infection. *Trends Parasitol.* **29,** 252–262 (2013).

182. Perlmann, P. & Troye-Blomberg, M. Malaria and the immune system in humans. *Chem. Immunol.* **80,** 229–42 (2002).

183. Winzeler, E. A. Applied systems biology and malaria. *Nat. Rev. Microbiol.* **4,** 145–151 (2006).

184. Falciparum, P., Vivax, P. & Thomson, J. G. Experiments on the Complement Fixation in Malaria with Antigens prepared from Cultures of Malarial Parasites.

185. Tobie, J. E., Kuvin, S. F., Contacos, P. G., Coatney, G. R. & Evans, C. B. Cross Reactions in Human and Simian Malaria. *JAMA J. Am. Med. Assoc.* **184,** 945 (1963).

186. Harris, A. & Reidel, L. M. Evaluation of the complement fixation test for malaria. *Am. J. Trop. Med. Hyg.* **28,** 787–95 (1948).

187. Meuwissen, J. H., Leeuwenberg, A. D. & Molenkamp, G. E. Studies on various aspects of the indirect haemagglutination test for malaria. *Bull. World Health Organ.* **46,** 771–82 (1972).

188. van den Hoogen, L. & Drakeley, C. in *Encyclopedia of Malaria* 1–8 (Springer New York, 2015). doi:10.1007/978-1-4614-8757-9_111-1

189. Voller, A. & Bruce-Chwatt, L. J. Serological malaria surveys in Nigeria. *Bull. World Health Organ.* **39,** 883–97 (1968).

190. Bruce-Chwatt, L. J., Draper, C. C., Dodge, J. S., Topley, E. & Voller, A. Sero-epidemiological studies on population groups previously exposed to malaria. *Lancet* **299,** 512–515 (1972).

191. Lelijveld, J., Otieno, L. H. & Meuwissen, J. H. Serological studies of malaria in East Africa. II. Serological indices as parameters of progress of malaria control and eradication. *Trop. Geogr. Med.* **25,** 75–83 (1973).

192. Collins, W. E. & Skinner, J. C. The Indirect Fluorescent Antibody Test for Malaria. *Am. J. Trop. Med. Hyg.* **21,** 690–695 (1972).

193. Skinner, J. C., Collins, W. E. & Warren, M. Serological Malaria Survey in the Ethiopian Highlands. *Am. J. Trop. Med. Hyg.* **20,** 199–205 (1971).

194. Multiplex Immunoassays | LSR | Bio-Rad. Available at: http://www.bio-rad.com/en-uk/applications-technologies/multiplex-immunoassays?ID=LUSM0E8UU#2. (Accessed: 11th June 2018)

195. Schena, M. *Protein microarrays*. (Jones and Bartlett, 2005).

196. Phillips-Howard, P. A. Malaria. Principles and Practice of Malariology. Vol 1 & 2. *J. R. Soc. Med.* **82,** 636 (1989).

197. Greenwood, B. M. *et al.* Mortality and morbidity from malaria among children in a rural area of The Gambia, West Africa. *Trans. R. Soc. Trop. Med. Hyg.* **81,** 478–86 (1987).

198. Caputo, B. *et al.* Anopheles gambiae complex along The Gambia river, with particular reference to the molecular forms of An. gambiae s.s. *Malar. J.* **7,** 182 (2008).

199. Giles, G. M. J. & Giles, G. M. J. *A handbook of the gnats or mosquitoes; giving the anatomy and life history of the Culicidæ together with descriptions of all species noticed up to the present date, by Lieut.-Col. Geo. M. Giles.* (J. Bale, sons & Danielsson, ltd., 1902). doi:10.5962/bhl.title.8549

200. Bertram, D. ., McGregor, I. . & McFadzean, J. . Mosquitoes of the colony and protectorate of the Gambia. *Trans. R. Soc. Trop. Med. Hyg.* **52,** 135–151 (1958).

201. Snow, W. F. Studies of house-entering habits of mosquitoes in The Gambia, West Africa: experiments with prefabricated huts with varied wall apertures. *Med. Vet. Entomol.* **1,** 9–21

(1987).

202. Snow, W. F. Mosquito production and species succession from an area of irrigated rice fields in The Gambia, West Africa. *J. Trop. Med. Hyg.* **86,** 237–45 (1983).

203. Gillies, M. T. & Wilkes, T. J. A comparison of the range of attraction of animal baits and of carbon dioxide for some West African mosquitoes. *Bull. Entomol. Res.* **59,** 441–56 (1969).

204. Gillies, M. T. & Wilkes, T. J. The vertical distribution of mosquitoes flying over open farmland in the Gambia. *Trans. R. Soc. Trop. Med. Hyg.* **68,** 268–9 (1974).

205. Lindsay, S. W., Adiamah, J. H., Miller, J. E., Pleass, R. J. & Armstrong, J. R. Variation in attractiveness of human subjects to malaria mosquitoes (Diptera: Culicidae) in The Gambia. *J. Med. Entomol.* **30,** 368–73 (1993).

206. Dutton, J. E., Dutton, J. E., Theobald, F. V., Medicine., L. S. of T. & Medicine., L. S. of H. and T. *Report of the malaria expedition to the Gambia 1902, of the Liverpool School of Tropical Medicine and Medical Parasitology*. (Longmans, Green for the University Press of Liverpool,).

207. Howard, R. J. *et al.* Antigenic diversity and size diversity of Plasmodium falciparum antigens in isolates from Gambian patients. I. S-antigens. *Parasite Immunol.* **8,** 39–55 (1986).

208. Marsh, K., Otoo, L., Hayes, R. J., Carson, D. C. & Greenwood, B. M. Antibodies to blood stage antigens of Plasmodium falciparum in rural Gambians and their relation to protection against infection. *Trans. R. Soc. Trop. Med. Hyg.* **83,** 293–303

209. Pasternak, N. D. & Dzikowski, R. PfEMP1: an antigen that plays a key role in the pathogenicity and immune evasion of the malaria parasite Plasmodium falciparum. *Int. J. Biochem. Cell Biol.* **41,** 1463–6 (2009).

210. Polley, S. D. *et al. Plasmodium falciparum* Merozoite Surface Protein 3 Is a Target of Allele-Specific Immunity and Alleles Are Maintained by Natural Selection. *J. Infect. Dis.* **195,** 279–287 (2007).

211. Conway, D. J. *et al.* A principal target of human immunity to malaria identified by molecular population genetic and immunological analyses. *Nat. Med.* **6,** 689–692 (2000).

212. Akpogheneta, O. J. *et al.* Duration of Naturally Acquired Antibody Responses to Blood-Stage Plasmodium falciparum Is Age Dependent and Antigen Specific. *Infect. Immun.* **76,** 1748–1755 (2008).

213. Drakeley, C. J., Secka, I., Correa, S., Greenwood, B. M. & Targett, G. A. Host haematological factors influencing the transmission of Plasmodium falciparum gametocytes to Anopheles gambiae s.s. mosquitoes. *Trop. Med. Int. Health* **4,** 131–8 (1999).

214. Drakeley, C., Sutherland, C., Bousema, J. T., Sauerwein, R. W. & Targett, G. A. T. The epidemiology of Plasmodium falciparum gametocytes: weapons of mass dispersion. *Trends Parasitol.* **22,** 424–430 (2006).

215. Bousema, T. *et al.* Human immune responses that reduce the transmission of Plasmodium falciparum in African populations. *Int. J. Parasitol.* **41,** 293–300 (2011).

216. Ceesay, S. J. *et al.* Continued Decline of Malaria in The Gambia with Implications for Elimination. *PLoS One* **5,** e12242 (2010).

217. WHO | World malaria report 2017. *WHO* (2018).

218. Mwesigwa, J. *et al.* On-going malaria transmission in The Gambia despite high coverage of control interventions: a nationwide cross-sectional survey. *Malar. J.* **14,** 314 (2015).

219. Okebe, J. *et al.* School-Based Countrywide Seroprevalence Survey Reveals Spatial

Heterogeneity in Malaria Transmission in the Gambia. *PLoS One* **9,** e110926 (2014).

220. Mwesigwa, J. *et al.* Residual malaria transmission dynamics varies across The Gambia despite high coverage of control interventions. *PLoS One* **12,** e0187059 (2017).

221. Thomson, M. *et al.* Geographical perspectives on bednet use and malaria transmission in The Gambia, West Africa. *Soc. Sci. Med.* **43,** 101–12 (1996).

222. Elimination 8. *Annual Report 2016*. (2016).

223. Smith Gueye, C. *et al.* Namibia's path toward malaria elimination: a case study of malaria strategies and costs along the northern border. *BMC Public Health* **14,** 1190 (2014).

224. Smith, J. L. *et al.* Malaria risk in young male travellers but local transmission persists: a case–control study in low transmission Namibia. *Malar. J.* **16,** 70 (2017).

225. Noor, A. M. *et al.* Malaria Control and the Intensity of Plasmodium falciparum Transmission in Namibia 1969–1992. *PLoS One* **8,** e63350 (2013).

226. Chanda, E. *et al.* Strengthening tactical planning and operational frameworks for vector control: the roadmap for malaria elimination in Namibia. *Malar. J.* **14,** 302 (2015).

227. Namibia Statistics Agency. *Government Republic of Namibia National Planning Commission: Namibia 2011 Population and Housing Census, Preliminary Report*. (2012).

228. Alegana, V. A. *et al.* Estimation of malaria incidence in northern Namibia in 2009 using Bayesian conditional-autoregressive spatial-temporal models. *Spat. Spatiotemporal. Epidemiol.* **7,** 25–36 (2013).

229. Noor, A. M. *et al.* The receptive versus current risks of Plasmodium falciparumtransmission in Northern Namibia: implications for elimination. *BMC Infect. Dis.* **13,** 184 (2013).

230. Trans-Kunene Anti-Malaria Initiative. Cross-Border Collaboration Initiative to Combat Malaria Trans-Kunene Anti-Malaria Initiative, Ministry of Health Republic of Angola and Ministry of Heath and Social Services Republic of Namibia. (2010).

231. Hay, S. I., Smith, D. L. & Snow, R. W. Measuring malaria endemicity from intense to interrupted transmission. *Lancet. Infect. Dis.* **8,** 369–78 (2008).

232. Wu, L. *et al.* Comparison of diagnostics for the detection of asymptomatic Plasmodium falciparum infections to inform control and elimination strategies. *Nature* **528,** S86-93 (2015).

233. Mbogo, C. M. *et al.* Spatial and temporal heterogeneity of Anopheles mosquitoes and Plasmodium falciparum transmission along the Kenyan coast. *Am. J. Trop. Med. Hyg.* **68,** 734–42 (2003).

234. Okell, L. C. *et al.* Factors determining the occurrence of submicroscopic malaria infections and their relevance for control. *Nat. Commun.* **3,** 1237 (2012).

235. Bousema, T., Okell, L., Felger, I. & Drakeley, C. Asymptomatic malaria infections: detectability, transmissibility and public health relevance. *Nat. Rev. Microbiol.* **12,** 833–840 (2014).

236. Cook, J. *et al.* Mass Screening and Treatment on the Basis of Results of a Plasmodium falciparum-Specific Rapid Diagnostic Test Did Not Reduce Malaria Incidence in Zanzibar. *J. Infect. Dis.* **211,** 1476–1483 (2015).

237. Rowe, A. K. *et al.* Caution is required when using health facility-based data to evaluate the health impact of malaria control efforts in Africa. *Malar. J.* **8,** 209 (2009).

238. Andrews, L. *et al.* Quantitative real-time polymerase chain reaction for malaria diagnosis and its use in malaria vaccine clinical trials. *Am. J. Trop. Med. Hyg.* **73,** 191–198 (2005).

239. Alegana, V. A. *et al.* Malaria prevalence metrics in low- and middle-income countries: an assessment of precision in nationally-representative surveys. *Malar. J.* **16,** 475 (2017).

240. Gerardin, J. *et al.* Effectiveness of reactive case detection for malaria elimination in three archetypical transmission settings: a modelling study. *Malar. J.* **16,** 248 (2017).

241. Sturrock, H. J. W. *et al.* Reactive Case Detection for Malaria Elimination: Real-Life Experience from an Ongoing Program in Swaziland. *PLoS One* **8,** e63830 (2013).

242. Smith, D. L. & Hay, S. I. Endemicity response timelines for Plasmodium falciparum elimination. *Malar. J.* **8,** 87 (2009).

243. Rogier, E. *et al.* Multiple comparisons analysis of serological data from an area of low Plasmodium falciparum transmission. *Malar. J.* **14,** 436 (2015).

244. Elliott, S. R. *et al.* Research priorities for the development and implementation of serological tools for malaria surveillance. *F1000Prime Rep.* **6,** 100 (2014).

245. Corran, P. H. *et al.* Dried blood spots as a source of anti-malarial antibodies for epidemiological studies. *Malar. J.* **7,** 195 (2008).

246. Smith, D. L., Dushoff, J., Snow, R. W. & Hay, S. I. The entomological inoculation rate and Plasmodium falciparum infection in African children. *Nature* **438,** 492–495 (2005).

247. Battle, K. E. *et al.* Global database of matched Plasmodium falciparum and P. vivax incidence and prevalence records from 1985–2013. *Sci. Data* **2,** 150012 (2015).

248. Drakeley, C. J. *et al.* Estimating medium- and long-term trends in malaria transmission by using serological markers of malaria exposure. *Proc. Natl. Acad. Sci. U. S. A.* **102,** 5108–13 (2005).

249. Sepúlveda, N. & Drakeley, C. Sample size determination for estimating antibody seroconversion rate under stable malaria transmission intensity. *Malar. J.* **14,** 141 (2015).

250. Supargiyono, S. *et al.* Seasonal changes in the antibody responses against Plasmodium falciparum merozoite surface antigens in areas of differing malaria endemicity in Indonesia. *Malar. J.* **12,** 444 (2013).

251. Cook, J. *et al.* Sero-epidemiological evaluation of changes in Plasmodium falciparum and Plasmodium vivax transmission patterns over the rainy season in Cambodia. *Malar. J.* **11,** 86 (2012).

252. Cruz Marques, A. Human migration and the spread of malaria in Brazil. *Parasitol. Today* **3,** 166–170 (1987).

253. Erhart, A. *et al.* Epidemiology of forest malaria in central Vietnam: a large scale cross-sectional survey. *Malar. J.* **4,** 58 (2005).

254. Ondigo, B. N. *et al.* Estimation of Recent and Long-Term Malaria Transmission in a Population by Antibody Testing to Multiple Plasmodium falciparum Antigens. *J. Infect. Dis.* **210,** 1123–1132 (2014).

255. Tongren, J. E. *et al.* Target antigen, age, and duration of antigen exposure independently regulate immunoglobulin G subclass switching in malaria. *Infect. Immun.* **74,** 257–64 (2006).

256. Ferreira, M. U., da Silva Nunes, M. & Wunderlich, G. Antigenic diversity and immune evasion by malaria parasites. *Clin. Diagn. Lab. Immunol.* **11,** 987–95 (2004).

257. Kilama, M. *et al.* Estimating the annual entomological inoculation rate for Plasmodium falciparum transmitted by Anopheles gambiae s.l. using three sampling methods in three sites in Uganda. *Malar. J.* **13,** 111 (2014).

258. Smith, D. L., Guerra, C. A., Snow, R. W. & Hay, S. I. Standardizing estimates of the Plasmodium falciparum parasite rate. *Malar. J.* **6,** 131 (2007).

259. Smith, D. L., Drakeley, C. J., Chiyaka, C. & Hay, S. I. A quantitative analysis of transmission efficiency versus intensity for malaria. *Nat. Commun.* **1,** 108 (2010).

260. van den Hoogen, L. L. *et al.* Serology describes a profile of declining malaria transmission in Farafenni, The Gambia. *Malar. J.* **14,** 416 (2015).

261. Churcher, T. S. *et al.* Public health. Measuring the path toward malaria elimination. *Science* **344,** 1230–2 (2014).

262. Helb, D. A. *et al.* Novel serologic biomarkers provide accurate estimates of recent Plasmodium falciparum exposure for individuals and communities. *Proc. Natl. Acad. Sci. U. S. A.* **112,** E4438-47 (2015).

263. Crompton, P. D. *et al.* A prospective analysis of the Ab response to Plasmodium falciparum before and after a malaria season by protein microarray. *Proc. Natl. Acad. Sci. U. S. A.* **107,** 6958–63 (2010).

264. Kerkhof, K. *et al.* Serological markers to measure recent changes in malaria at population level in Cambodia. *Malar. J.* **15,** 529 (2016).

265. White, M. T. *et al.* Dynamics of the Antibody Response to Plasmodium falciparum Infection in African Children. *J. Infect. Dis.* **210,** 1115–1122 (2014).

266. Mayor, A. *et al.* Changing Trends in *P. falciparum* Burden, Immunity, and Disease in Pregnancy. *N. Engl. J. Med.* **373,** 1607–1617 (2015).

267. Ahmed Ismail, H. *et al.* Subclass responses and their half-lives for antibodies against EBA175 and PfRh2 in naturally acquired immunity against Plasmodium falciparum malaria. *Malar. J.* **13,** 425 (2014).

268. Jacobson, J. O. *et al.* Surveillance and response for high-risk populations: what can malaria elimination programmes learn from the experience of HIV? *Malar. J.* **16,** 33 (2017).

269. Davies, D. H., Duffy, P., Bodmer, J.-L., Felgner, P. L. & Doolan, D. L. Large screen approaches to identify novel malaria vaccine candidates. *Vaccine* **33,** 7496–7505 (2015).

270. Morita, M. *et al.* Immunoscreening of Plasmodium falciparum proteins expressed in a wheat germ cell-free system reveals a novel malaria vaccine candidate. *Sci. Rep.* **7,** 46086 (2017).

271. Smits, G. P., van Gageldonk, P. G., Schouls, L. M., van der Klis, F. R. M. & Berbers, G. A. M. Development of a bead-based multiplex immunoassay for simultaneous quantitative detection of IgG serum antibodies against measles, mumps, rubella, and varicella-zoster virus. *Clin. Vaccine Immunol.* **19,** 396–400 (2012).

272. Perraut, R. *et al.* Comparative analysis of IgG responses to Plasmodium falciparum MSP1p19 and PF13-DBL1α1 using ELISA and a magnetic bead-based duplex assay (MAGPIX®-Luminex) in a Senegalese meso-endemic community. *Malar. J.* **13,** 410 (2014).

273. Basile, A. J. *et al.* Multiplex Microsphere Immunoassays for the Detection of IgM and IgG to Arboviral Diseases. *PLoS One* **8,** e75670 (2013).

274. Cham, G. K. K. *et al.* A semi-automated multiplex high-throughput assay for measuring IgG antibodies against Plasmodium falciparum erythrocyte membrane protein 1 (PfEMP1) domains in small volumes of plasma. *Malar. J.* **7,** 108 (2008).

275. Ondigo, B. N. *et al.* Standardization and validation of a cytometric bead assay to assess antibodies to multiple Plasmodium falciparum recombinant antigens. *Malar. J.* **11,** 427 (2012).

276. Luminex Corporation. Manual, xMAP Antibody Coupling Kit User, English - Luminex Corporation. (2015). Available at: https://www.luminexcorp.com/download/xmap-antibody-coupling-kit-user-manual/. (Accessed: 8th February 2018)

277. Nibsc. First WHO Reference Reagent for Anti-malaria (Plasmodium falciparum) human serum.

278. Burghaus, P. A. & Holder, A. A. Expression of the 19-kilodalton carboxy-terminal fragment of the Plasmodium falciparum merozoite surface protein-1 in Escherichia coli as a correctly folded protein. *Mol. Biochem. Parasitol.* **64,** 165–169 (1994).

279. Collins, C. R. *et al.* Fine mapping of an epitope recognized by an invasion-inhibitory monoclonal antibody on the malaria vaccine candidate apical membrane antigen 1. *J. Biol. Chem.* **282,** 7431–41 (2007).

280. Theisen, M., Vuust, J., Gottschau, A., Jepsen, S. & Høgh, B. Antigenicity and Immunogenicity of Recombinant Glutamate-Rich Protein of Plasmodium falciparum Expressed in Escherichia coli. **2,** 30–34 (1995).

281. Richards, J. S. *et al.* Association between Naturally Acquired Antibodies to Erythrocyte-Binding Antigens of *Plasmodium falciparum* and Protection from Malaria and High-Density Parasitemia. *Clin. Infect. Dis.* **51,** e50–e60 (2010).

282. Crosnier, C. *et al.* Basigin is a receptor essential for erythrocyte invasion by Plasmodium falciparum. *Nature* **480,** 534–537 (2011).

283. Triglia, T. *et al.* Identification of proteins from Plasmodium falciparum that are homologous to reticulocyte binding proteins in Plasmodium vivax. *Infect. Immun.* **69,** 1084–92 (2001).

284. Reiling, L. *et al.* The Plasmodium falciparum Erythrocyte Invasion Ligand Pfrh4 as a Target of Functional and Protective Human Antibodies against Malaria. *PLoS One* **7,** e45253 (2012).

285. Spielmann, T., Fergusen, D. J. P. & Beck, H.-P. etramps, a new Plasmodium falciparum gene family coding for developmentally regulated and highly charged membrane proteins located at the parasite-host cell interface. *Mol. Biol. Cell* **14,** 1529–44 (2003).

286. Raj, D. K. *et al.* Antibodies to PfSEA-1 block parasite egress from RBCs and protect against malaria infection. *Science* **344,** 871–7 (2014).

287. Polley, S. D. *et al.* High levels of serum antibodies to merozoite surface protein 2 of Plasmodium falciparum are associated with reduced risk of clinical malaria in coastal Kenya. *Vaccine* **24,** 4233–4246 (2006).

288. Pearce, J. A., Mills, K., Triglia, T., Cowman, A. F. & Anders, R. F. Characterisation of two novel proteins from the asexual stage of Plasmodium falciparum, H101 and H103. *Mol. Biochem. Parasitol.* **139,** 141–51 (2005).

289. Grüring, C. *et al.* Development and host cell modifications of Plasmodium falciparum blood stages in four dimensions. *Nat. Commun.* **2,** 165 (2011).

290. Kastenmüller, K. *et al.* Full-length Plasmodium falciparum circumsporozoite protein administered with long-chain poly(I·C) or the Toll-like receptor 4 agonist glucopyranosyl lipid adjuvant-stable emulsion elicits potent antibody and CD4+ T cell immunity and protection in mice. *Infect. Immun.* **81,** 789–800 (2013).

291. Kerkhof, K. *et al.* Serological markers to measure recent changes in malaria at population level in Cambodia. *Malar. J.* **15,** 529 (2016).

292. Gottschalk, P. G. & Dunn, J. R. The five-parameter logistic: A characterization and comparison with the four-parameter logistic. *Anal. Biochem.* **343,** 54–65 (2005).

293. Sanz, H. *et al.* drLumi: An open-source package to manage data, calibrate, and conduct quality control of multiplex bead-based immunoassays data analysis. *PLoS One* **12,** e0187901 (2017).

294. Motulsky, H. & Christopoulos, A. Fitting Models to Biological Data using Linear and Nonlinear Regression Contents at a Glance.

295. Smyth, G. K. & Speed, T. Normalization of cDNA microarray data. *Methods* **31,** 265–273 (2003).

296. de Jager, W., te Velthuis, H., Prakken, B. J., Kuis, W. & Rijkers, G. T. Simultaneous detection of 15 human cytokines in a single sample of stimulated peripheral blood mononuclear cells. *Clin. Diagn. Lab. Immunol.* **10,** 133–9 (2003).

297. Dunbar, S. A. Applications of Luminex® xMAP™ technology for rapid, high-throughput multiplexed nucleic acid detection. *Clin. Chim. Acta* **363,** 71–82 (2006).

298. Sarr, J. *et al.* Assessment of exposure to Plasmodium falciparum transmission in a low endemicity area by using multiplex fluorescent microsphere-based serological assays. *Parasit. Vectors* **4,** 212 (2011).

299. Dobaño, C. *et al.* Age-dependent IgG subclass responses to Plasmodium falciparum EBA-175 are differentially associated with incidence of malaria in Mozambican children. *Clin. Vaccine Immunol.* **19,** 157–66 (2012).

300. Koffi, D. *et al.* Analysis of antibody profiles in symptomatic malaria in three sentinel sites of Ivory Coast by using multiplex, fluorescent, magnetic, bead-based serological assay (MAGPIX™). *Malar. J.* **14,** 509 (2015).

301. Kerkhof, K. *et al.* Serological markers to measure recent changes in malaria at population level in Cambodia. *Malar. J.* **15,** 529 (2016).

302. Fouda, G. G. *et al.* Multiplex assay for simultaneous measurement of antibodies to multiple Plasmodium falciparum antigens. *Clin. Vaccine Immunol.* **13,** 1307–13 (2006).

303. Elshal, M. F. & McCoy, J. P. Multiplex bead array assays: Performance evaluation and comparison of sensitivity to ELISA. *Methods* **38,** 317–323 (2006).

304. Helb, D. A. *et al.* Novel serologic biomarkers provide accurate estimates of recent Plasmodium falciparum exposure for individuals and communities. *Proc. Natl. Acad. Sci. U. S. A.* **112,** E4438-47 (2015).

305. Fonseca, A. M. *et al.* Multiplexing detection of IgG against Plasmodium falciparum pregnancy-specific antigens. *PLoS One* **12,** e0181150 (2017).

306. Rogier, E. *et al.* Multiple comparisons analysis of serological data from an area of low Plasmodium falciparum transmission. *Malar. J.* **14,** 436 (2015).

307. Nagelkerke, N. J. D., Borgdorff, M. W. & Kim, S. J. Logistic discrimination of mixtures of M. tuberculosis and non-specific tuberculin reactions. *Stat. Med.* **20,** 1113–1124 (2001).

308. Rota, M. C. *et al.* Measles serological survey in the Italian population: Interpretation of results using mixture model. *Vaccine* **26,** 4403–4409 (2008).

309. Hardelid, P. *et al.* Analysis of rubella antibody distribution from newborn dried blood spots using finite mixture models. *Epidemiol. Infect.* **136,** 1698 (2008).

310. Migchelsen, S. J. *et al.* Defining Seropositivity Thresholds for Use in Trachoma Elimination Studies. *PLoS Negl. Trop. Dis.* **11,** e0005230 (2017).

311. Irion, A., Beck, H. P. & Smith, T. Assessment of positivity in immuno-assays with variability in background measurements: a new approach applied to the antibody response to Plasmodium

falciparum MSP2. *J. Immunol. Methods* **259,** 111–8 (2002).

312. Zhao, X., Siegel, K., Chen, M. I.-C. & Cook, A. R. Rethinking thresholds for serological evidence of influenza virus infection. *Influenza Other Respi. Viruses* **11,** 202–210 (2017).

313. Kompithra, R. Z. *et al.* Immunogenicity of a three dose and five dose oral human rotavirus vaccine (RIX4414) schedule in south Indian infants. *Vaccine* **32,** A129–A133 (2014).

314. Ubillos, I., Campo, J. J., Jiménez, A. & Dobaño, C. Development of a high-throughput flexible quantitative suspension array assay for IgG against multiple Plasmodium falciparum antigens. *Malar. J.* **17,** 216 (2018).

315. Dümmler, A., Lawrence, A.-M. & de Marco, A. Simplified screening for the detection of soluble fusion constructs expressed in E. coli using a modular set of vectors. *Microb. Cell Fact.* **4,** 34 (2005).

316. Dodig, S. Interferences in quantitative immunochemical methods. *Biochem. Medica* 50–62 (2009). doi:10.11613/BM.2009.005

317. Golden, A. *et al.* A Recombinant Positive Control for Serology Diagnostic Tests Supporting Elimination of Onchocerca volvulus. *PLoS Negl. Trop. Dis.* **10,** e0004292 (2016).

318. McCallum, F. J. *et al.* Differing rates of antibody acquisition to merozoite antigens in malaria: implications for immunity and surveillance. *J. Leukoc. Biol.* **101,** 913–925 (2017).

319. França, C. T. *et al.* An Antibody Screen of a Plasmodium vivax Antigen Library Identifies Novel Merozoite Proteins Associated with Clinical Protection. *PLoS Negl. Trop. Dis.* **10,** e0004639 (2016).

320. Bureau, A. *et al.* Identifying SNPs predictive of phenotype using random forests. *Genet. Epidemiol.* **28,** 171–182 (2005).

321. Strobl, C., Boulesteix, A.-L., Zeileis, A. & Hothorn, T. Bias in random forest variable importance measures: Illustrations, sources and a solution. *BMC Bioinformatics* **8,** 25 (2007).

322. Lunetta, K. L., Hayward, L. B., Segal, J. & Van Eerdewegh, P. Screening large-scale association study data: exploiting interactions using random forests. *BMC Genet.* **5,** 32 (2004).

323. Gregorutti, B., Michel, B. & Saint-Pierre, P. Correlation and variable importance in random forests. *Stat. Comput.* **27,** 659–678 (2017).

324. The Gambia Demographic and Health Survey. (2013).

325. Drakeley, C. J. *et al.* Altitude-dependent and -independent variations in Plasmodium falciparum prevalence in northeastern Tanzania. *J. Infect. Dis.* **191,** 1589–98 (2005).

326. Baum, E. *et al.* Protein Microarray Analysis of Antibody Responses to Plasmodium falciparum in Western Kenyan Highland Sites with Differing Transmission Levels. *PLoS One* **8,** e82246 (2013).

327. Aponte, J. J. *et al.* Age Interactions in the Development of Naturally Acquired Immunity to Plasmodium falciparum and Its Clinical Presentation. *PLoS Med.* **4,** e242 (2007).

328. Osier, F. H. A. *et al.* Breadth and Magnitude of Antibody Responses to Multiple Plasmodium falciparum Merozoite Antigens Are Associated with Protection from Clinical Malaria. *Infect. Immun.* **76,** 2240–2248 (2008).

329. Dent, A. E. *et al. Plasmodium falciparum* Protein Microarray Antibody Profiles Correlate With Protection From Symptomatic Malaria in Kenya. *J. Infect. Dis.* **212,** 1429–1438 (2015).

330. Marsh, K. & Howard, R. J. Antigens induced on erythrocytes by P. falciparum: expression of

diverse and conserved determinants. *Science* **231,** 150–3 (1986).

331. Tran, T. M. *et al.* Naturally Acquired Antibodies Specific for Plasmodium falciparum Reticulocyte-Binding Protein Homologue 5 Inhibit Parasite Growth and Predict Protection From Malaria. *J. Infect. Dis.* **209,** 789–798 (2014).

332. Partey, F. D. *et al.* Kinetics of antibody responses to PfRH5-complex antigens in Ghanaian children with Plasmodium falciparum malaria. *PLoS One* **13,** e0198371 (2018).

333. Kinyanjui, S. M., Conway, D. J., Lanar, D. E. & Marsh, K. IgG antibody responses to Plasmodium falciparum merozoite antigens in Kenyan children have a short half-life. *Malar. J.* **6,** 82 (2007).

334. Cavanagh, D. R. *et al.* Differential patterns of human immunoglobulin G subclass responses to distinct regions of a single protein, the merozoite surface protein 1 of Plasmodium falciparum. *Infect. Immun.* **69,** 1207–11 (2001).

335. Morell, A., Terry, W. D. & Waldmann, T. A. Metabolic properties of IgG subclasses in man. *J. Clin. Invest.* **49,** 673–680 (1970).

336. Vidarsson, G., Dekkers, G. & Rispens, T. IgG Subclasses and Allotypes: From Structure to Effector Functions. *Front. Immunol.* **5,** (2014).

337. Wipasa, J. *et al.* Long-Lived Antibody and B Cell Memory Responses to the Human Malaria Parasites, Plasmodium falciparum and Plasmodium vivax. *PLoS Pathog.* **6,** e1000770 (2010).

338. Slifka, M. K., Antia, R., Whitmire, J. K. & Ahmed, R. Humoral immunity due to long-lived plasma cells. *Immunity* **8,** 363–72 (1998).

339. Manz, R. A., Hauser, A. E., Hiepe, F. & Radbruch, A. Maintenance of serum antibody levels. *Annu. Rev. Immunol.* **23,** 367–386 (2005).

340. Portugal, S., Pierce, S. K. & Crompton, P. D. Young lives lost as B cells falter: what we are learning about antibody responses in malaria. *J. Immunol.* **190,** 3039–46 (2013).

341. Nduati, E. W. *et al.* Distinct Kinetics of Memory B-Cell and Plasma-Cell Responses in Peripheral Blood Following a Blood-Stage Plasmodium chabaudi Infection in Mice. *PLoS One* **5,** e15007 (2010).

342. Ndungu, F. M. *et al.* Functional Memory B Cells and Long-Lived Plasma Cells Are Generated after a Single Plasmodium chabaudi Infection in Mice. *PLoS Pathog.* **5,** e1000690 (2009).

343. Takala, S. L. & Plowe, C. V. Genetic diversity and malaria vaccine design, testing and efficacy: preventing and overcoming 'vaccine resistant malaria'. *Parasite Immunol.* **31,** 560–573 (2009).

344. Scherf, A., Lopez-Rubio, J. J. & Riviere, L. Antigenic Variation in *Plasmodium falciparum*. *Annu. Rev. Microbiol.* **62,** 445–470 (2008).

345. Neafsey, D. E. *et al.* Genetic Diversity and Protective Efficacy of the RTS,S/AS01 Malaria Vaccine. *N. Engl. J. Med.* **373,** 2025–2037 (2015).

346. Franks, S. *et al.* Genetic Diversity and Antigenic Polymorphism in Plasmodium falciparum: Extensive Serological Cross-Reactivity between Allelic Variants of Merozoite Surface Protein 2. *Infect. Immun.* **71,** 3485–3495 (2003).

347. Krishnarjuna, B. *et al.* Strain-transcending immune response generated by chimeras of the malaria vaccine candidate merozoite surface protein 2. *Sci. Rep.* **6,** 20613 (2016).

348. Casares, S., Brumeanu, T.-D. & Richie, T. L. The RTS,S malaria vaccine. *Vaccine* **28,** 4880–94 (2010).

349. RTS,S Clinical Trials Partnership *et al.* A phase 3 trial of RTS,S/AS01 malaria vaccine in African

infants. *N. Engl. J. Med.* **367,** 2284–95 (2012).

350. RTS,S Clinical Trials Partnership *et al.* First Results of Phase 3 Trial of RTS,S/AS01 Malaria Vaccine in African Children. *N. Engl. J. Med.* **365,** 1863–1875 (2011).

351. Webster, D. P. *et al.* Enhanced T cell-mediated protection against malaria in human challenges by using the recombinant poxviruses FP9 and modified vaccinia virus Ankara. *Proc. Natl. Acad. Sci. U. S. A.* **102,** 4836–41 (2005).

352. Bejon, P. *et al.* A phase 2b randomised trial of the candidate malaria vaccines FP9 ME-TRAP and MVA ME-TRAP among children in Kenya. *PLoS Clin. Trials* **1,** e29 (2006).

353. Moorthy, V. S. *et al.* A randomised, double-blind, controlled vaccine efficacy trial of DNA/MVA ME-TRAP against malaria infection in Gambian adults. *PLoS Med.* **1,** e33 (2004).

354. Sanchez-Mazas, A. *et al.* The HLA-B landscape of Africa: Signatures of pathogen-driven selection and molecular identification of candidate alleles to malaria protection. *Mol. Ecol.* **26,** 6238–6252 (2017).

355. Schaible, U. E. & Kaufmann, S. H. E. Malnutrition and Infection: Complex Mechanisms and Global Impacts. *PLoS Med.* **4,** e115 (2007).

356. Hartgers, F. C. & Yazdanbakhsh, M. Co-infection of helminths and malaria: modulation of the immune responses to malaria. *Parasite Immunol.* **28,** 497–506 (2006).

357. Tran, T. M., Samal, B., Kirkness, E. & Crompton, P. D. Systems immunology of human malaria. *Trends Parasitol.* **28,** 248–257 (2012).

358. Fowkes, F. J. I., Boeuf, P. & Beeson, J. G. Immunity to malaria in an era of declining malaria transmission. *Parasitology* **143,** 139–153 (2016).

359. Snow, R. W., Rowan, K. M. & Greenwood, B. M. A trial of permethrin-treated bed nets in the prevention of malaria in Gambian children. *Trans. R. Soc. Trop. Med. Hyg.* **81,** 563–567 (1987).

360. Snow, R. W., Lindsay, S. W., Hayes, R. J. & Greenwood, B. M. Permethrin-treated bed nets (mosquito nets) prevent malaria in Gambian children. *Trans. R. Soc. Trop. Med. Hyg.* **82,** 838–842 (1988).

361. Snow, R. W., Rowan, K. M., Lindsay, S. W. & Greenwood, B. M. A trial of bed nets (mosquito nets) as a malaria control strategy in a rural area of The Gambia, West Africa. *Trans. R. Soc. Trop. Med. Hyg.* **82,** 212–5 (1988).

362. Alonso, P. L. *et al.* A malaria control trial using insecticide-treated bed nets and targeted chemoprophylaxis in a rural area of The Gambia, West Africa: 6. The impact of the interventions on mortality and morbidity from malaria. *Trans. R. Soc. Trop. Med. Hyg.* **87,** 37–44 (1993).

363. D'Alessandro, U. *et al.* Mortality and morbidity from malaria in Gambian children after introduction of an impregnated bednet programme. *Lancet* **345,** 479–483 (1995).

364. The Republic of The Gambia. *The Gambia National Health Sector Strategic Plan*. (2014).

365. Cameron, E. *et al.* Defining the relationship between infection prevalence and clinical incidence of Plasmodium falciparum malaria. *Nat. Commun.* **6,** 8170 (2015).

366. Metselaar D; van Thiel P.H. Classification of Malaria. *Trop. Geogr. Med.* **11,** 157–61 (1959).

367. Stevenson, J. C. *et al.* Reliability of School Surveys in Estimating Geographic Variation in Malaria Transmission in the Western Kenyan Highlands. *PLoS One* **8,** e77641 (2013).

368. Chen, I. *et al.* "Asymptomatic" Malaria: A Chronic and Debilitating Infection That Should Be

Treated. *PLOS Med.* **13,** e1001942 (2016).

369. WHO Global Malaria Programme. *WHO malaria terminology*. (2016).

370. Bousema, T., Okell, L., Felger, I. & Drakeley, C. Asymptomatic malaria infections: detectability, transmissibility and public health relevance. *Nat. Rev. Microbiol.* **12,** 833–40 (2014).

371. Parker, D. M. *et al.* Limitations of malaria reactive case detection in an area of low and unstable transmission on the Myanmar–Thailand border. *Malar. J.* **15,** 571 (2016).

372. WHO Malaria Policy Advisory Committee. *Mass drug administration, mass screening and treatment and focal screening and treatment for malaria, Meeting report of the Evidence Review Group*. (2015).

373. Pinchoff, J. *et al.* Targeting indoor residual spraying for malaria using epidemiological data: a case study of the Zambia experience. *Malar. J.* **15,** 11 (2016).

374. World Health Organization (WHO). *An operational manual for indoor residual spraying (IRS) for malaria transmission control and elimination. 2nd edition*. (2015).

375. Alegana, V. A. *et al.* Advances in mapping malaria for elimination: fine resolution modelling of Plasmodium falciparum incidence. *Sci. Rep.* **6,** 29628 (2016).

376. National Vector-borne Disease Control Programme (Namibia). *Malaria Strategic Plan, 2010-2016l*. (Directorate: Special Programmes, National Vector-borne Diseases Control Programme, 2010, 2010).

377. University of California, S. F. Evaluation of Targeted Parasite Elimination (TPE) in Namibiae. *ClinicalTrials.cov* Available at: https://clinicaltrials.gov/ct2/show/NCT02610400.

378. Medzihradsky, O. F. *et al.* Study protocol for a cluster randomised controlled factorial design trial to assess the effectiveness and feasibility of reactive focal mass drug administration and vector control to reduce malaria transmission in the low endemic setting of Namibia. *BMJ Open* **8,** e019294 (2018).

379. *National malaria case management guidelines*. (Republic of Namibia, Ministry of Health and Social Services, 2014).

380. Brady, O. J. *et al.* Role of mass drug administration in elimination of Plasmodium falciparum malaria: a consensus modelling study. *Lancet Glob. Heal.* **5,** e680–e687 (2017).

381. Stuckey, E. M., Miller, J. M., Littrell, M., Chitnis, N. & Steketee, R. Operational strategies of anti-malarial drug campaigns for malaria elimination in Zambia's southern province: a simulation study. *Malar. J.* **15,** 148 (2016).

382. Maude, R. J., Nguon, C., Dondorp, A. M., White, L. J. & White, N. J. The diminishing returns of atovaquone-proguanil for elimination of Plasmodium falciparum malaria: modelling mass drug administration and treatment. *Malar. J.* **13,** 380 (2014).

383. Newby, G. *et al.* Review of mass drug administration for malaria and its operational challenges. *Am. J. Trop. Med. Hyg.* **93,** 125–34 (2015).

384. Parker, D. M. *et al.* Scale up of a Plasmodium falciparum elimination program and surveillance system in Kayin State, Myanmar. *Wellcome Open Res.* **2,** 98 (2017).

385. Landier, J. *et al.* Effect of generalised access to early diagnosis and treatment and targeted mass drug administration on Plasmodium falciparum malaria in Eastern Myanmar: an observational study of a regional elimination programme. *Lancet* **391,** 1916–1926 (2018).

386. Use of serology to validate health facility-based data for prioritizing IRS in the central highlands of Madagascar | MESA. Available at: http://www.malariaeradication.org/mesa-

track/use-serology-validate-health-facility-based-data-prioritizing-irs-central-highlands-0. (Accessed: 19th June 2018)

387. Epi Info™ | CDC. Available at: https://www.cdc.gov/epiinfo/index.html. (Accessed: 19th June 2018)

388. ClinEpiDB. Available at: https://clinepidb.org/ce/app. (Accessed: 19th June 2018)

389. Afgan, E. *et al.* The Galaxy platform for accessible, reproducible and collaborative biomedical analyses: 2016 update. *Nucleic Acids Res.* **44,** W3–W10 (2016).

390. Priest, J. W. *et al.* Integration of Multiplex Bead Assays for Parasitic Diseases into a National, Population-Based Serosurvey of Women 15-39 Years of Age in Cambodia. *PLoS Negl. Trop. Dis.* **10,** e0004699 (2016).

391. WHO. *Situation Report Ebola Virus Disease*. (2016).

392. Plucinski, M. M. *et al.* Effect of the Ebola-virus-disease epidemic on malaria case management in Guinea, 2014: a cross-sectional survey of health facilities. *Lancet. Infect. Dis.* **15,** 1017–1023 (2015).

393. Walker, P. G. T. *et al.* Malaria morbidity and mortality in Ebola-affected countries caused by decreased health-care capacity, and the potential effect of mitigation strategies: a modelling analysis. *Lancet. Infect. Dis.* **15,** 825–32 (2015).

394. Preventive malaria treatment for contacts of patients with Ebola virus disease in the context of the west Africa 2014–15 Ebola virus disease response: an economic analysis. *Lancet Infect. Dis.* **16,** 449–458 (2016).

395. WHO | Guidance on temporary malaria control measures in Ebola-affected countries. *WHO* (2015).